PLACENTATION AND BARRIER TRANSPORTERS:

REGULATION BY ENDOGENOUS AND EXOGENOUS FACTORS

By

Ludwik Janusz Gorczyca

A dissertation submitted to

The School of Graduate Studies

Rutgers, The State University of New Jersey

In partial fulfillment of the requirements

For the degree of

Doctor of Philosophy

Joint Graduate Program in Toxicology

Written under the direction of

Dr. Lauren M. Aleksunes

And approved by

_____

_____

_____

_____

_____

New Brunswick, New Jersey

October, 2020

ABSTRACT OF THE DISSERTATION

Placentation and Barrier Transporters:

Regulation by Endogenous and Exogenous Factors

By: LUDWIK JANUSZ GORCZYCA

Dissertation Director: Lauren Aleksunes, PharmD, PhD, DABT

During pregnancy, the placenta serves as a critical interface between the fetal and maternal circulations and facilitates nutrient-waste exchange to support normal fetal development. Once established, the placenta regulates hormone secretion, xenobiotic metabolism, and expression of transporters to maintain overall barrier integrity. Uptake and efflux transporters are localized to the syncytiotrophoblast cells and in part regulate the disposition of endogenous signaling molecules, hormones, chemicals, and drugs across the placenta. Development of the placenta can be affected by both endogenous (i.e. low oxygen, cyclic nucleotide signaling) and xenobiotic (i.e. mycotoxin zearalenone) influences. Due to the critical role of the placenta in supporting normal fetal development, more work is urgently needed to further characterize its physiology and susceptibility to insults. The purpose of this dissertation was to investigate the impact of endogenous (i.e. hypoxia, cyclic nucleotide signaling) and exogenous (i.e. zearalenone) factors on placentation with a focus on endobiotic and xenobiotic disposition through transporter-mediated mechanisms. Physiologically relevant low oxygen tension, observed during the 1st and 2nd trimesters, altered the transcriptional regulatory pathways and drug transporter profiles in two *in vitro* placental models (BeWo choriocarcinoma cells, human placental explants). Altered functionality of drug transporters may not only impact the disposition of xenobiotics but also endogenous molecules that activate/regulate downstream signaling cascades and overall placentation. Cyclic adenosine monophosphate (cAMP)-mediated signaling regulates the process of syncytialization whereby giant multinucleated syncytiotrophoblasts arise from the fusion of progenitor cytotrophoblast cells.

Multidrug resistance-associated protein (MRP) transporters are localized to the syncytiotrophoblast cell layer and regulate intracellular cAMP levels through active efflux. Studies using both pharmacological and genetic loss-of-function approaches targeting the MRP5 transporter revealed enhanced intracellular concentration of cAMP and syncytialization in placental explants and/or BeWo cells. Zearalenone, an estrogenic mycotoxin, is a known substrate of the BCRP efflux drug transporter. *In vivo* studies using Bcrp heterozygous mice demonstrated that zearalenone increased maternal weight gain and embryo resorption as well as decreased placental weight and area. Further examination revealed that markers responsible for placental differentiation were globally down-regulated in zearalenone-treated placentas. Zearalenone exposure differentially regulated placental xenobiotic transporter expression and decreased placental antioxidant defense genes. Together, these data demonstrate that endogenous and exogenous factors may influence placental transporter expression and function, and in turn, lead to altered disposition of endobiotics and xenobiotics and impact placenta and fetal development.

DEDICATION

This dissertation is dedicated to my dearest wife, Sylwia Gorczyca, my daughter Emilia Eve Gorczyca, and my parents, Agata and Boguslaw Prawdzik, Ewa and Marek Denko.

ACKNOWLEDGEMENTS

First and foremost, I would like to acknowledge my mentor and Ph.D. advisor, Dr. Lauren Aleksunes. Thank you so much for taking a chance on me and allowing me to join your lab 6 years ago. I always like to reflect and see how things have changed over time to truly appreciate the current moment and the progress achieved. I entered the graduate program not sure of myself and whether I even belonged at this stage of academia. While I was always able to memorize and regurgitate facts, I knew that if I were to succeed in this program I would need to learn how to think, interpret, and analyze. Through every one-on-one meeting that we had, I tried to take away even the smallest bit of your problem-solving skills and try to understand how you approach unique challenges that arise during various experimental designs. As the years progressed, I felt myself continuously grow as an independent thinker and scientist. Complicated problems that would have previously stressed me out and caused me worry became fun puzzles that simply needed a novel approach to attain resolution. It is safe to say that without your guidance and mentorship I would not have achieved this transformation. I am graduating with the utmost confidence that I can meet and overcome any challenges that arise during my next career stage. A welcome change from how I began my graduate studies. I can only hope to impart a similar type of influence onto my future mentees as you have onto me. To my thesis committee, Drs. Brian Buckley, Grace Guo, Phoebe Stapleton, and Marie Fortin, thank you from the bottom of my heart for your continuous support and time. Without your contribution my thesis would not have been anywhere close to what it is today. Your insight has facilitated the development of not only my aims but also my growth and development as a Toxicologist.

To all the past and present Aleksunes Lab members, it was truly an amazing experience to work alongside you! I would especially like to thank Drs. Kristin Bircsak and Xia Wen. I truly appreciate your friendship and the time you took away from your own studies to teach me the various assays

and models our laboratory uses day in and day out. While I may have asked a million questions during my first year (which may or may not have caused some hearing loss or at least the desire for some :p), please know that I remember all of your suggestions and answers to this day. I was able to pass along these insights to many of our present members and hope that they will do the same with the next generation of members. Without your help I would have been a life-long graduate student.

To the Rutgers Pharmacology/Toxicology Department and EOHSI staff, thank you for all your help. You have ensured that this process went as smoothly as possible. I would especially like to thank Liz, Eva, and Linda who worked tirelessly behind the scenes to make sure everything course- and grant-wise was taken care of. To the RATS, thank you for all the great experiences and fun times away from the lab.

Finally, I would like to thank my family. To the love of my life, my best friend, my wife, Sylwia Gorczyca: Thank you for your unconditional love, support, and endless laughter even during the hardest of times. You are my motivation to strive to be better every day. I cannot express enough how special you are and how much I cherish every moment that we spend together. To my parents, Agata Prawdzik and Boguslaw Prawdzik. Thank you for all the sacrifices you have made over the years to make sure that I could reach the goals I set out to accomplish so many years ago. It is because of your support, love, and guidance that I was able to continue to grow and become the person that I am today. Without you I would not be here. To my parents, Ewa and Marek Denko. Thank you for your endless love and help. It is because of you that Sylwia and I were able to start our life together with such ease. I cannot image the last few years without all the laughs we have shared. I love you all so much and hope that I have made you proud.

ACKNOWLEDGEMENT OF PUBLICATIONS

CHAPTER 1.2

Ludwik Gorczyca and Lauren M. Aleksunes (2020) Transcription factor-mediated regulation of the BCRP/ABCG2 efflux transporter: A review across tissues and species. *Expert Opin Drug Metab Toxicol. doi: 10.1080/17425255.2020.1732348. PMID: 32077332*

CHAPTER 2

Ludwik Gorczyca, Jianyao Du, Kristin M. Bircsak, Xia Wen, Anna M. Vetrano, and Lauren M. Aleksunes (2020) Low oxygen tension differentially regulates expression of placental SLC and ABC transporters. *Under review for FEBS Letter Special Issue on ABC Transporters*.

CHAPTER 3

Ludwik Gorczyca, Bingbing Wang, Todd Rosen, Lauren M. Aleksunes (2020) Novel regulation of human placental cell syncytialization by cyclic nucleotide-transporter interactions. *In preparation***.**

CHAPTER 4

Ludwik Gorczyca and Lauren M. Aleksunes (2020) Expression of the Bcrp transporter influences placental responses to the mycoestrogen zearalenone. *In preparation*.

APPENDIX 1

John T. Szilagyi, **Ludwik Gorczyca**, Anita Brinker, Brian Buckley, Jeffrey D. Laskin, Lauren M. Aleksunes (2019) Placental BCRP/ABCG2 transporter prevents fetal exposure to estrogenic mycotoxin zearalenone. *Toxicol Sci. 168(2):394-404. PMID: 30576553*

APPENDIX 2

Kristin M. Bircsak, Vivek Gupta, Poi Yu Sofia Yuen, **Ludwik Gorczyca**, Barry I Weinberger, Anna M. Vetrano, Lauren M. Aleksunes (2016) Genetic and dietary regulation of glyburide efflux by the human placental BCRP transporter. *J Pharmacol Exper Ther. 357:103-113. PMID: 26850786*

APPENDIX 3

Dahea You, Xia Wen, **Ludwik Gorczyca**, Ayeshia Morris, Jason R Richardson, Lauren M. Aleksunes (2019) Increased MDR1 transporter expression in human brain endothelial cells through enhanced histone acetylation and activation of aryl hydrocarbon receptor signaling. *Mol Neurobol. 56(10):6986-7002. PMID: 30963442*

APPENDIX 4

Yixin Lin, Kristin M. Bircsak, **Ludwik Gorczyca**, Xia Wen, Lauren M. Aleksunes (2017) Regulation of the placental BCRP transporter by PPAR gamma. *J Biochem Mol Toxicol. 31(5):10. PMID: 27879033*

APPENDIX 5

Lissa N Francois, **Ludwik Gorczyca**, Jianyao Du, Kristin M. Bircsak, Elizabeth Yen, Xia Wen, Mei-Juan Tu, Ai-Ming Yu, Nicholas P Illsley, Stacy Zamudio, Lauren M. Aleksunes (2017) Down-regulation of placental BCRP/ABCG2 transporter in response to hypoxia signaling. *Placenta. 51:57-63. PMID: 28292469*

APPENDIX 6

Le Zhan, Ill Yang, Bo Kong, Jianliang Shen, **Ludwik Gorczyca**, Naureen Memon, Brian T Buckley, Grace L Guo (2016) Dysregulation of bile acid homeostasis in parenteral nutrition mouse model. *Am J Physiol Gastrointest Liver Physiol. 310(2):G93-G102. PMID: 26564717*

Table of Contents

LIST OF FIGURES

LIST OF TABLES

CHAPTER 1: INTRODUCTION

1.1 Human Placenta Physiology

Normal fetal growth and development during pregnancy is reliant upon proper establishment and attachment of the placenta to the maternal endometrium. The placenta supports a healthy pregnancy through regulation of endocrine signaling, metabolism, endogenous immune response, and restricted accumulation of xenobiotics and fetal waste. Implantation and development of the placenta is a tightly regulated process centered around close interaction between embryonic and maternal cells. Due to the direct contact of the placental cells with maternal blood, the human placenta is considered to be hemochorial. The following overview of placental structure and function has been adapted from Williams Obstetrics (Cunningham 2014).

1.1.1 Structure and Development

The establishment and development of placental cells occurs within the first 3-4 days following fertilization. Continuous cleavage and differentiation of the zygote results in the formation of the blastocyst that is comprised of the inner cell mass, blastocyst cavity, and placental trophoblast cells. The inner cell mass contains stem cells that ultimately give rise to embryonic and extraembryonic structures. Various cytokines and hormones secreted by the blastocyst influence the receptivity of the maternal endometrium and enable implantation of the blastocyst to occur within 5-8 days following conception. Implantation is in part mediated by placental trophoblast cells that invade the maternal endometrium and remodel uterine vasculature to increase blood supply needed to sustain the growth and development of both the fetus and placenta.

The mature placenta is an organ composed of fetal and maternal tissue derived from the chorionic sac and endometrium, respectively. The fetal portion, referred to as the chorionic plate, contains

fetal umbilicus vasculature. The maternal region of the placenta is called the basal plate and is in direct contact with the uterus. In between the fetal and maternal regions of the placenta is the intervillous space which houses chorionic villi. Chorionic villi are villous tree structures that contain fetal capillaries and consist of an inner cytotrophoblast core surrounded by an outer layer of syncytiotrophoblasts. The chorionic villi are the primary site of exchange between fetal and maternal circulations as maternal blood, flowing from the uterine spiral arteries, envelops them.

Trophoblast Differentiation.

Placentation relies upon differentiation and proliferation of mononuclear progenitor cells called cytotrophoblasts. Cytotrophoblasts differentiate into two specific terminal cell types referred to as syncytiotrophoblasts and extravillous trophoblasts (EVTs). Multinucleated syncytiotrophoblasts line the outermost layer of chorionic villi and arise from aggregation and fusion of the underlying mononuclear cytotrophoblasts. Once formed, syncytiotrophoblasts perform a wide variety of placental functions including hormone secretion, metabolism, and protection against xenobiotic accumulation through the expression of efflux drug transporters. The syncytial epithelium exists in a post-mitotic state and relies on fusion with cytotrophoblasts for replenishment following cell turnover. The turnover of syncytiotrophoblasts occurs through apoptosis where apoptotic nuclei are shed into the maternal blood in tightly packed syncytial knots or sprouts. The turnover rate of syncytiotrophoblasts remains constant throughout pregnancy and is estimated to be about 4.5 million cells per day. With term placenta containing 6×10^9 cytotrophoblasts, only 0.8% have to proliferate each day to maintain the syncytial epithelial lining (Mayhew et al. 2001).

The cyclic adenosine monophosphate (cAMP) signaling pathway is one of the major regulators of syncytialization. This pathway is activated when human chorionic gonadotropin (hCG), secreted by syncytiotrophoblasts, binds to the luteinizing hormone receptor and increases intracellular cAMP levels by activating the adenylyl cyclase enzyme. Increased cAMP leads to protein kinase

A (PKA) activation and phosphorylation of the transcription factor cAMP response element binding protein (CREB). Phosphorylated CREB acts as a transcriptional co-activator and enables for the transcription of various fusogenic genes such as Glial Cell Missing 1 (GCM1), Syncytin 1, and Syncytin 2 to occur (Gerbaud et al. 2015a). Syncytins are fusogenic proteins encoded by the human endogenous defective retroviral genes, *ERVW-1* and *-2*, and localized to the syncytiotrophoblast cell layer (Knerr et al. 2002; Mi et al. 2000). Neutral amino acid transporters, ASCT-1 and -2, function as receptors for syncytins and enable their binding to facilitate adjacent cell aggregation and induction of the fusion process. Although the exact mechanism of syncytialization has not been established, it is hypothesized that initiation of cell fusion occurs through up-regulation of syncytin proteins in cytotrophoblasts, down-regulation of ASCT receptors in existing syncytiotrophoblasts, and/or up-regulation of syncytins in syncytiotrophoblasts (Colman et al. 2003). Once bound to its receptor, Syncytin, acting as a class I retroviral envelope protein, is thought to insert a hydrophobic fusion loop into the target plasma membrane to form a trimer. This trimeric intermediate then folds into a hairpin conformation and brings the target plasma membrane into close proximity of the original plasma membrane. The folding of the hairpin conformation results in plasma membrane distortions leading to the formation of small openings called fusion pores. These fusion pores allow for the joining of the plasma membranes to occur (Harrison 2008). The process of syncytialization can be stimulated *in vitro* with chemical agents such as 8-bromo-cAMP, a membrane permeable cAMP derivative, and forskolin, an activator of the adenylyl cyclase synthetic enzyme (Ogura et al. 2000; Wice et al. 1990).

The pathology of gestational disorders such as preeclampsia have recently been linked to trophoblast cell dysfunction. Preeclampsia, a disorder that affects 5-8% of all pregnancies worldwide, is characterized by incomplete spiral artery remodeling and increased maternal blood pressure and proteinuria. Elevated levels of human chorionic gonadotropin during second and third trimesters are associated with increased risk for preeclampsia, an observation that suggests major

dysfunction in syncytialization (Asvold et al. 2014; Barjaktarovic et al. 2019; Basirat et al. 2006; Heinonen et al. 1996; Taher et al. 2019; Wald et al. 2001). Interestingly, preeclamptic placentas exhibited significantly reduced mRNA expression of fusogenic markers, GCM1 and Syncytin-1 (Chen et al. 2004; Lapaire et al. 2012; Lee et al. 2001; Sitras et al. 2009). Disrupting the rate and extent of syncytialization can result in altered nutrient and xenobiotic metabolism, transport, and placental hormone production during pregnancy and in turn deleterious fetal outcomes.

The two subtypes of the extravillous trophoblasts, invasive endovascular cytotrophoblasts (eCTBs) and interstitial cytotrophoblasts (iCTBs), have distinct roles during placentation. During the 1st trimester, eCTBs occlude the terminal portions of the maternal spiral arteries. This occlusion limits blood flow from the arteries into the intervillous space of the placenta and results in a hypoxic environment (20 mmHg, 3% O_2) (Schneider 2011). As pregnancy progresses to the 2nd trimester, the eCTBs remodel the maternal spiral arteries to promote their dilation. These wider arteries allow for an increase in blood supply to the intervillous space which in turn results in an increase of oxygen tension to about 60 mmHg or 8% O_2 (Schneider 2011). Alternatively, iCTBs invade the maternal decidua and function to anchor the placenta onto the maternal endometrium. Secretion of matrix metalloproteinases, aminopeptidases, cathepsin B, and type IV collagenase by the iCTBs allows them to infiltrate the maternal decidua and degrade its extracellular matrix.

Placental pathologies have also been closely associated with abnormal invasion of trophoblasts. Placenta accreta, characterized by excessive invasion of extravillous trophoblast cells, is considered a high-risk pregnancy complication. This complication is marked by poor placental detachment following childbirth which can cause severe blood loss. Alternatively, inadequate trophoblast invasion during early stages of pregnancy can result in preeclampsia. Insufficient remodeling of the spiral arteries leads to hypoperfusion of the placenta and in turn reduced oxygen and nutrient

delivery to the fetus causing downstream deleterious pathologies such as intrauterine growth restriction (Gathiram et al. 2016).

Blood Flow.

The umbilical cord, which contains two arteries and one vein, mediates the blood flow within the feto-placental unit. Fetal vasculature enters the chorionic plate through the umbilical cord and branches into capillaries that are confined in chorionic villi. Unlike normal human circulation, oxygenated fetal blood flows from the placenta to the fetus via the umbilical vein while deoxygenated blood flows back via umbilical arteries. The oxygen/CO_2 exchange occurs at the villous syncytial epithelium that is bathed in oxygen rich maternal blood.

Fetal Membranes.

The amnion and chorion are fetal-facing and maternal-facing fetal membranes, respectively, that comprise the chorionic plate. The amniotic membrane is composed of five distinct layers with the innermost epithelium being in direct contact with the amniotic fluid. The other layers include the fibroblast layer, the spongy layer, and the compact layer. The chorionic membrane contains a basement membrane, reticular layer, and extravillous trophoblast layer which helps to adhere the placenta onto the maternal endometrium (Gude et al. 2004).

1.1.2 **Placental Function**

Serving as an interface between the feto-maternal circulations, the placenta plays significant roles in maintaining healthy development of a fetus. Roles include regulation of endocrine and immune responses as well as nutrient-waste and chemical exchange including nutrients and steroids.

Endocrine.

Human trophoblasts produce both steroid and protein hormones which function together to help sustain a normal and healthy fetal development during pregnancy. The human chorionic gonadotropin (hCG) is a glycoprotein secreted by synyctiotrophoblasts and acts via the luteinizing hormone-hCG receptor. Two dissimilar subunits, hCGα and hCGß, are held together by electrostatic and hydrophobic forces to make up the hCG molecule. The hCGα subunit is shared among other glycoprotein hormones such as the luteinizing hormone, follicle stimulating hormone, and thyroid stimulating hormone. Alternatively, the hCGß subunit is distinct from the other glycoproteins and has a specific amino acid sequence. Although the synthesis of the subunits is regulated separately, dimerization is required to bind the LH-hCG receptor and elicit biological function. This hormone not only regulates syncytialization but also initiates progesterone secretion to maintain the corpus luteum. Maternal plasma concentration of hCG reaches a peak level of 50,000-100,000 mlU/mL at around 10 weeks gestation and declines thereafter till term.

The placenta becomes the predominant source of progesterone production by the 8th week of pregnancy. At this time, plasma progesterone levels reach a concentration of ~40 ng/mL and steadily rises to ~200 ng/mL at term. Some of the functions mediated by progesterone include thickening of the maternal uterus lining, decreasing prostaglandin formation, stimulating decidualization, and relaxing smooth muscle to inhibit contraction (Chatuphonprasert et al. 2018). Progesterone exerts its functional roles by binding to the progesterone receptor-A (PR-A) and -B (PR-B) isoforms which have different activities, functions, and expression profiles across various tissues (Shao 2013). Similar to progesterone production, the 8th week of pregnancy marks the luteal-placental transition of estrogen production. In the placenta, the dehydroepiandrosterone (DHEA) steroid and its sulfated conjugate serve as estrogen precursors and are produced primarily by fetal liver and adrenal glands. Cytochrome P450 aromatase, 3ß-hydroxysteroid dehydrogenase type 1, and 17ß-hydroxysteroid dehydrogenase type I work together to convert DHEA to estradiol in the placenta. Just as observed with progesterone, estradiol plasma concentrations steadily rise

until term to reach a maximum concentration of ~30 ng/mL. Main function of estrogens during pregnancy is to maintain uterine lining and vasodilation of the maternal uterine blood vessels. Estrogens elicit their functions by binding to estrogen receptors ERα and ERß.

Syncytiotrophoblasts also produce human placental lactogen (hPL) and corticotropin releasing hormone (CRH). Human placental lactogen is a single, non-glycosylated polypeptide chain with a highly similar sequence homology to the human growth hormone. Secretion of the hPL is proportional to the placental mass which results in its plasma concentration to steadily rise up to 15 µg/mL at term. hPL functions to increase fetal concentrations of glucose by regulating free fatty acid lipolysis and decreasing maternal glucose utilization. hPL aids in fetal and placental angiogenesis by binding to the prolactin receptor, mimicking the action prolactin. CRH is a stress response hormone that stimulates the pituitary synthesis of adrenocorticotropic hormone and in turn secretion of glucocorticoid steroid hormones. Maternal serum CRH levels rise to ~500 pmol/L towards end of term and are thought to play important roles in smooth-muscle relaxation in both vascular and myometrial tissues.

Transport.

During pregnancy, the placenta regulates the bidirectional transfer of nutrients, gases, waste byproducts, and xenobiotics between feto-maternal circulations. The main site of exchange is centered around the chorionic villi found in the intervillous space of the placenta. There, the syncytium surrounding the chorionic villi acts as the main physical barrier between the two circulations. The chemical properties of a given molecule determine the route of transport across lipid bilayer of syncytiotrophoblasts.

Small (<500 Da) and uncharged molecules can cross the syncytium via passive diffusion. In this mode of transfer, the molecule moves down its concentration gradient and as a result does not have

any energy requirements. Some small molecules are also transferred down a concentration gradient via facilitated diffusion whereby a specific transporter mediates the transfer. For example, glucose transport requires help from glucose transporters to move from a high to low concentration gradient and cross the synctiotrophoblast plasma membrane. Other molecules that move against the concentration gradient require primary or secondary active transport. Primary active transport utilizes energy derived from ATP hydrolysis to drive a give molecule across a plasma membrane. Alternatively, secondary active transport utilizes an electrochemical gradient derived from the movement of an ion such as Na^+ or H^+ down its concentration gradient to move another molecule against its own concentration gradient and into the cell.

Various uptake and efflux drug transporters mediate the active transepithelial transport of numerous substrates against their concentration gradients and across the syncytiotrophoblast cell layer. Multinucleated syncytiotrophoblasts express both uptake and efflux transporters on their apical (maternal-facing) and basolateral (fetal-facing) membranes. The solute carrier (SLC) superfamily of transporters mediates the facilitated uptake of organic anions and cations, serotonin and nucleosides among others. Uptake transporters such as concentrative nucleoside transporters (CNT), equilibriative nucleoside transporters (ENT), organic anion transporters (OAT), organic cation transporters (OCT), carnitine transporters (CNT), multidrug and toxin extrusion protein (MATE), and organic anion-transporting polypeptides (OATP) are localized to both the apical and basolateral membrane of syncytiotrophoblasts. The ATP-binding cassette (ABC) transporter superfamily utilizes ATP hydrolysis to efflux substrates (i.e. xenobiotics, endogenous waste) across the plasma membrane and out of the cell. The efflux transporters most highly expressed in the syncytiotrophoblasts include the breast cancer resistance protein (BCRP), multidrug resistance protein 1 (MDR1), and multidrug resistance-associated proteins (MRPs). The BCRP and MDR1 efflux transporters are localized to the apical membrane of syncytiotrophoblasts and function to protect the fetus from xenobiotics present in maternal circulation.

Immune Response.

Complex interactions between maternal decidual immune cells and fetal trophoblasts are required to allow for implantation, placental development, and ultimately fetal growth to occur. Placental trophoblasts are the only fetal cells in direct contact with maternal blood and tissues. These cells express and secrete specific factors that facilitate tolerance by the endogenous maternal immune system. For instance, villous trophoblasts lack human leukocyte antigens (HLAs) and are immunologically dormant with limited recognition by the maternal immune system. Alternatively, EVTs do express major histocompatibility complex class I molecules that are hypothesized to regulate the invasion depth of the trophoblasts during the implantation process. During the first trimester, natural killer cells, found in the endometrium and decidua, express killer Ig-like receptors (KIR) that facilitate binding to EVTs via their HLA antigens and protect them against cytotoxicity. Decidual natural killer cells secrete proangiogenic factors such as vascular endothelial growth factor (VEGF) which stimulate angiogenesis in the decidua. Fetal macrophages, called Hofbauer cells, are also found in the fetal vasculature of the villous stroma as early as 4 weeks post-conception. Hofbauer cells secrete anti-inflammatory cytokines such as transforming growth factor beta 1 (TGF-ß1) and interleukin 10 (IL-10) and therefore display an M2-like phenotype. Similar to decidual natural killer cells, Hofbauer cells also secrete VEGF and Sprouty (Spry) proteins which facilitate angiogenesis and stimulate chorionic villous branching, respectively. Other functions of Hofbauer cells include phagocytosis of apoptotic and necrotic debris as well as regulation of stromal water content. As a result of their multiple roles within the placenta, disruption of Hofbauer cell homeostasis has been association with obstetric complications such as villitis of unknown etiology (VUE), preeclampsia, and chorioamnionitis.

1.2 The Breast Cancer Resistance Protein (BCRP/ABCG2) Transporter

The breast cancer resistance protein (human *ABCG2*/BCRP and rodent *Abcg2/*Bcrp), a 75 kDa membrane transporter, was first identified in a human breast cancer cell line, MCF-7/AdrVp, following the observation of an ATP-dependent mechanism that reduced the intracellular accumulation and toxicity of the chemotherapeutic drug, mitoxantrone (Doyle et al. 1998). A member of the human ABC transporter superfamily (G subfamily), BCRP utilizes ATP hydrolysis to actively transport substrates against an electrochemical gradient. The functional unit of the ABC transporters is characterized by two nucleotide binding domains (NBDs) and two transmembrane domains (TMDs) which together form the substrate translocation pathway. ATP hydrolysis in the cytoplasmic NBD region drives conformational changes in the TMD region that allow for substrate transport across the lipid bilayer. Unlike other members of this transporter superfamily, the *ABCG2* gene encodes for a half transporter with a single cytoplasmic NBD region followed by a single TMD region composed of six α-helices required for substrate recognition and transport. Recent crystal structure analysis has shown that BCRP exists in dimeric as well as higher order tetrameric states composed of two BCRP dimers (Khunweeraphong et al. 2017; Rosenberg et al. 2010). It is thought that these higher order complexes are required in order for BCRP to be functional.

Human BCRP and rodent Bcrp isoforms transport a wide array of structurally- and chemically-unrelated substrates ranging from drugs to environmental contaminants as well as endogenous molecules (Reviewed in Mao 2008). Commonly used chemotherapeutic drugs that are substrates of BCRP include mitoxantrone, methotrexate, doxorubicin, and topotecan (Reviewed in Mao 2008; and in Ni et al. 2010). Other BCRP substrates include the diabetes drug glyburide, antihypertensive prazosin, antibiotic nitrofurantoin, and anticancer tyrosine kinase inhibitors as well as porphyrins, bile acids, and estrones (Reviewed in Mao 2008; and in Ni et al. 2010). BCRP is most highly expressed in tissues regulating pharmacokinetics (colon, small intestine, liver, kidney) and blood-tissue barriers (brain, testis, placenta). Localized on the maternal surface of placental syncytiotrophoblasts as well as the luminal surface of hepatocyte canaliculi, proximal convoluted

tubules, enterocytes and brain capillaries, BCRP serves a crucial protective role by limiting the cellular, and often tissue, accumulation of xenobiotics (Maliepaard et al. 2001a; Reviewed in Mao 2008; and in Natarajan et al. 2012).

1.2.1 Pharmacological and physiological functions of BCRP

BCRP functions as an efflux transporter to limit the intracellular accumulation of various agents and toxicants. BCRP-mediated transport of drugs including topotecan, mitoxantrone, daunorubicin, and doxorubicin is often one of the factors responsible for poor oral bioavailability, resistance in tumor cells, and prevention of fetal exposure (Imai et al. 2002; Jonker et al. 2000; Reviewed in Mao et al. 2015). Interestingly, the *ABCG2* gene contains several polymorphisms and splicing variants that affect BCRP protein expression and function. The C421A variant results in a lysine for glutamine substitution in position 141 (Q141K) that markedly decreases BCRP protein function (Bircsak et al. 2018; Imai et al. 2002). Such polymorphisms may have therapeutic implications for various drugs that are BCRP substrates. Patients heterozygous for the CA allele exhibit a 1.3-fold higher oral bioavailability of topotecan when compared to patients with the wild-type allele (Sparreboom et al. 2005). Similarly, intravenous administration of diflomotecan resulted in 3-fold higher plasma concentrations in patients heterozygous for the CA allele when compared to patients with the wild-type allele (Sparreboom et al. 2004).

In the placenta, mononuclear progenitor cells called cytotrophoblasts fuse together to form giant multinucleated syncytiotrophoblasts through the process of syncytialization. Syncytiotrophoblasts are critical for the production of pregnancy-related hormones, metabolism of xenobiotics, and expression of placental barrier transporters including BCRP. Notably, as primary trophoblasts differentiate into syncytiotrophoblasts, a concurrent increase in BCRP mRNA and protein expression occurs (Evseenko et al. 2006). Likewise, forskolin-mediated stimulation of cell fusion

in human BeWo choriocarcinoma cells, a model of first trimester trophoblasts, not only enhances syncytialization markers, but also induces BCRP mRNA and protein levels (Lye et al. 2018; Prouillac et al. 2009). Interestingly, a genetic knockdown of BCRP in BeWo cells not only reduces transporter expression, but also decreases the expression of syncytialization markers (Evseenko et al. 2007c). Consistent with these results is the observation that BCRP mRNA levels as well as syncytialization markers are decreased in placentas obtained from gestational pathologies including preeclampsia and intrauterine growth restriction (Evseenko et al. 2007a; Jebbink et al. 2015a; Ruebner et al. 2012). Taken together, these data suggest that BCRP may play an endogenous physiological role in regulating human placentation.

While the majority of studies have focused on the ability of BCRP to confer cellular protection by removing substrates such as drugs and toxicants, there is growing evidence that this transporter may possess an intrinsic role in preventing cellular stress from non-substrates as well. For example, silencing of BCRP in BeWo cells and primary trophoblasts significantly increased cytokine- and ceramide-induced apoptosis (Evseenko et al. 2007a; Evseenko et al. 2007c). Similarly, subpopulations of cancer cell lines MCF-7 and H460, selected for resistance to the BCRP substrate mitoxantrone, exhibited a higher survival rate and decreased apoptosis in response to nutrient starvation as compared to their non-selected counterparts (Ding et al. 2016). BCRP-expressing human embryonic stem cells were also more resistant to ultraviolet light-induced cell death, an effect that was abolished in the presence of a known BCRP inhibitor, KO143 (Erdei et al. 2013). Moreover, subpopulations of the bladder cancer line T24 and medulloblastoma cells that contained high levels of BCRP were also more resistant to radiation treatment (Ingram et al. 2013; Ning et al. 2009). Under basal conditions and following gamma radiation, Ding et al., 2016 observed that protein expression of autophagy markers, LC3-II and SQSTM1, was significantly higher in BCRP-expressing MCF7 and H460 cell lines (Ding et al. 2016). Together, these data indicate that BCRP

has an important cellular role in promoting survival, possibly by regulating cell stress and autophagy.

This introduction summarizes the tissue-specific regulation of BCRP across species using nuclear receptor and transcription factor signaling (Figure 1.1). Understanding how these signaling pathways influence BCRP expression and function can be used to improve therapeutic outcomes while reducing the toxicity of drugs that are substrates of this efflux transporter.

1.2.2 Regulation by Estrogen Receptors (NR3A1/2)

Steroid hormones, such as 17ß-estradiol, influence development, differentiation, and growth in various cell types and tissues. Responses to 17ß-estradiol are largely mediated by two nuclear estrogen receptors, ERα and ERß, as well as the membrane-bound GPR30. The nuclear ER isoforms have distinct and overlapping patterns of expression and modulation of transcription. Ligand-bound estrogen receptors undergo conformational changes that enable dissociation from chaperone proteins in the cytoplasm. Upon dissociation, ligand-bound estrogen receptors translocate to the nucleus, dimerize, and bind to estrogen response elements (ERE) found in the promoters of target genes (Li et al. 2004; Reviewed by Marino et al. 2006; Monroe et al. 2005). Studies demonstrate that estrogens have the ability to regulate BCRP expression in human breast cancer cell lines, primary and immortalized cells of the placenta, as well as animal models (Table 1.1).

Human breast cancer cell lines

Although an ERE sequence has been identified in the promoter region of *ABCG2* (between nucleotides -243 and -115), the influence of estrogen on BCRP transcription in various models has been conflicting (Ee et al. 2004b). Treatment of ER-positive human breast cancer T47D:A18 cells

with 10 nM 17ß-estradiol for 24 h induced BCRP mRNA by 3-fold. Furthermore, mutations and deletions of the ERE in the *ABCG2* promoter attenuated and abrogated, respectively, this induction suggesting a direct regulatory role for estrogen (Ee et al. 2004b). By comparison however, a T47D cell line transfected with an *ABCG2* promoter luciferase construct revealed that 17ß-estradiol (0.1-10,000 nM) treatment for 24 h had no effect on luciferase activity (Yasuda et al. 2009). The authors hypothesized that the lack of promoter activity could be attributed to a low endogenous level of ERα in these cells. Transfection of the T47D cell line with an ERα construct resulted in a significant induction of luciferase activity following 17ß-estradiol treatment, suggesting that the endogenous expression of nuclear receptors in model cell lines should be taken into careful consideration (Yasuda et al. 2009). Likewise, treatment of human breast cancer MCF-7 cells with 17ß-estradiol (0.03-3 nM) for 72 h induced BCRP mRNA between 2.7- to 8-fold. This response was abolished by concomitant treatment with tamoxifen, a selective estrogen receptor modulator (Zhang et al. 2006). By comparison, work by a separate laboratory observed a time- and dose-dependent decrease in BCRP protein in MCF-7 cells treated with estrone (0.01-10 nM) and 17ß-estradiol (0.003-3nM), for up to 96 h. A similar decrease in BCRP protein expression was also observed with diethylstilbestrol (0.001-0.1 nM) treatment (Imai et al. 2005a). The ability of estradiol to inhibit BCRP expression was partially reversed by co-incubation with tamoxifen. Furthermore, genetic down-regulation of ERα in MCF-7 cells using siRNA prevented the repression of BCRP by estradiol, whereas, ERα-negative A549 cells exhibited no changes in BCRP protein expression following exposure to 17ß-estradiol (Imai et al. 2005a). Ultimately, these studies suggest that cell lineage, type of cell lines, duration of treatment, and the endogenous expression of ERα may impact estrogen receptor-mediated regulation of BCRP in breast cancer cell lines.

Placenta

During pregnancy, the plasma concentration of 17ß-estradiol increases steadily over 60-fold from preovulatory peaks to term gestation (Reviewed in Bukovsky et al. 2003b). 17ß-estradiol

participates in the onset of parturition, production of progesterone, maturation of the fetal adrenal glands, angiogenesis of placental villi, and differentiation of trophoblasts (Reviewed in Albrecht et al. 2010; Bukovsky et al. 2003b). ERα protein is expressed in villus cytotrophoblasts, amniotic fibroblasts, and vascular pericytes, whereas ERß expression is confined to differentiated syncytiotrophoblasts (Reviewed in Bukovsky et al. 2003a). Similar to breast cancer cells, divergent findings have been observed in estrogen-mediated regulation of BCRP expression and function in *in vitro* primary and immortalized trophoblast models.

Primary trophoblasts isolated from human term placentas were treated with 100 nM 17ß-estradiol for 12 and 48 h. Estradiol induced BCRP mRNA (12 h) and protein (48 h) by 1.5-fold as compared to vehicle controls (Evseenko et al. 2007b). It is important to note that only modest changes in BCRP protein expression were observed at the 24 h time point. As in the case of breast cancer cells, the duration of treatment is an important aspect to consider when studying the effects of estrogen-mediated regulation of placental transporters in primary trophoblasts (Evseenko et al. 2007b; Wang et al. 2006b). Treatment of human BeWo choriocarcinoma cells with 1-10 µM estriol for 48 h also induced BCRP mRNA and protein by 2-fold (Wang et al. 2008b). Transporter up-regulation was abolished by concomitant treatment with the ICI-182,780 estrogen receptor antagonist. The positive regulatory role of estrogens was also observed by Yasuda et al., 2006, where BeWo cells treated with different forms and concentrations of estrogen such as estrone (10 nM – 10 µM), estriol (10 nM – 10 µM), and 17ß-estradiol (10 nM – 10 µM) for 72 h exhibited a concentration-dependent induction of BCRP mRNA and protein (Yasuda et al. 2006).

Conversely, a study by Wang et al. noted that treatment of BeWo cells with 1 µM 17ß-estradiol for 72 h reduced BCRP mRNA and protein levels (Wang et al. 2006b). The same laboratory confirmed this effect in 2008, as treatment of BeWo cells with an even lower concentration of 5 nM 17ß-estradiol for 72 h reduced BCRP mRNA and protein by half (Wang et al. 2008b). It has also recently

shown that treatment of BeWo cells with 1– 10 µM genistein, a soy isoflavone that acts as a phytoestrogen, results in the dose-dependent down-regulation of BCRP mRNA, protein, and function as measured by cellular accumulation of the substrate ^{3}H-glyburide. Down-regulation of BCRP expression by genistein was attenuated by ICl 182,780 (1 µM) (Bircsak et al. 2016). As gestation progresses, estrogen secretion from the placenta increases whereas BCRP protein expression is thought to decrease (Mathias et al. 2005; Yasuda et al. 2006). While only an association, it supports the ability of estrogens to reduce BCRP expression.

Secretion of other pregnancy hormones, such as progesterone, by the placental models can potentially explain disparities across studies. Concomitant treatment of BeWo cells with progesterone and estradiol together augmented the induction of BCRP mRNA and protein expression when compared to progesterone treatment alone (Wang et al. 2006b). Consequently, endogenous production and secretion of progesterone by primary trophoblasts and BeWo cells may influence data in studies examining the ability of estrogens to regulate BCRP in the placenta.

Subsequent studies have interrogated which ER receptor is responsible for regulating BCRP in the placenta. Unlike breast cancer cells, the transcriptional regulation of BCRP by estradiol in BeWo cells was primarily mediated through ERß. Reduction of ERα expression using siRNA did not alter the estradiol-mediated induction of BCRP expression, suggesting that ERß is the main regulatory ER isoform in BeWo cells (Wang et al. 2008b). Treatment of BeWo cells with 17ß-estradiol (1 µM) down-regulated ERß mRNA expression and had no significant effect on ERα mRNA, further pointing towards ERß as the predominant regulatory isoform (Wang et al. 2006b). In pregnant mice, the highest levels of placental Bcrp mRNA are on gestational day (GD) 15 (Wang et al. 2006a). As compared to GD10, the placental mRNA expression of ERα and ß is significantly lower and higher, respectfully, on GD15 (Wang et al. 2006a). This correlation further supports the likely involvement of ERß isoform in regulating BCRP expression in the placenta.

Brain Capillaries

Due to the presence of aromatase, an enzyme responsible for the synthesis of 17ß-estradiol (Kellis et al. 1987), and estrogen receptors in the cerebral microvasculature (Stirone et al. 2003), the expression of BCRP in brain endothelial cells also makes this transporter a target of estrogen-mediated regulation. Unlike breast cancer and placenta models, isolated mouse and rat brain capillaries exhibit a consistent reduction of Bcrp mRNA, protein, and function in response to 17ß-estradiol treatment. Isolated rat brain capillary membranes exposed to 17ß-estradiol (1-10 nM) for 1 h and 6 h exhibited reduced Bcrp function, as measured by luminal accumulation of a fluorescent Bcrp substrate, BODIPY FL prazosin (Hartz et al. 2010a; Hartz et al. 2010b; Mahringer et al. 2010; Nickel et al. 2014). This reduction in activity was comparable to treatment with a known Bcrp inhibitor, fumitremorgin C (Hartz et al. 2010a; Hartz et al. 2010b). Inhibition of Bcrp was attributed to ERß signaling as rat brain capillaries incubated with 10 nM diarylpropionitrile, a selective ERß agonist, demonstrated decreased Bcrp protein expression and function that mirrored responses to 17ß-estradiol (Hartz et al. 2010a; Mahringer et al. 2010). By comparison, exposure of rat brain capillaries to an ERα-specific agonist (1 nM propyl pyrazole triol) or antagonist (100 nM methyl-piperidino-pyrazole) had no effect on Bcrp levels (Hartz et al. 2010a; Mahringer et al. 2010; Nickel et al. 2014). The authors speculated that initial estradiol signaling occurred through both ER isoforms leading to internalization of the Bcrp protein and thus a loss of function at early time points whereas the down-regulation of Bcrp protein expression was mediated directly through ERß activation and proteasomal degradation (Hartz et al. 2010a; Hartz et al. 2010b; Mahringer et al. 2010). In comparison to breast cancer and placenta models, expression of Bcrp in rodent brain capillaries appears to be significantly more sensitive to regulation by estrogen as much lower concentrations and exposure times elicit transcriptional and functional responses.

1.2.3 Regulation by Progesterone Receptors (NR3C3)

Progesterone is a critical regulator of embryogenesis, menstruation, metabolism, and transcriptional regulation of membrane transporters. In humans, the progesterone receptor exists as two isoforms, PR-A and PR-B, which arise from alternate translation of a single precursor progesterone receptor mRNA (Kastner et al. 1990). While both PR-A and PR-B mediate gene transcription, each isoform acts as an independent transcription factor with divergent properties (Reviewed in Dressing et al. 2009; Edwards et al. 1995). Upon progesterone binding, the receptors undergo conformational changes that enable translocation, dimerization, and binding to progesterone response elements in the promoter regions of target genes to either induce or repress transcription. A progesterone response element has been identified in the promoter region of *ABCG2*, suggesting this hormone can regulate BCRP expression and activity (Wang et al. 2008a).

Placenta

Incubation of BeWo cells with progesterone (1 - 10 μM) for up to 72 h induced BCRP mRNA and protein expression up to 2-fold (Table A-1.2) (Wang et al. 2008a; Wang et al. 2006b). Furthermore, progesterone decreased the intracellular accumulation of a classical BCRP substrate, mitoxantrone, consistent with enhanced BCRP activity (Wang et al. 2008a). Human BeWo choriocarcinoma cells express both PR isoforms (Wang et al. 2008a). Progesterone stimulation of PR-B-overexpressing BeWo cells preferentially stimulated BCRP protein expression when compared to PR-A-transfected cells, suggesting that PR-B is the major regulatory isoform (Wang et al. 2008a). As aforementioned, induction of BCRP was further enhanced with concomitant estradiol treatment and resulted in a 2-fold induction of PR-B mRNA expression, signifying additive roles in regulating BCRP levels (Wang et al. 2006b). Up-regulation of BCRP protein by progesterone was reversible through co-administration with the PR and glucocorticoid receptor antagonist, RU-486 (Wang et al. 2008a). It is important to note that progesterone-mediated regulation was concentration- and time-dependent in BeWo and primary human trophoblast cells. Exposure to progesterone at

concentrations lower than 10 µM or for less than 24 h had no effect on BCRP expression (Evseenko et al. 2007b; Wang et al. 2006b; Yasuda et al. 2009).

Human Breast Cancer Cell Lines

The ability of progesterone to regulate BCRP in human breast cancer cell lines is less consistent compared to regulation in placental cell lines. To examine the responsiveness of BCRP to progesterone, Yasuda et al., 2009 transfected the T47D cell line with an *ABCG2* promoter-luciferase plasmid. Following exposure to a range of progesterone concentrations (1 nM – 10 µM) for 24 h, a ~2.6-fold induction in luciferase activity was demonstrated. Activation of luciferase activity could be reversed by concomitant exposure to 100 nM RU-486 (Yasuda et al. 2009). Interestingly, following treatment with progesterone (0.0001 nM – 10 µM) for a longer time period (48 h), BCRP expression and activity were significantly down-regulated in both T47D and MCF7 cell lines (Wu et al. 2013; Wu et al. 2012b). As a result of progesterone treatment, T47D cells were approximately 5-fold more sensitive to mitoxantrone-induced cytotoxicity (LC_{50} control: 1.36 µM; LC_{50} progesterone: 0.26 µM) (Wu et al. 2013). The discrepancy between progesterone-mediated changes in promoter activity and BCRP mRNA and protein expression may be explained by the ability of progesterone to signal through posttranscriptional (Joyeux et al. 1989; Lan et al. 1999; Park et al. 1996; Wu et al. 1991) and posttranslational mechanisms (Gapter et al. 2006; Inoue et al. 1991, 1995; Pasqualini et al. 1983). Likewise, BCRP is known to be highly regulated by posttranscriptional (Pan et al. 2009; To et al. 2009; To et al. 2008b; Wang et al. 2010a) and posttranslational modifications (To et al. 2006; Turner et al. 2006; Xie et al. 2008). More studies are required to determine the direct effect of hormones such as progesterone on the posttranscriptional and posttranslational regulation of BCRP expression.

1.2.4 Regulation by Peroxisome proliferator-activated receptors (NR1C1/2/3)

Peroxisome proliferator-activated receptors (PPAR) are nuclear hormone receptors with three predominant isoforms denoted as PPARα, PPARß, and PPARγ. Upon ligand binding, PPARs translocate to the nucleus, heterodimerize with retinoid x receptor alpha, and bind to PPAR response elements in the promoter regions of target genes and, in turn, modulate their expression. PPARs regulate lipid and glucose homeostasis, metabolic enzyme activity, and expression of drug transporters including BCRP (Hirai et al. 2007; Moffit et al. 2006; Muerhoff et al. 1992).

1.2.4.1 PPARα

Brain

A number of studies have observed a consistent induction of BCRP mRNA, protein, and function in response to PPARα signaling (Table 1.3). Treatment of immortalized human cerebral microvascular endothelial hCMEC/D3 cells with PPARα ligands, GW7647 (20 nM) and clofibrate (100 μM), induced BCRP mRNA. Consistent with PPARα-mediated induction of BCRP mRNA, treatment of hCMEC/D3 cells with increasing GW7647 (1.25 nM – 20 nM) and clofibrate (200 nM – 125 μM) concentrations for 6-72 h revealed a concentration- and time-dependent induction of BCRP protein and function (Hoque et al. 2012). Targeted knockdown of PPARα with siRNA in hCMEC/D3 cells reduced BCRP protein expression further confirming a mechanistic role for PPAR (Hoque et al. 2012).

Induction of Bcrp mRNA and protein by clofibrate has also been observed in isolated brain capillaries from CD-1 mice treated with 125 μM clofibrate for 6 h (Hoque et al. 2015b). Interestingly, while the up-regulation of BCRP in human hCMEC/D3 cells was attenuated with known PPARα antagonists, MK886 (500 nM) and GW6471 (500 nM), the clofibrate-induced transport activity of Bcrp in CD-1 mouse brain capillaries was not, suggesting some potential species differences (Hoque et al. 2012; Hoque et al. 2015b). Treatment of isolated rat brain capillaries with other PPARα agonists including linoleic acid (10 μM), perfluorooctanoic acid (10

nM), and perfluorooctane sulfonate (10 nM) similarly increased Bcrp protein expression and transport activity. This induction was abrogated with by the PPARα antagonist GW6471 (More et al. 2017). Taken together, these data suggest that PPARα can regulate both rodent and human Bcrp/BCRP expression in the brain.

Liver, small intestine, and kidney

The ability of PPARα to regulate Bcrp expression extends beyond the brain to the liver, intestine, and kidney. Mice administered PPARα agonists, including clofibrate (500 mg/kg/d for 10 days i.p.), Wy14643 (0.1% enriched diet, *ad libitum* for 3 days), GW7647 (0.01% enriched diet, *ad libitum* for 3 days), or the environmental contaminant perfluorooctanoic acid (3 mg/kg/day for 7 days by oral gavage), demonstrated consistent up-regulation of hepatic Bcrp mRNA and protein up to 3-fold (Eldasher et al. 2013; Hirai et al. 2007; Moffit et al. 2006). As expected, administration of these agonists to PPARα-null mice had no effect on the mRNA and protein expression of Bcrp in the liver. In fact, PPARα null mice exhibit significantly lower constitutive expression of hepatic Bcrp protein when compared to the wild-type mice, suggesting that PPARα also influences basal Bcrp regulation (Eldasher et al. 2013; Hirai et al. 2007; Moffit et al. 2006). PPARα agonists also up-regulate Bcrp expression in the intestines and kidneys. Wild-type C57BL mice fed a diet containing 0.1% Wy14643 for 3 days exhibited a 1.5-fold induction in intestinal Bcrp mRNA when compared to mice on a control diet (Hirai et al. 2007). Similarly, exposure to perfluorooctanoic acid induced expression of renal Bcrp protein by 1.5-fold (Eldasher et al. 2013). Taken together, these data support the ability of PPARα to up-regulate BCRP/Bcrp across a wide array of tissues in rodents and humans.

1.2.4.2 PPARγ

Ligand-activated PPARγ can also induce BCRP mRNA and protein expression in a number of cell types. Treatment of human dendritic cells and colorectal adenocarcinoma Caco-2 cells with PPARγ

agonists, rosiglitazone (25 nM-10 μM), GW7845 (100 nM), and troglitazone (1000 nM), induced BCRP mRNA and protein (Szatmari et al. 2006; Wright et al. 2011). As expected, co-treatment of dendritic cells with the PPARγ antagonist, GW9662, attenuated BCRP up-regulation (Szatmari et al. 2006). Lin et al., 2016 has similarly shown that BCRP expression in the placenta is regulated in part by PPARγ. Treatment of human BeWo trophoblasts with the PPARγ agonist, rosiglitazone, resulted in the induction of BCRP mRNA, protein, and function. By comparison, treatment with a PPARγ antagonist T0070907 down-regulated expression of BCRP mRNA and protein (Lin et al. 2016). From the available data, it appears that activation of PPARα and PPARγ can induce the transcription of BCRP expression across numerous primary and immortalized cell lines as well as in rodent tissues.

1.2.5 Regulation by Constitutive androstane receptor (NR1I3)

The constitutive androstane receptor (CAR) regulates energy homeostasis, drug metabolism, and xenobiotic transport (Huang et al. 2005; Phillips et al. 2007; Yamamoto et al. 2004; Reviewed in Yang et al. 2014). Upon ligand binding, CAR undergoes translocation to the nucleus where it forms a heterodimer with the retinoid X receptor alpha and binds to *cis* elements in the promoter region of target genes to augment their transcription (Benoki et al. 2012; Lemmen et al. 2013a; Reviewed in Yang et al. 2014). As an orphan receptor, CAR is activated by a wide variety of xenobiotic chemicals often at micromolar concentrations. This differs from typical steroid hormone receptors that respond to nanomolar concentrations of endogenous ligands (Reviewed by Yang et al. 2014). CAR also differs from classical steroid hormone receptors as its activation can occur through a ligand-independent mechanism, as in the case of phenobarbital. Phenobarbital induces the nuclear translocation of CAR by competitively binding to the epidermal growth factor receptor and causing dephosphorylation of CAR (Benoki et al. 2012; Lemmen et al. 2013a; Reviewed in Yang et al. 2014).

Several studies have pointed to the involvement of CAR in the transcriptional regulation of human efflux transporters including Bcrp (Table 1.4). Treatment of isolated rat brain capillaries with the CAR agonist, phenobarbital, increased Bcrp protein expression (Wang et al. 2010b). Accordingly, isolated rat and mouse brain capillaries treated with phenobarbital and 3,3′,5,5′-tetrachloro-1,4-bis(pyridyloxy) benzene (TCPOBOP) exhibited a significant enhancement of transport activity of Bcrp, as measured by the luminal accumulation of BODIPY-prazosin (Wang et al. 2010b). The induction of Bcrp by phenobarbital and TCPOBOP was attenuated using okadaic acid (10 nM), a protein phosphatase 2A inhibitor; together, these data support a regulatory role of CAR in Bcrp expression (Wang et al. 2010b). Isolated capillaries from CAR-null mice did not exhibit enhanced Bcrp function in response to TCPOBOP (Wang et al. 2010b). These data were further confirmed *in vivo* where mice and rats treated with TCPOBOP or phenobarbital, exhibited up to 2-fold induction of Bcrp protein expression in brain capillary and liver membranes (Wang et al. 2010b).

While TCPOBOP induced Bcrp protein expression and transporter activity in mice and rats, it had no effect on expression or activity in isolated porcine brain capillary endothelial cells (Lemmen et al. 2013a). Alternatively, the same cells treated with a different CAR agonist, 6-(4-chlorophenyl)imidazo[2,1-b][1,3]thiazole-5-carbaldehyde O-(3,4-dichlorobenzyl) oxime (CITCO), exhibited significant and concentration-dependent increases in Bcrp mRNA, protein, and function (Lemmen et al. 2013a). Thus, selection of an appropriate ligand is important as receptor activation of CAR is species-specific. Similar results were observed in primary human hepatocytes infected with a human CAR expressing adenovirus. Treatment of these cells with 0.3 μM CITCO for 24 h increased BCRP mRNA expression by 1.7-fold (Benoki et al. 2012). Similarly, exposure of primary human hepatocytes (from three male and four female donors) to phenobarbital (3.2 mM) for 72 h up-regulated BCRP mRNA by over 3-fold (Jigorel et al. 2006). Although not statistically significant, human HuH-7 hepatoma cells treated with phenobarbital (2 mM) up-regulated BCRP

mRNA (Jouan et al. 2016). Together, these data indicate that CAR positively regulates BCRP transcription and expression across species and tissues.

1.2.6 Regulation by Pregnane X receptor (NR1I2)

The pregnane X receptor (PXR), a member of the nuclear hormone receptor superfamily of transcription factors, regulates genes involved in xenobiotic and endobiotic oxidation, metabolism, transport, and conjugation (Reviewed in Kliewer et al. 2002; Lemmen et al. 2013b). Similar to the mechanism of CAR, ligand binding initiates PXR translocation to the nucleus where it forms a heterodimer with retinoid X receptor alpha, binds to a xenobiotic responsive enhancer (XRE) element located upstream of the transcriptional start site and regulates transcription of target genes (Reviewed in Timsit et al. 2007).

Accumulating evidence suggests that PXR regulates BCRP expression in a species- and tissue-specific manner (Table 1.5). Isolated mouse, rat, and porcine brain capillaries treated with PXR ligands *in vivo* (pregnenolone 16α-carbonitrile (PCN; 50mg/kg/d; 2 days)) or *in vitro* (hyperforin (1 μM; 24h); rifampicin (5 μM; 24 h)) exhibited increased Bcrp expression and function (Lemmen et al. 2013b; Wang et al. 2010b). PXR-mediated regulation of Bcrp was also observed in mouse TM4 Sertoli cells. Treatment of TM4 cells with dexamethasone (100 μM) and PCN (50 μM) for 24 h induced Bcrp mRNA and protein expression, which was abrogated by the PXR antagonist, ketoconazole (10 μM). Genetic knockdown of PXR in TM4 cells using siRNA also reduced Bcrp protein expression, further confirming the direct regulatory role of PXR in testis (Whyte-Allman et al. 2017). The PXR-mediated regulation of Bcrp expression was also evident in mouse placentas. Treatment of pregnant C57BL/6 mice with 50 mg/kg i.p. PCN from gestational days 13 to 17 resulted in higher placental Bcrp mRNA levels when compared to PXR-null and heterozygous controls (Gahir et al. 2011).

Still, discrepancies in the PXR-mediated regulation of hepatic Bcrp expression have been reported (Anapolsky et al. 2006; Han et al. 2006; Teng et al. 2005). BALB/c mice treated with PCN (400 mg/kg i.p. for 4 days) had unaltered expression of liver Bcrp mRNA (Han et al. 2006). Similarly, C57BL/6 mice treated with the PXR agonist, PCN (50 mg/kg i.m.), and antagonist, RU486 (50mg/kg i.m.), for 3 days had no change in liver Bcrp mRNA (Teng et al. 2005). Interestingly, treatment of C57BL/6 mice with 2-acetylaminofluorene (150 mg/kg and 300 mg/kg i.p.) for 7 days resulted in a 2-2.5 fold induction of liver Bcrp mRNA (Anapolsky et al. 2006). This induction was prevented in PXR-null mice, supporting the direct involvement of this nuclear receptor in the up-regulation of Bcrp (Anapolsky et al. 2006). Discrepancies in mouse liver studies may be due to the dose of the PXR agonist, the duration of treatment, and potentially the strain of mice used.

The ability of PXR to regulate BCRP expression was examined in various human cell lines. Hepatocytes, obtained from three male and four female donors, exhibited a ~2.7-fold increase in BCRP mRNA after treatment with the PXR ligand rifampicin (50 μM) for 72 h (Jigorel et al. 2006). Similarly, HepG2 cells, a human liver cancer cell line, over-expressing PXR exhibited 7-fold higher BCRP mRNA expression when compared to parental cells (Naspinski et al. 2008). Moreover, PXR-mediated regulation of BCRP expression was also observed in MCF and MDA-MD-231 breast cancer cells as treatment with SR12813 (0.3 μM), a PXR agonist, for 24 h resulted in ~3-fold induction of BCRP mRNA in both lines (Qiao et al. 2014). By comparison, human cerebral hCMEC/D3 endothelial cells exposed to rifampicin (25 μM) for 24 h had no observable change in BCRP mRNA expression (Dauchy et al. 2009). The authors of the study noted that while PXR mRNA was detectable in hCMEC/D3 cells, the expression was low potentially explaining the absence of PXR-mediated regulation (Dauchy et al. 2009). Future studies should also take into consideration the endogenous expression of nuclear receptors in models of interest as that may alter the extent of regulation observed.

1.2.7 Regulation by Aryl hydrocarbon receptor (AHR)

The aryl hydrocarbon receptor (AHR) is a member of the basic helix-loop-helix/PER-AHR nuclear translocator superfamily of transcriptional factors. AHR regulates genes involved in cell proliferation, vascular and immune system functioning, phase I/II drug metabolism, and more recently, xenobiotic transport (Deng et al. 2001; Granberg et al. 2003; Jigorel et al. 2006; Reviewed in Kawajiri et al. 2007). AHR is bound by several chaperone proteins in the cytoplasm and remains in an inactive state (Petrulis et al. 2002). Upon ligand binding, AHR dissociates from chaperones and translocates to the nucleus where it forms a heterodimer with the aryl hydrocarbon nuclear translocator and regulates the transcription of various target genes. AHR ligands include several toxicants such as dioxins and polychlorinated biphenyls (Bradfield et al. 1991; Kafafi et al. 1993).

AHR ligands positively regulate human intestinal expression and function of BCRP across several primary and immortalized cell models (Table 1.6). Treatment of human Caco-2 cells with benzo[a]pyrene (10 µM), 2,3,7,8-tetrachlorodibenzo-*p*-dioxin (TCDD, 50 nM), benzo[*k*]fluoranthene (5 µM), and indolo[3,2-*b*]carbazole (2.5 µM) for 24 h induced BCRP mRNA expression between 3- and 6-fold (Ebert et al. 2005). By 72 h, a similar degree of induction was observed in BCRP protein (Ebert et al. 2005). Up-regulation of BCRP was abolished using the AHR antagonists, PD98059 (10 µM) and 3'-methoxy-4'-nitroflavone (10 µM) (Ebert et al. 2005). Significant induction of BCRP mRNA and protein expression has also been reported in C2bbe1 (subclone of Caco-2), LS180 (colorectal adenocarcinoma), LS174T (colorectal adenocarcinoma), MCF-7, HuH-7, HepaRG (human hepatoma cells), and HepG2 cells, as well as primary human colonocytes and hepatocytes in response to 10 nM TCDD treatment for 24 to 72 h (Jigorel et al. 2006; Jouan et al. 2016; Sayyed et al. 2016; Tan et al. 2010; Tompkins et al. 2010). This response was abrogated by the AHR antagonist, 3,4-dimethoxyflavone (10 µM) (Tan et al. 2010). Moreover, siRNA knockdown of AHR in LS174T and MCF7 cells attenuated the up-regulation of BCRP

mRNA by 3-methylcholanthrene (3MC; 1 µM) and TCDD (10 nM) (Tan et al. 2010; Tompkins et al. 2010). Likewise, site-directed mutagenesis of various AHR response elements in the *ABCG2* promoter region resulted in significant reduction of 3MC-mediated activation in LS1274T cells further pointing to the involvement of AHR in the transcriptional regulation of this transporter (Tompkins et al. 2010).

The ability of AHR to regulate BCRP in the placenta has also been reported. Univariate regression analysis of BCRP and AHR mRNA expression across 137 racially and ethnically diverse term placentas revealed significant correlation (b= 0.29; P < 0.0001) between the transcription factor and transporter (Bircsak et al. 2018). Pharmacological inhibition (3 µM CH223191) and genetic knockdown (shRNA) of AHR in primary human villous trophoblasts and immortalized placental *in vitro* models (BeWo, JEG3) significantly attenuated the 3MC-mediated induction of BCRP mRNA (Neradugomma et al. 2017).

While AHR-mediated regulation of Bcrp was demonstrated in immortalized porcine brain microvascular endothelial cells as well as isolated rat spinal cord and brain capillaries, various *in vivo* and *in vitro* mouse studies observed no changes in Bcrp expression in response to prototypical AHR agonists (Campos et al. 2012; Han et al. 2006; Neradugomma et al. 2017; Tan et al. 2010; Wang et al. 2011). Mouse mammary (EMT-6), hepatic (hepa1c1c7), and intestinal (CMT93) carcinoma cell lines exhibited no change in Bcrp mRNA expression in response to TCDD treatment (Tan et al. 2010). Additionally, no significant changes in Bcrp mRNA levels were observed in the small intestine, liver, and colon of pregnant C57BL/6N mice treated with TCDD (30 µg/kg, i.p.) on gestational day 16 and evaluated 24 hr later (Tan et al. 2010). The strain of mice does not seem to play a factor in this phenomenon as BALB/c mice treated with 3MC (30 mg/kg/d i.p. for 4 days) similarly had unchanged Bcrp levels in the liver and small intestine (Han et al. 2006). Comparison of the human *ABCG2* and mouse *Abcg2* genes revealed that although majority of the exons are

conserved, most of the noncoding regions, such as the intron and 5'-flanking regions, are not (Tan et al. 2010). From these studies, it can be concluded that AHR-mediated transcriptional regulation of BCRP appears to be species-specific.

1.2.8 Regulation by Nuclear factor erythroid 2-related factor 2 (NFE2L2)

Nuclear Factor Erythroid 2-Related Factor 2 (NRF2), a basic region-leucine zipper type transcription factor, protects against inflammation, oxidative injury, apoptosis, and environmental toxins through activation of target genes involved in antioxidant and detoxification pathways (Reviewed in Kensler et al. 2007; Morito et al. 2003; Rangasamy et al. 2004). Under basal conditions, Kelch like ECH associated protein (KEAP1) negatively regulates this pathway by sequestering NRF2 in the cytoplasm and targeting it for proteasomal degradation. In response to oxidative stress or electrophilic attack, NRF2 dissociates from KEAP1, translocates to the nucleus where it heterodimerizes with small Maf proteins, and initiates transcription of antioxidant target genes (Hagiya et al. 2008; Singh et al. 2010).

Recently several studies have suggested that BCRP can be regulated by NRF2 (Table 1.7). Luciferase reporter assays and CHIP analysis revealed an antioxidant response element (ARE) located -431 to -420 bp upstream of the *ABCG2* transcriptional start site, direct binding of NRF2 to the ARE element (Singh et al. 2010). Treatment of primary human hepatocytes, HepG2, HuH-7, and NuLi cells (human epithelial cells) with NRF2 inducers, tert-butylhydroquinone (20 µM-200 µM; 24-48 h) and oltipraz (50 µM; 72 h), enhanced BCRP mRNA and protein expression in a concentration-dependent manner. Induction of BCRP was accompanied by increased expression of classical NRF2 target genes, NAD(P)H quinone oxidoreductase 1 and the glutamate-cysteine ligase modifier subunit (Adachi et al. 2007; Jigorel et al. 2006; Jouan et al. 2016; Singh et al. 2010). Transfection with NRF2-specific shRNA also significantly lowered BCRP mRNA (up to ~5-fold)

and protein expression and function in A548 cells (Singh et al. 2010). Knockdown of NRF2 in DU145 cells (human prostate cancer model), SKOV3 cells (ovarian cancer model), HCT116 cells (human colorectal carcinoma), MDA-MB-231 (human breast carcinoma) and HepG2 cells also significantly reduced BCRP expression (Adachi et al. 2007; Choi et al. 2014a; Choi et al. 2017; Ryoo et al. 2016; Singh et al. 2010). Consistent with these findings, transfection of NuLi and HF-2 cells with shRNAs targeted against KEAP1, the negative regulator of NRF2, up-regulated BCRP mRNA and protein expression (Jeong et al. 2015; Singh et al. 2010). In addition, univariate regression analysis of genes in 137 human placentas revealed a strong correlation between NRF2 and BCRP mRNA levels (b = 0.85; P < 0.0001) (Bircsak et al. 2018). Taken together, NRF2 is a consistent inducer of human BCRP expression across numerous tissues and species.

1.2.9 Post -transcriptional and -translational regulation

Beyond transcriptional regulation, the expression, trafficking, and function of the BCRP transporter also relies on post-transcriptional and –translational mechanisms. A proximal miRNA response element has been identified in the 3'-untranslated region (3'-UTR) region of the *ABCG2* gene (Li et al. 2011). Transfection of MCF-7 breast cancer cells with miRNA-328 or miRNA-519c expression plasmids resulted in a ~1.35-fold reduction of BCRP protein expression (Li et al. 2011). This reduction correlated with an accelerated ABCG2 mRNA degradation in the transfected cells suggesting the contribution of an mRNA-specific decay mechanism. Post-translational regulation of BCRP, including phosphorylation and glycosylation, has also been reported. With respect to N-glycosylation, a study has shown that mutation of a glycosylation site, Asn596, results in enhanced ubiquitination and subsequent decrease in BCRP protein expression (Nakagawa et al. 2009). The functionality of the Bcrp transporter has also been shown to be affected by N-glycosylation as maximal Bcrp activity correlated with its fully N-glycosylated isoform, as observed by excretion of fluorescently tagged methotrexate into a canalicular network of a sandwich-cultured rat

hepatocyte model (Draheim et al. 2010). Trafficking of the BCRP transporter is also regulated by post-translational mechanisms as proper translocation to the plasma membrane depends on a phosphorylated threonine 362 (Xie et al. 2008). Likewise, localization of BCRP protein to detergent-resistant lipid rats within the plasma membrane is important for its function in the placenta (Szilagyi et al. 2017).

1.2.10 Conclusion

Over the past decade, numerous studies have highlighted the involvement of hormones, nuclear receptors, and transcription factors in regulating drug transporter expression and function. As described in this review, BCRP expression can be regulated by steroid receptors (ER, PR), xenobiotic receptors (CAR, PXR, PPAR), and transcription factors (AHR, NRF2). The relative contribution of each receptor alone or combined to the basal and inducible expression of BCRP is not entirely clear and likely differs across tissues. Nonetheless, it is clear that multiple signaling pathways can up-regulate BCRP expression and function. Moving forward, additional research is needed to understand the impact of this transcriptional regulation on the overall pharmacokinetics, pharmacodynamics, and toxicity of BCRP substrates.

1.2.11 Expert Opinion

Localized across several blood-tissue interfaces, BCRP actively limits the intracellular accumulation of numerous toxic xenobiotics by extruding them across cell membranes. During pregnancy, the BCRP transporter is localized to the placental syncytiotrophoblasts and limits fetal drug exposure by effluxing various drugs back into the maternal circulation. Correspondingly, the gestation diabetes drug and BCRP-substrate, glyburide, is prescribed during pregnancy due to its low fetal accumulation.

While this self-defense mechanism offers crucial protection under normal physiological circumstances, it is also a main component of multidrug resistance in cancer cells. Multidrug resistance in cancer therapy is often characterized by the overexpression of ABC efflux transporters and complicated by the broad substrate overlap between them. The pharmacokinetics of several chemotherapeutic drugs, including methotrexate, doxorubicin, and daunorubicin, have been shown to be altered due to their recognition and elimination by the BCRP, MDR1, and MRP transporters (Choi et al. 2014b; Liu et al. 2014; Sparreboom et al. 2005). Additionally, ABC transporters share distinct overlap not only in their substrates but also in their transcriptional machinery. Similar to BCRP, the multidrug resistance protein 1 (*ABCB1*/MDR1/P-gp) and multidrug resistance-associated proteins (*ABCC*/MRPs) have been shown to be transcriptionally regulated by the estrogen receptor (Chen et al. 2018a; Coles et al. 2009; Edavana et al. 2013; Evseenko et al. 2007b; Kim et al. 2004; Shi et al. 2014; Zampieri et al. 2002), progesterone receptor (Coles et al. 2009; Evseenko et al. 2007b; Kim et al. 2004), peroxisome proliferator activated receptors (Alexander et al. 2006; Konieczna et al. 2015; Maher et al. 2008; Maher et al. 2005; Manceau et al. 2010; Moffit et al. 2006; Wang et al. 2018b; Zhang et al. 2015a), pregnane x receptor (Kullak-Ublick et al. 2003; Maher et al. 2005; Manceau et al. 2010; Olinga et al. 2008), aryl hydrocarbon receptor (Maher et al. 2005; Olinga et al. 2008), nuclear factor erythroid 2-related factor 2 (Maher et al. 2008; Maher et al. 2005), and constitutive androstane receptor (Lu et al. 2004; Maher et al. 2005; Olinga et al. 2008) across species and tissues. Extrapolation of data from models investigating the regulatory capacity of transcriptional factors requires careful characterization of other proteins and signaling pathways potentially affected. Unwarranted activation of transporters by ligands targeting a mutual regulatory transcription factor may result in confounding data with respect to changes in transporter functionality, especially when a test substrate recognized by multiple transporters is affected. This is of particular concern in drug resistance as simultaneous activation of multiple transporters via transcriptional pathways may render the translocation of substrate drugs not feasible.

Understanding the mechanisms that govern BCRP expression enables for identification of new molecular targets and greater expansion of precision medicine. Knockout mouse models targeting the Bcrp transporter observed a significantly higher area under the curve of plasma concentration-time curve (AUC) for orally administered ciprofloxacin, afatinib, rucaparib, methotrexate, and vemurafenib, to name a few (Durmus et al. 2015; Durmus et al. 2012; Merino et al. 2006; van Hoppe et al. 2017; Vlaming et al. 2011). Similar effect was observed in individuals carrying common single nucleotide polymorphisms (SNPs) of the *ABCG2* gene. SNPs, such as the C421A/Q141K, result in decreased BCRP protein expression and function (Bircsak et al. 2016; Bircsak et al. 2018). Accordingly, individuals carrying the C421A/Q141K SNP also had higher plasma AUC or C_{max} of orally administered BCRP substrate drugs such as sulfasalazine, gefitinib, rosuvastatin, and atorvastatin (Reviewed in Mao et al. 2015). With respect to transcriptional regulation, more studies are still needed to determine whether the transcriptional modifiers of BCRP discussed in this review alter the pharmacokinetic profiles of various BCRP substrates *in vivo*. While decreased BCRP expression and/or loss of its function typically correlates with enhanced plasma concentration of orally administered substrates, the transcriptional factors discussed regulate not only transporters but also other major xenobiotic disposition pathways including those involved in Phase I and II metabolism. In the 2020 US FDA guidance for metabolizing enzyme- and transporter-mediated drug interactions, no models or methods are recommended for the evaluation of transporter induction despite the known ‘cross-talk’ between regulators of metabolism and transport. It is clear that additional investigation and validation of *in vitro* models specifically for transporters is needed.

With respect to its critical role in drug disposition, BCRP has also been recognized by the U.S. Food and Drug Administration as a key transporter to consider in the evaluation of potential drug-drug interactions (DDIs) during drug development and prescribing (Prueksaritanont et al. 2013). Several DDIs between BCRP substrate drugs and BCRP inhibitors in humans have been identified.

These include interactions between rosuvastatin and cyclosporine (Simonson et al. 2004), sulfasalazine and curcumin (Kusuhara et al. 2012), and atorvastatin and ritonavir (Pham et al. 2009), to name a few. It is also important to note that the expression and function of BCRP may be affected by pharmaceutical agents and toxicants alike, further complicating these interactions. Pharmaceutical agents such as gefitinib, topotecan, mitoxantrone, venlafaxine, promazine, etoposide, ifenprodil, among others, have been shown to affect the expression and/or function of the BCRP transporter (Badolo et al. 2015; Chen et al. 2011a; Washio et al. 2018). Similarly environmental toxicants such as cadmium chloride, bisphenol A (BPA), genistein, and daidzein, to name a few, are also implicated in regulating BCRP expression and/or function (Bircsak et al. 2016; Kummu et al. 2012; Liu et al. 2016; Nickel et al. 2014; Rigalli et al. 2019). Additional preclinical and clinical studies are warranted to determine whether drug interactions can be observed with drugs that induce or repress BCRP expression.

Review of current literature concerning the transcriptional regulation of BCRP revealed several aspects to consider when designing and evaluating studies across tissues and species. Many of the discrepancies between studies can be attributed to either 1. Inappropriate model selection or 2. A lack of an extensive model characterization. With respect to selection of an inappropriate model, several studies did not take into account the endogenous expression of target nuclear receptors or transcription factors. Accordingly, treatment with an agonist targeting a nuclear receptor that is not present in a given cell line or expressed at very low levels could result in a false negative and affect data interpretation across tissues and species. Another aspect to consider is the endogenous hormone secretion of a primary or immortalized cell line. Differences in the amount and type of hormones secreted between models may affect the observed transcriptional and translational changes in response to various agonists and become a confounding factor.

In terms of model characterization, disparate results observed by several studies can be attributed to the duration of agonist/antagonist treatment and/or their concentration. Future studies should consider including time courses and dose responses for each compound utilized as sensitivity and responsiveness may vary across different cell lines and tissues. Time courses are of particular importance when comparing changes in mRNA and protein expression. Moreover, genetic variability is another aspect to take into account especially when comparing results obtained from human primary cells and immortalized cell lines. Primary cells may contain single nucleotide polymorphisms spanning the promoter, exon, and intron regions of the target gene. With respect to transcriptional regulation of BCRP expression, the promoter region of the BCRP gene should be screened for any potential polymorphisms that could affect transcriptional factor and/or nuclear receptor binding. Without this consideration, data obtained from primary cells may be significantly different from immortalized cell models.

Crosstalk between transcription factors and nuclear receptors has been identified in numerous species and tissues and hence adds another level of complexity. With numerous pharmaceuticals and toxicants affecting multiple signaling pathways, future studies need to examine the combined regulatory effect of multiple transcription factors of BCRP at the same time. Site directed mutagenesis targeting one or more of the response elements found in the promoter region of *ABCG2* can identify the transcription factors that predominantly regulate BCRP expression. Ultimately, establishment of guidelines which cover each of the aforementioned concerns during the initial experimental design and characterization would aid in the standardization, translatability, and consistency of data regarding transcriptional regulation of proteins.

1.3 The Multidrug Resistance-Associated Protein (MRP/*ABCC*) Transporters

The Multidrug Resistance-Associated Proteins belong to the ATP-binding Cassette (ABC) superfamily of efflux drug transporters. Similar to the BCRP transporter, MRPs utilize ATP hydrolysis as an energy source to translocate various substrates against their concentration gradient and across the plasma membrane. MRP proteins transport both endogenous (prostaglandins, glutathione, bile salt, steroids, cyclic nucleotides) and exogenous molecules (antiviral/anticancer drugs) (Russel et al. 2008; Sampath et al. 2002). MRP isoforms expressed in the human placenta include MRP1, -2, -3, and -5 (Meyer Zu Schwabedissen et al. 2005a; Pascolo et al. 2003; St-Pierre et al. 2000; Williams et al. 2012).

1.3.1 Structure, Localization, and Function

Structure

MRP (*ABCC*) transporters are 190 kDa transmembrane proteins that contain both cytoplasmic and transmembrane regions. The core segment of all MRP transporters contains two hydrophobic transmembrane domains (TMDs/MSDs) and two cytosolic nucleotide-binding domains (NBDs). The TMDs consist of six transmembrane alpha helices that form the substrate translocation region while the NBDs bind and hydrolyze ATP required to facilitate substrate transport. Substrate translocation by the MRPs is similar to that of other mammalian ABC proteins. That is, upon substrate recognition and binding by the TMDs, the MRP proteins transition from an inward cytoplasmic-facing to an outward-facing conformation to translocate the substrate across the plasma membrane. In addition to the core segment, MRP isoforms 1, 2, and 3 also contain a third extracellular NH2-terminal transmembrane domain, TMD0. TMD0 consists of five transmembrane helices and is connected to the core domain through a cytoplasmic linker element, L0. The linker element has been shown to be a critical component in MRP transport function whereas the TMD0 domain enables proper folding, trafficking, and retention of the MRP1 transporter at the plasma membrane (Bakos et al. 1998; Mason et al. 2002; Westlake et al. 2005). In contrast, MRP5 does

not contain the TMD0 domain and functions similar to the MDR1/P-gp transporter with an intracellular N-terminal end.

Localization

MRP1

MRP1, the ATP binding cassette subfamily C member 1 (*ABCC1*), is universally expressed in humans with highest expression found in testes, lung, placenta, kidney, cardiac, and skeletal muscles (Cole et al. 1992; Flens et al. 1996; Kruh et al. 1995; St-Pierre et al. 2000). MRP1 predominantly localizes to the basolateral membrane of Sertoli cells, Leydig cells, proximal tubule cells, fetal endothelium, and syncytiotrophoblasts (Atkinson et al. 2003; Bart et al. 2004; Klein et al. 2014; Nagashige et al. 2003). Although the exact mechanism regulating the basolateral localization of MRP1 within epithelial cells is not yet established, contributing factors such as the cytoplasmic loop (CL3), TMD0, and the COOH-terminal region are all implicated to have significant roles in the process (Westlake et al. 2005; Westlake et al. 2003). In addition, MRP1 localizes to intracellular organelles including mitochondria, endocytic vesicles, and endoplasmic reticulum, where it is postulated to serve protective and sequestering functions (Laochariyakul et al. 2003; Rajagopal et al. 2003; Roundhill et al. 2012).

MRP2

The MRP2/*ABCC2* isoform is most highly expressed in the liver, gallbladder, kidney, gastrointestinal tract, and the placenta (Meyer zu Schwabedissen et al. 2005b; Rost et al. 2001; Sandusky et al. 2002). Unlike MRP1, the MRP2/*ABCC2* isoform is predominantly localized to the apical membrane of polarized cells including syncytiotrophoblasts, hepatocytes, intestinal epithelia, gall bladder epithelia, and proximal tubule cells (Meyer zu Schwabedissen et al. 2005b; Rost et al. 2001; Sandusky et al. 2002; Schaub et al. 1999). Similar to MRP1, the main components

implicated in MRP2 trafficking to the apical membrane are also TMD0 and a lysine-rich element in the cytoplasmic loop 3 (CL3) (Bandler et al. 2008; Fernandez et al. 2002).

MRP3

The MRP3/*ABCC3* isoform is highly expressed in gallbladder, pancreas, kidney, liver, gastrointestinal tract, and adrenal gland. In comparison to these tissues, placental MRP3 expression is low (Ortiz et al. 1999; Scheffer et al. 2002; van de Wetering et al. 2009). MRP3 has been shown to localize to both apical and basolateral membranes of polarized cells. In the placenta, MRP3 expression was found on the apical membrane of human syncytiotrophoblasts (St-Pierre et al. 2000). Meanwhile, in hepatocytes, gall bladder epithelia, cholangiocytes, pancreas, and distal convoluted tubules the MRP3 protein localized to the basolateral membrane (Konig et al. 1999; Kool et al. 1999; Rost et al. 2001; Scheffer et al. 2002). Often, MRP3 works in concert with MRP2 do to largely overlapping substrate profiles.

MRP5

The MRP5/*ABCC5* isoform is ubiquitously expressed in humans with highest expression in liver, skeletal muscle, placenta, kidney, colon, and brain endothelial cells (Kool et al. 1997; McAleer et al. 1999; Meyer Zu Schwabedissen et al. 2005a; Zhang et al. 2004b). Similar to MRP3, the MRP5 isoform has been shown to localize to both the apical and basolateral membranes of polarized cells. In human placental syncytiotrophoblasts and skeletal muscle fibers, MRP5 is expressed basolaterally (Knauer et al. 2010; Meyer Zu Schwabedissen et al. 2005a). Alternatively, in primary cultured bovine brain microvessel endothelial cells MRP5 was localized to the apical membrane (Zhang et al. 2004b).

Function

MRP1

The MRP1 drug transporter was discovered in 1992 as the primary mechanism conferring doxorubicin resistance to the human small cell lung carcinoma cell line, H69AR (Cole et al. 1992). Since its identification, the list of MRP1 substrates has become extensive and includes organic anion conjugates, unconjugated anionic drugs, dyes, amphipathic neutral and basic drugs, as well as oxyanions. In particular, MRP1 has been shown to transport endogenous conjugates such as 17ß-estradiol glucuronide, bile salt, bilirubin glucuronides, cysteinyl leukotriene C4, dehydroepiandrosterone, estrone-3-sulfate, and glutathione-S-conjugates of prostaglandins, to name a few (Bartosz et al. 1998; Evers et al. 1997; Jedlitschky et al. 1997; Loe et al. 1996; Qian et al. 2001). MRP1 also transports unconjugated endogenous molecules such as bilirubin, reduced and oxidized glutathione, and folic acid (Jedlitschky et al. 1997; Rigato et al. 2004; Zeng et al. 2001). Free glutathione is an important co-factor in MRP1-mediated transport of various substrates, including estrone-3 sulfate and etoposide glucuronide (Qian et al. 2001). MRP1-mediated transport is reduced by buthione sulfoximine, an agent that prevents gluthatione synthesis via y-glutamylcysteine synthase inhibition (Schneider et al. 1995). Exogenous xenobiotic substrates of MRP1 include arsenic, methotrexate, anthracyclines, antimony, the mycotoxin aflatoxin B_1, and antiviral protease inhibitors ritonavir and saquinavir (Jones et al. 2001; Koike et al. 2004; Leslie et al. 2004; Loe et al. 1997; Salerno et al. 2002).

The MRP1 transporter has been theorized to serve a multitude of protective functions during pregnancy despite its counterintuitive subcellular localization in fetal endothelial cells and placental syncytiotrophoblasts. That is, MRP1 is localized to the abluminal (syncytiotrophoblast-facing) and basolateral (fetal-facing) expression in fetal endothelium and syncytiotrophoblasts, respectively. However, the protective function of MRP1 is still possible due to its higher relative expression in fetal endothelial cells when compared to syncytiotrophoblasts (Atkinson et al. 2003; Nagashige et al. 2003; St-Pierre et al. 2000). Some of the protective functions of MRP1 during pregnancy include fetal bilirubin elimination and regulation of cellular signaling through modulation of intracellular

levels of secondary messengers. As gestation progresses, circulating fetal bilirubin concentrations rise and correlate to increases in MRP1 mRNA levels in term placenta as compared to first trimester (Pascolo et al. 2003; Sikkel et al. 2004). The rise in MRP1 expression may constitute a protective mechanism to aid in bilirubin elimination. MRP1 has also been postulated to regulate placental cell fusion by modulating intracellular levels of the secondary messenger cyclic adenosine monophosphate (cAMP). Treatment of placental JAR cells with a pharmacological inhibitor of MRPs, MK571, resulted in an enhanced fusion phenotype (Biondi et al. 2010). It is important to note, however, that the MK571 inhibitor is not specific to MRP1 and can inhibit other MRP isoforms as well (Kucka et al. 2010; Myint et al. 2015). More work is required to determine whether 1.) MRP1-mediates transport of cAMP in trophoblasts, 2.) there is involvement of other MRP isoforms in cAMP efflux, and 3.) the various MRP isoforms regulate cAMP-dependent processes such as trophoblast cell fusion.

Interestingly, changes in the expression and trafficking of MRP1 have been associated with preeclampsia. Pathological abnormalities of preeclamptic placentas include increased number of syncytial knots and small sclerotic villi (Roberts et al. 2012). These abnormalities correlated with increased MRP1 mRNA expression and decreased apical trafficking of the transporter in preeclamptic placentas (Afrouzian et al. 2018). Nonetheless, more research is needed to determine the exact role of MRP1 in potentially mediating placental changes during preeclampsia.

MRP2

The MRP2/*ABCC2* isoform was first identified as the canalicular multispecific organic anion transporter (cMOAT) in human liver (Paulusma et al. 1996). Studies have shown that MRP2 has a similar substrate specificity as MRP1. Various endogenous substrates include glutathione, glucuronide, and sulfate conjugates of bile acids, bilirubin, leukotrienes, and steroids (Joshi et al. 2016). Cell Lines (MDCKII, HepG2, Caco-2) stably transfected with an MRP2 construct exhibited

a similar drug resistance profile as MRP1. Xenobiotics examined included vinca alkaloids, epipodophyllotoxins, anthracyclins, camptothecins, and cisplatin (Cui et al. 1999; Ishikawa et al. 1993; Kawabe et al. 1999; Koike et al. 1997). Likewise, MRP2-mediated transport has been shown to be GSH-dependent (Dietrich et al. 2001; Van Aubel et al. 1999).

Although the exact role of MRP2 during pregnancy is still unknown, its expression increases nearly two fold from preterm to term human placenta, suggesting the potential for physiological significance (Meyer zu Schwabedissen et al. 2005b). Interestingly, the increase of MRP2 expression also correlates with higher production of steroid hormones (estrogen, progesterone), fetal bilirubin, and fetal bile acids (Joshi et al. 2016; Marin et al. 2005; St-Pierre et al. 2000). Considering that MRP2 is localized to the apical membrane of syncytiotrophoblasts, it may play a more classical protective barrier role in limiting fetal exposure to various endogenous and exogenous molecules found in the maternal blood.

MRP3

The human MRP3/*ABCC3*, while sharing considerable amino acid similarity with MRP1 and 2, has significantly lower affinity for substrates also transported by its sister isoforms (Zeng et al. 2000). The MRP3 transporter cannot transport GSH, hence any substrates requiring the GSH as a cofactor for transport will be effluxed at much lower rates (Choudhuri et al. 2006). Overexpression of MRP3 has been shown to offer much lower resistance to drugs commonly co-transported with GSH such as etoposide, vincristine, methotrexate, and teniposide (Kool et al. 1999; Zeng et al. 1999). Similar to MRP1 and 2, MRP3 transports endogenous molecules such as unconjugated and conjugated bile acids (taurocholate, glycocholate) and steroid glucuronides (estradiol-17ß-glucuronide). Interestingly, MRP3 has the ability to transport non-sulfonated bile acids, a feature unique to this isoform (Hirohashi et al. 2000; Zeng et al. 2000).

MRP5

MRP5/*ABCC5*, an organic anion pump, transports cyclic and acyclic nucleoside monophosphates as well as their analogs. Overexpression of MRP5 in intact HEK293 cells and membrane vesicles isolated from V79 hamster lung fibroblasts resulted in an enhanced ATP-dependent cAMP efflux when compared to parent cell lines and membranes (Jedlitschky et al. 2000; Wielinga et al. 2003). ATP-dependent cAMP efflux by MRP5 was also shown in basolateral membrane vesicles isolated from human placenta (Meyer Zu Schwabedissen et al. 2005a). MRP5 has the ability to transport both cAMP (K_m = 379μM) and cyclic guanosine monophosphate (cGMP; K_m = 2.1 μM) (Jedlitschky et al. 2000). The MRP5-mediated transport of cyclic nucleotides is GSH independent (Wielinga et al. 2003).

Syncytialization is a process of placental cell differentiation where mononuclear cytotrophoblasts fuse together to form multinucleated syncytiotrophoblasts. Once formed, syncytiotrophoblasts perform a wide variety of placental functions including metabolism, hormone secretion, and xenobiotic transport via the expression of drug transporters such as MRP5. A correlation between MRP5 expression and placental cell differentiation has been previously explored. Compared to term human placentas, MRP5 mRNA expression is 6-fold higher in preterm placentas (<32 weeks), a gestational stage associated with placental development. Accordingly, *ex vivo* differentiation of primary human trophoblasts over time is accompanied by marked increases in MRP5 mRNA expression (Meyer Zu Schwabedissen et al. 2005a). In addition, polarized BeWo cells, a choriocarcinoma cell line, had a 1500-fold higher MRP5 mRNA expression than non-polarized cells (Pascolo et al. 2003). The process of placental syncytialization is inducible *in vitro* through stimulation of intracellular cAMP and cGMP levels by various pharmacological agents (Sawai et al. 1996). Consequently, the involvement of MRP5 in syncytialization may be through its functional ability to regulate the intracellular levels of cyclic nucleotides.

1.3.2 Regulation

Transcriptional Regulation

The MRP transporters contain several response elements in their promoter regions to which various transcription factors can bind and regulate their expression. Characterization of the rat *Mrp2/Abcc2* promoter revealed binding sites for the farnesoid X receptor (Fxr), pregnane X receptor (Pxr), and constitutive androstane receptor (Car), establishing the potential for transcriptional regulation of MRP drug transporters by nuclear receptors and transcriptional factors (Kast et al. 2002). Activation of PXR signaling is achieved through treatment with pharmacological agents such as dexamethasone, rifampicin, pregnenolone 16α-carbonitrile, and spironolactone. The MRP1, -2, and -3 transporter isoforms were found to be inducible in *in vitro* models such as human hepatoma HepG2 cells, primary hepatocytes, rat hepatocytes, and human intestinal Caco-2 cells following Pxr/PXR activation (Jigorel et al. 2006; Kast et al. 2002; Kauffmann et al. 2002; Martin et al. 2008). Similarly, female and male rodents treated with classical Pxr ligands also exhibited induction of liver MRP2 and 3 mRNA and protein (Aleksunes et al. 2012; Johnson et al. 2002; Maher et al. 2005). The transcription of MRP transporters is also reliant on FXR- and CAR-mediated transcription. Classical activators of FXR (GW4064) and CAR (phenobarbital) signaling induce MRP1,-2, and -3 mRNA and protein expression in numerous *in vitro* and *in vivo* human and rodent models (Aleksunes et al. 2012; Jigorel et al. 2006; Johnson et al. 2002; Kast et al. 2002; Maher et al. 2005; Martin et al. 2008). Mrp2, -3, and -5 transporters are also up-regulated in response to pharmacological agents (TCDD; ß-naphthoflavone) that activate the aryl hydrocarbon receptor (AhR) (Johnson et al. 2002; Maher et al. 2005). The nuclear factor eythroid 2-related factor-2 (NRF2) is a basic region-leucine zipper type transcription factor involved in mediating cellular response to inflammation and oxidative injury (Reviewed in Kensler et al. 2007; Morito et al. 2003; Rangasamy et al. 2004). Pharmacological stimulation (oltipraz; ethoxyquin; sulforaphane) and genetic ablation of NRF2 has established this factor as another agonistic regulatory element

controlling MRP1, -2, -3,and -5 transcription (Adachi et al. 2007; Aleksunes et al. 2012; Aleksunes et al. 2008; Hayashi et al. 2003; Ibbotson et al. 2017; Jigorel et al. 2006; Johnson et al. 2002; Maher et al. 2005; Song et al. 2009). Recently, studies were able to modulate MRP-dependent drug resistance and toxicant sensitivity in diverse cell lines through stimulation of NRF2 signaling (Gao et al. 2019; Li et al. 2019b; Udasin et al. 2016; Wang et al. 2018c; Xia et al. 2015; Yao et al. 2016). Transcriptional regulation by peroxisome proliferator-activated receptor (PPARα) has also been shown with respect to MRPs. Treatment with PPARα agonists (WY14643, GW7647, clofibric acid, perfluorodecanoic acid) results in a down-regulation of Mrp1 and Mrp2 and an induction of Mrp3 expression (Hirai et al. 2007; Johnson et al. 2002; Maher et al. 2005). Taken together, these studies exhibit that MRP transporters can be regulated by numerous transcriptional factors across different systems and models.

Post-transcriptional Regulation

In addition to transcriptional modulators, the expression and function of MRP transporters is also affected by post-transcriptional and –translational mechanisms. microRNAs (miRNAs) have been recognized as major contributors in drug resistance of multiple cancers. In particular, miRNAs -122, -128, -134, -199a, -206, -297, and -326 are associated with down-regulation of MRP1, -2, and -5 protein expression and recognized as potential targets to alter drug resistance across various cancer cell lines (Borel et al. 2012; Chang et al. 2018b; Liang et al. 2010; Liu et al. 2019; Xu et al. 2012a; Xu et al. 2011). Post-translational mechanisms are also implicated in regulating the expression, function, and trafficking of MRP transporters. Phosphorylation of MRP1 is associated with modulation of its function capability by affecting the binding affinity to various substrates such as tubulin, arsenic triglutathione, and estradiol 17ß-glucuronide (Ambadipudi et al. 2017; Shukalek et al. 2016; Stolarczyk et al. 2012). N-glycosylation also directly affects the functional capability of the MRP1 transporter by altering the binding affinity and V_{max} of arsenic triglutathione transport (Shukalek et al. 2016). Ubiquitination, a process which targets proteins for proteasomal

degradation, is another major regulatory component involved in the degradation of the internalized MRP2 transporter (Aida et al. 2014). The MRP2 transporter is also regulated by SUMOylation, as absence of the SUMO modification resulted in decreased protein expression in rat hepatoma-derived McARH7777 cells (Minami et al. 2009).

1.3.3 Genetic Polymorphisms

In human populations, interindividual variability in drug metabolism and resistance can be in part a result of genetic polymorphisms that alter enzyme and transport expression and/or kinetics. A large number of single nucleotide polymorphisms (SNPs) have been identified in the *ABCC1* gene. Many of the SNPs are nonsynonymous and result in amino acid substitutions across all five domains of MRP1 (Conrad et al. 2001; Leslie et al. 2003). While their occurrence varies significantly across different ethnical groups, only some have been identified to affect expression, function, and trafficking of the MRP1 transporter (Wang et al. 2005). Specifically, the 1299G>T (Arg433Ser) MRP1 mutant, located at the COOH-proximal end of the cytoplasmic loop, exhibited a ~2-fold higher doxorubicin-resistance when compared to wild type MRP1 (Conrad et al. 2002). Additionally, a TMD1 128G>C (Cys43Ser) mutant affected MRP1 trafficking to the plasma membrane and displayed a 2.5-fold decrease in arsenite and vincristine resistance in HeLa cells (Leslie et al. 2003). Other missense mutations such as 218C>T (Thr73Ile), 2168G>A (Arg723Gln), and 3173G>A (Arg1058Gln) were also shown to affect transport capability of MRP1 and drug resistance to its substrates (Gao et al. 1998).

Genetic analysis of patients with the autosomal recessive Dubin-Johnson syndrome has identified several MRP2 SNPs as major contributing factors preventing hepatic bilirubin clearance. *In vitro* studies have identified homozygous mutations 2302C>T (Arg768Trp) and 4145A>G (Gln1382Arg), located in NBD1 and 2, respectfully, to disrupt function and trafficking of the MRP2

transporter (Hashimoto et al. 2002). Of the known MRP3 polymorphisms, most are localized in the non-coding regions (Conseil et al. 2005). The 202C>T (Lys13Asn) promoter polymorphism resulted in significantly lower *ABCC3* transcript levels (Lang et al. 2004). Although 76 SNPs of the *MRP5/ABCC5* gene were identified in a Japanese population, none resulted in a nonsynonymous mutation (Saito et al. 2002). Further work is still needed to characterize whether any of the identified SNPs affect MRP5 expression, function, or trafficking.

1.4 Zearalenone

Zearalenone (ZEN), a phenolic resorcyclic acid lactone (Figure 1.2), is an estrogenic mycotoxin produced by *Fusarium* fungal species that commonly grow on cereal crops such as wheat, sorghum, rye, barley, and maize (Caldwell et al. 1970). Contaminated foods of note include cereal, noodles, popcorn, beef, and infant formula. Zeranol, a semi-synthetic nonsteroidal estrogenic metabolite of zearalenone, is widely used as a livestock growth promoter in the United States under the veterinary brand name Ralgro®, (Mader 1994). Zearalenone, zeranol, and their metabolites are often referred to as mycoestrogens due to their strong binding affinity for both isoforms of the estrogen receptor, ERα and ERß, and the ability to disrupt estrogenic signaling (Fitzpatrick et al. 1989; Mueller et al. 2004; Takemura et al. 2007b). Perinatal exposure of mice and rats to zearalenone and zeranol resulted in accelerated mammary gland development disrupted estrous cycles, earlier vaginal opening times, shortened anogenital distances, and decreased serum estradiol in exposed offspring (Belli et al. 2010; C. et al. 2016). Studies have also begun to identify zearalenone as a substrate of the BCRP efflux transporter, which may serve a protective role against fetal and placental accumulation of the mycoestrogen (Szilagyi et al. 2019; Xiao et al. 2015a). While data regarding the toxicological profile of mycoestrogens is emerging, further characterization of their disposition and activity in the placenta is still urgently needed.

1.4.1 Sources and Exposure

In 2016, the United Nations Environmental Program identified fungal contamination of food supply as one of the top 6 emerging issues of environmental concern (Chatuphonprasert et al. 2018). Increasing global temperatures promote the growth of fungi and in turn their production of toxic by-products such as ZEN. Foods in Korea (3-17µg/kg), Pakistan, United Kingdom (8-231.8µg/kg), Germany (3-67µg/kg) and Brazil (70µg/kg) routinely exceed the European Union (EU) set allowable limit for ZEN (4µg/kg) (2006; (FSA) 2003; Iqbal et al. 2014b; Ok et al. 2014; Schollenberger et al. 2005; Tralamazza et al. 2016). ZEN or its metabolites have been detected in the urine of pregnant women and infants (1.5-4.5 years old) at concentrations ranging from 0.055 to 1.82 ng/mL (Ali et al. 2019; Fleck et al. 2016; Njumbe Ediage et al. 2013). Domestically, ZEN has also been detected in the urine of 78% of NJ girls tested (n=163; 9-10 years old) at a range of 0.2-8.4 ng/mL. Detection of ZEN or its metabolites, such as alpha-zearalanol, correlated with delayed onset of breast development and shorter height (Bandera et al. 2011; Rivera-Nunez et al. 2019).

1.4.2 Pharmacokinetics and Pharmacodynamics

Pharmacokinetics

Absorption and Bioavailability

Plasma concentration analyses following oral administration of zearalenone revealed rapid and extensive absorption in rabbits, rats, pigs, and humans (Kuiper-Goodman et al. 1987). In pigs, a single oral dose of ZEN (10 mg/kg b.w.) was estimated to be 80-85% absorbed (Biehl et al. 1993). Pharmacokinetic comparison of oral versus intravenous ZEN administration (1-8mg/kg b.w.) in rats revealed only 2.7% absolute bioavailability of the parent mycoestrogen compound (Shin et al. 2009). This is consistent with known extensive enteric metabolism of zearalenone prior to reaching the systemic circulation.

Distribution

Oral administration of zearalenone to male, bile duct-cannulated rats revealed a ~42% shorter elimination half-life (7 h) when compared to control rats (16.8 h), demonstrating enterohepatic recirculation as a major pharmacokinetic factor. Within male rats, zearalenone was most prominently detected in the gastrointestinal tract followed by the kidney, liver, adipose, lung, heart, spleen, muscle, brain, and testes, respectfully (Shin et al. 2009). Pregnancy studies have also characterized the placental and fetal accumulation of zearalenone in mice and rat models following i.v. administration. In rats, i.v. administration of zearalenone (740 µg/kg b.w.) resulted in placental and fetal zearalenone concentrations of 117 µg/kg and 58 µg/kg at 0.3 h, respectfully, further exhibiting the protective role of the placenta in restricting mycoestrogen distribution (Bernhoft et al. 2001). Our laboratory has shown that the Bcrp transporter contributes to the transplacenta disposition of zearalenone. Intravenous administration of zearalenone (10 mg/kg b.w.) in Bcrp -/- mice revealed 118% and 100% higher fetal and placental concentrations of free zearalenone, respectfully, as compared to wild-type controls (Szilagyi et al. 2019). BCRP-mediated transport of zearalenone has also been established in BeWo choriocarcinoma and HEK cells (Xiao et al. 2015a). Other xenobiotic transporters involved in cellular efflux of zearalenone are multidrug resistance-associated proteins 1 and 2 (MRP1, -2) (Videmann et al. 2009). Cellular uptake of zearalenone and its metabolites is mediated mainly through solute carrier (SLC) transporters, namely the organic anion transporters 1 and 3 (OAT1, -3). Zearalenone-mediated inhibition of human OAT1-4 transporters as well as the related organic cation transporters 1 and 2 (OCT1, -2) was noted in transfected *Drosophila* cells, with greatest sensitivity for the OCT1 transporter (IC_{50}= 0.62µM) (Tachampa et al. 2008).

Metabolism

The major biotransformation pathways of zearalenone include Phase I and II enzymatic reduction, hydroxylation, and conjugation (Described in Mukherjee et al. 2014). Enzymatic reduction of

zearalenone is achieved by 3α- and 3ß-hydroxysteroid dehydrogenases that catalyze the reduction of the ketone group to an alcohol group. This conversion results in the production of α-,ß-zearalenol metabolites. The primary reduced α-, ß- zearalenol forms and the parent compound, zearalenone, have different estrogenic properties. That is, α-zearalenol has been shown to have the highest estrogen receptor binding affinity followed by zearalenone and ß-zearalenol, respectfully. With humans primarily producing the more estrogenic metabolite, α-zearalenol, this species may be more sensitive to the estrogenic toxicities of zearalenone than rats which produce the less estrogenic metabolite, ß-zearalenol. Cytochrome P450 (CYP450) enzymes catalyze the hydroxylation of zearalenone at the 6/8- and 13/15 positions to form catechol metabolites. The major human CYP isoforms responsible for this conversion are -1A2, -2C8, -3A4, and -3A5 (Bravin et al. 2009; Pfeiffer et al. 2009).

Sulfotransferases (SULTs) and uridinediphosphate-glucuronosyltransferases (UGTs) catalyze the Phase II conjugation of zearalenone and its reduced metabolites, with glucuronidation being the major conjugation pathway of detoxification in the liver. *In vitro* microsomal incubation of zearalenones revealed high levels of glucuronide conversion of zearalanone (ZAN; 93%), zearalenone (ZEN; 99%), 7-ß-hydroxy-zearalanol (ß-ZAL; 64%), 7-ß-hydroxy-zearalenol (ß-ZOL; 51%), and 7-α-hydroxy-zearalenol (α-ZOL; 88%) (Slobodchikova et al. 2019). The primary human UGT isoforms responsible for Phase II glucuronidation of zearalenone and its metabolites are -1A1, -1A3, -1A8, and -2B7.

While the liver is the main organ involved in the metabolism of zearalenone, recent studies also implicate the placenta as a contributing factor in its biotransformation as well. *In vitro* and *ex vivo* human placental models, including term placental subcellular fractions, chorion carcinoma JEG-3 cells, and dually perfused placenta, revealed the presence of five major Phase I and II metabolites

(α-zearalenol, ß-zearalenol, α-zearalanol, ß-zearalanol, ZEN-14-sulfate) following ZEN treatment (Huuskonen et al. 2015; Warth et al. 2019).

Excretion

Excretion of zearalenone and its metabolites varies across species. In humans, the predominant mode of excretion is by urine, whereas in rats zearalenone is eliminated through feces. Evaluation of zearalenone elimination half-life also exhibited species-specific differences. Rats administered zearalenone intravenously showed a 0.6 to 2.8 hour elimination half-life for the unconjugated parent compound (Shin et al. 2009). Alternatively, the New Jersey Girl Study estimated the elimination half-life of zearalenone to be significantly longer at ~12 h (Bandera et al. 2011). This further suggests that human sensitivity to zearalenone may be significantly higher than in rodent species due to prolonged exposure times.

Pharmacodynamics

Zearalenone, at nanomolar concentrations, can bind to estrogen receptors alpha and beta (ERα, -ß) and disrupt estrogen signaling by acting as both an agonist and antagonist (Fitzpatrick et al. 1989; Kowalska et al. 2018; Mueller et al. 2004; Takemura et al. 2007b). It is important to note that zearalenone metabolites such as zeranol and α-zearalenol have higher binding affinity for the estrogen receptor isoforms than the parent compound. Zeranol had significantly lower K_d values for ERα (22nM) and ERß (43nM) than zearalenone (ERα = 240nM, ERß = 166nM) (Fitzpatrick et al. 1989; Takemura et al. 2007b). Zearalenone and α-zearalenol are also implicated in altering cellular signaling through inhibition of the non-classical estrogen membrane receptor GPR30 in pig pituitary and bovine cells (He et al. 2018; Nakamura et al. 2015).

A number of studies have shown the potential for zearalenone and its metabolites to alter estrogen signaling and act as developmental toxicants across species (Table 1.8). The ability of zearalenone

to cross the placenta and accumulate in the fetal compartment has been established in CBA mice and Sprague-Dawley rats (Appelgren et al. 1982; Bernhoft et al. 2001). *In utero* exposure to zearalenone and zeranol has led to accelerated mammary gland development at postnatal day 30, disrupted estrous cycles, earlier vaginal opening times, shortened anogenital distances, and decreased serum estradiol in exposed offspring (Belli et al. 2010; C. et al. 2016; Nikaido et al. 2004). Reduction of fetus size, an increase in number of resorptions, and placental abnormalities were also noted in mice following zearalenone or zeranol treatment (Li et al. 2019a; Perez-Martinez et al. 1995; Wang et al. 2013). In pigs, reproductive dysfunction observed in response to ZEN is characterized by ovarian atrophy, pseudopregnancy, disruption of hormone metabolism and secretion, endometrium abnormalities, sterility, decreased maturation rate of oocytes, and decreased proliferation rate of granulosa cells (Reviewed by Cortinovis et al. 2013; Table 1). In cows, the reproductive dysfunction of ZEN is characterized by reduced milk production, infertility, decreased maturation rate of oocytes, and hyperestrogenism (Reviewed by Cortinovis et al. 2013; Table 1.8). Although equine species is more resistant to ZEN-mediated reproductive effects, ZEN treatment of granulosa cells obtained from ovaries of cycling mares resulted in an enhanced cellular proliferation rate and apoptosis (Minervini et al. 2006). With respect to the human placenta, treatment of BeWo choriocarcinoma cells with 10 μM ZEN revealed changes in cell fusion and secretion of the human chorionic gonadotropin hormone (Prouillac et al. 2009).

1.5 Research Objective and Hypothesis

A central hypothesis was developed based on aforementioned literature: Disruption of placental transporter function can negatively impact the feto-placental unit by increasing and/or decreasing: 1) transplacental disposition of xenobiotics and 2) intracellular concentrations of cyclic nucleotides that regulate syncytialization. Three specific aims were developed to address this hypothesis:

Aim 1. Characterize the regulation of placental SLC and ABC transporter expression in response to low oxygen concentrations.

Aim 2. Assess the contribution of transporter-mediated efflux of cyclic nucleotides on syncytialization.

Aim 3. Determine the effect of zearalenone on placental cell differentiation and transporter expression in mice.

This research is the first study to examine the endogenous role of drug transporters in placentation. Namely, it tests the novel hypothesis that MRP transporters regulate placental cell fusion by controlling the intracellular concentration of cyclic nucleotides. This is important as we show that drug transporters profiles are influenced by both endogenous and exogenous factors such as, hypoxia and the estrogenic mycoestrogen zearalenone, respectfully. Dysregulation of drug transporter homeostasis can alter the placental integrity and increase fetal susceptibility to xenobiotic exposure. This work aims to expand current drug transporter, developmental toxicology, and environmental science literature and offer a potentially novel mechanism for altered placentation with respect to abnormal drug transporter function.

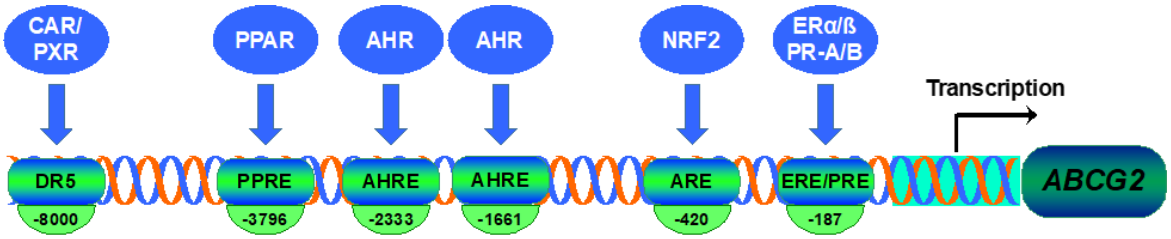

Fig 1.1. Transcription Factor-Mediated Activation of ABCG2 Gene. The location of response elements for nuclear hormone receptors and transcription factors involved in regulating the transcription of *ABCG2/BCRP* are shown relative to the transcriptional start site.

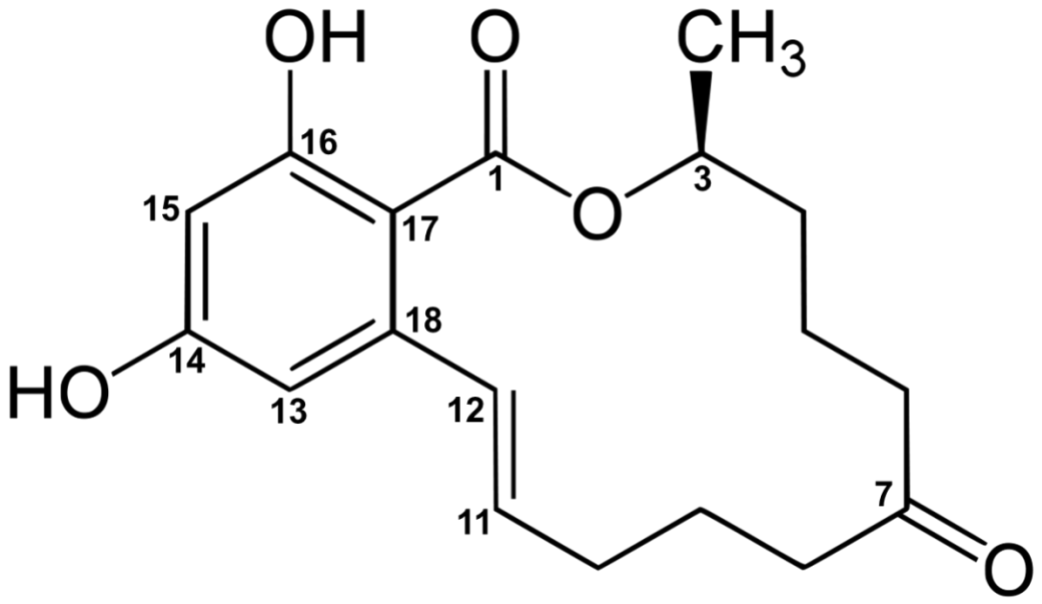

Figure 2.2. Numbered structure of zearalenone.

Table 1.1. Estrogen Receptor Regulation of BCRP/Bcrp Expression and Function

Model	Species	Agonists	Genetic Targeting	mRNA	Protein	Function	References
MCF-7 Breast Cancer Cells	Human	Estrone (10 nM), Estradiol (3 nM), and Diethylstilbestrol (0.1 nM)	siRNA	↑↔	↑↓	↓; Topotecan	(Imai et al. 2005a; Zhang et al. 2006)
T47D Breast Cancer Cells	Human	17-ß estradiol (0.1-10,000 nM)		↑↔			(Ee et al. 2004b; Yasuda et al. 2009)
BeWo Choriocarcinoma Cells	Human	Estriol (10 nM-100 µM), Estradiol (10 nM-10 µM), Estrone (10 nM-10 µM)		↑↓↔	↑↓	↓; Mitoxantrone	(Ee et al. 2004a; Wang et al. 2008b; Wang et al. 2006b; Yasuda et al. 2006)
Primary Trophoblasts	Human	Estradiol (100 nM)		↑	↑		(Evseenko et al. 2007b)
PA-1 Ovarian Cancer Cells	Human	Estradiol (10 nM)		↑			(Ee et al. 2004b)
Brain Capillaries	Rat	Propylpyrazoletriol (1 nM), Diarylpropionitrile (10 nM), Estradiol (1 nM-10 nM)			↓	↓↔; BODIPY FL prazosin	(Hartz et al. 2010a; Hartz et al. 2010b; Mahringer et al. 2010)
Brain Capillaries	Mouse	Estradiol (0.1 mg/kg)/(10 nM)	ERα and ERß Knockout Models		↓↔	↓↔; BODIPY FL prazosin	(Hartz et al. 2010a; Mahringer et al. 2010)

Table 1.2. Progesterone Receptor Regulation of BCRP/Bcrp Expression and Function

Model	Species	Agonists	mRNA	Protein	Function	References
T47D Breast Cancer Cells	Human	Progesterone (10 nM-100 µM)	↑			(Yasuda et al. 2009)
BeWo Choriocarcinoma Cells	Human	Progesterone (10 nM-100µM)	↑↔	↑	↑; Mitoxantrone	(Wang et al. 2006b; Yasuda et al. 2009)
Primary Trophoblasts	Human	Progesterone (100 nM)	↔	↔		(Evseenko et al. 2007b)
Placenta	Mouse	Progesterone (16 mg/kg)	↔	↔		(Kalabis et al. 2007)

Table 1.3. Peroxisome Proliferator-Activated Receptor Regulation of BCRP/Bcrp Expression and Function

Model	Species	Agonists	Genetic Targeting	mRNA	Protein	Function	References
hCMEC/D3 Blood Brain Barrier Cells	Human	Clofibrate, GW7647	siRNA	↑	↑	↑; Mitoxantrone	(Hoque et al. 2012)
Dendritic cells	Human	Rosiglitazone, Troglitazone, GW7845		↑	↑	↑; Hoechst	(Szatmari et al. 2006)
CD-1 Brain Capillaries	Mouse	Clofibrate		↑	↑	↑; BODIPY FL prazosin	(Hoque et al. 2015b)
Liver	Mouse	Wy14643, GW7647, Clofibrate		↑	↑		(Hirai et al. 2007; Moffit et al. 2006)
Small Intestine	Mouse	Wy14643, GW7647		↑	↑		(Hirai et al. 2007)

Table 1.4. Constitutive Androstane Receptor Regulation of BCRP/Bcrp Expression and Function[1]

Model	Species	Agonists	mRNA	Protein	Function	References
Primary Hepatocytes	Human	Phenobarbital, CITCO	↑	↑		(Benoki et al. 2012; Jigorel et al. 2006)
Liver	Mouse	TCPOBOP		↑		(Wang et al. 2010b)
Brain Capillaries	Porcine	CITCO	↑	↑	↑; Hoechst	(Lemmen et al. 2013a)
Brain Capillaries	Rat	Phenobarbital		↑	↑; BODIPY FL prazosin	(Wang et al. 2010b)
Brain Capillaries	Mouse	TCPOBOP		↑	↑; BODIPY FL prazosin	(Wang et al. 2010b)

[1]Abbreviations: CITCO (6-(4-chlorophenyl)imidazo[2,1-b][1,3]thiazole-5-carbaldehyde O-(3,4-dichlorobenzyl) oxime), TCPOBOP (3,3′,5,5′-tetrachloro-1,4-bis(pyridyloxy) benzene)

Table 1.5. Pregnane X Receptor Regulation of BCRP/Bcrp Expression and Function

Model	Species	Agonists	mRNA	Protein	Function	References
Primary Hepatocytes	Human	Rifampicin	↑			(Jigorel et al. 2006)
Liver	Human	Carbamazepine	↑			(Oscarson et al. 2006)
Liver	Mouse	Pregenolone-16 alpha-carbonitrile, 2-acetylaminofluorene	↑↔			(Anapolsky et al. 2006; Han et al. 2006)
hCMEC/D3 Blood Brain Barrier Cells	Human	Rifampicin	↔			(Dauchy et al. 2009)
Brain Capillaries	Porcine	Rifampicin	↑	↑	↑; Hoechst	(Lemmen et al. 2013b)
Small Intestine	Mouse		↔			(Han et al. 2006)

Table 1.6. Aryl Hydrocarbon Receptor Regulation of BCRP/Bcrp Expression and Function[1]

Model	Species	Agonists	Genetic Targeting	mRNA	Protein	Function	References
Primary Trophoblasts	Human	3MC		↔			(Stejskalova et al. 2011)
Primary Hepatocytes	Human	TCDD		↑			(Jigorel et al. 2006; Tan et al. 2010)
Hepa1c1c7 Liver Hepatoma Cells	Mouse	TCDD		↔			(Tan et al. 2010)
Liver	Mouse	3MC		↔			(Han et al. 2006)
Primary Colonocytes	Human	TCDD		↑			(Tan et al. 2010)
Caco-2 Colorectal Adenocarcinoma Cells	Human	TCDD, BP, indolo[3,2-b]carbazole, benzo[k]fluoranthene		↑	↑		(Ebert et al. 2005)
C2bbe1 Colorectal Adenocarcinoma Cells	Human	TCDD, DBA, and 3MC	siRNA	↑	↑	↑; Mitoxantrone	(Tan et al. 2010)
LS180 Colorectal Adenocarcinoma Cells	Human	TCDD		↑			(Tan et al. 2010)
LS174T Colorectal Adenocarcinoma Cells	Human	TCDD		↑			(Tan et al. 2010; Tompkins et al. 2010)
CMT93 Rectal Carcinoma Cells	Mouse	TCDD		↔			(Tan et al. 2010)
Small Intestine	Mouse	TCDD (30 μg/kg on GD16)		↔			(Tan et al. 2010)
Small Intestine	Mouse	3MC		↔			(Han et al. 2006)
hCMEC/D3 Blood Brain Barrier Cells	Human	TCDD		↑	↔		(Dauchy et al. 2009)
Brain Capillaries	Rat	TCDD			↑	↑; BODIPY FL prazosin	(Wang et al. 2011)
MCF-7 Breast Cancer Cells	Human	TCDD		↑			(Tan et al. 2010)
EMT 6 Breast Cancer Cells	Mouse	TCDD		↔			(Tan et al. 2010)

[1] Abbreviations: 3MC (3-methylcholanthrene), TCDD (2,3,7,8-tetrachlorodibenzo-*p*-dioxin), BP (benzo[a]pyrene), DBA (dimethyl-benzo[a]pyrene), GD (gestational day)

Table 1.7. Nuclear Factor Erythroid 2-Related Factor 2 Regulation of BCRP/Bcrp Expression and Function

Model	Species	Agonists	Genetic Targeting	mRNA	Protein	Function	References
Primary Hepatocytes	Human	Oltipraz		↑			(Jigorel et al. 2006)
HepG2 Liver Carcinoma Cells	Human	tert-Butylhydroquinone	siRNA	↑			(Adachi et al. 2007)
Brain capillaries	Rat	Sulforaphane			↑	↑; BODIPY-prazosin	(Wang et al. 2014)

Table 3.8. Zearalenone and Metabolite Reproductive Studies

Model/Species	Exposure	Observations	References
Mouse			
Mouse (CD-1)	Toxin: Zearalenone, zearalanol Dose: 0.01 & 10 mg/kg/d Route: Subcutaneous Period: GD15-19; 3 consecutive days following Postnatal day 17	**Maternal Endpoints** • ↑ uterine weight • ↑ uterine gland number **Fetal Endpoints** • Accelerated vaginal opening • ↑ length of estrous cycle • Lack of corpora lutea and vaginal cornification • Accelerated differentiation of mammary glands	Jefferson et al. (2002); Nikaido et al. (2004)
Mouse (NMRI)	Toxin: Zeranol Dose: 150 mg/kg/d Route: Subcutaneous Period: GD9-10	• ↓ fetal weight • ↓ fetal size • ↓ number of male pups	Perez-Martinez et al. (1995)
Mouse (ICR)	Toxin: Zeranol Dose: 1-100 mg/kg/d Route: Oral Period: GD13.5-16.5	• ↑ resorptions • ↑ preterm birth • ↓ placental expression of Cdk2/4, Cyclin D1, Bcl-xL • ↑ placental expression of pErk-1/2	Wang et al. (2013)
Mouse (C57BL/6)	Toxin: Zearalenone Dose: 0.8-40 ppm Route: Subcutaneous Period: GD5.5-13.5	• ↓ maternal weight gain • ↓ placental weight • ↓ fetal weight • ↑ resorptions • ↑ placental hemorrhage • Disruption of placental labyrinth layer • ↑ oil red staining of placenta	Li et al. (2019a)
Rat			
Rat (Wistar)	Toxin: Zearalenone Dose: 0.2 µg/kg/d - 5 mg/kg/d Route: Subcutaneous Period: Maternal: GD9-Delivery; Pups: Postnatal day 1-5 Observations: Postnatal day 30 and 180	**Fetal Endpoints** • Accelerated differentiation of mammary glands • ↑ necrosis of mammary glands	Belli et al. (2010)
Rat (Sprague-Dawley)	Toxin: Zearalenone Dose: 0.03 - 1 mg/kg/d Route: Oral Period: Postnatal day 21; 3 consecutive days	• ↑ thickness of uterine epithelial layer • ↑ uterine weight	Heneweer et al. (2007)
Rat (Sprague-Dawley)	Toxin: Zearalenone Dose: 1-8 mg/kg/d Route: Oral Period: GD6-19	• ↑ liver-body weight ratio • ↓ FSH in blood serum • ↓ Progesterone in blood serum **Fetal Endpoints** • ↓ fetal weight • ↓ skeletal ossification • ↑ fetal anogenital index	Collins et al. (2006)

		• ↓ fetal viability	
Horse			
Horse	Toxin: Zearalenone Dose: 7 mg Route: Oral Period: 10 consecutive days following ovulation	• ↔ length of interovulatory intervals • ↔ progesterone profile • ↔ follicular activity • ↔ uterine oedema	Juhasz et al. (2001)
Horse *Granulosa cells were collected from ovaries of cyclic mares*	Toxin: Zearalenone, α-zearalenol, ß-zearalenol Dose: 1 x 10^{-7} – 0.1 µM Period: 3 days	• ↑ cell proliferation • ↑ apoptosis	Minervini et al. (2006)
Pig			
Pig	Toxin: Zearalenone Dose: 1-100 mg/kg/d Route: Oral Period: Preestrous, gestational, or preestrous + gestational periods, Puberty to mating	• Constant estrous • Pseudopregnancy • Infertility • ↓ litter size • Fetal malformation and resorption • ↑ degeneration of blastocysts • Pseudopregnancy • No estrous detected within 50 days after puberty	Chang et al. (1979); Etienne et al. (1982); Long et al. (1992); Young et al. (1986)
Pig	Toxin: Zearalenone Dose: 1-20 mg Route: Intramuscular Period: Days 1-20 estrous cycle	• ↑ inter-estrous intervals • ↑ plasma progesterone levels	Edwards et al. (1987); Flowers et al. (1987)
Porcine oocytes and zygotes	Toxin: α-, ß-zearalenol Dose: 3.75-120 µM Period: 48-120 h	• ↓ maturation rate • ↑ degeneration rate • ↓↑ progesterone synthesis in FSH or forskolin stimulated cells • ↓ cell viability in FSH stimulated cells • ↓ expression of *P450scc* and *3ß-HSD* genes in forskolin and FSH stimulated cells • ↓ proliferation rate • ↑ apoptosis and necrosis	Alm et al. (2002); Ranzenigo et al. (2008); Tiemann et al. (2003); Zhu et al. (2012b)
Cow			
Cow	Toxin: zearalenone Dose: 250 mg Route: Oral Period: Daily over 3 estrous cycles	• ↓ conception rate • ↔ plasma progesterone • ↔ sex ratio	Weaver et al. (1986)
Bovine oocytes	Toxin: zearalenone Dose: 1-1000 µg/L Period: 21 h	• ↓ maturation rate	Takagi et al. (2008)
Bovine granulosa cells	Toxin: α-zearalenol Dose: 0.09-3.1 µM Period: 24-48 h	• ↑ cell growth • ↑ estradiol secretion in FSH and IGH1 stimulated cells	Pizzo et al. (2015)

CHAPTER 2: LOW OXYGEN TENSION DIFFERENTIALLY REGULATES EXPRESSION OF PLACENTAL SLC AND ABC TRANSPORTERS

Ludwik Gorczyca,[a,b] Jianyao Du,[c] Kristin M. Bircsak,[a,b] Xia Wen,[a]

Anna M. Vetrano,[d] and Lauren M. Aleksunes[a,e,f]

Affiliations:

[a] Rutgers University, Ernest Mario School of Pharmacy, Department of Pharmacology and Toxicology, Piscataway, NJ

[b] Rutgers University, Joint Graduate Program in Toxicology, Piscataway, NJ

[c] China Pharmaceutical University, Gulou, Nanjing, Jiangsu, People's Republic of China

[d] Rutgers University, Robert Wood Johnson Medical School, Department of Pediatrics, Division of Neonatology, New Brunswick, NJ

[e] Rutgers Center for Lipid Research, New Jersey Institute for Food, Nutrition, and Health, Rutgers University, New Brunswick, NJ

[f] Environmental and Occupational Health Sciences Institute, Piscataway, NJ

2.1 Abstract

Low oxygen concentration, or hypoxia, is an important physiological regulator of placental function including chemical disposition. The current study compared the ability of low oxygen tension to alter expression of SLC and ABC transporters in two human placental models (BeWo cells and term placental explants). Exposure of BeWo cells to low oxygen concentration differentially regulated transporter expression including down-regulation (ENT1, OATP4A1, OCTN2, BCRP, MRP2/3/5) and induction (CNT1, OAT4, OATP2B1, SERT, SOAT, MRP1). Similar up-regulation of MRP1 and down-regulation of MRP5 and BCRP was observed in explants whereas uptake transporters were decreased or unchanged. Screening of transcriptional regulators of transporters revealed declines in AHR, NRF2, and RXRα. These data suggest that transporter expression is differentially regulated by oxygen concentration across experimental human models. The ability of physiologically relevant low oxygen conditions to alter transporter expression and/or function should be given consideration during pharmacokinetic modeling of xenobiotic disposition across the placenta.

2.2 Introduction

The movement of drugs, chemicals, and hormones across the placenta is mediated in part by uptake and efflux transporters expressed on syncytiotrophoblasts. Placental uptake transporters from the solute carrier (SLC) superfamily include the concentrative and equilibrative nucleoside transporters, CNT1/*SLC28A1* and ENT1/*SLC29A1*, organic anion transporter 4 (OAT4/*SLC22A11*), organic anion transporting polypeptide 4A1 (OATP4A1/*SLCO4A1*) and 2B1 (OATP2B1/*SLCO2B1*), sodium-dependent organic anion transporter (SOAT/*SLC10A6*), organic cation transporter 2 (OCTN2/*SLC22A5*), and the serotonin transporter (SERT/*SLC6A4*). SLC transporters localize to different portions of the syncytiotrophoblast membrane including the apical or maternal-facing surface (CNT1, ENT1, OATP4A1, OCTN2, SOAT, SERT) (Balkovetz et al. 1989; Errasti-Murugarren et al. 2011; Grube et al. 2005; Loubiere et al. 2010; Schweigmann et al. 2014) as well as the basolateral or fetal-facing surface (OAT4, OATP2B1) (Grube et al. 2007; Ugele et al. 2003). Likewise, transporters from the ATP-binding cassette (ABC) superfamily export substrates from placental cells using energy garnered from the hydrolysis of ATP. In particular, the breast cancer resistance protein (BCRP/*ABCG2*) and multidrug resistance protein 1 (MDR1/*ABCB1/*P-glycoprotein) proteins localize to the apical surface of syncytiotrophoblasts and protect against fetal exposure to numerous xenobiotics through efflux back to the maternal circulation (MacFarland et al. 1994; Yeboah et al. 2006). Multidrug resistance-associated proteins (MRP/*ABCC*) are also expressed on syncytiotrophoblasts. MRP1 (*ABCC1*), MRP2 (*ABCC2*), and MRP3 (*ABCC3*) are predominantly found on the apical surface with some trafficking to the basolateral membrane as well (Meyer zu Schwabedissen et al. 2005b; Nagashige et al. 2003; St-Pierre et al. 2000). Alternatively, MRP5 (*ABCC5*) is notably expressed only on the basolateral side (Meyer Zu Schwabedissen et al. 2005a). In addition to the distinct patterns of trafficking to different portions of the plasma membrane, transporter expression is also regulated across gestation with some transporters expressed early in pregnancy (such as OCTN2, MDR1, MRP5) and others that

appear later (such as OATP2B1 and CNT1) (Table 2.1) (Jiraskova et al. 2018; Meyer zu Schwabedissen et al. 2006; Meyer Zu Schwabedissen et al. 2005a; Yasuda et al. 2005). Together, SLC and ABC transporters work together to regulate transepithelial transport of chemicals and hormones to and from the fetal circulation.

During the first trimester, the maternal uterine spiral arteries are occluded by invading extravillous trophoblasts. The occlusion limits the exchange of gases between the maternal and fetal blood and results in a partial oxygen tension in the human placenta of 20 mmHg (~3% O_2). Beginning from weeks 8 to 10 and onward, the spiral arteries undergo remodeling which increases uteroplacental blood flow resulting in a subsequent rise in oxygen concentration to about 60 mmHg (~8-10% O_2) during the second and third trimesters (Genbacev et al. 1997; Rodesch et al. 1992; Schneider 2011; Whitley et al. 2010). While low oxygen tension is a physiological feature of early placental development, reduced oxygen transfer to the placenta and fetus has also been implicated in the pathogenesis of diseases later in gestation (Stanek 2013). The dynamic nature of placental oxygenation influences expression and activity of key proteins and enzymes. Typically, transcriptional responses of cells to low oxygen concentrations are mediated by hypoxia-inducible factors (HIF). Under hypoxic conditions, the degradation of HIF-1α by pVHL-mediated ubiquitin proteases is prevented leading to its accumulation and subsequent translocation to the nucleus (Huang et al. 1996; Kallio et al. 1997). Once in the nucleus, HIF-1α forms a heterodimer with HIF-1β that binds hypoxia response elements found in the upstream promoter regions of target genes and enhances transcription (Patel et al. 2010). Hypoxic response elements have been identified in the promoter regions of uptake (ENT1/ *SLC29A1*) and efflux (MRP1*/ABCC1*; MDR1*/ABCB1*; BCRP*/ABCG2*) transporters implicating HIF-1α in their regulation (Chen et al. 2020; Comerford et al. 2002; Krishnamurthy et al. 2004; Lv et al. 2015). Regulation of transporters by HIF-1α may be one mechanism to explain changes in the expression of transporters from early to late gestation. For example, in mice, placental Bcrp expression corresponded with that of HIF-1α, where both

genes were maximally expressed at gestation day 15 (Wang et al. 2006a). In addition to HIF-1α, efflux transporters are also regulated by the nuclear factor erythroid 2-related factor 2 (NRF2), aryl hydrocarbon receptor (AHR), retinoid x receptor alpha (RXRα), estrogen receptor alpha (ERα), and peroxisome proliferator-activated receptor gamma (PPARγ) transcription factors (Adachi et al. 2007; Aleksunes et al. 2008; Anwar-Mohamed et al. 2011; Ee et al. 2004a; Ee et al. 2004b; Evseenko et al. 2007b; Ghanem et al. 2015; Han et al. 2006; Hartz et al. 2010a; Hartz et al. 2010b; Hayashi et al. 2003; Imai et al. 2005a; Jeong et al. 2015; Ji et al. 2013; Jigorel et al. 2006; Lin et al. 2016; Maher et al. 2005; Maher et al. 2007; Mahringer et al. 2010; Neradugomma et al. 2016; Rigalli et al. 2016; Song et al. 2009; Szatmari et al. 2006; Udasin et al. 2016; Vollrath et al. 2006; Wang et al. 2008b; Wang et al. 2014; Xu et al. 2014; Yasuda et al. 2006; Yasuda et al. 2009; Zhang et al. 2006). Response elements for these transcriptional factors have also been identified in the promoter regions of transporters (Ji et al. 2013; Maher et al. 2007; Singh et al. 2010; Tompkins et al. 2010; Yang et al. 2015). Moreover, these transcriptional regulators can also be regulated by HIF-1α signaling allowing for both direct and indirect regulation of transporters by low oxygen.

Early investigation into the ability of low oxygen to regulate efflux drug transporters such as MDR1 and BCRP within the placenta has yielded conflicting results (Francois et al. 2017; Javam et al. 2014; Krishnamurthy et al. 2004; Lye et al. 2013). One source of disparity between findings may be attributed to the selection of models for human placentation. Genetic variability between models and the gestational stage of the explants used may have altered the sensitivity to low oxygen tension. Therefore, the purpose of this study was to assess the regulation of xenobiotic and endobiotic transporter expression in two experimental models, namely, BeWo choriocarcinoma cells and healthy, term placental explants from uncomplicated pregnancies. This study expands the prior investigations by also comparing the regulation of uptake and efflux transporters by low oxygen tension across the two models.

2.3 Materials and Methods

Cell Culture

Human placental BeWo choriocarcinoma cells were purchased from the American Type Culture Collection (ATCC, Manassas, VA) and maintained in phenol-red free Dulbecco's Modified Eagle Medium: F-12 (ATCC) with 10% fetal bovine serum (Atlanta Biologicals, Flowery Branch, GA) and 1% penicillin-streptomycin (Life Technologies, Carlsbad, CA). Cells were incubated at 37°C with 20% O_2 and 5% CO_2 until they reached 70% confluence. Once confluent, cells were transferred to a modular incubator chamber (Billups-Rothenberg, Del Mar, CA) and sealed. Single flow meters were used to achieve a flow rate of 40 L/min and chamber was flushed with either 3% (similar to 1st trimester pregnancy) or 8% O_2 (similar to 2nd and 3rd trimester pregnancy) for six minutes. Once flushing was completed, clamps on the inlet and outlet ports were closed and the chamber was placed in an incubator at 37°C. Control cells were cultured under standard conditions (20% O_2). After 18 to 24 h, cells were processed for RNA, protein, or functional assays.

Fluorescent Substrate Accumulation Assay

The BCRP-specific fluorescent substrate, Hoechst 33342 (Sigma-Aldrich, St. Louis, MO), was used to assess BCRP activity in BeWo cells as previously described by our laboratory (Bircsak et al. 2013b). BeWo cells incubated in 3, 8, or 20% O_2 for 18 h were dissociated from culture plates using trypsin and centrifuged (500 x *g*, 5 min). Cell pellets were re-suspended with media containing Hoechst 33342 substrate (3 µM) with or without the BCRP-specific inhibitor, Ko143 (1 µM). Resuspended cells were then added to a 96-well plate and centrifuged once more (500 x *g*, 5 min). After centrifugation, cells were then placed in a 37°C cell culture incubator at 5% CO_2 for 30 min (*Uptake Phase*). Media containing the fluorescent substrate was then removed and cells were resuspended with substrate-free media with or without Ko143 and incubated for 1 h at 37°C and 5% CO_2 (*Efflux Phase*). After the efflux phase, cells were centrifuged (500 x *g*, 5 min, 5°C), washed,

and resuspended in cold phosphate-buffered saline (PBS) to allow for assessment of intracellular fluorescence using the Cellometer Vision cell counter (Nexcelom Bioscience, Lawrence, MA). Resuspended cells (20 µl) were added to a cell counting slide and analyzed for fluorescence intensity using a VB-450-302 filter (excitation/emission: 375/450 nm). The measured fluorescence intensity was normalized to size for each cell. Substrate and inhibitor were dissolved in dimethyl sulfoxide (DMSO), which did not exceed 0.1% in treatment media.

HIF-1α ELISA

BeWo cells were grown to 70% confluence on 6-well plates and exposed to 3%, 8%, and 20% O_2 for 18 h. Following incubation, cells were washed with PBS and lysed with 500 µl of chilled 1X Cell Extraction Buffer PTR. Cell lysate was scraped into a microcentrifuge tube and incubated on ice for 15 minutes. Cell lysates were centrifuged at 18,000 x g for 20 minutes at 4ºC and supernatant was extracted for analysis. HIF-1α protein concentration was determined by HIF-1α ELISA kit, as per manufacturer's protocol (ab171577, Abcam). Data were normalized to protein concentration.

Western Blot

Following treatment, BeWo cells were lysed using lysis buffer containing 20 mM Tris-HCl, 150 mM NaCl, 5 mM EDTA, 1% Triton X-100, and 2% protease inhibitor. The bicinchoninic acid assay was used to determine the protein concentration of cell lysates and placental explant homogenates. Total protein (30 µg) was loaded onto a SDS-polyacrylamide 4-12% Bis-Tris gel (Life Technologies) and resolved by electrophoresis. Proteins were transferred onto polyvinylidene fluoride membranes overnight using a Biorad Criterion Blotter (Biorad, Hercules, CA). Following the transfer, membranes were blocked in 5% non-fat milk in 0.5% Tween 20-PBS for 2 h. Membranes were then incubated with primary antibodies for 2 h at room temperature or overnight at 4ºC. Primary antibodies utilized included BCRP (BXP-53, 1:5000, Enzo Life Sciences, Farmingdale, NY), MDR1 (Mdr1a/b, 1:2000, Abcam, Cambridge, MA), GLUT1 (ab652, 1:10,000

Abcam), MRP1 (MRPr1, 1:2000, Enzo Life Sciences, Inc,), MRP2 (M_2III-5, 1:1000, Alexis), MRP3 (M_3II-9, 1:1000, Alexis), MRP5 (M_5I-10, 1:500, G. Scheffer, VU Medical Center, Amsterdam, Netherlands), and ß-Actin (ab8227, 1:2000, Abcam). All primary antibodies were diluted in 2% non-fat milk in 0.5% Tween 20-PBS. Primary antibodies were probed with species-appropriate secondary antibodies (Sigma-Aldrich). Chemiluminescent detection of protein signal was performed using SuperSignal West Dura blotting reagents (Pierce Biotechnology) and Fluorchem Imager (ProteinSimple, Santa Clara, CA). AlphaView Software (ProteinSimple) was used for semi-quantitation of protein bands. ß-ACTIN was used as a loading control.

Patient Selection

The inclusion criteria for placenta collection were healthy women aged 18-40 years scheduled for cesarean section with term pregnancies (>36 weeks) without labor. Exclusion criteria included maternal smoking, alcohol, or drug abuse, known fetal chromosomal abnormalities, medical conditions induced by pregnancy (i.e., hypertension, preeclampsia, gestational diabetes), medication use, maternal infection, and chronic medical conditions (i.e., autoimmune disorders, hypertension, diabetes) (Memon et al. 2014). Written informed consent was obtained from patients. The study was approved by the Institutional Review Boards of Robert Wood Johnson Medical School (Protocol #0220100258) and Rutgers University (Protocol #E12-024) (Memon et al. 2014).

Placental Explants

Information regarding the demographics of the patients along with the weight, size, and age of the placentas are provided in Table 2.2. Placentas were collected within 10 min of delivery, kept on ice, and processed within 2 h. Sections of villous tissue were obtained after removal of the maternal decidua and the chorionic plate. Villous tissue was washed three times in PBS to remove maternal blood and sectioned into 8 mm^3 pieces. Sectioned villous tissue was cultured in DMEM: F12 media with 10% FBS (Atlanta Biologicals) and 1% penicillin-streptomycin (Life Technologies). Explants

were cultured for 5 days to allow for complete degeneration and regeneration of the syncytium (Siman et al. 2001). Media was changed and collected every 24 h. On day 5, placental explants were incubated in 3%, 8%, or 20% O_2 for 24 h as described above for BeWo cells. After 24 h, cells were washed with PBS and frozen in liquid nitrogen.

Hormone Secretion

Placental explants were exposed to low oxygen concentration for 24 h and cell culture media was collected to determine explant viability. Hormone secretion into the media was quantified using a human chorionic gonadotropin ELISA kit ß (DY9034-05, R and D Systems, Minneapolis, MN) according to the manufacturer's protocol. Hormone secretion was normalized to protein concentration as determined by the bicinchoninic acid protein assay kit (Thermo Fisher).

RNA Isolation, cDNA preparation,and Quantitative Polymerase Chain Reaction

Following treatment, BeWo cells were lysed using Buffer RLT (Qiagen, Germantown, MD) containing 1% β-mercaptoethanol. Alternatively, 30 mg of placental explant tissue was added to 700 ml of Buffer RLT with 1% β-mercaptoethanol and a 5-mm stainless steel bead in a 2-ml round bottom polypropylene tube. Samples were homogenized in solution for 5 min at 40 Hz in the TissueLyser II (Qiagen). Total RNA from both BeWo cells and placental explants was isolated using the RNeasy mini kit (Qiagen). RNA concentrations were measured using a Nanodrop 2000 spectrophotometer (Thermo Scientific, Wilmington, DE). cDNA was generated using the High-Capacity cDNA Reverse Transcription Kit (Life Technologies). mRNA expression was determined by quantitative PCR (qPCR) using specific forward and reverse primers (Integrated DNA Technologies, Inc., Coralville, IA) and SYBR Green dye (Life Technologies). qPCR was performed using the ViiA7 Real-Time PCR machine (Life Technologies). CT values were converted to delta delta CT values with β-ACTIN serving as a reference gene for normalization (Livak et al. 2001).

Statistical Analysis

Data are presented as mean ± SE and analyzed using Graphpad Prism 6.0 (Graphpad Software, Inc., La Jolla, CA). An unpaired Student's t-test or a one-way ANOVA followed by a Newman-Keuls multiple comparison post hoc test were used to assess statistical significance. * $p \leq 0.05$ compared with cells treated with 20% O_2. † $p \leq 0.05$ compared with cells treated with 8% O_2.

2.4 Results

Activation of HIF-1α signaling in BeWo cells and placental explants exposed to reduced oxygen concentrations.

BeWo cells were exposed to 3%, 8%, and 20% O_2 for up to 24 h. As compared to 20% O_2, exposure of BeWo cells to 8% and 3% O_2 resulted in 60% and 75% induction of HIF-1α mRNA, respectively (data not shown). Similarly, total cellular HIF-1α protein was enhanced by 26% after exposure to 3%, but not 8% O_2 (Figure 2.1A). Increased mRNA expression of two prototypical HIF-1α target genes, VEGF and GLUT1 was also observed (Figure 2.1C). Exposure of BeWo cells to 8% and 3% O_2 for 24 h resulted in a 2-fold and 6.4-fold induction of GLUT1 mRNA expression, respectively. Correspondingly, the level of GLUT1 protein in BeWo cells was elevated by 34 and 69% after exposure to 8% and 3% O_2, respectively (Figure 2.1B). Expression of VEGF mRNA was also increased by 2.4- and 5.5-fold exposure to 8% and 3% O_2, respectively (Figure 2.1C).

Placental explants undergo degeneration (Day 2) and regeneration (Days 3-5) of syncytium (Supplemental Figure 2.1). Explants obtained from term, uncomplicated pregnancies were cultured for 5 days to allow for regeneration of the syncytiotrophoblast cell layer prior to a 24 h treatment with 20%, 8%, or 3% O_2 beginning on the 5^{th} day. Integrity of the placental explant syncytiotrophoblast layer under 20% and 3% O_2 conditions was confirmed by histology and detection of hCG secretion into media (Supplemental Figure 2.2). Explants exhibited numerous multinucleated syncytiotrophoblasts on the outermost layer of the chorionic villi that was not different between treatment groups. Activation of the HIF-1α signaling pathway in placental explants exposed to hypoxic conditions for 24 h was confirmed by induction of GLUT1 and VEGF mRNA expression although to a lesser magnitude than observed in BeWo cells (Figure 2.1C).

Differential expression of transporters in BeWo cells and placental explants exposed to reduced oxygen concentrations.

Exposure of BeWo cells to 3% O_2 for 24 h revealed significant induction of CNT1 (333%), OAT4 (20%), OATP2B1 (211%), SERT (361%), and SOAT (220%) mRNA as compared to the 20% O_2 control. In response to 8% O_2, OAT4 and OATP2B1 transporter mRNAs were similarly induced by 25% and 75%, respectively (Figure 2.2). In contrast, the mRNA expression of ENT1, OATP4A1, and OCTN2 was down-regulated by 36%, 41%, and 27%, respectively, under 3% O_2 conditions. A significant reduction in OATP4A1 and OCTN2 mRNA expression was also observed after 8% O_2 exposure (Figure 2.2). Placental explants exposed to low oxygen conditions for 24 h had reduced expression of OAT4 and OATP2B1 mRNA (up to 55%) (Figure 2.2). Examination of other uptake transporters revealed no significant mRNA changes in placental explants following low oxygen tension exposure.

Compared to 20% O_2, MRP1 mRNA was increased by 41% and 18% in BeWo cells exposed to 8% and 3% O_2 for 24 h, respectively (Figure 2.3). Examination of MRP1 protein level revealed no significant change following low oxygen tension exposure (3% and 8% O_2) for 18 h (Figure 2.4A/B). MRP2 and MRP3 mRNAs were also significantly down-regulated in BeWo cells after a 24 h exposure to a low oxygen environment (Figure 2.3). Notably, MRP2 and MRP3 proteins were not detected in BeWo cells similar to prior reports (Evseenko et al. 2006; Pascolo et al. 2003). MRP5 mRNA expression was consistently down-regulated in BeWo cells following exposure to low oxygen concentrations (Figure 2.3). A corresponding decrease in MRP5 protein level was also seen after an 18 h exposure to 3% and 8% O_2 (Figure 2.4A/B), with a maximal decline to 30% of control levels (20% O_2). Exposure of BeWo cells to reduced oxygen concentrations for 24 h also revealed a consistent reduction in BCRP mRNA expression (20-30%) (Figure 2.3). BCRP protein decreased 20% in BeWo cells after exposure to 3% O_2 for 18 h (Figure 2.4A/B). The Hoechst accumulation assay was used to assess whether low oxygen tension altered the function of BCRP (Figure 2.4C). Accordingly, in response to 3% O_2, cellular retention of the prototypical BCRP substrate Hoechst 33342 increased by 25%, which was consistent with decreased transport activity

of this efflux transporter. MDR1 mRNA was not detected by qPCR in BeWo cells, similar to previous publications (Atkinson et al. 2003; Ceckova et al. 2006; Magnarin et al. 2008). Low oxygen-mediated changes observed in MRP drug transporters in the BeWo cell models correlated well with term explants exposed to similar conditions. Following a 24 h exposure to 3% O_2, term explants exhibited up to a 50% and 30% reduction of MRP5 and BCRP mRNA expression, respectively, as well as a 20% induction of MRP1 mRNA expression (Figure 2.3). While expression of the MDR1 transporter was quantifiable in placental explants, there were no observed changes in its mRNA expression under hypoxic conditions (data not shown).

Differential expression of transcription factors in placental models exposed to reduced oxygen concentrations.

mRNA expression of multiple transcription factors known to regulate efflux transporters was also quantified in BeWo cells and placental explants following exposure to low oxygen levels for 24 h (Figure 2.5). A global reduction of AHR, NRF2, RXRα, and PPARγ mRNAs between 25 and 85% was observed after treatment of BeWo cells with 3% O_2. Conversely, there was a 6-fold induction of ERα mRNA in BeWo cells after a 3% O_2 exposure for 24 h. Consistent with changes observed in BeWo cells exposed to reduced oxygen concentrations, the mRNA expression of AHR, NRF2, and RXRα was also lower in placental explants exposed to 3% O_2 (Figure 2.5). In contrast to BeWo cells, the mRNA expression of PPARγ in placental explants was induced by 39% under reduced oxygen concentrations (Figure 2.5). Taken together, these data point to similar down-regulation of AhR and NRF2 mRNAs in the two placental models following exposure to low oxygen whereas other regulators exhibited differential changes that were dependent on the placenta model.

2.5 Discussion

In this study, we examined the impact of reduced oxygen concentrations (3% and 8% O_2) on the mRNA expression of placental drug transporters. We employed two widely used human placental *in vitro* models, BeWo choriocarcinoma cells and term placental explants, to directly compare the responses of transporters to low oxygen tension. This was achieved by incubating cells and explants with 3% and 8% O_2 to mimic physiological concentrations observed at the first and second/third trimester, respectively. Activation of HIF-1α was denoted by induction of two target genes, VEGF and GLUT1, in both models. In BeWo cells, hypoxic conditions resulted in the induction (CNT1, OAT4, OATP2B1, SERT, SOAT) and down-regulation (ENT1, OATP4A1, OCTN2) of uptake transporter mRNAs. Notably, low oxygen tension largely did not influence expression of uptake transporters in term placental explants to the same extent as observed in BeWo cells. The only significant changes in uptake transporter expression in placental explants were reduced levels of OAT4 and OATP2B1 mRNA. A global reduction of efflux drug transporter gene expression (MRP-2, 3, 5, BCRP), protein levels (MRP5, BCRP) and function (BCRP) was observed in BeWo cells incubated with 3% O_2. Meanwhile, placental explants exposed to 3% O_2 revealed differential changes in efflux transporter expression. Specifically, treatment with low oxygen tension resulted in the significant induction of MRP1 and down-regulation of BCRP and MRP5 mRNA expression. Relationships between efflux transporters and known regulatory transcription factors were also evaluated in response to low oxygen concentrations and revealed a down-regulation of AHR, NRF2, PPARγ, and RXRα as well as an induction of ERα mRNA expression in BeWo cells. Alternatively, the same conditions decreased AHR and NRF2 and induced PPARγ mRNA levels in placental explants. Taken together, these data suggest that low oxygen conditions alter transcriptional pathways that may regulate placental drug transporter expression, and possibly function, during early fetal development and diseases of pregnancy.

The two experimental models revealed several similarities in the regulation of some transcription

factors and transporters following exposure to low oxygen. Still, there were some clear differences, namely in the regulation of OAT4, OATP2B1, and PPARγ (Table 2.3). The BeWo cell line is one of the most commonly used placenta models due to its ability to secrete hormones and undergo syncytial fusion, both properties exhibited by human placental villous trophoblasts (Orendi et al. 2011). Despite the recapitulation of some critical trophoblast functions, BeWo cells are still an immortalized cancer cell line. Therefore, data from studies examining gene changes have to be assessed carefully as the immortalization of cell lines is dependent on gene silencing through promoter specific methylation (Novakovic et al. 2011). Analysis of DNA methylation profiles of primary trophoblast cell populations and derived cell lines revealed that choriocarcinoma-derived cell lines exhibit an overall methylation profile that reflects unrelated solid cancers, rather than untransformed human trophoblast cells (Novakovic et al. 2011). As an alternative to choriocarcinoma cell lines, placental explants allow for greater translation of data since DNA methylation profiles and transcriptional regulation mirror *in vivo* human placenta biology. Still, term placental explants are genetically diverse and may have single nucleotide polymorphisms and insertion-deletion variants that can alter transporter expression and regulation (Bircsak et al. 2018). The small amount of explant tissue available limited our analyses to only mRNA expression. Furthermore, placental explants contain a variety of cells including stem-cell like cytotrophoblasts, syncytiotrophoblasts, fetal endothelial cells, and invasive extravillous cytotrophoblasts. These cell populations differ in morphology, function, as well as gene expression profiles (Huppertz 2008). OAT4, OATP2B1, MRP-1, 3, 5 and BCRP have all been shown to be localized to the syncytiotrophoblast layer as well as stem cell-like cytotrophoblasts and/or fetal endothelium (Ceckova et al. 2006; Lye et al. 2013; Meyer Zu Schwabedissen et al. 2005a; St-Pierre et al. 2000; Ugele et al. 2008). The presence of transporters on different cell types may also explain differences in low oxygen tension-mediated changes (OAT4, OATP2B1) between the two experimental models.

The effect of low oxygen tension on MRP efflux transporter mRNA and protein expression has been previously investigated in tissues other than placenta. Induction of MRP1 mRNA and protein level has been observed in HepG2 and Lovo cell lines in response to hypoxic conditions or following treatment with a hypoxia-mimetic agent, cobalt chloride (Lv et al. 2015; Sakulterdkiat et al. 2012; Zhu et al. 2005; Zhu et al. 2012a). This induction was comparable to the up-regulation of MRP1 mRNA in placental explants under 3% O_2 suggesting that low oxygen has a prominent role in regulating MRP1 expression. Interestingly, while MRP2 mRNA was induced in HepG2 cells in response to low oxygen concentration, its expression in cultured hepatocytes isolated from Wistar rats was reduced after hypoxic exposure (Fouassier et al. 2007; Sakulterdkiat et al. 2012). A similar disconnect in terms of low oxygen-mediated regulation of MRP2 expression was seen in our study where MRP2 mRNA decreased in BeWo cells but not in placental explants, suggesting that species, cellular model, and tissue type determine responses to low oxygen levels.

Conflicting results suggested that BCRP mRNA and protein can be differentially regulated in response to low oxygen (Javam et al. 2014; Lye et al. 2013). Exposure of JAR cells, a placental choriocarcinoma cell line, to hypoxic conditions for 24 h resulted in significant induction of BCRP mRNA and function (Krishnamurthy et al. 2004). Interestingly, term placental explants exposed to hypoxic conditions for 24 and 48 h revealed no changes in BCRP mRNA and protein expression (Javam et al. 2014). Still, the same laboratory found a significant decrease in BCRP mRNA expression after a 48 h incubation of 1st trimester placental explants in 3% O_2 (Lye et al. 2013). A disconnect between BCRP mRNA and protein expression changes under low oxygen was observed in this study, as low oxygen caused an increased immunohistochemical staining for BCRP in cytotrophoblasts and the microvillous membrane of the syncytium (Lye et al. 2013). Our laboratory, has also previously shown a reduction of BCRP mRNA, protein, and function in BeWo cells after a 24 or 48 h exposure to cobalt chloride (200 µM) or 3% O_2 as well as in placentas from healthy pregnant women who give birth at high altitudes (Francois et al. 2017). The conflicting

results between these studies, specifically regarding placental explants, may be attributed to genetic variability between models as well as different stages of gestation that may render explants more or less sensitive to oxygen-induced changes.

Potential regulatory crosstalk between the hypoxia signaling pathway and transcription factors, specifically AHR, PPARγ, NRF2, and ERα, has been examined. For example, hypoxia reduces the expression of AHR target genes CYP1A1 and CYP1B1 in brain endothelial hCMEC/D3 cells and hepatoma HepG2 cells (Jacob et al. 2015; Vorrink et al. 2014). Treatment of JEG3, BeWo, and HVT cells with 3-methylcholanthrene, an AHR agonist, resulted in a global induction of BCRP mRNA expression (Neradugomma et al. 2016). Similarly, HMEC-1 cells, a dermal microvasular endothelium cell line, treated with a hypoxic mimetic, dimethyloxaloylglycine, had a significant reduction in the mRNA expression of NRF2 as well as its target gene, HO-1 (Loboda et al. 2009). NRF2 is involved in the transcriptional up-regulation of MRP1, 2, 3, 5 and BCRP in numerous tissues, cell lines, and species (Adachi et al. 2007; Aleksunes et al. 2008; Anwar-Mohamed et al. 2011; Ghanem et al. 2015; Hayashi et al. 2003; Jeong et al. 2015; Ji et al. 2013; Jigorel et al. 2006; Maher et al. 2005; Maher et al. 2007; Rigalli et al. 2016; Song et al. 2009; Udasin et al. 2016; Vollrath et al. 2006; Wang et al. 2014; Xu et al. 2014). Furthermore, HepG2 hepatoma cells exposed to hypoxia exhibit induction of PPARγ mRNA and protein (Zhao et al. 2014). Chromatin immunoprecipitation assays also revealed HIF-1α binding to an HRE element found upstream of a PPARγ transcriptional start site, further exhibiting a potential regulatory role of HIF-1α (Zhao et al. 2014). While this does not correlate with our results in the BeWo cell model, it is parallel with the induction of PPARγ mRNA expression seen in our placental explant model, further demonstrating the importance of cell type and tissue specific responses to hypoxic conditions. A PPAR response element has also been identified upstream of the *ABCG2* transcriptional start site and our laboratory has shown that the PPARγ agonist, rosiglitazone, induces BCRP mRNA and protein expression in BeWo cells (Lin et al. 2016; Szatmari et al. 2006). Hypoxic conditions as

well as a siRNA knockdown of HIF-1α caused a significant reduction in ERα protein level in MCF7 cells, displaying the interdependence of these two signaling pathways (Wolff et al. 2017). The ability of ERα to regulate transporter expression is varied and can depend upon cell lineage, cell type, duration of treatment, and endogenous expression of ER isoforms (Ee et al. 2004b; Imai et al. 2005a; Wang et al. 2008b). Ultimately, future studies using promoter binding assays, such as ChIP and knockout cell line models of noted transcription factors, would further elucidate the extent of their specific contribution to the regulation of efflux drug transporters under hypoxia.

Taken together, these data suggest that low oxygen conditions observed during the 1st and 2nd trimesters may regulate transcriptional regulatory pathways which in turn govern placental drug transporter expression and function. With the increasing development of physiologically-based pharmacokinetic models of pregnancy, the importance of hypoxia in regulating transporter expression across gestation or in response to pathology should be considered. In vitro to in vivo extrapolation of drug transporter expression and function under physiologically relevant low oxygen tension may improve the pharmacokinetic modeling of xenobiotic disposition across the placenta.

Table 4.1. Human Placental Transporter Localization, Substrates, and Expression Across Gestation.

Transporter	Syncytiotrophoblast Localization	Substrates	Expression Across Gestation[1]	References
CNT1/3 (*SLC28A1/3*)	Apical	Adenosine, uridine, thymine, cytosine	↑	(Jiraskova et al. 2018; Ritzel et al. 2001; Ritzel et al. 1997)
ENT1 (*SLC29A1*)	Apical	Adenine, adenosine, cytidine, cytosine, guanine, guanosine, hypoxanthine, inosine, thymidine, uracil, uridine	↔	(Boswell-Casteel et al. 2017; Cerveny et al. 2018)
OAT4 (*SLC22A11*)	Basolateral	Sulfated steroids, prostaglandins, uric acid, NSAIDs, antihypertensives	NA[2]	(Nigam et al. 2015)
OATP4A1 (*SLCO4A1*)	Apical	Estradiol-17ß- glucuronide, estrone 3-sulfate, thyroxine, triiodothyronine, prostaglandin, and taurocholate	↔	(Dallmann et al. 2019; Roth et al. 2012)
SOAT (*SLC10A6*)	Apical	DHEAS, oestrone sulfate, pregnenolone sulfate, and methylpyrene sulphates	NA[2]	(Vahakangas et al. 2009)
OATP2B1 (*SLCO2B1*)	Basolateral	Estrone-3-sulfate, pregnenolone sulfate, dehydroepiandrosterone sulfate, xenobiotics (cholesterol, blood pressure, and diabetes drugs)	↑	(Kalliokoski et al. 2009; Mikheev et al. 2008)
OCTN2 (*SLC22A5*)	Apical	Quinidine, verapamil, choline, lysine, carnitine	↓	(Grube et al. 2005; Ohashi et al. 1999)
SERT (*SLC6A4*)	Apical	Serotonin	NA[2]	(Kekuda et al. 2000)
BCRP (*ABCG2*)	Apical	Chemotherapeutic drugs, tyrosine kinase inhibitors, prazosin, glyburide, nitrofurantoin, dietary flavonoids, statins, porphyrins	↑↔↓	(Iqbal et al. 2012; Mathias et al. 2005; Meyer zu Schwabedissen et al. 2006; Ni et al. 2010; Yeboah et al. 2006)
MDR1 (*ABCB1*)	Apical	Steroids, lipids, bilirubin, bile acids, digoxin, fexofenadine, doxorubicin, vinblastine, chemotherapeutic drugs	↓	(Mathias et al. 2005; Sun et al. 2006)
MRP1 (*ABCC1*)	Apical	Etoposide, vinblastine, cisplatin, mitoxantrone, folate, bilirubin, leukotrienes,	↔	(Dallmann et al. 2019; Mason et al. 2011; Ni et al. 2011)

		prostaglandins, sulfate and glucuronide conjugates		
MRP2 (*ABCC2*)	Apical	Pravastatin, bilirubin, sulfated bile salts, estrone-3-sulfate, glutathione and glucuronide conjugates, chemotherapeutic drugs	↑↔	(Dallmann et al. 2019; Mason et al. 2011; Meyer zu Schwabedissen et al. 2005b)
MRP3 (*ABCC3*)	Apical	Methotrexate, bile salts, estradiol-17ß-glucuronide, fexofenadine, vincristine	NA[2]	(Dallmann et al. 2019)
MRP5 (*ABCC5*)	Basolateral	cAMP, cGMP, folate, 6-mercaptopurine, methotrexate	↓	(Dallmann et al. 2019; Jedlitschky et al. 2000; Meyer Zu Schwabedissen et al. 2005a)

[1]Changes in transporter expression across gestation in healthy human placentae. [2]NA=Information currently unavailable.

Table 2.2. Subject Demographics.

Subject Demographics	
Maternal Age (y, range)	Mean: 33.5 (31-39)
Gestational Age (weeks, range)	Mean: 38.44 (37 - 39)
Placenta weight (g, range)	Mean: 684.78 (531.1 - 927.2)
Baby Gender	8 Male; 1 Female
Maternal Race/Ethnicity	Caucasian (7) and African American (2)
Paternal Race/Ethnicity	Caucasian (7) and African American (2)

Table 2.3. Hypoxia-Mediated Regulation of Drug Transporter and Transcription Factor mRNAs in Placental Cells and Cultured Placental Explants.

Gene	BeWo Cells	Placental Explants
CNT1	↑	↔
ENT1	↓	↔
OAT4	↑	↓
OATP2B1	↑	↓
OATP4A1	↓	↔
OCTN2	↓	↔
SERT	↑	↔
SOAT	↑	↔
MRP1	↑↔	↑
MRP2	↓	↔
MRP3	↓	↔
MRP5	↓	↓
BCRP	↓	↓
MDR1	ND[1]	↔
VEGF	↑	↑
GLUT1	↑	↑
AHR	↓	↓
NRF2	↓	↓
PPARγ	↓	↑
ERα	↑	↔
RXRα	↓	↔

[1] ND: not detected

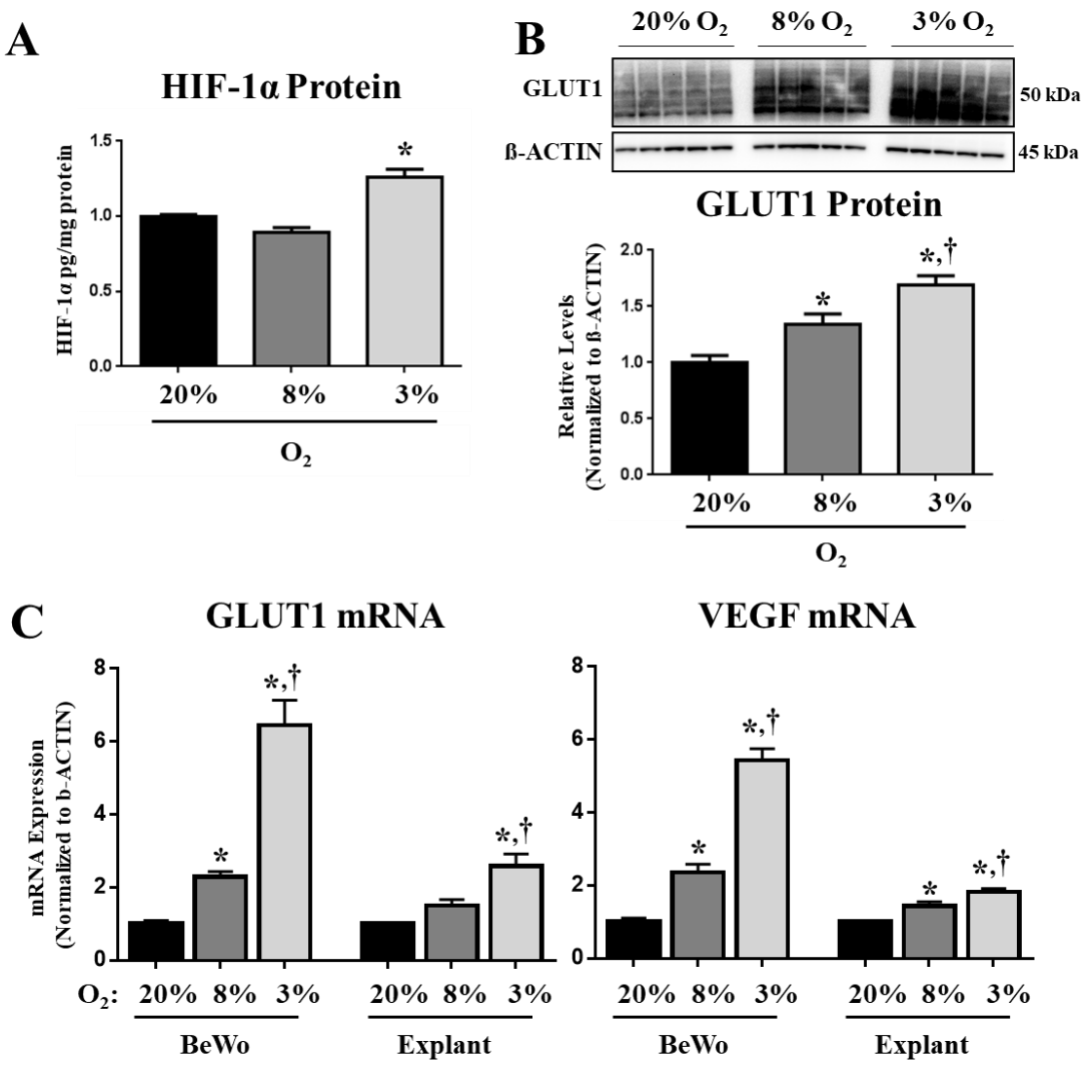

Fig 2.1. Activation of HIF-1α signaling in BeWo cells and placental explants. BeWo cells and placental explants were exposed to a range of oxygen concentrations for up to 24 h. (A) Changes in HIF-1α protein level in BeWo cells were measured at 18 h using an ELISA according to the manufacturer's protocol. (B) GLUT1 protein level in BeWo cells at 18 h was semi-quantified by western blot. ß-Actin was used as a loading control. (C) Placental explants were exposed to a range of oxygen concentrations on the 5th day of culture. Activation of HIF-1α target genes (VEGF and GLUT1) in BeWo cells and placental explants at 24 h was assessed by qPCR and normalized to ß-Actin. BeWo cell data are presented as mean ± SE of a single representative run with at least three replicates (n=3). Placental explant data are presented as the mean of 3-6 placentas (4-5 samples

from each placenta per treatment) ± SE. * $p \leq 0.05$ compared with cells or explants treated with 20% O_2. † $p \leq 0.05$ compared with cells or explants treated with 8% O_2.

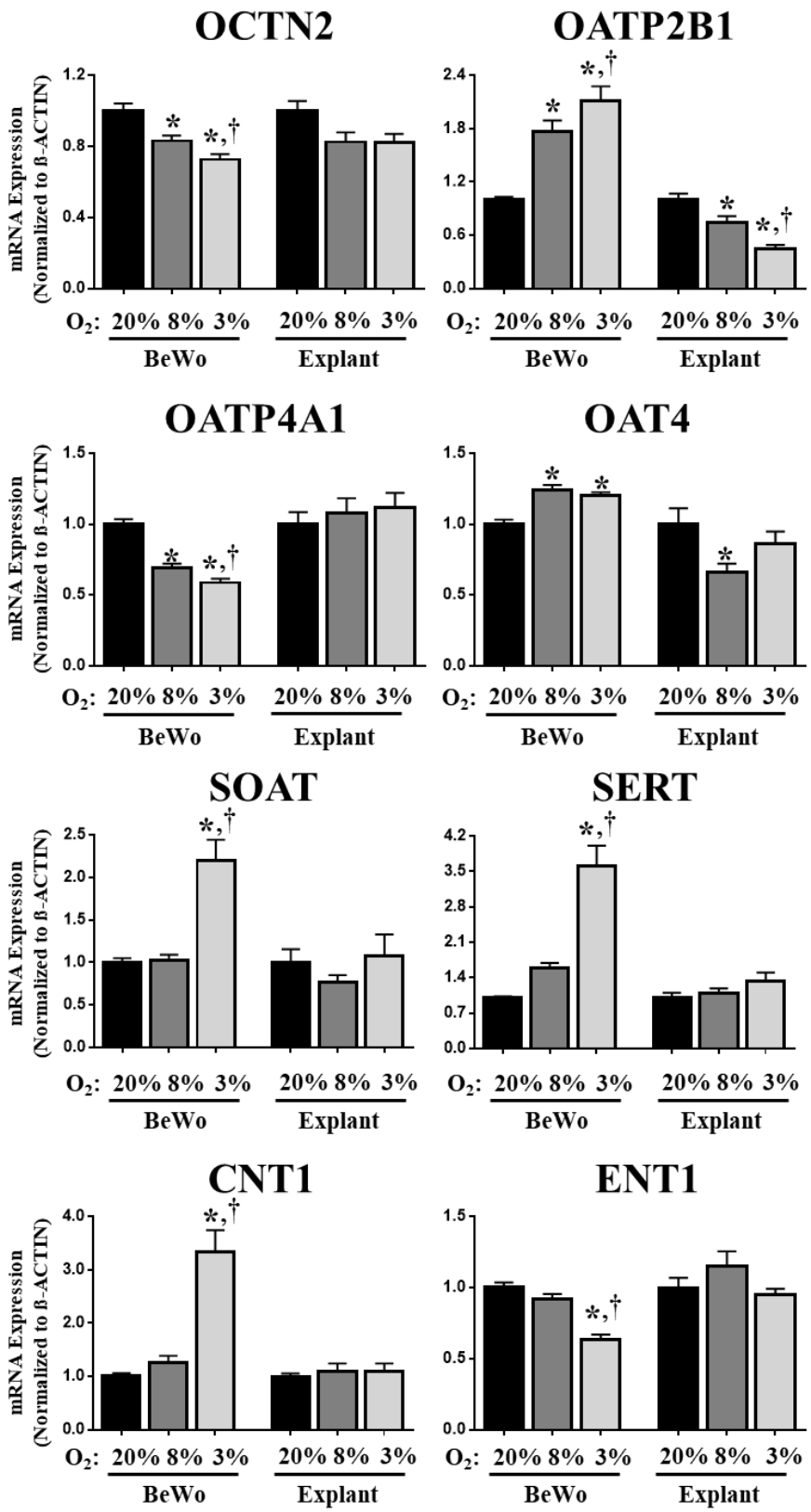
OCTN2
OATP2B1
OATP4A1
OAT4
SOAT
SERT
CNT1
ENT1
mRNA Expression (Normalized to ß-ACTIN)
O2: 20% 8% 3% 20% 8% 3%
BeWo
Explant
*
*,†

Fig 2.2. mRNA expression of uptake transporters in BeWo cells and placental explants under low oxygen. BeWo cells were exposed to a range of oxygen concentrations for 24 h. Placental explants were exposed to a range of oxygen concentrations for 24 h on the 5th day of culture. Quantitative analysis of mRNA expression was performed by qPCR and normalized to ß-Actin. BeWo cell data are presented as mean ± SE of a single representative run with at least three replicates (n=3). Placental explant data are presented as the mean of 3-6 placentas (4-5 samples from each placenta per treatment) ± SE. * $p \leq 0.05$ compared with cells or explants treated with 20% O_2. † $p \leq 0.05$ compared with cells or explants treated with 8% O_2.

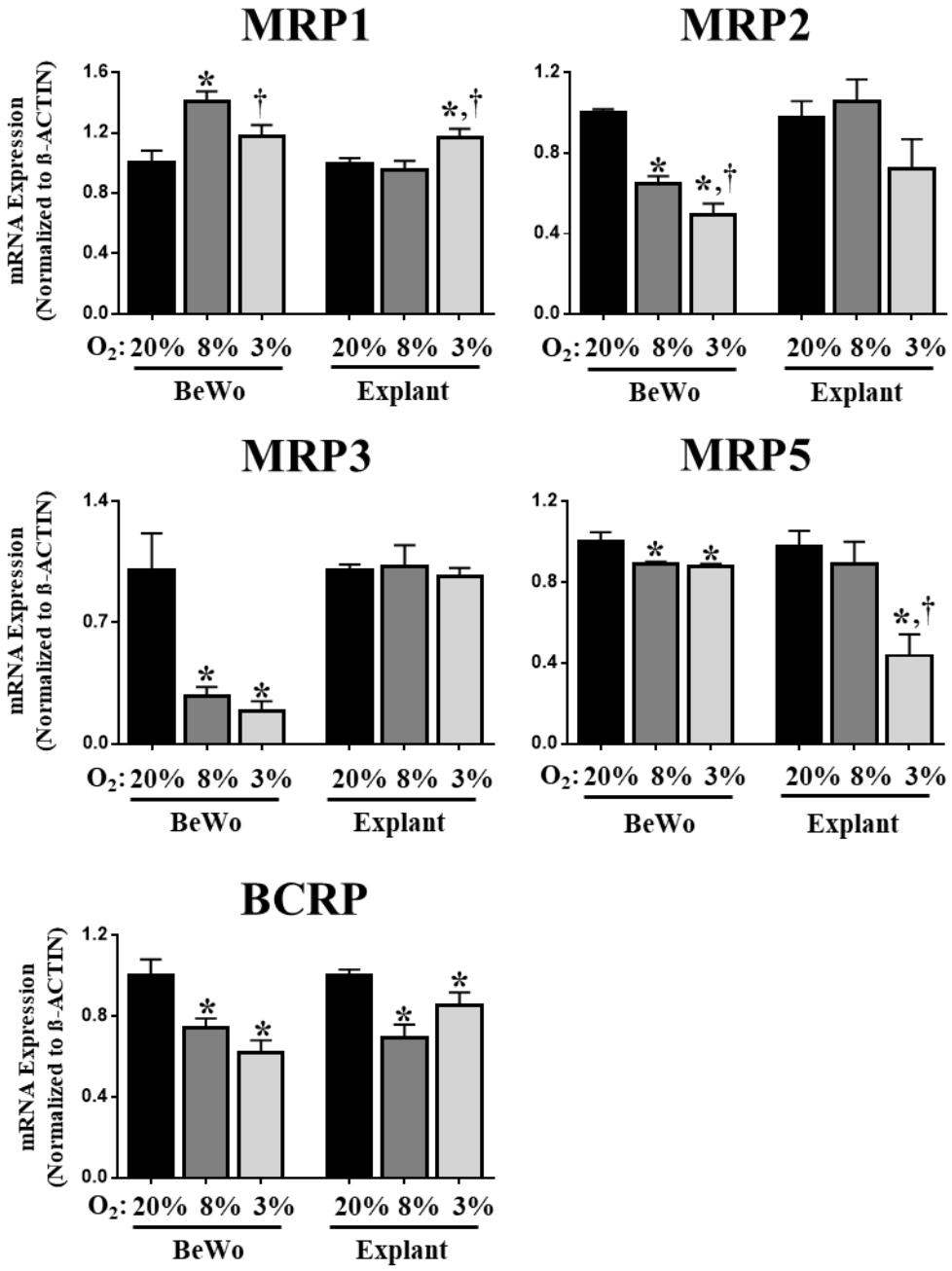
MRP1
MRP2
MRP3
MRP5
BCRP
mRNA Expression
(Normalized to ß-ACTIN)
O2: 20% 8% 3% 20% 8% 3%
BeWo
Explant

Fig 2.3. mRNA expression of efflux transporters in BeWo cells under low oxygen.

BeWo cells were exposed to a range of oxygen concentrations for 24 h. Placental explants were exposed to a range of oxygen concentrations for 24 h on the 5th day of culture. Quantitative analysis of mRNA expression was performed by qPCR and normalized to ß-Actin. BeWo cell data are presented as mean ± SE of a single representative run with at least three replicates (n=3). Placental explant data are presented as the mean of 3-6 placentas (4-5 samples from each placenta per treatment) ± SE. * $p \leq 0.05$ compared with cells or explants treated with 20% O_2. † $p \leq 0.05$ compared with cells or explants treated with 8% O_2.

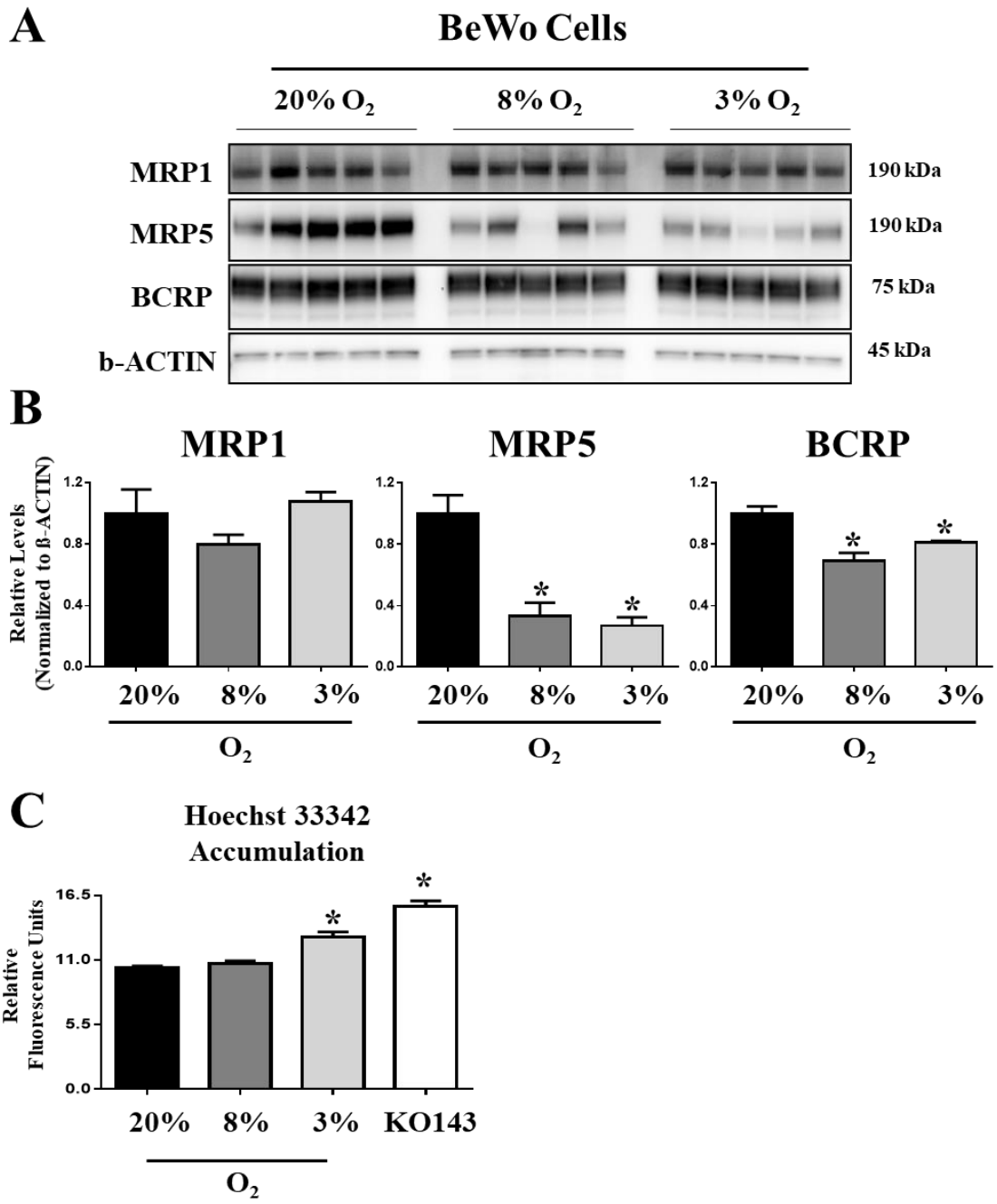
A
BeWo Cells
20% O2
8% O2
3% O2
MRP1
MRP5
BCRP
b-ACTIN
190 kDa
190 kDa
75 kDa
45 kDa
B
MRP1
MRP5
BCRP
Relative Levels
(Normalized to ß-ACTIN)
1.2
0.8
0.4
0.0
20%
8%
3%
O2
C
Hoechst 33342
Accumulation
Relative
Fluorescence Units
16.5
11.0
5.5
0.0
KO143

Fig 2.4. Protein levels of efflux transporters in BeWo cells under low oxygen. BeWo cells were exposed to a range of oxygen concentrations for 18h. (A) Representative Western blots exhibit changes in transporter protein levels. ß-Actin was used as a loading reference. (B) Raw densitometry of transporter protein levels. (C) BCRP function was measured by examining the cellular retention of a fluorescent BCRP substrate, Hoechst 33342 (3 µM), in the presence and absence of a BCRP-specific inhibitor (1 µM KO143). A Cellometer Vision automated cell counter was used to quantify intracellular fluorescence. Fluorescence intensity was normalized to cell size. Data are presented as a mean ± SE of a representative single run with at least three replicates (n=3). * $p \leq 0.05$ compared with cells treated with 20% O2.

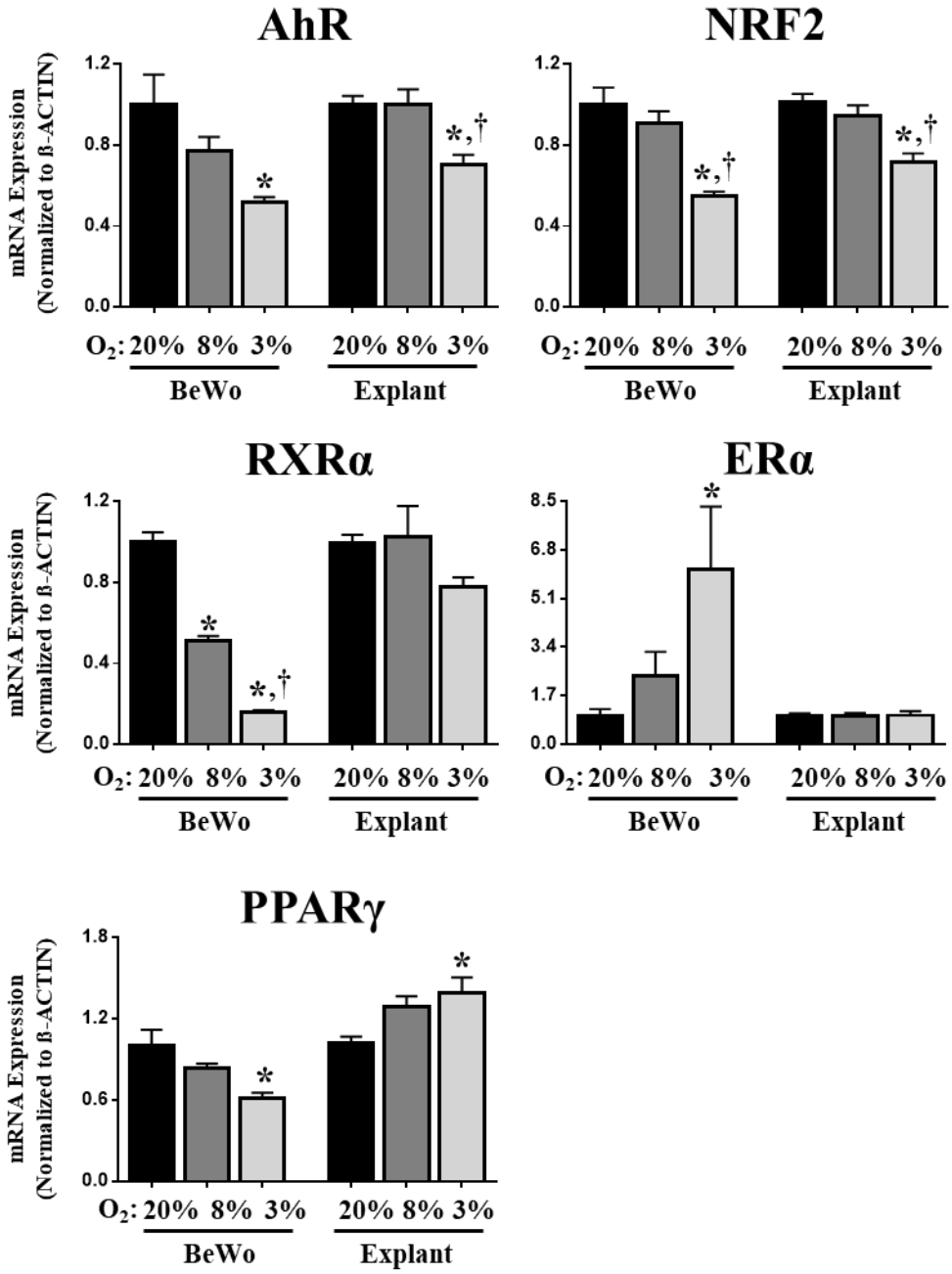

Fig 2.5. mRNA expression of transcription factors in BeWo cells under low oxygen.

Five transcription factors were selected based on their known ability to regulate transporter expression. BeWo cells were exposed to a range of oxygen concentrations for 24 h. Placental explants were exposed to a range of oxygen concentrations for 24 h on the 5th day of culture. mRNA expression of transcription factors was assessed by qPCR. BeWo cell data are presented as mean ±

SE of a single representative run with at least three replicates (n=3). Placental explant data are presented as the mean of 3-6 placentas (4-5 samples from each placenta per treatment) ± SE. * $p \leq 0.05$ compared with cells or explants treated with 20% O_2. † $p \leq 0.05$ compared with cells or explants treated with 8% O_2.

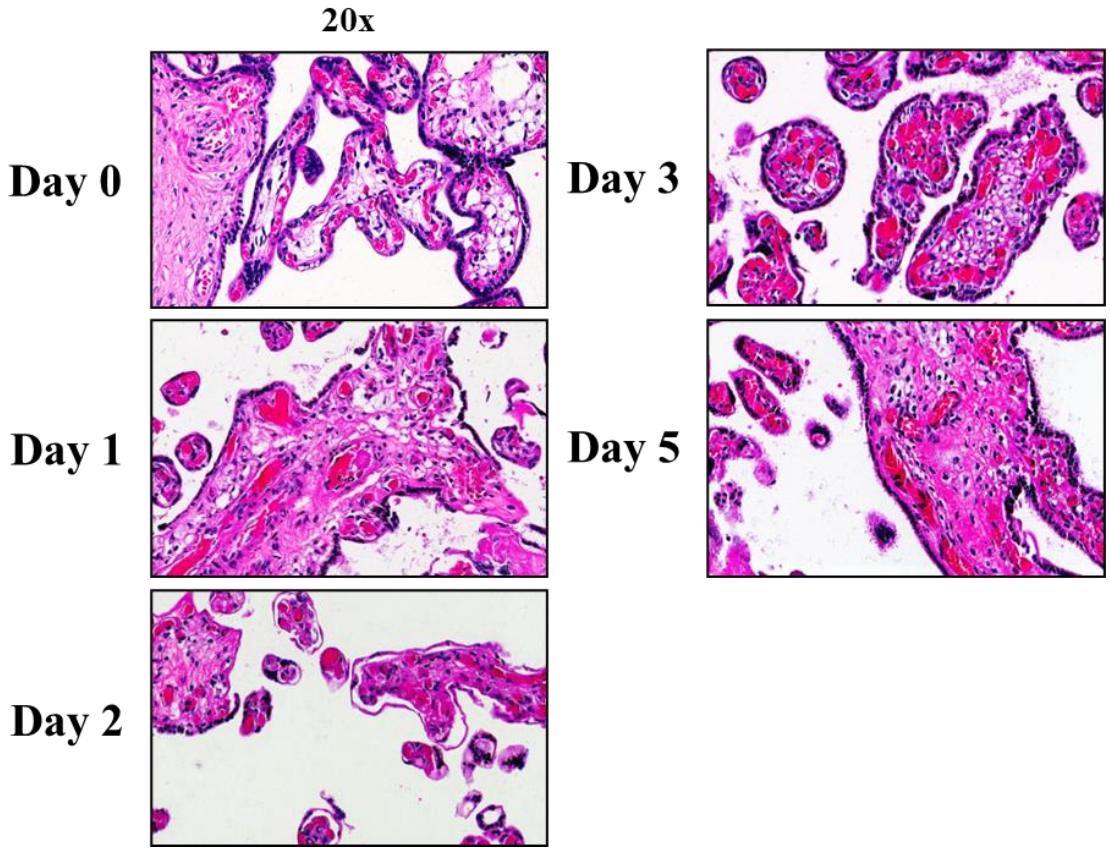

Supplemental Fig 2.1. Characterization of trophoblast turnover in placental explants. Explants undergo degeneration (Day 2) and regeneration (Day 5) of the syncytiotrophoblast cell layer. The degree of syncytiotrophoblast regeneration was determined using histological analysis prior to initiation of treatments with low oxygen concentrations.

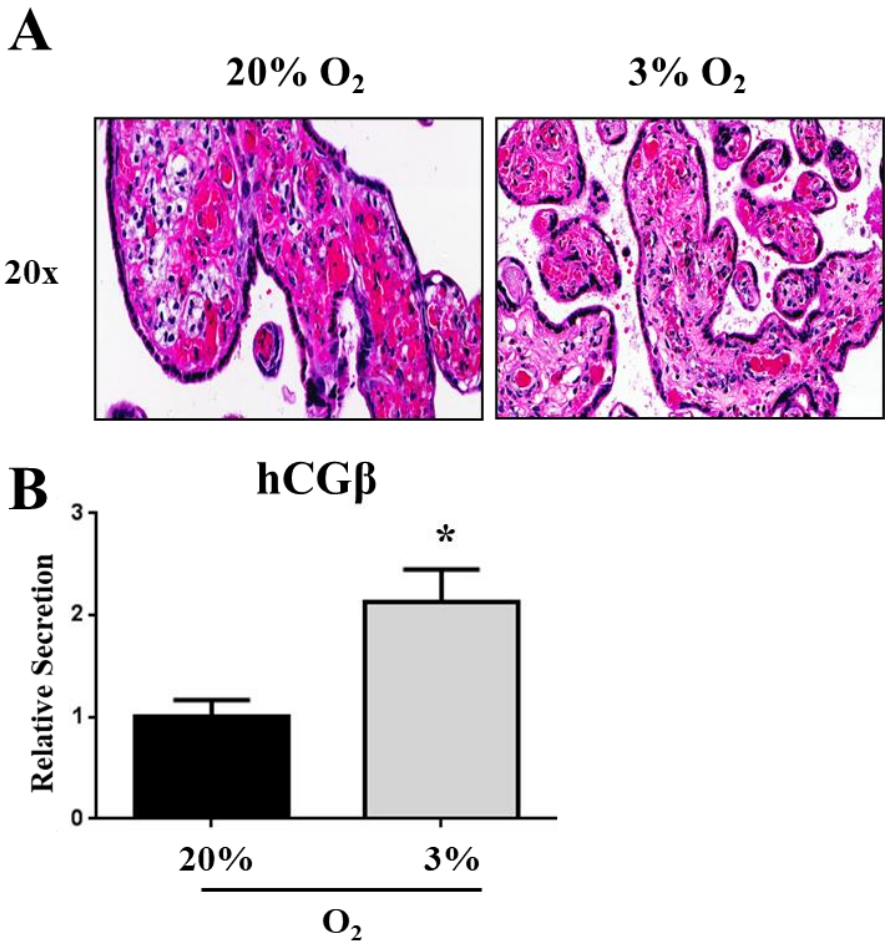

Supplemental Fig 2.2. Placental explant model viability under hypoxia. Healthy human term placentas were processed within two hours of delivery. Placental explants were cultured for 5 days to allow for shedding and syncytialization prior to a 24h treatment with 3% O_2 beginning on the 5th day. (A) Tissue histology was assessed using hematoxylin and eosin stained-slides following a 3% and 20% O_2 treatment for 24h (on Day 6). (B) Viability of placental explants under low oxygen concentration was determined through examination of hCG secretion into the media. Data are presented as the mean of 6 placentas (4-5 samples from each placenta) ± SE. * $p \leq 0.05$ compared with placental explants treated with 20% O2.

CHAPTER 3: NOVEL REGULATION OF HUMAN PLACENTAL CELL SYNCYTIALIZATION BY CYCLIC NUCLEOTIDE-MRP TRANSPORTER INTERACTIONS

Ludwik Gorczyca[a,b], Bingbing Wang[c], Todd Rosen[c], Lauren M. Aleksunes[a,d,e]

Affiliations:

[a] Rutgers University, Ernest Mario School of Pharmacy, Department of Pharmacology and Toxicology, 170 Frelinghuysen Road, Piscataway, NJ 08854, USA

[b] Rutgers University, Joint Graduate Program in Toxicology, 170 Frelinghuysen Road, Piscataway, NJ 08854, USA

[c] Division of Maternal-Fetal Medicine, Department of Obstetrics, Gynecology and Reproductive Sciences, Rutgers Robert Wood Johnson Medical School, New Brunswick, NJ, 08901, USA.

[d] Rutgers Center for Lipid Research, New Jersey Institute for Food, Nutrition, and Health, Rutgers University, New Brunswick, New Jersey 08901

[e] Environmental and Occupational Health Sciences Institute, 170 Frelinghuysen Rd, Piscataway, NJ 08854, USA

3.1 Abstract

Syncytiotrophoblasts arise from the fusion of cytotrophoblasts, a process regulated by cyclic nucleotide signaling. Syncytiotrophoblasts express transporters, including the multidrug resistance-associated proteins (MRP) 1, 3, and 5, which regulate the intracellular concentration of cyclic nucleotides through active efflux. Here, we sought to assess the ability of MRP transporters to regulate intracellular concentration of cyclic adenosine monophosphate (cAMP) and in turn cytotrophoblast fusion. Placental explants obtained from healthy, term pregnancies were treated with vehicle (DMSO) or the MRP inhibitor MK-571 (25 µM) for 24 hr. Human BeWo b30 trophoblasts were treated with vehicle (DMSO), MK-571 (25 µM), 8-Bromo-cAMP (100 µM), forskolin (10, 25 µM), IBMX (200 µM), H89 (5µM) or their combination for up to 72 hr. Markers of trophoblast cell fusion (*GCM1*; *syncytin 2*) and hormone secretion (*hCGα* and *hCGß*) were quantified by qPCR. Stable BeWo b30 cell lines with reduced expression of MRP5 were generated using targeted shRNAs. Changes in cell size and expression of the tight junction protein E-cadherin were quantified using immunofluorescence. Treatment of trophoblast cells with MK-571 increased intracellular concentrations of cAMP and cGMP by 15- and 19-fold, respectively. Moreover, MK-571 treatment up-regulated cell fusion and hormone secretion markers (*GCM1*, *hCGα*, *hCGß*, *syncytin 2*) by 20-200%. Similarly, MRP inhibition with MK-571 further enhanced syncytialization and hormone markers following 1) stimulation with the permeable cAMP analog 8-Bromo-cAMP (2- to 6-fold), 2) activation of cAMP synthesis with forskolin (20-160%), or 3) inhibition of cAMP/cGMP breakdown by IBMX (50-130%). In response to treatment with forskolin for 18 hr, induction of *syncytin 2, hCGα,* and *hCGß* mRNA expression was higher in MRP5 knockdown (KD) cells compared to control cells. Furthermore, MRP5 KD cells were 35% larger in size due to greater numbers of multinucleated cells and exhibited decreased staining of E-cadherin, pointing to enhanced syncytialization. In conclusion, MRP transporters participate in trophoblast cell fusion, which likely represents a novel mechanism regulating placentation.

Keywords: Syncytialization; Placenta; Cyclic Nucleotides; Transporters; Multidrug Resistance-Associated Proteins

Highlights:

- Pharmacological modulators of cAMP signaling stimulate syncytialization in placental cells
- Inhibition of MRP transport induces markers of syncytialization in placental cells and explants
- Protein kinase A mediates enhanced syncytialization in placental cells following MRP inhibitor treatment
- Genetic knockdown of MRP5 increases intracellular concentration of cAMP and induces hormone secretion by placental cells
- MRP5 KD stimulates syncytialization and increases the number of multinucleated cells in response to modulators of cAMP signaling
- MRP transporters participate in trophoblast cell fusion

3.2 Introduction

The establishment and maintenance of a healthy pregnancy requires proper placental development. Serving as an interface between the fetal and maternal circulations, the placenta allows for the exchange of nutrients, wastes and gases and, in turn, supports normal fetal growth. One of the major processes responsible for placental development is syncytialization whereby giant multinucleated syncytiotrophoblasts arise from the fusion of mononuclear progenitor placental cytotrophoblasts (Chang et al. 2018a; Midgley et al. 1963). Syncytiotrophoblasts line the outside surface of chorionic villi and establish the maternal-fetal circulatory interface within the placenta (Figure 3.1). Once formed, syncytiotrophoblasts also facilitate a variety of critical functions during pregnancy. These include xenobiotic metabolism, hormone secretion (estrogen, human placental lactogen (hPL), human chorionic gonadotropin (hCG) as well as formation of the placental barrier through the expression of xenobiotic and endobiotic transporters (Costa 2016; Syme et al. 2004).

One of the major molecular mediators regulating cell fusion is cyclic adenosine monophosphate (cAMP). Signal transduction is stimulated when hCG binds to the G-protein coupled luteinizing hormone receptor on the surface of trophoblasts. In response, adenylyl cyclase is activated and converts ATP to cAMP thereby increasing the intracellular concentrations of the secondary messenger. cAMP binds to the regulatory subunits of protein kinase A (PKA) and causes conformational changes that enable the release and activation of the catalytic subunits of PKA. Catalytically active PKA dimer then phosphorylates the cAMP response element binding protein (CREB) and enables its interaction with other transcriptional activators such as P300 and CREB binding protein (CBP) (Figure 3.2). The CREB/P300/CBP complex enhances the expression of fusogenic genes such as Glial Cell Missing 1 (GCM1), Syncytin 1, and Syncytin 2 (Gerbaud et al. 2015a). The fusion of human BeWo choriocarcinoma trophoblasts, an *in vitro* placental cell fusion model, has been shown to be stimulated with pharmacological agents that modulate intracellular levels of cAMP, namely IBMX, a phosphodiesterase inhibitor, 8-bromo-cAMP, a cell permeable

chemical analog of cAMP, and forskolin, an activator of the adenylyl cyclase enzyme (Delidaki et al. 2011; Dubey et al. 2018; Gerbaud et al. 2015b; Knerr et al. 2005; Ogura et al. 2000; Omata et al. 2013b; Wice et al. 1990).

The aberrant differentiation and fusion of cytotrophoblasts is associated with gestational disorders such as preeclampsia and intrauterine growth restriction (IUGR). Preeclampsia, affecting 2-8% of pregnant women, is characterized by proteinuria (≥ 300 mg/24 h) and hypertension (≥ 140/90 mmHg). This pathology is through to arise from the incomplete remodeling of the maternal spiral arteries by invading trophoblast cells. The resulting hypoperfusion of the placenta leads to decreased oxygen and nutrient delivery and ultimately fetal growth restriction. Evidence suggests that abnormal syncytialization may contribute to the pathogenesis of this disorder. For example, primary villous cytotrophoblasts obtained from patients with preeclampsia or associated disorders such as IUGR exhibited significantly reduced mRNA and protein expression of syncytialization markers (Syncytin-1, -2), a decreased ability to syncytialize *in vitro*, as well as altered hormone secretion (hCG, hPL) (Chen et al. 2006; Knerr et al. 2002; Langbein et al. 2008; Newhouse et al. 2007; Pijnenborg et al. 1996; Ruebner et al. 2010). More work is urgently needed to further characterize placental cAMP signaling to help elucidate the potential link between altered syncytialization and adverse placental/neonatal outcomes.

The multidrug resistance-associated proteins (MRPs/*ABCC*) are a subfamily of ATP-binding cassette efflux transporters highly expressed in the placenta. MRP1 (*ABCC1*), MRP2 (*ABCC2*), and MRP3 (*ABCC3*) are primarily localized on the apical (maternal-facing) membrane of syncytiotrophoblasts with some basolateral (fetal-facing) membrane expression (Meyer zu Schwabedissen et al. 2005b; Nagashige et al. 2003; St-Pierre et al. 2000). Meanwhile, MRP5 (ABCC5) is solely expressed on the basolateral membrane of syncytiotrophoblasts (Meyer Zu Schwabedissen et al. 2005a; Rubinchik-Stern et al. 2012). MRP proteins transport a wide variety

of substrates including nucleoside-derived antiviral drugs as well as endogenous molecules such as prostaglandins, glutathione, bile salt, steroids and cyclic nucleotides to name a few (Russel et al. 2008; Sampath et al. 2002). In particular, MRP5, can efflux cyclic AMP and GMP with K_m values of 379 and 2.1 μM, respectively (Biondi et al. 2010; Jedlitschky et al. 2000; Meyer Zu Schwabedissen et al. 2005a; Nagashige et al. 2003). MRP5-mediated export of cAMP and cGMP may play a role in regulating signal transduction by controlling the intracellular concentration of cyclic nucleotides. While MRP function in controlling cellular efflux of cyclic nucleotides has been established, there are currently no data examining the endogenous regulatory role of these transporters in placental cell fusion. Understanding the interplay of cyclic nucleotides, efflux transporters, and syncytialization may offer a novel mechanism explaining the pathogenesis of gestational disorders and xenobiotic toxicities associated with abnormal cytotrophoblast differentiation and placental development. Therefore, the purpose of this study was to characterize the ability of MRP transporters, specifically MRP5, to regulate intracellular cyclic nucleotide accumulation and in turn trophoblast cell fusion.

3.3 Materials and Methods

Chemicals

All chemicals were purchased from Sigma-Aldrich (St. Louis, MO), unless stated otherwise.

Patient Selection

Healthy placentas were obtained from women aged 18-40 years following term (>36 weeks) delivery by scheduled Cesarean section. Exclusion criteria included medical conditions induced by pregnancy (i.e. gestational diabetes, hypertension, preeclampsia), maternal smoking, alcohol, or drug abuse, medication use, chronic medical conditions (i.e., autoimmune disorders, hypertension, diabetes), known fetal chromosomal abnormalities, and maternal infection (Memon et al. 2014; Wang et al. 2018a). The study was approved by the Institutional Review Board of Robert Wood Johnson Medical School (Protocol #E12-024; 20150001445).

Placental Explants

Placentas were processed within 2 h of delivery. After removal of the maternal decidua and chorionic plate, sections of villous tissue were extracted and washed three times in PBS buffer to remove maternal blood. Villous tissue was further sectioned into 8 mm^3 pieces and cultured in DMEM: F12 media with 10% FBS (Atlanta Biologicals) and 1% penicillin-streptomycin (Life Technologies). Explants were cultured for 3 days to allow for degeneration and regeneration of the syncytium (Siman et al. 2001). Media was changed every 24 h. On day 3, placental explants were treated with 25 μM MK-571, a pharmacological inhibitor of MRP function, for 24 h. After 24 h, explants were washed with PBS and frozen in liquid nitrogen.

Cell Culture

Human placental BeWo b30 choriocarcinoma cells were provided by Dr. Nicholas Illsley (Hackensack University Medical Center) and maintained in DMEM:F12 media (Life Technologies,

Carlsbad, CA) supplemented with 10% fetal bovine serum (Atlantic Biologicals, Fredrick, MD) and 1% penicillin-streptomycin (Life Technologies) (Vardhana et al. 2002). Cells were grown to 50-70% confluence in 12-well cell culture plates prior to initiating treatments with 25 µM MK-571, a pharmacological inhibitor of MRP function, 200 µM IBMX (Cayman Chemical, Ann Arbor, MI), a phosphodiesterase inhibitor, 10 µM or 25 µM forskolin, an activator of adenylyl cyclase, 100 µM 8-bromo-cyclic adenosine monophosphate (8-bromo-cAMP), 5 µM H89 dihydrochloride, a PKA inhibitor, or their combination for up to 72 h. All chemicals were dissolved in DMSO, the final concentration of which did not exceed 0.1% (v/v) in culture media.

Generation of Knockdown Cell Lines

Control (sc-108080, Santa Cruz Biotechnology, Santa Cruz, CA) and transporter-specific (ABCC5: sc-35965-V, Santa Cruz Biotechnology) shRNA lentiviral particles were used to generate stable BeWo b30 knockdown cell lines. Cells were seeded on a 96-well plate and allowed to reach 70% confluence prior to the initiation of transfection protocol. The transfection media (DMEM:F12) contained control and transporter-specific shRNA lentiviral particles (2 viral particles/cell; 60,000 particles/well) as well as 5 µg/ml Polybrene (Santa Cruz Biotechnology), as per manufacturer's protocol. The cells were cultured in the transfection media for 24 h. Transfected cells were washed with PBS and sub-cultured with fresh medium, absent of lentiviral particles and polybrene, for 72 h. Stable clones were selected and maintained using growth media supplemented with 5 µg/ml puromycin (Santa Cruz Biotechnology).

RNA Isolation and Analysis Using Quantitative Polymerase Chain Reaction (qPCR)

BeWo b30 cells were collected and lysed using 500 µl of the RNAzol reagent. Nuclease-free water (200 µl) was added to the cell lysates to precipitate DNA, proteins, and lipids. Samples were centrifuged for 15 min at 12,000 x g to obtain the aqueous phase containing RNA. To precipitate the RNA, the aqueous phase (500 µl) was transferred to new Eppendorf tubes containing 500 µl of

100% isopropanol. Samples were vortexed and centrifuged for 15 min at 12,000 x g to obtain an RNA pellet. The resulting pellet was washed twice with 75% ethanol (200 µl) and resuspended with 50 µl of nuclease-free water. Alternatively, placental explant tissue (30 mg) was lysed with 700 µl of Buffer RLT (1% β-mercaptoethanol). A 5-mm stainless steel bead was added to a 2-ml round bottom polypropylene tube containing the explant tissue and lysis buffer. Samples were homogenized in solution for 5 min at 50 Hz in the TissueLyser II (Qiagen). Total RNA from placental explants was isolated using the RNeasy mini kit (Qiagen). The integrity and purity of isolated RNA was confirmed by measuring absorbance at 260 and 280 nm with the NanoDrop 2000 spectrophotometer (Thermo Scientific, Wilmington, DE) and examining the A260/A280 ratios. cDNA was generated from total RNA (1000 ng) using the High-Capacity cDNA Reverse Transcription Kit (Life Technologies) and a MultiGene OptiMax Thermal Cycler (Labnet International Inc., Edison, NJ). Cycle conditions were as follows: 10 min at 25°C, 120 min at 37°C, 5 min at 85°C, and held at 4°C. mRNA expression was determined by qPCR using specific forward and reverse primers (Table 1) (Integrated DNA Technologies, Inc., Coralville, IA) and SYBR Green dye (Life Technologies). qPCR was performed using the ViiA7 Real-Time PCR machine (Life Technologies). CT values were converted to delta delta CT values with Ribosomal protein l13a (RPL13a) serving as a reference gene for normalization.

Western Blot

Following transfection and generation of stable clones, BeWo b30 control and knockdown cells were lysed using lysis buffer containing 20 mM Tris-HCl, 150 mM NaCl, 5 mM EDTA, 1% Triton X-100, and 2% protease inhibitor. The bicinchoninic acid assay was utilized to quantify protein concentrations within cell lysates. Total protein (50 µg) was loaded onto a SDS-polyacrylamide 4-12% Bis-Tris gel (Life Technologies) and resolved by electrophoresis. The Biorad Criterion Blotter (Biorad, Hercules, CA) was used to transfer proteins onto polyvinylidene fluoride membranes overnight. Following transfer, membranes were blocked in 5% non-fat milk in 0.5% Tween 20-

PBS for 2 h. Membranes were then incubated with the MRP5 (MA1-35683, 1:1000, ThermoFisher) and ß-Actin (ab8227, 1:2000, Abcam) primary antibodies overnight at 4ºC. All primary antibodies were diluted in 2% non-fat milk in 0.5% Tween 20-PBS. Species-appropriate secondary antibodies (Sigma-Aldrich) were used to probe the primary antibodies. Chemiluminescent detection of protein signal was performed using SuperSignal West Dura blotting reagents (Pierce Biotechnology) and Fluorchem Imager (ProteinSimple, Santa Clara, CA).

Calcein-AM Accumulation Assay

Intracellular accumulation of the MRP-specific fluorescent substrate, calcein-AM, was used to assess MRP loss of function in BeWo b30 cells as previously described by our laboratory (Bircsak et al. 2013b). BeWo b30 control cells and MRP5 KD cells were grown to 70% confluence in 96-well plates. *Uptake Phase*. Control cells were incubated with media containing calcein-AM (1 µM) with or without the MRP pharmacological inhibitor, MK-571 (25 µM). In parallel, MRP KD cells incubated with media containing just Calcein-AM (1 µM). Cells were placed in a 37ºC cell culture incubator at 5% CO_2 for 30 min to allow for uptake of the fluorescent substrate. *Efflux Phase*. Substrate-containing media was replaced with substrate-free media with or without MK-571 and incubated for an additional 1 h at 37ºC and 5% CO_2. This allows for MRP-mediated efflux of calcein-AM. Following incubation, cells were washed with cold phosphate-buffered saline (PBS) (200 µl). Intracellular accumulation of calcein-AM was assessed using the Cellometer Vision cell counter (Nexcelom Bioscience, Lawrence, MA). Resuspended cells (20 µl) were added to a cell counting slide and analyzed for fluorescence intensity using a VB-535-402 filter (excitation/emission: 475/535 nm). The measured fluorescence intensity was normalized to cell size for each cell.

Intracellular Concentration of Cyclic Nucleotides

BeWo b30 cells were grown to 70% confluence on 12-well culture plates and treated with DMSO (0.1%) or MK-571 (25 µM) for 1 h at 37°C. Following a wash with 2 ml PBS, cells were trypsinized (500µl) and placed in an Eppendorf tube containing equal amount of cell culture media (500 µl). Cells were centrifuged for 3 min at 3000 rpm (1,811 x g) to form pellets. Cell pellets were washed with 1 ml of PBS and centrifuged once more. Washed cell pellets were re-suspended with 200 µl of 0.1M HCl and incubated for 20 min at room temperature. Concentrations of cAMP and cGMP were determined using cyclic nucleotide-specific enzyme-linked immunosorbent assay kits (ELISA, Cayman Chemical). Data were normalized to protein concentration as determined by the bicinchoninic acid protein assay kit (Thermo Fisher).

Hormone Secretion

BeWo b30 control and knockdown cells were grown to 70% confluence on 12-well culture plates. Media was changed and collected following a 24 h incubation period. Hormone secretion into the media was determined using human chorionic gonadotropin ß (DY9034-05, R and D Systems, Minneapolis, MN) and progesterone (582601, Cayman Chemical) ELISA kits, according to manufacturer's protocols. Hormone secretion was normalized to protein concentration.

Immunofluorescence

BeWo b30 control and knockdown cells were seeded on glass chamber slides (Thermo Fisher) at a concentration of 200,000 cells/well. Cells were placed in a 37ºC cell culture incubator for 24 h to allow for adherence. On day two, treatments with DMSO (0.1%), MK-571 (25 µM), IBMX (200 µM) or forskolin (10 µM) for 72 h were initiated. Treatment media was changed every 24 h. After 72 h, cells were washed with PBS (300 µl/well) and subsequently fixed with 4% paraformaldehyde (300 µl/well) for 5 min at room temperature. Slides were then washed twice with PBS and once with 0.1% Triton X in PBS for 5 minutes each at room temperature. Non-specific binding sites were blocked by incubating fixed cells with 5% normal goat serum (Thermo Fisher) in 0.1% Triton

X in PBS for 1 h. A mouse monoclonal antibody against human E-cadherin (13-1700, Thermo Fisher) was added at 1:100 in 5% goat serum in 0.1% Triton X in PBS and slides were incubated overnight at 4°C. Slides were then rinsed three times with 0.1% Triton X in PBS and incubated with goat anti-mouse immunoglobulin G (IgG)-Alexa Fluor 488 conjugate (A11029, Life Technologies) at 1:100 in 5% goat serum in 0.1% Triton X in PBS for 1 h at room temperature. Slides were then washed three times with PBS for 5 min and cured overnight with Prolong Gold Antifade Mountant with DAPI (P36941, Life Technologies). Digital images for signal quantification were captured with a Zeiss Axio Observer D1 fluorescent microscope (Carl Zeiss, Gottingen, Germany) using an emission of 430 nm and 520 nm for DAPI and E-cadherin (GFP), respectively. Representative images shown were taken with a Leica SP5 confocal microscope (Leica Microsystems, Wetzlar, Germany). All images obtained contain identical laser power, gain, and offset settings.

Cell Size Analysis

Cell size was quantified using ImageJ software. All digital images were quantified using the same protocol described below. Four digital images (20X magnification), each depicting various areas of a well, were taken and quantified for each treatment group. The images were converted to greyscale. Single cell nuclei were identified and outlined using the Isodata threshold method. With all the nuclei outlined, the size (in pixels squared) was analyzed.

Signal Quantification

Signal quantification of fluorescence intensity was performed using ImageJ software. All digital images were quantified using the same protocol described below. Four digital images (20X magnification), each depicting various areas of a well, were taken and quantified for each treatment group. Quantification is based on the number of pixels showing antibody expression compared to the total number of pixels in each converted grayscale image. The merged digital image, containing

both DAPI and E-cadherin staining, was converted to three separate grayscale images with each representing a red, green (E-cadherin), and blue (DAPI) channel. Single cell nuclei were identified and outlined in the blue channel using the Isodata threshold method. To normalize the amount of E-cadherin signal with respect to each cell, all nuclei on the blue channel were selected and the mean gray value was analyzed in the green channel.

Multinucleatation Analysis

BeWo b30 control and knockdown cells were plated on a 96-well Corning black/clear plate coated with Poly-D-Lysine (62406-036, VWR, Bridgeport, NJ) at a concentration of 4,000 cells/well. Cells were placed in a 37ºC cell culture incubator for 24 h to allow for adherence. On day two, treatments with DMSO (0.1% v/v), MK-571 (25 μM), or forskolin (2 μM) in media containing 100nM Hoechst 33342 were initiated for up to 60 h. Images were taken every 12 h using the Cytation 5 Cell Imaging Multi-Mode Reader (BioTek) with the DAPI filter cube (excitation/emission: 377/447 nm). Cells in the obtained images were counted and their average size quantified using the Gen5 software (BioTek). Multinucleated cells were characterized as cells having an average cell size that was 2 standard deviations above the average cell size of DMSO-treated BeWo b30 control cells. Percent multinucleated cells was achieved by dividing the number of multinucleated cells by the total number of cells per well.

Statistical Analysis

Data are presented as mean ± SE and analyzed using Graphpad Prism 6.0 (Graphpad Software, Inc., La Jolla, CA). According to the number of variables and comparisons, a one-way ANOVA followed by a Newman-Keuls multiple comparison post hoc test or an unpaired Student's t-test were used to assess statistical significance ($p<0.05$).

3.4 Results

Pharmacological inhibition of MRP function induces syncytialization markers in human placental explants and BeWo trophoblast cells.

In order to assess the endogenous role of MRP efflux drug transporters in mediating placental cell fusion, healthy, term human placental explants were exposed to MK-571, a pharmacological inhibitor of MRP function. Once placental explants are placed into culture, they undergo degeneration and subsequent *de novo* regeneration of the syncytiotrophoblast cell layer on days 2-5 following collection (Siman et al. 2001). In order to examine the ability of MRP inhibition to further induce the re-syncytialization process, treatments were initiated on day 3 of culture. Classical syncytialization markers that regulate placental cell fusion include Glial cell missing 1a (GCM1), Syncytin-1/2, hCGα, and hCGß. Exposure of human placental explants to 25 µM MK-571 for 24 h induced the mRNA expression of GCM1, Syncytin-1, Syncytin-2, hCGα, and hCGß between 20-50% (Figure 3.3A) suggesting a potential role for MRPs in regulating syncytialization.

The BeWo choriocarcinoma cell line, a widely used *in vitro* placental model, recapitulates features of 1st trimester trophoblasts such as hormone secretion, syncytialization, and high transporter expression (Avery et al. 2003; Correia Carreira et al. 2011; Evseenko et al. 2006; Magnarin et al. 2008; Milane et al. 2009; Mitra et al. 2010; Pattillo et al. 1971; Poulsen et al. 2009; Xiao et al. 2015a). This model was employed in subsequent studies to further test the mechanism by which MK-571 induced syncytialization in placental explants. Within 1 h treatment of BeWo b30 cells with 25 µM MK-571, intracellular concentrations of cAMP were increased 5.5-fold higher (Figure 3.4A). Similar to explants, BeWo b30 cells treated with 25 µM MK-571 for 18 h resulted in an up-regulation of GCM1, hCGα, and hCGß mRNA expression by 50-100% (Figure 3.4B). Likewise, these data positively correlate with a 16% higher number of multinucleated cells following a 24 h exposure to 25 µM MK-571, as compared to control (Figure 3.4C).

Modulation of cAMP signaling enhances MRP-dependent induction of syncytialization markers in human trophoblast cells.

BeWo b30 cells were treated with known modulators of intracellular cAMP in the presence or absence of 25 µM MK-571 to determine whether MRP inhibition could alter known responses to cAMP activators including a phosphodiesterase inhibitor (200 µM IBMX) which prevents cAMP breakdown, an activator of adenylate cyclase (25 µM forskolin), and a membrane permeable chemical analog of cAMP (100 µM 8-bromo-cAMP). As expected, all modulators of cAMP levels induced mRNA expression of syncytialization markers by up to ~13-fold (Figure 3.5A). Interestingly, MK-571 further up-regulated the IBMX-, forskolin-, and 8-Bromo-cAMP-mediated induction of GCM1 by up to ~10-fold (Figure 3.5A).

Inhibition of PKA prevents MRP-dependent induction of syncytialization markers in human trophoblast cells.

To demonstrate that cAMP-PKA signaling was mediating the induction of syncytialization genes by MK-571, BeWo b30 cells were treated with a PKA inhibitor (5 µM H89) along with MK-571. The PKA inhibitor, H89, significantly reduced the MK-571-mediated induction of GCM1, hCGα, and hCGß by up to 65% (Figure 3.6) confirming that the observed data are due to changes in intracellular cAMP levels and PKA-mediated signaling.

Knockdown of the MRP5 transporter enhances fusion of human trophoblast cells.

The pharmacological inhibitor MK-571 inhibits the transport capability of multiple MRP isoforms known to be expressed in BeWo cells including MRP1-3 and 5 (Bertollotto et al. 2018; Chen et al. 2018b; Jedlitschky et al. 2000; Kucka et al. 2010; Liu et al. 2010; Myint et al. 2015; Tivnan et al. 2015). Because of the known ability of MRP5 to transport cyclic nucleotides, lentiviral-based transfections with control or MRP5-specific shRNA were performed to further examine the role of this transporter in placental cell fusion. Following transfection, the mRNA and protein expression

of MRP5 was down-regulated by ~75% and ~85%, respectively (Figure 3.7A). The impact of the shRNA knockdown on MRP5 function was analyzed using an MRP-specific fluorescent substrate, Calcein-AM (1 μM). Compared to control cells, MRP5 KD cells retained a 16% higher accumulation of Calcein-AM suggesting decreased efflux function. This was comparable to the 20% higher retention of Calcein-AM dye in control cells treated with 25 μM MK-571 inhibitor (Figure 3.7A). Likewise, further characterization revealed a 5-fold higher intracellular accumulation of cAMP in the MRP5 KD cells as compared to control cells. Retention of cAMP in MRP5 KD cells was comparable to the 6-fold higher accumulation of cAMP observed in cells treated with MK-571 (Figure 3.7B). A hallmark of syncytialized human trophoblast cells is greater secretion of hCGß and progesterone into media. Compared to control cells, MRP5 KD cells exhibited increased secretion of hCGß (3.5-fold) and progesterone (2-fold) (Figure 3.7C). The shRNA-based knockdown of MRP5 did not significantly change the mRNA expression of other MRP isoforms, including MRP1, -2, and -3 (data not shown).

Expression of syncytialization genes in control and MRP5 KD cells were also assessed in the presence and absence of cAMP modulators. As expected, all cAMP modulators including IBMX (200 μM), forskolin (10 μM), and 8-bromo-cAMP (100 μM) significantly induced the mRNA expression of GCM1, Syncytin-2, hCGα, and hCGß in control cells. Treatment of MRP5 KD cells with cAMP modulators further increased GCM1, Syncytin-2, hCGα, and hCGß mRNA expression by up to 18-fold, as compared to their treated control counterparts (Figure 3.8). Taken together, these data indicate that the genetic knockdown of the MRP5 transporter increases cellular concentrations of cAMP and primes BeWo cells for induction of syncytialization genes.

The observed genetic changes also translate to a cellular phenotype. Cell size analysis by ImageJ revealed that the MRP5 KD cells are 35% larger in size when compared to control. This was comparable to the forskolin-treated cells which were 58% larger than the control (Figure 3.9B). E-

cadherin is a tight junction protein localized to the membrane of cytotrophoblasts and known to disappear during trophoblast fusion (Coutifaris et al. 1991; Getsios et al. 2000). Accordingly, MRP5 KD cells exhibited 44% lower e-cadherin staining intensity as compared to BeWo control cells (Figure 3.9B). This is similar to the 50% reduction of e-cadherin staining observed in BeWo control cells treated with forskolin. Representative images of cells are shown (Figure 3.9C). A time course was performed to further characterize the change in percent multinucleated cells over time between control and MRP5 KD cells stimulated with 10 μM forskolin. The time course demonstrated that knockdown of the MRP5 transporter resulted in a significantly higher percentage of multinucleated cells across numerous timepoints when compared to control cells (Figure 3.9A).

3.5 Discussion

Proper placentation is reliant on continual syncytialization whereby mononuclear progenitor cells termed cytotrophoblasts fuse to form giant, multinucleated syncytiotrophoblasts. Disruption of syncytialization has been linked to the pathogenesis of gestational disorders including preeclampsia and intrauterine growth restriction (Chen et al. 2006; Knerr et al. 2002; Langbein et al. 2008; Newhouse et al. 2007; Pijnenborg et al. 1996; Ruebner et al. 2010). Recognizing the significance of this cellular event, additional research is warranted to further elucidate the underlying mechanisms governing trophoblast fusion during healthy and pathological conditions. While the role of cAMP/PKA-mediated signaling in syncytialization and MRP functionality (Evseenko et al. 2006) in BeWo cells have been established, there is currently no research examining the endogenous ability of MRPs to alter trophoblast fusion by regulating the intracellular concentration of cyclic nucleotides through active efflux. To our knowledge this is the first study to establish the capability of cyclic nucleotide-MRP transporter interactions to regulate human placental trophoblast fusion. Human BeWo b30 choriocarcinoma cells and term placental explants were employed as human placental *in vitro* models to study the relationship between MRP transporters and cellular fusion. BeWo b30 cells recapitulate the signaling of first trimester trophoblasts and are a widely used human placental *in vitro* model (Pattillo et al. 1968c). Alternatively, the human term placental explant model allows for additional translatability of data as transcriptional regulatory pathways and DNA methylation profiles mirror that of *in vivo* human placenta. Importantly, both models express MRP transporters and are known to undergo syncytialization *in vitro* (Al-Nasiry et al. 2006; Bircsak et al. 2016; Evseenko et al. 2006; Ikeda et al. 2012; Pascolo et al. 2003; Siman et al. 2001). Treatment of BeWo cells and human term placental explants with the pharmacological inhibitor of MRP function, MK-571, resulted in the significant induction of cell fusion markers (GCM1, Syncytin-1/2, hCGα/ß) in both models. Similar to previous reports, BeWo cells treated with various modulators of cAMP signaling including the phosphodiesterase inhibitor, IBMX, the adenylate cyclase activator, forskolin, and the membrane permeable chemical analog, 8-Bromo-

cAMP, exhibited enhanced syncytialization as evidenced by significantly increased mRNA expression of cell fusion markers (GCM1, Syncytin-2, hCGα/ß) (Delidaki et al. 2011; Dubey et al. 2018; Gerbaud et al. 2015b; Knerr et al. 2005; Ogura et al. 2000; Omata et al. 2013b; Wice et al. 1990). Combination treatments of intracellular cAMP modulators (IBMX, forskolin, 8-Bromo-cAMP) with MK-571 resulted in even greater induction of cell fusion markers when compared to the induction observed with cAMP modulators alone. In order to validate that the observed MK-571-mediated changes in cell fusion markers are PKA-specific, BeWo cells were exposed to a concomitant treatment of MK-571 and H89, a selective, potent, and cell permeable PKA inhibitor. As expected, the induction of cell fusion markers (GCM1, hCGα/ß) by MK-571 was significantly truncated in combination treatments with H89. Collectively, these data demonstrate the ability of MK-571 to inhibit MRP function, increase the intracellular concentration of cAMP, and in turn induce the syncytialization markers in a PKA-dependent manner.

Although the induction of cell fusion markers by MK-571 was PKA-specific, it has been shown that MK-571 targets and globally inhibits all MRP isoforms, including MRP1,-2, -3, -4, and -5 (Bertollotto et al. 2018; Chen et al. 2018b; Jedlitschky et al. 2000; Kucka et al. 2010; Liu et al. 2010; Myint et al. 2015; Tivnan et al. 2015). In order to elucidate the isoform specific contribution of MRP5, a transporter that has a high affinity for cAMP, BeWo cells were transfected with MRP5-specific shRNA lentiviral particles. The MRP5 KD cells had significantly lower mRNA and protein expression of MRP5 which also translated to decreased functionality as depicted by the elevated intracellular levels of cAMP and Calcein AM. Knockdown of the MRP5 transporter in BeWo cells resulted in higher sensitivity to pharmacological inducers of syncytialization, elevated hormone secretion, larger cell size, and an elevated number of multinucleated cells, all hallmarks of syncytialized trophoblasts. Together, these data demonstrate that reducing expression and function of the MRP5 transporter in BeWo cells results in increased intracellular cAMP accumulation, downstream activation of PKA signaling, and syncytialization.

While the primary focus of this study was to examine the contribution of MRP transporters in regulating cell fusion through modulation of intracellular cAMP levels, it is also important to consider the potential effect of MRP inhibition on cGMP signaling and how that may also influence the syncytialization process. Notably, treatment of BeWo cells with the MK-571 inhibitor resulted in a significantly higher intracellular concentration of both cAMP and cGMP (Figure 3.2A; Supplementary Figure 3.1B). In the nitric oxide (NO)-cGMP pathway, the nitric oxide synthase (NOS) enzyme converts L-arginine to NO, which in turn binds and activates the soluble guanylate cyclase (sGC) enzyme. Once activated, the guanylate cyclase enzyme catalyzes the conversion of guanosine 5'-triphosphate (GTP) to cGMP, which then activates cGMP-dependent protein kinases leading to the expression of numerous target genes. There is conflicting literature examining the ability of NO-cGMP coupled signaling to induce syncytialization. The main source of inconsistency between studies has been centered around the gestational stage at which the placentas were obtained. Treatment of primary cytotrophoblasts isolated from first trimester placentas with 8-bromo-cGMP increased hCGß release into media (Hilf et al. 1985; Sachs et al. 1978). In contrast, term primary cytotrophoblasts and placental explants treated with 8-bromo-cGMP revealed no changes in hCGß secretion (Feinman et al. 1986; Lambot et al. 2005; Rodway et al. 1988). The lack of response can be attributed to low levels or complete absence of hCGß in term placentas (Lin et al. 1995). To explore potential underlying genetic changes in syncytialization, we treated BeWo cells with the membrane-permeable chemical analog of cGMP, 8-bromo-cGMP or a NO donor, sodium nitroprusside (SNP), in the presence and absence of MK-571. In the absence of MK-571, treatment of BeWo cells with 8-bromo-cGMP and SNP had little effect on syncytialization marker expression (Supplementary Figure 3.1A). Interestingly, stimulation with SNP caused a significant down-regulation of hCGß mRNA expression similar to the observation by Myat et al., 1996 who noted decreased hCGß secretion by BeWo and JEG-3 cells in response to 8-bromo-cGMP stimulation (Myat et al. 1996). Although the NO-cGMP stimulators did not induce pronounced changes in syncytialization markers by themselves, the combination treatment of SNP

and MK-571 significantly induced GCM1 mRNA expression (Supplementary Figure 3.1A). Considering that GCM1 is one of the global regulatory genes of syncytialization, this may warrant additional studies examining time course- and concentration-dependent changes of NO-cGMP stimulators on markers of syncytialization in BeWo cells and first trimester cytotrophoblasts.

Phosphodiesterase enzymes hydrolyze the 3'-phosphodiester bond of cAMP and cGMP to form 5' AMP or 5' GMP, respectfully, which terminates downstream signaling of cyclic nucleotides. In addition to phosphodiesterases, MRP 4 and 5 transporters act as negative regulators through active efflux od cAMP/cGMP (Copsel et al. 2011; Pattabiraman et al. 2013; Sassi et al. 2012; Sassi et al. 2008). There is growing evidence that phosphodiesterase enzymes and MRP transporters are interdependent, where the expression and function of one is affected by the other. For example, IBMX, a phosphodiesterase inhibitor, can induce MRP4 mRNA expression in primary cultures of human coronary smooth muscle cells as well as decrease and increase cGMP efflux of MRP4 and MRP5, respectfully, in HEK293 cells (Sassi et al. 2008; Wielinga et al. 2003). Additionally, treatment of human colon carcinoma T84 cells with the MRP inhibitor MK-571 significantly reduced their PDE activity (Xie et al. 2011). In the current study, MK-571 significantly induced (cAMP: PDE4C, PDE8A) and down-regulated (cGMP: PDE5A) the mRNA expression of PDE cyclic nucleotide-specific isoforms. Interestingly, the MRP5 KD cells exhibited gross down-regulation of PDE isoforms (cAMP: PDE4D, PDE7A; cGMP: PDE5A, PDE9A) regardless of cAMP/cGMP specificity (Supplemental Figure 3.2). Investigation into the ability of MK-571 to inhibit phosphodiesterase catalytic activity revealed significant down-regulation of cAMP- and cGMP hydrolysis, as compared to vehicle-treated control (Supplemental Figure 3.3A). However, vehicle-treated MRP5 KD cells and BeWo control cells pretreated with MK-571 for 18 h did not exhibit altered phosphodiesterase activity (Supplemental Figure 3.3B). While the mRNA expression of PDE5A was reduced in both models and could potentially contribute to elevated intracellular cAMP level, the disparity between the other PDE isoforms affected by genetic and

pharmacological MRP inhibition supports the observation that enhanced cell fusion was not solely due to indirect effects on PDEs. This contention was further confirmed by the MRP5 KD cell lysates, which did not exhibit any alteration in PDE activity (either cAMP or cGMP). Taken together, it is important to note that phosphodiesterases and MRP transporters work in tandem to effectively limit the intracellular concentration of cyclic nucleotides and limit their signal transduction.

Preeclampsia is a disorder marked by maternal proteinuria and hypertension and affects 2-8% of pregnancies worldwide (Ananth et al. 2013; Duley 2009). While the mechanisms underlying preeclampsia are yet to be fully understood, the pathogenesis is centered around improper trophoblastic remodeling of maternal uterine spiral arteries which leads to decreased blood flow and ultimately uteroplacental ischemia (Phipps et al. 2019). Investigation into potential serum markers to help identify pregnancies at risk for preeclampsia revealed that elevated human chorionic gonadotropin (hCG) levels in the second and third trimester are associated with increased risk for preeclampsia (Asvold et al. 2014; Barjaktarovic et al. 2019; Basirat et al. 2006; Heinonen et al. 1996; Taher et al. 2019; Wald et al. 2001). The human chorionic gonadotropin hormone is produced by syncytiotrophoblasts and maintains the corpus luteum during early pregnancy. This hormone is also responsible for feedback regulation of trophoblast fusion and formation of multinucleated syncytiotrophoblasts (Malhotra et al. 2015). Once formed, hCGß binds to the luteinizing hormone receptor on the surface of cytotrophoblasts and initiates the activation of adenylyl cyclase to increase the intracellular production of cyclic AMP. Analysis of markers regulating trophoblast fusion in preeclamptic placentas revealed a significant down-regulation of GCM1 and Syncytin-1 as well as an induction of hCGß mRNA expression (Chen et al. 2004; Lapaire et al. 2012; Lee et al. 2001; Sitras et al. 2009). The induction of hCGß mRNA expression may be a compensatory mechanism to rescue the expression of downstream target genes, GCM1 and Syncytin-1. Interestingly, MRP1 and MRP5 transporters, both known to efflux cyclic

nucleotides, have been shown to be altered in preeclamptic placentas as well. Specifically, the mRNA expression of MRP1 is significantly induced while the promoter of MRP5 is hypomethylated, suggesting enhanced expression in preeclamptic placentas (Afrouzian et al. 2018; Jia et al. 2012). These data show that increased MRP transporter expression is correlated with decreased expression of trophoblast fusion markers in preeclamptic placentas. This may offer a novel mechanism to aid in the understanding of preeclampsia pathogenesis. Current proposed drug remedies for preeclampsia target the dysregulation of the nitric oxide-cGMP signaling cascade and vasoconstriction through specific PDE inhibitors, albeit with mixed results (Samangaya et al. 2009; Sharp et al. 2018; Trapani et al. 2016; Wareing et al. 2005). Future studies should consider PDE inhibitors that are also capable of inhibiting MRP function. Selection of such compounds will aid two-fold as inhibition of PDE activity and MRP function will more effectively increase the intracellular concentration of cAMP and cGMP to further enhance the resolution of vasoconstriction as well as abnormal trophoblast fusion.

The current study demonstrates the ability of the MRP5 efflux transporter to regulate trophoblast cell fusion and hormone secretion through efflux of cyclic nucleotides. This finding may provide a novel mechanism explaining the pathogenesis of gestational disorders and xenobiotic toxicities associated with abnormal cytotrophoblast differentiation and placental development.

Table 3.1. Primers used for gene expression analysis.

Gene	Primer sequence (5' → 3')
Reference/Housekeeping	
RPL13a	**Fwd:** GGTGCAGGTCCTGGTGCTTGA
	Rev: GGCCTCGGGAAGGGTTGGTG
Efflux Transporter	
MRP5/*ABCC5*	**Fwd:** AGTGGACCAGCCTTCATGGTGAAA
	Rev: AGCGGACACCGGTTCGGTAATT
Syncytialization Markers	
GCM1	**Fwd:** TGAGGCTGCTCTCAAACTCCTGAT
	Rev: AGACGGGACAGGTTTCCATTCCTT
Syncytin-1	**Fwd:** CCCCATCGTATAGGAGTCTT
	Rev: CCCCATCAGACATACCAGTT
Syncytin-2	**Fwd:** GCCTGCAAATAGTCTTCTTT
	Rev: ATAGGGGCTATTCCCATTAG
hCGα	**Fwd:** CAGAATGCACGCTACAGGAA
	Rev: CGTGTGGTTCTCCACTTTGA
hCGß	**Fwd:** GCACCAAGGATGGAGATGTT
	Rev: GCACATTGACAGCTGAGAGC
cAMP-Specific PDEs	
PDE4A	**Fwd:** CCACGCTGTCAGAAGAAACG
	Rev: GAGCTCACGGTTCAACATCC
PDE4C	**Fwd:** ACTCTGGAGGAGGCAGAGGAA
	Rev: AGGCAACTCCAAGGCCTCTT
PDE4D	**Fwd:** GGCAGGGTCAAACTGAGAAATT
	Rev: TGACTGCCACTGTCCTTTTCC
PDE7A	**Fwd:** TGTGCCTGTTGCTGTTAACTT
	Rev: GCTCGGACTGAGTAAACATCTG
PDE7B	**Fwd:** TCTCAACTGCCTTCCCATGT

	Rev: AGGCTTGTTGAAGGGTCTCA
PDE8A	**Fwd:** GTGTAGTACGCAGGGTGGATA
	Rev: GCCCTGAGTTTCAGTTGTGAT
PDE8B	**Fwd:** AGCCATTTTTCACTCCCAACA
	Rev: AGATTGTCCTTGCCTCAAGC
cGMP-Specific PDEs	
PDE5A	**Fwd:** TGTTCTTCTGAGGGACGGAC
	Rev: TGACCATTTCTCTGGTGGCT
PDE6A	**Fwd:** CCGAATCTAAGTATGTTCTGGCA
	Rev: GGACAAGTGTAACAAATTGACTTGC
PDE9A	**Fwd:** AGTAAAAAGTCCGAGTGCAGC
	Rev: GAACAGGTCCATGATGTCGC
cAMP/cGMP PDEs	
PDE1B	**Fwd:** TCTCTGCTGCGCTACATGG
	Rev: TGCTGGGTGAAGGTGGAG
PDE10A	**Fwd:** TCTAATAATGCGAGCTGCTTCC
	Rev: TCTTCCTCTTCAGCCATTTCTCT

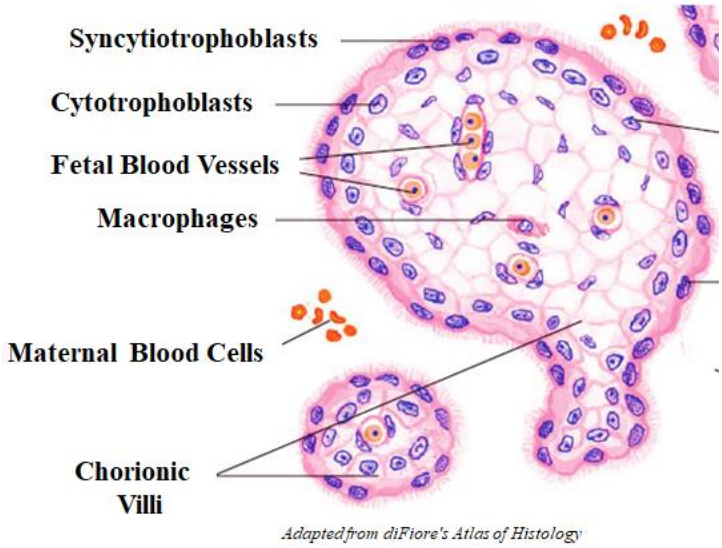

Fig 3.1. Cross section of placental chorionic villi. Different cell types found in the human chorionic villi.

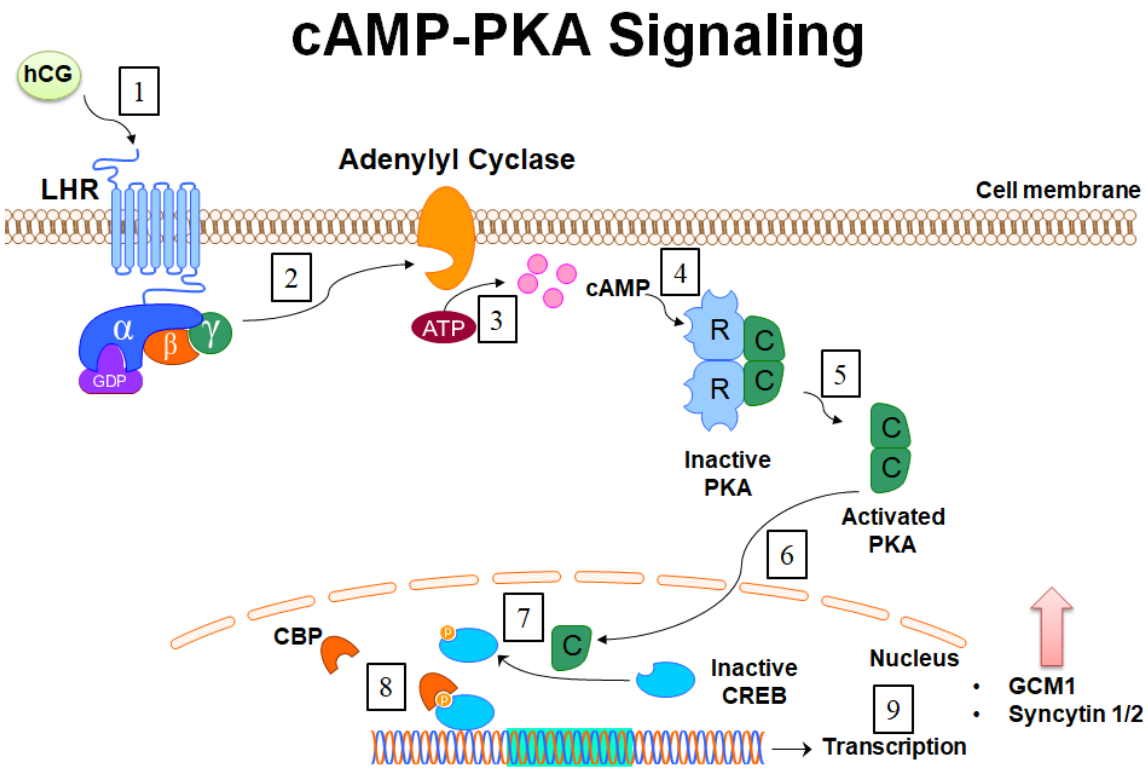

Fig 3.2. Cyclic adenosine monophosphate-protein kinase A signaling pathway.

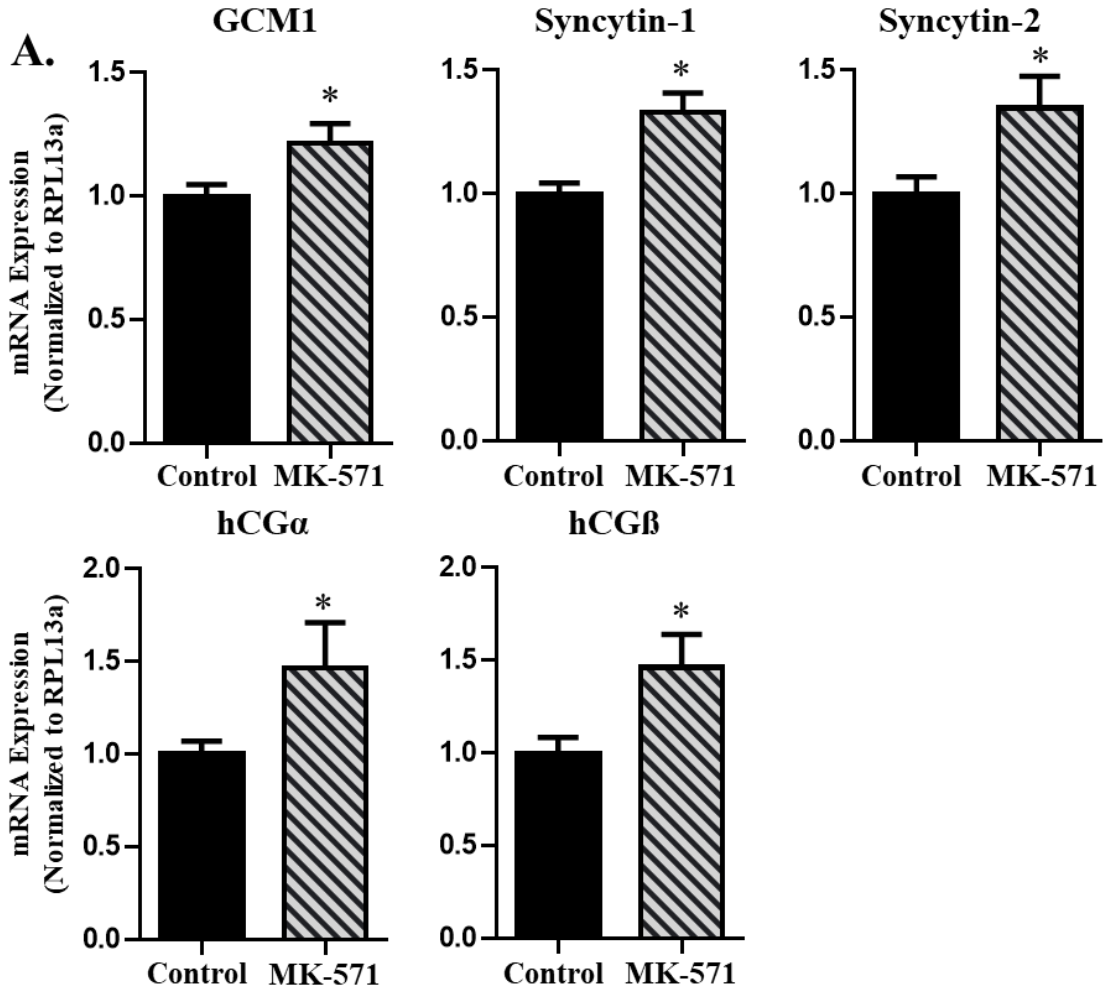

Fig 3.3. Expression of syncytialization markers following pharmacological inhibition of MRP function in human placental explants. (A) Healthy human term placentas were processed within two hours of delivery. Placental explants were cultured for 3 days to allow for shedding and re-syncytialization prior to a 24 h treatment with 25 μM MK-571 beginning on the 3rd day. Induction of syncytialization markers in placental explants was assessed by qPCR and normalized to RPL13a. Data are presented as the mean of 6-8 placentas (4-5 samples from each placenta per treatment) ± SE. * $p \leq 0.05$ compared with vehicle-treated explants.

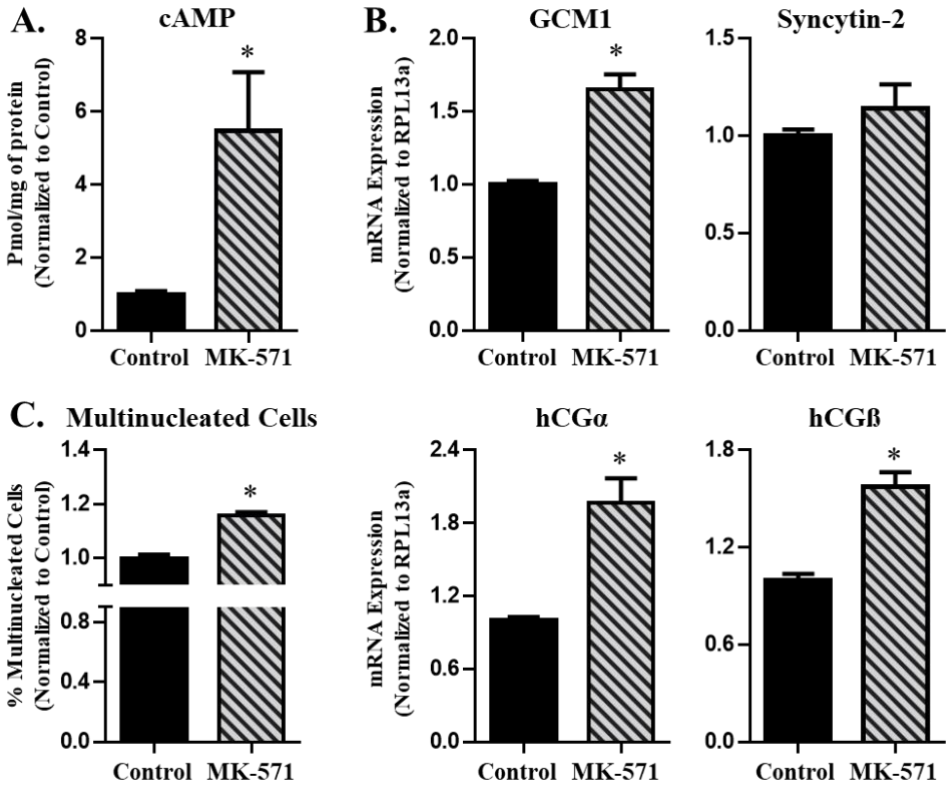

Fig 3.4. Expression of syncytialization markers following pharmacological inhibition of MRP function in human trophoblasts. (A) Effect of MK-571 on intracellular cAMP accumulation. BeWo b30 cells were treated with 25 µM MK-571 for 1 h and lysed with 0.1 M HCl. Changes in the intracellular concentration of cAMP were determined with an ELISA and normalized to protein concentration. (B) BeWo b30 cells were treated with 25 µM MK-571 for 18 h. Quantitative analysis of changes in the mRNA expression of syncytialization markers was performed by qPCR and normalized to RPL13a. (C) Increased presence of multinucleated cells following MK-571 treatment. BeWo b30 cells were treated with 25 µM MK-571 for 24 h. Percent of multinucleated cells was determined as described in Materials and Methods and normalized to vehicle-treated controls. Data are presented as mean ± SE (n=3-4). * $p \leq 0.05$ compared with vehicle-treated cells.

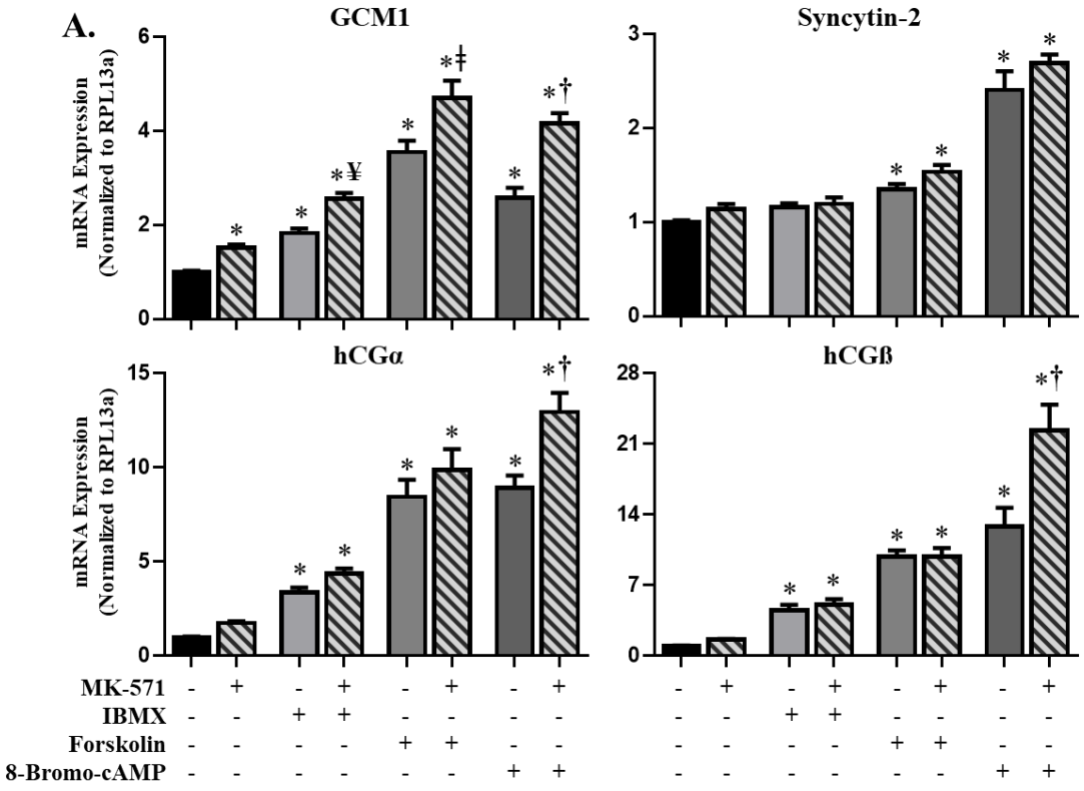

Fig 3.5. Expression of syncytialization markers following pharmacological modulation of intracellular cAMP and MRP function in human trophoblasts. (A) Induction of syncytialization markers following stimulation with pharmacological cAMP modulators is further enhanced in MK-571 combination treatments. BeWo b30 cells were treated with the MRP inhibitor MK-571 (25 µM), the phosphodiesterase inhibitor IBMX (200 µM), the adenylyl cyclase activator forskolin (25 µM), the analog 8-Bromo-cAMP (100 µM), or their combination for 18 h. Quantitative analysis of mRNA expression was performed by qPCR and normalized to RPL13a. Data are presented as mean ± SE (n=3) * $p \leq 0.05$ compared with cells treated with vehicle. ¥ $p \leq 0.05$ compared with cells treated with IBMX. ǂ $p \leq 0.05$ compared with cells treated with Forskolin. † $p \leq 0.05$ compared with cells treated with 8-Bromo-cAMP.

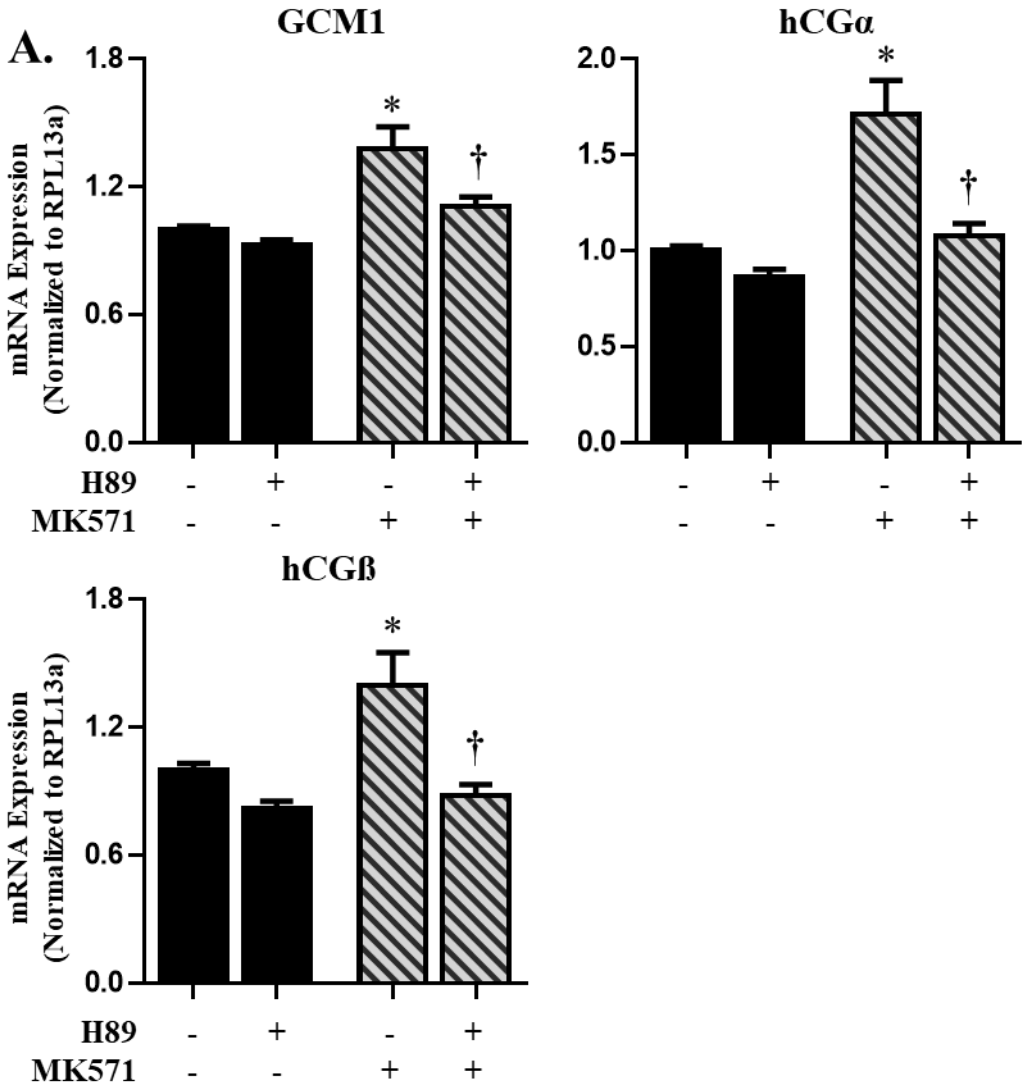

Fig 3.6. Induced expression of syncytialization markers following pharmacological MRP inhibition is PKA-dependent. PKA inhibitor prevents MK-571-mediated induction of syncytialization markers. (A) BeWo b30 cells were treated with 5 µM H89, a PKA inhibitor, 25 µM MK-571, or their combination for 18 h. Quantitative analysis of mRNA expression was performed by qPCR and normalized to RPL13a. Data are presented as mean ± SE (n=3-4). * $p \leq 0.05$ compared with vehicle-treated cells. † $p \leq 0.05$ compared with MK-571-treated cells.

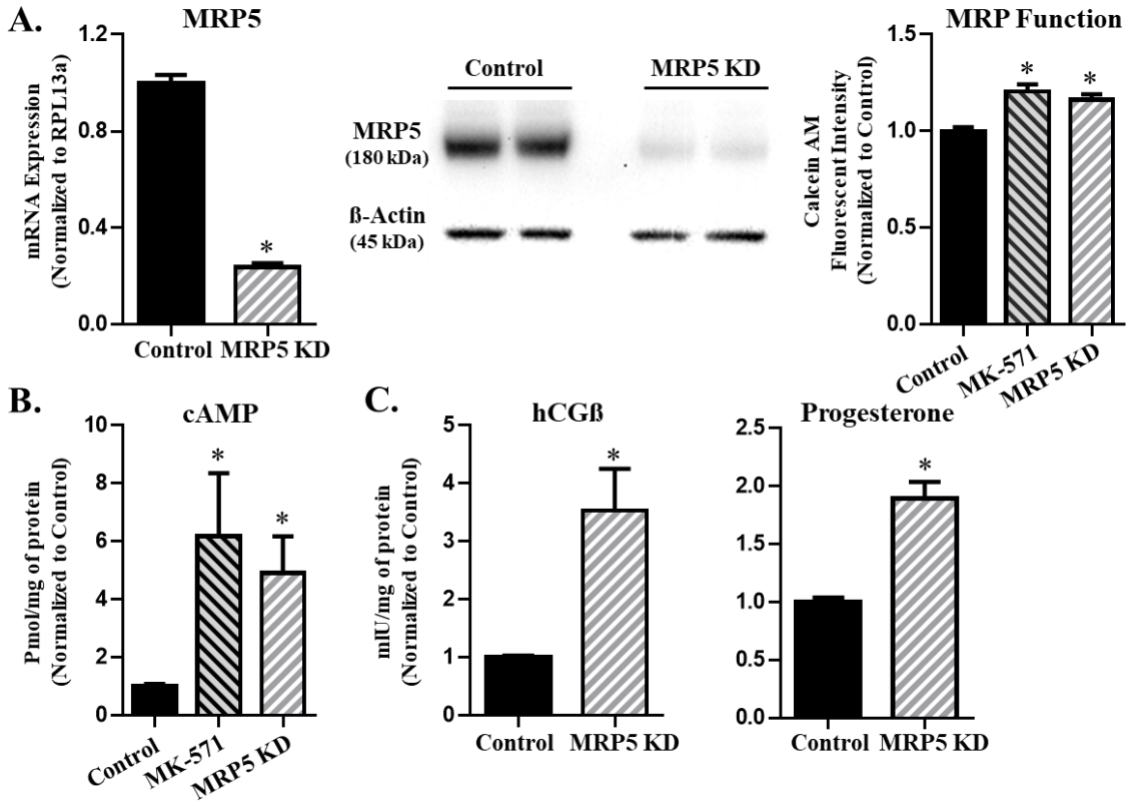

Fig 3.7. Characterization of MRP5 KD in human trophoblast cells. BeWo B30 cells were transfected with lentiviral shRNA particles specific for human MRP5 (or non-specific shRNAs) and stable knockdown (KD) lines were generated. (A) mRNA Analysis. Quantitative analysis of MRP5 mRNA expression in knockdown cells was performed by qPCR and normalized to RPL13a. Protein Analysis. Representative image of MRP5 protein in transfected BeWo b30 control and MRP5 KD cells. Protein homogenates were prepared from BeWo b30 control and MRP5 KD cells and analyzed for MRP5 (180 kDa) expression by Western blot. ß-Actin (42 kDa) was used as a loading control. Function Analysis. BeWo b30 cells (control and MRP5 KD) were incubated with 1 µM Calcein AM and intracellular retention of the fluorescent dye was determined as described in Materials and Methods. Control cells were also treated with MK-571 as a positive control for MRP inhibition. (B) Effect of shRNA MRP5 KD on intracellular cAMP accumulation. Control cells were treated with 25 µM MK-571 for 1 h as a positive control for MRP inhibition. Changes in the intracellular concentration of cAMP were determined with an ELISA and normalized to

protein concentration. (C) Syncytialized human trophoblast cells secrete hormones at a higher extent than their cytotrophoblast progenitor counterparts. Changes in hormone secretion by the MRP5 KD cells were quantified by ELISA and normalized to protein concentration. Data are presented as mean ± SE (n=3). * $p \leq 0.05$ compared with vehicle-treated control cells.

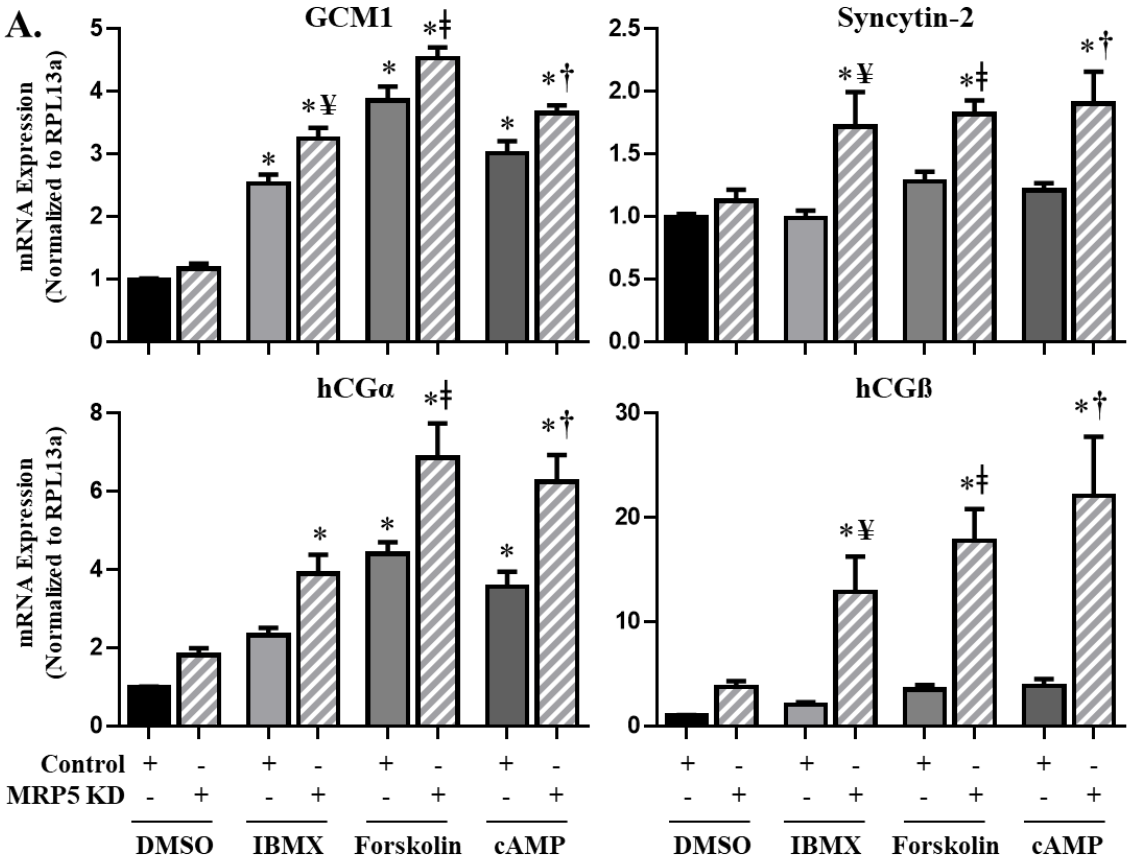

Fig 3.8. Expression of syncytialization markers in MRP5 KD trophoblasts following pharmacological modulation of intracellular cAMP. Induction of syncytialization markers following stimulation with pharmacological cAMP modulators is further enhanced in MRP5 KD cells. BeWo b30 control and MRP5 KD cells were treated with the MRP inhibitor MK-571 (25 µM), the phosphodiesterase inhibitor IBMX (200 µM), the adenylyl cyclase activator forskolin (10 µM), or the analog 8-Bromo-cAMP (100 µM) for 18 h. Quantitative analysis of mRNA expression was performed by qPCR and normalized to RPL13a. Data are presented as mean ± SE (n=3) * $p \leq 0.05$ compared with control cells treated with vehicle. ¥ $p \leq 0.05$ compared with control cells treated with IBMX. ǂ $p \leq 0.05$ compared with control cells treated with Forskolin. † $p \leq 0.05$ compared with control cells treated with 8-Bromo-cAMP.

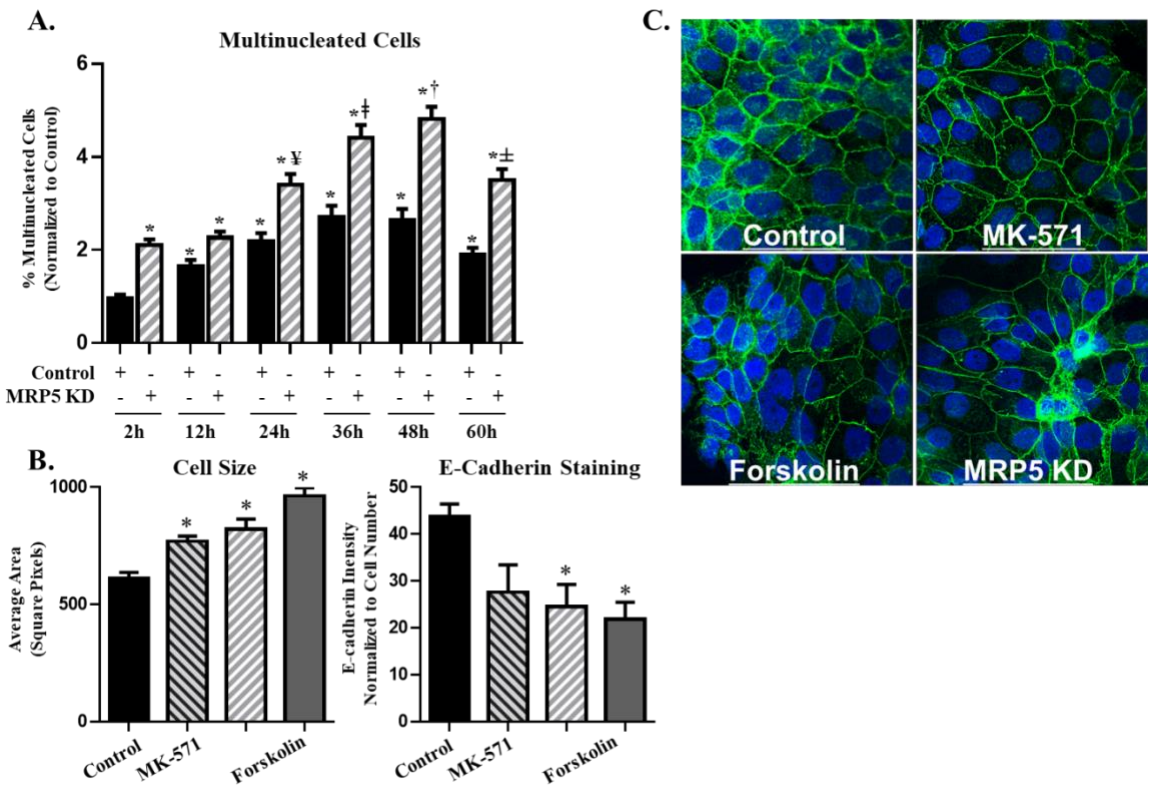

Fig. 3.9. Cellular fusion of MRP5 KD human trophoblasts. (A) Change in percent multinucleated cells over time was assessed with control and MRP5 KD trophoblast cells. Control and MRP5 KD cells were treated with media containing 10 µM Forskolin and 100 nM Hoechst 33342 for 60 h. Images were taken every 12 h. Percent of multinucleated cells was normalized to control cells at 2 h and analyzed as described in Materials and Methods. Data are presented as mean ± SE (n=3) * p≤0.05 compared with control cells treated with DMSO at 2 h. ¥ p≤0.05 compared with control cells treated with Forskolin at 24 h. ǂ p≤0.05 compared with control cells treated with Forskolin at 36 h. † p≤0.05 compared with control cells treated with Forskolin at 48 h. ± p≤0.05 compared with control cells treated with Forskolin at 60 h. (B/C) Indirect immunofluorescent staining of BeWo B30 control and MRP5 KD cells at 72 h. BeWo b30 control were treated with the MRP inhibitor MK-571 (25 µM) or the adenylyl cyclase activator forskolin (25 µM) for 72 h. Fusion of trophoblast cells decreases tight junction markers. Cells were stained for the tight junction marker E-cadherin (*green*). Nuclei were stained with DAPI (*blue*). 20X magnification of

representative images are shown. Signal quantification and analysis of cell size was determined as described in Materials and Methods. Data are presented as mean ± SE (n=3) * $p \leq 0.05$ compared with control cells treated with vehicle.

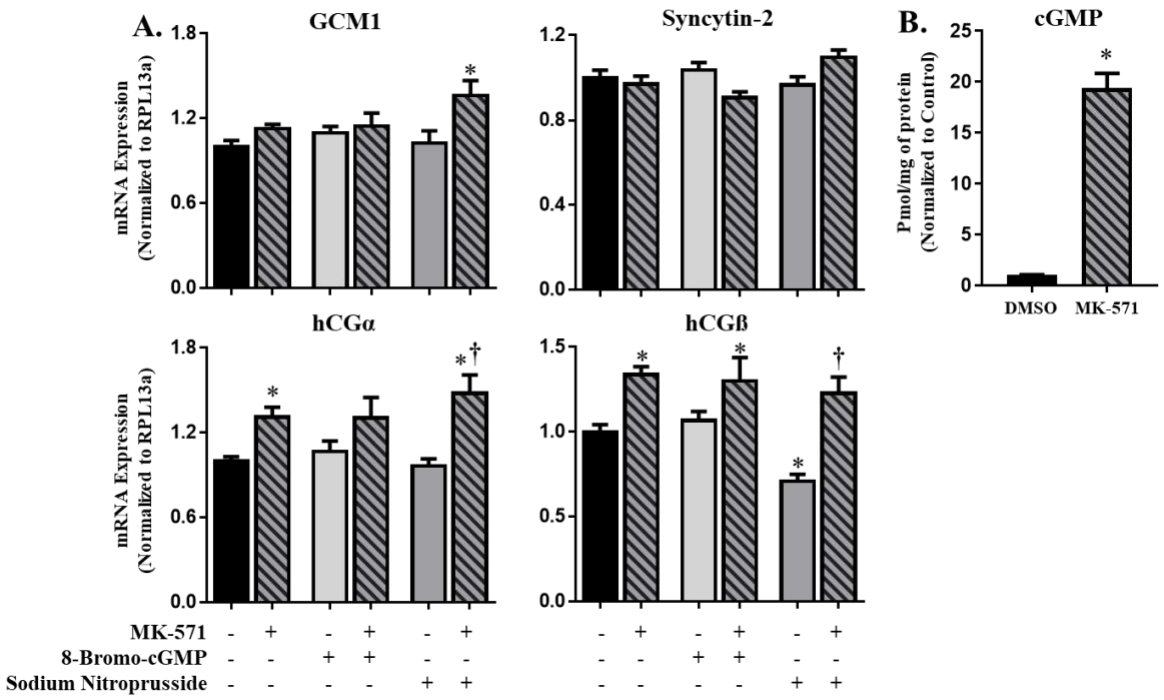

Supplementary Fig. 3.1. Expression of syncytialization markers following pharmacological modulation of intracellular cGMP and MRP function in human trophoblasts. (A) BeWo b30 cells were treated with the MRP inhibitor MK-571 (25 µM), the activator of guanylate cyclase sodium nitroprusside (100 µM), the analog 8-Bromo-cGMP (100 µM), or their combination for 18 h. Quantitative analysis of mRNA expression was performed by qPCR and normalized to RPL13a. Data are presented as mean ± SE (n=3) * $p \leq 0.05$ compared with cells treated with vehicle. † $p \leq 0.05$ compared with cells treated with sodium nitroprusside. (B) Effect of MK-571 on intracellular cGMP accumulation. Control cells were treated with 25 µM MK-571 for 1 h and lysed with 0.1 M HCl as a positive control for MRP inhibition. Changes in the intracellular concentration of cGMP were determined with an ELISA and normalized to protein concentration. Data are presented as mean ± SE (n=1) * $p \leq 0.05$ compared with cells treated with vehicle.

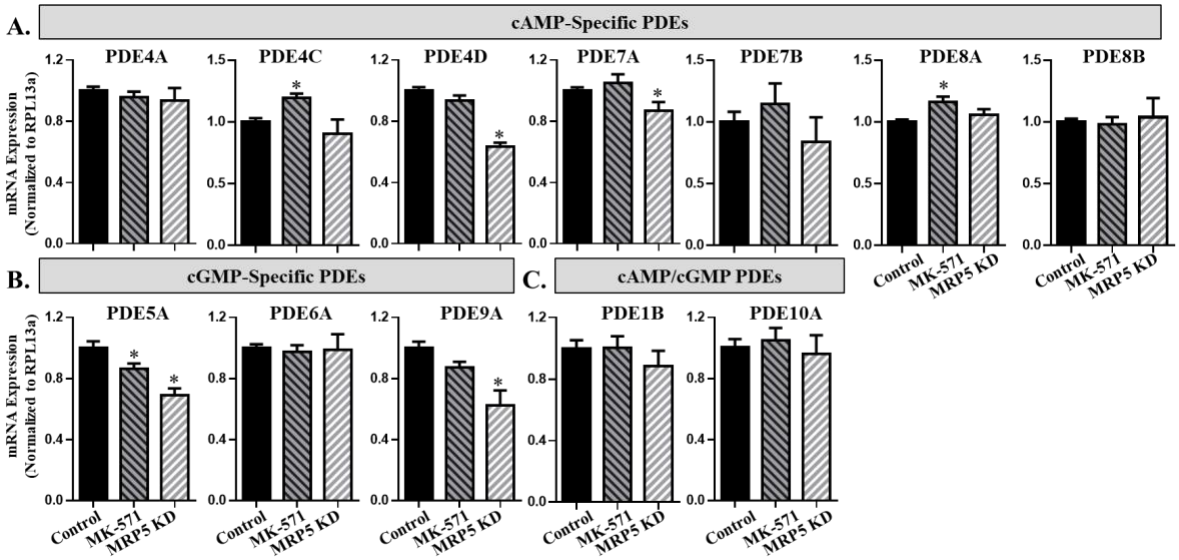

Supplementary Fig. 3.2. Expression of phosphodiesterase isoforms following genetic and pharmacological inhibition of MRP function. Expression of phosphodiesterase isoforms in BeWo b30 control cells treated with 25 µM MK-571 for 18 h and MRP5 KD cells. (A) cAMP-specific phosphodiesterase isoforms. (B) cGMP-specific phosphodiesterase isoforms. (C) cAMP/cGMP phosphodiesterase isoforms. Quantitative analysis of mRNA expression was performed by qPCR and normalized to RPL13a. Data are presented as mean ± SE (n=3) * $p \leq 0.05$ compared with control cells treated with vehicle.

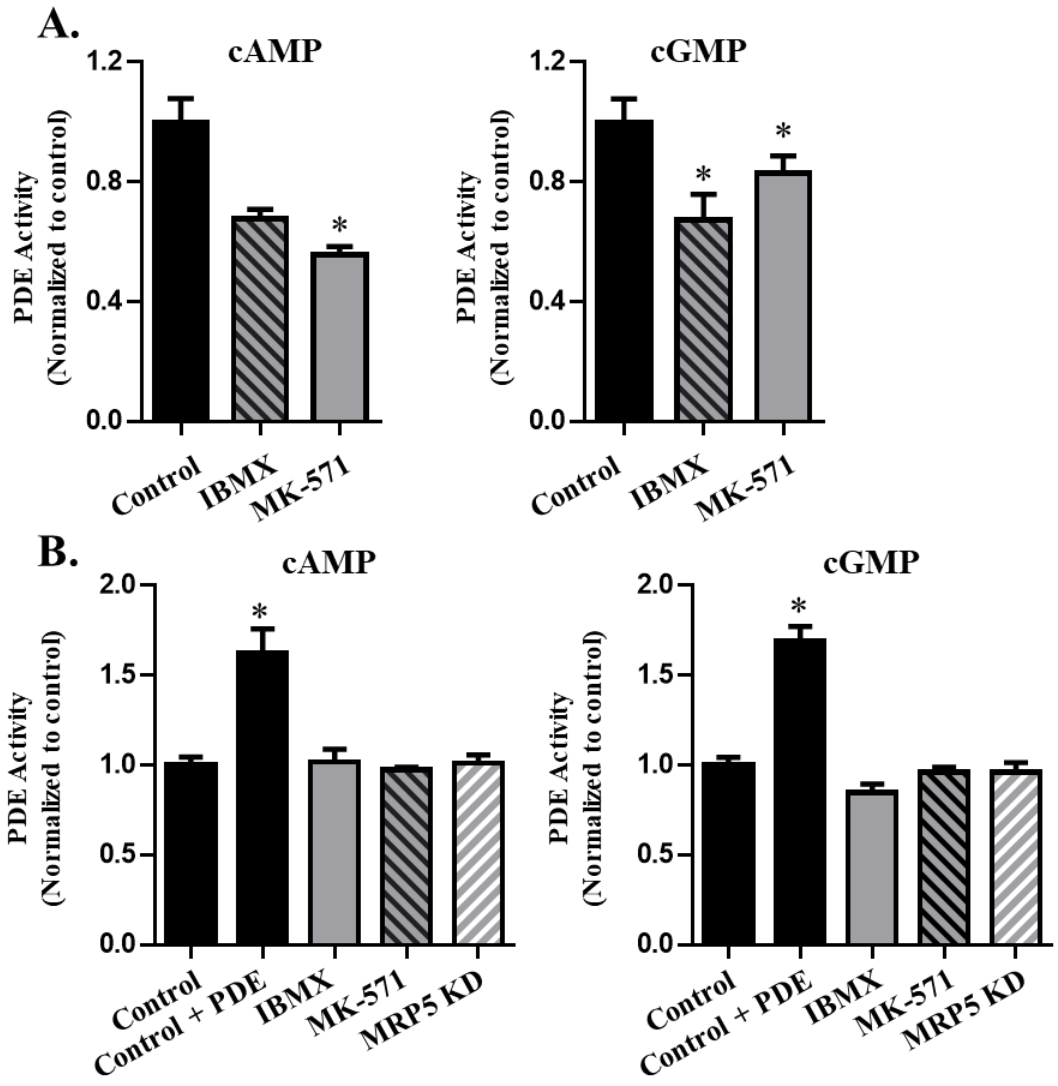

Supplementary Fig. 3.3. Phosphodiesterase activity following genetic and pharmacological inhibition of MRP function. (A) The ability of MK-571 to inhibit phosphodiesterase activity was measured using a colorimetric phosphodiesterase kit (ab139460). Reaction mixture (50 µl/well) containing cAMP/cGMP substrate (200 µmol/l), 5′-nucleotidase (50 kU/well), PDE enzyme (20 mU/well), and MK-571 (25µM) was incubated for 30 minutes at 30°C. Addition of Green Assay Reagent (100 µl/well) at the 30 minute mark terminated the reaction. Plate was incubated for an additional 30 minutes at room temperature after which the colorimetric phosphate-dependent reaction was measured by reading absorbance at 620 nm in a microplate-reading

spectrophotometer. (B) BeWo b30 control cells pre-treated with 25 µM MK-571 or 200 µM IBMX for 18 h and MRP5 KD cells were tested for altered phosphodiesterase catalytic activity. Desalted cell lysates were assayed for altered phosphodiesterase activity as described above. Data are presented as mean ± SE (n=1-2) * $p \leq 0.05$ compared with control cells treated with vehicle.

CHAPTER 4: EXPRESSION OF THE BCRP TRANSPORTER INFLUENCES PLACENTAL RESPONSES TO THE MYCOESTROGEN ZEARALENONE

Ludwik Gorczyca[a,b] and Lauren M. Aleksunes[a,c,d]

Affiliations:

[a] Rutgers University, Ernest Mario School of Pharmacy, Department of Pharmacology and Toxicology, 170 Frelinghuysen Road, Piscataway, NJ 08854, USA

[b] Rutgers University, Joint Graduate Program in Toxicology, 170 Frelinghuysen Road, Piscataway, NJ 08854, USA

[c] Rutgers Center for Lipid Research, New Jersey Institute for Food, Nutrition, and Health, Rutgers University, New Brunswick, New Jersey 08901, USA

[d] Environmental and Occupational Health Sciences Institute, 170 Frelinghuysen Rd, Piscataway, NJ 08854, USA

4.1 Abstract

During pregnancy, the placenta limits the maternal-to-fetal translocation of xenobiotics. This barrier is established in part by the presence of efflux transporters, such as the breast cancer resistance protein (BCRP/ABCG2), which actively extrude compounds from the placenta back towards the maternal circulation. Zearalenone is an estrogenic mycotoxin and reproductive toxicant that has been identified as a substrate of BCRP/Bcrp in the placenta. In the present study, we sought to 1) assess the impact of prenatal zearalenone administration on placental development and signaling and 2) determine whether placental Bcrp genotype influences responses to zearalenone. Bcrp heterozygous mice were mated to generate all three Bcrp genotypes (Wild-type, Heterozygous, Knockout) *in utero*. Based on Food and Drug Administration's acceptable daily intake for zeranol (1.25 µg/kg/d), dams received vehicle or ZEN (1.25, 3.75 µg/kg/d; 5 ml/kg) absorbed into soy-free peanut butter from gestational day 6 to 17. Changes in expression of markers of syncytialization (Catenin ß1, Cebpa, Gcma), spongiotrophoblasts (Ascl2, Hand1, Tpbpa, Cx31.1, Igf2, Pcdh12), giant trophoblasts (Prl-2c2, -3b1, Ctsq, Plap), placental barrier uptake transporters (Oatp-2b1, -4a1, -5a1), efflux transporters (Bcrp, Mdr1a, Mdr1b, Mrp-1,-4,-5), as well as antioxidant defense (Nrf2, Ho-1, Sod1, Sod2) were quantified by qPCR. Treatment with zearalenone enhanced maternal weight gain, decreased placental weight and area, and increased the number of resorptions. Moreover, zearalenone administration globally down-regulated mRNA markers of syncytiotrophoblasts, spongiotrophoblasts, and giant trophoblasts in Wt fetuses up to 90% while increasing expression of Erα. Treatment of dams with zearalenone down-regulated placental Bcrp mRNA expression in Wt fetuses by up to 63%. Moreover, zearalenone exposure differentially regulated placental transporter expression including down-regulation (Oatp2b1, Oatp4a1, Mdr1b, Mrp4) and induction (Oatp5a1) in Wt fetuses with little to no change in Bcrp Het and Ko placentas. Zearalenone globally down-regulated antioxidant defense genes by 32-57% in

placentas from Wt and Het fetuses. Together, these data suggest that prenatal zearalenone exposure alters the placental development, differentiation, and barrier homeostasis during pregnancy.

Keywords: Placenta; zearalenone; mycotoxin; BCRP; transporters

4.2 Introduction

The development and growth of a healthy fetus is reliant on the ability of the placenta to limit the transfer of potentially toxic environmental contaminants, pharmaceuticals, and even endogenous compounds into the fetal compartment. This feto-maternal barrier is mediated, in part, by the expression of efflux drug transporters on the maternal-facing membrane of syncytiotrophoblast cells lining the chorionic villi of the placenta (Iqbal et al. 2012). The Breast Cancer Resistance Protein (BCRP/*ABCG2*) is a member of the ATP-binding cassette superfamily of efflux transporters that uses ATP hydrolysis to actively translocate xenobiotics back toward maternal circulation, in turn limiting fetal exposure (Hahnova-Cygalova et al. 2011). Substrates of the BCRP transporter include various chemicals that have the potential to disrupt fetal development and growth. Some of these include known endocrine active chemicals such as bisphenol A, a plastic contaminant and glyburide, a drug prescribed for gestational diabetes (Mazur et al. 2012; Zhou et al. 2008a). Taken together, these data suggest that changes to the expression and/or function of BCRP may facilitate fetal drug and chemical exposure. Elevated levels of xenobiotics in the fetal compartment can heighten the risk of various developmental disorders, structural malformations, preterm birth, low birth weight and metabolic disorders (Brent 2001; Gluckman et al. 2004; Stillerman et al. 2008). Further studies examining the effect of impaired placental BCRP function on the downstream activity of endocrine active environmental contaminants are urgently needed.

Mycotoxin exposure has become a growing concern over the last two decades. In 2016, the United Nations Environmental Program identified fungal contamination of food supply as one of the top emerging issues of environmental concern (Erkan et al. 2005). Increasing global temperatures promote the growth of fungi and in turn their production of toxic by-products such as zearalenone (ZEN). ZEN is a nonsteroidal estrogenic mycotoxin produced by the *Fusarium* species of fungi that commonly grow on cereal crops such as maize and wheat (Marin et al. 2013). Foods in Korea

(3-17 µg/kg), United Kingdom (8-231.8 µg/kg), Germany (3-67 µg/kg) and Brazil (70 µg/kg) routinely exceed the European Union (EU) allowable limit for ZEN (4 µg/kg) (2006; (FSA) 2003; Iqbal et al. 2014b; Ok et al. 2014; Schollenberger et al. 2005; Tralamazza et al. 2016). ZEN can disrupt hormonal signaling through interactions with estrogen receptors alpha and beta (Fitzpatrick et al. 1989; Mueller et al. 2004; Takemura et al. 2007b). *In utero* exposure to ZEN accelerated the onset of puberty and altered the mammary gland development in both C57BL/6 mice and Wistar rats (Belli et al. 2010; Hilakivi-Clarke et al. 1998). ZEN has been detected in the urine of 78% of adolescent girls tested and exposures correlated with changes in height, weight, and breast development (Bandera et al. 2011; Rivera-Nunez et al. 2019). Notably, ZEN has also been detected in the urine of pregnant women and infants (Fleck et al. 2016; Njumbe Ediage et al. 2013). While data regarding the impact of high dose ZEN on the feto-placental unit is emerging (Andersen et al. 2018; Belli et al. 2010; C. et al. 2016; Collins et al. 2006; Gao et al. 2017; Li et al. 2019a), there is still little known about the impact of ZEN during the prenatal period at doses relevant to dietary exposures.

Rodents are routinely used to study mechanisms of developmental toxicity and to assess the risk of exposure to humans. Rodent and human placentas are both hemochorial but possess a number of anatomical differences (Carter 2007). In humans, progenitor cytotrophoblast cells line the basement membrane of chorionic villi and fuse together to form giant multinucleated cells called syncytiotrophoblasts. Syncytiotrophoblasts perform the majority of placental functions including hormone synthesis and metabolism, nutrient and gas exchange, and feto-maternal transport. Cytotrophoblasts also detach from the basement membrane of chorionic villi and aggregate as extravillous trophoblasts in multilayered columns that invade the maternal endometrium and spiral arteries. This invasion anchors the placenta onto the uterine wall and through remodeling of spiral arteries enables delivery of oxygenated blood into the placenta. By comparison, the mouse placenta is composed of three distinct layers, the maternal decidua, junctional zone, and labyrinth zone. The

decidua is in direct contact with the uterus and is comprised of trophoblast giant cells that exhibit endocrine and invasive properties, similar to extravillous trophoblasts in human placentas. Adjacent to the decidua is the junctional zone comprised of spongiotrophoblast cells, glycogen cells, and trophoblast giant cells. Spongiotrophoblasts serve as precursors to trophoblast giant cells and maintain overall placental structure and integrity during gestation. The innermost labyrinth is comprised of three layers of trophoblasts. Two layers of syncytiotrophoblasts are in direct contact with the fetal endothelium while the precursor cytotrophoblasts make up the third layer and are in direct contact with maternal blood. As in humans, mouse syncytiotrophoblasts facilitate the feto-maternal exchange of nutrients and waste between maternal sinuses and the fetal endothelium (Reviewed in Malassine et al. 2003; Soncin et al. 2015; Woods et al. 2018). Distinct markers of the different trophoblasts can be used to evaluate effects of xenobiotics or genetic manipulation on the murine placenta (Table 4.1). Furthermore, the subcellular localization of drug transporters such as Bcrp across the species remains largely similar (Myllynen et al. 2010). Together, the hemochorial nature, similarity in cell type and function, and xenobiotic transporter expression/localization supports the use of a mouse model to investigate prenatal exposures to xenobiotics and their effect on the fetus and placenta.

Limited transplacental transfer of ZEN into the fetal compartment has been observed in rodents and in perfused human placentas (Appelgren et al. 1982; Bernhoft et al. 2001; Koraichi et al. 2012; Warth et al. 2019). Recently, our laboratory identified ZEN as a substrate of the human and mouse BCRP/Bcrp transporter in the placenta and observed higher ZEN concentrations in placentas and fetuses lacking Bcrp expression (Szilagyi et al. 2019; Xiao et al. 2015a). However, the ability of Bcrp to modulate the impact of ZEN on placental development has not been evaluated. Therefore, the purpose of this present study was to two-fold: 1) assess whether prenatal ZEN administration alters placental and fetal development and 2) determine whether Bcrp genotype in the placenta alters responses to ZEN.

4.3 Materials and Methods

Chemicals

All chemicals were purchased from Sigma-Aldrich (St. Louis, MO), unless stated otherwise.

Generation of Bcrp Heterozygous Mice and Treatment

Wild-type (Wt) C57BL/6 mice 7 weeks of age were purchased from Charles River Laboratories (Wilmington, MA). Bcrp knockout (KO) mice were obtained from Taconic Biosciences (Taconic, NY) and backcrossed to the C57BL/6 background (027 strain, Charles River Laboratories, Wilmington, MA) until >99% congenic (Rutgers RUCDR Infinite Biologics, Piscataway, NJ). Bcrp heterozygous (Het) were generated in house by crossing adult Wt female mice with Bcrp KO male mice. To reduce exposure to potential phytoestrogen contamination, the adult Bcrp Het female mice were housed in cages containing Alpha-Dri bedding and given the 2020X Teklad global soy protein-free extruded diet (T.2020X.15, Envigo, Madison, WI) *ad libitum* as primary feed for the duration of the experiment. Adult female and male Bcrp Het mice were mated overnight to generate all three fetal Bcrp genotypes (Wt, Het, KO). The presence of a vaginal sperm plug the following morning denoted gestation day (GD) 0. Female mice with a vaginal sperm plug were separated and housed individually for the duration of the experiment. Beginning on GD6 (after implantation) (McCormack et al. 1974), dams (n=6-8) were orally administered vehicle (dimethyl sulfoxide: polyethylene glycol PEG400: Saline, 1:5:4 ratio)(Shin et al. 2009) or ZEN (1.25, 3.75 µg/kg/day; 5 ml/kg) until GD17. To minimize maternal stress, vehicle or ZEN was absorbed into 0.5 g of soy-free organic peanut butter (8441497020621; Vitacost, Las Vegas, NV). Peanut butter was placed inside the cages each morning and dams were observed until all peanut butter was consumed. Weights of dams were recorded on GD6, GD10, GD13, GD15, and GD17 and normalized to litter size, as previously reported (Gupta et al. 2014).

Fetuses and placentas were collected from vehicle- and ZEN-treated pregnant mice 4 hours after the consumption of peanut butter on GD17. Tissues were collected within 60 min, snap frozen in liquid nitrogen, and stored at -80ºC. All mice were housed in an Association for Assessment and Accreditation of Laboratory Animal Care accredited facility in temperature-, light-, and humidity-controlled rooms. This study was approved by the Rutgers University Institutional Animal Care and Use Committee under protocol #09-038.

Genotyping/Sexing

The genotype of fetal pups was confirmed via western blot and PCR genotyping. Western blots served to identify Bcrp KO fetuses while standard PCR genotyping differentiated between Bcrp Wt and Het fetuses. To isolate protein, ~20 mg of fetal rump tissue was homogenized in sucrose-Tris buffer (pH 7.5) using the TissueLyser II Adapter (Qiagen LLC, Germantown, MD), per manufacturer's protocol. Protein concentration of tissue homogenates was obtained using the bicinchoninic acid assay. Total protein (50 µg) was loaded onto a SDS-polyacrylamide 4-12% Bis-Tris gel (Life Technologies, Grand Island, NY) and resolved by electrophoresis. The Biorad Criterion Blotter (Biorad, Hercules, CA) was used to transfer proteins onto polyvinylidene fluoride membranes overnight. Following the transfer, membranes were blocked in 5% non-fat milk in 0.5% Tween 20-PBS for 2 h. Membranes were then incubated with the Bcrp (BXP-53, 1:5000, Enzo Life Sciences, Farmingdale, NY) or ß-Actin (ab8227, 1:2000, Abcam) primary antibodies for 2 h at room temperature. All primary antibodies were diluted in 2% non-fat milk in 0.5% Tween 20-PBS. Species-appropriate secondary antibodies (Sigma-Aldrich) were used to probe primary antibodies. Chemiluminescent detection of protein signal was performed using SuperSignal West Dura blotting reagents (Pierce Biotechnology) and Fluorchem Imager (ProteinSimple, Santa Clara, CA). ß-Actin served as a loading control.

Genomic DNA was isolated from fetal rump samples using the DNeasy Blood and Tissue Kit (69506; Qiagen LLC) according to manufacturer's protocol. The quantity and quality of isolated DNA was verified using the NanoDrop 2000 spectrophotometer (Thermo Scientific, Wilmington, DE). Genotyping was determined by PCR and appropriate primers (Table 4.1). Cycle conditions were as follows: 15 min at 95°C, 45 sec at 94°C, 1 min at 60°C, 1 min at 72°C, 5 min at 72°C, for 35 cycles and held at 4°C.

Sexing of the fetuses was performed via quantitative PCR. Total RNA was isolated from fetal rumps and cDNA was generated as described below. Quantitative PCR was perfomed with cDNA, SYBR Green dye (Life Technologies), male-specific primers (Integrated DNA Technologies, Inc., Coralville, IA) (Table 4.1), and a ViiA7 RT-PCR System (Life Technologies). Undertermined C_t values denoted female fetuses.

RNA Isolation and Analysis Using Quantitative Polymerase Chain Reaction (qPCR)

RNA was isolated using the QIAshredder and Qiagen RNeasy Mini Kits (79654; 74104, Qiagen LLC) according to manufacturer's protocols. Briefly, ~20 mg of tissue was added to a 2-ml round bottom polypropylene tube containing 700 µl of Buffer RLT (1% β-mercaptoethanol) and a 5-mm stainless steel bead. Homogenization of samples was performed for 5 min at 50 Hz using the TissueLyser II (Qiagen LLC). Homogenate was transferred to QIAshredder tubes and centrifuged at 16.3 x g for 2 min to further break down the lysate. Flow through was added to a 1.7 ml eppendorf tube containing 70% ethanol (1:1 ratio) and briefly vortexed. Total RNA was purified using the RNeasy mini kit (Qiagen LLC) spin columns. The A260/A280 ratios were obtained for each sample using the NanoDrop 2000 spectrophotometer (Thermo Scientific) to confirm the integrity and purity of isolated RNA. The High-Capacity cDNA Reverse Transcription Kit (Life Technologies) and a MultiGene OptiMax Thermal Cycler (Labnet International Inc., Edison, NJ) were used to generate cDNA from 1000 ng of total RNA. The cycle conditions were as follows: 10 min at 25°C,

120 min at 37°C, 5 min at 85°C, and held at 4°C. mRNA expression was determined by quantitative PCR (qPCR) using specific forward and reverse primers (Integrated DNA Technologies, Inc.) and SYBR Green dye (Life Technologies). qPCR was performed using the ViiA7 Real-Time PCR machine (Life Technologies). CT values were converted to delta delta CT values with beta-2-microglobulin (ß2m) serving as a reference gene for normalization purposes.

Statistical Analysis

Data are presented as mean ± SE and analyzed using Graphpad Prism 6.0 (Graphpad Software, Inc., La Jolla, CA). A 1-way ANOVA or 2-way ANOVA was selected depending on number of variables compared. Dunnett's multiple comparison post-hoc test determined group significance. * $p \leq 0.05$ compared with litters treated with vehicle (genotype/sex-specific).

4.4 Results

Prenatal zearalenone administration increases maternal weight gain and resorptions and decreases placental size.

Pregnant mice heterozygous for the *Bcrp* gene were administered 0, 1.25, or 3.75 µg/kg/d ZEN from GD6 to 17 and weighed on GD -1, 6, 10, 13, 15, and 17. As expected, maternal weight increased over gestation with notably greater percent weight change in dams receiving 3.75 µg/kg/d ZEN compared to vehicle controls (Figure 4.1A). Treatment with 1.25 µg/kg/d ZEN did not alter maternal weight gain.

Daily oral administration of 1.25 and 3.75 µg/kg/d ZEN resulted in 8% and 11% lower placental weights, respectfully (Figure 4.1B). This correlated with an 11% smaller placental area of dams treated with 3.75 µg/kg/d ZEN (Figure 4.1C). No notable differences in placental weight and area were observed after accounting for fetal Bcrp genotype or sex (Figure 4.1B/C, Supplemental Figure 4.1A/B). In response to 3.75 µg/kg/d ZEN, the number of resorptions per pregnant dam was ~2-fold higher as compared to vehicle control (Figure 4.2A). No statistical changes were observed in the total number of viable fetuses per pregnancy, fetal sex ratio, fetal weight, or fetal crown-rump length following ZEN treatment. Similarly, neither fetal Bcrp genotype nor sex altered fetal weight or crown-rump length in response to ZEN treatment (Figure 4.2B/C; Supplemental Figure 4.1C/D).

BCRP/Bcrp expression can be altered by estrogen receptor mediated signaling (Reviewed in Gorczyca et al. 2020), which is important as mycoestrogens and their metabolites are known ERα and ERß agonists/antagonists (Fitzpatrick et al. 1989; Mueller et al. 2004; Takemura et al. 2007b). Oral administration of 3.75 µg/kg/d ZEN induced the mRNA expression of Erα in Wt placentas by ~50% (Figure 4.3A). Accordingly, administration of 1.25 and 3.75 µg/kg/d ZEN down-regulated

placental Bcrp mRNA expression in Wt fetuses by 53% and 62%, respectfully (Figure 4.3B). ZEN treatment did not significantly impact Bcrp mRNA expression in Het fetuses (data not shown).

Reduced expression of placental differentiation markers in response to zearalenone exposure.

Placental development can similarly be impacted by alterations in estrogen receptor signaling (Bechi et al. 2006; Guo et al. 2012; Rajakumar et al. 2015; Tait et al. 2015; Wang et al. 2016; Xu et al. 2015). Notably, in Bcrp Wt placentas, the mRNA expression of syncytialization markers Cebpa, Catenin ß1, and Gcma was down-regulated following 1.25 and 3.75 µg/kg/d ZEN treatment (Figure 4.4). Interestingly, expression of Gcma tended to be reduced ($p = 0.08$) in Bcrp Het and KO placentas. Likewise, in Bcrp Het and KO placentas, ZEN did not significantly alter the expression of Erα, Cebpa, Catenin ß1, or Gcma.

Spongiotrophoblast markers, including Ascl2, Hand1, Tpbpa, Cx31.1, Igf2, and Pcdh12, were similarly expressed in all three Bcrp genotypes. However, effects of ZEN on their expression were typically only observed in Bcrp Wt placentas (Figure 4.5). All six spongiotrophoblast mRNAs were reduced up to 50% in Bcrp Wt placentas at either or both doses of ZEN. Similar to Wt placentas, the expression of Hand1 and Ascl2 mRNAs was also down-regulated in Bcrp Het placentas following ZEN administration (Figure 4.5). ZEN did not significantly alter the expression of spongiotrophoblast markers in Bcrp Het placentas.

A panel of four markers, Prl2c2, Prl3b1, Ctsq, and Plap, were used to characterize enrichment of giant trophoblasts within the placentas. Similar to the syncytiotrophoblast and spongiotrophoblast markers, the mRNA expression of all four giant trophoblast markers Prl2c2 was also significantly down-regulated in Bcrp Wt placentas by ZEN with little to no change in Bcrp Het or KO placentas (Figure 4.6). Taken together, these data suggest that ZEN induces estrogen receptor signaling and alters placental cell differentiation.

Differential expression of placental transporters in response to zearalenone exposure.

The ability of ZEN and/or its metabolites to differentially regulate the expression of placental transporters has been reported in rats (Koraichi et al. 2012). Prenatal administration of ZEN down-regulated placental Oatp2b1, Oatp4a1, Mdr1b, and Mrp4 mRNA expression in Wt fetuses by up to 63% at either or both doses. Alternatively, placental Oatp5a1 mRNA expression was significantly induced by up to 44% in Wt fetuses exposed to ZEN (Figure 4.7). No notable differences were observed in the mRNA expression of placental Mrp1 and Mdr1a transporters in Wt fetuses exposed to ZEN (data not shown). Although not statistically significant, the mRNA expression of placental Oatp4a1, Mdr1b, and Mrp5 tended to be reduced in Bcrp Het and KO fetuses following ZEN exposure.

Down-regulation of placental antioxidant pathways in response to zearalenone exposure.

In addition to transporters in the placental barrier, antioxidant enzymes are important for proper placenta homeostasis and protection. While not statistically significant, there tended to be lower expression of the heat shock protein Ho-1 and superoxide dismutase-1 and -2 in Bcrp KO placentas. In Bcrp Wt placentas, expression of Ho-1, Sod-1/2, and the transcription factor Nrf2 was reduced 30-40% by ZEN (Figure 4.8). Similarly, 1.25 µg/kg/d ZEN reduced expression of Nrf2, Ho-1, and Sod-1 in Bcrp Het placentas.

4.5 Discussion

Disruption to the development of the endocrine and reproductive systems due to *in utero* xenobiotic exposures has become an increasing concern over the last two decades. The risk of precocious puberty, obesity, and diabetes is heightened through prenatal exposure to endocrine active chemicals. While data regarding human exposure to mycoestrogens is emerging, there is still little known about ZEN's impact during the prenatal period. In the present study, Bcrp heterozygous mice were mated to generate all three fetal Bcrp genotypes (Wt, Het, KO) to determine the influence of Bcrp-mediated disposition and activity of ZEN in the placenta. This model allows for direct comparison of all three genotypes in the same dam following gestational toxicant exposure. Our data demonstrate that prenatal ZEN exposure induced physical changes in both the pregnant dams and their fetuses. Specifically, ZEN increased maternal weight gain, decreased placental weight and area, and increased fetal resorptions. Interestingly, low doses of ZEN only increased the mRNA expression of Erα in Bcrp Wt placentas. Moreover, ZEN administration globally down-regulated syncytialization (Cebpa, Catenin ß1, Gcma), spongiotrophoblast (Ascl2, Hand1, Tpbpa, Cx31.1, Igf2, Pcdh12), and giant trophoblast (Prl2c2, -3b1, Ctsq, Plap) markers – changes most notably observed in Bcrp Wt fetuses. Further, ZEN increased (Oatp5a1) and down-regulated (Oatp2b1, -4a1, Bcrp, Mdr1b, Mrp4) placental drug transporter mRNA expression. Likewise, the mRNA expression of antioxidant genes (Nrf2, Ho-1, Sod-1, -2) was significantly decreased in response to ZEN. There were fewer notable changes in Bcrp Het placentas as only spongiotrophoblast (Ascl2, Hand1), and antioxidant (Nrf2, Ho-1, Sod-1, -2) markers were significantly down-regulated following ZEN exposure. Similarly, Bcrp KO placentas only exhibited significant down-regulation of Sod-1 mRNA expression in response to ZEN. Although the fetal BCRP genotype did not exaggerate the zearalenone insult as expected, collectively, these data demonstrate the ability of environmentally relevant ZEN exposures to alter placental estrogen signaling as well as the molecular and anatomic profiles of the murine placenta.

The overall hypothesis of the present study was that fetal genotypes with Bcrp Het or KO genotype would exacerbate the impact of ZEN due its presumed higher placental accumulation. Administration of ZEN to pregnant rats results in lower fetal concentrations of ZEN and its metabolites when compared to their concentrations in maternal tissues (Bernhoft et al. 2001; Koraichi et al. 2012). These data suggest that the placental barrier limits the transfer of ZEN into the fetal compartment. Recently, our laboratory identified ZEN as a substrate of the human and murine BCRP/Bcrp transporters (Szilagyi et al. 2019; Xiao et al. 2015a). After an intravenous injection of a single dose of 10 mg/kg ZEN, greater placental accumulation and maternal-to-fetal transfer of ZEN and two metabolites was observed in pregnant Bcrp KO mice compared to Wt counterparts (Szilagyi et al. 2019). These data suggest that Bcrp limits *in utero* exposure to ZEN through active efflux of the mycotoxin back toward the maternal circulation. Somewhat surprisingly, in the present study Wt Bcrp placentas exhibited more pronounced molecular changes. This may potentially be explained by 1) ZEN decreasing Bcrp expression in Wt placentas and therefore limiting genotype-specific impact, 2) the endogenous role of Bcrp in placentation and its impact on the molecular integrity of the murine placenta, and/or 3) lower sensitivity of the Bcrp Het and KO genotypes to estrogen-mediated signaling.

Expression of xenobiotic transporters is sensitive to estrogen-mediated signaling (Reviewed in Chan et al. 2013a; Gorczyca et al. 2020; Yacovino et al. 2012). In fact, the promoter region of the human *ABCG2* gene contains estrogen response elements that allow for interaction with estrogen receptors α and ß (Ee et al. 2004b). Exposure of term placental explants and BeWo cells to estrogenic chemicals bisphenol A (BPA; estrogenic plasticizer) and genistein (phytoestrogen) has resulted in significant down-regulation of BCRP mRNA and protein expression (Lin et al. 2017; Sieppi et al. 2016). In the present study, oral administration of ZEN to pregnant Bcrp Het dams induced Erα mRNA expression by 50% and correspondingly down-regulated Bcrp mRNA expression by up to 64% in Bcrp wild type placentas. The ability of ZEN to decrease Bcrp

expression may result in a similar level of mycotoxin accumulation in placental and fetal compartments when compared to the Bcrp knockdown/knockout genotypes. This could explain the absence of Bcrp genotype-specific impact on ZEN activity in the placenta in this study. Ongoing studies are evaluating ZEN concentrations using LC-MS/MS analysis to determine whether Bcrp genotype altered ZEN accumulation in placental and fetal compartments at these low doses.

Although BCRP is largely recognized for its ability to efflux xenobiotics, it is important to consider potential endogenous role in placentation despite the fecundity of Bcrp-knockout mice (Reviewed in Gorczyca et al. 2020). Basal and stimulated syncytialization of primary trophoblast and BeWo cells is characterized by increased expression of BCRP mRNA and protein (Evseenko et al. 2006; Lye et al. 2018; Prouillac et al. 2009). Moreover, the mRNA expression of syncytialization genes (hCGß, Syncytin-1) was significantly down-regulated following siRNA-based genetic knockdown of BCRP in BeWo cells (Evseenko et al. 2007c). Accordingly, gestational pathologies of placental origin, preeclampsia and intrauterine growth restriction, exhibit reduced expression of BCRP and syncytialization genes in the placenta (Evseenko et al. 2007a; Jebbink et al. 2015a; Ruebner et al. 2012). In the present study, control Bcrp Het and KO fetuses tended to have lower expression of syncytialization markers (Cebpa, Catenin ß1, Gcma), spongiotrophoblast markers (Hand1, Tpbpa, Cx31.1, Igf2), and trophoblast giant cell markers (Prl2c2, -3b1, Ctsq) when compared to their wild-type vehicle controls. Possibly, the genetic knockdown of Bcrp limited any further down-regulation of these pathways in response to ZEN.

Studies have begun to show that xenobiotic-induced placental dysfunction, namely hormone secretion and cell fusion, can be attributed to alterations in antioxidant and estrogen receptor signaling mechanisms (Bechi et al. 2006; Guo et al. 2012; Ponniah et al. 2015; Rajakumar et al. 2015; Tait et al. 2015; Wang et al. 2016; Xu et al. 2015; Zhang et al. 2015b). Estrogen receptor α (ERα) and ß (ERß) are expressed in human cytotrophoblasts and syncytiotrophoblasts, respectively

(Bechi et al. 2006). Meanwhile, murine estrogen receptor staining is observed in all placental cell types (decidua, spongiotrophoblast, labyrinth, trophoblast giant cells), albeit to varying degrees of enrichment (Iguchi et al. 1993). BeWo cells (human choriocarcinoma cells), primary cytotrophoblasts, or placental explants exposed to 17ß-estradiol exhibit increased human chorionic gonadotropin ß (hCGß) secretion (marker of syncytialization) and apoptosis, an effect reversed by the estrogen receptor antagonist ICI-182780 (Bechi et al. 2006; Bukovsky et al. 2003b; Cronier et al. 1999; Prouillac et al. 2009). Interestingly, intraperitoneal infusion of estradiol benzoate into pregnant Wistar rats resulted in a dose-dependent decrease in placental weights and enhanced labyrinth degeneration and presence of apoptotic bodies (Matsuura et al. 2004). Although lower than 17ß-estradiol, mycoestrogens and their metabolites have strong binding affinity for both ERα and ERß (17ß-estradiol ERα/ß IC_{50}= ~10nM; ZEN ERα IC_{50} = 240 nM, ERß IC_{50}= 166 nM) (Fitzpatrick et al. 1989; Mueller et al. 2004; Takemura et al. 2007b). Treatment of BeWo cells with ZEN (5-10µM) enhanced cell fusion and increased hCGß secretion (Prouillac et al. 2009). Notably, exposure of pregnant mice to high doses of ZEN (40 mg/kg) from GD 5.5 to 13.5 increased the number of resorptions, decreased placental and fetal weights, reduced placental layers (decidua, junction zone, labyrinth), and disorganized labyrinth vascular spaces (Li et al. 2019a). Exposure of pregnant mice to zeranol, a semi-synthetic zearalenone metabolite, increased apoptosis in the placentas, increased fetal resorption rate, reduced murine fetal size and weight, and decreased expression of cell cycle proteins (Cdk2, Cyclin D1, Bcl-xL) (Perez-Martinez et al. 1995; Wang et al. 2013). Together, these data strongly suggest that prenatal exposure to ZEN and/or its metabolites can significantly alter placenta homeostasis and integrity. In the present study, the Bcrp Hets and KOs did not exhibit overt changes in markers of placental differentiation. This correlated with an absence of increased Erα mRNA expression following ZEN administration, an outcome unique to the Bcrp Het and KO placentas. It is possible that the Bcrp knockdown/knockout may have decreased the overall estrogenic responsiveness of the placenta and accordingly decreased the overall impact of the ZEN insult.

Collectively, these data show that exposure to environmentally relevant ZEN concentrations during the prenatal period alters the expression of drug transporters, markers of placental differentiation, and antioxidant genes in a Bcrp Het mouse model. Disruption of the placental barrier integrity may render the fetus susceptible to xenobiotic exposures and heightened risk for the development of the endocrine and reproductive system abnormalities. Further studies investigating the *ex vivo* consequences of mycoestrogen exposure on human placenta health at relevant exposure levels are urgently needed.

Table 4.1. Primers used for genotyping, sex determination, and gene expression analysis.

Gene	Primer sequence (5' → 3')
Genotyping	
Bcrp/*Abcg2*	**Fwd:** CTTCTCCATTCATCAGCCTCG
	Rev: CAGTCGATGGATCCACTTAGG
	KO: GGAGCAAAGCTGCTATTGGC
Sex Determination	
Sry/*Sry*	**Fwd:** TCATCGGAGGGCTAAAGTGT
	Rev: CAACAGGCTGCCAATAAAAGC
Ssty1/*Ssty1*	**Fwd:** AGAAGGATCCAGCTCTCTATGCT
	Rev: CCAGTTACCAATCAACACATCAC
Reference/Housekeeping Gene	
ß2m/*ß2m*	**Fwd:** ACGTAACACAGTTCCACCCG
	Rev: CAGTCTCAGTGGGGGTGAAT
Uptake Transporters	
Oct2/*Slc22a2*	**Fwd:** ATTTCTGGTGCATACCGGAGTCTCC
	Rev: AGGGGTTCTGACCAAGTCCAGGA
Oatp2b1/*Slc21a9*	**Fwd:** CTCAGGACTCACATCAGGATGC
	Rev: CTCTTGAGGTAGCCAGAGATCA
Oatp4a1/*Slc21a12*	**Fwd:** CCAGCGCTACGTTGTTATGAGAG
	Rev: CAATGAGTGTGGCTTCAGTGG
Oatp5a1/*Slc21a15*	**Fwd:** CACCCTGGGACCAACCTATT
	Rev: ACTCCACCAGTTTCCGATGA
Efflux Transporters	
Bcrp/*Abcg2*	**Fwd:** GCGGAGGCAAGTCTTCGTTGC
	Rev: TCTCTCACTGTCAGGGTGCCCA
Mdr1a/*Abcb1a*	**Fwd:** TGCCCCACCAATTTGACACCCT
	Rev: ATCCAGTGCGGCCTGAACCA
Mdr1b/*Abcb1b*	**Fwd:** GTGTTAAAGGGGCGATGGGCG
	Rev: AGGCTTGGCCAGACAACAGCTT
Mrp1/*Abcc1*	**Fwd:** GCTGTGGTGGGCGCTGTCTA
	Rev: CCCAGGCTCAGCCACAGGAA
Mrp4/*Abcc4*	**Fwd:** CCAGACCCTCGTTGAAAGAC
	Rev: TGAAGCCGATTCTCCCTTC
Mrp5/*Abcc5*	**Fwd:** AGGGCAGCTTGTGCAGGTGG
	Rev: TGCTGTTCCCGCTTCCTTGCT
Labyrinthine Differentiation Markers	
Catenin ß1/*Ctnnb1*	**Fwd:** GGGAACAGTCGAAGTACGCT
	Rev: CAAGCAAAGTCAGCACCACTA
Cebpa/*Cebpa*	**Fwd:** ACTCGGTGCGTCTAAGATGA
	Rev: ACCCTTCATTTTTCTCACGGG
Gcma/*Gcm1*	**Fwd:** GGCGGACAGGCTTTGAAAAA
	Rev: ACTCCTGGAACCAGTCAGTC

Syncytin a/*Syna*	**Fwd:** GCCATGCCAGGGTCTAAATG
	Rev: CGGCTCGAATAGGGTGAGAT
Syncytin b/*Synb*	**Fwd:** AGGCTAACAGCTACCTCAGTT
	Rev: GCTTTCCTGGAGAGAACCTGT
Ly6e/*Ly6e*	**Fwd:** GACCCCTGTCGTAGTCTCAG
	Rev: GGTCCTGGAGGATCACCAAA
Cx26/*Gjb2*	**Fwd:** ATGCTACGACCACCACTTCC
	Rev: TACGGACCTTCTGGGTTTTG
Spongiotrophoblast and Glycogen Cell Markers	
Ascl2/*Ascl2*	**Fwd:** CGAGGATTTTTCGAGGACGC
	Rev: GAAGTGGACGTTTGCACCTT
Hand1/*Hand1*	**Fwd:** TCCACGAACCCTTCCTGTTT
	Rev: TTCTTGGGTCCTGAGCCTTT
Tpbpa/*Tpbpa*	**Fwd:** GAGACGGAAGGCTCCAACAT
	Rev: CGCTCGTTGCCTAACTTCAT
Cx31.1/*Gjb5*	**Fwd:** CCCTCTTTGCTTGTGGTCAT
	Rev: CCTTGAACGAGAGGCTGAAG
Igf2/*Igf2*	**Fwd:** CGTTTGGCCTCTCTGAACTC
	Rev: GACGACTTCCCCAGATACCC
Pcdh12/*Pcdh12*	**Fwd:** CTTCACCTCATCACGCTCAA
	Rev: TGCCCTCTGTCCTCTGCTAT
Giant Trophoblast Markers	
Prl2c2/*Prl2c2*	**Fwd:** TGAGGAATGGTCGTTGCTTT
	Rev: TCTCATGGGGCTTTTGTCTC
Prl3b1/*Prl3b1*	**Fwd:** CCAACGTGTGATTGTGGTGT
	Rev: TCTTCCGATGTTGTCTGGTG
Prl3d1/*Prl3d1*	**Fwd:** AGCCTACATTGTGGTGGATCT
	Rev: ATACAGGTCTTCAGTGGGCA
Ctsq/*Ctsq*	**Fwd:** GGAAACGTGCACTTGGTAGT
	Rev: AGTGGGATCAGTTTGCCTGT
Plap/*Alpl*	**Fwd:** TGAGGGCAATGAGGTCACAT
	Rev: CCTCTGGTGGCATCTCCTTA
Antioxidant Markers	
Nrf2/*Nfe2l2*	**Fwd:** AATTCAGCCGGCCCAGCACA
	Rev: TCCAGGGCAAGCGACTCATGG
Ho-1/*Hmox1*	**Fwd:** GGTGACAGAAGAGGCTAAGACCGC
	Rev: GCAGTATCTTGCACCAGGCTAGCA
Sod1/*Sod1*	**Fwd:** CACTTCGAGCAGAAGGCAAG
	Rev: CGGGCCACCATGTTTCTTAG
Sod2/*Sod2*	**Fwd:** TAACGCGCAGATCATGCAGCTG
	Rev: AGGCTGAAGAGCGACCTGAGTT
Estrogen Receptor	
Erα/*Esr1*	**Fwd:** GACCAGATGGTCAGTGCCTT
	Rev: ACTCGAGAAGGTGGACCTGA

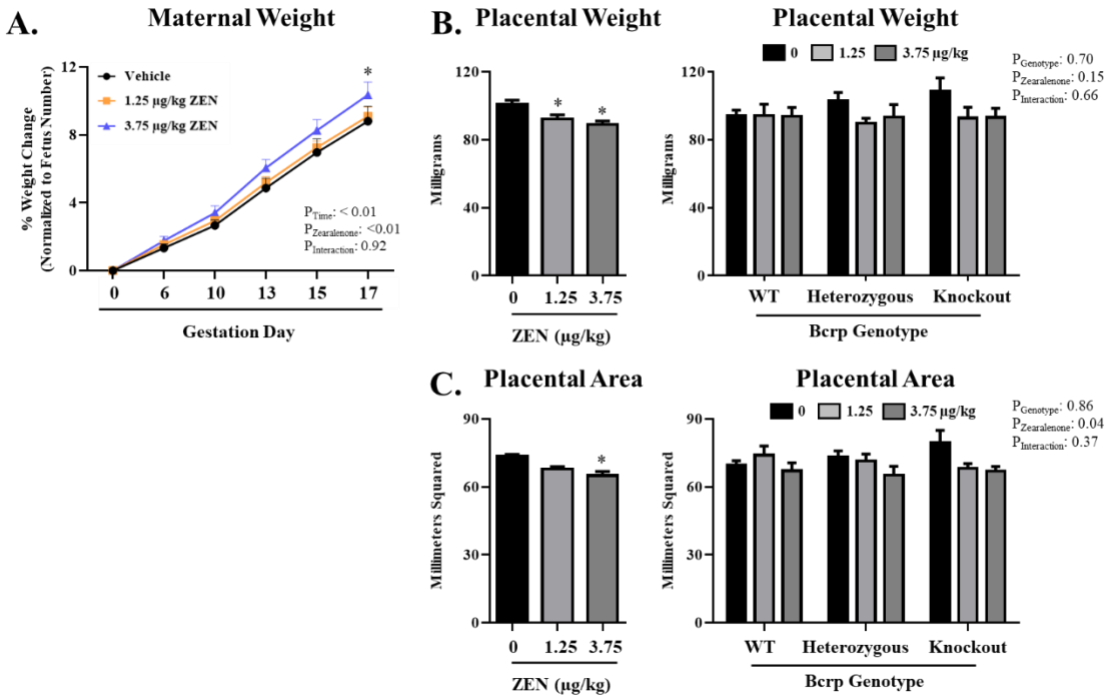

Fig 4.1 Changes in maternal weight and placental size following prenatal zearalenone administration. Bcrp Het dams were treated with zearalenone (1.25, 3.75 µg/kg/d; 5ml/kg) absorbed into 0.5 g of soy-free peanut butter from GD6-17. (A) Maternal body weight was measured on mating day, GD6, -10, -13, -15, and -17. Body weight was normalized to litter size. (B/C) Placental weight and area were measured on GD17. Data are presented as mean (6-8 dams per treatment) ± SE. * $p \leq 0.05$ compared with vehicle-treated dams. No differences in placental weight and area were observed between fetal Bcrp genotypes following zearalenone treatment. Data are expressed as mean (N=3-8 litters per genotype) ± SE.

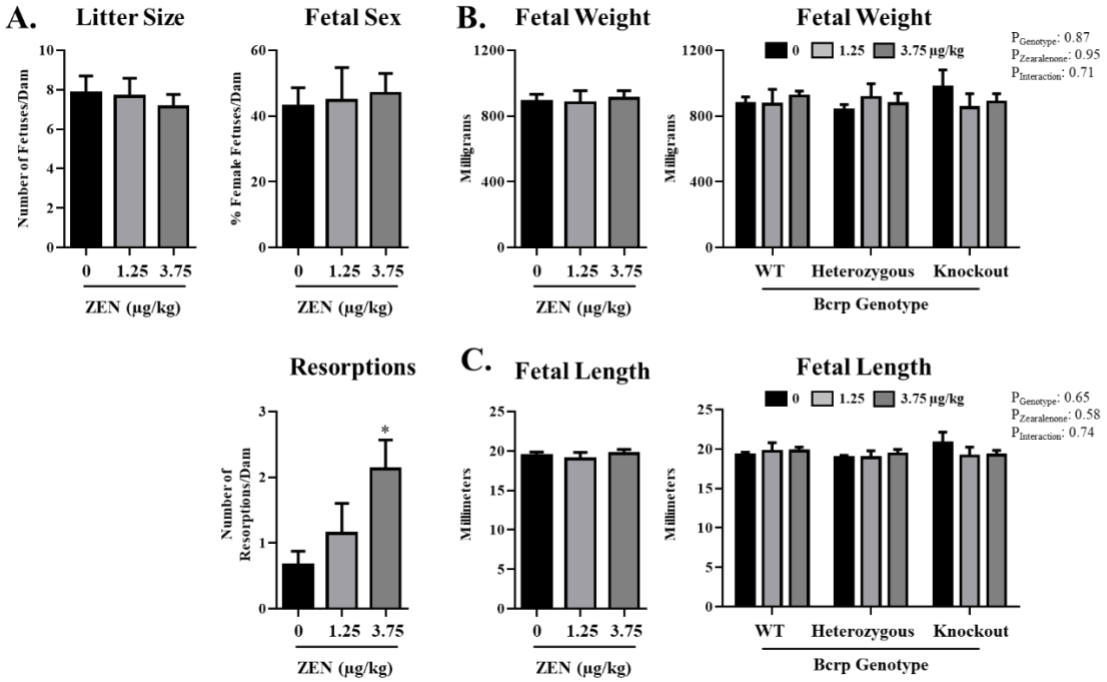

Fig 4.2. Changes in gestational outcomes following prenatal zearalenone administration.

(A) Fetal sex, litter size, and number of resorptions, (B) fetal weight, and (C) fetal crown-rump length were noted on GD17 after prenantal treatment with vehicle or zearalenone (1.25, 3.75 µg/kg/d; 5ml/kg; GD6-17). (A) Fetus sex was determined by qPCR via the mRNA expression of male-specific genes, Sry and Ssty1. Data are presented as mean (6-8 dams per treatment) ± SE. * $p \leq 0.05$ compared with vehicle-treated dams. No differences in (B) fetal weight and (C) crown-rump length were observed between fetal Bcrp genotypes following zearalenone administration. Data are expressed as mean (N=3-8 litters per genotype) ± SE.

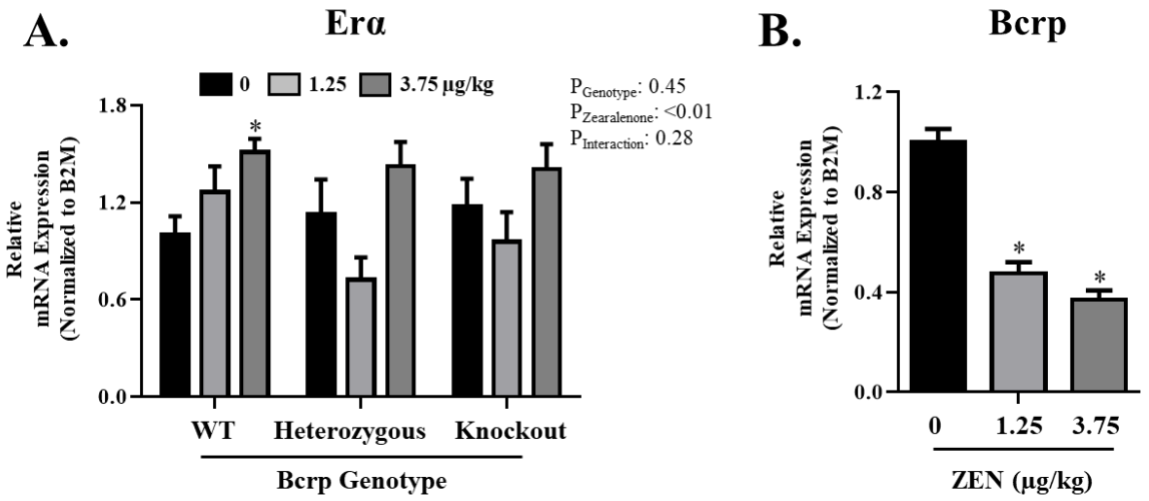

Fig 4.3. Expression of placental estrogen receptor alpha and Bcrp following prenatal zearalenone administration. Placental mRNA expression of (A) estrogen receptor alpha and (B) Bcrp was quantified in vehicle and zearalenone-treated (1.25, 3.75 µg/kg/d; 5ml/kg; GD6-17) dams. Bcrp expression in (B) represents mRNA levels in WT placentas only. Ct values were converted to ΔΔCt by comparing to the reference gene ß2m. Data are expressed as mean (N=3-8 litters per genotype) ± SE. * $p \leq 0.05$ compared with litters treated with genotype-specific vehicle control.

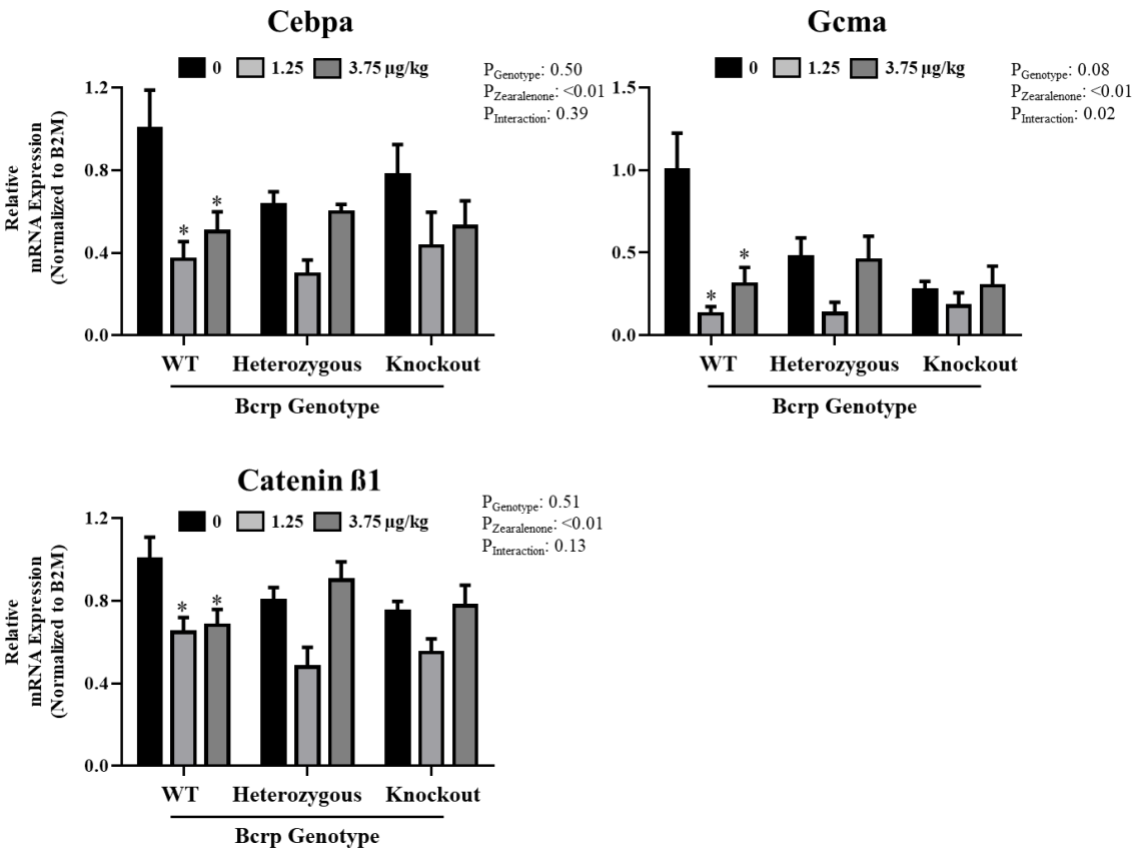

Fig 4.4. Expression of placental labyrinth markers following prenatal zearalenone administration. Placental mRNA expression of labyrinth markers was quantified in vehicle and zearalenone-treated (1.25, 3.75 µg/kg/d; 5ml/kg; GD6-17) dams. Ct values were converted to ΔΔCt by comparing to the reference gene ß2m. Data are expressed as mean (N=3-8 litters per genotype) ± SE. * $p \leq 0.05$ compared with litters treated with genotype-specific vehicle control.

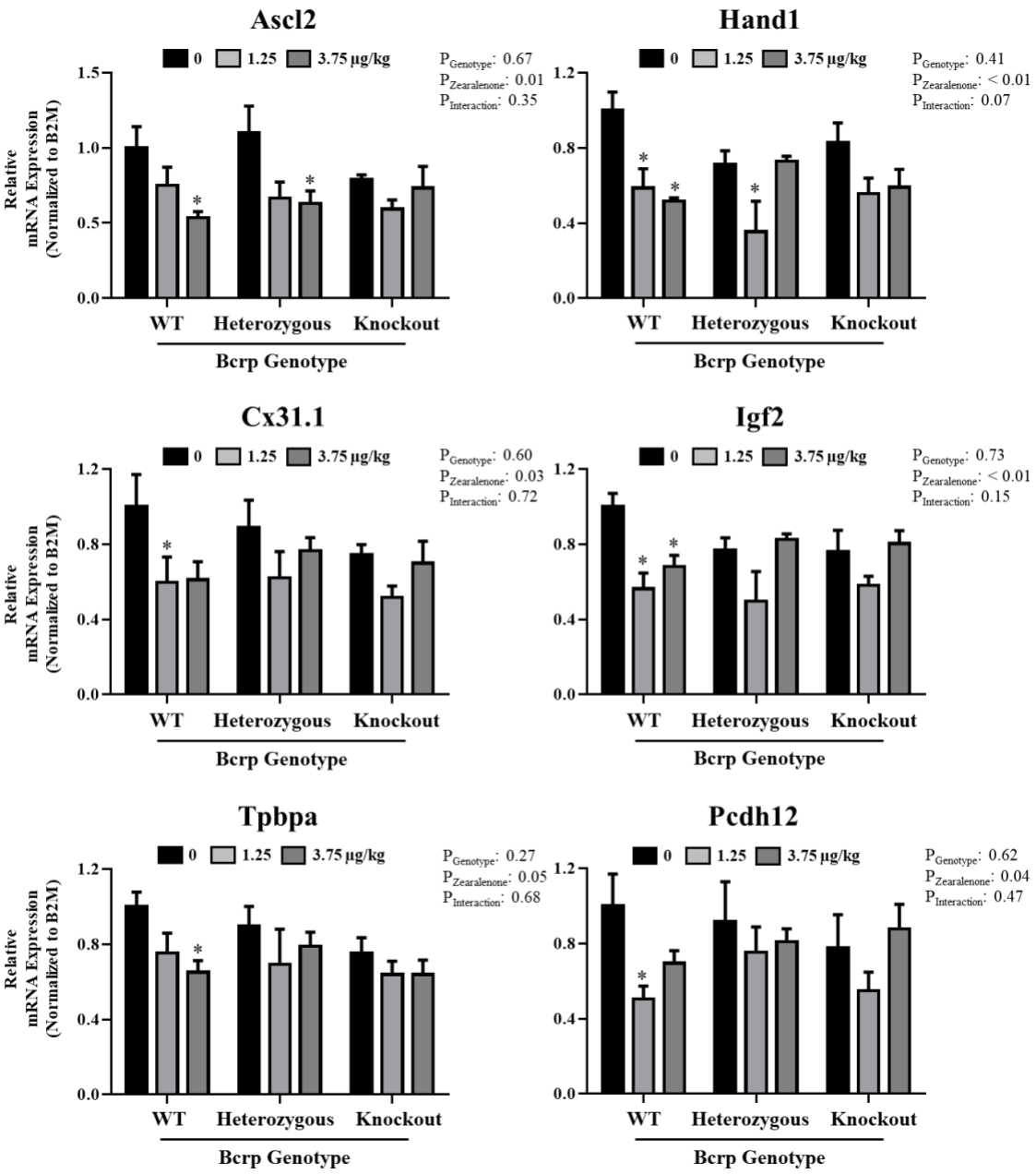

Fig 4.5. Expression of placental spongiotrophoblast markers following prenatal zearalenone exposure. Placental mRNA expression of spongiotrophoblast markers was quantified in vehicle and zearalenone-treated (1.25, 3.75 µg/kg/d; 5ml/kg; GD6-17) dams. Ct values were converted to ΔΔCt by comparing to the reference gene ß2m. Data are expressed as mean (N=3-8 litters per genotype) ± SE. * $p \leq 0.05$ compared with litters treated with genotype-specific vehicle control.

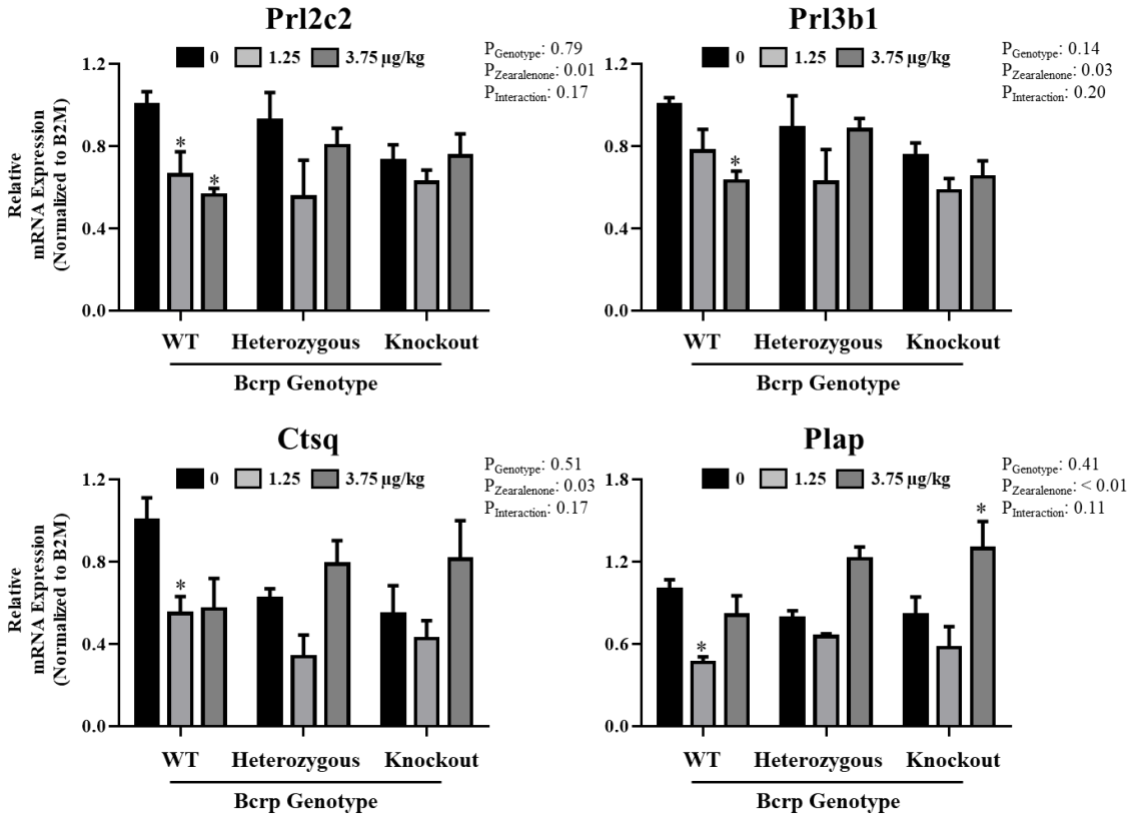

Fig 4.6. Expression of placental giant trophoblast markers following prenatal zearalenone exposure. Placental mRNA expression of giant trophoblast markers was quantified in vehicle and zearalenone-treated (1.25, 3.75 µg/kg/d; 5ml/kg; GD6-17) dams. Ct values were converted to ΔΔCt by comparing to the reference gene ß2m. Data are expressed as mean (N=3-8 litters per genotype) ± SE. * $p \leq 0.05$ compared with litters treated with genotype-specific vehicle control.

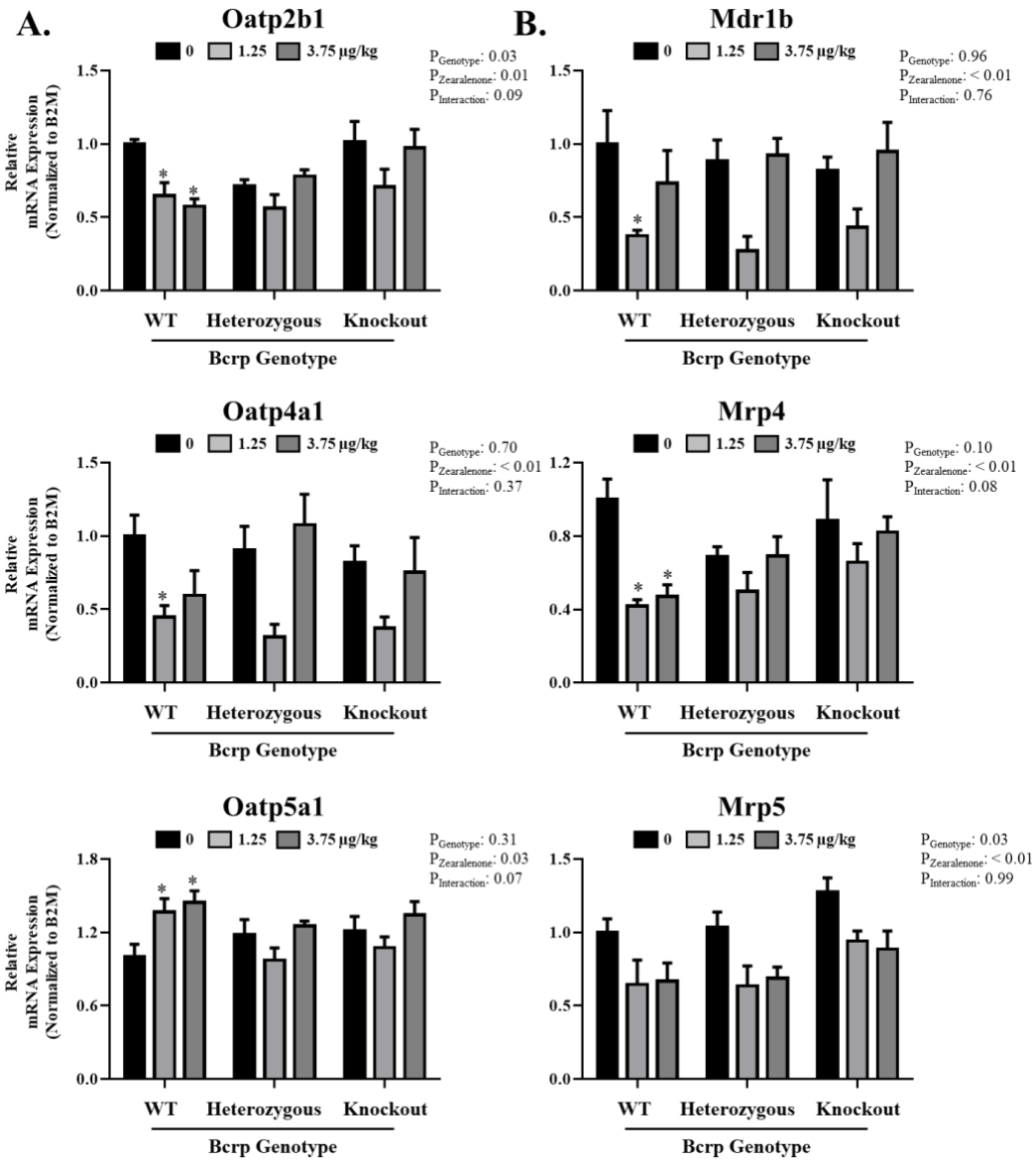

Fig 4.7. Expression of placental uptake and efflux transporters following prenatal zearalenone exposure. Placental mRNA expression of (A) uptake and (B) efflux transporters was quantified in vehicle and zearalenone-treated (1.25, 3.75 µg/kg/d; 5ml/kg; GD6-17) dams. Ct values were converted to ΔΔCt by comparing to the reference gene ß2m. Data are expressed as mean (N=3-8 litters per genotype) ± SE. * $p \leq 0.05$ compared with litters treated with genotype-specific vehicle control.

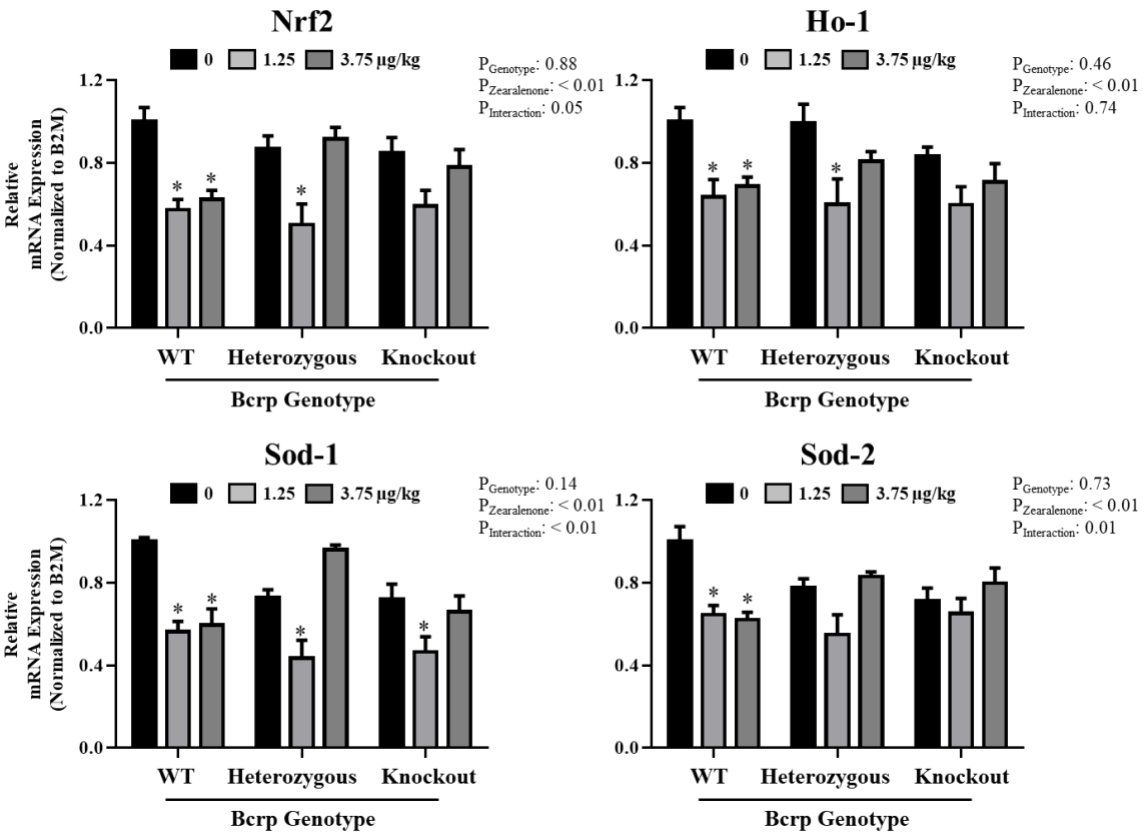

Fig 4.8. Expression of placental antioxidant markers following prenatal zearalenone exposure. Placental mRNA expression of antioxidant markers was quantified in vehicle and zearalenone-treated (1.25, 3.75 µg/kg/d; 5ml/kg; GD6-17) dams. Ct values were converted to ΔΔCt by comparing to the reference gene ß2m. Data are expressed as mean (N=3-8 litters per genotype) ± SE. * $p \leq 0.05$ compared with litters treated with genotype-specific vehicle control.

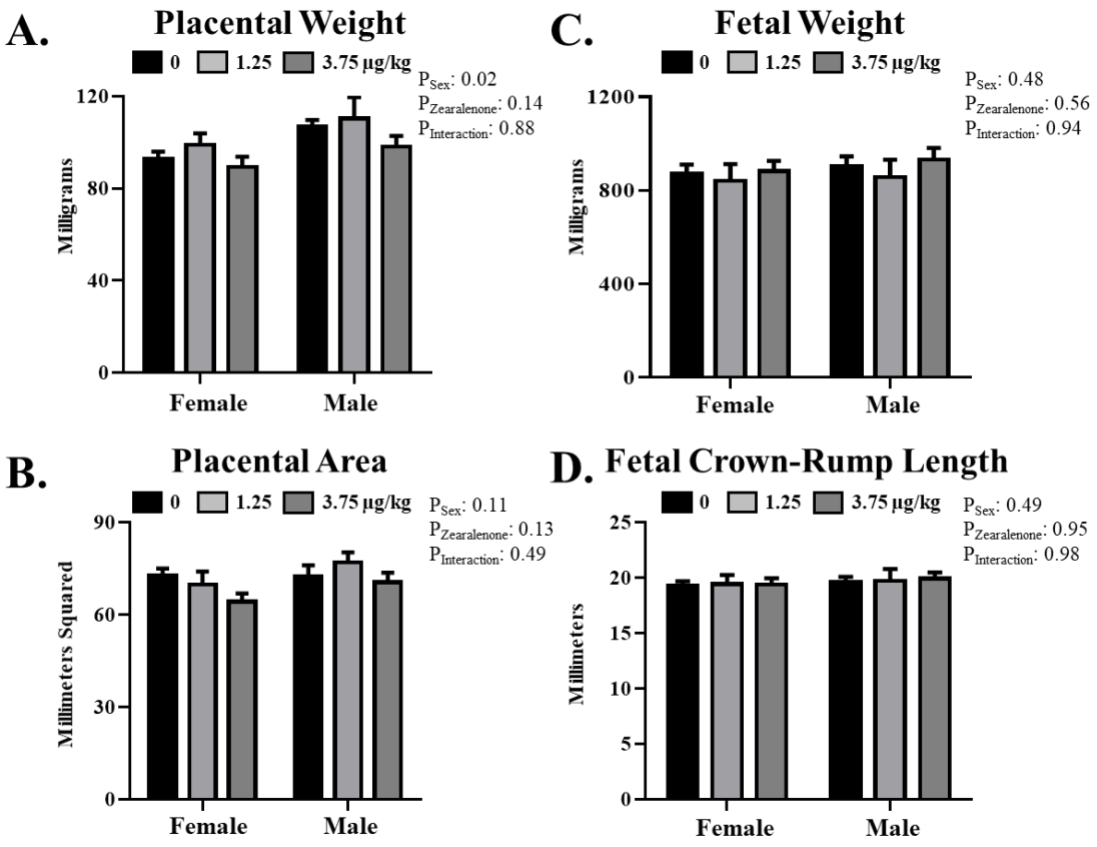

Supplemental Fig 4.1. Sex-specific changes in placental and fetal size following prenatal zearalenone administration. Fetus sex was determined by qPCR via the mRNA expression of male-specific genes, Sry and Ssty1. (A/B) Placental weight and area were measured on GD17. No differences in placental weight and area were observed between fetal sexes following zearalenone treatment. (C/D) No differences in (C) fetal weight and (D) crown-rump length were observed between fetal sexes following zearalenone administration. Data are expressed as mean (N=3-8 litters per genotype/sex) ± SE.

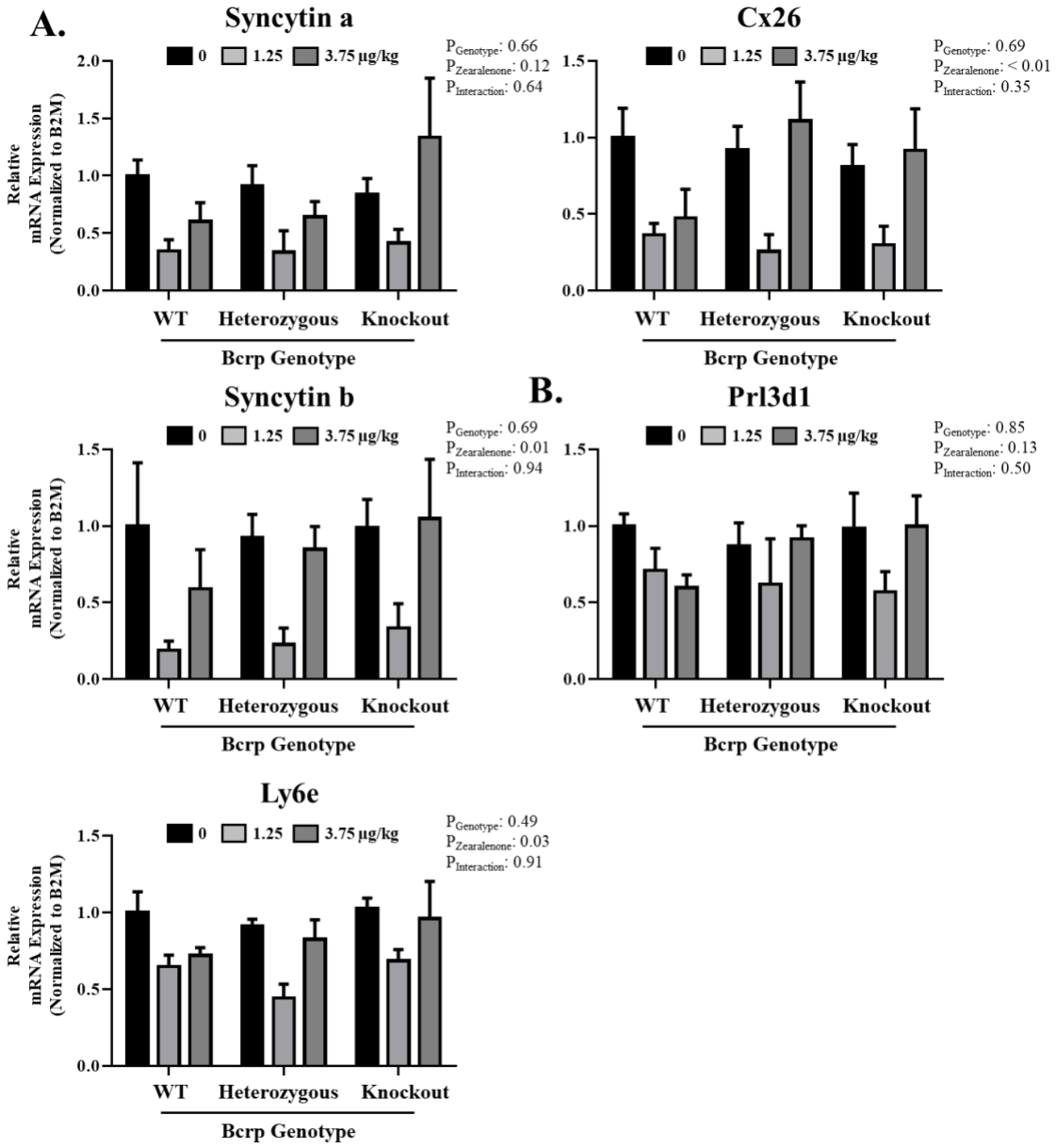

Supplemental Fig 4.2. Expression of placental differentiation markers following prenatal zearalenone exposure. Placental mRNA expression of (A) syncytialization and (B) giant trophoblast markers was quantified in vehicle and zearalenone-treated (1.25, 3.75 µg/kg/d; 5ml/kg; GD6-17) dams. Ct values were converted to ΔΔCt by comparing to the reference gene ß2m. Data are expressed as mean (N=3-8 litters per genotype) ± SE. * $p \leq 0.05$ compared with litters treated with genotype-specific vehicle control.

CHAPTER 5: OVERALL DISCUSSION

Summary

The purpose of this dissertation was to characterize the impact of *endogenous* (i.e., hypoxia, cyclic adenosine monophosphate) and *exogenous* (i.e., mycoestrogen zearalenone) factors on placentation and the placental barrier. Hypoxia is a physiological regulator of placental function and xenobiotic and nutrient disposition. Secondary messengers, such as cyclic nucleotides, are known transporter substrates and govern molecular signaling regulating syncytialization or cell fusion within the placenta. Zearalenone, an estrogenic mycotoxin, can cross the placental barrier and disrupt fetal development. Disruption of placental transporter function can negatively impact the feto-placental unit by: 1) altering transplacental disposition of xenobiotics and 2) influencing the intracellular concentration of cyclic nucleotides and in turn, syncytialization. Elucidating transporter functions within the placenta contributes to our understanding of developmental biology and may be relevant for the pathogenesis of placenta-associated gestational disorders.

I hypothesized that altered expression of transporters could not only influence the maternal-fetal disposition of chemicals, but also the process of placentation by affecting the accumulation of endogenous cellular mediators. Three specific aims were developed to address this hypothesis: 1) Characterize the regulation of placental SLC and ABC transporter expression under low oxygen conditions (**Chapter 2**), 2) Assess the contribution of transporter-mediated efflux of cyclic nucleotides on syncytialization (**Chapter 3**), and 3) Determine the effect of zearalenone on placental differentiation and transporter genes (**Chapter 4**).

The first aim characterized the ability of physiologically-relevant concentrations of oxygen to alter transporter expression in the human placenta. Previous studies observed the ability of low oxygen conditions to alter human BCRP and MDR1 transporter expression in the placenta, albeit with

conflicting results (Javam et al. 2014; Krishnamurthy et al. 2004; Lye et al. 2013). Our laboratory has also previously observed a reduction of BCRP mRNA, protein, and function in BeWo cells after exposure to the hypoxia mimetic, cobalt chloride, or 3% O_2 (Francois et al. 2017). We employed two placental models, BeWo choriocarcinoma cells and term placental explants, to directly compare the expression of drug transporters in response to hypoxia. Activation of HIF-1α signaling was observed in both models following hypoxic incubations. In BeWo cells, hypoxia down-regulated (ENT1, OATP4A1, OCTN2, BCRP, MRP2/3/5) and induced (CNT1, OAT4, OATP2B1, SERT, SOAT, MRP1) drug transporter mRNA expression. Similarly, placental explants exposed to hypoxia exhibited down-regulation of BCRP and MRP5 as well as an induction of MRP1 mRNA expression. In explants, uptake transporters were decreased or unchanged. Both models revealed global reduction in AHR, NRF2, and RXRα mRNAs at low oxygen concentrations which may mediate differential expression of transporters. Together, these data confirm that hypoxia differentially regulates transporter expression across experimental human placenta models.

The second aim sought to determine the ability of MRP efflux drug transporters to regulate intracellular concentration of cyclic nucleotides and in turn, placental syncytialization. Previous studies demonstrated the ability of MRP drug transporters to efflux cyclic adenosine monophosphate (cAMP), a key secondary messenger involved in regulating placental cell fusion, but none examined their direct role in syncytialization (Biondi et al. 2010; Jedlitschky et al. 2000; Meyer Zu Schwabedissen et al. 2005a; Nagashige et al. 2003). Here, I utilized MRP-specific pharmacologic (MK-571) and genetic (MRP5 shRNA) loss-of-function approaches and demonstrated enhanced syncytialization in placental explants and BeWo cells. Treatment of BeWo cells with MK-571 increased the intracellular concentration of cAMP. This coincided with induced expression of cell fusion and hormone markers in both placental models. Similarly, combination treatments of MK-571 with cAMP stimulants, 1) permeable cAMP analog, 8-Bromo-cAMP, 2)

activator of cAMP synthesis, forskolin, and 3) inhibitor of cAMP breakdown, IBMX further induced the expression of cell fusion and hormone markers when compared to the stimulators alone. Moreover, MRP5 knockdown cells exhibited significantly higher expression of cell fusion and hormone markers following treatment with stimulants when compared to control cells. MRP5-knockdown cells were also larger in size (including greater numbers of multinucleated cells) and exhibited decreased staining of E-cadherin, pointing to enhanced syncytialization. Together, these data demonstrate for the first time the ability of MRP transporters to regulate trophoblast cell fusion and offer a novel mechanism regulating placentation.

The third aim examined the impact of prenatal exposure to the estrogenic mycotoxin zearalenone on placental differentiation markers and xenobiotic transporter expression. Previous studies by our laboratory identified zearalenone as a substrate of the human and mouse BCRP/Bcrp transporter (Szilagyi et al. 2019; Xiao et al. 2015a). While zearalenone does cross the placental barrier, the fetal concentration of the mycotoxin is much lower when compared to maternal tissue suggesting that placental efflux transporters may play a protective role in limiting fetal exposure (Appelgren et al. 1982; Bernhoft et al. 2001; Koraichi et al. 2012; Warth et al. 2019). Here, we mated female and male Bcrp heterozygous mice to generate all three placental/fetal Bcrp genotypes (Wt, Het, KO) to evaluate whether Bcrp protects against zearalenone-induced toxicity. This was an advantageous experimental approach to study placental/fetal genotypes. It is possible that the heterozygous status of the dams may have increased overall ZEN absorption in the intestines compared to wild-type dams. Nonetheless, treatment with zearalenone increased maternal weight gain, decreased placental weight and area, and increased fetal resorptions. Zearalenone globally down-regulated placental differentiation markers of the labyrinth, junctional, and decidual zones in Wt fetuses. Exposure to zearalenone differentially regulated placental drug transporter expression including down-regulation (Oatp2b1, Oatp4a1, Bcrp, Mdr1b, Mrp4) and up-regulation (Oatp5a1) in Wt fetuses. Furthermore, zearalenone globally down-regulated placental markers of apoptosis

and cellular stress in Wt and Het fetuses. Although the fetal Bcrp genotype did not exaggerate the zearalenone responses as I had expected, together, these data suggest that prenatal zearalenone exposure alters the placental development (i.e. decreased weight/area), differentiation, and transporter homeostasis during pregnancy and increases resorptions.

Hypoxia

Our data demonstrate the ability of low oxygen tension to induce hypoxia molecular signaling and alter the transcription factor and drug transporter mRNA expression in human placenta models. Although gestational changes in placental oxygenation (1st trimester: 1-3% O_2; 2nd/3rd trimester: 8-10% O_2) coincide with altered transporter expression (Lye et al. 2013; Mathias et al. 2005; Yeboah et al. 2006), conflicting results have been reported in *in vitro* and *ex vivo* studies (Fouassier et al. 2007; Javam et al. 2014; Krishnamurthy et al. 2004; Lv et al. 2015; Lye et al. 2013; Sakulterdkiat et al. 2012; Zhu et al. 2005; Zhu et al. 2012a). Differences in species, cellular model, tissue-type, gestational stage of placenta, and genetic variability can all highly influence the sensitivity and responsiveness to low oxygen tension. Specifically, the Matthews laboratory observed the disparate ability of low oxygen tension to alter BCRP expression in first and term placental explants (Javam et al. 2014; Lye et al. 2013). While first trimester explants revealed significant down-regulation of BCRP mRNA expression in response to hypoxia, exposure of term explants to similar conditions exhibited no such change. At first glance, the major confounding factor in between the two studies is the gestational stage of the placental explants utilized. However, our data demonstrated the ability of hypoxia to down-regulate BCRP expression in term placental explants, suggesting additional factors may have contributed to the disparate results.

Differences in genetic variability and maternal demographics of placental explants may have contributed to the disparate results. The expression level of the BCRP transporter has been shown to be significantly modified by single nucleotide polymorphisms. Specifically, our laboratory has

found that placentas with the nonsynonymous variant rs2231142 (421 A/A and 421 A/C), present in 17% of pregnancies, had 50% less BCRP protein when compared to wild-type (421 C/C) (Bircsak et al. 2018). Additionally, the C421A SNP was most frequent in Hispanic and Asian populations, occurring at 20 and 32%, respectfully (Hispanic N=11, Asian N=9) (Bircsak et al. 2018). It is plausible that increased presence of the single nucleotide polymorphism C421A in sample tissues tested may have prevented hypoxia-mediated regulation and/or impacted the basal BCRP expression level. Although the maternal demographics were not provided by the Matthews laboratory, additional investigation into maternal ethnicity and/or screening for the nonsynonymous variant of tested samples is warranted.

Moreover, a closer examination of the cell culture methodology revealed differences in insulin supplementation of growth medium. Altered BCRP expression in response to hypoxia was observed in placental explants cultured in growth medium supplemented with either insulin or fetal bovine serum (FBS) (Lye et al. 2013). Alternatively, placental explants which did not exhibit hypoxia-mediated changes in BCRP expression were cultured in growth medium supplemented with both insulin and FBS (Javam et al. 2014). Under standard cell culture conditions (20% O_2), HIF-1α expression has been demonstrated to be inducible by various stimuli including cytokines, growth factors, and hormones (Gorlach et al. 2001; Hellwig-Burgel et al. 1999; Richard et al. 2000; Wolf 2005; Zelzer et al. 1998). Previous reports have described crosstalk between hypoxia and insulin signaling pathways (Biswas et al. 2013; Feldser et al. 1999; Fukuda et al. 2002; Regazzetti et al. 2009; Taniguchi et al. 2013; Treins et al. 2002; Wang et al. 2007; Zelzer et al. 1998). Insulin and insulin-like growth factor increase HIF-1α protein expression in a dose dependent manner across tissues and induce the expression of prototypical HIF-1α target genes, GLUT1 and VEGF (Biswas et al. 2013; Fukuda et al. 2002; Treins et al. 2002; Wang et al. 2007; Zelzer et al. 1998). Interestingly, a time course revealed that chronic hypoxia (BE(2)C cells) or a prolonged incubation with insulin (ARPE-19 cells) actually lead to the reduction of HIF-1α protein after an initial

induction (Lin et al. 2011; Treins et al. 2002). It is now understood that when HIF-1α protein level reaches a certain threshold a negative feedback mechanism takes over where the HIF-1α proteins negatively regulate HIF-1α gene expression by activating antisense HIF-1α transcripts. These antisense transcripts bind to the 3'UTR region of HIF-1α mRNA and expose AU-rich elements which in turn increase mRNA degradation and ultimately reduce HIF-1α protein levels (Uchida et al. 2004). It is plausible that the additional insulin supplementation by Javam et al., 2014 resulted in a faster induction of HIF-1α protein and subsequent destabilization leading to disruption of downstream signaling and absence of BCRP expression change. Serum insulin levels have been shown to progressively rise as gestation progresses (Sonagra et al. 2014). Consequently, studies utilizing lower levels of insulin supplementation better recapitulate first trimester conditions. Future studies examining the regulatory impact of hypoxia should consider using charcoal-stripped and/or serum-free cell culture medium to limit unwarranted insulin-mediated activation of HIF-1α signaling.

Our present study and previous literature examined the contribution of HIF-1α signaling on transporter expression through stimulation of hypoxia signaling with low oxygen levels or hypoxia mimetics such cobalt chloride (Javam et al. 2014; Krishnamurthy et al. 2004; Lye et al. 2013). However, we have shown that exposure of BeWo cells or placental explants to hypoxia alters the expression of other transcription factors, such as NRF2 and AHR, that are known regulators of transporter expression (Adachi et al. 2007; Neradugomma et al. 2017). Altered expression of these transcriptional factors may significantly contribute to the observed changes in transporter expression under hypoxic conditions. Future mechanistic studies should consider chromatin immunoprecipitation assays to further characterize the binding of AHR and NRF2 to the associated promoter regions of the BCRP transporter under hypoxic conditions.

Chronic hypoxia, due to inadequate extravillous trophoblast invasion and improper spiral artery remodeling, has been associated with the pathogenesis of preeclampsia and intrauterine growth restriction (IUGR) during pregnancy (Reviewed in Chaddha et al. 2004). Notably, preeclamptic human placentas exhibit increased (MRP1) and decreased (OCTN2; BCRP) expression of uptake and efflux drug transporters (Chang et al. 2011; Evseenko et al. 2007a; Jebbink et al. 2015a; Williams et al. 2012). These findings are in accordance with our current study in which hypoxic conditions result in an induction of MRP1 and down-regulation of OCTN2 and BCRP mRNA expression in BeWo cells and/or healthy, term placental explants. This further supports the reliability and translatability of data obtained with current *in vitro* and *ex vivo* placental models utilized in our studies. Furthermore, our data indicate that low oxygen tension influences the expression of multiple uptake and efflux transporters, many of which are yet to be examined in pregnancies complicated with preeclampsia and intrauterine growth restriction. Future studies should consider treatment of isolated primary cytotrophoblast or placental explants in media supplemented with serum obtained from healthy vs. preeclamptic pregnancies. Such studies would aid in 1) enhanced characterization of altered drug transporter profiles under pathological conditions and 2) screening and identification of additional factors present in maternal serum which may alter drug disposition and placental integrity. Expanded screening of placenta-associated gestational disorders can aid in drug delivery and offer new therapeutic targets to support normal fetal development.

While changes in transporter mRNA and protein expression profiles can identify potentially altered transport dynamics, novel functional studies are also required to develop a complete profile of transplacental disposition under hypoxic and pathological conditions. Semi-permeable transwell inserts are widely utilized as tissue barrier models to screen bidirectional drug transport across a cell monolayer. Regarding the human placenta, a subclone of BeWo cells, BeWo b30, and isolated primary cytotrophoblasts have been employed as *in vitro* transport models to determine the apical-

to-basolateral and basolateral-to-apical transfer of various test substrates. Both models form highly differentiated polarized monolayers, tight junctions, and apical/basolateral localization of drug transporters (Hemmings et al. 2001; Huang et al. 2016; Li et al. 2013a; Liu et al. 1997). These models can be expanded to assess the relative transplacental disposition of different drug candidates under hypoxic conditions or pathological diseases. Specifically, isolated primary cytotrophoblasts and BeWo b30 cells can be grown under hypoxic conditions until a monolayer is reached. This will induce the hypoxia-mediated changes in transporter expression and allow for greater translatability of transcellular distribution of substrates across the placental trophoblast. Alternatively, both cell models could be grown under normal conditions until a monolayer is formed and primed with low oxygen tension or cobalt chloride, a hypoxia mimetic, for 24 h to induce transporter changes. Utilizing these models to screen commonly prescribed gestational drugs (i.e. glyburide, nitrofurantoin, cimetidine, acyclovir) could offer an enhanced understanding of their safety profile during early gestation and pregnancies at high altitude or complicated with preeclampsia.

Placentation and MRP Transporters

Our data suggest that MRP transporters function as a negative regulator of syncytialization by actively removing intracellular cyclic nucleotides and limiting downstream protein kinase A-mediated signaling. Although utilization of BeWo choriocarcinoma cells and placental explants allows for a thorough mechanistic analysis of MRP function in syncytialization, the translatability and relevance of our data could be further strengthened by additional *in vitro* and *in vivo* approaches. BeWo cells and placental explants contain innate confounding factors such as cancer-related methylation profiles and presence of numerous cell types, respectfully, which may impact cAMP-based signaling and trophoblast differentiation (Huppertz 2008; Novakovic et al. 2011). Isolated primary cytotrophoblasts offer individual assessment of the primary cell type involved in syncytialization without the confounding factors associated with whole tissue and immortalized cell line models. Still, the expression of drug transporters in primary cytotrophoblasts has not been

fully characterized and needs to be addressed prior to initiation of MRP-centered cell fusion studies. With respect to MRP transporters, the only isoforms that has been tested for and shown to be expressed in primary cytotrophoblasts is MRP1 and MRP5 (Atkinson et al. 2003). Still, the ability of isolated primary cytotrophoblasts to undergo *de novo* syncytialization in culture (Li et al. 2015) ultimately warrants additional investigation into pharmacologic (MK-571) and genetic (siRNA) loss of function approaches to test MRP-mediated regulation of trophoblast differentiation. It is feasible that if MRP transporters are highly expressed in primary cytotrophoblasts, inhibiting their function will also result in a higher rate and extent of trophoblast differentiation.

Another approach to test the relevance of our current study would be a more comprehensive evaluation of MRP5 knockout mice. Although an MRP5 knockout mouse model did not demonstrate any overt outcomes concerning fertility or fetal viability, more pregnancy-centered analyses are warranted (Wijnholds et al. 1999). Analysis of placental and fetal endpoints discussed in our zearalenone study may reveal more granular deleterious phenotypes associated with the knockout. Similarly, immunohistochemical analysis of mouse placental zones through hematoxylin and eosin staining may reveal unbeknownst structural malformations. Alternatively, it is also possible that MRP substrate overlap and/or the presence of two syncytiotrophoblast layers would prevent MRP5 knockout mice from exhibiting any pregnancy-related phenotype. The two synyctiotrophoblast cell layers in the mouse placenta may function in tandem to ensure proper hormone secretion as well as nutrient and waste exchange between the fetal and maternal circulations. In the case of one synyctiotrophoblast layer malfunctioning, the redundancy of the second layer would allow for the overall functionality and structure of the placenta to remain intact and prevent adverse fetal outcomes. Still, even in the absence of a basal pregnancy-related phenotype in MRP5 knockout mice, it would be interesting to see how these animals respond to classical developmental and reproductive toxicants such as cadmium chloride and polychlorinated biphenols. It is plausible that with altered syncytialization layers, the knockout mice may not only

exhibit altered drug disposition but also become more sensitized to toxicant-induced changes concerning hormone secretion, placental differentiation and growth, and adverse fetal outcomes.

Moreover, MRP5 knockout animals may be utilized to generate improved models of preeclampsia. Current preeclampsia rodent models, such as endothelial nitric oxide synthase (eNOS) and catechol-*O*-methyltransferase (COMT) knockout mice, induce maternal preeclampsia outcomes such as hypertension, proteinuria, and uterine artery dysfunction which ultimately result in placental dysfunction and intrauterine growth restriction (Reviewed in Marshall et al. 2018). Generation of MRP5 and eNOS/COMT dual knockout mouse models may rescue or ameliorate deleterious fetal outcomes. Knocking out MRP5 may increase the intracellular accumulation of cyclic nucleotides, enhance syncytialization, hormone secretion, and nutrient/waste exchange to potentially improve placental dysfunction and fetal outcomes.

Understanding the impact of pharmaceuticals and environmental contaminants on human trophoblast differentiation and MRP transporter function can further the screening sensitivity of potential toxicants in developmental and reproductive toxicology studies. We have demonstrated that changes in intracellular cAMP level, syncytialization marker expression, cell size, percent multinucleation, and staining intensity of the tight junction protein, e-cadherin, can be effectively combined as a screening tool to investigate changes in trophoblast differentiation and fusion. These endpoints can be expanded to include cell cycle analysis following toxicant insult. It is widely understood that upon differentiation, syncytiotrophoblasts exist in a non-proliferative post-mitotic G_0 state (Chuprin et al. 2013; Lu et al. 2017; Taylor et al. 1991). Analysis of cell cycle marker expression and flow cytometry-based sorting can promote the identification of syncytiotrophoblasts and generate a more comprehensive cell population profile. Moreover, previous studies observed a link between syncytialization and apoptosis, albeit with conflicting results (Al-Nasiry et al. 2006; Chen et al. 2011b; Wei et al. 2012). More studies are needed to compare the relative sensitivity of

cytotrophoblasts and terminally differentiated syncytiotrophoblasts to toxicant-mediated insult. Still, immunofluorescence-based screening of syncytiotrophoblasts can be coupled with cellular stains targeting apoptotic nuclei to further characterize cellular stress. Together, identification of xenobiotics targeting MRP function and/or trophoblast differentiation can significantly increase the predictive power of safety assessments and allow for prioritization of chemicals for further hazard identification and characterization.

Zearalenone

Mouse models offer the ability to identify mechanisms of action for numerous toxicants during the perinatal period in a whole-body system. Still, careful consideration is required during strain selection. Different genetic backgrounds may influence the pharmacokinetic profile of a toxicant and in turn impact the overall sensitivity of the model (Goodman et al. 2006; Spearow et al. 1999a; Spearow et al. 1999b; Wadia et al. 2007). Compared to other mouse strains, CD-1 and C57BL/6 mice are significantly less and more responsive, respectfully, to estrogen-mediated changes concerning reproductive endpoints (Pepling et al. 2010; Spearow et al. 1999b). Ideally, the most sensitive strain should be utilized in endocrine disruptor research to minimize the likelihood of false negative results and identify the most adverse effects (Stokes 2004). In our study, we selected the inbred C57BL/6 strain to examine zearalenone activity in the placenta. C57BL/6 mice are one of the most commonly used strains in research and often serve as the background strain for transgenic and knockout mouse models. Screening of the PubMed database for literature concerning the C57BL strain and the term “endocrine” yielded over 10,000 papers. The next most common mouse strain, BALB/C, yielded only ~3,500 papers. The prevalent use of the C57BL/6 strain in literature concerning the endocrine system allows for greater interpretation and comparison of data across studies. Additionally, inbred strains, such as C57BL/6, offer the advantage of each animal being genetically identical, sharing the same homozygous allele for each gene sequence. Elimination of genetic variability as a confounding factor further simplifies data

interpretation in mechanistic studies concerning endocrine active compounds. Together, the extensive utilization of the C57BL/6 strain in endocrine literature as well as its inbred origin and sensitivity to estrogen stimulation render this an appropriate *in vivo* model to study zearalenone activity in the placenta.

Administration of zearalenone at high concentrations resulted in significant endocrine dysregulation and reproductive/developmental abnormality in rodent models. In these studies, zearalenone impacted both maternal and fetal endpoints. Exposed rodent dams exhibited accelerated mammary gland differentiation and necrosis, increased uterine weight and thickness, decreased serum progesterone levels, abnormal placental development, increased weight gain, and altered estrous cycle (Table 1.8). Zearalenone also decreased the viability, growth, and maturation of the fetus (Andersen et al. 2018; Belli et al. 2010; C. et al. 2016; Collins et al. 2006; Gao et al. 2017; Li et al. 2019a). Although these studies provided extensive data on the ability of zearalenone to act as a potent endocrine disruptor, the high doses (0.8 to 40 mg/kg) administered impacted the entire feto-placental unit and did not allow for the identification of the primary target of insult. Zearalenone can theoretically impact the feto-placental unit by three mechanisms. The placenta may be the primary target of zearalenone which induces major dysfunction and decreased integrity of the placental barrier. Decreased placental barrier function can result in 1) lower nutrient and waste exchange, 2) altered hormone secretion, and 3) higher accumulation of zearalenone in the fetal compartment leading to endocrine-related abnormalities. Alternatively, zearalenone has been shown to cross the placenta and may directly impact fetal growth and development. The observed reduction in placental weight and differentiation may simply be an adaptation to the reduced nutritional demands of the smaller fetus. Conversely, zearalenone may simultaneously impact the entire feto-placental unit and cause global endocrine dysfunction {Li, 2019 #20}. The lower and environmentally relevant concentrations utilized in our study clearly identified the placenta as the primary target of zearalenone toxicity. Our data demonstrate that zearalenone administration results

in decreased placental weight and area. Moreover, placental markers of labyrinth, junction, and decidual zones were all globally down-regulated in response to zearalenone. These data are observed in the absence of any significant differences in litter size, fetal weight, and fetal crown-rump length. Interestingly, the number of fetal resorptions was higher in the zearalenone group suggesting that certain embryos were unable to tolerate the zearalenone-induced placental dysfunction. It is plausable that the higher concentrations of zearalenone utilized in previous studies result in more pronounced placental insult, greater transplacental disposition of zearalenone, and correspondingly reduced fetal development. While zearalenone did not induce any pronounced physical changes (such as weight or length) in the fetuses in our study, future research should consider longitudinal observation of offspring development following exposure to environmentally-relevant zearalenone concentrations. Comparison of development of the reproductive system, estrous cycles, and serum hormone levels in F1 generations could provide greater clarity on the long-term impact of perinatal zearalenone administration and whether stricter guidelines are required to further limit exposure.

Although rodent models offer the advantage of a whole-body system to characterize toxicant activity and disposition, there are species differences between the murine and human placentas that need to be accounted for during data interpretation. Human placentas highly express the aromatase (CYP19A1) enzyme whereas mouse placentas do not (Anelli et al. 2019; Mendelson et al. 2005). Aromatase is involved in the conversion of androgens to estrogens in the placenta and has been identified in the metabolism of zearalenone and zearalanone to α-zearalenol (α-ZEL) and α-zearalanol (α-ZAL), respectfully (Huuskonen et al. 2015). The binding affinity of these zearalenone metabolites for estrogen receptors is higher than the parent zearalenone compound, suggesting even stronger estrogenic and endocrine disrupting profiles (Kuiper-Goodman et al. 1987; Minervini et al. 2005; Molina-Molina et al. 2014; Shier et al. 2001). Even in the absence of aromatase, our data demonstrate that low prenatal zearalenone exposure can still induce dysfunction in the molecular

and anatomic parameters of the placenta. It is plausible that zearalenone exposure in humans may be more hazardous than observed in mice due to the higher metabolic turnover of zearalenone by the placental aromatase. Utilization of *ex vivo* human placental models such as isolated primary cytotrophoblasts and placental explants can further our understanding of mycoestrogen placental toxicity. The data obtained from such models allows for enhanced translatability as there is no species-specific differences in metabolism of zearalenone. Moreover, placental *ex vivo* studies can be used as animal testing alternatives and provide more extensive comparative analysis with integrated positive (i.e. 17ß-estradiol) and negative (i.e. ICI-182,780) estrogen controls without the need to sacrifice additional animals.

Further, mechanistic studies examining the protective role of BCRP in zearalenone disposition and activity are still required. While our laboratory has shown that zearalenone is a substrate of the human and mouse BCRP/Bcrp transporter (Szilagyi et al. 2019; Xiao et al. 2015a), data regarding the ability of BCRP to transport zearalenone metabolites is urgently needed. Future studies should consider using HEK293 cells transfected with human and mouse BCRP/Bcrp transporters to test the relative affinity and intracellular accumulation of zearalenone and its metabolites. Alternatively, siRNA-based BCRP knockdown in isolated primary cytotrophoblasts can similarly offer another approach to test the relative affinity of mycoestrogens for the BCRP transporter and simultaneously allow for placental differentiation marker analysis.

I hypothesized that the knockdown/knockout of the placental Bcrp transporter will exaggerate the impact of ZEN insult due to presumably higher accumulation. However, our data demonstrate that Wt Bcrp placentas are more susceptible to changes in gene expression by ZEN. An important consideration to aid in understanding these data is the ability of Bcrp to transport sulfated estrogens (Imai et al. 2003). Sulfatase enzymes are expressed in both murine and human placentas (Reed et al. 2005; Salido et al. 1990; Szilagyi et al. 2019). These enzymes function in the intracrine

production of biologically active estrogens by hydrolyzing aryl and alkyl steroid sulfates. It is possible that Bcrp Het and KO placentas have a greater intracellular concentration of endogenous estrogens in the placenta which drive down the basal expression of placental differentiation markers. In comparison to endogenous estrogens, ZEN has a lower binding affinity for estrogen receptors (Fitzpatrick et al. 1989; Mueller et al. 2004; Takemura et al. 2007b) and the given concentration in this study may not be high enough to displace the endogenous estrogens and further alter molecular signaling.

Conclusion

The overall objective of this dissertation was to investigate novel endogenous and exogenous factors regulating placentation and placental functions. The data presented demonstrate the ability of physiologically-relevant low oxygen tension to alter placental drug transporter expression. Altered transporter expression may influence trophoblast differentiation and potentially placental integrity. This is of particular significance during evaluation of exogenous toxicants, such as zearalenone, which alter drug transporter expression and placental differentiation. The observations and future considerations discussed within will guide novel research concerning gestational pathologies and toxicant exposures to improve fetal outcomes and safety assessment guidelines.

APPENDIX 1: PLACENTAL BCRP/ABCG2 TRANSPORTER PREVENTS FETAL EXPOSURE TO THE ESTROGENIC MYCOTOXIN ZEARALENONE

John T. Szilagyi[a], Ludwik Gorczyca[a], Anita Baker[c], Brian Buckley[b,c], Jeffrey D. Laskin[b,c,d], Lauren M. Aleksunes[b,c]

[a] Joint Graduate Program in Toxicology, Rutgers University Graduate School of Biomedical Sciences, 170 Frelinghuysen Rd, Piscataway, NJ 08854, USA

[b] Department of Pharmacology and Toxicology, Rutgers University, 170 Frelinghuysen Rd, Piscataway, NJ 08854, USA

[c] Environmental and Occupational Health Sciences Institute, Rutgers University, 170 Frelinghuysen Rd, Piscataway, NJ 08854, USA

[d] School of Public Health, Rutgers University 170 Frelinghuysen Rd, Piscataway, NJ 08854, USA

A-1.1 Abstract

In the placenta, the BCRP/*ABCG2* efflux transporter is responsible for preventing the maternal-to-fetal transfer of chemicals. Previous research has pointed to the estrogenic mycotoxin, zearalenone as a potential substrate for BCRP. The purpose of this study was to assess the role of the BCRP transporter in the transplacental disposition of zearalenone during pregnancy. *In vitro* transwell transport assays employing BCRP/Bcrp-transfected MDCK cells and BeWo trophoblasts with reduced BCRP expression were used to characterize the impact of BCRP on the bidirectional transport of zearalenone. In transwell experiments, the presence of BCRP protein increased the basolateral-to-apical transport of the probe BCRP substrate glyburide by 42-89% after 2 h. The presence of BCRP protein in transwell cultures also decreased the apical-to-basolateral transport of zearalenone by and increased its basolateral-to-apical transport up to 24%. *In vivo* pharmacokinetics analyses were then performed on pregnant wild-type and Bcrp$^{-/-}$ mice after a single tail vein injection of zearalenone. Zearalenone and its metabolite α-zearalenol were detectable in serum, placentas, and fetuses from all animals, and β-zearalenol was detected in serum and fetuses but not placentas. There were no significant differences in the maternal serum concentrations of any analytes between the two genotypes. In Bcrp$^{-/-}$ mice, the free fetal concentrations of zearalenone, α-zearalenol, and β-zearalenol were increased by 115%, 84%, and 150%, respectively, when compared to wild-type mice. Placental concentrations of free zearalenone and α-zearalenol were increased by 145% and 78%, respectively, when compared to wild-type mice. Taken together, these data indicate that the placental BCRP transporter functions to prevent the fetal accumulation of zearalenone, which may impact susceptibility to developmental toxicities associated with *in utero* zearalenone exposure.

Abbreviations

ABC, ATP-binding cassette; MDCK, Marine-Darby canine kidney; BCRP, breast cancer resistance protein; CYP, cytochrome P450; ENT, equilibrative nucleoside transporter; GAPDH, glyceraldehyde 3-phosphate dehydrogenase; GusB, glucuronidase B; HEK, human embryonic kidney; MATE, multidrug and toxin extrusion protein;MDR, multidrug resistance protein; MRP, multidrug resistance-associated protein; OAT, organic anion transporter; OATP, organic anion transporting polypeptide; OCT, organic cation transporter; OCTN, organic cation transporter, novel; P_{app}, apparent permeability coefficient; RPL13a, ribosomal protein 13a; SULF, sulfatase; SULT, sulfotransferase; TEER, transepithelial electrical resistance.

A-1.2 Introduction

During pregnancy, the placenta develops from the blastocyst and regulates the flow of nutrients, waste, and gases between the maternal and fetal circulations. Trophoblasts, the parenchymal cell of the placenta, fuse to form a syncytium that inhibits direct contact of the two blood supplies providing a physical and biochemical barrier that protects the developing fetus (Gupta et al. 2016). The breast cancer resistance protein (BCRP/*ABCG2*) is an efflux transporter enriched on the maternal-facing surface of syncytiotrophoblasts. On the apical membrane, BCRP prevents the transepithelial passage of xenobiotics. Substrates of BCRP include endogenous chemicals, such as certain steroids and bile acids, pharmaceuticals, such as the diabetes drug glyburide and the antibiotic nitrofurantoin, and dietary contaminants, such as the plasticizer bisphenol A and phytoestrogen genistein. Compromised BCRP function in the placenta may consequently increase the risk of the fetus to chemical exposures during pregnancy. It is therefore critical to characterize the interaction of environmental and dietary contaminants with placental BCRP.

Recently, *in vitro* screening performed by our laboratory identified zearalenone as a substrate of the human BCRP transporter (Xiao et al. 2015b). Zearalenone is an estrogenic mycotoxin produced by *Fusarium* fungi that grows on cereal crops in moist climates. The European Union has determined the acceptable maximum for zearalenone in food at 4 μg/kg (Commision 2006), but multiple studies worldwide have demonstrated that commonly consumed foods often exceed this level (Iqbal et al. 2014a; Lahouar et al. 2018; Ok et al. 2014; Tralamazza et al. 2016). Further, analysis of urine from a cohort of pre-pubescent girls in New Jersey demonstrated that free zearalenone was present in the range of 0.2-8.4 ng/mL and was correlated with delayed puberty onset (Bandera et al. 2011). It should also be noted that α-zearalanone, a zearalenone metabolite marketed under the tradename Ralgro®, is commonly used to increase feed-to-weight ratios in cattle. Ralgro® is current used as a growth promoter in the United States but has been banned by

the European Union. Exposure to xenoestrogens *in utero* is well-understood to induce adverse developmental effects (Hines 2011). *In utero* exposure to zearalenone causes precocious puberty and mammary proliferation in both female Wistar rats and C57BL/6 mice (Belli et al. 2010; Hilakivi-Clarke et al. 1998). Zearalenone exposure is potentially common during pregnancy, with one study reporting detectable levels of zearalenone in the urine of 11 out of 30 pregnant women tested (Fleck et al. 2016).

From prior *in vivo* rodent studies, zearalenone does cross the placenta into the fetal compartment, but the transplacental transfer of zearalenone appears to be limited (Appelgren et al. 1982; Bernhoft et al. 2001; Koraichi et al. 2012). While multiple factors can regulate xenobiotic disposition, these data could point to placental efflux as a potential mechanism for regulating fetal exposure to zearalenone. To date, no studies have evaluated the ability of the BCRP transporter to regulate the fetoplacental disposition of zearalenone. Therefore, the purpose of this study was to comprehensively assess whether BCRP restricts the maternal-to-fetal transfer of zearalenone using *in vitro* and *in vivo* models of the human placental barrier.

A-1.3 Materials and Methods

Chemicals

Unless stated otherwise, all chemicals were purchased from Sigma-Aldrich (St. Louis, MO).

Cell Culture and Lentiviral Knockout of BCRP

All cell culture and transport experiments were performed in an incubator at 37°C with 5% CO_2 in HEPA-filtered air. Marine-Darby Canine Kidney (MCDK) cells transfected with human (hBCRP) or mouse (mBcrp) BCRP constructs or empty vector were provided by Dr. Alfred Schinkel (Netherlands Cancer Institute) and maintained in DMEM (Life Technologies, Carlsbad, CA) supplemented with 10% fetal bovine serum (Atlantic Biologicals, Frederick, MD) and 1% penicillin-streptomycin (Durmus et al. 2012). BeWo-b30 human choriocarcinoma cells were provided by Dr. Nicholas Illsley (Hackensack University Medical Center) and maintained in DMEM:F12 (Life Technologies) supplemented with 10% fetal bovine serum and 1% penicillin-streptomycin (Vardhana et al. 2002). Stable BeWo knockdown cells were generated using ABCG2 (sc-41151-V, Santa Cruz) or control (sc-108080) lentiviral shRNA particles. Cells were grown to 70% confluence on a 96-well plate before incubation for 24h in DMEM:F12 containing 5 μg/mL polybrene (Santa Cruz) and 2 viral particles per cell (60,000 particles/well). Subsequently, cells were sub-cultured in a 24-well plate, and stable transfected clones were selected using 6.5 μg/mL puromycin over 48 h.

Animal treatment

$Bcrp^{-/-}$ mice were obtained from Taconic Biosciences (Taconic, NY) and backcrossed to the C57BL/6 background (027 strain, Charles River Laboratories, Wilmington, MA) until >99% congenic (Rutgers RUCDR Infinite Biologics, Piscataway, NJ). Adult female and male C57BL/6 wild-type and $Bcrp^{-/-}$ mice were mated overnight with the same genotype. The presence of the sperm plug denoted gestational day 0. Mice were provided phytoestrogen-free food and water *ad*

libitum. At gestation day 14, mice were administered 10 mg/kg zearalenone dissolved in DMSO:PEG400:Saline (1:5:4 v/v) by tail vein injection (n = 6-8 dams per genotype). Two additional dams per genotype received vehicle to generate tissue matrices used for standard curves. At one hour post injection, dams were sacrificed by pentobarbital overdose, and blood (cardiac puncture), placentas, and fetuses were collected. Blood samples were centrifuged for 15 min at 600 x *g* to isolate sera. All samples were stored at -80°C until analysis by LC-MS.

Western Blotting

MDCK and BeWo cell lysates for Western Blot were collected and stored in buffer containing 20 mM Tris-HCl, 150 mM NaCl, 5 mM ethylenediaminetetraacetic acid, 1% Triton X-100 and a protease inhibitor cocktail (Sigma P8340, 1%, v/v). Mouse placenta homogenates were prepared in sucrose-Tris-HCl buffer (250 mM sucrose and 10 mM Tris-HCl, pH 7.5) supplemented with protease inhibitor cocktail (Sigma P8340, 1%, v/v) using a bead homogenizer (Tissue-Lyser LT, Qiagen) for 3 min at 40 Hz. Unless indicated otherwise, all Western blotting was performed with equipment from BioRad (Hercules, CA) as previously described (Zheng et al. 2013). All samples were spun down at 1000 x *g* for 10 min. Thirty μg of protein homogenates were loaded onto 4-12% Tris-HCl gels, electrophoretically separated, and transferred to nitrocellulose membranes. After blocking in 5% nonfat milk for 2 h, membranes were incubated overnight at 4°C in 2% nonfat milk containing primary antibodies used to detect BCRP (BXP-53, 1:5000; Enzo Life Sciences, Farmingdale, NY), β-actin (ab8227, 1:2000, Abcam, Cambridge, MA) or glyceraldehyde 3-phosphate dehydrogenase (GAPDH, ab9485, Abcam), followed by incubation with either HRP-linked rabbit or HRP-linked rat secondary antibodies (1:1000, 2 h, Cell Signaling Technologies, Danvers, MA). After incubating membranes briefly with Luminata Forte Western HRP substrate (Millipore, Billerica, MA), protein-antibody complexes were visualized using a Fluorchem Imager (ProteinSimple, Santa Clara, CA).

Hoechst 33342 Transport

For Hoechst 33342 transport studies, BeWo or MDCK cells were added to 96-well round-bottom plates (100,000 cells/well). *Uptake phase.* Cells were incubated in 100 µL DMEM (MDCK) or DMEM:F12 (BeWo) containing 5 µM Hoechst 33342, a fluorescent BCRP substrate, for 30 min. A parallel treatment group included cells also incubated with 1 µM Ko143, an established BCRP inhibitor (Bircsak et al. 2013a). *Efflux phase.* The substrate-containing media was removed and replaced with substrate-free media. Cells were then incubated an additional 1 h. The cells were then washed and re-suspended in 50 µL ice cold HBSS and set on ice for analysis. A Cellometer Vision automated cell counter (Nexcelom Bioscience, Lawrence, MA) fitted with a VB-450-302 filter (excitation/emission = 375/450 nm) was used to quantify intracellular fluorescence. The total number of cells analyzed for each sample ranged from 500-2000, and fluorescence was normalized for cell size.

Transwell Transport

MDCK or BeWo cells were seeded at a density of 100,000 and 200,000 cells per well, respectively, on a collagen-coated 24-well multiwall insert system (Cat# 351181, 1.0 µM pore, high density PET membrane, Corning, Tewksbury, MA). Transport assays were performed on day 3-4 post seeding on those wells with a TEER value greater than 250 Ω*cm^2 for MDCK cells (Yang et al. 2016) and 80-160 Ω*cm^2 for BeWo cells (Li et al. 2013a) as measured immediately before and after the experiment. Monolayer integrity was also assessed by measuring the rejection percentage of Lucifer Yellow (20 µM) (Hidalgo et al. 1989) using % Rejection = $(1 - C_r / (C_r + C_D) * 100$, where C_r is the final concentration in the receiver compartment and C_d is the final concentration in the donor compartment (Nkabinde et al. 2012). On the day of experiments, media in both the apical and basolateral compartment were replaced with HBSS. The test compound (1 µM BODIPY-glyburide, 50 µM zearalenone, or 10 µM Rhodamine 123) was added to the donor compartment at time = 0 and a 100 µL aliquot was collected from the receiver compartment every 30 min.

Fluorescence was measured using a SpectraMax M3 spectrophotometer (Molecular Devices, San Jose, CA). BODIPY-glyburide and Lucifer Yellow were measured using Ex/Em: 428/540 nm, and Rhodamine was measured using Ex/Em: 507/529 nm. Zearalenone was quantified by HPLC-UV. Permeability coefficients were calculated using P_{app} (cm/s) = (Q / t) / (A*C_0), where Q is glyburide (nmol) transported to the receiver compartment at time t (s), A is the cell surface area (cm^2) and C_0 is the initial concentration of test substrate (μM) (Li et al. 2013a).

Messenger RNA Quantification

Mouse placentas were homogenized using a bead homogenizer (Tissue-Lyser LT, Qiagen) for 4 min at 40 Hz in RNAzol RT. Total RNA was isolated from lysates according to the manufacturer's protocol. RNA content and purity was determined by measuring absorbance at 260 nm using a NanoDrop (Fisher Scientific). cDNA was generated from total RNA (1000 ng) with the High-Capacity cDNA Reverse Transcription Kit (ThermoFisher) and a MultiGene OptiMax Thermal Cycler (Labnet International Inc., Edison, NJ) according to the manufacturer's instructions. Quantitative PCR was performed with cDNA, Sybr Green dye (Life Technologies), forward and reverse primers (see Supplemental Table A-1.1) (Integrated DNA Technologies, Inc., Coralville, IA), and a ViiA7 RT-PCR System (Life Technologies). Ct values were converted to ΔΔCt values by comparison with the housekeeping gene ribosomal protein 13A (Rpl13A).

Quantification of Zearalenone and Metabolites

Quantification of free zearalenone (parent compound only) in aliquots from transwell transport experiments was performed using an HPLC-UV system (Jasco, Easton, MD) equipped with a PU-4185 binary pump, UV 4075 detector (254 nm), AS-2055 autosampler, Zorbax Eclipse 3 mm x 15 cm C18 column (Agilent, Santa Clara, CA) (adapted from De Baere et al. 2012). Peak areas were quantified using ChromNav V2 and compared to a standard curve. The mobile phase consisted of H_2O:acetonitrile (3:2, formic acid added to pH = 3.0).

In order to quantify free and total zearalenone and metabolites from in vivo experiments, analyte extracts were prepared and measured by LC-MS. For sera, samples were added onto ChemElut solid phase extraction columns (1 mL, unbuffered, 12198002, Agilent), and analytes were eluted using methyl tert-butyl ether. Samples were then dried under N_2, re-dissolved in methanol, added onto pre-conditioned Discovery DSC-NH_2 solid phase extraction columns, and eluted with methanol. Samples were dried again before being re-dissolved in LC-MS mobile phase (see below). Placentas and fetuses were first weighed and homogenized in sodium acetate buffer (0.2 M, pH 4.65) before incubating overnight in the presence or absence of β-glucuronidase (1000 U/sample) at 37°C with gentle shaking. Liquid-liquid extraction was then performed on the homogenates by adding methyl tert-butyl ether (2x volume of sample), vortexed for 30 sec, and centrifuged at 1000 x g for 10 min. The ether phase was removed and the extraction was repeated two more times. Extracts were dried under N_2, reconstituted in n-hexane:dichloromethane (3:2), and added onto pre-conditioned silica Sep-Pak solid phase extraction columns (500mg/3cc, 186004615, Waters, Milford, MA). Samples were washed with ethyl acetate:n-hexane (6:94), and then the analytes were eluted with ethyl acetate:n-hexane (25:75) then ethyl acetate (neat). Eluates were dried under N_2 before being re-dissolved in LC-MS mobile phase (see below).

Quantification of zearalenone and its metabolites in extracts prepared from mouse tissues and serum was performed using an LC-MS system (Thermo Fisher) equipped with an Accela UPLC pump and autosampler (4°C), a 100 x 4.6 mm betasil phenyl hexyl column (35°C) (Phenomenex, Torrance, CA), and an LTQ XL mass spectrometer with an atmospheric pressure chemical ionization source. The mobile phase used was water:methanol (0.1% formic acid added):acetonitrile (2:1:1). Spiked sample matrices were used for quality control (>80% recovery) and run with each sample batch. The inter/intra-day variability (%RSD) was 4.5/4.0, 3.2/3.1, and 2.6/2.5 for zearalenone, α-zearalenol, and β-zearalenol, respectively. The detection limit for this

method was 0.05 ng/mL. Peak areas were quantified using Xcalibur and normalized to mL (serum) or mg (tissues).

Statistical Analysis

Data are presented as mean ± SE and analyzed using GraphPad Prism 5.0 software (GraphPad Software Inc., La Jolla, CA). Depending upon the number of comparisons, either one-way or two-way analysis of variance with Newman-Keuls or Bonferroni post-test, respectively, or an unpaired student's t test was used to assess statistical significance ($p < 0.05$).

A-1.4 Results

Transporter Expression and Activity in Transfected hBCRP and mBcrp MDCK Cells

The ability of human BCRP and mouse Bcrp proteins to transport zearalenone was first assessed in MDCK cells transfected with full-length *BCRP/Bcrp* plasmids (Durmus et al. 2012). Western blot analysis of MDCK cells demonstrated that only the hBCRP and mBcrp transfected cell lines expressed BCRP/Bcrp protein, with no detectable bands in the empty vector control cells (Fig A-1.1A). H33342, a fluorescent substrate of BCRP, was used to assess BCRP activity using a cell accumulation assay. The intracellular retention of H33342 was reduced 80-90% in MDCK cells transfected with hBCRP and mBcrp (Fig A-1.1B). Ko143, an inhibitor of BCRP, increased the cellular accumulation of H33342 by 20%, 1000%, and 425% in control, hBCRP, and mBcrp MDCK cells, respectively (Fig A-1.1B).

Transepithelial Transport of Zearalenone in Transfected hBCRP and mBcrp MDCK Cells

As an efflux transporter that localizes to the apical membrane of cells, BCRP/Bcrp enables the basolateral-to-apical transport of chemicals in polarized epithelium. In transwell cultures, BODIPY-glyburide was used as a probe BCRP/Bcrp substrate (Bircsak et al. 2016; Gedeon et al. 2008b; Hemauer et al. 2010b; Zhou et al. 2008a) to confirm the polarization and activity of BCRP/Bcrp. For these experiments, BODIPY-glyburide was added to the donor compartment and fluorescence quantified in the receiver compartment. The time-dependent increase of glyburide in the receiver compartment was linear (Fig A-1.2, $R^2 = 0.95 – 0.99$). When grown in transwell inserts, MDCK cells exhibited minimal apical-to-basolateral transport of glyburide that was unaffected by expression of BCRP/Bcrp (Fig A-1.2A). As expected, both hBCRP and mBcrp MDCK cells significantly increased the basolateral-to-apical transport of glyburide (Fig A-1.2A).

Similar to experiments with glyburide, the increase of zearalenone in the receiver compartment was linear and time-dependent (Fig A-1.1B, $R^2 = 0.98 – 0.99$). While zearalenone was transported in

the apical-to-basolateral direction, this transfer was minimally affected by expression of BCRP/Bcrp (Fig A-1.2B). By comparison, both hBCRP- and mBcrp-transfected MDCK cells exhibited significantly increased basolateral-to-apical transport of zearalenone (Fig A-1.2B).

MDCK cells express endogenous canine multidrug resistance protein 1 (MDR1, P-glycoprotein) (Li et al. 2013b). In this study, we confirmed canine MDR1 activity using the MDR1 substrate, Rhodamine 123. In MDCK cells, the MDR1 inhibitor PSC833 significantly reduced the basolateral-to-apical transport of Rhodamine 123 at all time points (Supplemental Fig A-1.1A) but had no impact on the disposition of zearalenone (Supplemental Fig A-1.1B).

BCRP Expression and Activity in Human Placental Cells Following Lentiviral Knockdown

To recapitulate the human placental barrier, a second set of transwell studies were performed using human BeWo b30 trophoblast cells. Consistent with prior reports (Ceckova et al. 2006; Mitra et al. 2010), BeWo cells highly express BCRP protein (Fig A-1.3A). Lentiviral knockdown of BCRP in BeWo b30 cells using targeted shRNAs reduced BCRP protein to levels below detection (Fig A-1.3A). Similarly, compared to BeWo b30 cells infected with control shRNAs, BCRP mRNA expression was reduced 88% (data not shown). As a result of BCRP knockdown, H33342 retention was increased by 53% in BeWo b30 cells (Fig A-1.3B). The enhanced accumulation of H33342 in BCRP knockdown cells was similar to the pharmacological inhibitor of BCRP, Ko143 (Fig A-1.3B).

Transepithelial Transport of Zearalenone in Human Placental Cells Following Lentiviral Knockdown of BCRP

In the placenta, BCRP mediates the fetal (basolateral) to maternal (apical) translocation of xenobiotics. When grown in transwell inserts, BeWo b30 cells exhibited greater transfer of BODIPY-glyburide in the basolateral-to-apical direction compared to the apical-to-basolateral

direction. While there was no difference in the apical-to-basolateral transport of glyburide between control and shBCRP BeWo cells (Fig A-1.4A), the basolateral-to-apical transport of glyburide was significantly decreased by 50% in shBCRP BeWo cells (Fig A-1.4A). These data confirm that BCRP was properly polarized to the apical surface of BeWo b30 cells and functional in transferring the known substrate glyburide. By comparison, the apical-to-basolateral transport of zearalenone was significantly increased in shBCRP BeWo cells compared to control cells (Fig A-1.4B), and this difference was observed when the starting concentration was as low as 5 μM (Supplemental Fig A-1.2). The basolateral-to-apical transport of zearalenone also tended to decrease in shBCRP cells (Fig A-1.4B).

For all transwell experiments, the observed effects of BCRP on glyburide and zearalenone transport were reflected in the respective permeability coefficients and flux ratios, presented in Table A-1.1. Lucifer yellow was used in transwell experiments to confirm monolayer integrity (determined by TEER values), and the percent rejection of Lucifer yellow was 98.6 ± 1.5% and 95.0 ± 0.6% and in MDCK and BeWo cell transwell cultures, respectively. BCRP expression did not impact Lucifer yellow rejection in either MDCK or BeWo cells (data not shown).

Distribution of Zearalenone and its Metabolites in Wild-Type and Bcrp$^{-/-}$ Mice

After confirming that both mouse and human BCRP proteins could transport zearalenone and that BCRP can influence the directional transfer of the mycoestrogen in placental cells, the transplacental transfer of zearalenone was assessed in pregnant wild-type and Bcrp$^{-/-}$ mice. In placentas from gestation day 14, Bcrp protein was detected in wild-type but not Bcrp$^{-/-}$ mice (Fig A-1.5A). Placentas from Bcrp$^{-/-}$ mice also displayed a >99% reduction in Bcrp mRNA (data not shown).

After an IV injection of zearalenone to pregnant wild-type and Bcrp$^{-/-}$ mice, zearalenone and its metabolites were quantified in mouse serum, placenta, and fetuses by LC-MS. After 1 h, serum concentrations of free zearalenone, α-zearalenol, and β-zearalenol ranged from 108 – 588, 4 – 7, and 1 – 2 ng/mL, respectively (Fig A-1.5B). There were no significant differences in the serum concentrations of any analyte between wild-type and Bcrp$^{-/-}$ mice (Fig A-1.5B). For placental and fetal tissues, both free and total (free + deconjugated) zearalenone and its metabolites were quantified. In fetal tissues of Bcrp$^{-/-}$ mice, free/total zearalenone, α-zearalenol, and β-zearalenol increased by 115/118%, 84/53%, and 150/100%, respectively, compared to wild-type mice (Fig A-1.5C). In matched placentas of Bcrp$^{-/-}$ mice, free/total zearalenone and α-zearalenol were increased by 145/99% and 122/114%, respectively, compared to wild-type mice (Fig A-1.5D). β-zearalenol was not detected in placental samples of either genotype (data not shown). All samples were also assessed for the presence for zearalenone, α-zearalanol, and β-zearalanol, but these analytes were below the detectable limit (data not shown).

Relative Expression of Transporters and Drug Metabolizing Enzymes in Wild-Type and Bcrp$^{-/-}$ Mouse Placentas

To rule out compensatory changes in placental gene expression that could impact the metabolism and disposition of zearalenone *in vivo*, the mRNA expression of transporters and drug metabolizing enzymes were compared between wild-type and Bcrp$^{-/-}$ placentas (Table A-1.2). The majority of transcripts analyzed demonstrated no statistically significant difference between genotypes. Oatp2b1, Oatp3a1, and Oatp5a1 mRNA levels were significantly but minimally altered in Bcrp$^{-/-}$ placentas (+31%, +29%, and -27% compared to wild-type placentas, respectively). Cyp1a1 and sulfatase 1 were also significantly altered in Bcrp$^{-/-}$ placentas (+37% and -24%, respectively). Transcripts for Cyp3a11, Oatp1a5, and Oatp2a1 were also analyzed but could not be detected.

A-1.5 Discussion

In the placenta, BCRP protects the fetus from toxicant exposure by preventing transport from the maternal to the fetal circulation. Therefore, we sought to determine whether BCRP can prevent the maternal-to-fetal transfer of the mycotoxin, zearalenone. Previous work from our laboratory demonstrated that zearalenone is a novel substrate of BCRP using basic screening techniques including BCRP substrate retention and ATPase activity (Xiao et al. 2015b). Zearalenone inhibited BCRP activity in membrane vesicles (using ATPase activity with sulfasalazine and Lucifer yellow uptake) and in BeWo cells (using the H33342 retention assay) (Xiao et al. 2015b). Further, the presence of the BCRP inhibitor Ko143 increased zearalenone retention in BeWo cells (Xiao et al. 2015b). Building on these initial data, the current study employed complementary *in vitro* and *in vivo* approaches to address whether BCRP could limit the transplacental transfer of zearalenone. We compared transport of zearalenone by mouse Bcrp and human BCRP isoforms, utilized an *in vitro* model of the human placental barrier, and quantified placental and fetal zearalenone concentrations in wild-type and Bcrp$^{-/-}$ dams.

In order to determine if BCRP prevents fetal exposure to zearalenone, this study utilized techniques designed to more accurately represent the human placental barrier than cell retention-based transport methods. MDCK cells transfected with the *hBCRP* and *mBCRP* genes were used to elucidate the specific effect of BCRP on zearalenone disposition and to account for differences between homologues (human and mouse). After establishing that BCRP was present and functional in transfected MDCK cells, glyburide, a previously published substrate of BCRP in BeWo cells (Bircsak et al. 2016), was used to probe the impact of BCRP on vectoral transport. In MDCK cells, BCRP greatly increased the basolateral-to-apical transport of glyburide. The flux ratios of glyburide in control, hBCRP, and mBcrp MDCK cells were 6.38, 14.87, and 17.70, respectively. Only minimal glyburide was transported from the apical to the basolateral compartment, which could account for a lack of difference between the transfected and non-transfected MDCK cells. MDCK

cells also express the canine Mdr1 transporter, which can transport glyburide. In MDCK cells, the presence of BCRP increased the basolateral-to-apical transport and decreased the apical-to-basolateral transport of zearalenone. Importantly, the MDR1 inhibitor PSC833 had no impact on the basolateral-to-apical transport of zearalenone, indicating that our observations with MDCK cells are specific to BCRP/Bcrp.

B30 cells, a sub-clone of the BeWo cell line that can form a monolayer, were used to recapitulate syncytiotrophoblasts. It has been previously demonstrated that BeWo cells secrete hormones including human chorionic gonadotropin similar to syncytiotrophoblasts (Pattillo et al. 1968b; Pattillo et al. 1968c). After confirming that shBCRP knockdown successfully reduced BCRP protein expression and activity, we examined the impact of BCRP on the bidirectional transport of glyburide and zearalenone. Similar to our observations with MDCK cells, BCRP knockdown reduced the basolateral-to-apical transport of glyburide by BeWo cells but had no effect in the opposite direction. BeWo b30 cells have been reported to express MDR1 protein (Albekairi et al. 2015), but, contrary to those studies, we did not detect MDR1 protein or activity (data not shown). In BeWo cells, the genetic knockdown of BCRP decreased the basolateral-to-apical transport and increased the apical-to-basolateral transport of zearalenone.

The flux ratios of zearalenone ranged from 0.91-1.06 when BCRP was expressed and 0.59-0.65 when BCRP was absent or reduced. Traditionally, a flux ratio of >1.5 indicates active transport, but the results observed in this study make evident the importance of BCRP in zearalenone distribution during pregnancy. Further, in considering the data presented here, it is also important to recognize the potential role of other uptake and efflux transporters present at both the apical and basolateral membranes of either cell line. Zearalenone has also been shown to interact with MRP1-3, OAT1-4, OCT1 and OCT2 *in vitro* (Tachampa et al. 2008; Videmann et al. 2009). This study

focused specifically on the role of BCRP, and further work is needed to fully characterize involvement by other transporters in the transplacental disposition of zearalenone.

Pharmacokinetics studies with nitrofurantoin and glyburide in Bcrp$^{-/-}$ mice demonstrate that BCRP/Bcrp activity in the placenta prevents the fetal accumulation of BCRP substrates (Zhang et al. 2007; Zhou et al. 2008a). The findings from the *in vivo* experiments in this study reflect those observed from *in vitro* transwell assays. Bcrp$^{-/-}$ mice displayed greater placental retention and maternal-to-fetal transfer of zearalenone and its metabolites compared to control without any significant differences in sera concentrations, placental weights litter size, or fetal weights. It is therefore evident that Bcrp plays a role in protecting the fetus from exposure to zearalenone present in the maternal circulation. In considering the impact of BCRP on zearalenone pharmacokinetics, it is also important to note any compensatory transcriptional changes to transporters and enzymes that result from deleting the *Bcrp* gene. Bcrp$^{-/-}$ placentas displayed a similar transcriptional profile of transporters to those of wild-type mice, with a few exceptions. Oatp2b1 and 3a1 were both slightly up-regulated (29-31%) and Oatp5a1 was slightly down-regulated (27%). Oatp2b1 is basolateral transporter, and, if zearalenone is an Oatp2b1 substrate, an increase in transcript levels would decrease the transplacental transfer of zearalenone. However, the subcellular localization of Oatp3a1 and 5a1 in mouse syncytiotrophoblasts and their contribution to zearalenone disposition are not currently understood. It is also unclear in this study if the metabolites of zearalenone cross the placenta or are formed from fetal hepatic metabolism of the parent compound. By gestation day 17, fetal livers of C57BL/6 mice do express a number of Cyps, including 2d26, 2d10, 2c68, and 2c69, but these isoforms have not yet been shown to metabolize zearalenone (Peng et al. 2012). It is known that zearalenone is metabolized to α-zearalenol and β-zearalenol by 3α- and 3β-hydroxysteroid dehydrogenase, and both the parent compound and its metabolites can be glucuronidated in humans by UGT 1A1, 1A3, 1A8, and 2B7. Sulfonation of the parent compound also occurs but to a much lesser extent. BCRP is known to transport both glucuronidated and

sulfonated phase II metabolites of other compounds (An et al. 2011; Imai et al. 2003; Wu et al. 2012a; Zamek-Gliszczynski et al. 2011). While the glucuronidated metabolites have not been shown to be estrogenic, human fetal livers do express glucuronidase enzymes that can deconjugate the glucuronide-conjugated zearalenone metabolites. Additional work is therefore needed to thoroughly characterize the transport of these metabolites individually.

The effects of *in utero* exposure to zearalenone are not fully understood, but *in vivo* studies note developmental effects similar to other estrogens. Prior studies have demonstrated that zearalenone crosses the placenta and impacts reproductive development in both female Wister rats and C57BL/6 mice (Belli et al. 2010; Hilakivi-Clarke et al. 1998). Specifically, zearalenone (0.2-5000 µg/kg/day for Wistar rats on GD9-PND5 and 2 µg/day for C57BL/6 mice on GD15-20) induced precocious puberty and mammary proliferation in both studies, raising the concern that similar effects may be seen in humans. Conversely, however, urinary zearalenone concentration has been correlated to delayed puberty in a cohort of New Jersey girls (Bandera et al. 2011). It is possible, however, that urinary concentrations of zearalenone indicate an increase in excretion rather than an increase in consumption. Alternately, zearalenone may act as an antagonist to endogenous estrogens. Zearalenone interacts with all three isoforms of estrogen receptor (ERα, ERβ, and GPR30) but is not as potent as 17β-estradiol (Kuiper-Goodman et al. 1987; Takemura et al. 2007a; Zinedine et al. 2007). The specific effects of zearalenone, therefore, may depend on the presence of endogenous estrogens.

There exist genetic, pathological, and toxicological factors that decrease placental BCRP activity and may therefore increase fetal exposure to zearalenone. The 421C>A BCRP polymorphism, for instance, significantly decreases BCRP protein expression (40-50%) but not transcription (Bircsak et al. 2018). The 421C>A allele varies between ethnic groups, but is relatively common among Asian (32%) and Hispanic (28%) populations (Bircsak et al. 2018). Previous *in vitro* experiments

with Q141K BCRP expressing HEK cells demonstrate increased retention of H33342, glyburide, and zearalenone compared to those expressing wild-type BCRP protein (Bircsak et al. 2016; Xiao et al. 2015b). However, further studies are needed to determine the impact of the Q141K polymorphism on fetal drug accumulation *in vivo*. BCRP activity can also be directly inhibited by the previously mentioned substrates glyburide, genistein, and bisphenol A, which can all be encountered during pregnancy (Bircsak et al. 2016; Dankers et al. 2013). Moreover, BCRP expression is reduced by diseases of pregnancy involving placental dysfunction. Placentas from pregnancies with preeclampsia and intrauterine growth restriction, for instance, have demonstrated a marked reduction in BCRP mRNA and protein expression (Evseenko et al. 2007a; Jebbink et al. 2015b).

Using a complement of *in vitro* and *in vivo* approaches, we have demonstrated that zearalenone is a substrate of human BCRP and mouse Bcrp and that BCRP/Bcrp in the placenta reduces the maternal-to-fetal transfer of zearalenone. There are a number of conditions in which placental BCRP function can be compromised which could potentially increase the maternal-to-fetal transfer of zearalenone. Taken together, these data suggest that women with compromised BCRP efflux may be at risk for higher fetal zearalenone exposure during pregnancy. Therefore, further studies are needed to characterize the effects of real world *in utero* exposure to zearalenone.

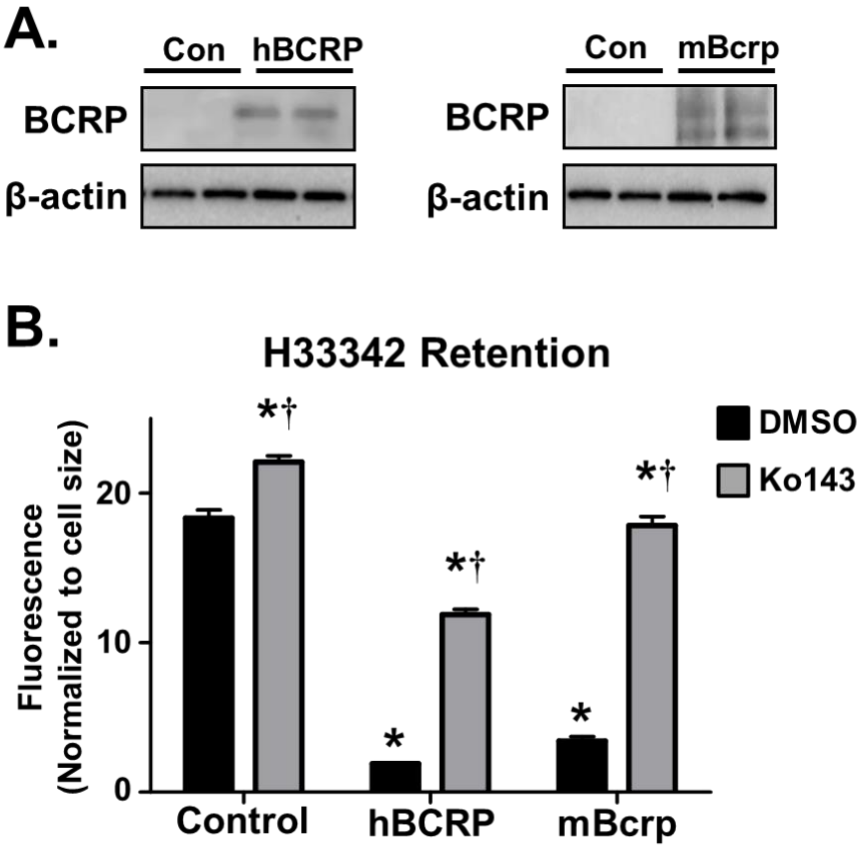

Fig A-1.1. Characterization of BCRP expression and activity in hBCRP- and mBcrp-transfected MDCK cells. **A.** Western Blot of transfected and control MDCK cells analyzing BCRP/Bcrp protein expression (72 kDa). β-actin (42 kDa) was used as a loading control. **B.** Retention of H33342 (10 μM) in empty vector control and transfected MDCK cells. Ko143 (1 μM) was used as a pharmacological inhibitor of BCRP/Bcrp. Data represent the mean ± SE (n = 6) and were analyzed using a two-way ANOVA followed by post-hoc Bonferroni analysis. Asterisks (*) represent statistically significant differences ($p < 0.05$) compared to control/vehicle (control black bar). Daggers (†) represent statistically significant differences ($p < 0.05$) compared to vehicle within treatment group (black bars within group).

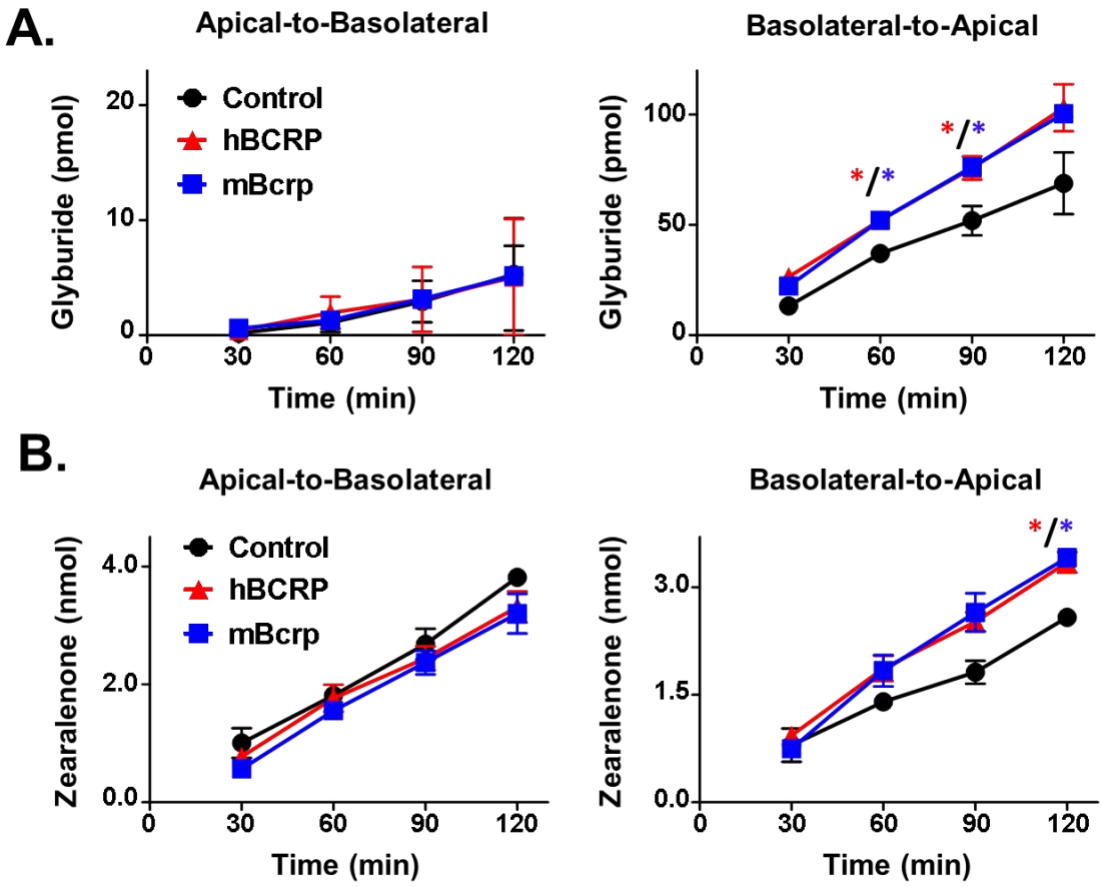

Fig A-1.2. Transport of glyburide and zearalenone by MDCK cells in transwell cultures. MDCK cells grown on transwell inserts were assessed for translocation of **A.** BODIPY-glyburide (1 μM) and **B.** zearalenone (50 μM) across cell monolayers for 2 h as described in the Materials and Methods. Data represent the mean pmol detected in the receiver compartment ± SE (n = 3 independent experiments) and were analyzed using a one-way ANOVA followed by post-hoc Newman-Keuls analysis (*$p < 0.05$ compared to control).

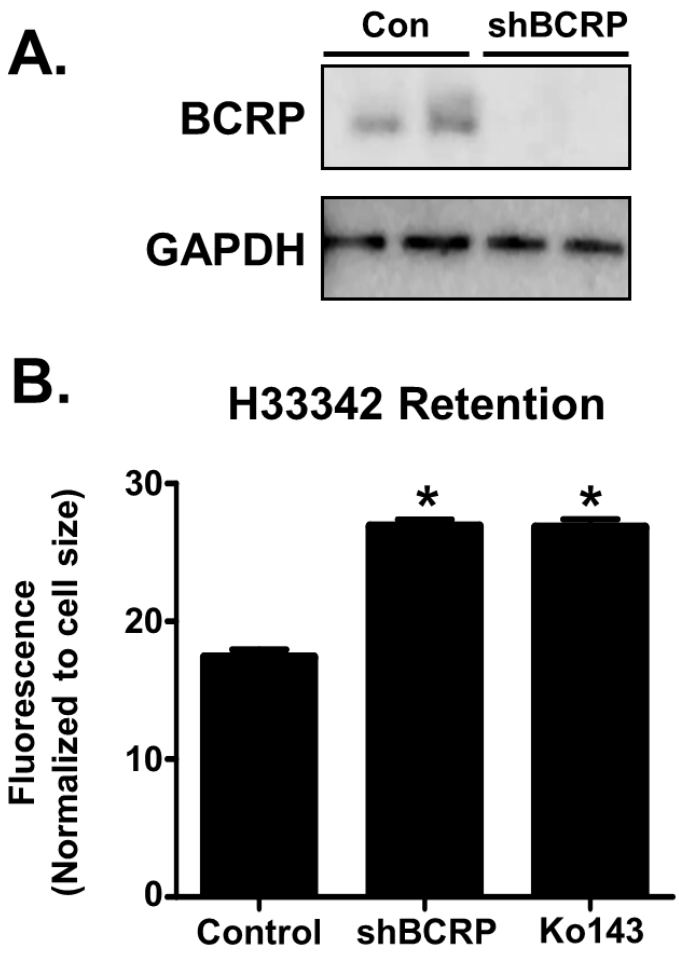

Fig A-1.3. Characterization of BCRP protein and activity in BeWo shBCRP cells.

A. Western blot of BCRP protein (72 kDa) in lysates from BeWo cells after treatment with control or shBCRP lentiviral particles. GAPDH (37 kDa) was used as a loading control. **B.** Retention of H33342 (10 μM) in control and shBCRP BeWo cells. Ko143 (1 uM) was used as a pharmacological inhibitor of BCRP. Data represent the mean ± SE (n = 6) and were analyzed using a one-way ANOVA followed by post-hoc Newman-Keuls analysis (*$p < 0.05$ compared to control).

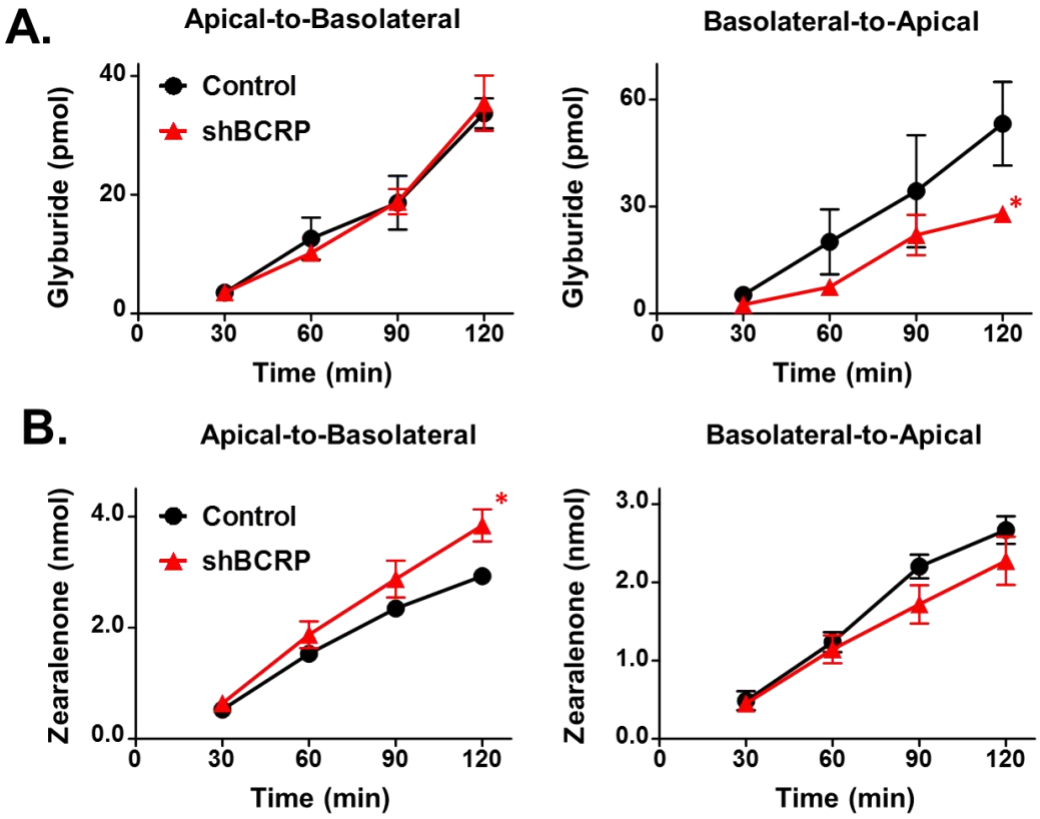

Fig A-1.4. Transport of glyburide and zearalenone by BeWo cells in transwell cultures.

BeWo cells grown on transwell inserts were assessed for translocation of **A.** BODIPY-glyburide (1 μM) and **B.** zearalenone (50 μM) across cell monolayers for 2 h as described in the Materials and Methods. Data represent the mean pmol/nmol detected in the receiver compartment ± SE (n = 3 independent experiments) and were analyzed using a Student's t-test (*$p < 0.05$ compared to control).

Table A-1.1 Permeability coefficients of glyburide and zearalenone in BeWo and MDCK transwell culture experiments

	Glyburide[a]		
	P_{app} A-B	P_{app} B-A	Flux Ratio
BeWo	1.42×10^{-5}	2.33×10^{-5}	**1.64**
BeWo BCRP-kd	1.49×10^{-5}	1.21×10^{-5}	**0.81**
MDCK	4.54×10^{-6}	2.90×10^{-5}	**6.38**
MDCK hBCRP	2.83×10^{-6}	4.21×10^{-5}	**14.87**
MDCK mBCRP	2.39×10^{-6}	4.23×10^{-5}	**17.70**

	Zearalenone[a]		
	P_{app} A-B	P_{app} B-A	Flux Ratio
BeWo	2.46×10^{-5}	2.25×10^{-5}	**0.91**
BeWo BCRP-kd	3.23×10^{-5}	1.92×10^{-5}	**0.59**
MDCK	3.34×10^{-5}	2.17×10^{-5}	**0.65**
MDCK hBCRP	2.79×10^{-5}	2.82×10^{-5}	**1.01**
MDCK mBCRP	2.69×10^{-5}	2.87×10^{-5}	**1.06**

[a] P_{app} expressed in cm/s

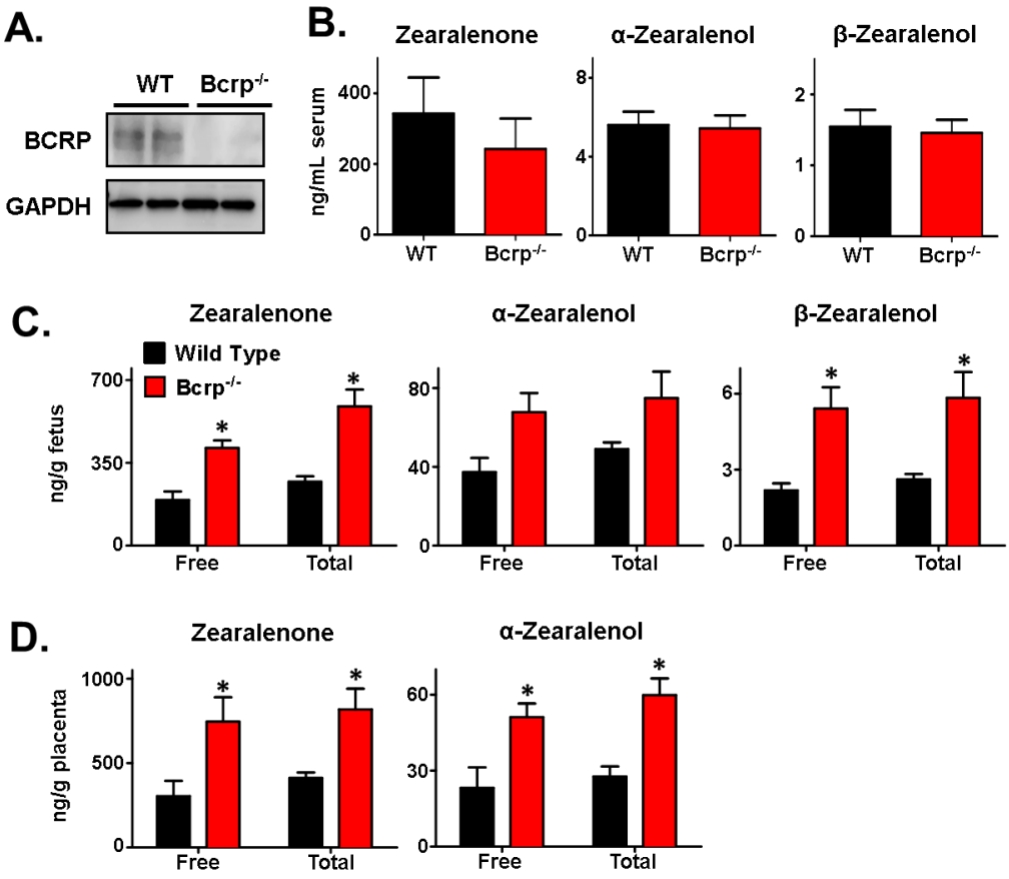

Fig A-1.5. Quantification of zearalenone and its metabolites in pregnant wild-type and Bcrp-/- mice. A. Western Blot of placental homogenates from pregnant wild-type and Bcrp$^{-/-}$ mice analyzing BCRP protein expression (72 kDa) on gestation day 14. GAPDH (37 kDa) was used as a loading control. B-D. Concentration of zearalenone and its metabolites detected in serum (B), fetuses (C), and matched placentas (D) 1 h after tail vein injection as determined by LC-MS. Total concentration was determined after incubation of samples with β-glucuronidase overnight at 37°C. Data represent the mean ± SE (n = 4-6 dams) and were analyzed using a two-way ANOVA followed by post-hoc Bonferroni analysis (*$p < 0.05$ compared to control).

Table A-1.2 Changes in mRNA transcription of transporters and drug metabolizing enzymes in placentas from Bcrp-/- mice versus wild-type mice.

Slc Transporters		
Gene	Fold Change	P < 0.05
Oct1	1.12	N
Oct2	0.87	N
Oct3	0.88	N
Oat1	0.95	N
Oat2	0.92	N
Oat3	1.13	N
Octn1	0.97	N
Octn2	0.97	N
Octn3	0.96	N
Ent1	1.07	N
Mate1	1.07	N
Mate2	0.96	N
Oatp1a4	0.89	N
Oatp2b1	1.31	Y
Oatp3a1	1.29	Y
Oatp4a1	1.05	N
Oatp5a1	0.73	Y

Abc Transporters		
Gene	Fold Change	P < 0.05
Abca1	1.19	N
Mdr1a	1.08	N
Mdr1b	1.13	N
Mrp1	1.16	N
Mrp2	0.79	N
Mrp3	1.27	N
Mrp4	1.23	N
Mrp5	1.14	N
Mrp6	1.19	N
Mrp7	1.13	N

Phase I & II Enzymes		
Gene	Fold Change	P < 0.05
Cyp1a1	1.37	Y
Cyp1a2	1.31	N
Cyp1b1	0.94	N
Cyp27a1	1.01	N
Cyp2b10	1.19	Y
Cyp2e1	1.57	N
Gusb	1.02	N
Sulf1	0.76	Y
Sulf2	1.02	N
Sult1a1	1.09	N
Sult1e1	1.03	N

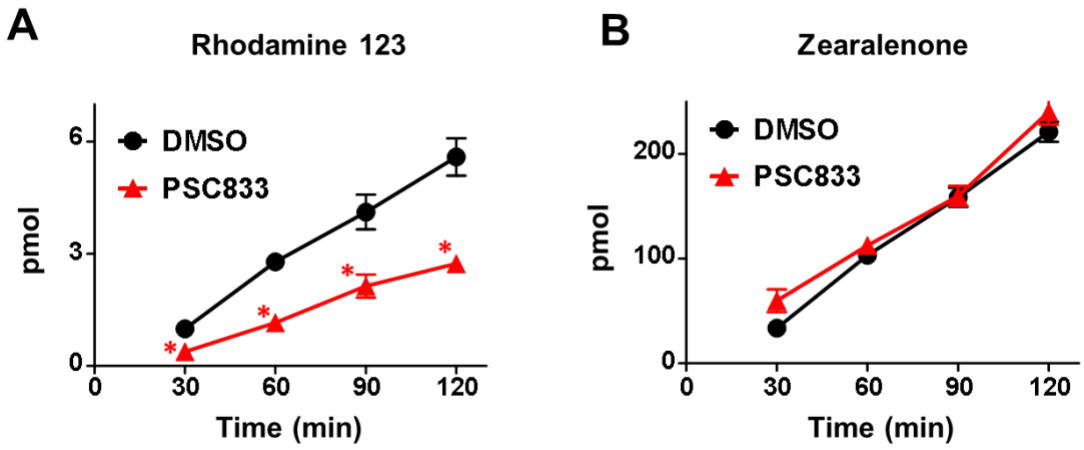

Supplemental Fig A-1.1. Basolateral-to-apical transport of zearalenone and Rhodamine 123 in MDCK cells in the presence of a MDR1 inhibitor. Control MDCK cells grown on transwell inserts were assessed for translocation of the MDR1 substrate Rhodamine 123 (10 μM, A) and zearalenone (50 μM, B) across cell monolayers for 2 h as described in the Materials and Methods. PSC833 (5 μM) was used as a pharmacological inhibitor of MDR1. Data represent the mean pmol detected in the receiver compartment ± SE (n = 3-4) and were analyzed using a Student's t-test (*$p < 0.05$ compared to control).

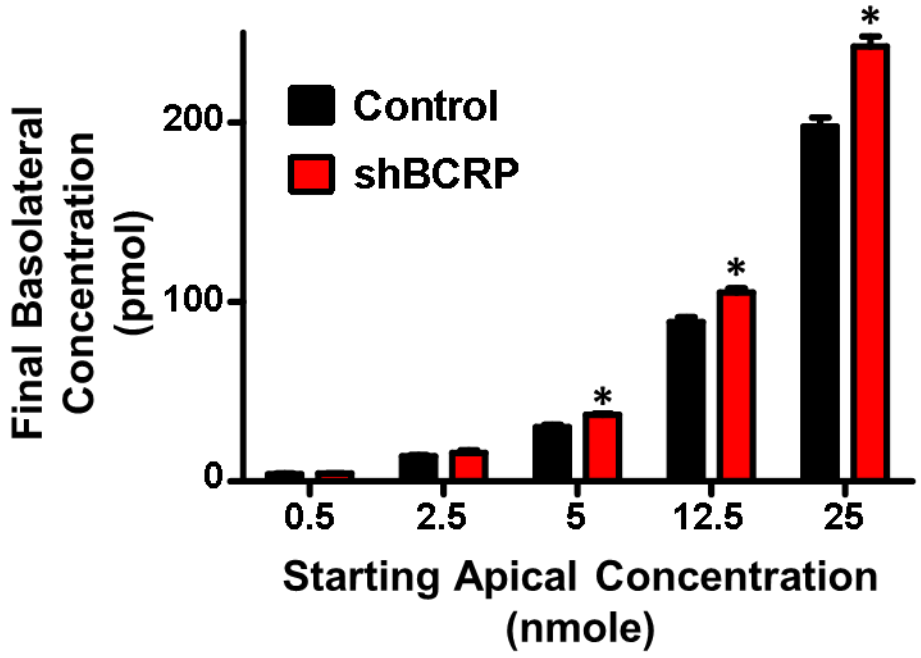

Supplemental Fig A-1.2. Concentration-dependent apical-to-basolateral transport of zearalenone by BeWo b30 cells in transwell cultures. Control and shBCRP BeWo b30 cells grown on transwell inserts were assessed for translocation of zearalenone across cell monolayers for 2 h as described in the Materials and Methods. Data represent the mean pmol detected in the receiver compartment at 2 h ± SE (n = 3-4) and were analyzed using a Student's t-test (*$p < 0.05$ compared to control).

Supplemental Table A-1.1. Primer Sequences for qPCR (5' → 3')

Abca1	AAAACCGCAGACATCCTTCAG	CATACCGAAACTCGTTCACCC
Bcrp/Abcg2	GCGGAGGCAAGTCTTCGTTGC	TCTCTCACTGTCAGGGTGCCCA
Cyp1a1	TGGAAGGGCATAGGCAGCCAC	ACCAATGAAGGGCAAGCCCCA
Cyp1a2	CCCTGCCCTTCAGTGGTACAGATG	TCCGGGTGGATTCTTCAGGCC
Cyp1b1	GCTCATCCTCTTTACCAGATACC	GCAAAAAGCTGGAGAATCGC
Cyp27a1	GCCTCACCTATGGGATCTTCA	TCAAAGCCTGACGCAGATG
Cyp2b10	TGCTGTCGTTGAGCCAACCTTCA	GGGGCTCCCTGGGATTTCCG
Cyp2e1	TTCTGCAGGAAAGCGCGTGTGT	GCGTGGGATACTGCCAAAGCCAA
Cyp3a11	TCACACACACAGTTGTAGGGAGAA	GTCCATCCCTGCTTGTTTGTC
Ent1	CAAGTATTTCACAAACCGCCTGGAC	GAAACGAGTTGAGGCAGGTGAAGAC
Gusb	GGGTGAATGGGATTCATGTGG	TTGGGATACATGGAGGTGTCAG
Mate1	GTTGGCCTTACGGAGAGGAC	AATCCCACCCACCAAGACTAA
Mate2	AGTGGAGCTCCTACACGCGC	AGGGCACCATGTAGGCGACAG
Mdr1a	TGCCCCACCAATTTGACACCCT	ATCCAGTGCGGCCTGAACCA
Mdr1b	GTGTTAAAGGGGCGATGGGCG	AGGCTTGGCCAGACAACAGCTT
Mrp1	GCTGTGGTGGGCGCTGTCTA	CCCAGGCTCAGCCACAGGAA
Mrp2	AGCAGGTGTTCGTTGTGTGT	AGCCAAGTGCATAGGTAGAGAAT
Mrp3	CTGGGTCCCCTGCATCTAC	GCCGTCTTGAGCCTGGATAAC
Mrp4	CCAGACCCTCGTTGAAAGAC	TGAAGCCGATTCTCCCTTC
Mrp5	AGGGCAGCTTGTGCAGGTGG	TGCTGTTCCCGCTTCCTTGCT
Mrp6	TGTCTGCAAGCCATCGGACTGTTTG	TGGAAAAGCGGTTCAGCAGGTTCC
Mrp7	TGGAAACCTCTACACCCCAC	TGAGGAGTCGATGCAGTAGG
Oat1	TAATACCGAGGGGCCATACA	ATGCTTATCAGTGGGCTCAC
Oat2	GTGCTCAGACAGACAGGAAT	AGCTGTGCTTTCTTCGTCTC
Oat3	CTTCAGAAATGCAGCTCTTG	ACCTGTTTGCCTGAGGACTG
Oatp1a4	GCTTTTCCAAGATCAAGGCATTT	GCTTTTCCAAGATCAAGGCATTT
Oatp1a6	GCTGTGTAGACTGAGTTCCAT	CCAACAGAAACACCTTGATCTT
Oatp2a1	CTGTGGAGACAATGGAATCGAG	CACGATCCTGTCTTTGCTGAAG
Oatp2b1	CTCAGGACTCACATCAGGATGC	CTCTTGAGGTAGCCAGAGATCA
Oatp3a1	CGTTTGTTGGGTTTCATCCC	GAGGATGAAGGCAAAGGACT
Oatp4a1	CCAGCGCTACGTTGTTATGAGAG	CAATGAGTGTGGCTTCAGTGG
Oatp5a1	CACCCTGGGACCAACCTATT	ACTCCACCAGTTTCCGATGA
Oct1	TGTCGGCTCTGGCTACAGGAGA	GGGGGATTCTGGGACAAACCAGTAA
Oct2	ATTTCTGGTGCATACCGGAGTCTCC	AGGGGTTCTGACCAAGTCCAGGA
Oct3	ATCCTGAGGCGCGTGGCTAA	GCGCTCGTGAACCAAGCAAACAT
Octn1	GCGCCTATAACAGACTCCTAC	TTTTTCCCACATCTGAACCCTC
Octn2	ACTTTGTTTACCTAGGTGCCTA	TTGTCTGGCTTTGGATTTGC
Octn3	CGTGGGTGTGCTCTTAGGC	CGTGGGTGTGCTCTTAGGC
Rpl13a	GGGCAGGTTCTGGTATTGGAT	GGCTCGGAAATGGTAGGGG
Sulf1	TGAGTGCTTGAGGACGTGTT	CCCTCAGCACCTGAAAATACTG
Sulf2	AAAGTGACCCATCGGTGCTA	TTGAGACGGCCTTTGTGTTG
Sult1a1	CCCGTCTATGCCCGGATAC	GGGCTGGTGTCTCTTTCAGAGT
Sult1e1	TAA AAA CTC ACC TGC CAC CCA	ACC ATA CGG AAC TTG CCC T

APPENDIX 2: INCREASED MDR1 TRANSPORTER EXPRESSION IN HUMAN BRAIN ENDOTHELIAL CELLS THROUGH ENHANCED HISTONE ACETYLATION AND ACTIVATION OF ARYL HYDROCARBON RECEPTOR SIGNALING

Dahea You,[a] Xia Wen,[b,c] Ludwik Gorczyca,[a] Ayeshia Morris,[a]

Jason R. Richardson,[c,d,§] Lauren M. Aleksunes[b,c,§]

[a]Joint Graduate Program in Toxicology, Rutgers, The State University of New Jersey, Piscataway, NJ, USA (DY, LG, AM)

[b]Department of Pharmacology and Toxicology, Rutgers, The State University of New Jersey, Ernest Mario School of Pharmacy, Piscataway, NJ, USA (XW, LMA)

[c]Environmental and Occupational Health Sciences Institute, Piscataway, NJ, USA (XW, JRR, LMA)

[d]Robert Stempel School of Public Health and Social Work, Florida International University, Miami, FL, USA (JRR)

§Denotes equal senior contributors

A-2.1. Abstract

Multidrug resistance protein 1 (MDR1, ABCB1, P-glycoprotein) is a critical efflux transporter that extrudes chemicals from the blood-brain barrier (BBB) and limits neuronal exposure to xenobiotics. Prior studies in malignant cells demonstrated that MDR1 expression can be altered by inhibition of histone deacetylases (HDAC), enzymes that modify histone structure and influence transcription factor binding to DNA. Here, we sought to identify the mechanisms responsible for the up-regulation of MDR1 by HDAC inhibitors in human BBB cells. Immortalized human brain capillary endothelial (hCMEC/D3) cells were treated with HDAC inhibitors and assessed for MDR1 expression and function. Of the HDAC inhibitors profiled, valproic acid (VPA), apicidin, and suberoylanilide hydroxamic acid (SAHA) increased MDR1 mRNA and protein levels by 30-200%, which corresponded with reduced intracellular accumulation of the MDR1 substrate rhodamine 123. Interestingly, induction of MDR1 mRNA by HDAC inhibitors mirrored increases in the expression of the aryl hydrocarbon receptor (AHR) and its target gene cytochrome P450 1A1. To explore the role of AHR in HDAC inhibitor-mediated regulation of MDR1, a pharmacological activator (β-naphthoflavone, βNF) and inhibitor (CH-223191, CH) of AHR were tested. The induction of MDR1 in cells treated with SAHA was amplified by βNF and attenuated by CH. Furthermore, SAHA increased the binding of acetylated histone H3K9/K14 and AHR proteins to regions of the *MDR1* promoter that contain AHR response elements. In conclusion, HDAC inhibitors up-regulate the expression and activity of the MDR1 transporter in human brain endothelial cells by increasing histone acetylation and facilitating AHR binding at the *MDR1* promoter.

Keywords: MDR1, HDAC, transport, blood brain barrier, aryl hydrocarbon receptor

A-2.2. Introduction

The exchange of xenobiotics between the circulation and brain is restricted by the blood-brain barrier (BBB). The BBB possesses tight junctions, few fenestrations, and efflux transporters that work in a coordinated fashion to limit the entry of chemicals into the brain. In particular, the multidrug resistance protein 1 (MDR1, *ABCB1*, P-glycoprotein) is a critical efflux transporter located at the apical surface of the capillary endothelial cells that limits the accumulation of xenobiotics in the brain (Abbott 2014; Abbott et al. 2010). MDR1 transports structurally-diverse chemicals including anticancer agents, pesticides, antipsychotic drugs, and analgesics (Loscher et al. 2005; Nakanishi et al. 2012). As a result, MDR1 plays a critical role in determining the efficacy or toxicity of chemicals in the brain (Sadhasivam et al. 2015; Xie et al. 1999). For example, brain concentrations of the MDR1 substrate, morphine, are elevated in knockout mice lacking the *Mdr1a/1b* ortholog genes (Xie et al. 1999). Similarly, in humans, a genetic polymorphism in *MDR1* that results in transporter loss-of-function has been associated with more significant adverse events following treatment with morphine (Sadhasivam et al. 2015). Consequently, MDR1 is important in regulating xenobiotic disposition and responses in the brain.

The expression of MDR1 is tightly controlled through multiple transcriptional and translational mechanisms. The *MDR1* promoter contains multiple response elements that can interact with a variety of transcription factors. Nuclear transcription factor Y (NF-Y), Sp1, and Sp3 interact with response elements, including an inverted CCAAT box (Y-box) and GC boxes, in the *MDR1* promoter. Likewise, response elements for xenobiotic-activated transcription factors, such as pregnane X receptor (PXR), constitutive androstane receptor (CAR), and aryl hydrocarbon receptor (AHR), are located near the transcriptional start site of the *MDR1* gene (Chan et al. 2013b; Cornwell 1990; Deng et al. 2001; Geick et al. 2001; Goldsmith et al. 1993; Gromnicova et al. 2012; Jin et al. 1998; Madden et al. 1993; Ogura et al. 1991; Scotto 2003; Ueda et al. 1987a; Ueda et al.

1987b). Collectively, multiple signaling pathways work in a coordinated fashion to control the basal and inducible expression of MDR1 in the BBB.

Recently, histone acetylation has gained attention as a potential epigenetic mechanism for regulating MDR1 transcription. The acetylation of histones loosens their interaction with DNA by neutralizing the positive charge in tail regions and reducing affinity to the negatively-charged DNA. As a result, histones as well as transcription factors gain greater access to DNA often resulting in the activation of gene expression (Cary et al. 1982; Hong et al. 1993; Sung et al. 1970). Histone deacetylases (HDACs) control the acetylation status of histones (Inoue et al. 1969; Lopez-Rodas et al. 1993). There are four classes of HDACs: class I (HDACs 1, 2, 3, 8), class IIA (HDACs 4, 5, 7, 9) and IIB (HDACs 6, 10), and class IV (HDAC 10), which are Zn^{2+}-dependent enzymes, and class III, which are Zn^{2+}-independent sirtuin enzymes (Glaser 2007; Harrison et al. 2013; Ni et al. 2015). Inhibitors of HDAC enzymes fall into different chemical classes as outlined in Table 1 (Dokmanovic et al. 2007; Harrison et al. 2013). HDAC inhibitors, including valproic acid (VPA), suberoylanilide hydroxamic acid (SAHA, Zolinza®), and romidepsin (Istodax®), have been approved by the US FDA for a variety of clinical indications, including the treatment of seizure disorders (VPA) and cancer (SAHA and romidepsin) (Kavanaugh et al. 2010; Liu et al. 2015; Terranova-Barberio et al. 2016; Tiffon et al. 2011). One consequence of HDAC inhibition is altered expression and/or activity of the MDR1 transporter in cancer cells (Duan et al. 2017a; El-Khoury et al. 2007; Jin et al. 1998; Xu et al. 2012b). Treatment of H69WT human small cell lung carcinoma cells with trichostatin A (TSA, 330 nM) increased the mRNA expression of MDR1 as well as the binding of acetylated histone H3 and H4 proteins at the *MDR1* promoter (El-Khoury et al. 2007). Furthermore, genetic knockdown of HDACs 1 and 2 using siRNA in cancer cells also enhanced MDR1 expression (Xu et al. 2012b). Moreover, recent studies showed that SAHA and TSA could induce MDR1 in human choriocarcinoma cells via HDAC2 inhibition (Duan et al. 2017a; Duan et al. 2017b). Collectively, these studies in cancer cells point to an epigenetic mechanism for regulating MDR1 expression through modulation of histone acetylation.

To date, no studies have systematically addressed the ability of HDAC inhibitors to regulate MDR1 expression and activity in the BBB. Therefore, the purpose of this study was to evaluate the effects of six different HDAC inhibitors, VPA, sodium butyrate (NaB), romidepsin, apicidin, SAHA and TSA, on the expression and functional activity of the MDR1 transporter in an *in vitro* model of the human BBB. These six HDAC inhibitors were selected based on differences in chemical structure and HDAC targets (Table A-2.1). We hypothesized that disruption of HDAC activity in human brain endothelial cells using pharmacological inhibitors would increase histone acetylation and up-regulate MDR1 expression and function and that modulation of transcriptional regulators, in particular AHR, could be responsible for transporter induction.

A-2.3. Materials and Methods

Chemicals and Reagents

VPA, NaB, apicidin, and SAHA were purchased from Sigma-Aldrich (St. Louis, MO). Romidepsin and TSA were purchased from Selleck Chemicals (Houston, TX) and Wako Chemicals USA, Inc. (Richmond, VA), respectively. All other chemicals were purchased from Sigma-Aldrich unless otherwise specified.

hCMEC/D3 Cell Culture

Human brain capillary endothelial cells (hCMEC/D3), obtained from Dr. Babette Weksler (Poller et al. 2008; Weksler et al. 2013; Weksler et al. 2005), were grown in EBM-2 basal medium (Lonza, Inc., Walkersville, MD) supplemented with 5% characterized fetal bovine serum (GE Healthcare Life Sciences, Logan, UT), 1% penicillin-streptomycin (Life Technologies, Carlsbad, CA), 1.4µM hydrocortisone, 5µg/mL ascorbic acid, 1% chemically defined lipid concentrate (Life Technologies), 10mM HEPES (Life Technologies), and 1ng/mL basic fibroblast growth factor). Cell culture dishes and plates were coated with rat collagen I (Trevigen, Gaithersburg, MD) at 5µg/cm^2. Cells were cultured at 37ºC in a humidified incubator with 5% CO_2.

Cell Viability Assay

To test the cytotoxicity of HDAC inhibitors, hCMEC/D3 cells were seeded in 96-well plates at a density of 8,000 cells per well, allowed to attach overnight, and then treated for 24 h with increasing concentrations of one of following treatments (n=5-10): vehicle, VPA, NaB, apicidin, romidepsin, SAHA or TSA. The vehicles consisted of sterile, distilled water for VPA and NaB and dimethyl sulfoxide (DMSO) for other chemicals. The final concentration of DMSO was 0.1%. Cell viability was measured using the AlamarBlue® assay (Life Technologies) according to the manufacturer's protocol.

Cell Treatments

To screen a panel of HDAC inhibitors for their ability to regulate MDR1 expression, hCMEC/D3 cells were seeded on 6-well plates at a density of 250,000 cells per well. On the following day, cells were incubated in media containing one of the following treatments (n=3-6): vehicle, 5mM VPA, 0.25mM NaB, 1nM romidepsin, 0.5μM apicidin, 10μM SAHA, or 0.25μM TSA. For select HDAC inhibitors, concentration-response experiments were also performed. After 12 and 24 h of treatment, cells were collected and further processed to isolate total RNA and protein as described below.

To assess the effects of the AHR modulators, hCMEC/D3 cells were seeded on 6-well plates at a density of 350,000 cells per well. On the following day, cells (n=3-4) were incubated in media containing one of the following treatments: vehicle (DMSO), 5μM β-naphthoflavone (βNF, AHR activator), 5μM CH-223191 (CH, AHR inhibitor), or 10μM SAHA (HDAC inhibitor) in the presence or absence of either 5μM βNF or 5μM CH. Total RNA was isolated after 6 and 12 h treatments whereas protein was obtained after 24 and 36 h treatments.

RNA Extraction, Reverse Transcription, and Real-Time Quantitative Polymerase Chain Reaction (qPCR)

Total RNA was isolated from the cells using RNAzol® RT reagent (Sigma-Aldrich) following the manufacturer's instructions. RNA purity and concentration were assessed using a Nanodrop 1000 spectrophotometer (Thermo Scientific, Rockford, IL). Complimentary DNA (cDNA) was obtained from total RNA using High-Capacity cDNA Reverse Transcription Kit with RNase Inhibitor (Applied Biosystems, Foster City, CA). Expression of *MDR1 (ABCB1), BCRP (ABCG2), MRPs (ABCCs), AHR, CYP1A1,* and different *HDAC* genes was analyzed by qPCR. Specific forward and reverse primers (Integrated DNA Technologies, Coralville, IA) for each gene

were added to one microgram of cDNA from each sample, and then amplified products were detected using SYBR Green (Applied Biosystems). Sequences of the primers are listed in Supplemental Table 1. qPCR was performed in a 384-well plate format using the ViiA™7 real-time PCR instrument (Applied Biosystems). Ct values were converted to delta delta Ct values by comparing to beta$_2$-microglobulin (β2M), which was used as a reference gene.

Western Blot Analysis

Vehicle- and chemical-treated hCMEC/D3 cells were lysed in cell lysis buffer containing 20mM Tris-HCl, 150mM NaCl, 5mM EDTA, 1% Triton 100 and 1% protease inhibitor cocktail, and then transferred to microcentrifuge tubes. Tubes were centrifuged for 10 min at 500 *g* and supernatants collected. Protein concentrations were determined using the Pierce™ bicinchonicic acid (BCA) protein assay kit (Thermo Scientific). Cell lysates (20 µg protein/well) were loaded on NuPAGE™ 4-12% Bis-Tris Midi Gel (Life Technologies) and then separated by SDS-PAGE electrophoresis. Proteins were then transferred overnight at 4ºC to Immobilon®-FL polyvinylidene fluoride transfer membranes (Millipore, Billerica, MA). Membranes were blocked for 1 h in 5% non-fat dry milk in phosphate-buffer saline (PBS) with 0.5% Tween-20 (PBS-T). Blocking was followed by incubation at room temperature for 3 h with the following primary antibodies diluted in 2% non-fat dry milk at 1:1000 concentration: MDR1 (C219, NB600-1036, Novus Biologicals, Littleton, CO), BCRP (BXP-53, ALX-801-036, Enzo Life Sciences, Inc., Farmingdale, NY), acetylated histone H3 lysine residues 9 and 14 (H3K9/14) (9677S, Cell Signaling Technology, Danvers, MA), and alpha-tubulin (T6199, Sigma-Aldrich). After washing in PBS-T, membranes were incubated with species-appropriate horseradish peroxidase-conjugated secondary antibodies (Sigma-Aldrich). Proteins were detected using SuperSignal® West Dura Extended Duration Substrate (Thermo Scientific) and a FluorChem E imager (Protein Simple, Santa Clara, CA). Protein expression was semi-quantified using AlphaView SA Ver. 3.4.0 (Protein Simple) and normalized to alpha-tubulin.

Rhodamine 123 Accumulation Assay

Cells were treated with vehicle, VPA (5mM), apicidin (0.5μM), or SAHA (10μM) for 24 h and then re-seeded in a 96-well plate to undergo transporter efflux assays as described in a previous protocol (Bircsak et al. 2013b). Briefly, hCMEC/D3 cells (n=4) were incubated for 30 min in medium containing the MDR1 fluorescent substrate rhodamine 123 (7.5μM) in the presence or absence of the functional inhibitor, verapamil (100μM) (*uptake phase*). Cells were then washed, centrifuged, resuspended, and incubated for 2 h in substrate-free medium in the presence or absence of the inhibitors (*efflux phase*). At the end of the efflux phase, cells were washed and re-suspended in cold PBS and evaluated for retention of rhodamine 123. Intracellular fluorescence intensity was quantified in relative fluorescence units (RFU) using the Cellometer Vision cell counter (Nexcelom Bioscience LLC., Lawrence, MA) with the filter cube VB-595-502 (Excitation/Emission: 525nm/595nm). The average for each treatment group was determined by the average fluorescence values of four independent samples.

Nuclear and Cytoplasmic Protein Extraction

Cells were seeded on 100mm dishes at a density of 2,000,000 cells per dish and allowed to attach for 24 h. On the following day, cells were incubated in media containing vehicle or SAHA (10μM). After 24 h, cells were harvested with trypsin-EDTA (Life Technologies) and centrifuged to obtain a cell pellet. The pellet was washed with PBS and underwent nuclear and cytoplasmic extraction using NE-PER™ Nuclear and Cytoplasmic Extraction Reagents (Thermo Scientific). Protein concentrations of the extracts were determined using BCA protein assay kit (Thermo Scientific), and western blot analysis was conducted as described previously with the following primary antibodies at 1:1000 concentration: MDR1 (C219, NB600-1036, Novus Biologicals), AHR

(D5S6H, 83200S, Cell Signaling Technology), histone H3 (D2B12, 4620S, Cell Signaling Technology), and acetylated histone H3K9/H3K14 (9677S, Cell Signaling Technology).

Chromatin Immunoprecipitation (ChIP)-qPCR

Cells were seeded on 150mm dishes at a density of 5,000,000 cells per dish and allowed to attach and grow for 24 h. On the following day, cells were incubated in the media containing vehicle or SAHA (10μM). After 24 h, cells were washed, and ChIP was performed using SimpleChIP® Enzymatic Chromatin IP Kit (Agarose Beads) (Cell Signaling Technology) according to the manufacturer's protocol. Briefly, cells were crosslinked in 1% formaldehyde for 10 min and the crosslinking was stopped with 0.125M glycine. Crosslinked cells were washed and lysed to isolate nuclear pellets. Pelleted nuclei were digested by micrococcal nuclease to obtain DNA fragments of 150 to 600bp, as confirmed by agarose gel electrophoresis (Supplemental Fig. A-2.3). Immunoprecipitation was performed using the following antibodies: acetylated histone H3K9/H3K14 (1:50, 9677S, Cell Signaling Technology), AHR (1:50, D5S6H, 83200S, Cell Signaling Technology), histone H3 (1:50, D2B12, 4620S, Cell Signaling Technology), or normal rabbit IgG (1:333, 2729S, Cell Signaling Technology) which served as a negative control. Immunoprecipitated DNA was purified and quantified by qPCR using specific primers for GAPDH exon 1 (5516S, Cell Signaling Technology), α-satellite repeats (4486S, Cell Signaling Technology), and proximal regions of the *MDR1*/*ABCB1* promoter (P1, P2, P3, P4, and P5). Sequences of the primers are listed in Supplemental Table 1. Amplified products were detected using SYBR Green (Applied Biosystems). Fold enrichment of the immunoprecipitation was calculated by comparing the PCR products of the immunoprecipitated samples to values obtained for input DNA.

Statistical Analysis

GraphPad Prism v5© was used for statistical analysis (GraphPad Software, La Jolla, CA). Differences between groups were compared using a two-tailed student's t-test, one-way analysis of

variance (ANOVA), or two-way ANOVA as appropriate for the number of comparisons and variables. Posthoc Tukey's and Bonferroni tests were performed for one-way and two-way ANOVA, respectively. Correlations and R-values were calculated using a two-tailed Pearson's correlation test. Statistical significance was set at $p < 0.05$.

A-2.4. Results

Viability of hCMEC/D3 Cells after Treatment with HDAC Inhibitors

The ability of HDAC inhibitors to alter hCMEC/D3 cell viability was evaluated using the AlamarBlue® assay. hCMEC/D3 cells were treated with increasing concentrations of each HDAC inhibitor for 24 h (Supplemental Fig. A-2.1). Ranges of HDAC inhibitor concentrations were selected based on previous *in vitro* studies (El-Khoury et al. 2007; Frommel et al. 1993; Galanis et al. 2009; Kelly et al. 2005; Shin et al. 2011; To et al. 2008a; Wang et al. 2010b; Xie et al. 1999; Xu et al. 2012b). For all HDAC inhibitors, the highest concentration that did not reduce cell viability or increase cell detachment was selected to perform further experiments. Therefore, 5mM VPA, 0.25mM NaB, 1nM romidepsin, 0.5µM apicidin, 10µM SAHA, and 0.25µM TSA were used for subsequent studies.

MDR1 Transporter Expression is Increased After HDAC Inhibition

To determine whether brain endothelial MDR1 expression was altered by HDAC inhibition, hCMEC/D3 cells were treated with one of six different HDAC inhibitors and analyzed for changes in the mRNA expression of MDR1 at 12 and 24 h (Fig. A-2.1a). At 12 h, four HDAC inhibitors (VPA, apicidin, SAHA, and TSA) increased MDR1 mRNA levels between 30 and 200%. Up-regulation of MDR1 mRNA by HDAC inhibitors was generally attenuated by 24 h, with the exception of apicidin. Western blotting revealed that HDAC inhibitors increased acetylated histone H3K9/14 protein levels by up to 330%, which confirmed the ability of the majority of chemicals to modify histone protein status. Similar to mRNA expression, inhibition of HDACs by VPA, apicidin, TSA, and SAHA for 24 h up-regulated MDR1 protein expression (Fig. A-2.1b).

HDAC inhibitors were also shown to alter the mRNA levels of other BBB transporters (Supplemental Fig. A-2.2). For example, breast cancer resistance protein (BCRP, *ABCG2)* mRNA expression was significantly induced by all HDAC inhibitors at both 12 and 24 h by up to 220%.

In contrast, the mRNA expression of other efflux transporters including multidrug resistance-associated proteins (MRPs, *ABCC*s) 1, 3, and 4 was moderately down-regulated after exposure to HDAC inhibitors for 12 h and/or 24 h.

Enhanced MDR1 Expression Leads to Increased Functional Activity Following HDAC Inhibition

To determine whether enhanced MDR1 protein expression corresponded with increases in transporter activity, a fluorescent dye accumulation assay was performed. hCMEC/D3 cells were treated with vehicle, VPA, apicidin, or SAHA for 24 h and then evaluated for the intracellular accumulation of the fluorescent substrate, rhodamine 123 (Fig. A-2.1c). Cells treated with VPA, apicidin, and SAHA exhibited reduced accumulation of rhodamine by 20 to 30%, indicating increased efflux function by MDR1. This enhanced activity was reversed by co-incubation with verapamil, a specific MDR1 inhibitor (Wang et al. 2006d). These data indicate that the reduced retention of rhodamine 123 after 24 h exposure to VPA, apicidin, and SAHA was due to the up-regulation of MDR1 expression.

MDR1 Up-Regulation Can Be Achieved at Lower Concentrations of HDAC Inhibitors

To determine whether lower concentrations of HDAC inhibitors could also alter MDR1 expression, hCMEC/D3 cells were treated with vehicle, VPA (1, 2, 5mM), apicidin (0.1, 0.25, 0.5 μM), or SAHA (2.5, 5, 10 μM) and analyzed for MDR1 mRNA and protein levels at 12 and 24 h, respectively. Even the lowest tested concentrations of apicidin and SAHA significantly increased MDR1 mRNA (Fig. A-2.2a). Interestingly, the magnitude of induction was largely similar at each concentration of apicidin or SAHA. On the other hand, the magnitude of MDR1 mRNA up-regulation by VPA was concentration-dependent. Similar to mRNA expression, the protein levels of MDR1 were similarly induced by 24 h at all tested concentrations of VPA, apicidin, and SAHA (Fig. A-2.2b). While the magnitude of MDR1 protein up-regulation was largely similar across all

concentrations, the extent of total histone H3 acetylation by VPA, apicidin, and SAHA increased in a concentration-dependent manner.

SAHA Increases Histone Acetylation at the MDR1 Promoter

SAHA was selected as a prototypical HDAC inhibitor for use in subsequent studies that investigated mechanisms responsible for MDR1 up-regulation. To determine whether HDAC inhibitors altered histone acetylation at the *MDR1* promoter in a manner that facilitates *MDR1* gene activation, we quantified the enrichment of acetylated histone H3K9/K14 proteins in cytoplasmic and nuclear fractions of hCMEC/D3 cells treated with SAHA (Fig. A-2.3a). Basal expression of acetylated histone H3 K9/K14 proteins was detectable in cytosolic and nuclear fractions from vehicle-treated cells. Treatment of hCMEC/D3 cells with SAHA increased acetylated histone H3 K9/K14 proteins by 100% in both nuclear and cytosolic fractions.

To investigate whether enrichment of acetylated histones in the nuclear fraction of hCMEC/D3 cells treated with SAHA enabled the induction of MDR1 mRNA, chromatin immunoprecipitation (ChIP) was performed using an antibody that recognizes acetylation of H3K9/14 and qPCR amplification of different segments of the *MDR1* promoter. Five different regions spanning the *MDR1* transcriptional start site (-182 to +339 bp), namely P1, P2, P3, P4, and P5, were selected based on previous studies highlighting the importance of these regions for efficient transcription of *MDR1* (Fig. A-2.3b). Prior data demonstrated the presence of key transcription factor binding sites within these regions and the critical role of corresponding response elements to mediate induction of MDR1 expression (Cornwell 1990; Goldsmith et al. 1993; Madden et al. 1993; Ueda et al. 1987b; van Groenigen et al. 1993). Treatment of hCMEC/D3 cells with SAHA for 24 h increased the enrichment of acetylated H3K9/14 protein binding at positions P1 and P2 (Fig. A-2.3c). In particular, binding of acetylated H3K9/14 protein was significantly increased by 50% within the P2 region where a putative dioxin response element (DRE) for AHR, a known regulator of MDR1 transporter, is located. Interestingly, P4 and P5 regions which also

include AHR-like DRE elements, suggested trends of reduced DNA binding by acetylated histone H3K9/14 proteins.

AHR Signaling Modulates HDAC Inhibitor-Mediated Induction of the MDR1 Transporter

The results in Fig. A-3.3 indicated that the transcriptional activation of MDR1 involves enhanced binding of acetylated histone proteins in the region of the *MDR1* promoter that contains AHR-like DRE elements. In hCMEC/D3 cells treated with a panel of HDAC inhibitors, we found a correlation between induction of mRNA levels of MDR1 and AHR as well as cytochrome P450 1A1 (CYP1A1), a target gene of AHR (Fig. A-2.4a and b). These data demonstrate increased expression and activity of AHR after HDAC inhibition. Furthermore, nuclear extracts of hCMEC/D3 cells treated with SAHA for 24 h exhibited significant enrichment of AHR protein (Fig. A-3.4c), suggesting that AHR may play a transcriptional role in regulating *MDR1* gene expression following exposure to HDAC inhibitors. It is important to note that the mRNA expression of other xenobiotic-activated MDR1 regulators, PXR and CAR, was barely detectable in hCMEC/D3 cells, as previously noted (Supplemental Table A-2.2) (Dauchy et al. 2009). Therefore, subsequent experiments investigated the role of AHR in HDAC inhibitor-mediated regulation of MDR1.

The effects of AHR activation on MDR1 expression in hCMEC/D3 cells were assessed using the pharmacological AHR agonist, β-naphthoflavone (βNF, 5μM), in combination with SAHA (Fig. A-2.5). Activation of AHR signaling by βNF was confirmed by a 290-370% increase of CYP1A1 mRNA at 6 and 12 h (Fig. A-2.5a). Likewise, treatment with SAHA enhanced CYP1A1 mRNA levels by 135-845% at 6 and 12 h which was further elevated to 910-2660% of control levels following combination with βNF. At 6 h, MDR1 mRNA expression was significantly increased 170% by SAHA and further up-regulated to 300% following combined treatment with SAHA and βNF. Notably, βNF on its own had no significant effect on MDR1 mRNA expression at either time point although there was a trend for 80% increase at 12 h. However, by 12 h, the

augmented induction of MDR1 mRNA in the cells treated with SAHA and βNF was no longer observed. Enhanced MDR1 expression by AHR activation and HDAC inhibition was also observed at the protein level (Fig. A-2.5b). After 24 h, treatment of hCEMC/D3 cells with βNF alone did not affect MDR1 protein expression while SAHA significantly up-regulated levels by 47% as expected. Importantly, the addition of βNF to SAHA further increased MDR1 protein expression by 85% compared to vehicle-treated cells.

To further elucidate the role of AHR in mediating the induction of MDR1 in hCMEC/D3 cells treated with HDAC inhibitors, we assessed whether inhibition of AHR using CH-223191 (CH, 5μM) altered the expression of MDR1 in cells co-treated with SAHA (Fig. A-2.6). Induction of CYP1A1 expression by SAHA at 6 h (82%) and 12 h (540%) was attenuated by co-treatment with CH confirming that AHR signaling was reduced by CH (Fig. A-2.6a). At 6 h, CH did not alter the up-regulation of MDR1 mRNA by SAHA. However, by 12 h, CH significantly suppressed SAHA-mediated induction of MDR1 (175% in SAHA cells; 120% in SAHA+CH cells) similar to that observed for CYP1A1 mRNA. Likewise, at 36 h, CH largely prevented SAHA-mediated induction of MDR1 protein (Fig. A-2.6b).

HDAC Inhibition by SAHA Increases AHR Binding to the MDR1 Promoter

To investigate the interaction of AHR at the *MDR1* gene, we performed a ChIP assay to assess the binding of AHR proteins to *MDR1* promoter regions, P1 through P5. Of these regions, P2, P4, and P5 contain putative AHR response elements as illustrated in Fig. A-2.7a. Treatment of hCMEC/D3 cells with SAHA for 24 h significantly increased AHR binding between 50 to 100% at the P2, P4, and P5 regions (Fig. A-2.7b). Of these regions, P2 also exhibited significant histone H3K9/14 acetylation as aforementioned (Fig. A-2.3c). The promoter of *CYP1A1*, a positive control gene, also exhibited significantly higher enrichment of AHR binding after SAHA treatment (Supplemental Fig. A-2.4). On the contrary, the enrichment of AHR did not change at the P1 and P3 regions of the *MDR1* promoter where no AHR response elements are found (Fig. A-2.7b).

A-2.5. Discussion

MDR1, which is tightly regulated by multiple mechanisms, confers protection to the brain by preventing the passage of numerous xenobiotics into the parenchyma (Abbott et al. 2010; Loscher et al. 2005; Nakanishi et al. 2012). Previous studies have identified several nuclear receptors and transcription factors as regulators of MDR1 (Bauer et al. 2004; Lemmen et al. 2013b; Wang et al. 2014; Wang et al. 2011; Wang et al. 2010b). Recent studies have revealed the ability of HDAC inhibitors to up-regulate the expression and function of MDR1 in various cancer cell lines. This induction occurs via histone acetylation at gene promoters, demonstrating a novel role for epigenetic modifications to control transporter expression (El-Khoury et al. 2007; Kim et al. 2009; To et al. 2008a). Since HDAC inhibitors have clinical utility in treating various brain diseases including epilepsy and glioblastoma, it is important to evaluate the effects of HDAC inhibitors on transporters at the BBB. Therefore, the purpose of this study was to investigate the ability of pharmacological inhibitors of HDAC enzymes to regulate the expression and function of the MDR1 transporter in human brain endothelial cells. Our findings demonstrated that: (1) HDAC inhibitors increased the mRNA and protein expression of MDR1 in hCMEC/D3 cells, an *in vitro* model of the human BBB; (2) up-regulated expression translated into increased functional activity of MDR1; and (3) enhanced histone acetylation and activation of AHR signaling are involved in MDR1 up-regulation.

Six different HDAC inhibitors were tested including three FDA-approved drugs, VPA, romidepsin and SAHA, as well as NaB, apicidin, and TSA. HDAC inhibitors are classified based upon chemical properties, which enable the targeting of different HDAC isoforms (Table A-2.1) (Harrison et al. 2013). Across classes, HDAC inhibitors differ in their potency. Whereas short chain fatty acids such as VPA and NaB are weak HDAC inhibitors typically effective at millimolar concentrations, hydroxamic acids (SAHA and TSA) and cyclic peptides (romidepsin and apicidin) are more potent, eliciting effects at nanomolar to micromolar concentrations (Dokmanovic et al.

2007). In the current study, HDAC inhibitors displayed differential abilities to regulate MDR1 expression in hCMEC/D3 cells. Generally, short chain fatty acids were less potent and/or effective at increasing HDAC acetylation and inducing MDR1 expression compared to other HDAC inhibitors. This observation likely results from the relatively weaker inhibition of HDACs as indicated by minimal changes in acetylated histone H3 level.

On the other hand, apicidin, a potent HDAC inhibitor that specifically targets class I HDACs, was effective in inducing both mRNA and protein levels of MDR1. Interestingly, romidepsin, also a potent HDAC inhibitor, which increased MDR1 mRNA expression and MDR1 promoter acetylation in acute promyelocytic leukemia NB4 cells (Tabe et al. 2006), did not alter MDR1 mRNA or protein levels in hCMEC/D3 cells despite detectable histone H3 acetylation. It is possible that the romidepsin-mediated changes of MDR1 expression are concentration- and time-specific. Alternatively, this disconnect may be due to: (1) different specificity of targeting HDAC isoforms between romidepsin and apicidin; or (2) the involvement of an alternative (non-histone), cell-specific mechanism that is not altered by romidepsin. In contrast, although TSA significantly induced MDR1 mRNA level, it did not affect histone acetylation status as observed with SAHA, which targets the same isoforms of HDACs. It is important to note that histone H3 acetylation is just one type of epigenetic modification and the possibility exists that other epigenetic events such as H4 acetylation may be involved. A study by Tabe and coworkers (2006) showed that romidepsin increased the acetylation of H4 but not H3K9, at the CCAAT box of *MDR1* promoter in NB4 acute promyelocytic leukemia cells (Tabe et al. 2006). Taken together, these data suggest that HDAC inhibitors can elicit highly specific patterns of histone acetylation.

The most likely mechanism for induction of MDR1 following treatment of hCMEC/D3 cells with HDAC inhibitors is through the binding of acetylated histones at the *MDR1* promoter and subsequent gene activation due to an open, accessible DNA conformation (Clayton et al. 1993; Lee et al. 1993; Turner 1991; Wolffe 1996). In fact, we observed a significant increase in the protein levels of acetylated histone H3 in nuclear fractions of hCMEC/D3 cells treated with SAHA. Further

analyses showed that these acetylated histone H3 proteins were highly enriched at the upstream region of the *MDR1* promoter (-182 to +8 bp relative to the TSS) which contains several response elements interacting with key transcription factors such as Sp1, Sp3, AP-1, and NF-Y (Goldsmith et al. 1993; Gromnicova et al. 2012; Jin et al. 1998; Ogura et al. 1991; Sundseth et al. 1997; Ueda et al. 1987b). In particular, significant enrichment of histone H3 K9/K14 binding was observed between -100 to +8 bp where an inverted CCAAT box (Y-box) and a potential DRE are located (Goldsmith et al. 1993; Madden et al. 1993; Ueda et al. 1987b). This finding was significant because it further supports that: (1) Y-box, which was identified as the critical element for the induction of MDR1 by TSA and apicidin in cancer cells (Jin et al. 1998; Kim et al. 2009), is an important sequence for the activity of HDAC inhibitors; and (2) AHR plays a role in inducing MDR1 transcription. Our results further demonstrated that there was a correlation between AHR and MDR1 mRNA upon HDAC inhibition, suggesting the possible involvement of AHR signaling. Enhanced histone acetylation at a DRE suggests that there is an increased accessibility for AHR to interact with this response element to facilitate *MDR1* gene activation.

By comparison, histone H3 acetylation at the "P3" region of the *MDR1* promoter (spanning from +11 to +110 bp), which does not have transcription factor binding sites, did not significantly change. This indicates that the binding of acetylated histone H3 preferentially occurs at regions that interact with transcription factors. Interestingly, there was a trend of reduced binding of acetylated histone H3 proteins in the P4 and P5 regions (spanning from +90 to + 339 bp) which also contains a DRE (Madden et al. 1993; Ueda et al. 1987b). However, it is possible that other markers of histone modification, such as acetylated histone H4, may have been enriched at these regions.

We performed further studies to investigate the importance of AHR activity in SAHA-mediated regulation of MDR1. First, we evaluated the effects of pharmacologic modulators of AHR activity on MDR1 induction by SAHA. βNF activation of AHR augmented MDR1 mRNA induced by SAHA at 6 h, suggesting that SAHA induces binding of acetylated histones at the *MDR1*

promoter to increase the accessibility of DRE, facilitate the binding of the ligand-activated AHR, and induce *MDR1* gene activation. By comparison, the AHR inhibitor CH attenuated the induction of MDR1 mRNA and protein by SAHA. Assessment of nuclear lysates of SAHA-treated cells showed that there was indeed a significant increase in AHR expression in the nucleus, suggesting the possibility of enhanced AHR binding to target genes. ChIP analysis revealed enrichment of AHR binding at the P2 (-100 to +8 bp), P4 (+90 to +245 bp), and P5 (+230 to +338 bp) regions of the *MDR1* promoter which contain putative DREs (Madden et al. 1993; Ueda et al. 1987b). On the other hand, no significant changes were observed at the P1 (-182 to -76 bp) and P3 (+11 to +110 bp) regions that do not possess AHR binding sites. These data point to a critical role of AHR in HDAC-mediated regulation of MDR1. Nonetheless, it is possible that additional mechanisms play a role. It is well-known that the regulation of MDR1 is complex and involves the interaction of multiple pathways. As discussed above, the promoter regions with significant histone H3 acetylation after SAHA treatment contain multiple response elements. It is plausible that other transcription factors, such as Sp1 and Sp3, also work cooperatively with AHR to regulate the transcriptional activation of *MDR1* in response to HDAC inhibition.

Interestingly, HDAC inhibition did not result in global up-regulation of efflux transporters as MRP mRNAs were either unchanged or down-regulated, suggesting that MRP regulation by HDAC inhibitors may be mediated via different mechanisms. Differences in the organization of the *MRP* promoter relative to the *MDR1* promoter is a likely cause for divergent responses to HDAC inhibitors. To address this question, it would be important to assess the characteristics of *MRP* promoters, such as the methylation status, baseline histone acetylation level, as well as the types and locations of the transcription factor binding sites. Alternatively, suppression of MRP expression may be compensatory response to the MDR1 up-regulation to maintain the overall transport properties of shared substrates.

Taken together, this study demonstrated that HDAC inhibitors, in particular VPA, apicidin, and SAHA, significantly up-regulated the mRNA and protein expression of MDR1 in a human

model of the BBB. Enhanced functional activity of MDR1 after HDAC inhibition was indicated by reduced accumulation of its substrate rhodamine. Transporter up-regulation was associated with histone acetylation as shown by increased levels of acetylated histone H3. Our mechanistic studies showed that SAHA induces the nuclear enrichment and binding of acetylated histones and AHR to the *MDR1* promoter. Concurrent exposure to an AHR activator further enhanced SAHA-mediated induction of MDR1 expression while an AHR inhibitor moderately reduced MDR1 mRNA and protein levels induced by SAHA. These results suggest that inhibition of HDAC activity by pharmacological inhibitors promotes the binding of acetylated histones at the *MDR1* promoter to make the region more accessible for transcription factors, such as AHR, to bind and activate *MDR1* gene transcription. A proposed mechanism is illustrated in Fig. 8.

It is important to note that although the hCMEC/D3 cells are a representative model of the BBB, it does not possess all properties of intact brain microvessels. For example, we were unable to achieve sufficient transendothelial electrical resistance (TEER), a key feature of the BBB, when these cells were cultured as a monolayer on transwell inserts (data not shown). Prior studies showed that the co-culture of brain microvascular endothelial cells with supporting cells, such as the astrocytes and pericytes, can improve tight junction formation as measured by TEER (Hatherell et al. 2011; Kulczar et al. 2017). Implementing this co-culture system to test the effects of HDAC inhibitors on transporters may provide a more translational platform. In addition, it would be advantageous to assess the effects of HDAC inhibitors using other types of BBB models. A recent *in vivo* study in our laboratory showed that HDAC inhibitors (apicidin and valproic acid) caused brain region-specific up-regulation of Mdr1 in mice, with the most notable induction in the striatum (You et al. 2019). Future studies are also needed to investigate the effects of HDAC inhibitors on MDR1-mediated efflux of pharmaceuticals and environmental chemicals using *ex vivo* mouse brain microvessels.

Collectively, our data suggest that the clinical administration of HDAC inhibitors may alter efflux properties at the BBB leading to reduced penetration of MDR1 substrates into the

parenchyma. This may be relevant for: (1) the concomitant administration of neuroactive drugs that are substrates of the MDR1 transporter; and (2) the treatment of neurological conditions caused by the neurotoxicants cleared by MDR1. Expanding our understanding of the epigenetic regulation of MDR1 transporters can aid in identifying specific molecular targets that are important for maintaining efflux transport properties of the human BBB. HDAC and AHR pathways may represent novel molecular targets to modulate the BBB transporter activity to either increase the brain concentration of psychoactive drugs or decrease the penetration of toxicants implicated in neurodegeneration.

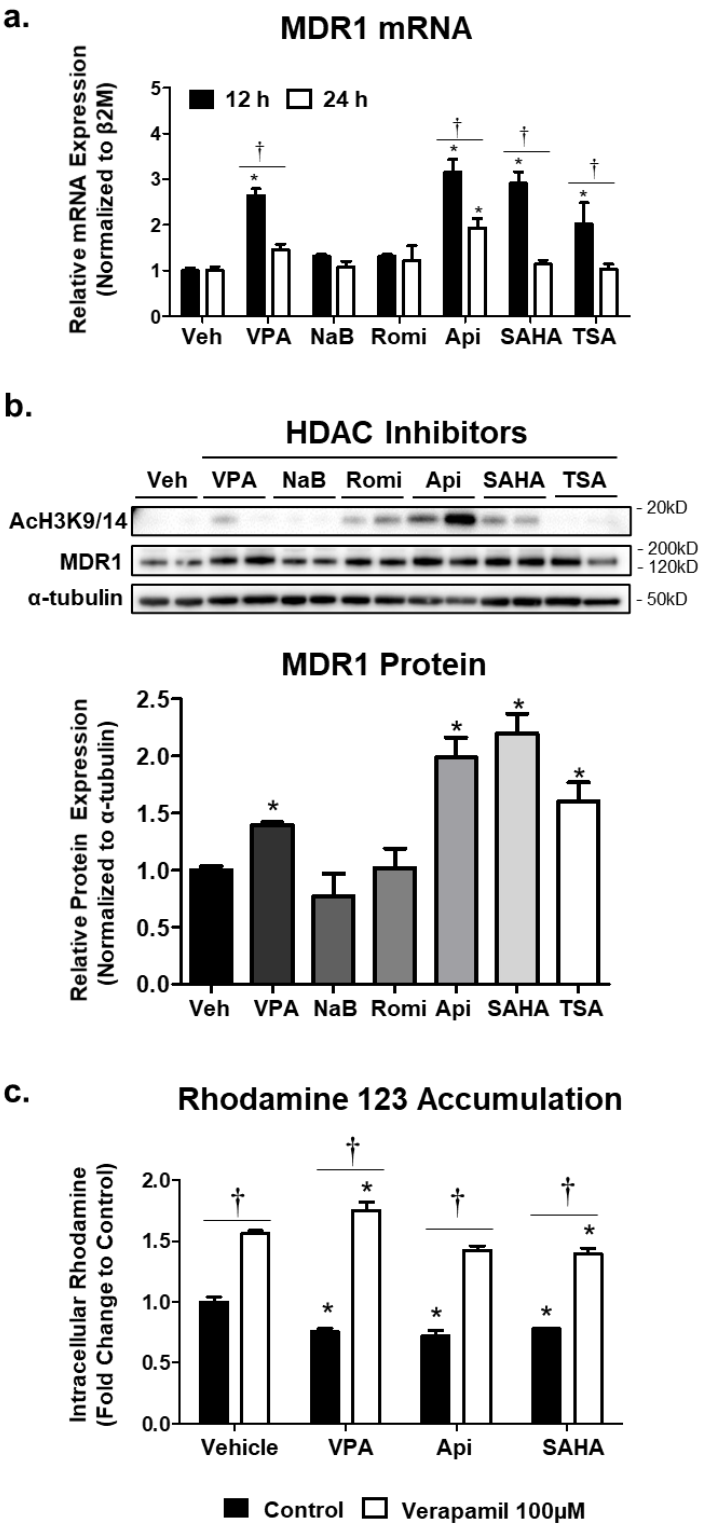
a.
MDR1 mRNA
Relative mRNA Expression (Normalized to β2M)
12 h
24 h
Veh
VPA
NaB
Romi
Api
SAHA
TSA
b.
HDAC Inhibitors
AcH3K9/14
MDR1
α-tubulin
20kD
200kD
120kD
50kD
MDR1 Protein
Relative Protein Expression (Normalized to α-tubulin)
c.
Rhodamine 123 Accumulation
Intracellular Rhodamine (Fold Change to Control)
Vehicle
Control
Verapamil 100μM

Fig A-2.1. MDR1 expression and function in human brain microvascular endothelial cells treated with HDAC inhibitors. (a) hCMEC/D3 cells (n=3-6) were treated with vehicle (veh) or six HDAC inhibitors (5mM VPA, 0.25mM NaB, 1nM romidepsin (Romi), 0.5μM apicidin (Api), 10μM SAHA, or 0.25μM TSA) for 12 h (black) or 24 h (white) and analyzed for mRNA expression of MDR1. Data were normalized to beta$_2$-microglobulin and presented as mean ± SEM. Data were analyzed by one-way ANOVA between treatments within each time point (*), and by two-way ANOVA to compare between the two time points (†), with statistical significance at $p < 0.05$; (b) hCMEC/D3 cells (n=3-4) were treated with vehicle or six HDAC inhibitors for 24 h and analyzed for protein expression of acetylated histone H3K9/14 or MDR1 by western blot analysis followed by densitometry to semi-quantify protein levels. Alpha-tubulin (α-tubulin) was used as a loading control. Data are presented as mean ± SEM and analyzed by one-way ANOVA. Asterisks (*) represent a statistical difference ($p < 0.05$) between vehicle- and HDAC inhibitor-treated cells; (c) MDR1 function after the exposure to HDAC inhibitors was assessed by measuring the cellular accumulation of a fluorescent MDR1 substrate, rhodamine 123 (7.5μM), in the presence or absence of the MDR1 inhibitor, verapamil (100μM), using the Nexcelom Cellometer Vision (n=4). Intracellular fluorescence was quantified as mean relative fluorescence intensity. The bar graph is presented with mean ± SEM as analyzed by 2-way ANOVA to compare each treatment group to vehicle (*) and within each treatment group (†), with statistical significance at $p < 0.05$

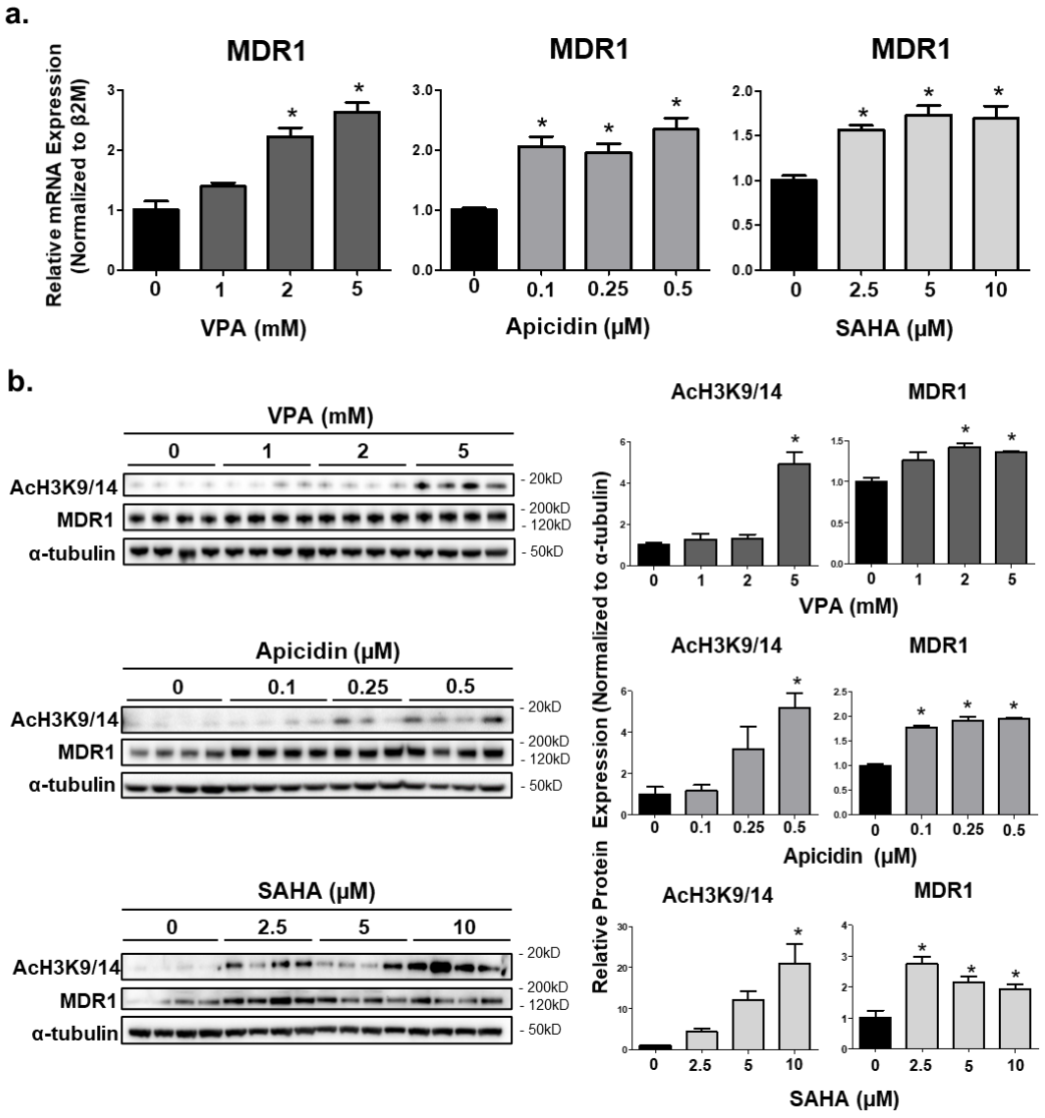

Fig A-2.2. Concentration-dependent regulation of MDR1 expression in human brain microvascular endothelial cells treated with HDAC inhibitors. hCMEC/D3 cells (n=3-6) were treated with vehicle or increasing concentrations of VPA, apicidin, or SAHA for 12 h and 24 h and analyzed for MDR1 mRNA (a) and protein (b), respectively. Data were normalized to beta$_2$-microglobulin for mRNA and alpha-tubulin (α-tubulin) for protein, and presented as mean ± SEM. Asterisks (*) represent a statistical difference ($p < 0.05$) between vehicle- and HDAC inhibitor-treated cells

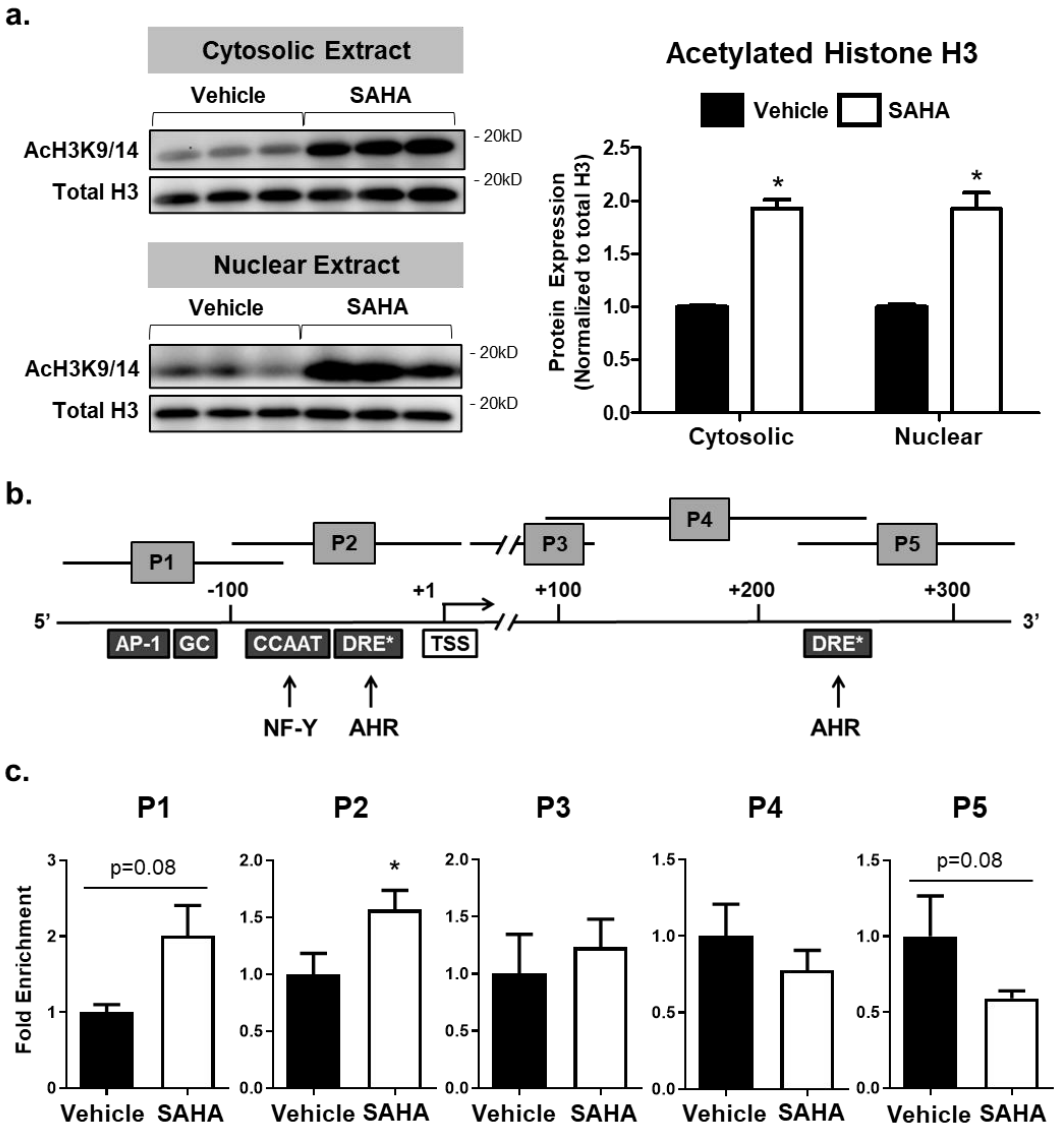

Fig A-2.3. The enrichment of acetylated histone H3 proteins and DNA binding in human brain microvascular endothelial cells treated with SAHA. (a) hCMEC/D3 cells (n=3-10) were treated with vehicle or 10μM SAHA for 24 h and cytosolic and nuclear extracts were collected. The relative protein expression of acetylated histone H3K9/14 in each compartment was analyzed by western blot analysis followed by densitometry to semi-quantify protein levels. Total histone H3 was used as a loading control. Data are presented as mean ± SEM and analyzed by a two-tailed Student's t-test compared to the vehicle control (*) for each compartment with statistical

significance at $p < 0.05$; (b) The locations of different response elements and transcription factor binding sites at human *MDR1/ABCB1* gene (NC_000007.14) promoter region. DRE: Dioxin Response Element; TSS: Transcription Start Site; AHR: Aryl Hydrocarbon Receptor; (c) hCMEC/D3 cells (n=3-6) were treated with vehicle or 10μM SAHA for 24 h and analyzed for relative histone H3K9/14 acetylation at different regions of the *MDR1*/*ABCB1* gene promoter. Data collected from qPCR amplification of ChIP samples were presented as mean ± SEM. Data were analyzed by two-tailed Student's t-test between treatment groups with statistical significance at $p < 0.05$. The graph titles correspond to the labels in Fig. 3b

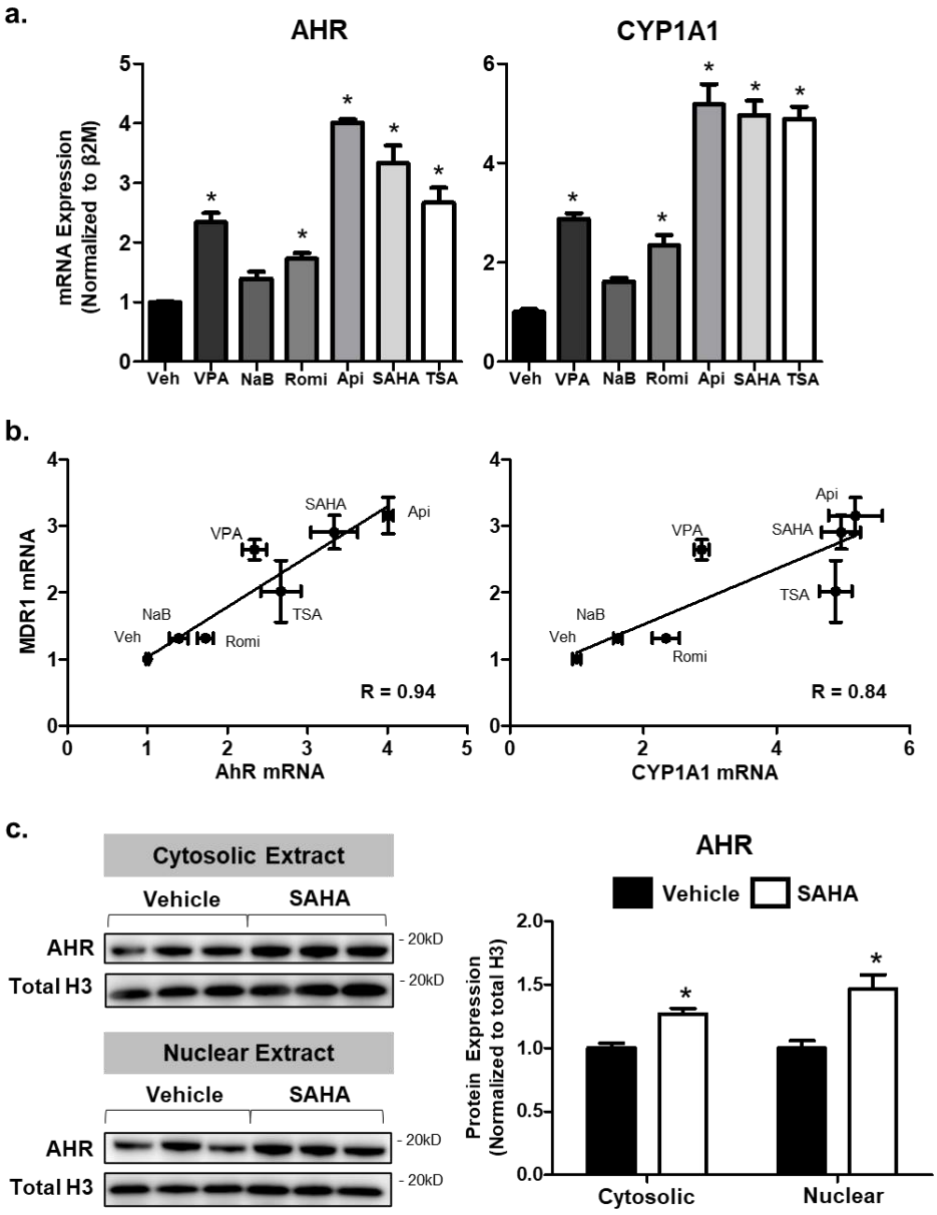

Fig A-2.4. AHR expression and activity in human brain microvascular endothelial cells treated with HDAC inhibitors. (a) hCMEC/D3 cells (n=3-6) were treated with vehicle (Veh) or six HDAC inhibitors (5mM VPA, 0.25mM NaB, 1nM romidepsin (Romi), 0.5µM apicidin (Api), 10µM SAHA, or 0.25µM TSA) for 12 h and analyzed for mRNA expression of AHR and CYP1A1. Data were normalized to beta2-microglobulin and presented as mean ± SEM. Data were analyzed by one-way ANOVA compared to the vehicle control (*) with statistical significance at $p < 0.05$;

(b) Correlation between changes in the expression of MDR1 and AHR and CYP1A1 mRNA levels after 12 h treatment with HDAC inhibitors was analyzed by Pearson's correlation test; (c) hCMEC/D3 cells (n=3-7) were treated with vehicle or 10μM SAHA for 24 h and cytosolic and nuclear extracts were collected. The relative protein expression of AHR in each compartment was analyzed by western blot analysis followed by densitometry to semi-quantify protein levels. Total histone H3 was used as a loading control. Data are presented as mean ± SEM and analyzed by a two-tailed Student's t-test compared to the vehicle control (*) for each compartment with statistical significance at $p < 0.05$

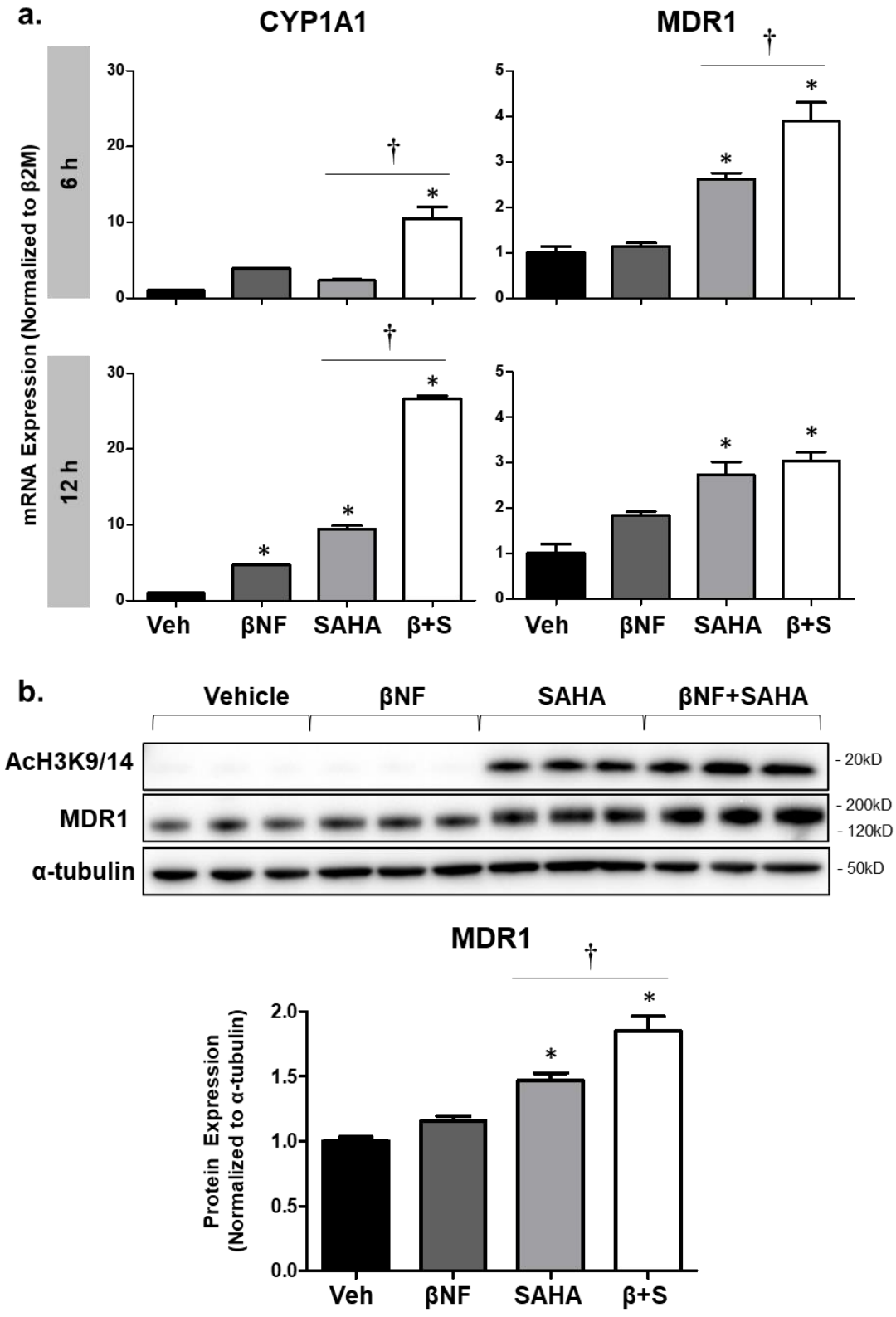
a.
CYP1A1
MDR1
6 h
12 h
mRNA Expression (Normalized to β2M)
Veh
βNF
SAHA
β+S
b.
Vehicle
βNF
SAHA
βNF+SAHA
AcH3K9/14
MDR1
α-tubulin
- 20kD
- 200kD
- 120kD
- 50kD
MDR1
Protein Expression (Normalized to α-tubulin)

Fig A-2.5. MDR1 expression in human brain microvascular endothelial cells treated with SAHA and an AHR activator. (a) hCMEC/D3 cells (n=3) were treated with vehicle (Veh), AHR activator (βNF, β-naphthoflavone 5μM) and/or 10μM SAHA for 6 h or 12 h. Total RNA was isolated and analyzed for mRNA expression of MDR1 and CYP1A1, the positive control, by qPCR. Data were normalized to beta$_2$-microglobulin and presented as mean ± SEM. Data were analyzed by one-way ANOVA compared to the vehicle control (*), and between SAHA and β+S (βNF + SAHA) (†) with statistical significance at $p < 0.05$; (b) hCMEC/D3 cells (n=3) were treated with Veh, βNF 5μM and/or 10μM SAHA for 24 h and analyzed for protein expression of acetylated histone H3K9/14 or MDR1 by western blot analysis followed by densitometry to semi-quantify protein levels. Alpha-tubulin (α-tubulin) was used as a loading control. Data are presented as mean ± SEM and analyzed by one-way ANOVA compared to the vehicle control (*), and between SAHA and β+S (†) with statistical significance at $p < 0.05$

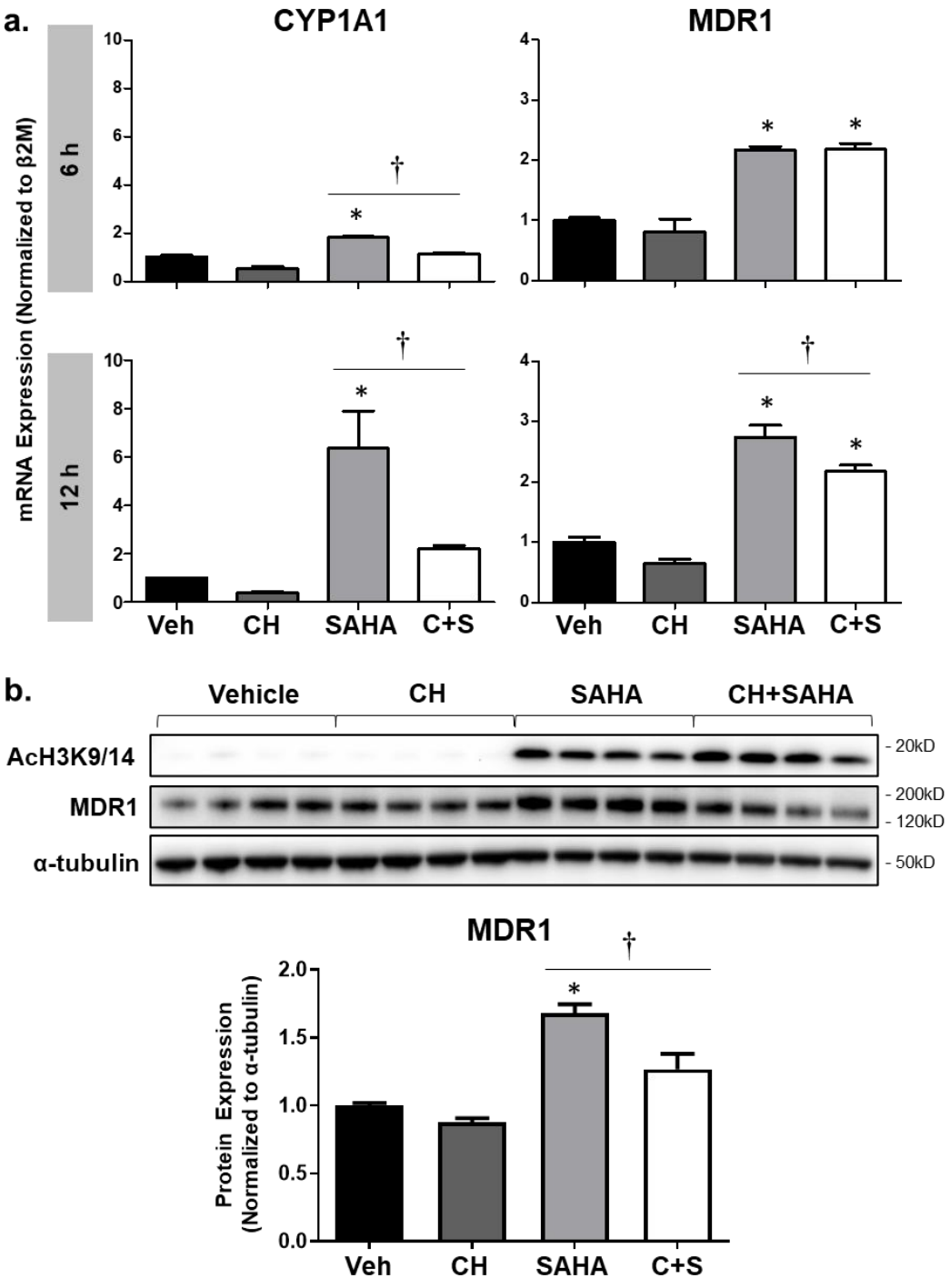
a.
CYP1A1
MDR1
6 h
12 h
mRNA Expression (Normalized to β2M)
Veh
CH
SAHA
C+S
b.
Vehicle
CH
SAHA
CH+SAHA
AcH3K9/14
MDR1
α-tubulin
- 20kD
- 200kD
- 120kD
- 50kD
MDR1
Protein Expression (Normalized to α-tubulin)

Fig A-2.6. MDR1 expression in human brain microvascular endothelial cells treated with SAHA and an AHR inhibitor. (a) hCMEC/D3 cells (n=3-4) were treated with vehicle (Veh), AHR inhibitor (CH, CH-223191 5μM) and/or 10μM SAHA for 6 h or 12 h. Total RNA was isolated at the end of the treatment and analyzed for mRNA expression of MDR1 and CYP1A1, the positive control, by qPCR. Data were normalized to beta$_2$-microglobulin and presented as mean ± SEM. Data were analyzed by one-way ANOVA compared to the vehicle control (*), and between SAHA and C+S (CH + SAHA) (†) with statistical significance at $p < 0.05$; (b) hCMEC/D3 cells (n=4) were treated with Veh, CH 5μM and/or 10μM SAHA for 36 h and analyzed for protein expression of acetylated histone H3K9/14 or MDR1 by western blot analysis followed by densitometry to semi-quantify protein levels. Alpha-tubulin (α-tubulin) was used as a loading control. Data are presented as mean ± SEM and analyzed by one-way ANOVA compared to the vehicle control (*), and between SAHA and C+S (†) with statistical significance at $p < 0.05$

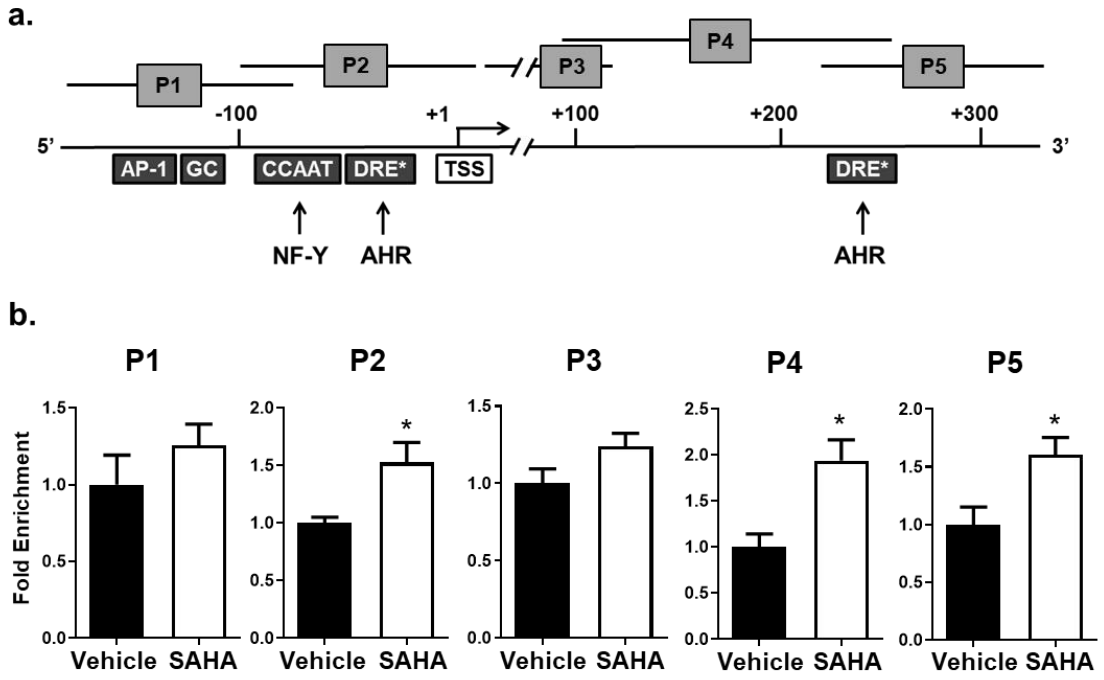

Fig A-2.7. Relative aryl hydrocarbon receptor binding at different regions of the *MDR1/ABCB1* gene promoter in human brain microvascular endothelial cells treated with SAHA. hCMEC/D3 cells (n=3-10) were treated with vehicle or 10μM SAHA for 24 h and analyzed for relative AHR binding at different regions of the *MDR1/ABCB1* gene promoter (a). Data collected from qPCR amplification of ChIP samples were presented as mean ± SEM (b). Data were analyzed by two-tailed Student's t-test between treatment groups with statistical significance (*) at $p < 0.05$. The graph titles correspond to the labels in Fig. 7a

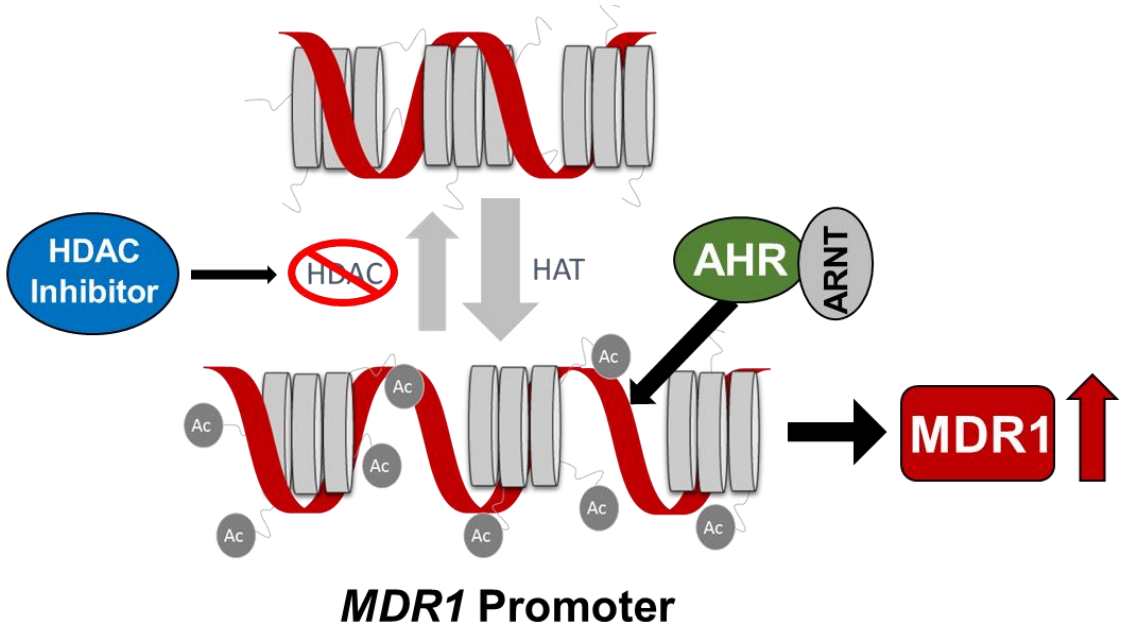

Fig A-2.8. Proposed mechanism of interaction between histone acetylation and AHR signaling in MDR1 regulation at the human blood-brain barrier. Pharmacological inhibition of HDACs promotes the acetylation of histones which consequently increases the accessibility of the *MDR1* promoter to AHR binding and transactivation of the *MDR1* gene

Table A-2.1. Classification of HDAC inhibitors (Harrison et al. 2013)

HDAC Inhibitor Class	HDAC targets	Example Compounds	Potency Range[a]
Short chain fatty acids	Classes I and IIA	▪ Valproic acid (VPA) ▪ Sodium butyrate (NaB)	mM
Cyclic peptides	Class I	▪ Romidepsin (Romi) ▪ Apicidin (Api)	nM
Hydroxamic acids	Classes I and II	▪ Suberoylanilide hydroxamic acid (SAHA) ▪ Trichostatin A (TSA)	nM – μM

[a]This potency range represents general IC_{50} values (50% inhibitory concentrations) for purified HDAC proteins as determined by HDAC activity assays.

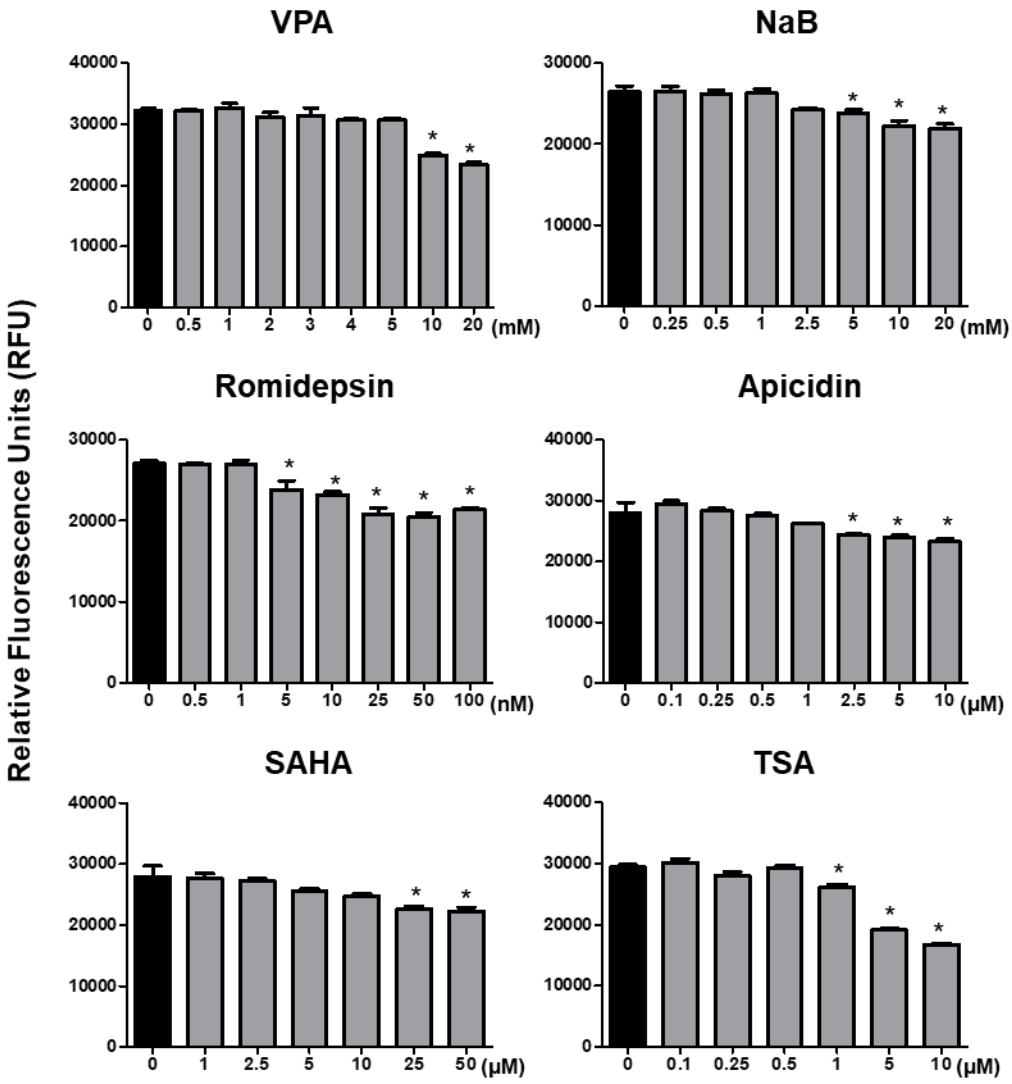

Supplemental Fig A-2.1. hCMEC/D3 cell viability after treatment with HDAC inhibitors. hCMEC/D3 cells (n=5-10) were treated with vehicle or increasing concentrations of six HDAC inhibitors for 24 h. Cell viability was assessed using the AlarmarBlue® assay and data recorded as relative fluorescence units (RFUs). Data are presented as mean ± SEM and analyzed by one-way ANOVA. Asterisks (*) represent a statistical difference ($p < 0.05$) of each treatment compared to the vehicle-treated control group

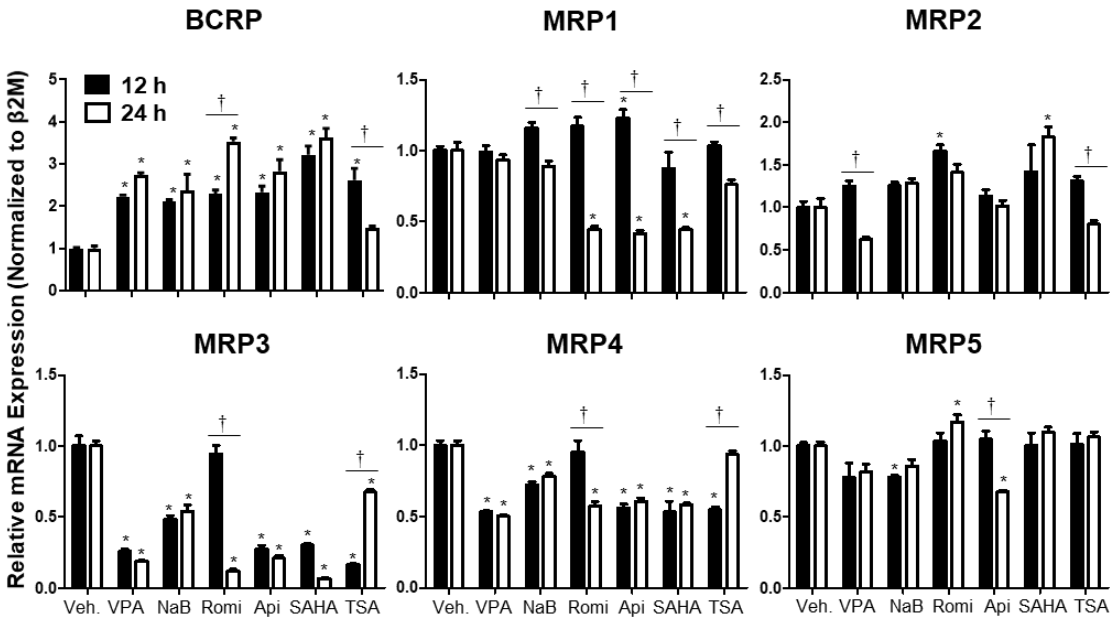

Supplemental Fig A-2.2. Efflux transporter mRNA expression in human brain microvascular endothelial cells treated with HDAC inhibitors. hCMEC/D3 cells (n=3-6) were treated with vehicle or six HDAC inhibitors for 12 h (black) or 24 h (white) and analyzed for mRNA expression of BCRP and MRP isoforms. Data were normalized to beta$_2$-microglobulin and presented as mean ± SEM. Data were analyzed by one-way ANOVA between treatments within each time point (*), and by two-way ANOVA to compare between the two time points (†), with statistical significance at $p < 0.05$

Supplemental Fig A-2.3. The chromatin fragmentation of digested nuclei from human brain microvascular endothelial cells. The digestion pattern of nuclei samples was analyzed by an agarose gel electrophoresis. The lengths of DNA fragments range from 150 to 600bp.

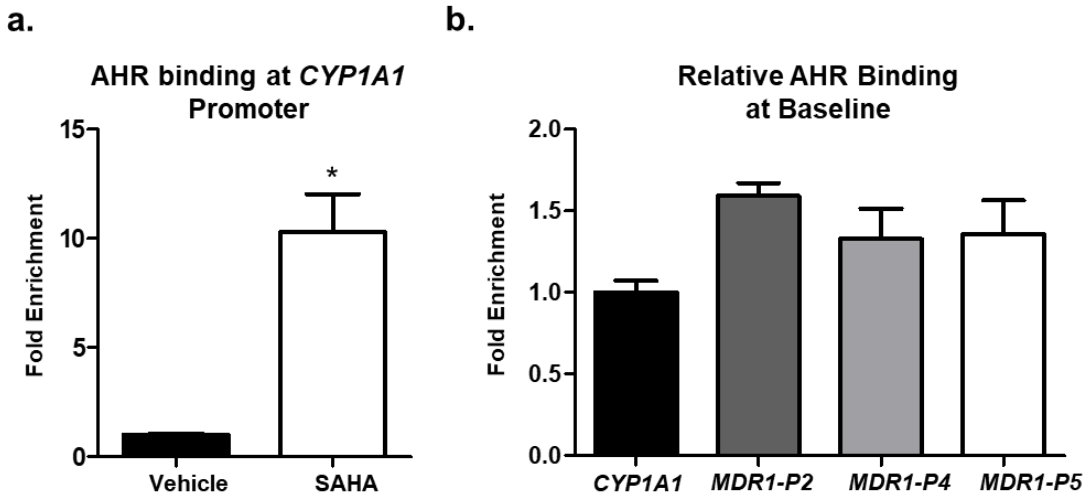

Supplemental Fig A-2.4 Relative aryl hydrocarbon receptor (AHR) binding at *CYP1A1* gene promoter in human brain microvascular endothelial cells treated with SAHA. (a) hCMEC/D3 cells (n=3-6) were treated with vehicle or 10μM SAHA for 24 h and analyzed for relative AHR binding at the *CYP1A1* gene promoter. Data collected from qPCR amplification of ChIP samples were presented as mean ± SEM. Data were analyzed by two-tailed Student's t-test between treatment groups with statistical significance (*) at $p < 0.05$; (b) Relative baseline AHR binding at *CYP1A1* gene promoter and different regions of *MDR1/ABCB1* gene promoter in untreated hCMEC/D3 cells (n=3-6) was assessed. Data collected from qPCR amplifications of ChIP samples were presented as mean ± SEM. The labels for the *MDR1/ABCB1* gene promoter regions are the same as in Fig. 3 and 7

Supplemental Table A-2.1. Primer Sequences for qPCR and ChIP

Target	Primer Sequence		Assay
MDR1, ABCB1	Forward	5' – TTG AAA TGA AAA TGT TGT CTG G – 3'	qPCR
	Reverse	5' – CAA AGA AAC AAC GGT TCG G – 3'	
BCRP, ABCG2	Forward	5' – ATC AGC TGG TTA TCA CTG TGA GGC C – 3'	qPCR
	Reverse	5' – AGT GGC TTA TCC TGC TTG GAA GGC – 3'	
AHR	Forward	5' – CAT ACC GAA GAC CGA GCT GA – 3'	qPCR
	Reverse	5' – TCA TTG CCA GAA AAC CAG ATG A– 3'	
HDAC1	Forward	5' – TAC GAC GGG GAT GTT GGA AA – 3'	qPCR
	Reverse	5' – TCG CTG TGG TAC TTG GTC AT – 3'	
HDAC2	Forward	5' – ACT GCA GTT GCC CTT GAT TG – 3'	qPCR
	Reverse	5' – ACA CCA GGT GCA TGA GGT AA – 3'	
HDAC3	Forward	5' – GAG ACA TCG CTG CTG GTA GA – 3'	qPCR
	Reverse	5' – TTT TCA AAG ATT GTC TGG CG – 3'	
β2M	Forward	5' – TCG CTC CGT GGC CTT AGC TG – 3'	qPCR
	Reverse	5' – CAA TGT CGG ATG GAT GAA ACC CAG – 3'	
MDR1 P1 (-182, -76)	Forward	5' – GAA GCC AGA ACA TTC CTC CT – 3'	ChIP
	Reverse	5' – CAA TCA GCC TCA CCA CAG AT – 3'	
MDR1 P2 (-100, +8)	Forward	5' – AGT CAT CTG TGG TGA GGC TGA T – 3'	ChIP
	Reverse	5' – TACTCGAATGAGCTCAGGCTTC – 3'	
MDR1 P3 (+11, +110)	Forward	5' – CGG CTC TTC CAA GCT CAA A – 3'	ChIP
	Reverse	5' – CAC CAA GAC GTG AAA TTT TGG AA – 3'	
MDR1 P4 (+90, +245)	Forward	5' – CAA AAT TTC ACG TCT TGG TGG C – 3'	ChIP
	Reverse	5' – TCA CAC TAT CCA CGC CTC AA – 3'	
MDR1 P5 (+230, +339)	Forward	5' – GCG TGG ATA GTGTGAAGTCCTCT	ChIP
	Reverse	5' – CAT GGT CCA GTG CCA CTA CG – 3'	
CYP1A1 (-350, -162)	Forward	5' – TGC CCA GGC GTT GCG TGA GAA G – 3'	ChIP
	Reverse	5' – ACC CGC CAC CCT TCG ACA GTT C – 3'	

Supplemental Table A-2.2. Average Ct Values for PXR and CAR genes

Gene	Ct Value
PXR	30.89
CAR	31.72

APPENDIX 3: GENETIC AND DIETARY REGULATION OF GLYBURIDE EFFLUX BY THE HUMAN PLACENTAL BCRP TRANSPORTER

Kristin M Bircsak, Vivek Gupta, Poi Yu Sofia Yuen, Ludwik Gorczyca, Barry I Weinberger, Anna M Vetrano, Lauren M Aleksunes

Department of Pharmacology and Toxicology, Rutgers, The State University of New Jersey, Ernest Mario School of Pharmacy, Piscataway, NJ, USA (K.M.B., L.M.A.), Department of Obstetrics and Gynecology, Rutgers University Robert Wood Johnson Medical School, New Brunswick, NJ, USA (V.G.), Department of Pediatrics, Rutgers University Robert Wood Johnson Medical School, New Brunswick, NJ, USA (P.Y.S.Y., A.M.V.), Hofstra North Shore-LIJ School of Medicine, Cohen Children's Medical Center of New York, New Hyde Park, NY, USA (B.I.W.), Environmental and Occupational Health Sciences Institute, Rutgers, The State University of New Jersey, Piscataway, NJ, USA (L.M.A.)

A-3.1 Abstract

Glyburide is frequently used to treat gestational diabetes due to its low fetal accumulation resulting from placental efflux by the BCRP/*ABCG2* transporter. Here we sought to determine how exposure to the dietary phytoestrogen genistein and expression of a loss-of-function polymorphism in the *ABCG2* gene (C421A) impacted the transport of glyburide by BCRP using stably-transfected human embryonic kidney 293 (HEK) cells, human placental choriocarcinoma BeWo cells and human placental explants. Genistein competitively inhibited the BCRP-mediated transport of ^{3}H-glyburide in both wild-type (WT) and C421A-BCRP HEK-expressing cells, with greater accumulation of ^{3}H-glyburide in cells expressing the C421A variant. In BeWo cells, exposure to genistein for 60 min increased the accumulation of ^{3}H-glyburide 30-70% at concentrations relevant to dietary exposure (IC_{50} ~180 nM). Continuous exposure of BeWo cells to genistein for 48 h reduced the expression of BCRP mRNA and protein by up to 40%, which impaired BCRP transport activity. Pharmacological antagonism of the estrogen receptor attenuated the genistein-mediated downregulation of BCRP expression, suggesting that phytoestrogens may reduce BCRP levels through this hormone receptor pathway in BeWo cells. Interestingly, genistein treatment for 48 h did not alter BCRP protein expression in explants dissected from healthy term placentas. These data suggest that while genistein can act as a competitive inhibitor of BCRP-mediated transport, its ability to down-regulate placental BCRP expression may only occur in choriocarcinoma cells. Overall, this research provides important mechanistic data regarding how the environment (dietary genistein) and a frequent genetic variant (*ABCG2*, C421A) may alter the maternal-fetal disposition of glyburide.

Abbreviations (alphabetical order):

ABC, ATP-binding cassette; BCA, bicinchoninic acid; BSA, bovine serum albumin; BCRP, breast cancer resistance protein; cDNA, complementary DNA; DMSO, dimethylsulfoxide; EV, empty vector; ER, estrogen receptor; GD, gestational diabetes; hCG, human chorionic gonadotropin; HEK, human embryonic kidney 293; IC_{50}, half maximal inhibitory concentration; INN, international nonproprietary name; J_{max}, maximum accumulation rate; K_m, substrate concentration of half the maximum accumulation rate; LDH, lactate dehydrogenase; MDR1, multidrug resistance protein 1; MRP, multidrug resistance-associated protein; qPCR, quantitative polymerase chain reaction; RPL13A, ribosomal protein L13A; WT, wild-type

A-3.2 Introduction

Gestational diabetes (GD) is on the rise worldwide (Dabelea et al. 2005; Ferrara 2007) and affects 5-10% of pregnant women in the United States (DeSisto et al. 2014). Glyburide (INN: glibenclamide) is a second-generation sulfonylurea drug used in the treatment of type II diabetes and more recently GD. In 2000, Langer et al. performed a prospective randomized clinical trial that demonstrated the efficacy and safety of glyburide in the treatment of GD as compared to insulin (Langer et al. 2000). Furthermore, glyburide was undetectable in cord serum (limit of detection < 10 ng/ml), suggesting limited fetal exposure. These findings launched additional investigations (Anjalakshi et al. 2007; Bertini et al. 2005; Jacobson et al. 2005; Ogunyemi et al. 2007) and ultimately a major shift in the management of GD. By 2011, over 50% of U.S. obstetricians were prescribing glyburide as first line pharmacotherapy for GD (Camelo Castillo et al. 2014).

Kraemer et al. (2006) were the first to demonstrate that glyburide is actively removed from the fetal to the maternal circulation, suggesting that transport plays a major role in the transplacental disposition of glyburide (Kraemer et al. 2006). While multiple transporters in the placenta interact with glyburide (Gedeon et al. 2008a; Gedeon et al. 2008b; Gedeon et al. 2006; Hemauer et al. 2010a), there is significant evidence that points to the breast cancer resistance protein (BCRP/*ABCG2*) as the major transporter responsible for the active extrusion of glyburide from the placenta. This has been demonstrated using BCRP-overexpressing cells, Bcrp knockout mice, pregnant rats, human placentas and human placental vesicles (Feinshtein et al. 2013; Pollex et al. 2008; Pollex et al. 2010; Zhou et al. 2008b).

BCRP is a transmembrane protein that moves xenobiotics and endogenous chemicals out of cells. In the intestine, liver and kidney, BCRP is expressed on the apical membrane of epithelial cells and promotes the excretion of drugs and chemicals from the body (Maliepaard et al. 2001b). In the placenta, BCRP is primarily localized to the apical membrane of syncytiotrophoblasts where it

transports substrates back to the maternal circulation, such that fetal exposure to various chemicals including glyburide is restricted (Maliepaard et al. 2001b). Although placental BCRP plays a critical role in protecting the fetus from exposure to glyburide, there is limited understanding of the potential consequences of reduced placental BCRP function in pregnant women prescribed glyburide for GD. Babies born to this population of women may be at an elevated risk of neonatal hypoglycemia as a result of fetal glyburide exposure, potentially leading to low birth weight, increased morbidity and impaired neurological development (reviewed in (Williams 1997)). BCRP function may be compromised by genetic single nucleotide polymorphisms, as well as environmental factors, including dietary constituents.

A single nucleotide polymorphism occuring at nucleotide 421 (C>A) in the *ABCG2* gene leads to an amino acid change from glutamine to lysine (Q141K). *In vitro*, the C421A genotype is associated with reduced BCRP function (Kondo et al. 2004; Pollex et al. 2010). Importantly, the C421A genotype occurs frequently in Asian (C/A: 30%, A/A: 10%) and Caucasian (C/A: 15%, A/A: 1%) populations (Imai et al. 2002; Kobayashi et al. 2005; Zamber et al. 2003).

Genistein is a soy isoflavone that is found naturally in plants of the *Leguminosae* family and occurs abundantly in soybeans (2014; 2008). Considering the increasing consumption of soy-containing products (i.e., tofu, soy formula, dietary supplements) over the last 10 years (2014), it is important to recognize that components of soy, including genistein, may interfere with the disposition of prescribed drugs. Genistein alone and in combination with other isoflavones has been shown to directly interfere with the BCRP-mediated disposition of drugs *in vivo* including BCRP substrates enrofloxacin and nitrofurantoin (Merino et al. 2010; Pulido et al. 2006). Genistein also interacts with proteins that may regulate placental BCRP expression, including the estrogen receptor and the epidermal growth factor receptor (Kuiper et al. 1998; Traxler et al. 1999). Considering this

evidence, genistein may reduce placental BCRP function in two distinct manners, by 1) direct inhibition of BCRP activity and 2) altered transcriptional regulation of BCRP.

Due to the increased use of glyburide in GD treatment and the sensitivity of the developing fetus, it is critical to consider separately and together the influence of genetic and environmental factors on the placental BCRP-mediated disposition of glyburide. The purpose of this study was to use complementary *in vitro* and *ex vivo* model systems to characterize the molecular mechanisms by which dietary-relevant concentrations of genistein impair the transport of glyburide by BCRP in placental trophoblasts.

A-3.3 Materials and Methods

Chemicals

Unless otherwise specified, all chemicals were obtained from Sigma-Aldrich (St. Louis, MO).

Cell Culture

Human embryonic kidney-293 (HEK) cells were stably transfected with an empty vector (EV, pcDNA 3.1), the human wild-type (WT) BCRP/*ABCG2* gene or the human C421A BCRP/*ABCG2* variant (kindly provided by Dr. Robert Robey, National Cancer Institute, National Institutes of Health, Bethesda, MD) (Morisaki et al. 2005). Cells were maintained in Dulbecco's Modified Eagle Medium (Life Technologies, Carlsbad, CA) with 10% fetal bovine serum (Atlanta Biologicals, Norcross, GA), 1% penicillin-streptomycin (Life Technologies) and 0.2 mg/ml geneticin (Life Technologies) to select for transfected cells. Human placental choriocarcinoma BeWo cells were purchased from American Type Culture Collection (ATCC, Manassas, VA) and grown in phenol-red free Dulbecco's Modified Eagle Medium: F-12 (Life Technologies) with 10% charcoal-stripped and dextran-treated fetal bovine serum (Atlanta Biologicals) and 1% penicillin-streptomycin (Life Technologies). All cells were maintained at 37°C with 5% CO_2 and used in experiments at 80-90% confluence. For the regulation studies, BeWo cells were incubated with genistein (0-10 μM) or ICI 182,780 (0-1 μM) for 48 h, after which they were processed for mRNA, protein, or functional analysis. All chemicals were dissolved in dimethyl sulfoxide (DMSO) such that the final percentage (% v/v) of DMSO did not exceed 0.1% of the treatment media.

Flow Cytometry

HEK cells overexpressing the EV, WT-BCRP or C421A-BCRP gene were suspended in cold isotonic PBS with 0.5% bovine serum albumin (BSA), centrifuged (500 *g*, 5 min) and washed three times in PBS with 0.5% BSA. Cells in suspension were blocked with human IgG (2 μg/500,000 cells in PBS/0.5% BSA) for 15 min at room temperature. Cells were then incubated for 45 min at

4°C with the monoclonal phycoerthyrin-labeled anti-BCRP antibody (5D3) or the phycoerthyrin-labeled negative control IgG antibody (R&D Systems, Minneapolis, MN) according to the manufacturer's protocol. Cells were washed three times (5 min with PBS/0.5% BSA) and resuspended in 2% paraformaldehyde/PBS for flow cytometry analysis using a Gallios/FC500 Cytometer with 488-nm wavelength laser excitation (Beckman Coulter, Indianapolis, IN) in the Flow Cytometry/Cell Sorting Core Facility at Rutgers University.

Hoechst 33342 Accumulation Assay

The BCRP-specific fluorescent substrate, Hoechst 33342, was used to quantify BCRP function in HEK and BeWo cells as previously described (Bircsak et al. 2013b). Briefly, HEK and BeWo cells were trypsinized and added to a 96-well plate. Following centrifugation (500 *g*, 5 min, 5°C) and removal of the media, cells were loaded with Hoechst 33342 (7-15 µM) in the presence or absence of the BCRP-specific inhibitor, Ko143 (1-3000 nM), or the test compound, genistein (0.1-100 µM) for 30 min at 37°C and 5% CO_2 (uptake phase). Cells were washed, centrifuged, and resuspended in substrate-free media with or without inhibitor for 1 h (efflux phase). During all phases, inhibitor compounds were initially dissolved in DMSO and did not exceed 1% (v/v) of the final treatment media. Following the efflux phase, cells were centrifuged, washed, and resuspended in cold PBS for quantification of intracellular fluorescence using the Cellometer Vision automated cell counter (Nexcelom Bioscience, Lawrence, MA). Cell suspension (20 µl) was added to the cell counting chamber and each sample was analyzed using bright-field images for cell size and cell number. A VB-450-302 filter (excitation/emission: 375/450) allowed for intracellular fluorescence detection of Hoechst 33342. The total number of cells analyzed for each sample ranged from 200 to 2000. In BeWo cells, raw fluorescence intensity for each cell was normalized to cell size.

^{3}H-Glyburide Accumulation Assay

HEK and BeWo cells were trypsinized and added to a 96-well plate. Following centrifugation (500 *g*, 5 min, 5°C) and removal of the media, cells were loaded with ^{3}H-glyburide (0.1-10 µM; Specific Activity: 40 µCi; Perkin Elmer, Waltham, MA) in the presence and absence of the BCRP-specific inhibitor, Ko143 (1-3000 nM), or the test compound, genistein (0.01-20 µM) for 1 h at 37 °C and 5% CO_2. Inhibitors were dissolved in DMSO such that the final concentration of DMSO did not exceed 1% (v/v) in the final treatment media. Following the 1 h incubation, cells were centrifuged, washed, and lysed using 1 M NaOH. Lysates were then neutralized using 1 M HCl and added to 4 ml ScintiSafe Econo 1 liquid scintillation fluid (Fisher Scientific, Waltham, MA) in 7 ml glass liquid scintillation vials (Perkin Elmer). Radioactivity was detected using a TriCarb 2100TR Liquid Scintillation Analyzer (Perkin Elmer-Packard, Waltham, MA). A standard curve was used to extrapolate glyburide concentrations. Accumulation of glyburide was normalized to the total protein concentration of cell lysates from representative wells using the bicinchoninic acid (BCA) assay (Pierce Biotechnology, Rockford, IL).

Western Blot

HEK and BeWo cells were lysed in lysis buffer (20 mM Tris-HCl, 150 mM NaCl, 5 mM EDTA, 1% Triton X-100 and 1% protease inhibitor cocktail). Protein concentrations of cell lysates and placental explant homogenates were determined by the BCA assay. Five to ten µg total protein were added to SDS-polyacrylamide 4-12% Bis-Tris gels (Life Technologies) which were resolved by electrophoresis. Transfer of proteins onto polyvinylidene fluoride membranes was completed using an overnight transfer apparatus (Biorad Criterion Blotter, Biorad, Hercules, CA). Membranes were blocked using 5% non-fat milk in 0.5% Tween-20-PBS, then incubated with primary antibodies in 2% non-fat milk in 0.5% Tween-20-PBS for 2 h. Primary antibodies detected proteins including BCRP (BXP-53, 1:5000, Enzo Life Sciences, Farmingdale, NY), β-Actin (Ab8227, 1:2000, Abcam, Cambridge, MA) and Na^{+}/K^{+} ATPase (Ab76020, 1:20000, Abcam). The membranes were washed and species-specific HRP-conjugated secondary antibodies were added

to the blots for 1 h. Supersignal West Dura Extended Duration Substrate (Pierce Biotechnology) was used for chemiluminescent detection of proteins with a Fluorchem Imager (ProteinSimple, Santa Clara, CA). Semi-quantitation of bands was performed using the AlphaView Software (ProteinSimple). β-Actin or Na^+/K^+ ATPase were used as loading controls where appropriate.

RNA Isolation and Real-Time Quantitative PCR

BeWo cells were collected in Buffer RLT provided in the RNeasy Mini Kit (Qiagen, Germantown, MD), plus 1% β-mercaptoethanol. Cells were lysed using QIAshredder columns (Qiagen), and total RNA was isolated with the RNeasy Mini Kit (Qiagen) according to the manufacturer's protocol. Total RNA concentration and purity (260/280) were determined using a Nanodrop spectrophotometer (Fisher Scientific). Complementary DNA (cDNA) was generated from total RNA (500 ng) using the High-Capacity cDNA Reverse Transcription Kit (Life Technologies) and a MultiGene OptiMax Thermal Cycler (Labnet International Inc., Edison, NJ). Quantitative PCR (qPCR) was performed with specific forward and reverse primers (Integrated DNA Technologies, Inc., Coralville, IA), cDNA, Sybr Green dye (Life Technologies) and a ViiA7 RT-PCR System (Life Technologies) in the Bionomics Research and Technology Center at Rutgers University. Ct values were converted to delta delta Ct values by comparison to ribosomal protein 13A (RPL13A) as a reference gene and the DMSO-treated control cells. Primer sequences for BCRP and RPL13A are provided in Supplemental Table A-3.1.

Patient Selection

Written informed consent was obtained and placentas were collected from five healthy women with uncomplicated pregnancies following term delivery by scheduled cesarean section. Inclusion criteria were healthy women, ages 18-40, term gestation (≥ 36 weeks) and scheduled cesarean section without labor. Exclusion criteria included chronic medical conditions (i.e., hypertension, diabetes, autoimmune disorders), pregnancy-induced medical conditions (i.e., pregnancy-induced

hypertension, preeclampsia, gestational diabetes), maternal infection, clinical chorioamnionitis, medication use (with the exception of prenatal vitamins), maternal smoking, alcohol or drug abuse and known fetal chromosomal abnormalities. All placentas expressed two wild-type alleles (C/C) at the 421 nucleotide position in the *ABCG2* gene as determined by a Fluidigm Biomark Genetic Analysis system in the Bionomics Research and Technology Center at Rutgers University. Other patient demographic information is provided in Supplemental Table A-3.2. The Institutional Review Boards of Robert Wood Johnson Medical School (RWJMS) (Protocol #0220100258) and Rutgers University (Protocol #E12-024) approved this study.

Placental Explants

All placentas were obtained within 10 min of delivery and processed within 2 h. Placentas were carefully inspected for any visible abnormalities and location of umbilical cord. Only placentas with central or eccentric cord insertion were used. The maternal decidua and the chorionic plate along the overlying membranes were removed and sections of villous tissue were washed in PBS three times to remove maternal blood before dissection into 2 x 2 x 2 mm (8 mm^3) pieces of tissue. In a 24-well dish, two pieces of 8 mm^3 villous tissue were cultured in DMEM:F12 media without phenol red (Life Technologies) and with 10% charcoal-stripped and dextran-treated fetal bovine serum (Atlanta Biologicals) and 1% penicillin-streptomycin (Life Technologies). To allow for complete degeneration and regeneration of the syncytium as described by other laboratories (Siman et al. 2001), explants were maintained in culture for 5 days, with the media changed and collected every 24 h. On day 5, genistein (0-10 μM) treatment began for 48 h (media not changed during 48 h treatment). Genistein was dissolved in DMSO and the final DMSO percentage was 0.1% (v/v) in the treatment media. Following the 48 h treatment, explants were washed in PBS and frozen in liquid nitrogen before homogenization in sucrose (250 mM)-Tris (10 mM) buffer (pH 7.4) with protease inhibitors (1%, v/v), using the TissueLyser LT (Qiagen) according to the manufacturer's protocol.

hCG ELISA and LDH Assay

Each day of explant culture, media was collected for assessment of syncytiotrophoblast function and overall tissue integrity by quantification of human chorionic gonadotropin (hCG) and lactate dehydrogenase (LDH), respectively. The hCG ELISA was completed using the manufacturer's protocol (Calbiotech, Spring Valley, CA). Activity of LDH in the media was determined using the manufacturer's protocol.

Statistical Analysis

Data are presented as mean ± SE of multiple independent experiments (n=3-5) and analyzed using Graphpad Prism 5.0 (Graphpad Software Inc., La Jolla, CA). Two-way ANOVA with Bonferroni post-test, One-way ANOVA with Newman-Keuls post-test, or a two-tailed student's t-test were used to assess statistical significance ($p<0.05$) according to the number of comparisons and variables. Nonlinear regression analysis (dose-response: [log] inhibitor vs response—Variable slope (four parameters) or Michaelis-Menten) was used to determine kinetic parameters (IC_{50}, K_m, J_{max}).

A-3.4 Results

Functional Inhibition of BCRP by Genistein

WT- and C421A-BCRP Overexpressing HEK Cells. Whole cell and cell surface protein expression of BCRP were assessed by western blot and flow cytometry, respectively. Three independent experiments revealed that BCRP protein expression in whole cell lysates was reduced by about 30% in C421A-BCRP expressing cells compared to WT-BCRP expressing cells (p=0.172) (Figure A-3.1A). At the cell surface, BCRP protein expression in the C421A-BCRP cells was significantly decreased by 50% compared to the WT cells (Figure A-3.1B). Both methods confirmed the absence of BCRP protein in HEK cells expressing the EV (data not shown).

Two substrate accumulation assays (Hoechst 33342 and ^{3}H-glyburide) were employed to examine modulation of BCRP transport activity by pharmacological inhibition and genetic variation. Initial experiments determined the optimal substrate concentrations for use in the two accumulation assays (Hoechst 33342, 7 µM and ^{3}H-glyburide, 10 µM unlabeled glyburide and 0.1 µM ^{3}H-glyburide; Supplemental Fig A-3.1). In the absence of inhibitor, there was a trend for the cells overexpressing the variant BCRP (C421A) to accumulate 50-100% more Hoechst 33342 or ^{3}H-glyburide than the respective WT-BCRP cells (Figure A-3.2). The BCRP-specific inhibitor Ko143 increased the accumulation of Hoechst 33342 and ^{3}H-glyburide in a concentration-dependent manner in both BCRP genotypes (Figures A-3.2A and A-3.2C), demonstrating the ability of the assays to detect inhibition of BCRP activity. Similar to Ko143, genistein increased the accumulation of Hoechst 33342 and ^{3}H-glyburide in WT- and C421A-BCRP expressing cells (Figures A-3.2B and A-3.2D). Confirming the involvement of the BCRP transporter in the genistein-induced substrate accumulation, EV cells lacking BCRP protein accumulated both substrates which was not altered by genistein (data not shown). It should be noted that Ko143 significantly increased the accumulation of both BCRP substrates in the C421A-BCRP cells at lower concentrations than in WT-BCRP cells. Further, the half-maximal inhibitory concentration (IC_{50}) value for the inhibition

of ^{3}H-glyburide transport in the C421A-BCRP (10.1 ± 1.79 nM) cells by Ko143 was 50% lower than the WT-BCRP cells (21.5 ± 1.04 nM) (Table A-3.1). For genistein, the IC_{50} values for the inhibition of ^{3}H-glyburide transport in both BCRP genotypes were comparable (WT: 4.56 ± 0.15, C421A: 3.92 ± 0.73) (Table A-3.1).

To determine the mechanism by which genistein inhibited the BCRP-mediated transport of glyburide, accumulation experiments were performed using varying concentrations of both glyburide and genistein. Genistein significantly decreased the K_m value for glyburide transport by 80% without changing the J_{max} in either BCRP genotypes (Figure A-3.3; Table A-3.2), suggesting that genistein competitively inhibited the BCRP-mediated efflux of glyburide.

Placental BeWo Cells. Expression and function of endogenous BCRP protein in placental BeWo cells was confirmed by western blot (Figure A-3.4A) and substrate accumulation assays (Hoechst 33342 and ^{3}H-glyburide) (Supplemental Fig A-3.2), respectively. Ko143 and genistein significantly increased the accumulation of both Hoechst 33342 and ^{3}H-glyburide by 30-100% in placental BeWo cells (Figure A-3.4B-E). Notably, concentrations as low as 0.01 μM genistein inhibited ^{3}H-glyburide transport (IC_{50}= 0.18 ± 0.11 μM). Prototypical inhibitors of other efflux transporters (MDR1: PSC833, 2 μM; MRPs: 25 μM MK571) did not alter the accumulation of ^{3}H-glyburide in the BeWo cells (data not shown), supporting the specific involvement of BCRP in the inhibition of glyburide transport by genistein.

Regulation of Placental BCRP Expression by Genistein

BeWo Cells. To determine whether genistein could alter the transcriptional regulation of BCRP expression, placental BeWo cells were incubated with genistein for 48 h. Compared to control cells, genistein significantly decreased the BCRP mRNA and protein expression up to 40% (Figure A-3.5A and B). Furthermore, 48 h exposure to genistein (5 μM) increased the accumulation of ^{3}H-

glyburide by 30% in placental BeWo cells, which was comparable to the pharmacological inhibition of glyburide transport by Ko143 (100 nM) (Figure A-3.5C). Notably, there was no effect of genistein on mRNA and protein expression of other efflux transporters including the multidrug resistance-associated protein 1 (MRP1) (data not shown). Because genistein is a phytoestrogen, the mechanism by which it downregulated BCRP mRNA and protein expression in BeWo cells was investigated using the estrogen receptor α antagonist ICI 182,780. Exposure to ICI 182,780 (1 μM) for 48 h did not alter BCRP protein expression; however, the combination of genistein and ICI 182,780 together abolished the down-regulation of BCRP protein expression caused by genistein alone (Figure A-3.6).

Placental Explants. Additional experiments aimed to determine whether genistein-mediated down-regulation of BCRP expression could occur in native placental tissue. Explants were obtained from healthy human term placentas and allowed to undergo shedding and syncytialization for 5 days prior to treatment with genistein on days 5-7. Viability of the explants was confirmed by a decrease in LDH activity in the media over seven days (Supplemental Figure A-3.3A; Siman et al., 2001). The degree of syncytialization was verified by detection of hCG in the media and by histologic analysis (Supplemental Figure A-3.3B; (Siman et al. 2001)). Genistein treatment did not affect LDH activity or hCG secretion. Furthermore, BCRP protein expression was not altered by genistein (1-10 μM, 48 h) in human term placental explants (Figure A-3.7).

A-3.5 Discussion

The present study demonstrated the influence of genetic and dietary factors on the BCRP-mediated transport of glyburide using complementary *in vitro* and *ex vivo* placenta model systems. The C421A-BCRP genotype alone reduced the transport of ^{3}H-glyburide compared to the WT-BCRP control cells, while genistein competitively inhibited ^{3}H-glyburide transport by BCRP to a similar extent in both genotypes. Confirming the potential for a placenta-specific glyburide accumulation, the BCRP-mediated transport of ^{3}H-glyburide was inhibited by a short-term exposure (1 h) to genistein in placental BeWo cells. Moreover, BCRP mRNA, protein and function were reduced in BeWo cells exposed to genistein for 48 h; however, the same genistein exposure did not alter BCRP protein expression in normal placental explant tissues. Results from the present study aim to direct future investigations to consider genetic and environmental (dietary genistein) influences when optimizing glyburide treatment in GD patients.

In this study, we confirmed the reduced capability of the C421A-BCRP protein to transport ^{3}H-glyburide in HEK cells that overexpress the mutated BCRP protein (Q141K), as compared to WT-BCRP overexpressing cells (Figure A-3.2, Table A-3.2). While Pollex et al. (2010) described BCRP protein cell surface expression to be equal between genotypes, we observed less total (30%) and cell surface (50%, $p<0.05$) BCRP protein expression in the C421A-BCRP HEK cells (Figure A-3.1). Considering these findings, altered BCRP function in our experiments may be due to reduced BCRP protein trafficking to the cell surface. This is in line with other studies reporting decreased BCRP protein expression and function in C421A-BCRP overexpressing cells (Furukawa et al. 2009; Imai et al. 2002; Kondo et al. 2004; Tamura et al. 2007; Woodward et al. 2013). In human tissue, the heterozygous variant genotype (421C/A) did not change BCRP protein expression in the intestine or placenta, but there was a significant decrease in BCRP protein expression in placentas of individuals homozygous for the SNP (421A/A) (Kobayashi et al. 2005; Urquhart et al. 2008; Zamber et al. 2003). Taken together, there may be differences in BCRP protein

expression in cells or tissue based on the copy number of the C421A gene. Furthermore, there may be a cell-type and/or tissue specific effect of C421A on BCRP protein expression. Most importantly, patients expressing one or two variant alleles exhibit increased blood concentrations (sulfasalazine, diflomotecan, rosuvastatin) and enhanced side effects (gefitinib) of drugs that are substrates for BCRP (Cusatis et al. 2006; Keskitalo et al. 2009; Sparreboom et al. 2004; Urquhart et al. 2008). Due to these clinical findings and the frequent occurrence of the SNP, the International Transporter Consortium named the C421A BCRP genetic variant as a clinically relevant transporter polymorphism that should be evaluated in drug development studies (Giacomini et al. 2013).

Over the past 10 years there has been an increase in the sale and consumption of soy in the United States, likely due to the growing number of reports which suggest that a soy diet provides health benefits (Bitto et al. 2008; Chen et al. 2003; Clarkson et al. 2011; Constantinou et al. 2005; Hussain et al. 2003; Squadrito et al. 2013; Strom et al. 1999). Taken together with the increase in the prescribing of glyburide for GD (Camelo Castillo et al. 2014), there is a need to investigate the impact of soy on glyburide transport. Genistein and its conjugated metabolites (genistein-sulfate and genistein-glucuronide) are substrates for BCRP, suggesting that they competitively inhibit BCRP transport (Alvarez et al. 2011; Enokizono et al. 2007a; Imai et al. 2004; Mease et al. 2012). However, others propose that genistein can non-competitively inhibit BCRP transport via disruption of ATP hydrolysis as well (Di Pietro et al. 2002; Randak et al. 1999). In both the WT-BCRP and the C421A-BCRP overexpressing cells, genistein competitively inhibited the BCRP-mediated transport of ^{3}H-glyburide to similar degrees (Fig 2D and 3, Table 2). While various studies demonstrated genistein to interfere with the transport of other BCRP substrates (i.e., mitoxantrone, enrofloxacin) (Pulido et al. 2006; Zhang et al. 2004a), this is the first report implicating genistein in the inhibition of ^{3}H-glyburide transport by BCRP. It is important to note that Ko143 significantly reduced ^{3}H-glyburide transport in the C421A-BCRP overexpressing cells at a lower concentration than the WT-BCRP overexpressing cells, while genistein equally inhibited

^{3}H-glyburide transport between cell types (Table A-3.1). This suggests that individuals with the C421A-BCRP genotype may be at a greater risk for chemically induced BCRP inhibition depending on the inhibitor compound.

BeWo cells are commonly used as a model of placental transport because they endogenously express functional BCRP protein and produce the placenta-specific hormone, hCG (Takeuchi et al. 1990). In placental BeWo cells, genistein increased the accumulation of Hoechst 33342 and ^{3}H-glyburide (Figure A-3.4). Interestingly, the concentrations of genistein which inhibited ^{3}H-glyburide transport out of the BeWo cells were quite low and within the range of those observed in the plasma or serum of people consuming a soy diet (0.01- 3 μM) (Arai et al. 2000; Frankenfeld et al. 2003; Gardner et al. 2009; Uehar et al. 2000). These data provide plausibility to the assertion that genistein may be able to inhibit BCRP transport of substrates *in vivo*. The BCRP-specific inhibitor, Ko143, was used as a positive control to confirm the involvement of BCRP in the genistein-mediated cellular accumulation of Hoechst 33342 and ^{3}H-glyburide.

Placental BCRP function may also be affected by chemical-mediated changes in mRNA and/or protein expression. Following 48 h exposure to genistein, BCRP mRNA and protein expression was decreased in BeWo cells compared to the vehicle treated cells **(**Fig A-3.5A and B**)**. In turn, this caused significant accumulation of ^{3}H-glyburide in cells that were exposed to genistein (5 μM, 48 h) **(**Fig A-3.5C**)**. Only one other study has reported a significant decrease in ABCG2 mRNA expression following an *in vitro* genistein exposure (15 μM, 24 h, gastric cancer cells, MGC803) (Huang et al. 2014), while many others detected no change in BCRP mRNA and/or protein expression in other cell types (Arias et al. 2014; Ebert et al. 2007; Imai et al. 2004).

In the 1960's, genistein was recognized as a phytoestrogen due to its ability to alter reproductive function in sheep (Barrett et al. 1965) and agonize both ERα and β with a greater affinity for ERβ

(Kuiper et al. 1998; Martin et al. 1978). Importantly, an estrogen response element has been identified in the promoter region of the *ABCG2* gene (Ee et al. 2004c). Furthermore, estradiol down-regulated BCRP protein expression in various cells and tissues including placental BeWo cells (Imai et al. 2005b; Mahringer et al. 2010; Wang et al. 2006c), which express both ERα and ERβ (Gambino et al. 2012). To explore the involvement of the ER signaling pathway in the genistein-mediated downregulation of BCRP expression in placental BeWo cells, the ERα antagonist ICI 182,780 was used (Peekhaus et al. 2004; Van Den Bemd et al. 1999). ICI 182,780 (1 μM) alone did not alter BCRP expression but was able to prevent the down-regulation of BCRP by genistein (Figure A-3.6). These findings suggest that ER signaling participates in the repression of BCRP expression in BeWo cells.

Placental explants are an *ex vivo* model of the human term placenta as they retain the morphology of the human placental villi, contain multiple cell types, and are frequently used in examining transporter regulation in normal human placenta (Atkinson et al. 2006; Javam et al. 2014). Genistein did not alter BCRP protein expression in human term placental explants (Figure A-3.7). While these findings contrast those observed in placental BeWo cells, it is important to note that extrapolation of gene regulation findings observed in choriocarcinoma cells to normal placenta must be made with caution. DNA methylation patterns vary between normal primary trophoblasts and choriocarcinoma cells, contributing to the overall differential gene expression and regulation profiles between the two types of cells (Novakovic et al. 2011). Altogether, results from this study indicate that the direct pharmacological inhibition of BCRP by genistein may have greater implications for BCRP-mediated transport of glyburide rather than modulation of transcription and/or translation.

The prescription of glyburide for management of GD has reached an all-time high as most initial reports found no differences in neonatal hypoglycemia rates between insulin and glyburide

managed GD (Anjalakshi et al. 2007; Jacobson et al. 2005; Langer et al. 2000). More recently, Schartz et al., described a weak, but significant negative correlation between neonatal blood glucose concentration and umbilical cord blood glyburide concentration (Schwartz et al. 2015). There were interindividual differences in the umbilical cord blood concentration to maternal blood concentration ratio of glyburide for which the authors named genetic differences in the BCRP/*ABCG2* gene as a likely contributor. Differences in diets, including those that are rich in soy may also contribute to this variability.

In summary, our data demonstrate that genistein inhibits the BCRP-mediated efflux of glyburide *in vitro* by direct inhibition and reduced protein expression in placental BeWo cells but not placental explants. To better optimize the individualized prescribing of glyburide for GD, future research should address the contribution of the C421A-BCRP genotype and genistein in the diet to the transplacental passage of glyburide.

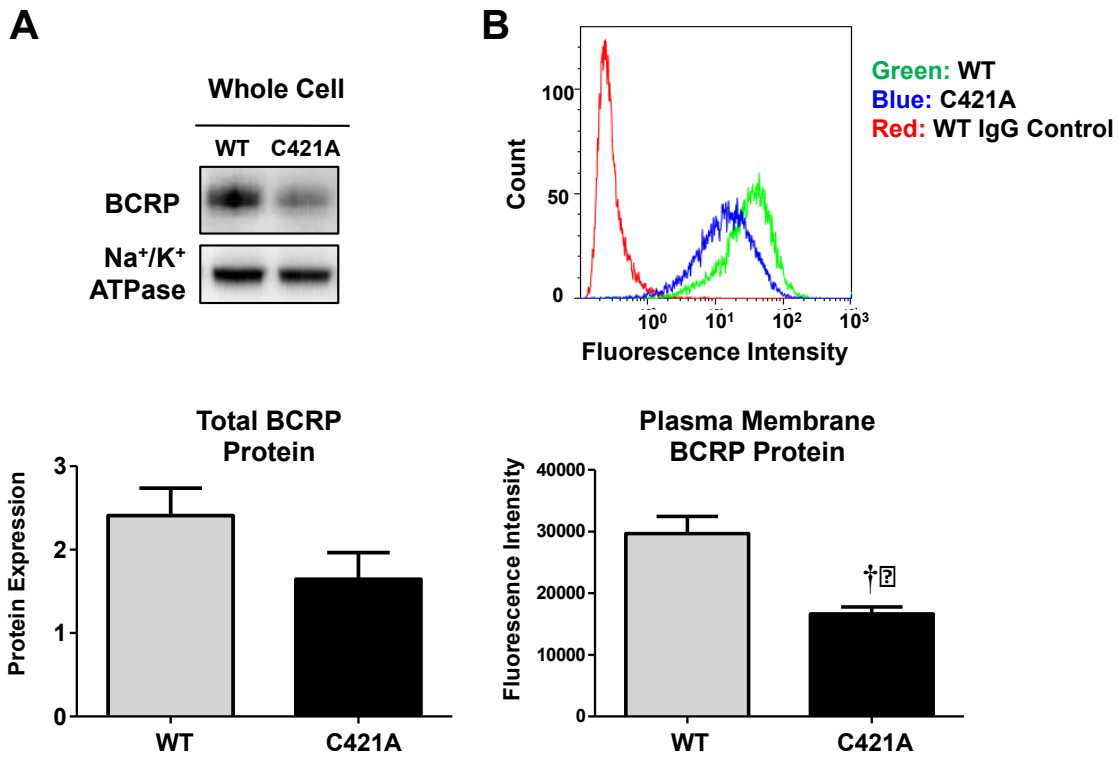

Fig A-3.1. Characterization of BCRP protein in WT- and C421A-BCRP overexpressing HEK cells. (A) BCRP protein expression in HEK whole cell lysates was determined by western blot (10 µg protein homogenate/lane). Na^+/K^+ ATPase was used as a loading control. Western blot data are presented as a representative western blot from one experiment. The bar graph shows the semiquantitation of band densities and represents the mean ± SE from three independent experiments. (B) BCRP protein expression on the cell surface of HEK cells was determined by flow cytometry. Cells were incubated for 45 min with the phycoerthyrin-labeled anti-BCRP antibody (5D3) or the phycoerthyrin-labeled negative control IgG antibody (green: WT-BCRP 5D3 stained cells, blue: C421A-BCRP 5D3 stained cells, red: WT-BCRP IgG control). Flow cytometry histogram data are presented as one representative experiment. Bar graph represents mean ± SE fluorescence intensity of individual cells from 3 independent experiments. Daggers (†) represent statistically significant differences ($p<0.05$) compared to WT-BCRP.

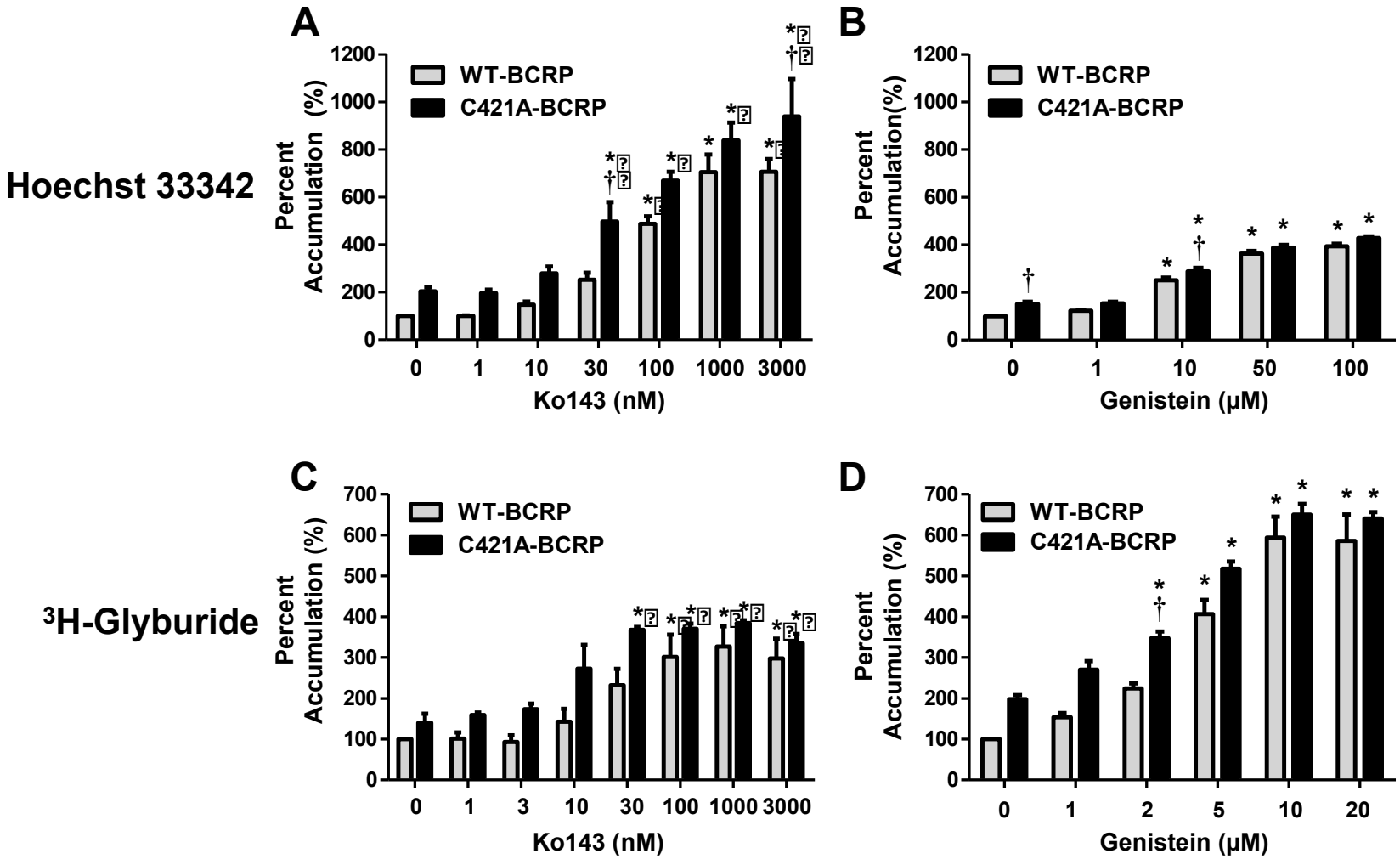
Hoechst 33342
3H-Glyburide
A
B
C
D
WT-BCRP
C421A-BCRP
Percent Accumulation (%)
Percent Accumulation(%)
Ko143 (nM)
Genistein (μM)
0 1 10 30 100 1000 3000
0 1 10 50 100
0 1 3 10 30 100 1000 3000
0 1 2 5 10 20

Fig A-3.2. Inhibition of BCRP transport in WT- and C421A-BCRP overexpressing HEK cells. BCRP function was assessed by measuring the cellular accumulation of (A and B) Hoechst 33342 (7 μM) or (C and D) ^{3}H-glyburide (10 μM unlabeled glyburide, 0.1 μM ^{3}H-glyburide) in the presence of increasing concentrations of the BCRP-specific inhibitor, Ko143 or genistein. Intracellular fluorescence and radioactivity were quantified by a Cellometer Vision or a liquid scintillation counter, respectively. Bar graphs represent mean ± SE (n=3 independent experiments). Asterisks (*) represent statistically significant differences ($p<0.05$) compared to 0 μM genotype control. Daggers (†) represent statistically significant differences ($p<0.05$) compared to WT-BCRP control.

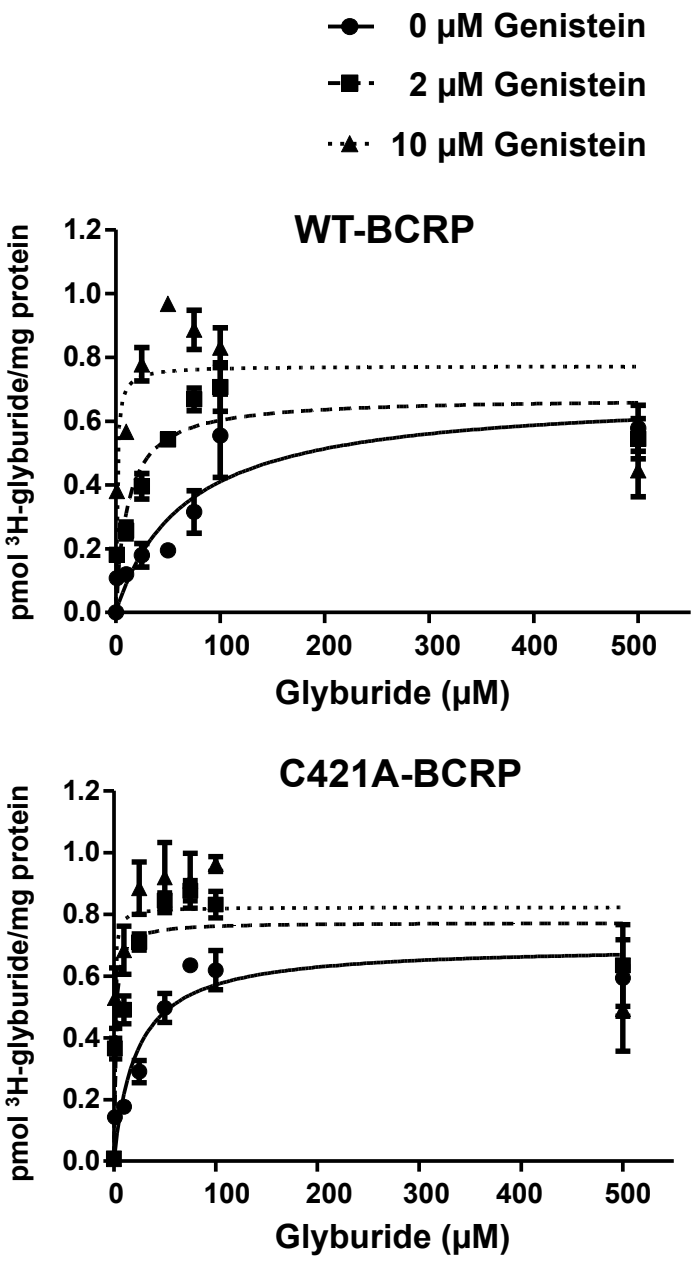

Fig A-3.3. Characterization of the genistein-glyburide interaction mediated by BCRP. BCRP function was assessed in WT- and C421A-BCRP HEK-expressing cells by measuring the cellular accumulation of ^{3}H-glyburide (0-500 μM unlabeled glyburide, 0.1 μM ^{3}H-glyburide) in the presence of increasing concentrations of genistein (0-10 μM) and was quantified using a liquid scintillation counter. Data represent mean ± SE (n=3 independent experiments). Nonlinear regression analysis (Michaelis-Menten) was used for curve-fitting analysis.

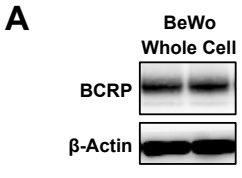
A
BeWo
Whole Cell
BCRP
β-Actin

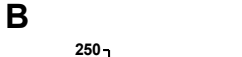
B

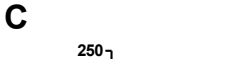
C

Fig A-3.4. Inhibition of BCRP transport in placental BeWo cells. (A) BCRP protein expression in placental BeWo whole cell lysates was determined by western blot (10 µg protein homogenate/lane). β-Actin was used as a loading control. (B-E) BCRP function was assessed in the presence of increasing concentrations of Ko143 (B and D) or genistein (C and E), by the accumulation of (B and C) Hoechst 33342 (15 µM) or (D and E) ^{3}H-glyburide (0.1 µM). Intracellular fluorescence or radioactivity was quantified using a Nexcelom Cellometer Vision or a liquid scintillation counter, respectively. Bar graphs represent mean ± SE (n=3-4 independent experiments). Asterisks (*) represent statistically significant differences ($p<0.05$) compared to the 0 µM control.

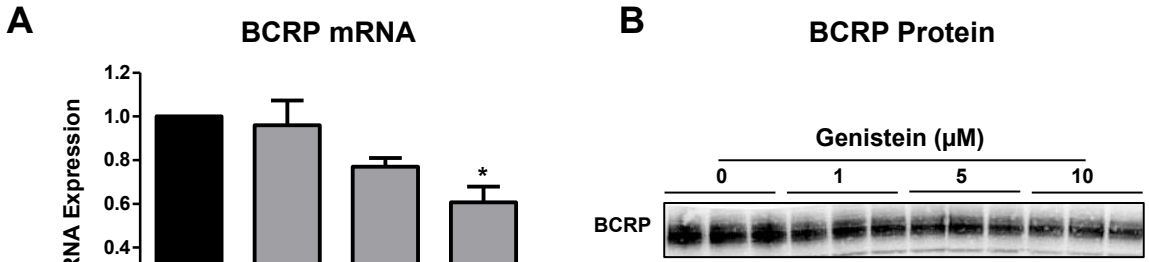

Fig A-3.5. Regulation of BCRP transporter expression and function in placental BeWo cells. Following a 48 h exposure to genistein (0-10 μM), (A) qPCR was used to quantify BCRP and housekeeping gene, ribosomal protein L13A (RPL13A), mRNA expression in placental BeWo cells. (B) BCRP protein expression in placental BeWo whole cell lysates was determined by western blot (10 μg protein homogenate/lane). β-Actin was used as a loading control. Western blot data are presented as a representative western blot from one experiment. (C) BCRP function was assessed by the cellular accumulation of ^{3}H-glyburide (0.1 μM) which was quantified using a liquid scintillation counter. All bar graphs represent mean ± SE (n=3-4 independent experiments). Asterisks (*) represent statistically significant differences ($p<0.05$) compared to the 0 μM genistein control.

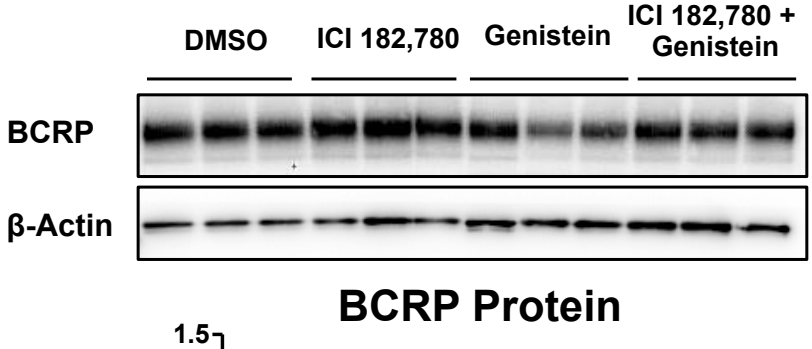

Fig A-3.6. Estrogen receptor-mediated regulation of the BCRP transporter in placental BeWo cells. BCRP protein expression in placental BeWo whole cell lysates was determined by western blot (10 µg protein homogenate/lane) following a 48 h exposure to the estrogen receptor antagonist, ICI 182,780 in the presence and absence of genistein. β-Actin was used as a loading control. All western blot data are presented as a representative western blot from one experiment. The bar graphs are the semiquantitation of band density and represent the mean ± SE from three independent experiments. Asterisks (*) represent statistically significant differences ($p<0.05$) compared to the 0 µM control.

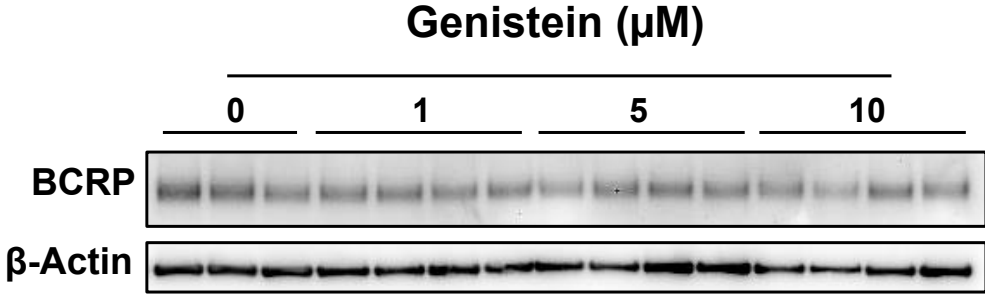

Fig A-3.7. Regulation of BCRP transporter expression in human term placental explants. Five healthy human term placentas were collected and processed within 2 h of delivery. Explants were cultured for 5 days with the media replaced every day, before treatment with genistein (1-10 μM) on day 5 for 48 h. BCRP protein expression in total explant lysates was determined by western blot (5 μg protein homogenate/lane). β-Actin was used as a loading control. Western blot data are presented as a representative western blot from one placenta. The scatter dot plot is the semiquantitation of band density and represent five individual placentas with mean ± SE.

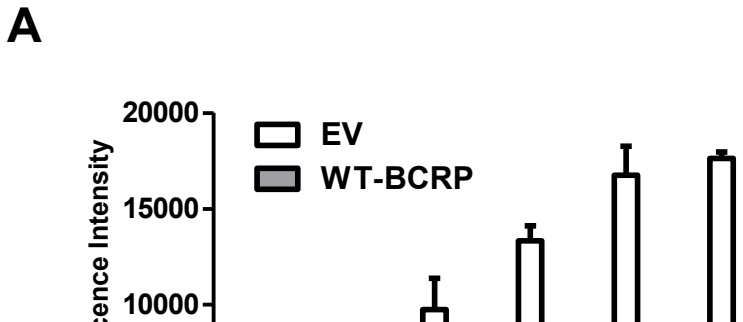

Supplemental Fig A-3.1. Characterization of Hoechst 33342 and ^{3}H-glyburide accumulation assays in HEK cells. Intracellular accumulation of (A) Hoechst 33342 or (B) ^{3}H-glyburide was determined in HEK cells overexpressing an EV or the WT-BCRP using a Cellometer Vision or liquid scintillation counter, respectively. Data are presented as mean ± SE.

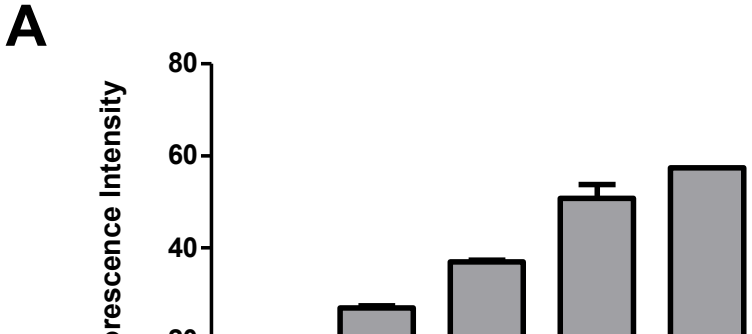

Supplemental Fig A-3.2. Characterization of Hoechst 33342 and ^{3}H-glyburide accumulation assays in placental BeWo cells. Intracellular accumulation of (A) Hoechst 33342 or (B) ^{3}H-glyburide was determined in placental BeWo cells using a Cellometer Vision or liquid scintillation counter, respectively. Data are presented as mean ± SE.

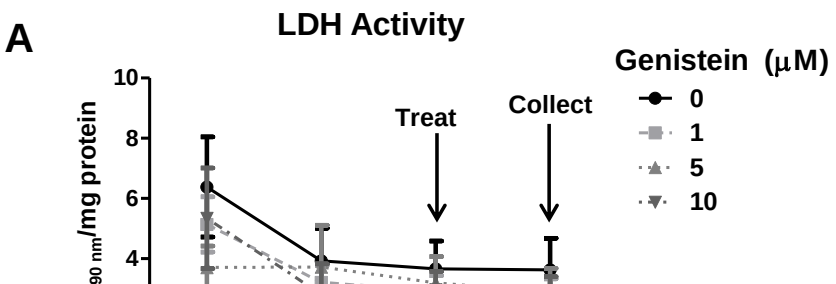

Supplemental Fig A-3.3. Characterization of human term placental explant viability and trophoblast function. (A) LDH activity in explant media was monitored over 7 days to confirm placental explant viability. Degree of syncytialization was assessed by (B) detection of hCG into the media and (C) histologic analysis (20x magnification). Data are presented as mean ± SE from five individual placentas. The image is from one representative placenta.

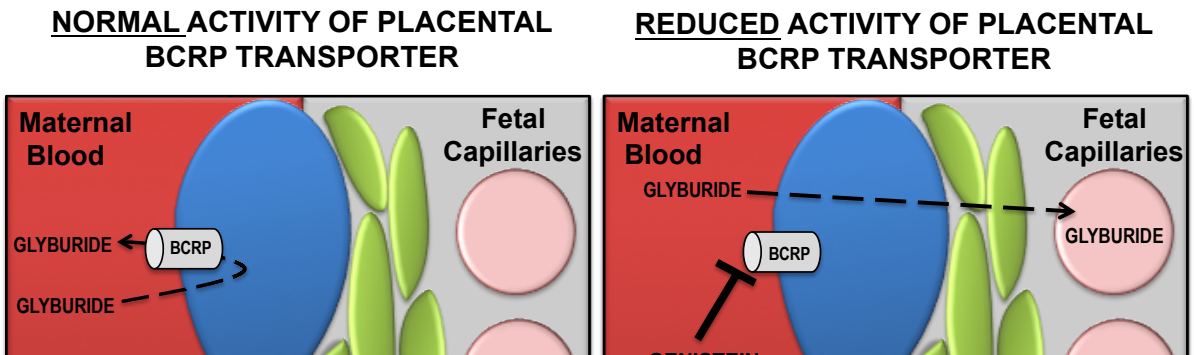

Supplemental Fig A-3.4. Visual abstract.

Table A-3.1. Inhibition of ^{3}H-glyburide transport in BCRP-overexpressing cells and placental BeWo cells.

	Transport IC_{50}[a]		
	HEK WT-BCRP	**HEK C421A-BCRP**	**BeWo**
Ko143 (nM)	21.5 ± 1.04	10.1 ± 1.79[b]	3.62 ± 2.0
Genistein (μM)	4.65 ± 0.15	3.92 ± 0.73	0.18 ± 0.11

[a]IC_{50} value calculated using Graphpad nonlinear regression analysis (dose-response: [log] inhibitor vs response—Variable slope (four parameters))

[b]$p<0.05$ compared to WT-BCRP control

Table A-3.2. Kinetic parameters of glyburide transport in HEK cells overexpressing BCRP protein (WT or C421A).[a]

	Genistein (μM)		
	0	**2**	**10**
WT-BCRP			
K_m (μM)	70.5 ± 9.8	12.1 ± 3.80[b]	1.0 ± 0.11[b]
J_{max} (pmol ^{3}H-glyburide/mg protein)	0.69 ± 0.10	0.68 ± 0.07	0.89 ± 0.13
C421A-BCRP			
K_m (μM)	14.5 ± 1.05[c]	2.52 ± 1.09[b]	0.61 ± 0.13[b]
J_{max} (pmol ^{3}H-glyburide/mg protein)	0.73 ± 0.12	0.79 ± 0.06	0.82 ± 0.08

[a] K_m and J_{max} values calculated using Graphpad nonlinear regression analysis (Michaelis-Menten)

[b] $p<0.05$ compared to 0 μM genotype control

[c] $p<0.05$ compared to 0 μM WT-BCRP control

Supplemental Table A-3.1. Primer sequences for human BCRP/*ABCG2* and RPL13A genes (5' to 3').

Gene	Forward Primer Sequence	Reverse Primer Sequence
ABCG2	ATCAGCTGGTTATCACTGTGAGGCC	AGTGGCTTATCCTGCTTGGAAGGC
RPL13A	GGTGCAGGTCCTGGTGCTTGA	GGCCTCGGGAAGGGTTGGTG

Supplemental Table A-3.2. Patient demographic information.

Results are presented as a range

[b] Wet, untrimmed weight

Gestational Age (weeks)	37-39[a]
Maternal Age (years)	34-39[a]
Maternal Race	Caucasian = 3 African American = 2
Paternal Ethnicity	Caucasian = 3 African American = 2
Birth Weight (grams)	2610-3545[a]
Placental Weight (grams)[b]	552-771[a]
Baby's Sex	Female = 2 Male = 3

APPENDIX 4: REGULATION OF THE PLACENTAL BCRP TRANSPORTER BY PPAR GAMMA

Yixin Lin[1], Kristin M. Bircsak[1], Ludwik Gorczyca[1],

Xia Wen[1], Lauren M. Aleksunes[1,2]

[1] Rutgers University Ernest Mario School of Pharmacy, Department of Pharmacology and Toxicology, 170 Frelinghuysen Rd. Piscataway, NJ 08854, USA

[2] Environmental and Occupational Health Sciences Institute, 170 Frelinghuysen Rd. Piscataway, NJ 08854, USA

Running Title: Placental BCRP and PPAR Gamma

Keywords: Placenta, Trophoblast, BCRP, ABCG2, PPAR gamma

Non-Standard Abbreviations: breast cancer resistance protein (BCRP); control (CON); hemolysis, elevated liver enzymes, low platelet count (HELLP); glial cells missing homolog 1 (GCM1); human chorionic gonadotropin beta (hCGβ); peroxisome proliferator-activated receptor γ (PPARγ); ribosomal protein 13a (RPL13A); rosiglitazone (ROSI); T0070907 (T00)

A-4.1 Abstract

Identifying regulators of placental breast cancer resistance protein (BCRP) expression is critical as down-regulation of this transporter may increase exposure of the fetus to xenobiotics. Here we sought to test whether the nuclear receptor peroxisome proliferator-activated receptor γ (PPARγ) regulates BCRP expression in the placenta. To test this, human BeWo placental choriocarcinoma cells were cultured with the PPARγ agonist rosiglitazone or the PPARγ antagonist T0070907 for 24 h. Messenger RNA (mRNA) expression of syncytialization markers, GCM1 and hCGβ, as well as BCRP increased with PPARγ agonist treatment. Conversely, BCRP mRNA and protein expression decreased 30-50% with PPARγ antagonist treatment. Rosiglitazone enhanced BCRP protein expression and transport activity, resulting in a 20% greater efflux of the substrate Hoechst 33342 compared to control cells. These results suggest that PPARγ can up-regulate BCRP expression in the placenta, which may be important in understanding mechanisms that protect the fetus from xenobiotic exposure during development.

A-4.2 Introduction

The human placenta supports the normal growth and development of the fetus. Placental villi are lined with syncytiotrophoblasts that produce hormones such as human chorionic gonadotropin beta (hCGβ) and also express transporters that regulate the maternal-to-fetal and fetal-to-maternal transfer of chemicals. One such transporter is the breast cancer resistance protein (BCRP, *ABCG2*), which is highly enriched within the placenta on the apical (maternal) surface of syncytiotrophoblasts and is an important part of the blood-placental barrier (Allikmets et al. 1998; Ceckova et al. 2006; Doyle et al. 1998; Maliepaard et al. 2001a). BCRP is a half-transporter protein that requires the formation of homodimers and oligomers to function properly (Henriksen et al. 2005). BCRP has over 100 substrates (reviewed in (Klaassen et al. 2010)) including environmental chemicals (perfluorooctanoic acid, bisphenol A) (Dankers et al. 2013; Mazur et al. 2012), mycotoxins (zearalenone, aflatoxin B1) (van Herwaarden et al. 2006; Xiao et al. 2015a), chemotherapeutic drugs (mitoxantrone, doxorubicin, daunorubicin) (Doyle et al. 1998), photosensitizers (pheophorbide A, protoporphyrin IX) (Jonker et al. 2002) and others such as cimetidine (Pavek et al. 2005), glyburide (Gedeon et al. 2008b), phytoestrogens (genistein and daidzein) (Enokizono et al. 2007b), nitrofurantoin (Zhang et al. 2007), and rosuvastatin (Huang et al. 2006). Previous studies show that mouse fetuses lacking the Bcrp transporter have elevated concentrations of glyburide, nitrofurantoin, and genistein (Enokizono et al. 2007b; Zhang et al. 2007; Zhou et al. 2008a). In addition to xenobiotics, BCRP has been shown to transport the fluorescent dye Hoechst 33342 (Scharenberg et al. 2002), which is often used as a marker of BCRP function. Human BeWo choriocarcinoma cells express transporters and secrete hormones such as hCGβ. BeWo cells highly express BCRP (Bailey-Dell et al. 2001; Evseenko et al. 2006) and have been shown to transport BCRP substrates including Hoechst 33342 (Evseenko et al. 2006), mitoxantrone (Ceckova et al. 2006), and glyburide (Bircsak et al. 2016). Thus, BeWo cells are

routinely used to study the regulation and function of the placental BCRP transporter (Pattillo et al. 1968a; Pattillo et al. 1971).

A number of nuclear receptor pathways including the progesterone and estrogen receptors have been explored as potential regulators of BCRP expression in BeWo cells (Wang et al. 2008a; Wang et al. 2006b). However, little attention has been placed on the ability of xenobiotic-activated receptors to transactivate the *ABCG2* gene in the placenta. For example, a study using human brain dendritic cells has identified the peroxisome proliferator activated receptor gamma (PPARγ) as a novel regulator of BCRP (Szatmari et al. 2006). Ligand-activated PPARγ binds to a 150-bp portion (-3946/-3796) of a conserved region in the promoter of the human *ABCG2* gene (Szatmari et al. 2006). PPARγ is an important regulator of placenta development such that mice lacking expression of PPARγ do not develop. Placentas lacking *PPARγ* exhibit altered terminal differentiation of trophoblasts and placental vascularization. PPARγ homozygous null ($^{-/-}$) embryos cannot be detected on gestation day 12.5 and beyond (Barak et al. 1999). A second study found that no *PPARγ*$^{-/-}$ pups were born in 62 offspring of heterozygous *PPARγ* intercrosses; likewise, no viable *PPARγ*$^{-/-}$ embryos were detected 11.5 days post coitum pointing to an indispensible role for this nuclear receptor in placental development (Kubota et al. 1999). Preliminary studies suggest that PPARγ can activate BCRP mRNA expression in placental cells in coordination with the induction of syncytialization genes, including the transcriptional regulator of syncytin genes known as glial cells missing homolog 1 (GCM1), and the secretion of hCGβ (Ruebner et al. 2012; Tarrade et al. 2001). Moreover, mouse trophoblast stem cells lacking PPARγ have reduced expression of syncytin A and lower numbers of multinucleated syncytiotrophoblasts (Tache et al. 2013). The fact that placenta is highly enriched in both BCRP and PPARγ expression led us to consider whether this transcriptional pathway could be activated by an exogenous ligand and further increase BCRP levels. Therefore, the purpose of this study was to determine whether PPARγ regulates BCRP

expression and function in placental cells. This was accomplished by treating BeWo cells with a pharmacological agonist (rosiglitazone) and an antagonist (T0070907) and evaluating BCRP mRNA and protein expression as well the ability to efflux the prototypical substrate Hoechst 33342 (Lee et al. 2002; Scharenberg et al. 2002).

A-4.3 Materials and Methods

Chemicals. Unless otherwise specified, chemicals were obtained from Sigma-Aldrich (St. Louis, MO).

Cell Culture. BeWo choriocarcinoma placenta cells were obtained from the American Type Culture Collection (ATCC, Manassas, VA) and grown in Dulbecco's Modified Eagle Medium: F-12 (1:1, ATCC) with 10% fetal bovine serum (Atlanta Biologicals, Norcross, GA) and 1% penicillin-streptomycin (Life Technologies, Carlsbad, CA). Cells were incubated at 37°C with 5% CO_2 and were used in experiments when they reached 80 to 90% confluence.

BeWo cells (3×10^4 cells/well) were grown on six-well plates for 3 days. Fresh media was supplied on the second day. For the dose-response study, rosiglitazone (1-30 μM) was dissolved in 0.24% DMSO and applied to cells for 24 h. For other studies, BeWo cells were treated with vehicle (0.1% DMSO), rosiglitazone (15 μM), T0070907 (1 or 10 μM) or the combination of rosiglitazone (15 μM) and T0070907 (1 μM) for 24 h.

RNA Isolation and Real-Time Quantitative PCR. After an 24 h incubation with vehicle, rosiglitazone, and/or T0070907, cells were rinsed with phosphate-buffered saline (PBS) and lysed with buffer RLT (QIAGEN, Valencia, CA) containing 1% β-mercaptoethanol. Total RNA was isolated using the RNeasy Mini kit (QIAGEN) according to the manufacturer's instruction. Integrity and concentration of RNA were assessed with a Nanodrop 1000 spectrophotometer (Thermo Fisher Scientific, Waltham, MA). Complementary DNA was generated with the High Capacity cDNA Reverse Transcription kit with 500 ng total RNA (Applied Biosystems, Foster City, CA). SYBR Green (Applied Biosystems) was used for detection of amplified products. qPCR

was performed in a 384-well plate using a ViiA7 RT-PCR system (Applied Biosystems). Primer sequences have been provided in Table 1. C_t values were converted to delta C_t values by comparing to the reference gene, ribosomal protein 13a (RPL13A) and further to delta delta C_t by comparing to the respective control-treated cells (Livak et al. 2001).

Western Blot. BeWo cells were treated with vehicle (0.1% DMSO), rosiglitazone (15 μM), or T0070907 (10 μM). After 24 h, cells were harvested and centrifuged for 10 min at the speed of 1500 rpm to obtain cell pellets. Lysis buffer (20 mM Tris-HCl, 150 mM NaCl, 5 mM EDTA, 1% Triton X-100 and 1% protease inhibitor cocktail) was added to the cell pellets. Samples were centrifuged for 3 min at 1000 rpm before performing analysis. Protein concentrations were determined by the bicinchoninic acid assay (Pierce Biotechnology, Rockford, IL). Western blot analysis was performed by loading 10 μg protein homogenate per sample on polyacrylamide 4–12% Bis–Tris gels (Life Technologies), which were resolved by electrophoresis. Proteins were transferred from gels onto a PVDF membrane overnight. The membrane was then blocked in 5% non-fat dry milk in PBS with 0.5% Tween-20 for 1 h. BCRP (BXP-53, Abcam, Cambridge, MA) and β-ACTIN (ab8227, Abcam) primary antibodies were diluted in 2% non-fat dry milk in PBS with 0.5% Tween-20 and incubated with the membranes at dilutions of 1:5000 and 1:2000, respectively. After washing, the membrane was incubated with species-specific HRP-conjugated secondary antibodies (Sigma Aldrich, St. Louis, MO): anti-rat IgG (BCRP) and anti-rabbit (β-ACTIN) at dilutions of 1:2000. SuperSignal West Dura Extended Duration Substrate (Pierce Biotechnology) was added to the blots for 2 min. Detection and semiquantitation of protein bands were performed with a FluorChem imager (ProteinSimple, Santa Clara, CA). The density of bands was assessed using an Alpha Viewer (ProteinSimple) and normalized to β-ACTIN levels.

Fluorescent Substrate Transport and Cell Size Assays. The BCRP-specific fluorescent substrate, Hoechst 33342, was used to quantify BCRP function (Bircsak et al. 2016). Following treatments, BeWo cells were trypsinized and added to a 96-well plate. Following centrifugation (500x*g*, 5 min, 8°C) and removal of the media, cells were loaded with Hoechst 33342 (3 μM) for 30 min at 37°C and 5% CO_2 (*uptake phase*). A subset of control cells were incubated with the BCRP-specific inhibitor, Ko143 (1 μM). Media was removed and cells were resuspended in substrate-free media with or without Ko143 for 1 h (*efflux phase*). Following the efflux phase, cells were centrifuged (500x*g*, 5 min, 8°C), washed, and resuspended in cold PBS for quantification of intracellular fluorescence using the Cellometer Vision automated cell counter (Nexcelom Bioscience, Lawrence, MA). Because BeWo cells stimulated to undergo cell fusion are larger in size (Kudo et al. 2003), cell suspensions (20 μl) were added to the cell counting chamber and analyzed for cell size and cell number using bright field images. A similar number of cells (between 750-1500) were counted for each treatment group. A VB-450-302 filter (excitation/emission: 375/450 nm) allowed for intracellular fluorescence detection of Hoechst 33342.

Immunocytochemistry. BeWo cells (2 x 10^5 cells/well) were seeded in chamber slides and grown until 90% confluent. After treatment with vehicle (0.1% DMSO), rosiglitazone (15 μM), or T0070907 (1 μM) for 24 h, cells were washed with PBS and fixed in 4% paraformaldehyde, then blocked with 5% goat serum in 0.1% Triton X in PBS for 1 h. The primary antibody against Na^+/K^+ ATPase (ab76020, Abcam) was diluted 1:200 in 5% goat serum in PBS-Triton X and applied overnight. After washing, a goat anti-rabbit IgG 594 (*red*) (Life Technologies, Carlsbad, CA) was diluted 1:200 in 5% goat serum in PBS-Triton X and applied for 1 h. Slides were rinsed in PBS-Triton X, PBS, and deionized water. One drop of Prolong Gold with DAPI was added to each slide and covered with a coverslip. Images were acquired at 320X magnification (objective 20X, eye

objective 10X, 1.6X setting) using an Olympus OlyVIA VS120 microscope (Olympus Corp., Center Valley, PA).

Statistical Analysis. Data were expressed as mean ± SE and all statistical analyses were performed using GraphPad Prism 5.0 (GraphPad Software, Inc., San Diego, CA). Data were analyzed by one-way ANOVA with a Newman-Keuls post-hoc test. Statistical significance was set at $p<0.05$.

A-4.4 Results

GCM1 and hCGβ mRNA Expression in Response to PPARγ Agonism and Antagonism. Rosiglitazone was used to activate PPARγ at concentrations (1-30 μM, 24 h) that did not alter cell viability or cytotoxicity as determined by the alamarBlue assay and lactate dehydrogenase release, respectively (data not shown). Similarly, PPARγ was inhibited using T0070907 at concentrations (1-10 μM, 24 h) that did not change cell viability or cytotoxicity (data not shown).

Markers of placental trophoblast syncytialization (GCM1 and hCGβ) were quantified using qPCR analysis. Treatment of BeWo cells with rosiglitazone increased GCM1 mRNA by 66% and tended to elevate hCGβ mRNA by 18% mRNA although not statistically significant (Figure A-4.1). Conversely, treatment with T0070907 decreased both GCM1 and hCGβ mRNAs by 55% and 60%, respectively (Figure A-4.1).

Cell Morphology and Size in Response to PPARγ Agonism and Antagonism.

Previous studies demonstrate that induction of syncytialization in BeWo cells leads to an increase in mean cell size (Kudo et al. 2003). Therefore, we assessed the degree of syncytialization using immunofluorescence and cell size measurements. Morphological analysis showed a similar degree of multinucleated cells between vehicle-, rosiglitazone-, and T0070907-treated groups (Figure A-4.2A). A slight but significant increase in BeWo cell size as determined by an automated cell counter (Nexcelom Cellometer) was observed following treatment with rosiglitazone (Figure A-4.2B). Conversely, T0070907 decreased BeWo cell size.

BCRP mRNA Expression in Response to PPARγ Agonism and Antagonism.

BCRP mRNA was quantified in BeWo cells treated with increasing concentrations of rosiglitazone for 24 h. Compared to vehicle-treated cells, a 50% increase in BCRP mRNA expression was observed in the cells treated with rosiglitazone concentrations as low as 1 μM (Figure A-4.3A). BCRP mRNA expression was not enhanced much further at higher concentrations of rosiglitazone. Quantification of BCRP mRNA was also performed following exposure to rosiglitazone, T0070907, and the combination of rosiglitazone with T0070907 for 24 h (Figure A-4.3B). BCRP mRNA expression was increased by 50% in cells treated with rosiglitazone, decreased by 50% with T0070907, and was unchanged following the combination treatment (Figure A-4.3B).

BCRP Protein Expression and Transporter Function in Response to PPARγ Agonism and Antagonism.

Western Blot analysis was performed on BeWo cell lysates following treatment with vehicle, rosiglitazone, or T0070907 for 24 h. Changes in BCRP protein mirrored the regulation of mRNA. BCRP protein expression was increased by 20% in cells treated with rosiglitazone and decreased by 30% in cells treated with T0070907 (Figure A-4.4A).

The Hoechst 33342 accumulation assay was used to assess BCRP activity in BeWo cells after rosiglitazone or T0070907 treatment for 24 h. The BCRP specific inhibitor Ko143 (1 μM) was used as a positive control and revealed a 175% increase in the retention of Hoechst (Figure A-4.4B). Consistent with the induction of BCRP protein and presumably activity, the intracellular concentration of Hoechst 33342 was reduced by 20% in BeWo cells treated with rosiglitazone. Despite the down-regulation of BCRP expression by T0070907, no change in Hoechst 33342 accumulation was observed.

A-4.5 Discussion

Because BCRP is a critical part of the blood-placental barrier, there is interest in understanding how transcriptional pathways regulate this transporter's expression and function. PPARγ is a candidate for regulating BCRP transcription since its ligands can induce expression in human dendritic (Szatmari et al. 2006) and intestinal cells (Wright et al. 2011). More recent data also suggest that BCRP mRNA can be induced by the PPARγ activator troglitazone in primary human cytotrophoblasts (Ruebner et al. 2012). Therefore, we assessed the ability of a PPARγ agonist and antagonist to up- and down-regulate BCRP expression and function, respectively. We observed that enhanced BCRP expression and function was associated with induction of GCM1 and hCGβ, two markers of syncytialization, as well as a modest increase in placental BeWo cell size. Moreover, inhibition of basal PPARγ activity reduced BCRP mRNA and protein levels although no change in function, as assessed by Hoechst 33342 retention, was observed. Collectively, these data point to PPARγ as a novel regulator of the blood-placental barrier.

Induction of BCRP expression is a feature of syncytializing trophoblasts (Prouillac et al. 2009). Treatment with forskolin increases cyclic AMP concentrations resulting in cell fusion and increased expression of BCRP (Prouillac et al. 2009). Similarly, the mycoestrogens zearalenone was able to stimulate both syncytialization of BeWo cells as well as induction of BCRP (Prouillac et al. 2009). Moreover, down-regulation of BCRP in BeWo cells has demonstrated an intrinsic role for this transporter in the up-regulation of syncytialization markers (Evseenko et al. 2007c).

A disconnect between BCRP protein down-regulation by T0070907 and no change in intracellular Hoecsht concentrations was surprising. These data suggest that sufficient BCRP function was present despite the significant decline in protein levels. Further studies characterizing the kinetics

of Hoescht efflux or employing an alternate BCRP substrate may suggest a reduction in BCRP function following treatment with T0070907.

There is great interest in determining whether placental BCRP expression is altered in diseases of pregnancy. Abnormal placentation can result in preeclampsia, HELLP syndrome (hemolysis, elevated liver enzymes, low platelet count), and intrauterine growth restriction (reviewed in (Uzan et al. 2011; Zhang et al. 2015c). Reduced BCRP mRNA expression in placentas has been observed in preeclamptic pregnancies complicated by HELLP syndrome (Jebbink et al. 2015a; Ruebner et al. 2012). Likewise, BCRP mRNA is reduced in placentas from pregnancies with intrauterine growth restriction (Evseenko et al. 2007a). This corresponds with a down-regulation of syncytin-1 mRNA in both diseases of pregnancy (Ruebner et al. 2012) and a decrease in PPARγ expression in placentas from preeclamptic women (Memon et al. 2014). Interestingly, recent data point to a potential role for PPARγ agonists as a therapeutic intervention for the treatment of gestational hypertension and preeclampsia by enhancing signaling through the regulator of G protein (heterotrimeric guanine nucleotide-binding protein) (Holobotovskyy et al. 2015). Collectively, these data suggest that targeting of PPARγ to treat disorders of pregnancy may also restore BCRP expression and function.

There is growing interest in environmental chemicals that function as PPARγ agonists and contribute to obesity and altered lipid signaling. Phthalates, such as monoethylhexylphthalate, have been recognized as PPARγ agonists (Feige et al. 2007) although they have little interaction with BCRP directly (Dankers et al. 2013). Likewise, emerging research has pointed to organotins, including tributyltin and triphenyltin, as activators of PPARγ signaling and stimulators of adipocyte differentiation (Hiromori et al. 2009; Inadera et al. 2005). Recent analysis has revealed that components of house dust can activate PPARγ signaling (Fang et al. 2015a; Fang et al. 2015b).

Chemicals in house dust include flame retardants triphenyl phosphate and metabolites such as diphenyl phosphate, tetrabromobenzoic acid, and tetrabromo mono(2-ethylhexyl)phthalate, which all exhibit an affinity for PPARγ (Fang et al. 2015a). In particular, binding of tetrabromo mono(2-ethylhexyl)phthalate was similar to that of rosiglitazone (Fang et al. 2015a). Because of the widespread exposure to these chemicals, it will be important to determine whether these chemicals stimulate placental hormone secretion and BCRP expression by enhancing PPARγ signaling and triggering syncytialization.

As an efflux pump, BCRP is an important component of the blood-placenta barrier. The current findings build upon prior investigations pointing to sex steroid receptors as modulators of BCRP expression in placenta (Wang et al. 2008a; Wang et al. 2006b). We have identified PPARγ as a novel transcription factor that can induce BCRP mRNA, protein, and activity in placental cells. Future studies aim to understand the ability of PPARγ to enhance placental BCRP function *in vivo*, particularly in animal models of pregnancy disorders.

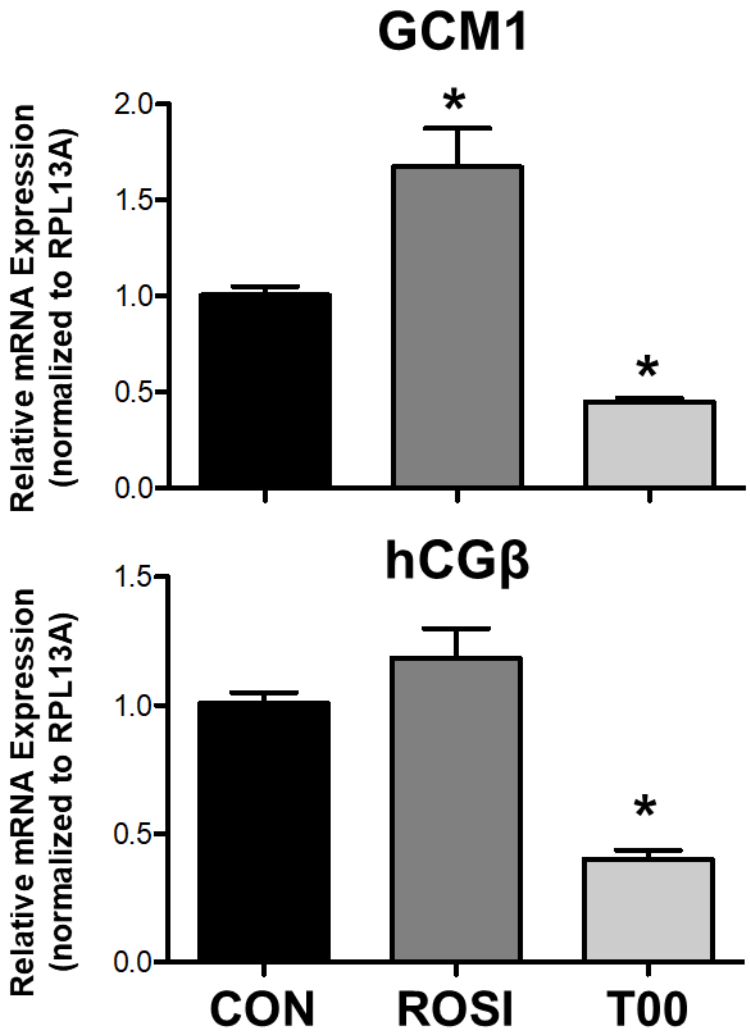

Fig A-4.1. GCM1 and hCGβ mRNA Expression in Response to PPARγ Agonism and Antagonism. BeWo cells were treated with the PPARγ agonist rosiglitazone (ROSI, 15 μM) and PPARγ antagonist T0070907 (T00, 10 μM) for 24 h. Quantitative real-time PCR analysis of GCM1 and hCGβ mRNA was performed with SYBR Green fluorescence detection using a ViiA7 RT-PCR system. Ribosomal protein L13a (RPL13A) was used as a reference gene (n=2 experiments, 4 replicates/experiment). Data are presented as mean ± S.E. * $p < 0.05$ compared to control (CON).

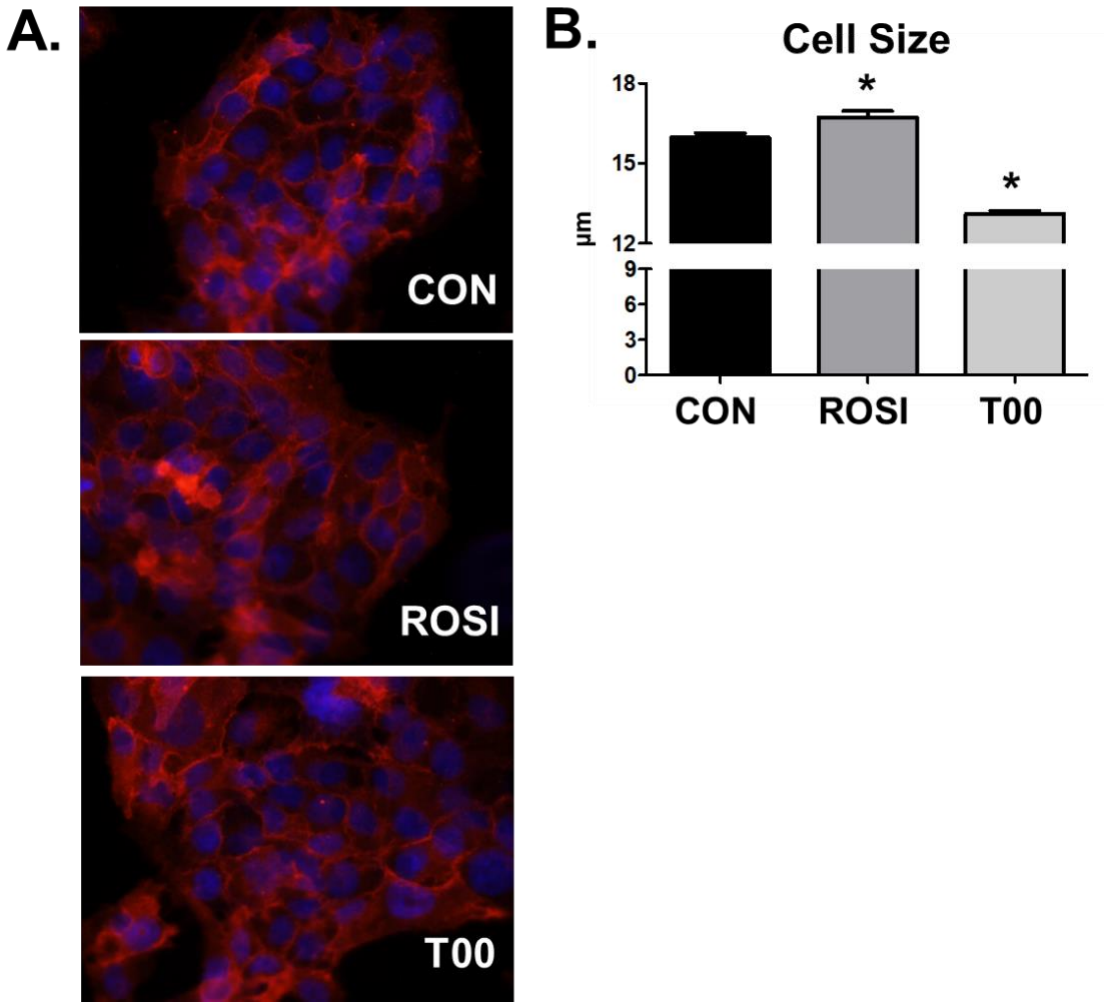

Fig A-4.2. Cell Morphology and Size in Response to PPARγ Agonism and Antagonism. (A) The number of nuclei per cell, an indicator of syncytialization, was qualitatively assessed after treatment with rosiglitazone (ROSI, 15 µM) and T0070907 (T00, 1 µM). Neither treatment differed from control (CON) cells. Plasma membranes were stained for the Na^+/K^+ ATPase (*red*) and nuclei were stained with DAPI (*blue*). Magnification 320X. (B) Cell size was quantified using a Nexcelom Cellometer cell counter and presented as mean ± S.E. * $p < 0.05$ compared to control (CON).

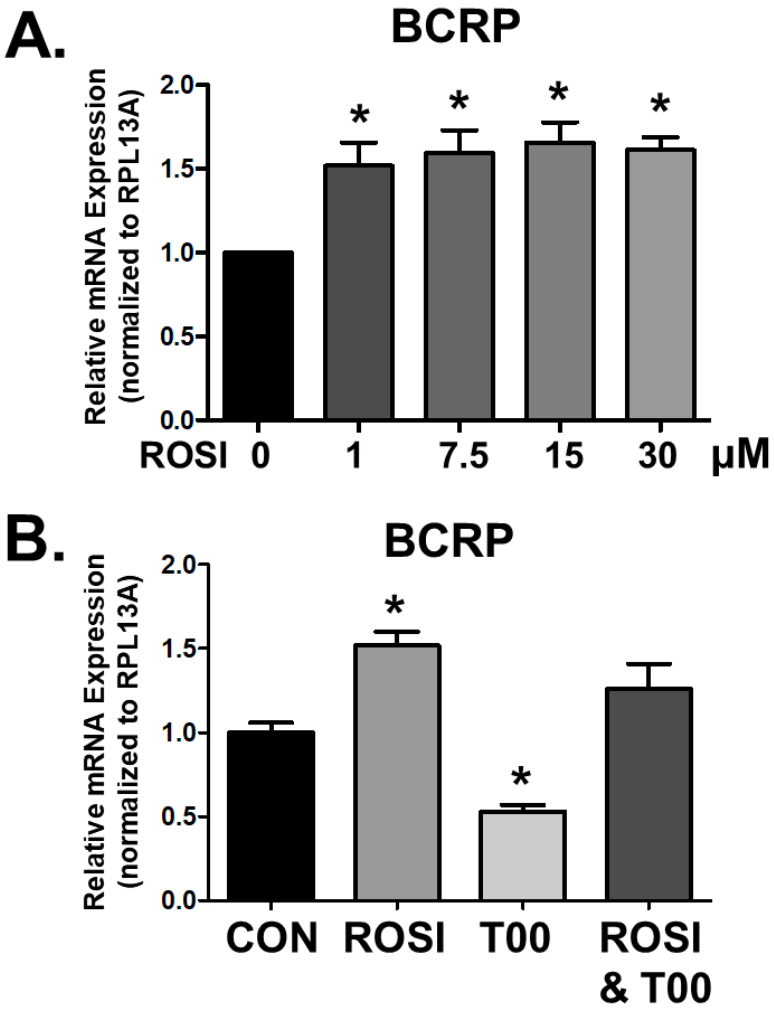

Fig A-4.3. BCRP mRNA Expression in Response to PPARγ Agonism and Antagonism. (A) BeWo cells were treated with increasing concentrations of PPARγ agonist, rosiglitazone, and incubated for 24 h (n=5 experiments, 4 replicates/experiment). (B) BeWo cells were treated with the PPARγ agonist rosiglitazone (ROSI, 15 μM), PPARγ antagonist T0070907 (T00, 1 μM), and the combination of rosiglitazone (15 μM) and T0070907 (1 μM) for 24 h (n=1 experiment, 4 replicates/experiment). Quantitative real-time PCR analysis of BCRP mRNA was performed with SYBR Green fluorescence detection using a ViiA7 RT-PCR system. Ribosomal protein L13a (RPL13A) was used as a reference gene. Data are presented as mean ± S.E. * $p < 0.05$ compared to control (CON, 0 μM).

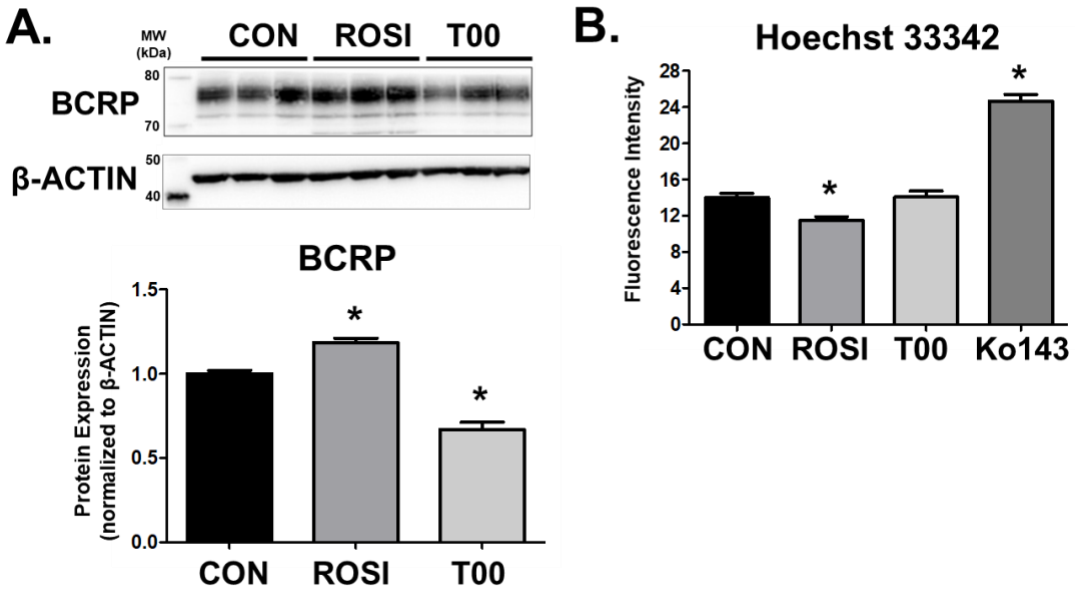

Fig A-4.4. BCRP Protein Expression and Transporter Function in Response to PPARγ Agonism and Antagonism. (A) BCRP protein expression in BeWo cells was determined 24 h after PPARγ agonism (rosiglitazone, ROSI, 15 μM) and PPARγ antagonism (T0070907, T00, 10 μM). β-ACTIN was used as the loading control. BCRP expression was compared to control cells (CON, set to 1.0). n=2 experiments, 3 replicates/experiment. (B) Fluorescence intensity of Hoechst 33343 dye retained in BeWo cells was quantified 24 h after PPARγ agonism (ROSI, 15 μM) and PPARγ antagonism (T0070907, T00, 1 μM). Ko143 (1 μM) was used as positive control inhibitor of BCRP function. n=2 experiments, 5-6 replicates/experiment. Data are presented as mean ± S.E. * $p < 0.05$ compared to control (CON).

Table A-4.1. Primer Sequences for qPCR

Genes	Forward	Reverse
BCRP	ATCAGCTGGTTATCACTGTGAGGCC	AGTGGCTTATCCTGCTTGGAAGGC
GCM1	TGAGGCTGCTCTCAAACTCCTGAT	AGACGGGACAGGTTTCCATTCCTT
hCGβ	GCACCAAGGATCGAGATGTT	GCACATTGACAGCTGAGAGC
RPL13A	GGTGCAGGTCCTGGTGCTTGA	GGCCTCGGGAAGGGTTGGTG

APPENDIX 5: DOWN-REGULATION OF THE PLACENTAL BCRP/ABCG2 TRANSPORTER IN RESPONSE TO HYPOXIA SIGNALING

Lissa N. Francois[a], Ludwik Gorczyca[b], Jianyao Du[c], Kristin M. Bircsak[b], Elizabeth Yen[d], Xia Wen[b], Mei-Juan Tu[e], Ai-Ming Yu[e], Nicholas P. Illsley[f], Stacy Zamudio[f], Lauren M. Aleksunes[b,g]

Affiliations:

[a] Rutgers University, Robert Wood Johnson Medical School, Department of Obstetrics, Gynecology and Reproductive Sciences, Maternal-Fetal Medicine Division, 125 Paterson St. New Brunswick, NJ 08091, USA

[b] Rutgers University, Ernest Mario School of Pharmacy, Department of Pharmacology and Toxicology, 170 Frelinghuysen Rd. Piscataway, NJ 08854, USA

[c] China Pharmaceutical University, Gulou, Nanjing, Jiangsu, China

[d] Rutgers University, Robert Wood Johnson Medical School, Department of Pediatrics, Division of Neonatology, 1 Robert Wood Johnson Place. New Brunswick, NJ 08903, USA

[e] University of California, Davis, Department of Biochemistry and Molecular Medicine, 2700 Stockton Blvd. Sacramento, CA 95817, USA

[f] Hackensack University Medical Center, Department of Obstetrics and Gynecology, 30 Prospect Ave. Hackensack, NJ 07601, USA

[g] Environmental and Occupational Health Sciences Institute, 170 Frelinghuysen Rd., Piscataway, NJ 08854, USA

[h] Rutgers Center for Lipid Research, New Jersey Institute for Food, Nutrition, and Health, Rutgers University, New Brunswick, New Jersey 08901

Highlights

- Cobalt chloride and low oxygen activate HIF-1α signaling in BeWo placental cells.
- BCRP expression and function are reduced by HIF-1α signaling in BeWo placental cells.
- BCRP protein expression is reduced in placentas from high altitude pregnancies.
- Down-regulation of BCRP in the placenta may increase fetal exposure to chemicals.

A-5.1 Abstract

Introduction: The BCRP/*ABCG2* efflux transporter protects the developing fetus by limiting the transplacental transfer of drugs and chemicals and prevents the apoptosis of trophoblasts. The purpose of this study was to determine whether hypoxia-related signaling alters placental BCRP expression and function *in vitro* and in human pregnancies.

Methods: Human BeWo choriocarcinoma cells were treated with the hypoxia mimetic, cobalt chloride ($CoCl_2$), or 3% oxygen for 24-48 h. Activation of HIF-1α signaling and regulation of BCRP was assessed using qPCR, ELISA, western blotting and a fluorescent substrate transport assay. In addition, healthy term placentas from high altitude pregnancies with chronic hypoxia were assessed for BCRP expression.

Results: $CoCl_2$ and 3% oxygen increased HIF-1α protein signaling and decreased the mRNA and protein expression of BCRP by 30-75% in BeWo cells. Reduced BCRP expression corresponded with impaired efflux activity during hypoxia as evidenced by accumulation of the substrate Hoechst 33342. A number of transcription factors known to regulate BCRP, including AHR, NRF2 and PPARγ, were also coordinately down-regulated by 3% oxygen in BeWo cells. Moreover, women who gave birth at a high altitude (3100 m) exhibited signs of chronic placental hypoxia, including enhanced protein expression of the HIF-1α target GLUT1, and had reduced BCRP levels in microvillous membranes compared to women at a moderate altitude (1600 m).

Discussion: This study provides novel insight into the regulation of the placental BCRP transporter by hypoxia, which may be important for exposure of the fetus to chemicals during early development and in hypoxia-related pregnancy disorders.

Keywords: BCRP, ABCG2, placenta, transporter, hypoxia

A-5.2 Introduction

The breast cancer resistance protein (BCRP/*ABCG2*) is an efflux transporter that is highly expressed on the apical membrane of placenta syncytiotrophoblasts and fetal endothelial cells (Allikmets et al. 1998; Maliepaard et al. 2001a). BCRP actively transports xenobiotics and endogenous chemicals away from the fetus and into the maternal circulation (Jonker et al. 2002). BCRP substrates include many compounds that may be relevant during pregnancy such as the gestational diabetes drug glyburide, the antibiotic nitrofurantoin, the acid reflux medication cimetidine, and the dietary phytoestrogen genistein (Enokizono et al. 2007b; Gedeon et al. 2006; Merino et al. 2005; Pavek et al. 2005). Mouse fetuses lacking Bcrp expression in the placenta exhibit elevated concentrations of glyburide, nitrofurantoin, and genistein (Enokizono et al. 2007b; Gedeon et al. 2006; Merino et al. 2005; Pavek et al. 2005). In addition to serving as a key component of the blood-placental barrier, BCRP critically prevents cytokine-induced apoptosis and enhances syncytial formation in placental cells (Ebert et al. 2005; Tompkins et al. 2010). Reductions in BCRP expression lead to greater cytokine-induced damage and lower expression of human chorionic gonadotropin beta and syncytin-1 (Ebert et al. 2005; Tompkins et al. 2010). Due to the important role of BCRP in maintaining placental health and protecting the fetus from xenobiotic exposure, it is critical to understand factors and conditions that may compromise its function.

While the placental environment is maintained under low oxygen tension relative to the maternal circulation throughout gestation the influence of hypoxia on placental BCRP expression remains unclear. Importantly, oxygen tension is quite low in the first trimester and increases during the 2nd and 3rd trimesters (1st trimester: 2-3% O_2, ~20 mmHg; 2nd trimester: 8-10% O_2, ~60 mmHg, 3rd trimester 40-60 mmHg, 5-8% O_2) (Rodesch et al. 1992). A previous study has demonstrated an up-

regulation of Bcrp protein expression in mouse hematopoietic stem cells under hypoxic conditions following direct transactivation by the hypoxia inducible factor-1 alpha (Hif-1α) transcription factor (Krishnamurthy et al. 2004). Furthermore, a direct relationship between Hif-1α and Bcrp mRNA levels has been reported in mouse placentas (Wang et al. 2006a). However, more recent evidence suggests that hypoxia may have the opposite effect in the human placenta. In fact, expression of BCRP mRNA was shown to be directly related to oxygen levels in human 1st trimester placental explants, such that lower *BCRP* expression was observed in explants exposed to 3% O_2 as compared to greater expression at 20% O_2 (Lye et al. 2013). These divergent results suggest that additional mediators may be involved in the regulation of BCRP in the human placenta during hypoxia.

In addition to HIF-1α, a number of transcription factors have been shown to directly bind to the promoter and transactivate the *ABCG2* gene that encodes the BCRP protein leading to increased mRNA expression. Of these factors, those expressed in placenta include the aryl hydrocarbon receptor (AHR) (Ebert et al. 2005; Tompkins et al. 2010), estrogen receptor-α (ERα) (Ee et al. 2004b; Wang et al. 2006b), nuclear factor (erythroid-derived 2)-like 2 (NRF2) (Hagiya et al. 2008; Singh et al. 2010), peroxisome proliferator-activated receptors (PPAR) (Hoque et al. 2015a; Szatmari et al. 2006), and retinoid X receptor-α (RXRα). More recent studies into the dynamic mechanisms regulating BCRP mRNA have demonstrated that levels can also be inversely related to the expression of certain miRNAs, including miR-519c, miR-520h, and miR-328, that target the *ABCG2* gene (Li et al. 2011; Wang et al. 2010a). Specifically, methylation of the miR-328 5'-flanking region correlated negatively with miR-328 levels and positively with BCRP mRNA expression in human placentas (Saito et al. 2013). These pathways provide potential mechanisms by which hypoxia could alter BCRP expression.

There are a number of experimental approaches to study hypoxia-related signaling. For example, the hypoxia mimetic cobalt chloride ($CoCl_2$) has been shown to prevent the breakdown of HIF-1α protein and enhance the expression of target genes such as the glucose transporter 1 (GLUT1) in placental choriocarcinoma BeWo cells (Baumann et al. 2007; Hayashi et al. 2004). Similar to $CoCl_2$, exposure of BeWo cells to 1-5% O_2 increases expression of GLUT1 protein (Baumann et al. 2007). Analogous results have been observed *in vivo* from placentas obtained from healthy pregnant women at different elevations. Interestingly, placentas from women living at high altitudes (3100m in Colorado) exhibited higher HIF-1α protein expression and the neonates had reduced birth weights compared to those at moderate altitudes (1600m in Colorado) (Zamudio et al. 2007). Across both altitudes HIF-1α protein levels were strongly, negatively associated with the placental:birth weight ratio, indicating that greater HIF-1α stimulation is related to lower placental efficiency, i.e. a larger placenta is required to sustain a certain level of fetal growth where HIF-1α levels are elevated.

Using complementary models of placental hypoxia, the purpose of this study was to 1) characterize the effect of HIF-1α activation on BCRP expression and function in human placental BeWo cells, 2) identify potential regulatory factors controlling BCRP expression during hypoxia, and 3) quantify BCRP protein expression during chronic hypoxia using maternal-facing microvillus membranes from healthy, term human placentas from high altitude pregnancies.

A-5.3 Materials and Methods

Chemicals. All chemicals were obtained from Sigma-Aldrich (St. Louis, MO) unless otherwise specified.

BeWo cell culture. The BeWo choriocarcinoma cell line was maintained in DMEM: F-12 containing 10% fetal bovine serum (Atlanta Biologicals, Flowery Branch, GA) and 1% penicillin-streptomycin at 37°C and 5% CO_2 (atmospheric O_2, ~20%). *$CoCl_2$ Studies.* BeWo cells were cultured in DMEM:F-12 with 0.5% bovine serum albumin, 5mM glucose and 1% penicillin-streptomycin 24 h prior to $CoCl_2$ treatment (Baumann et al. 2007). Cells were then treated with $CoCl_2$ (200 µM) for 24 to 48 h. *Hypoxia Chamber Studies.* BeWo cells in normal culture media were placed in the Modular Incubator Chamber (MIC-101) (Billups-Rothenberg, Inc, Del Mar, CA) and gas (3% O_2, 5% CO_2) was flushed through the chamber at a regulated flow rate of 25-50 liters/min for 6 min in order to obtain a 100% exchange of gases. After flushing was completed, the chamber was placed into the cell culture incubator at 37°C for 24 h. A separate set of BeWo cells were placed into the same cell culture incubator and incubated for 24 h under standard culture conditions (37°C, 20% O_2, 5% CO_2).

Placental microvillous membranes. Placenta microvillous membranes were prepared from frozen tissue as described (Zamudio et al. 2006). The high altitude samples (3100 m, Leadville, CO) were previously characterized for markers of hypoxia compared to the moderate altitude samples (1600 m, Denver, CO) (Zamudio et al. 2006). The current study was approved by the Rutgers Institutional Review Board (exempt protocol E15-729). Subjects included n=8 from the moderate altitude (n=2 male, n=6 female) and n=7 from the high altitude (n=2 male, n=5 female). The race of all mothers was Caucasian. The race of fathers was Caucasian with two fathers in the

high altitude group who identified their ethnicity as Hispanic. Both groups were similar with regards to maternal age (range 18-36 y, p=0.783), pre-pregnancy BMI (range 19.4-25.7, p=0.530), weight gain during pregnancy (range 8.2-24 kg, p= 0.624), and gestational age at delivery (range 37.1-41.1 weeks, p=0.797).

Alamar Blue Assay. BeWo cell viability was assessed using the Alamar Blue Assay (Life Technologies) with fluorescence detection using a Spectramax M5 plate reader (Molecular Devices, Sunnyvale, CA).

HIF-1α ELISA. The HIF-1alpha Human SimpleStep ELISA Kit (Abcam, Cambridge, MA) was used.

RNA isolation and real-time quantitative PCR. RNA was isolated and qPCR performed as previously described (Bircsak et al. 2016). Stem-loop reverse transcription real-time qPCR for microRNA (miRNA) was performed using the primers and methods as reported (Li et al. 2011). Primer sequences are listed in Supplemental Table 1. Cycle threshold (Ct) values were first converted to delta Ct values by comparing to the reference genes, RPL13A (for mRNA) and U6 (for miRNA) and then to delta delta Ct values by comparing to the respective control-treated cells (Livak et al. 2001).

Western blot analysis. Proteins from cell homogenates (10µg) or placental microvillous membranes (15µg) were separated on SDS-polyacrylamide 4-12% Bis-Tris gels (Life Technologies) by electrophoresis (Bircsak et al. 2016). The following antibodies were used: BCRP (BXP-53 Enzo LifeSciences, Farmingdale, NY, 1:5000), GLUT1 (Ab652 Abcam, Cambridge, MA, 1:1000) and β-ACTIN (Ab8227 Abcam, 1:2000). BCRP and GLUT1 protein levels in BeWo cells

were normalized to β-Actin levels. Due to changes in protein loading controls in the high altitude placentas, raw luminescence values for BCRP and GLUT1 staining were presented after confirming equal protein loading with Coomassie blue dye.

Hoechst 33342 retention assay. Transporter function was quantified using a Nexcelom Cellometer fluorescent cell counter (Lawrence, MA) and the fluorescent substrate Hoechst 33342 (5 μM) as previously described (Bircsak et al. 2013b).

Statistical Analysis. Data are expressed as mean ± SE and analyzed using Graphpad Prism 6.0 (GraphPad Software, Inc., La Jolla, CA). One-way ANOVA followed by a Newman-Keuls multiple comparison post hoc test was used when comparing 3 or more groups, while an unpaired Student's t-test was used when comparing 2 groups. Statistical significance was set at $p<0.05$.

A-5.4 Results

Regulation of HIF-1α signaling and BCRP expression by the hypoxia mimetic $CoCl_2$ in BeWo cells. Treatment of BeWo cells with $CoCl_2$ (200 μM) increased total cellular HIF-1α protein at 24 h (4-fold) (Fig. A-5.1A) compared to control cells. Prototypical HIF-1α target genes, VEGF and GLUT1, as well as GLUT1 protein were also induced by $CoCl_2$ at 48 h (Fig. A-5.1B and A-5.1C). Conversely, $CoCl_2$ treatment reduced BCRP mRNA and protein expression at 48 h to 25% and 70% of control levels, respectively (Fig. A-5.2A and B). Reduced BCRP protein expression in BeWo cells corresponded with impaired transport activity as evidenced by a 2-fold increase in the cellular retention of the fluorescent BCRP substrate, Hoechst 33342 (Fig. A-5.2C). The BCRP inhibitor Ko143 (1 μM) was used as a positive control and increased Hoechst 33342 retention 3-fold. It should be noted that the concentration of $CoCl_2$ used in these studies did not alter cell viability at 48 h as determined by the Alamar Blue Assay (data not shown).

Regulation of HIF-1α signaling and BCRP expression by low oxygen content (3% O_2) in BeWo cells. Compared to standard culture conditions (20% O_2), exposure of BeWo cells to low oxygen levels (3% O_2) for 24 h increased HIF-1α protein levels by 50% (Fig. A-5.3A). Corresponding increases in VEGF and GLUT1 mRNAs (2- and 4-fold, respectively) as well as GLUT1 protein were observed in cells exposed to 3% O_2 (Fig. A-5.3B and 3C). Low oxygen levels (3% O_2, 24 h) down-regulated BCRP mRNA and protein by 60% and 40%, respectively (Figs. A-5.4A and B). Consequently, BCRP function was reduced by 3% O_2 as demonstrated by a 2-fold increase in the cellular retention of Hoechst 33342 (Fig. A-5.4C).

To elucidate a potential mechanism for the reduction of BCRP expression following activation of the HIF-1α pathway, we quantified the expression of critical miRNAs and transcription factors. All

three BCRP regulatory miRNAs were reduced by 25 to 30% in response to hypoxia (Fig. A-5.5A) suggesting that they were not responsible for the decrease in BCRP expression. By comparison, exposure of BeWo cells to 3% O_2 for 24 h significantly lowered the mRNA expression of AHR, NRF2, PPARγ and RXRα between 20-60% (Fig. A-5.5B). Meanwhile, there was a trend for a 3-fold induction of ERα mRNA in response to 3% O_2 (Fig. A-5.5B).

Regulation of GLUT1 and BCRP expression in placentas from a high altitude. Placentas were obtained from women at moderate (1600m, n=8) and high altitudes (3100 m, n=7) as previously described (Zamudio et al. 2006). Placentas from the 3100m altitude exhibited greater weights compared to the moderate altitude placentas (Fig. A-5.6A) and infants born at the higher altitude tended to have reduced birth weights similar to published findings (Zamudio et al. 2006). Western blot analysis of microvillous membranes revealed that placentas from a high altitude (3100 m) exhibited 30% higher GLUT1 protein expression than moderate altitude (1600 m) placentas (Fig. A-5.6B). Additionally, BCRP protein expression was reduced by approximately 20% in high altitude (3100 m) placentas as compared to those from a moderate altitude (1600 m).

A-5.5 Discussion

The current study characterized the influence of hypoxic conditions on placental BCRP expression and function. Treatment of BeWo cells with $CoCl_2$ or 3% O_2 activated the HIF-1α transcription factor pathway, while reducing BCRP expression and function. Altered expression of known transcription factors following 3% O_2 exposure, likely underlie the hypoxia-mediated down-regulation of BCRP in placental cells. Finally, microvillous membranes isolated from term placentas of high-altitude pregnancies (3100 m), exhibited reduced levels of BCRP concurrently with the up-regulation of the HIF-1α target, GLUT1. Our data shed light on the regulation of the human placental BCRP transporter by hypoxia, which may be important in hypoxia-related pathologies of pregnancy such as preeclampsia and growth restriction.

Proper human placental development is dependent upon tightly-regulated oxygen concentrations (Caniggia et al. 2000; Genbacev et al. 1997). Through the 1st trimester, placental invasion occurs at a low oxygen tension (~20 mmHg, 2-3% O_2) as the uterine spiral arterioles are plugged by extravillous trophoblasts. During this period, the HIF-1α protein is preferentially located in villous cytotrophoblasts, as syncytiotrophoblasts contain the von Hippel-Lindau tumor suppressor protein, which ubiquitinates HIF-1α and targets it for proteasomal degradation (Ietta et al. 2006). By weeks 10 to 12, maternal blood flow to the placenta is established, thereby increasing the placental oxygen tension (~55 mmHg, 8% to 10% O_2). Immunohistochemical analysis suggests that BCRP staining is less intense in cytotrophoblasts and syncytiotrophoblasts from 1st trimester placentas than in term placentas (Lye et al. 2013). Western blot analysis has also revealed lower BCRP protein expression earlier in pregnancy compared to term in whole tissue homogenates (Yeboah et al. 2006). Others have reported variable BCRP expression between placentas that precluded analysis of gestational age-related changes (Mathias et al. 2005). Nonetheless, these data generally support a trend for

lower BCRP protein levels early in gestation when oxygen levels are low which is consistent with our observations that activation of HIF-1α is inversely related to the expression of BCRP in placental cells.

More recent work has begun to address the ability of hypoxia to regulate BCRP expression in placental explants. Exposure of 1st trimester explants to varying levels of O_2 (3, 8 and 20%) revealed that higher O_2 tension was associated with greater BCRP mRNA expression (Lye et al. 2013). These data are consistent with the findings in the current study. However, immunohistochemical analysis demonstrated BCRP protein expression to be up-regulated in 1st trimester explants at low O_2 levels (Lye et al. 2013). The disconnect between the mRNA and protein findings in this prior study were not clear and may represent an acute stress of explants to the substantial change in oxygen concentrations. Time-dependent differences in acute and chronic responses to hypoxia have been demonstrated previously, operating through distinct signaling pathways (Koritzinsky et al. 2006). Using term placental explants, the same laboratory demonstrated that low O_2 concentrations (3%) had no effect on BCRP mRNA or protein expression, suggesting that responses to hypoxia are dependent upon the stage of placental development (Javam et al. 2014).

In the present studies, the down-regulation of BCRP in the placenta by hypoxia was somewhat surprising since investigations in other cell types and tissues demonstrated that HIF-1α can directly transactivate the human *ABCG2* gene at specific response elements (-1059 to -1055 bp, -194 bp to -190 bp, and -116 to -112 bp) (Cheng et al. 2012; Krishnamurthy et al. 2004). Because of this disconnect, we explored the expression of transcriptional and epigenetic pathways that could explain BCRP down-regulation in placental cells during hypoxia. We anticipated the up-regulation of miR-328, -519c, and -520h, which could lead to BCRP mRNA; however, the opposite was

observed suggesting that altered miRNA regulation was an unlikely mechanism in the current study.

Transcription factors directly regulate BCRP expression through activation of response elements in the promoter of the *ABCG2* gene. These factors include NRF2 (Hagiya et al. 2008; Singh et al. 2010), AHR (Ebert et al. 2005; Tompkins et al. 2010), PPARγ (Hoque et al. 2015a; Szatmari et al. 2006), ERα (Ee et al. 2004b; Wang et al. 2006b), as well as RXRα, a common nuclear receptor partner for activated transcription factors. Interestingly, the mRNA expression of these transcription factors, with the exception of ERα, decreased in response to 3% O_2 and provide candidate regulators that may underlie the down-regulation of BCRP during hypoxia. Prior work by Wang et al. has demonstrated that mRNA levels of Bcrp in mouse placentas correlate with a number of transcription factors including HIF-1α, AhR and ERβ (Wang et al. 2006a). While these data infer a relationship, the ability of some transcription factors such as HIF-1α to regulate expression of a transgene is dependent upon activation of the signaling pathway rather than the relative abundance of mRNAs. Notably, when trophoectoderm cells were exposed to low oxygen conditions, HIF-1α protein was increased but no change in mRNA expression was observed suggesting little dependence upon transcriptional regulation (Jeong et al. 2016). Like Wang et al., we have observed a coordinated regulation of AHR and BCRP mRNAs. Both genes declined in response to hypoxia in BeWo cells as well as explants obtained from third trimester healthy placentas (data not shown). It is important to note that while Wang et al. observed a correlation between AhR and Bcrp mRNAs in mice, prior work has shown that pharmacological activation of AhR does not alter *Abcg2* transcription in mice (including placenta) whereas the human AHR receptor can transactivate the *ABCG2* gene and increase expression (Tan et al. 2010). Supporting AHR as a mediator of BCRP down-regulation, it is known that hypoxia reduces the transcriptional activity of AHR (Khan et al. 2007; Vorrink et al. 2014) in part due to competition for the common

heterodimer partner, aryl hydrocarbon receptor nuclear translocator (Vorrink et al. 2014). Therefore, dysregulation of placental AHR signaling by HIF-1α activation is a likely mechanism for the decline in BCRP expression and function in BeWo cells.

A number of gestational disorders that are complicated by low oxygen tension result in reduced placental BCRP expression. For example, BCRP expression was reduced in placentas from preeclamptic pregnancies that were accompanied by HELLP syndrome (Jebbink et al. 2015a). This finding corresponded with a significant decrease in birth weight (~25%) in infants born to mothers with preeclampsia and HELLP. Likewise, levels of BCRP mRNA were reduced ~40% in placentas from pregnancies affected by fetal growth restriction in the absence of preeclampsia compared to placentas from gestational age matched controls (Evseenko et al. 2007a). The authors postulated that reduced BCRP expression in fetal growth restriction may sensitize the placenta to increased apoptosis due to altered responses to cytokines. The general association between reduced birth weight and lower BCRP expression was also observed in the current study investigating healthy placentas from high altitude that experience preplacental hypoxia in the *absence* of pathological disease. Taken together, these findings suggest that activation of human HIF-1α signaling reduces placental BCRP expression *in vitro* and *in vivo* likely by dysregulating critical transcriptional pathways, such as AHR.

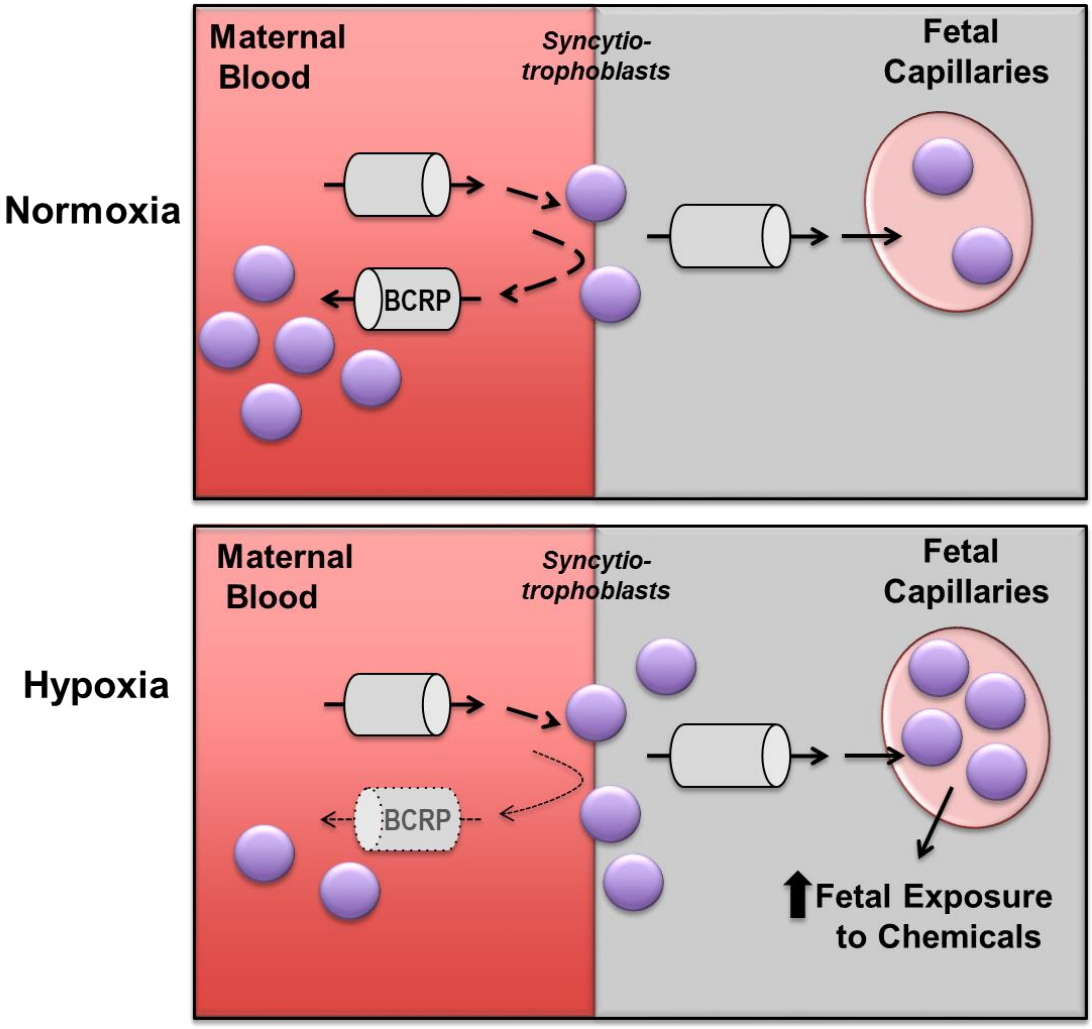

Graphical Abstract

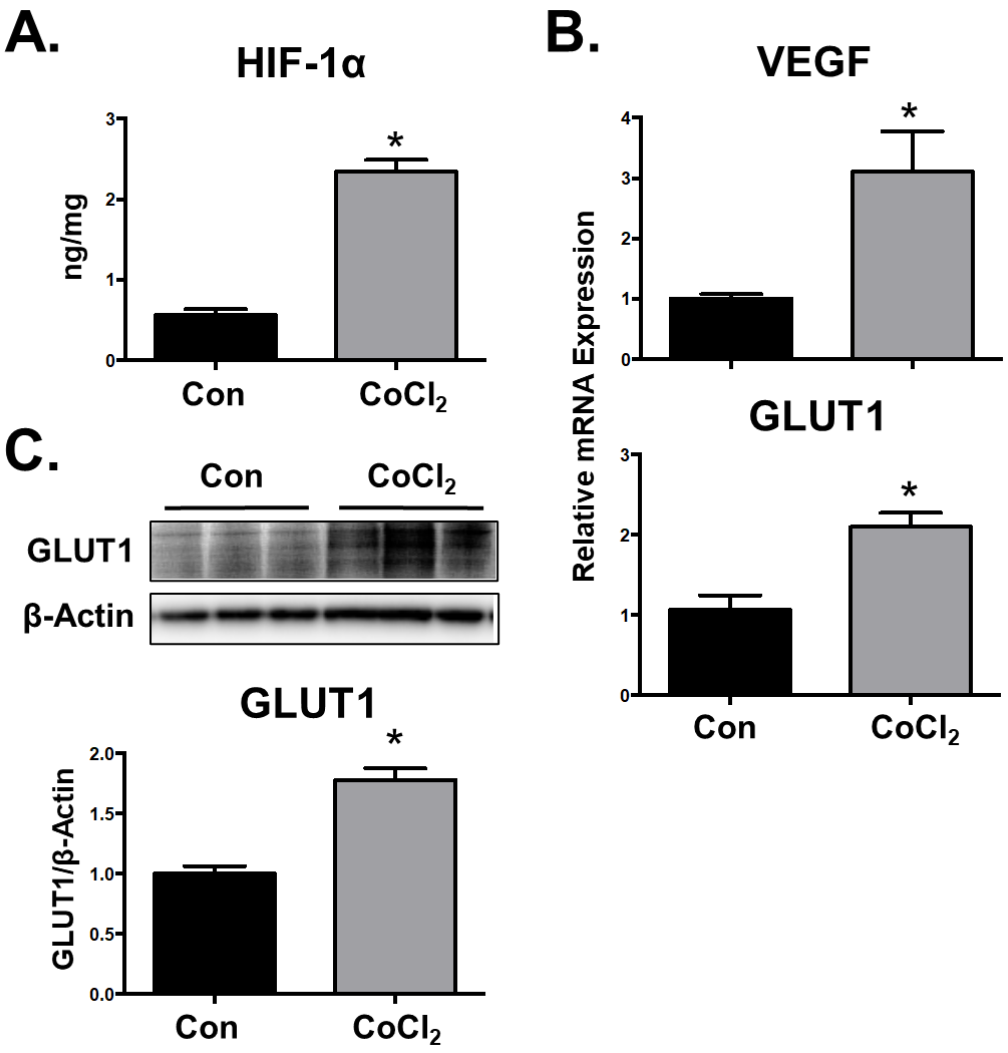

Fig A-5.1. Activation of HIF-1α signaling in BeWo cells by $CoCl_2$. Following treatment of BeWo cells with $CoCl_2$ (200 μM) (A) HIF-1α protein levels were quantified by ELISA at 24 h. (B) HIF-1α target gene (VEGF and GLUT1) expression was assessed at 48 h by qPCR and normalized to RPL13A. (C) GLUT1 protein expression was determined by western blot and β-ACTIN was used as a loading control. Data are presented as mean ± SE (n=3-4). Asterisks (*) represent statistically significant differences ($p<0.05$) compared to control cells (Con).

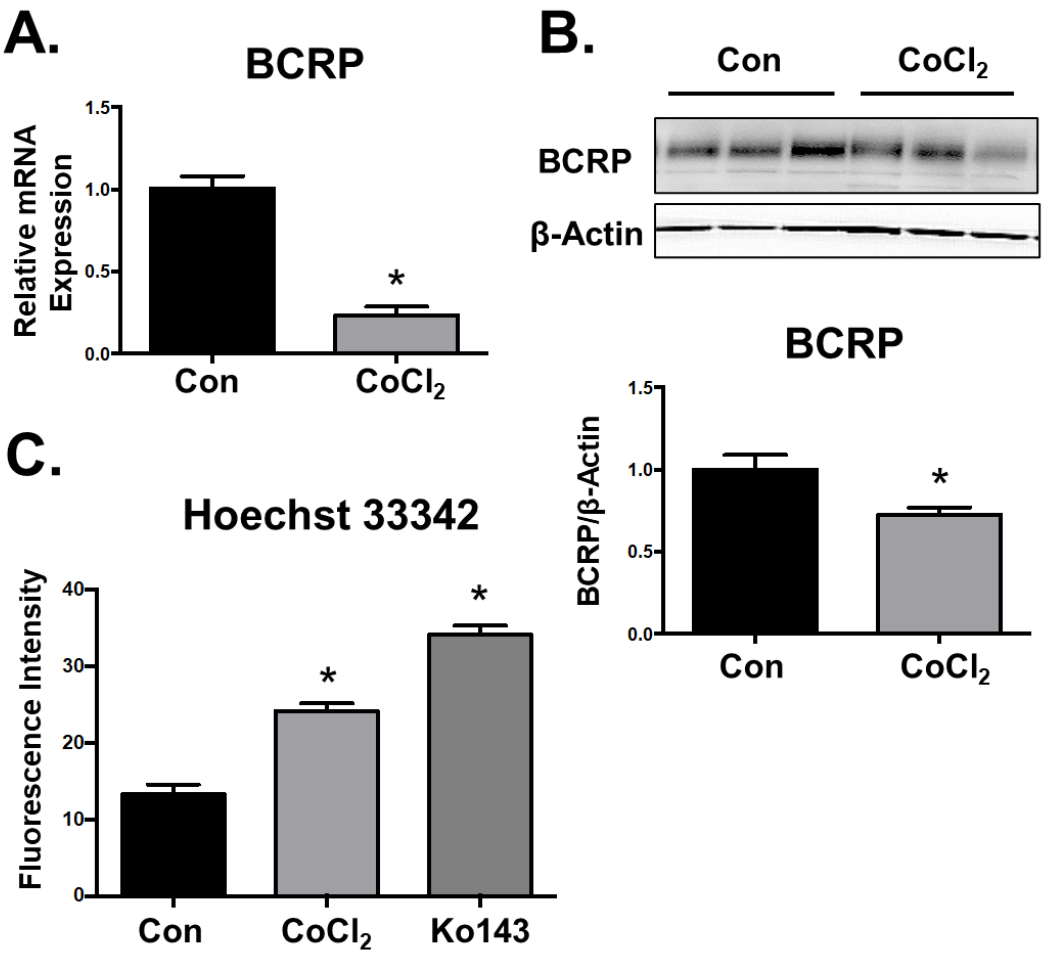

Fig A-5.2. Down-regulation of BCRP in BeWo cells by $CoCl_2$. BeWo cells were treated with $CoCl_2$ (200 µM) for 48 h, following which they were processed for (A) BCRP and RPL13A mRNA expression by qPCR. (B) Protein expression of BCRP was determined by western blot and β-ACTIN was used as a loading control. (C) BCRP function was assessed by measuring the cellular retention of Hoechst 33342 (5 µM) in the presence or absence of the BCRP-specific inhibitor (1 µM Ko143). Intracellular fluorescence was quantified by a Cellometer Vision automated cell counter. Data are presented as mean ± SE (n=3-4). Asterisks (*) represent statistically significant differences ($p< 0.05$) compared to control cells (Con).

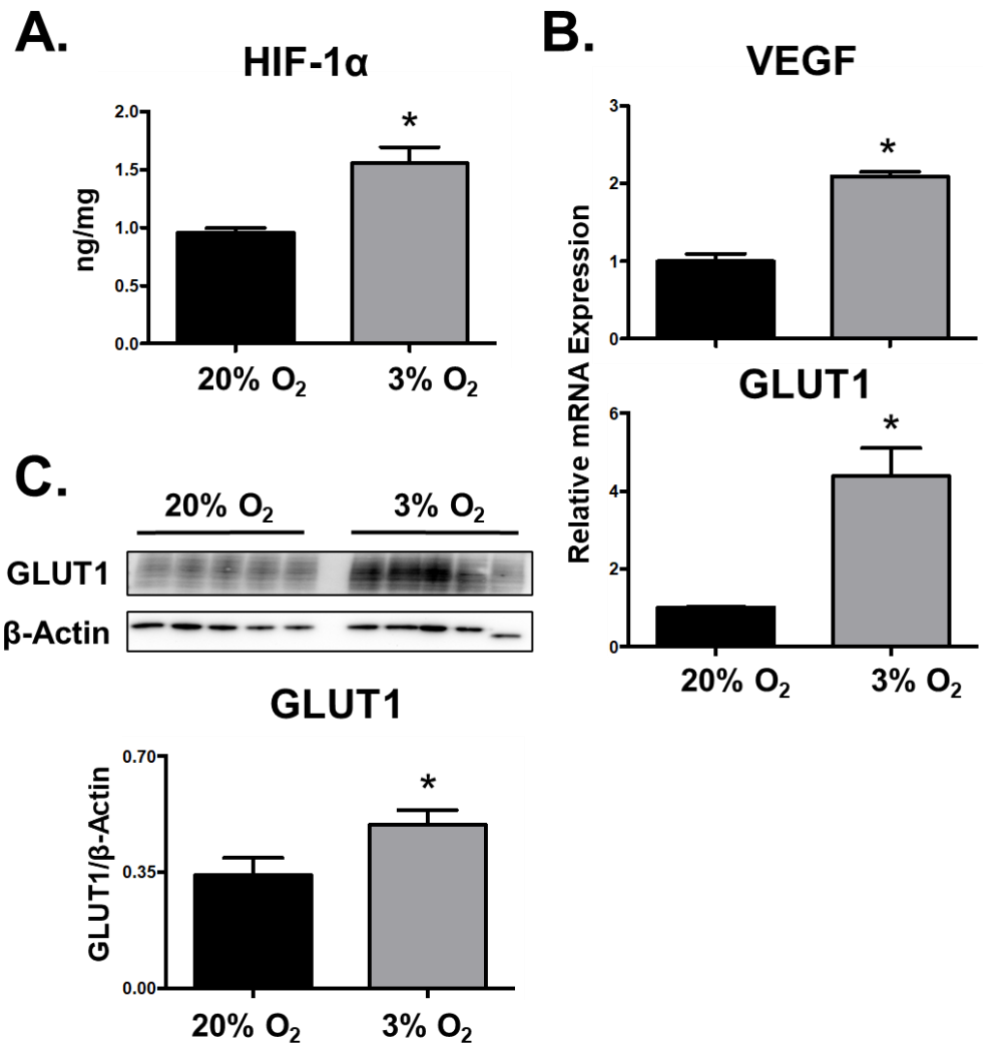

Fig A-5.3. Activation of HIF-1α signaling in BeWo cells by hypoxia. Following 24 h exposure of BeWo cells to hypoxia (3% O_2), (A) HIF-1α protein levels were quantified by ELISA. (B) HIF-1α target gene (VEGF and GLUT1) expression was assessed by qPCR and normalized to RPL13A. (C) GLUT1 protein expression was determined by western blot and β-ACTIN was used as a loading control. Data are presented as mean ± SE (n=3-4). Asterisks (*) represent statistically significant differences ($p<0.05$) compared to 20% O_2 cells.

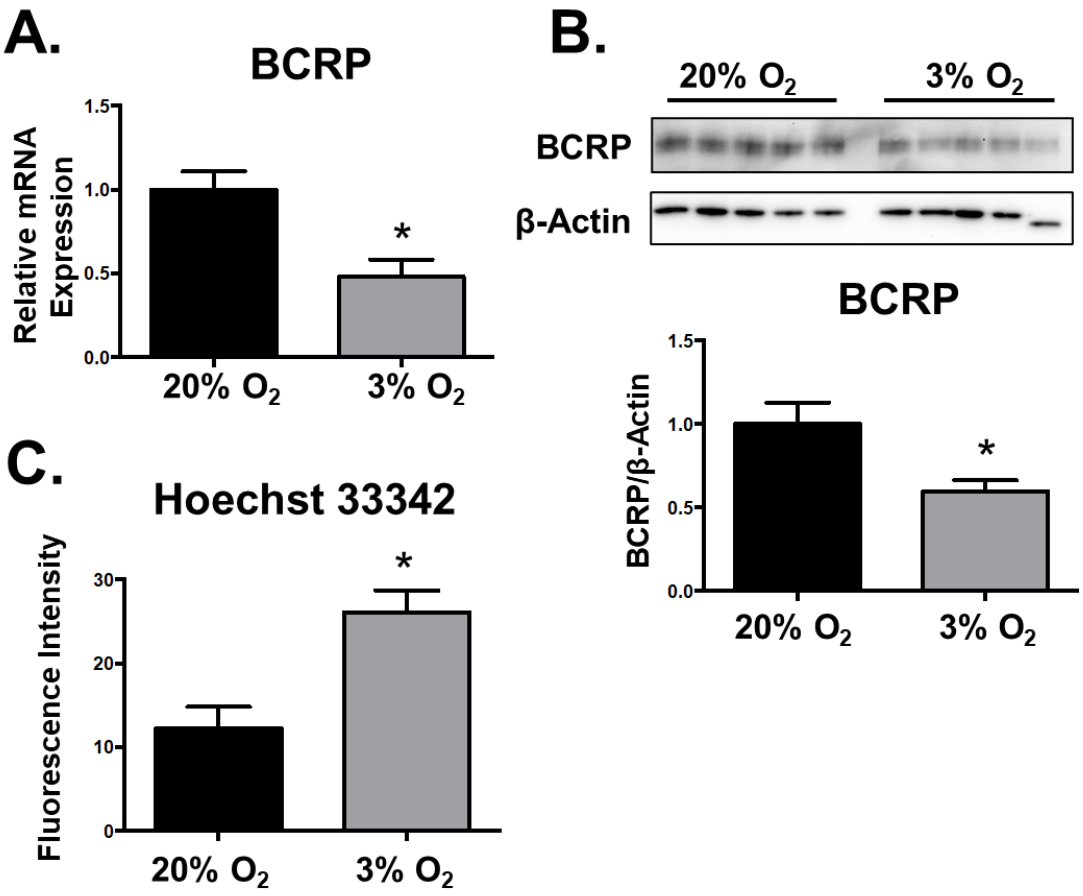

Fig A-5.4. Down-regulation of BCRP in BeWo cells by hypoxia. BeWo cells were exposed to hypoxia (3% O_2) for 24 h, following which the cells were processed for (A) BCRP and RPL13A mRNA expression by qPCR. (B) Protein expression of BCRP was determined by western blot and β-ACTIN was used as a loading control. (C) BCRP function was assessed by measuring the cellular retention of Hoechst 33342 (5 μM). Intracellular fluorescence was quantified by a Cellometer Vision automated cell counter. Data are presented as mean ± SE (n=3-4). Asterisks (*) represent statistically significant differences ($p< 0.05$) compared to 20% O_2 cells.

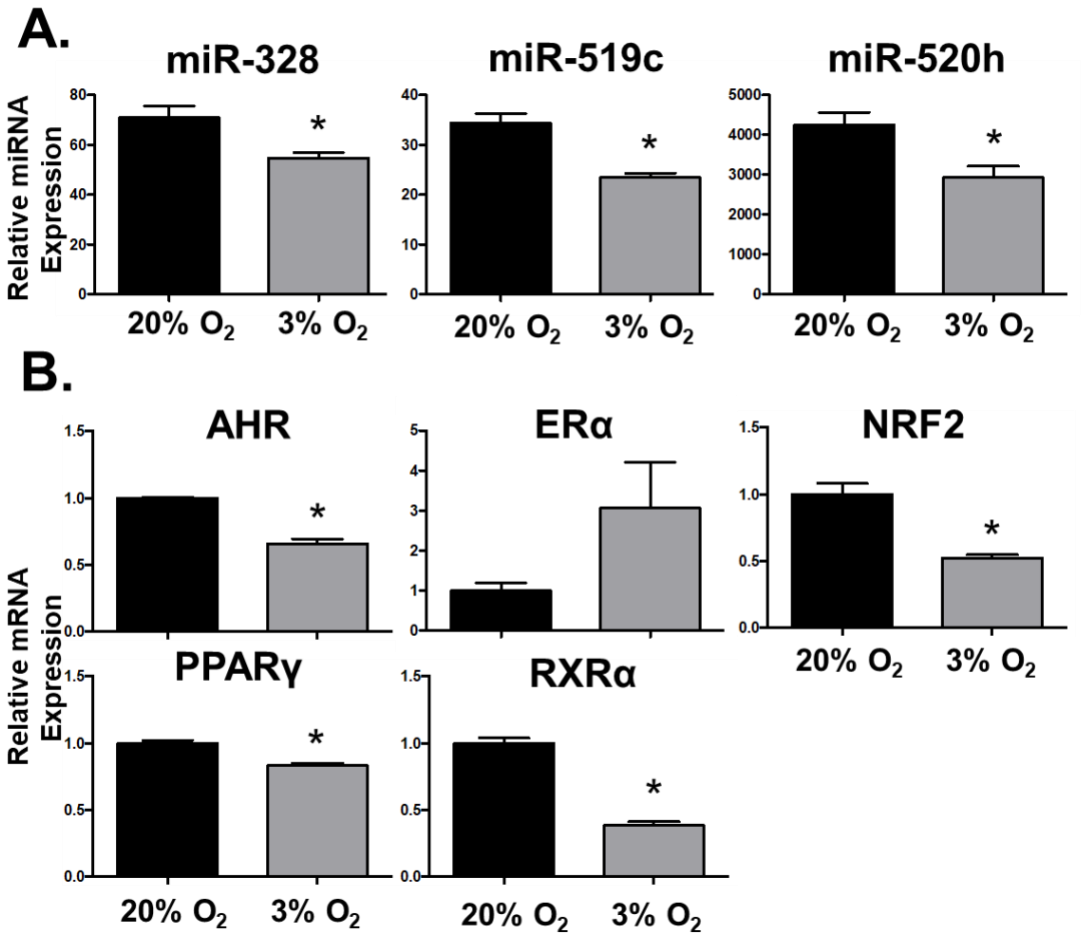

Fig A-5.5. Effect of hypoxia on BCRP-related miRNA and transcription factor mRNA expression in BeWo cells. Following 24 h exposure of BeWo cells to hypoxia (3% O_2), (A) BCRP-targeted miRNA (miR-328, -519c, and -520) expression and (B) mRNA expression of transcription factors (AhR, ERα, NRF2, PPARγ, RXRα) was determined by qPCR. miRNAs were normalized to U6 and mRNAs were normalized to RPL13A. Data are presented as mean ± SE (n=3-5). Asterisks (*) represent statistically significant differences ($p < 0.05$) compared to 20% O_2 cells.

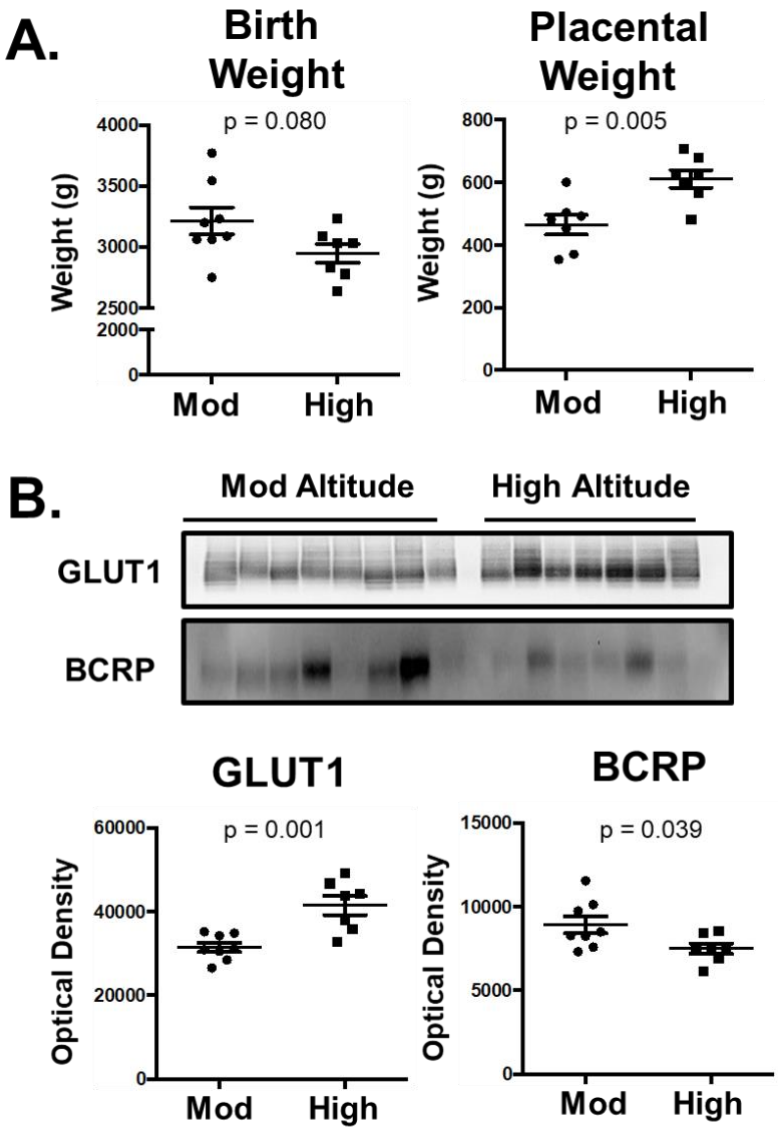

Fig A-5.6. **Regulation of BCRP and GLUT1 expression in high altitude placentas**. In microvillous membranes isolated from placentas from women living at a moderate (Mod, 1600 m) or high altitude (3100 m), GLUT1 and BCRP protein expression was determined by western blot. Equal protein loading was confirmed after staining western blots with Coomassie blue dye. Data are presented as mean ± SE (n=7-9) Asterisks (*) represent statistically significant differences ($p < 0.05$) compared to moderate altitude samples (Mod).

Supplemental Figure A-5.1. Primer sequences use for qPCR (5' to 3').

Gene	Forward Primer Sequence	Reverse Primer Sequence
AHR	CATACCGAAGACCGAGCTGA	TCATTGCCAGAAAACCAGATGA
BCRP	ATCAGCTGGTTATCACTGTGAGGCC	AGTGGCTTATCCTGCTTGGAAGGC
ERα	AAAGGTGGGATACGAAAAGACC	CCAACAAGGCACTGACCATC
GLUT1	CCCTACGTCTTCATCATCTTC	GACTCACACTTGGGAATCAG
miR-328	ATATCTGGCCCTCTCTGCCC	GTGCAGGGTCCGAGGT
miR-519c	GGCGGGAAAGTGCATCTTTTT	GTGCAGGGTCCGAGGT
miR-520h	GGCGACAAAGTGCTTCCCTT	GTGCAGGGTCCGAGGT
NRF2	TCCCAGCAGGACATGGATTT	TCTTCATCTAGTTGTAACTGAGCG
PPARγ	GTCGTGTCTGTGGAGATAAA	ACCTGATGGCATTATGAGAC
RPL13A	GGTGCAGGTCCTGGTGCTTGA	GGCCTCGGGAAGGGTTGGTG
RXRα	CTTGGGAACTTTGTCGTTTC	CCAACAGCACTGTACAACTA
U6	CTCGCTTCGGCAGCACA	AACGCTTCACGAATTTGCGT
VEGF	CAGAATCATCACGAAGTGGT	GGTTTGATCCGCATAATCTG

APPENDIX 6: DYSREGULATION OF BILE ACID AND LIPID HOMEOSTASIS IN PARENTERAL NUTRITION MOUSE MODEL

Authors and Affiliations:

Le Zhan[1] (zhanle999@gmail.com)

Ill Yang[2] (hillyang@eohsi.rutgers.edu)

Bo Kong[1] (kong@eohsi.rutgers.edu)

Jianliang Shen[1] (jianliangs@gmail.com)

Ludwik Gorczyca [1] (ljgorczyca@gmail.com)

Naureen Memon[3] (memonna@rwjms.rutgers.edu)

Brian T. Buckley[2] (bbuckley@eohsi.rutgers.edu)

Grace L. Guo[1] (guo@eohsi.rutgers.edu)

1. Department of Pharmacology and Toxicology, School of Pharmacy, Rutgers University, Piscataway, NJ, USA, 08854

2. EOHSI/ Chemical Analytical Core Laboratory, Rutgers University, Piscataway, NJ, USA, 08854

3. Department of Pediatrics, Rutgers Robert Wood Johnson Medical School, New Brunswick, NJ, USA, 08901

A-6.1 Abstract

Long-term parenteral nutrition (PN) administration can lead to PN associated liver diseases (PNALD). While multiple risk factors have been identified for PNALD, to date, the roles of bile acids (BAs) and the pathways involved in BA homeostasis in the development and progression of PNALD are still unclear. We have established a mouse PN model with IV infusion of PN solution containing soybean oil based lipid emulsion (SOLE). Our results showed that PN altered the expression of genes involved in a variety of liver functions at the mRNA levels. PN increased liver gene expression of *Cyp7a1* and markedly decreased that of *Cyp8b1, Cyp7b1, Bsep, and Shp.* CYP7A1 and CYP8B1 are important for synthesizing the total amount of BAs and regulating the hydrophobicity of BAs, respectively. Consistently, both the levels and the percentages of primary BAs as well as total non-12α-OH BAs increased significantly in the serum of PN mice when compared to saline controls, while liver BA profiles were largely similar. The expression of several key genes involved in lipid synthesis was also increased in PN mouse livers. RORα has been shown to induce the expression of *Cyp8b1* and *Cyp7b1*, as well as to suppress LXRα function. Our results showed significantly reduced nuclear migration of RORα protein in PN mouse livers. **CONCLUSIONS:** This study shows that continuous PN infusion with SOLE in mice leads to dysregulation of BA and lipid homeostasis. Alterations of liver RORα signaling in PN mice may be one of the mechanisms implicated in the pathogenesis of PNALD.

Keywords: parenteral nutrition, liver, bile acid, *Cyp7a1*, *Cyp8b1*, RORα

A-6.2 Introduction

Long-term PN infusion has been shown to be associated with a spectrum of hepatobiliary disorders, including cholestasis, steatosis, fibrosis, and end stage liver complication, cirrhosis, collectively known as PNALD (Kumpf 2006). Among these disorders, steatosis, cholestasis, and cholelithiasis (i.e. gallbladder sludge/stones) are most common (Kumpf 2006). PN associated steatosis occurs mostly in adults and is generally benign (Kumpf 2006). PN associated cholestasis (PNAC) occurs predominantly in term and preterm infants (Peyret et al. 2011). Given the immature livers and intestines, infants with PNALD can rapidly develop devastating liver diseases if they are not able to be weaned off of PN in a timely fashion. There are no effective preventative or therapeutic approaches to PNALD other than discontinuation of PN and advancement to full enteral food intake, which is challenging and often impossible in patients dependent on PN because of their poor intestinal function (Ziegler et al. 2006).

PNALD is multifactorial in etiology, with many associated risk factors including lack of enteral feeding (i.e. nutrition obtained by mouth), inflammation, infection, micronutrient deficiencies, contaminants in PN products, and the composition and/or source of macronutrients such as intravenous fat emulsions (Waitzberg et al. 2006). A significant amount of research has been conducted on SOLE. The presence of plant phytosterols, large amounts of pro-inflammatory ω-6 polyunsaturated fatty acids (PUFAs), and the lack of anti-inflammatory ω-3 PUFAs in SOLE have all been implicated in the pathogenesis of PNALD (Vlaardingerbroek et al. 2014). In recent years, newer generations of lipid emulsion, including the fish oil based lipid emulsion (FOLE), which mainly contains ω-3 PUFAs, and SMOFlipid [a mixture of soybean oil, medium chain triglycerides (MCTs), olive oil, and fish oil] have been shown to be beneficial to improve or even reverse the PNALD in both pediatric and adult patients (Waitzberg et al. 2006).

Intra- or extra-hepatic bile acid (BA) accumulation in the liver leads to cholestatic liver disorders. The farnesoid X receptor (FXR) is the BA sensor, playing an essential role in maintaining enterohepatic BA homeostasis (Zhu et al. 2011). To date, changes in liver and intestine FXR function as well as BA signaling pathways within PNALD are still not fully understood. It has been shown that toll like receptor 4 (TLR4) signaling mediated immune responses were critically involved in PN induced liver injury when PN mice were pretreated with dextran sulphate sodium (DSS) (El Kasmi et al. 2012). DSS is a toxic chemical agent which could induce intestinal damage to mimic human clinical conditions. The same group also showed that plant sterols contained in SOLE, particularly stigmasterols, were associated with cholestatic liver injury by inhibiting FXR function in PN mouse livers (El Kasmi et al. 2013). However, studies from PN piglet models do not support the idea that phytosterols are associated with suppression of hepatic FXR function and pathogenesis of PNALD (Vlaardingerbroek et al. 2014). Therefore, a comprehensive understanding of the BA homeostasis and FXR function under PN is urgently needed.

To test our hypothesis that PN infusion will disrupt BA homeostasis, especially entero-hepatic circulation of BAs, we have established a valid mouse PN model. We characterized the expression profiles for liver genes critically involved in BA homeostasis, as well as the serum and liver BA profiles for the PN mice. The results of this study will aid in determining contributing factors involved in the development and management of PNALD in the future.

A-6.3 Materials and Methods

Animals and Surgery

All animal protocols and procedures were approved by the Institutional Animal Care and Use Committee (IACUC) of the Rutgers University. Unless otherwise specified, all mice used for the PN study were maintained in the pathogen-free animal facilities in the Comparative Medicine Resources at the Nelson Animal Facility at Rutgers University, under a standard 12-hr light/dark cycle (6 AM/6 PM) with temperature-, humidity-controlled conditions. Mice were fed at *ad libitum* with standard mouse chow and autoclaved tap water before initiation of PN infusion. Wild-type (WT) C57BL/6J mice were obtained from the Jackson Laboratory (Bar Harbor, ME). Male mice, between 8 to 20 weeks of age were used for the study.

For jugular vein catheterization, mice were anesthetized via i.p. injection with 80mg/kg ketamine and 10 mg/kg xylazine, followed by placement of a central venous catheter (polyurethane tubing, 1F in O.D.,) (SAI Infusion Technologies, IL) into the right jugular vein. Minimal amount of blood was carefully withdrawn to verify the catheter patency. Afterwards, the saline solution in the catheter was replaced by heparin/glycerol catheter lock solution (SAI Infusion Technologies, IL). The proximal end of the catheter was then tunneled subcutaneously, exited between the shoulder blades and properly secured. On the next day, fully recovered surgical mouse was placed in a plastic harness (SAI Infusion Technologies, IL) and the catheter was connected to an infusion pump (Harvard Apparatus, MA) through the extension lines (SAI Infusion Technologies, IL). Catheterized mice were then kept on intravenous infusion of normal saline (NS, 0.9%) at an initial rate of 6ml/d and had free access to food and water. The next day, mice in the PN group (here after referred to as PN mice) started to receive intravenous PN infusion prepared by CAPS, Inc. (Englewood, NJ), and still had free access to water but not food. Saline control mice (hereafter referred to as saline mice) continued to receive saline infusion and have free access to food and

water. One day after, the infusion rates for both saline and PN mice were increased to 8ml/d, and kept as 8ml/d throughout the study period with the PN solution providing an adequate caloric intake of 10.62 kcal/d (Table A-6.1). This regimen was based on the report that graded infusion period is necessary for the mice to adapt to the continuous infusion of fluid and nutrients (Omata et al. 2013a). All saline and PN mice were housed individually in metabolic cages to prevent PN mice from coprophagia. Since metabolic cages were maintained in non-sterile environment, all surgical mice were allowed at least one week to acclimatize. After 8 days of PN infusion, mice were sacrificed and tissues were harvested for analysis.

Serum Biochemical Analysis

Commercially available testing kits were used to measure serum levels of biomarkers, including alanine transaminase (ALT), aspartate transaminase (AST), alkaline phosphatase (ALP) (Pointe Scientific, MI), and total serum bile acids (TSBA) (Diazyme Laboratories, CA). Procedures were scaled up or down based on the manufacturer's instructions.

RNA Isolation, RT-qPCR and Microarray Analysis

Total RNA was isolated using TRI reagent (Sigma, St. Louis, MO) according to the manufacturer's instructions. Liver gene expression at mRNA level was analyzed by Reverse Transcriptase (RT) quantitative PCR (RT-qPCR). After rigorous analysis of gene expression in saline and PN mice, RNA samples (n=3) obtained from the livers from saline and PN mice were pooled, respectively, for microarray analysis (Microarray-PN/Saline). Liver mRNA microarray analysis was determined using Mouse Gene 2.0 ST Array system manufactured by Affymetrix, Inc (Santa Clara, CA). Microarray data were analyzed using the Affymetrix Power Tools (http://www.affymetrix.com). Data retrieved from the microarray analysis were further validated by RT-qPCR analysis. All the primer sequences for RT-qPCR were listed in Table A-6.2. The raw

and processed data files for microarray analysis have been deposited in NCBI's Gene Expression Omnibus (Edgar et al. 2002), and are accessible through GEO Series accession number GSE71286 (http://www.ncbi.nlm.nih.gov/geo/query/acc.cgi?token=ylmficimlhexpcj&acc=GSE71286).

Organic Extraction and Ultra Performance Liquid Chromatography/Mass Spectrometry (UPLC/MS) Profiling of Serum and Liver BAs

Serum and liver total BAs were extracted as previously described (Zhang et al. 2010). Final BA extracts were introduced to the Thermo Finnigan Ultra Performance Liquid Chromatography (UPLC) system (Thermo Fisher Scientific, Waltham, MA) coupled with a Thermo Finnigan LTQ XL Ion Trap Mass Spectrometer (Thermo Fisher Scientific, Waltham, MA). An Electrospray (ESI)/ITMS was operated in multiple MS/MS and SRM (Selective Reaction Monitoring) modes for simultaneous determination of 23 BAs including: cholic acid (CA), chenodeoxycholic acid (CDCA), deoxycholic acid (DCA), lithocholic acid (LCA), ursodeoxycholic acid (UDCA), taurocholic acid (TCA), taurochenodeoxycholic acid (TCDCA), taurodeoxycholic acid (TDCA), taurolithocholic acid (TLCA), tauroursodeoxycholic acid (TUDCA), glycocholic acid (GCA), glycochenodeoxycholic acid (GCDCA), glycodeoxycholic acid (GDCA), glycolithocholic acid (GLCA), β-muricholic acid (β-MCA), α-muricholic acid (α-MCA), ω-muricholic acid (ω-MCA), tauro-β-muricholic acid (T-β-MCA), tauro-α-muricholic acid (T-α-MCA), tauro-ω-muricholic acid (T-ω-MCA), hyodeoxycholic acid (HDCA), taurohyodeoxycholic acid (THDCA), and glycohyodeoxycholic acid (GHDCA).

For BA standards, CA, GCA, TCA, DCA, GDCA, TDCA, CDCA, GCDCA, TCDCA, LCA, TLCA, UDCA, and TUDCA were purchased from Sigma-Aldrich (St. Louis, MO); GLCA, β-MCA, α-MCA, ω-MCA, T-β-MCA, T-α-MCA, T-ω-MCA, HDCA, THDCA, and GHDCA were purchased from Steraloids, Inc. (Newport, RI). For internal standards, chenodeoxycholic-2,2,4,4-

$d_4$acid ($^2H_4$-CDCA) and glycochenodeoxycholic-2,2,4,4-d_4 acid ($^2H_4$-GCDCA) were purchased from C/D/N Isotopes, Inc. (Pointe-Claire, Quebec, Canada).

Western blot

Nuclear, cytoplasmic and total protein extraction and western blot analysis were performed as previously described (Maran et al. 2009). Antibodies against lamin a/c (Developmental Studies Hybridoma Bank, Iowa City, IA) and β-actin (Santa Cruz Biotechnology, Santa Cruz, CA) were used as the loading controls for nuclear and total proteins, respectively. Antibody for RORα was purchased from BioLegend (San Diego, CA).

Oil Red O Staining

The O.C.T. compound embedded frozen livers were sectioned at 8μM and stained with Oil Red O with a standard protocol (Kong et al. 2009).

Statistical Analysis

Data are presented as mean ± SEM (standard error of the mean). Student's *t*-test was used to compare the data obtained from the saline and PN groups. $P < 0.05$ was considered statistically significant.

A-6.4 Results

PN mice had decreased body and liver weight. Upon infusion system setup, average body weight (BW) for saline and PN mice was 21.28 and 21.22 g, respectively (Table A-6.3). The initial infusion rate for PN mice was set to 7 ml/d, which was adapted from a previous study and provided a calorie intake of 8.4 kcal/d (El Kasmi et al. 2012). After 8 days of PN infusion, mice consistently exhibited an average BW loss of around 20% (data not shown). Therefore, the lipid content in the PN solution was increased from 2g per 100ml to 3g per 100ml. The infusion rate was also increased from 7 ml/d to 8 ml/d for mice with an initial BW around 22 g (Table A-6.3). After receiving the modified PN for 8 days (6 ml/d for day1, 8 ml/d afterwards), average BW change for PN mice was -2.10 g (range 0.06 to -3.44 g, Table A-6.3), whereas the average BW change for saline mice was -0.06 g (range 1.28 to -2.02 g, Table A-6.3). PN mice had around 10% BW loss (Table A-6.3). This trend of BW change is similar to the trend reported previously (El Kasmi et al. 2012). In addition to BW loss, final liver weight (LW) and the ratio of LW to BW also decreased in PN mice (Table A-6.3). Upon animal sac, the gallbladders of PN mice were substantially smaller than those found in saline mice (data not shown).

PN mice had altered serum biochemical parameters. Serum levels of ALT were similar between saline and PN mice (Figure A-6.1A). However, PN mice had significantly increased serum levels of AST (Figure A-6.1B) and TSBA (Figure A-6.1D), and significantly decreased serum levels of ALP (Figure A-6.1C), when compared to saline controls. Decreased ALP levels and empty gallbladders observed in PN mice indicate that PN infusion was associated with diminished bile flow from the hepatocytes into the biliary tract. This suggests that PN mice may have an increased risk of developing intra-hepatic cholestatic complications after long-term PN infusion, especially

when other risk factors, such as intestinal inflammation coupled with LPS infiltration, are presented.

PN altered gene expression for BA homeostasis and lipid metabolism. Substantial changes in the expression of genes involved in BA homeostasis and lipid metabolism were detected in the livers of PN mice. Relative mRNA levels of *Cyp7a1*, which encodes the rate-limiting enzyme in BA synthesis, showed significant increase in the livers of PN mice compared to saline mice (around 3 fold, $P < 0.005$) (Figure A-6.2A). Relative mRNA levels of *Cyp27a1*, *Fxr*, bile salt export pump (*Bsep*) and small heterodimer partner (*Shp*) decreased significantly in PN mice ($P < 0.05$, 0.05, 0.0005, 0.05, respectively) (Figure A-6.2A). Relative mRNA levels of *Cyp7b1* and multidrug related protein 3 (*Mrp3*) decreased more than 70% ($P < 0.005$ for both), whereas relative mRNA levels of *Cyp8b1* decreased more than 90% ($P < 0.005$) (Figure A-6.2A). CYP8B1 is critical in determining BA hydrophobicity as it functions to generate CA, a more water-soluble BA. Relative mRNA levels of genes involved in cholesterol and lipid metabolism were also quantified (Figure A-6.2B). Relative mRNA levels of *Cd36*, which encodes a long-chain fatty acid uptake transporter, decreased 50% ($P < 0.05$), whereas relative mRNA levels of fatty acid synthase (*Fas*), lipoprotein lipase (*Lpl*) and sterol regulatory element-binding protein-1c (*Srebp-1c*) increased significantly in the livers of PN mice ($P < 0.005$, 0.05, 0.005, respectively) (Figure A-6.2B).

In the distal ileum, while the relative mRNA levels of *Fxr*, ileum bile acid binding protein (*Ibabp*), and organic solute transporter beta (*Ost-β*) were similar between saline and PN mice, the relative mRNA levels of fibroblast growth factor 15 (*Fgf15*) increased in 4 out of 7 of the PN mice (Figure A-6.2C, $P > 0.05$). Nevertheless, no correlation between the mRNA levels of ileal *Fgf15* and liver *Cyp7a1* was found when the data from individual mice was examined.

PN altered serum BA profiles, but not liver BA profiles. Among all the 23 BAs tested, serum and liver concentrations of GDCA, LCA, and GUDCA in both saline and PN samples were below the UPLC-MS detection limits. The analyzed serum concentration for each of the other 20 BAs in the saline (n=5) and PN mice (n=6) was plotted in Figure A-6.3. For most BAs, levels of glycol-conjugates were the lowest, whereas tauro-conjugates were much higher when compared to the unconjugated forms. Calculated total serum concentrations of the 20 BAs increased 5 fold in PN mice compared to saline mice (mean ± SEM, ng/ml: saline mice, 1601.2 ± 417.9; PN mice, 8112.4 ± 605). Compared to saline mice, serum levels of TCDCA, β-MCA, T-β-MCA, T-α-MCA, ω-MCA, T-ω-MCA, TLCA, TUDCA increased significantly in PN mice ($P < 0.05$), whereas serum levels of GLCA in PN mice decreased dramatically below the detection limit (Figure A-6.3). Among these, levels of TCDCA, T-β-MCA, T-α-MCA, TLCA increased more than 10 fold in PN mice. Levels of CDCA increased 3 fold in PN mice, though without significance (P=0.09). Levels of TCA, GCA, α-MCA, and THDCA also increased dramatically ($P < 0.07$) in PN mice (Figure A-6.3). The total serum concentration and percentage of each BA species (unconjugated BA and its conjugates), total primary BAs and total secondary BAs, as well as total 12α-OH BAs (CA, DCA and their conjugates) and total non-12α-OH BAs (CDCA, MCA, LCA, HDCA, UDCA and their conjugates) in the total BA pool were summarized in Table A-6.4. The percentage of total CDCA increased more than 3 fold, and the percentage of total α/β-MCA increased almost 1 fold in PN mice. The percentage of total primary and secondary BAs was similar in saline mice (mean: 56.93% versus 43.07%), whereas in PN mice, the percentage of total primary BAs was 3.1 fold when compared to the secondary BAs (mean: 75.75% versus 24.25%). In addition, the percentage of total 12α-OH BAs and non-12α-OH BAs was also similar in saline mice (mean: 44.45% versus 55.55%), whereas the percentage of total non-12α-OH BAs was 2.8 fold of that of total 12α-OH BAs in PN mice (mean: 73.73% versus 26.27%).

In contrast, levels of total BAs and individual BAs were overall similar in the livers of PN and saline mice. Levels of TCDCA, T-β-MCA, T-α-MCA and TUDCA increased significantly in the livers of PN mice, while the fold changes were substantially smaller when compared to the changes detected in serum samples (Figure A-6.4). Nevertheless, compared to unconjugated BAs, these tauro-conjugated BAs are not toxic to the liver (Li et al. 2014). Consistent with these relatively normal liver BA profiles, H&E staining showed relatively normal liver histology of PN mice (data not shown), despite altered gene expression and slightly altered liver biochemistry parameters.

PN altered the expression of genes in many biological pathways. To determine the changes of gene expression in pathways altered by PN, other than the previously mentioned BA and lipid pathways, a microarray was performed. Genes with fold change ≥ 4 (up-regulated) or ≤ -4 (down-regulated) obtained from the microarray analysis, with their full names and the corresponding fold changes, are presented in Table A-6.5. RT-qPCR was performed to validate the microarray results (Figure A-6.5). Both up-regulated and down-regulated genes were tested. Among these, the relative mRNA levels of ATP-binding cassette, sub-family d (ALD), member 2 (*Abcd2*), *Nocturnin* and macrophage receptor with collagenous structure (*Marco*) increased significantly in PN mice compared to saline controls (2.2, 5, and 6.8 fold, $P < 0.0005$, 0.05, 0.05, for *Abcd2*, *Nocturnin*, and *Marco*, respectively). Relative mRNA levels of *Cyb2b10* decreased more than 20 fold in PN mice ($P < 0.005$). However, for the other genes tested, the means of fold changes were less than 2, and without significance (Figure A-6.5).

Kyoto Encyclopedia of Genes and Genomes (KEGG) pathway analysis was used to further categorize the altered genes found in the microarray analysis (Table A-6.6**)**. Many genes, which are related to immune and inflammatory responses, were up-regulated, including genes involved in cytokine-cytokine receptor interaction (19 out of 28), Janus kinase-signal transducer and activator of transcription (JAK-STAT) signaling pathway (12 out of 15), and natural killer cell mediated

cytotoxicity (11 out of 15). Most genes in the category of fat digestion and absorption as well as biosynthesis of unsaturated fatty acids (FAs) were up-regulated (10 out of 11). On the contrary, majority of the genes involved in metabolism of endobiotics and xenobiotics were down-regulated (13 out of 19 in drug metabolism - cytochrome P450, 10 out of 14 in retinol metabolism, 8 out of 12 in arachidonic acid metabolism, all the 8 in glutathione metabolism, and all the 6 in fatty acid metabolism).

PN altered liver RORα signaling. Previous studies have shown that retinoid acid-related orphan receptor alpha (RORα) plays a key role in regulating the gene expression of *Cyp8b1* and *Cyp7b1* in mouse liver (Kang et al. 2007; Pathak et al. 2013; Wada et al. 2008). A detailed comparison of our microarray data (Microarray-PN/Saline) with previously published microarray data, obtained from RORα and retinoic acid-related orphan receptor gamma (RORγ) double KO (DKO) mice (Microarray-DKO/WT) (Kang et al. 2007), revealed similar trends of alterations for a number of genes in the two datasets. A few genes with different trends were also identified (Table A-6.7). As shown in Table A-6.7, the mRNA expression of RORα also slightly decreased in the livers of PN mice. As a nuclear receptor, RORα protein level, especially nuclear localization of RORα, is more important in determining its physiological function. Western blot analysis showed that nuclear levels of RORα protein decreased significantly in the livers of PN mice, while total RORα protein levels actually increased (Figure A-6.6).

PN mice had increased hepatic lipid accumulation. Consistent with increased mRNA expression of lipid synthesis genes (Figure A-6.2), Oil Red O staining showed that PN mouse livers had significantly increased levels of lipid staining (Figure A-6.7), but not reaching the levels of steatosis.

A-6.5 Discussion

The PN regimen, based on a previous publication (El Kasmi et al. 2012), was modified to maintain sufficient calorie intake for adult mice in order to prevent excessive BW loss. One interesting change observed in this model was increased extent of liver weight loss in the PN mice. Future studies will be needed to uncover the underlying mechanisms.

Similar to the previous study (El Kasmi et al. 2012), serum ALT levels were not increased in the PN mice, whereas serum AST levels increased significantly in our model, but were still in the normal range. TSBA levels increased significantly in the PN mice. Interestingly, serum ALP levels decreased significantly in the PN mice. It has been shown that FGF15 is essential for gallbladder refill in mice (Inagaki et al. 2005). Without normal food intake, the lack of enteral stimulus in PN mice will lead to impaired BA release into the GI track. This could further impair enterohepatic FGF15 signaling, causing diminished gallbladder refilling from the liver and subsequently less biliary BA exposure, leading to less biliary injury indicated by decreased serum ALP levels. In addition, recent studies also showed that elevated levels of ALP in patients with intestinal failure and PNALD can be caused by metabolic bone diseases (MBD), rather than liver diseases (Nandivada et al. 2014). From the KEGG pathway analysis, we did see that 10 out of 11 genes in the category of osteoclast differentiation were up-regulated in the Microarray-PN/Saline (**Table A-7.6**). These findings from the microarray analysis can potentially provide novel insights into the association of long-term PN induced liver dysfunction to the development of MBD, for which, the underlying mechanisms are still poorly understood (Nandivada et al. 2014).

The lack of enterohepatic FGF15 signaling could also be responsible for the upregulation of *Cyp7a1* gene expression seen in the PN mice. It has been shown that WT mice with bile duct ligation had a 3 fold increase in *Cyp7a1* expression, while the expression of small heterodimer partner (*Shp*) was not changed (Inagaki et al. 2005). The increased mRNA levels of *Cyp7a*1 in PN

mice may lead to the accumulation of cholesterol metabolites in the liver, which could in turn, activate LXRα and induce the expression of LXRα target genes. Indeed, we have observed upregulation of LXRα target genes in PN mouse livers, including *Lpl, Srebp-1c, a*nd *Fas* (Figure A-6.2B**)**. Long-term LXRα activation coupled with upregulation of its target genes could be responsible for PN induced liver steatosis in adults, even though PN mice tend to lose body weight.

Similar to prior findings from PN piglets (Vlaardingerbroek et al. 2014), we also detected decreased gene expression of *Fxr*, *Bsep* and *Mrp3* in the livers of PN mice. A previous report did show reduced expression of *Fxr* and *Bsep* in DSS pretreated PN mice (PN/DSS), however the expression of these genes in PN-only mice was not reported (El Kasmi et al. 2012; El Kasmi et al. 2013). Consistent with the downregulation of *Fxr* and FXR target genes (*Bsep, Cd36*), we also detected a reduced gene expression of *Shp* in the livers of PN mice. Though a previous study has shown that intestinal FXR and FGF15 play a major role in suppressing *Cyp7a1* gene expression (Kong et al. 2012), the downregulation of *Shp* could also contribute to the upregulation of *Cyp7a1*. Interestingly, similar to the findings in PN piglets, ileum *Fgf15* gene expression also increased in the distal ileums of PN mice. Nevertheless, previous report has shown that plasma FGF19 level actually decreased in the PN piglets measured by ELISA (Vlaardingerbroek et al. 2014). Due to the lack of a good ELISA antibody for FGF15 protein, the data for portal FGF15 levels is not provided. Nevertheless, similar trends of decreased gene expression in the adult mice and preterm piglets suggest common underlying mechanisms in different species, which are most likely PN dependent. Future studies will be needed to uncover the underlying mechanisms, especially the downregulation of *Fxr* gene expression and FXR signaling. The increase of *Cyp7a1* and decrease of *Fxr*, *Bsep*, *Shp* and *Mrp3* gene expression, taken together with the lack of hepatic bile flow into the gallbladder, could lead to BA accumulation in hepatocytes, causing the elevation of TSBA in PN mice. BA accumulation in hepatocytes of PN mice could lead to cholestasis after long-term PN, especially with the presence of additional risk factors, such as catheter related infections or

intestinal tract inflammation. These risk factors could magnify liver stress and cause severe liver damage in a relatively short time, as detected in PN/DSS mice (El Kasmi et al. 2012).

Results from serum BA profiling by UPLC-MS were consistent with gene expression results. PN mice exhibited a 3 fold increase of *Cyp7a1* gene expression as well as an increase in serum levels of the total and individual BAs. CYP8B1 determines the ratio of 12α-OH BAs versus non-12α-OH BAs. As expected, the lack of intestinal FXR-FGF15 signaling and the decreased mRNA expression of *Cyp8b1* in PN mice could lead to a dramatic increase of the levels and percentages of serum TCDCA, T-β-MCA, and T-α-MCA in PN mice (Figure A-6.3, Table A-6.4). Although serum levels of CA, TCA, DCA, and TDCA also increased in PN mice, their percentage in the total serum BA pool actually decreased. As a result, the percentage of total non-12α-OH BAs was much higher in PN mice (Table A-6.4). The decrease in the percentage of total secondary BAs in PN mice could also be caused by decreased bile flow from the liver into the intestinal tract, leading to a proportional decrease of secondary BA formation in the gut. While the levels of unconjugated secondary BAs in saline and PN mice were similar (Figure A-6.3), the levels of conjugated secondary BAs were much higher in PN mice, except for GLCA (undetectable). Since fecal excretion is mainly responsible for the direct loss of secondary BAs, the increased levels of conjugated secondary BAs in PN mice could be caused by the decreased fecal loss of BAs (Li et al. 2014). Studies in germ-free mice suggest that T-β-MCA and T-α-MCA are FXR antagonists (Sayin et al. 2013). Indeed, the most significant changes detected in the PN mice were the increased levels of T-β-MCA and T-α-MCA in both mouse serum and liver extracts, which could explain the downregulation of FXR signaling in the PN mice, even without DSS pretreatment. Of note, liver TCDCA also increased significantly, but the concentration was much lower compared to T-β-MCA or T-α-MCA.

RORα has been shown to play critical roles in regulating the expression of many genes involved in phase I and phase II metabolism (Kang et al. 2007). The expression patterns of many

genes involved in cellular metabolism in the liver are also regulated by the fast-feed circadian rhythm (Xu et al. 2012c; Zhang et al. 2011). It has been shown that the expression of RORα exhibited an oscillatory pattern consistent with the liver circadian rhythm (Kang et al. 2007)**.** Under continuous PN infusion, it is very likely that the normal fast-feed circadian rhythm, maintained in saline control mice, is disrupted in PN mice. It has also been shown that glucagon/protein kinase A (PKA) signaling could phosphorylate and stabilize RORα protein upon fasting, to induce *Cyp8b1*gene expression and diurnal rhythm (Pathak et al. 2013). The continuous supply of dextrose in the PN solution could potentially lead to a downregulation of PKA signaling, and therefore cause a suppression of RORα target genes, such as *Cyp7b1* and *Cyp8a1*. Furthermore, many indirect target genes were also altered in the PN mice (Table A-6.7), due to the suppression of RORα by the continuous PN infusion, as exhibited by significantly decreased nuclear protein levels of RORα in PN mouse livers. Previous studies have also shown that RORα and LXRα could mutually suppress the function of each other (Wada et al. 2008). Therefore, the dramatic downregulation of RORα signaling could also lead to the upregulation of LXRα target genes as well as the subsequent lipid accumulation in the livers of PN mice. It has been shown that RORα and RORγ could redundantly regulate the expression of many genes involved in phase I and phase II metabolism (Kang et al. 2007). However, nuclear protein levels of RORγ by western blot didn't show any correlation (data not shown) with the alterations of the gene expression of RORγ targets.

It is also important to note that the expression of several genes listed in Table A-6.7 showed opposite trends of alterations (*Cyp2b10, Cyp4a10, Ccnb1, etc.*). These changes could be mediated by additional transcriptional factors altered by PN infusion. For example, the expression of *Cyp2b10* has been shown to be directly regulated by both CAR and PXR (Park et al. 2012). In this case, the potential alterations of CAR and/or PXR signaling could explain the dramatic decrease of *Cyp2b10* expression in PN mice.

In summary, combining liver gene expression profiling and serum/liver BA profiling, we characterized detailed molecular and cellular alterations in WT PN mice. We showed altered gene expression, altered serum/liver profiles for BA homeostasis, and increased hepatic lipid accumulation in mice after 8 days of PN infusion. We provided mechanistic evidence of altered RORα signaling in PN mice. We further showed additional alterations of gene expression in various functional pathways in the livers of PN mice. These novel results will provide critical insights for future studies of PN induced cholestasis (BA homeostasis), steatosis (LXRα and lipid metabolism), MBDs, etc., when PN infusion is combined with genetic, pharmacological, or toxicological manipulations in mice or other animal models.

Table A-6.1. Components of Parenteral Nutrition per 100 ml

Component	Amount	Unit
Concentrated amino acids *	4	g
Dextrose	25.5	g
Lipid [#]	3	g
Sodium phosphate	1.34	mM
Potassium chloride	1.6	mEq
Sodium chloride	3.2	mEq
Potassium acetate	12	mEq
Magnesium sulphate	0.8	mEq
Calcium gluconate	1.32	mEq
Multitrace®-5 concentrate [§]	0.1	ml
Heparin	500	U
Multi-vitamin [¥]	2	ml
Protein content (amino acid)	4	g
Nitrogen content	0.632	g
Non-protein calorie	116.7	kcal
Carbohydrate calorie	86.7	kcal
Lipid calorie	30.0	kcal
Protein calorie	16	kcal
Total calorie	132.7	kcal

***** Clinisol 15%, obtained from Baxter International Inc., Deerfield, IL.
[#] Intralipid 20%, obtained from Baxter International Inc., Deerfield, IL.
[§] Multitrace®-5 concentrate, contains zinc, copper, manganese, chromium, and selenium, obtained from American Regent, Inc. Shirley, NY.
[¥] Infuvite Adult, obtained from Baxter International Inc., Deerfield, IL.

Table A-6.2. List of qPCR Primers

Gene	Forward Primer Sequence (5' - 3')	Reverse Primer Sequence (5' - 3')
Abcd2	CACAGCGTGCACCTCTAC	AGGACATCTTTCCAGTCCA
Abcg5	TGGATCCAACACCTCTATGCTAAA	GGCAGGTTTTCTCGATGAACTG
Acc	TGACAGACTGATCGCAGAGAAAG	TGGAGAGCCCCACACACA
β-actin	GCGTGACATCAAAGAGAAGC	CTCGTTGCCAATAGTGATGAC
Bsep	CTGCCAAGGATGCTAATGCA	CGATGGCTACCCTTTGCTTCT
Cd36	GATGACGTGGCAAAGAACAG	TCCTCGGGGTCCTGAGTTAT
Cyp2b10	GACTTTGGGATGGGAAAGAG	CCAAACACAATGGAGCAGAT
Cyp27a1	GCCTCACCTATGGGATCTTCA	TCAAAGCCTGACGCAGATG
Cyp7a1	AACAACCTGCCAGTACTAGATAGC	GTGTAGAGTGAAGTCCTCCTTAGC
Cyp7b1	CAGCTATGTTCTGGGCAATG	TCGGATGATGCTGGAGTATG
Cyp8b1	AGTACACATGGACCCCGACATC	GGGTGCCATCCGGGTTGAG
Fas	GCTGCGGAAACTTCAGGAAAT	AGAGACGTGTCACTCCTGGACTT
Fgf15	GCCATCAAGGACGTCAGCA	CTTCCTCCGAGTAGCGAATCAG
Fxr	TCCGGACATTCAACCATCAC	TCACTGCACATCCCAGATCTC
Lepr-b	GCATGCAGAATCAGTGATATTTGG	CAAGCTGTATCGACACTGATTTCTTC
Lpl	AGGACCCCTGAAGACAC	GGCACCCAACTCTCATA
Mrp3	AGAGCTGGGCTCCAAGTTCT	TGGTGTCTCAGGTAAAACAGGTAGCA
Pgc-1α	CGGAAATCATATCCAACCAG	TGAGGACCGCTAGCAAGTTTG
Marco	GCACTGCTGCTGATTCAAGTTC	AGTTGCTCCTGGCTGGTATG
Nocturnin	ACCAGCCAGACATACTGTGC	CTTGGGGAAAAACGTGCCT
Nurr77	AGCTTGGGTGTTGATGTTCC	AATGCGATTCTGCAGCTCTT
Scd1	CCGGAGACCCCTTAGATCGA	TAGCCTGTAAAAGATTTCTGCAAACC
Shp	CGATCCTCTTCAACCCAGATG	AGGGCTCCAAGACTTCACACA
Srebp1c	GGAGCCATGGATTGCACATT	GCTTCCAGAGAGGAGGCCAG

Table A-6.3. Summary of Body and Liver Weight for PN and Saline Mice*

Group	Initial BW (g)	Final BW (g)	BW Change (g)	BW Change	LW (g)	LW/BW Ratio
Saline	21.28 (± 0.51)	21.22 (± 0.55)	-0.06 (± 0.50)	-0.17 (± 2.36)%	1.11 ± 0.08	0.052 ± 0.003
PN	21.22 (± 0.53)	19.12 (± 0.67)	-2.10 (± 0.34)	-10.03 (± 1.70)%	0.75 ± 0.10	0.038 ± 0.004

Abbreviations: BW, body weight; LW, liver weight.

* $P<0.05$, PN group compared to saline group, student's *t*-test, for all the categories in this table except for "initial BW". Data were presented as mean ± SEM. Initial BW was recorded upon infusion setup; final BW and LW were recorded upon animal sac (PN mice had gone through 8 days of PN infusion, corresponding saline controls were sacrificed at the same time).

Table A-6.4. Summary of Serum BAs in PN and Saline Mice

	Concentration (ng/ml)			Percentage	
Total BA (s)	**Saline**	**PN**	**Fold #**	**Saline**	**PN**
Total CA	384.071	1802.12	4.69	29.55%	22.03%
Total CDCA	20.557	440.13 *	21.41	1.46%	6.36%
Total α/β-MCA	409.629	4137.79 *	10.10	27.38%	53.44%
Total DCA	276.050	407.79	1.48	14.90%	4.24%
Total LCA	5.234	1.89 *	0.36	0.37%	0.03%
Total ω-MCA	361.724	1108.15 *	3.06	21.42%	17.14%
Total HDCA	59.056	94.53	1.60	3.95%	1.30%
Total UDCA	34.828	129.12 *	3.71	2.43%	1.83%
Total Primary BAs	793.700	5939.91 *	7.48	56.93%	75.47%
Total Secondary BAs	736.892	1741.48 *	2.36	43.07%	24.53%
Total Unconjugated BAs	873.506	1744.56	2.00	49.84%	25.21%
Total Conjugated BAs	657.087	5936.83 *	9.04	50.16%	74.79%
Total 12α-OH BA	660.121	2209.91	3.35	44.45%	26.27%
Total non-12α-OH BA	870.472	5471.48 *	6.29	55.55%	73.73%
Total BAs	1530.592	7681.39 *	5.02		

Total BAs from UPLC/MS analysis for saline (n=5) and PN mice (n=6). Full names of the 20 BAs are described in "Materials and Methods". Data for concentration and percentage were expressed as mean for each category of BAs in saline or PN mice.

"Fold" was calculated by dividing the averaged total serum concentration of BAs in each category detected in PN mice by that in saline mice. * $P < 0.05$, compared to saline group, student's *t*-test.

Table A-6.5. Top Up- and Down-regulated Liver Genes from Microarray-PN/Saline

Gene	Fold Change	Direction	Full Transcript Name
Sult1e1	17.17	Up	Sulfotransferase family 1E, member 1, mRNA
Fmo3	7.68	Up	Flavin containing monooxygenase 3 (Fmo3), mRNA
Lepr	7.05	Up	Leptin receptor (Lepr), transcript variant 2, mRNA
Abcd2	5.97	Up	ATP-binding cassette, sub-family D (ALD), member 2, mRNA
Cyp17a1	5.28	Up	Cytochrome P450, family 17, subfamily a, polypeptide 1 (Cyp17a1), mRNA
Nr4a1	5.16	Up	Nuclear receptor subfamily 4, group A, member 1, mRNA
Marco	5.15	Up	Macrophage receptor with collagenous structure (Marco), mRNA
Egr1	5.1	Up	Early growth response 1 (Egr1), mRNA
Ccrn4l	5.02	Up	NOCTURNIN (Nocturnin)
Btg2	4.64	Up	B-cell translocation gene 2, anti-proliferative (Btg2), mRNA
Cyp4a12a	9.17	Down	Cytochrome P450, family 4, subfamily a, polypeptide 12a, mRNA
Ces2	8.37	Down	Carboxylesterase 2 (Ces2), mRNA
Cyp2b10	6.72	Down	Cyp2b10-like pseudogene, mRNA sequence
Orm3	6.61	Down	Orosomucoid 3, mRNA
Hist1h2bg	6.28	Down	Histone cluster 1, H2bg, mRNA
Clec2h	6.12	Down	C-type lectin domain family 2, member h (Clec2h), mRNA
Orm2	6.07	Down	Orosomucoid 2 (Orm2), mRNA
Cyp4a12b	4.87	Down	highly similar to CYTOCHROME P450 4A8
Cml5	4.85	Down	Camello-like 5 (Cml5), mRNA
Selenbp2	4.49	Down	Selenium binding protein 2, mRNA
Cyp2c55	4.28	Down	Cytochrome P450, family 2, subfamily c, polypeptide 55, mRNA

Table A-6.6. KEGG Pathway Analysis for Microarray-PN/Saline

KEGG Pathway	List	Up	Down	Gene Set
Cytokine-cytokine receptor interaction	28	19	9	243
Neuroactive ligand-receptor interaction	16	11	5	309
Jak-STAT signaling pathway	15	12	3	146
Natural killer cell mediated cytotoxicity	15	11	4	132
Osteoclast differentiation	11	10	1	107
Staphylococcus aureus infection	11	9	2	48
Glycolysis / Gluconeogenesis	9	6	3	58
p53 signaling pathway	9	7	2	65
Inositol phosphate metabolism	7	7	0	55
Fat digestion and absorption	6	6	0	41
Biosynthesis of unsaturated fatty acids	5	4	1	24
Steroid biosynthesis	4	4	0	18
Drug metabolism - cytochrome P450	19	6	13	74
Retinol metabolism	14	4	10	64
Steroid hormone biosynthesis	13	5	8	46
Arachidonic acid metabolism	12	4	8	82
Complement and coagulation cascades	11	4	7	70
Glutathione metabolism	8	0	8	53
Pentose and glucuronate interconversions	7	1	6	22
Fatty acid metabolism	6	0	6	45
Circadian rhythm - mammal	4	1	3	21
Bile secretion	16	9	7	65
PPAR signaling pathway	15	8	7	74

Total number of genes retrieved from Microarray-PN/Saline for each KEGG category was listed in the “List” column. Total number of genes for each category in the mouse genome in the database for DAVID was listed in the “Gene set” column.

Table A-6.7. Comparison of Microarray Analysis

		Microarray-PN/Saline		Microarray- RORα$^{sg/sg}$/WT	
Functional Category	Gene	Fold Change	Direction	Fold Change	Direction
Cytochrome P450	Cyp2b9	9.4	Up	7.2	Up
	Cyp8b1	3.56	Down	1.8	Down
	Cyp7b1	2.22	Down	4.2	Down
	Cyp2b10	**6.72**	**Down**	**1.2**	**Up**
	Cyp4a10	**2.74**	**Down**	**3.3**	**Up**
Steroid	**Hmgcr**	**2.61**	**Up**	**1.1**	**Down**
	Hsd17b7	**1.68**	**Up**	**1.3**	**Down**
	Hsd3b4	2.45	Down	1.9	Down
	Hsd3b5	2.39	Down	2.8	Down
Lipid and fatty acid	Scd2	2.11	Up	1.0	Up
	Elovl6	1.66	Up	1.3	Up
	Elovl3	3.01	Down	2.2	Down
Cell signaling	**Igfbp1**	**2.88**	**Up**	**1.1**	**Down**
Transport	Abcd2	5.97	Up	1.3	Up
	Apoa4	3.87	Up	1.4	Up
Carbohydrate	Ppp1r3c	3.55	Down	1.7	Down
Circadian rhythm	Rora	1.6	Down	2.6	Down
	Rorc	**1.61**	**Down**	**1.2**	**Up**
	Ccrn4l	5.02	Up	1.7	Up
Miscellaneous	Keg1	2.22	Down	1.6	Down
	Lpin2	2.57	Up	1.4	Up
	Selenbp2	4.49	Down	3.1	Down
	Ccnb1	**2.22**	**Up**	**1.3**	**Down**

Selected genes with the corresponding fold changes and directions of change were retrieved from Microarray-PN/Saline and Microarray- RORα$^{sg/sg}$ /WT (Kang et al. 2007). The functional categories of these genes were obtained from the previous microarray study (Kang et al. 2007). The genes with different directions of changes in the two microarray datasets were highlighted in bold.

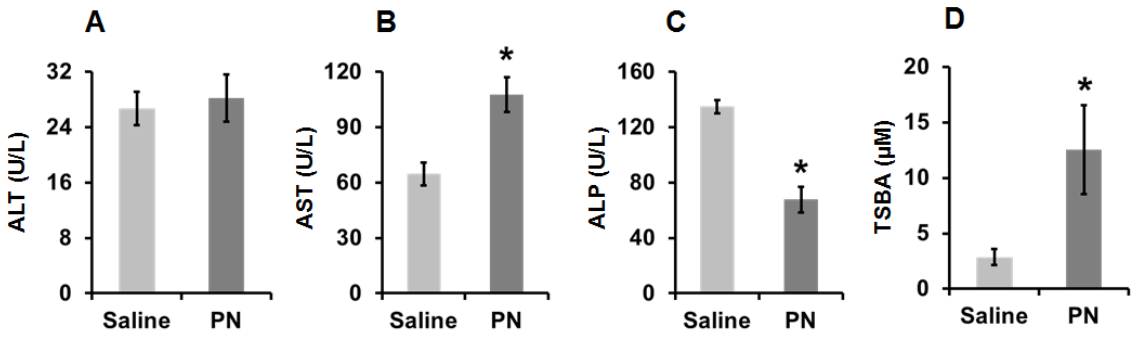

Fig A-6.1. PN mice had altered serum biochemistry. Serum levels of ALT (A), AST (B), ALP (C), and TSBA (D) in saline and PN mice (n=6 to 8). Data were expressed as mean ± SEM. **P* < 0.05, compared with saline group, student's *t*-test.

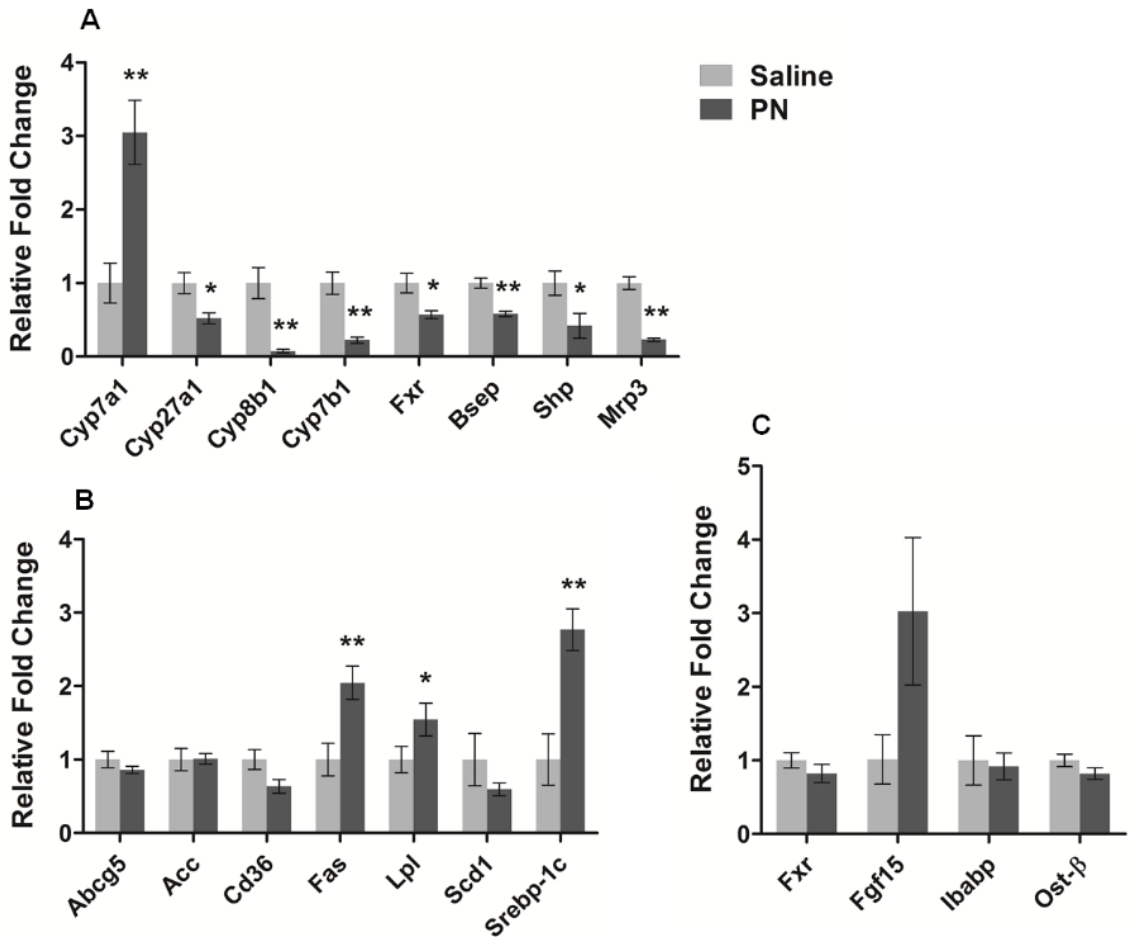

Fig A-6.2. PN altered the expression of genes involved in BA homeostasis and lipid metabolism. RT-qPCR analysis of relative mRNA levels of genes in the livers for BA homeostasis (A) and lipid metabolism (B), and genes in the distal ileums (C) of saline and PN mice (n=6 to 8). Gene expression data were expressed as mean ± SEM. Relative mRNA levels were first normalized to mouse β-actin, and then relative fold changes were normalized to saline group. **P* < 0.05, ***P* < 0.005, compared with saline group, student's *t*-test.

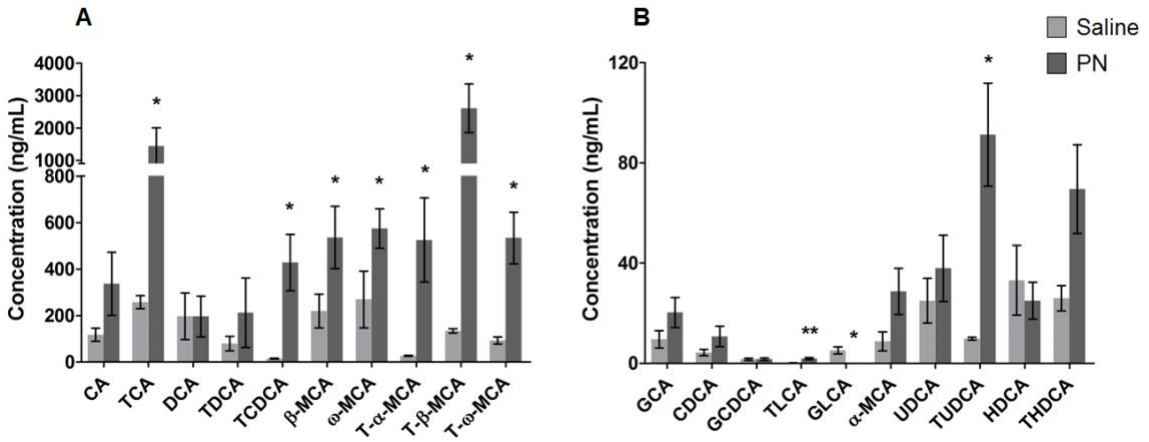

Fig A-6.3. PN altered serum BA profiles in mice. Quantified serum concentrations (ng/ml of serum sample) of the 20 BAs by UPLC/MS for saline (n=5) and PN mice (n=6). Full names of the 20 BAs are described in "Materials and Methods". Data were presented as mean ± SEM. **P* < 0.05, compared with saline group, student's *t*-test.

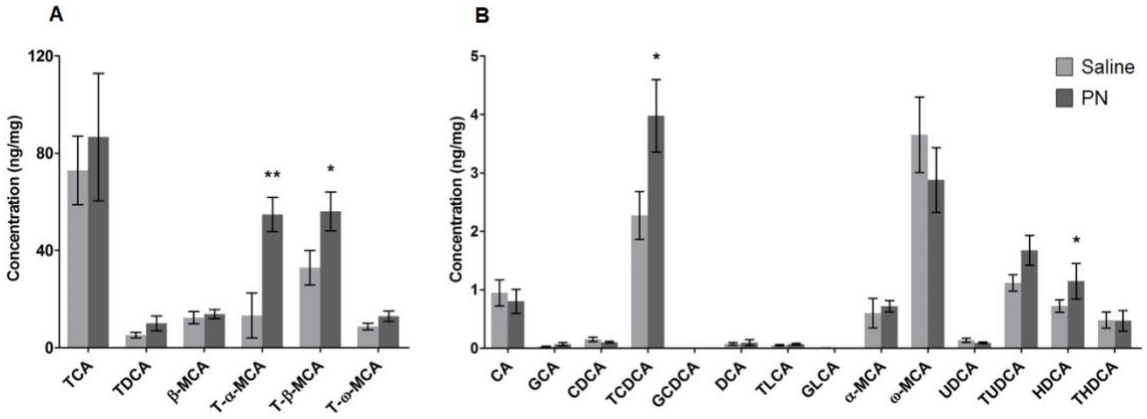

Fig A-6.4. Liver BA profiles were similar between PN and saline mice. Quantified liver concentrations (ng/mg of liver tissue) of the 20 BAs by UPLC/MS for saline (n=6) and PN mice (n=6). Full names of the 20 BAs are described in "Materials and Methods". Data were presented as mean ± SEM. **P* < 0.05, compared with saline group, student's *t*-test.

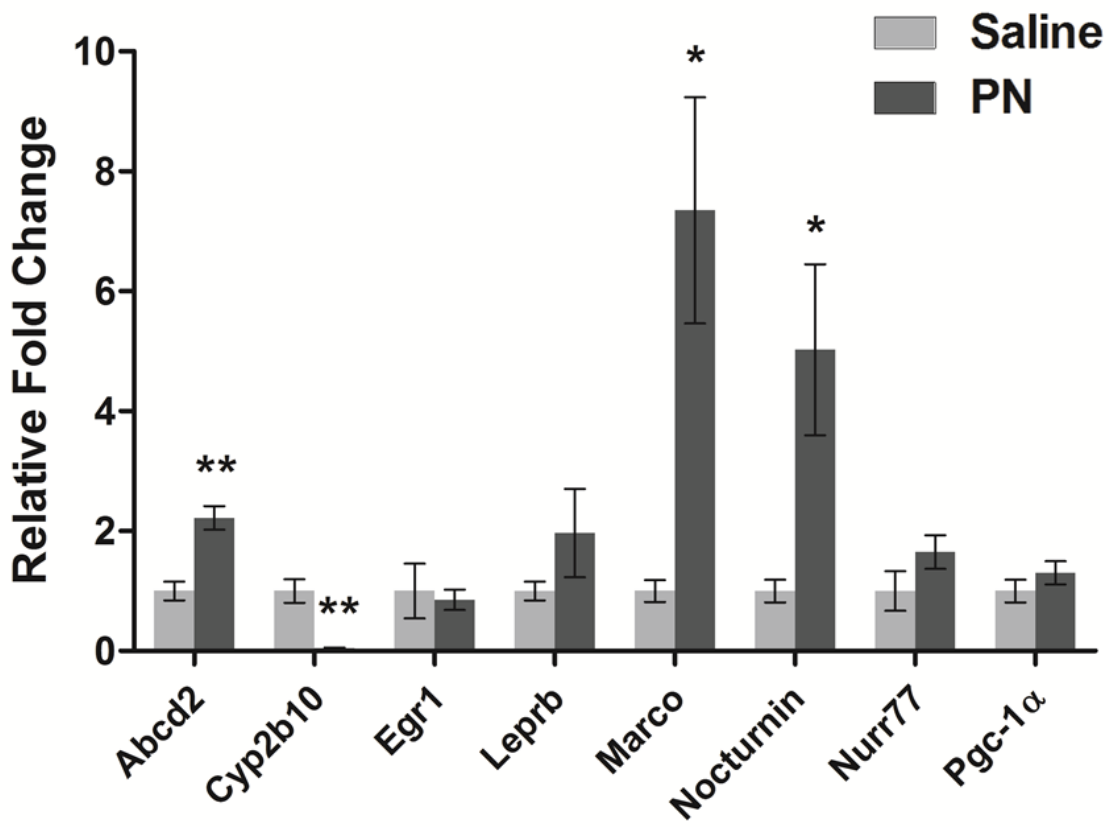

Fig A-6.5. Validation of microarray analysis (Microarray-PN/Saline). RT-qPCR validation of selected genes retrieved from Microarray-PN/Saline (genes with full names were shown in Table A-6.5, *Nur77* is for *Nr4a1*). Hepatic gene expression data were expressed as mean ± SEM. Samples from the same mice were used as in Figure A-6.2. Relative mRNA levels were first normalized to β-actin, and then relative fold changes were normalized to saline mice. **P* < 0.05, ***P* < 0.005, compared with saline group, student's *t*-test.

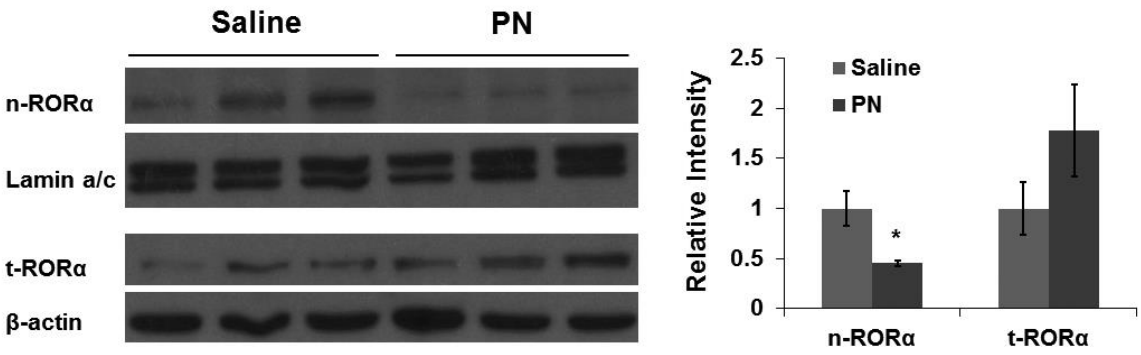

Fig A-6.6. PN decreased liver nuclear protein levels of RORα. Left: Western blot analysis of RORα protein in saline and PN mouse livers (n-RORα: nuclear fraction of RORα; t-RORα: total cellular RORα). Lamin a/c and β-actin were used as the loading controls for nuclear and total protein, respectively. Each band represents one single mouse sample in the indicated treatment group. Right: the relative band density was determined using the ImageJ software. Data were presented as mean ± SEM. The relative intensity of RORα for each mouse samples was first normalized to the corresponding loading control, then the results from PN mice was normalized to the saline mice. Results from saline mice were set as arbitrary 1. *$P < 0.05$, compared with saline group, student's *t*-test.

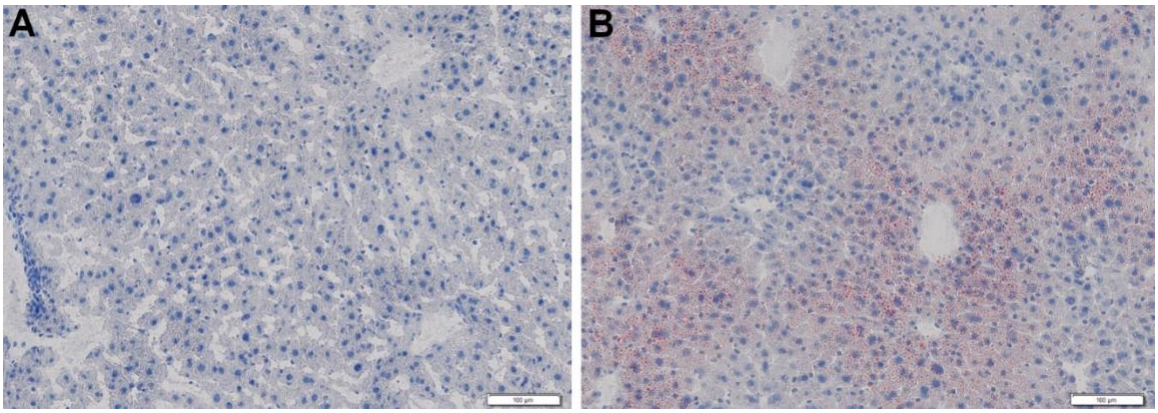

Fig A-6.7. PN increased hepatic lipid deposition in mice. Representative low-throughput images from Oil Red O staining of frozen mouse liver sections from saline (A) and PN (B) mice. Scale bar is 100μm.

REFERENCES

2006. Commision E: Commission Regulation (Ec) No 1881/2006 of 19 December 2006 Setting Maximum Levels
for Certain Contaminants in Foodstuffs. Off J Eur Union L364, 5-24.

(FSA), F.S.A. 2003. Survey of retail cereal products for trichothecenes and zearalenone (Number 35/03).

Abbott, N.J. 2014. Anatomy and Physiology of the Blood-Brain Barriers. In: M. Hammarlund-Udenaes, E. de Lange and R.G. Thorne (Eds), Drug Delivery to the Brain: Physiogial Concepts, Methodologies and Approaches, Springer-Verlag New York, pp. xx, 731.

Abbott, N.J., Patabendige, A.A., Dolman, D.E., Yusof, S.R. and Begley, D.J. 2010. Structure and function of the blood-brain barrier. Neurobiol Dis 37, 13-25.

Adachi, T., Nakagawa, H., Chung, I., Hagiya, Y., Hoshijima, K., Noguchi, N., Kuo, M.T. and Ishikawa, T. 2007. Nrf2-dependent and -independent induction of ABC transporters ABCC1, ABCC2, and ABCG2 in HepG2 cells under oxidative stress. Journal of experimental therapeutics & oncology 6, 335-348.

Afrouzian, M., Al-Lahham, R., Patrikeeva, S., Xu, M., Fokina, V., Fischer, W.G., Abdel-Rahman, S.Z., Costantine, M., Ahmed, M.S. and Nanovskaya, T. 2018. Role of the efflux transporters BCRP and MRP1 in human placental bio-disposition of pravastatin. Biochem Pharmacol 156, 467-478.

Aida, K., Hayashi, H., Inamura, K., Mizuno, T. and Sugiyama, Y. 2014. Differential roles of ubiquitination in the degradation mechanism of cell surface-resident bile salt export pump and multidrug resistance-associated protein 2. Mol Pharmacol 85, 482-491.

Al-Nasiry, S., Spitz, B., Hanssens, M., Luyten, C. and Pijnenborg, R. 2006. Differential effects of inducers of syncytialization and apoptosis on BeWo and JEG-3 choriocarcinoma cells. Human reproduction 21, 193-201.

Albekairi, N.A., Al-Enazy, S., Ali, S. and Rytting, E. 2015. Transport of digoxin-loaded polymeric nanoparticles across BeWo cells, an in vitro model of human placental trophoblast. Therapeutic Delivery 6, 1325-1334.

Albrecht, E.D. and Pepe, G.J. 2010. Estrogen regulation of placental angiogenesis and fetal ovarian development during primate pregnancy. Int J Dev Biol 54, 397-408.

Aleksunes, L.M. and Klaassen, C.D. 2012. Coordinated regulation of hepatic phase I and II drug-metabolizing genes and transporters using AhR-, CAR-, PXR-, PPARalpha-, and Nrf2-null mice. Drug Metab Dispos 40, 1366-1379.

Aleksunes, L.M., Slitt, A.L., Maher, J.M., Augustine, L.M., Goedken, M.J., Chan, J.Y., Cherrington, N.J., Klaassen, C.D. and Manautou, J.E. 2008. Induction of Mrp3 and Mrp4 transporters during acetaminophen hepatotoxicity is dependent on Nrf2. Toxicology and applied pharmacology 226, 74-83.

Alexander, R.L., Bates, D.J., Wright, M.W., King, S.B. and Morrow, C.S. 2006. Modulation of nitrated lipid signaling by multidrug resistance protein 1 (MRP1): glutathione conjugation and MRP1-mediated efflux inhibit nitrolinoleic acid-induced, PPARgamma-dependent transcription activation. Biochemistry 45, 7889-7896.

Ali, N. and Degen, G.H. 2019. Biomonitoring of zearalenone and its main metabolites in urines of Bangladeshi adults. Food Chem Toxicol 130, 276-283.

Allikmets, R., Schriml, L.M., Hutchinson, A., Romano-Spica, V. and Dean, M. 1998. A human placenta-specific ATP-binding cassette gene (ABCP) on chromosome 4q22 that is involved in multidrug resistance. Cancer Res 58, 5337-5339.

Alm, H., Greising, T., Brussow, K.P., Torner, H. and Tiemann, U. 2002. The influence of the mycotoxins deoxynivalenol and zearalenol on in vitro maturation of pig oocytes and in vitro culture of pig zygotes. Toxicol In Vitro 16, 643-648.

Alvarez, A.I., Vallejo, F., Barrera, B., Merino, G., Prieto, J.G., Tomas-Barberan, F. and Espin, J.C. 2011. Bioavailability of the glucuronide and sulfate conjugates of genistein and daidzein in breast cancer resistance protein 1 knockout mice. Drug Metab. Dispos. 39, 2008-2012.

Ambadipudi, R. and Georges, E. 2017. Sequences in Linker-1 domain of the multidrug resistance associated protein (MRP1 or ABCC1) bind to tubulin and their binding is modulated by phosphorylation. Biochem Biophys Res Commun 482, 1001-1006.

An, G. and Morris, M.E. 2011. The sulfated conjugate of biochanin A is a substrate of breast cancer resistant protein (ABCG2). Biopharmaceutics & drug disposition 32, 446-457.

Ananth, C.V., Keyes, K.M. and Wapner, R.J. 2013. Pre-eclampsia rates in the United States, 1980-2010: age-period-cohort analysis. BMJ 347, f6564.

Anapolsky, A., Teng, S., Dixit, S. and Piquette-Miller, M. 2006. The role of pregnane X receptor in 2-acetylaminofluorene-mediated induction of drug transport and -metabolizing enzymes in mice. Drug metabolism and disposition: the biological fate of chemicals 34, 405-409.

Andersen, C., Zhao, F. and Ye, X.-Q. 2018. Effects of Mycoestrogens on Female Reproduction. Reproductive and Developmental Medicine 2, 52-58.

Anelli, G.M., Mando, C., Letizia, T., Mazzocco, M.I., Novielli, C., Lisso, F., Personeni, C., Vago, T. and Cetin, I. 2019. Placental ESRRG-CYP19A1 Expressions and Circulating 17-Beta Estradiol in IUGR Pregnancies. Front Pediatr 7, 154.

Anjalakshi, C., Balaji, V., Balaji, M.S. and Seshiah, V. 2007. A prospective study comparing insulin and glibenclamide in gestational diabetes mellitus in Asian Indian women. Diabetes Res Clin Pract 76, 474-475.

Anwar-Mohamed, A., Degenhardt, O.S., El Gendy, M.A., Seubert, J.M., Kleeberger, S.R. and El-Kadi, A.O. 2011. The effect of Nrf2 knockout on the constitutive expression of drug metabolizing enzymes and transporters in C57Bl/6 mice livers. Toxicology in vitro : an international journal published in association with BIBRA 25, 785-795.

Anzai, N., Kanai, Y. and Endou, H. 2007. New insights into renal transport of urate. Curr Opin Rheumatol 19, 151-157.

Appelgren, L.E., Arora, R.G. and Larsson, P. 1982. Autoradiographic studies of [3H]zearalenone in mice. Toxicology 25, 243-253.

Arai, Y., Uehara, M., Sato, Y., Kimira, M., Eboshida, A., Adlercreutz, H. and Watanabe, S. 2000. Comparison of isoflavones among dietary intake, plasma concentration and urinary excretion for accurate estimation of phytoestrogen intake. J Epidemiol 10, 127-135.

Arias, A., Rigalli, J.P., Villanueva, S.S., Ruiz, M.L., Luquita, M.G., Perdomo, V.G., Vore, M., Catania, V.A. and Mottino, A.D. 2014. Regulation of expression and activity of multidrug resistance proteins MRP2 and MDR1 by estrogenic compounds in Caco-2 cells. Role in prevention of xenobiotic-induced cytotoxicity. Toxicology 320, 46-55.

Asvold, B.O., Eskild, A. and Vatten, L.J. 2014. Human chorionic gonadotropin, angiogenic factors, and preeclampsia risk: a nested case-control study. Acta Obstet Gynecol Scand 93, 454-462.

Atkinson, D.E., Greenwood, S.L., Sibley, C.P., Glazier, J.D. and Fairbairn, L.J. 2003. Role of MDR1 and MRP1 in trophoblast cells, elucidated using retroviral gene transfer. Am J Physiol Cell Physiol 285, C584-591.

Atkinson, D.E., Sibley, C.P., Fairbairn, L.J. and Greenwood, S.L. 2006. MDR1 P-gp expression and activity in intact human placental tissue; upregulation by retroviral transduction. Placenta 27, 707-714.

Avery, M.L., Meek, C.E. and Audus, K.L. 2003. The presence of inducible cytochrome P450 types 1A1 and 1A2 in the BeWo cell line. Placenta 24, 45-52.

Badolo, L., Jensen, B., Sall, C., Norinder, U., Kallunki, P. and Montanari, D. 2015. Evaluation of 309 molecules as inducers of CYP3A4, CYP2B6, CYP1A2, OATP1B1, OCT1, MDR1,

MRP2, MRP3 and BCRP in cryopreserved human hepatocytes in sandwich culture. Xenobiotica 45, 177-187.

Bailey-Dell, K.J., Hassel, B., Doyle, L.A. and Ross, D.D. 2001. Promoter characterization and genomic organization of the human breast cancer resistance protein (ATP-binding cassette transporter G2) gene. Biochim Biophys Acta 1520, 234-241.

Bakos, E., Evers, R., Szakacs, G., Tusnady, G.E., Welker, E., Szabo, K., de Haas, M., van Deemter, L., Borst, P., Varadi, A. and Sarkadi, B. 1998. Functional multidrug resistance protein (MRP1) lacking the N-terminal transmembrane domain. J Biol Chem 273, 32167-32175.

Balkovetz, D.F., Tiruppathi, C., Leibach, F.H., Mahesh, V.B. and Ganapathy, V. 1989. Evidence for an imipramine-sensitive serotonin transporter in human placental brush-border membranes. J Biol Chem 264, 2195-2198.

Bandera, E.V., Chandran, U., Buckley, B., Lin, Y., Isukapalli, S., Marshall, I., King, M. and Zarbl, H. 2011. Urinary mycoestrogens, body size and breast development in New Jersey girls. Sci Total Environ 409, 5221-5227.

Bandler, P.E., Westlake, C.J., Grant, C.E., Cole, S.P. and Deeley, R.G. 2008. Identification of regions required for apical membrane localization of human multidrug resistance protein 2. Mol Pharmacol 74, 9-19.

Barak, Y., Nelson, M.C., Ong, E.S., Jones, Y.Z., Ruiz-Lozano, P., Chien, K.R., Koder, A. and Evans, R.M. 1999. PPAR gamma is required for placental, cardiac, and adipose tissue development. Mol Cell 4, 585-595.

Barjaktarovic, M., Korevaar, T.I.M., Jaddoe, V.W.V., de Rijke, Y.B., Peeters, R.P. and Steegers, E.A.P. 2019. Human chorionic gonadotropin and risk of pre-eclampsia: prospective population-based cohort study. Ultrasound Obstet Gynecol 54, 477-483.

Barrett, J., George, J. and Lamond, D. 1965. Reproductive performance of Merino ewes grazing red clover (*Trifolium pratense* L.), improved pasture, or native pasture. Aust J Agric Res 16, 189-200.

Bart, J., Hollema, H., Groen, H.J., de Vries, E.G., Hendrikse, N.H., Sleijfer, D.T., Wegman, T.D., Vaalburg, W. and van der Graaf, W.T. 2004. The distribution of drug-efflux pumps, P-gp, BCRP, MRP1 and MRP2, in the normal blood-testis barrier and in primary testicular tumours. Eur J Cancer 40, 2064-2070.

Bartosz, G., Konig, J., Keppler, D. and Hagmann, W. 1998. Human mast cells secreting leukotriene C4 express the MRP1 gene-encoded conjugate export pump. Biol Chem 379, 1121-1126.

Basirat, Z., Barat, S. and Hajiahmadi, M. 2006. Serum beta human chorionic gonadotropin levels and preeclampsia. Saudi Med J 27, 1001-1004.

Bauer, B., Hartz, A.M., Fricker, G. and Miller, D.S. 2004. Pregnane X receptor up-regulation of P-glycoprotein expression and transport function at the blood-brain barrier. Mol Pharmacol 66, 413-419.

Baumann, M.U., Zamudio, S. and Illsley, N.P. 2007. Hypoxic upregulation of glucose transporters in BeWo choriocarcinoma cells is mediated by hypoxia-inducible factor-1. American journal of physiology. Cell physiology 293, C477-485.

Bechi, N., Ietta, F., Romagnoli, R., Focardi, S., Corsi, I., Buffi, C. and Paulesu, L. 2006. Estrogen-like response to p-nonylphenol in human first trimester placenta and BeWo choriocarcinoma cells. Toxicol Sci 93, 75-81.

Belli, P., Bellaton, C., Durand, J., Balleydier, S., Milhau, N., Mure, M., Mornex, J.F., Benahmed, M. and Le Jan, C. 2010. Fetal and neonatal exposure to the mycotoxin zearalenone induces phenotypic alterations in adult rat mammary gland. Food and chemical toxicology : an international journal published for the British Industrial Biological Research Association 48, 2818-2826.

Benoki, S., Yoshinari, K., Chikada, T., Imai, J. and Yamazoe, Y. 2012. Transactivation of ABCG2 through a novel cis-element in the distal promoter by constitutive androstane receptor but not pregnane X receptor in human hepatocytes. Archives of biochemistry and biophysics 517, 123-130.

Bernhoft, A., Behrens, G.H., Ingebrigtsen, K., Langseth, W., Berndt, S., Haugen, T.B. and Grotmol, T. 2001. Placental transfer of the estrogenic mycotoxin zearalenone in rats. Reprod Toxicol 15, 545-550.

Bertini, A.M., Silva, J.C., Taborda, W., Becker, F., Lemos Bebber, F.R., Zucco Viesi, J.M., Aquim, G. and Engel Ribeiro, T. 2005. Perinatal outcomes and the use of oral hypoglycemic agents. J Perinat Med 33, 519-523.

Bertollotto, G.M., de Oliveira, M.G., Alexandre, E.C., Calmasini, F.B., Passos, G.R., Antunes, E. and Monica, F.Z. 2018. Inhibition of Multidrug Resistance Proteins by MK 571 Enhances Bladder, Prostate, and Urethra Relaxation through cAMP or cGMP Accumulation. J Pharmacol Exp Ther 367, 138-146.

Biehl, M.L., Prelusky, D.B., Koritz, G.D., Hartin, K.E., Buck, W.B. and Trenholm, H.L. 1993. Biliary excretion and enterohepatic cycling of zearalenone in immature pigs. Toxicol Appl Pharmacol 121, 152-159.

Biondi, C., Ferretti, M.E., Lunghi, L., Medici, S., Cervellati, F., Pavan, B., Vesce, F., Morano, D., Adinolfi, E., Bertoni, F. and Abelli, L. 2010. cAMP efflux from human trophoblast cell lines: a role for multidrug resistance protein (MRP)1 transporter. Mol Hum Reprod 16, 481-491.

Bircsak, K.M., Gibson, C.J., Robey, R.W. and Aleksunes, L.M. 2013a. Assessment of drug transporter function using fluorescent cell imaging. Curr Protoc Toxicol 57, Unit 23.26.

Bircsak, K.M., Gibson, C.J., Robey, R.W. and Aleksunes, L.M. 2013b. Assessment of drug transporter function using fluorescent cell imaging. Current protocols in toxicology / editorial board, Mahin D. Maines 57, Unit 23 26.

Bircsak, K.M., Gupta, V., Yuen, P.Y., Gorczyca, L., Weinberger, B.I., Vetrano, A.M. and Aleksunes, L.M. 2016. Genetic and Dietary Regulation of Glyburide Efflux by the Human Placental Breast Cancer Resistance Protein Transporter. The Journal of pharmacology and experimental therapeutics 357, 103-113.

Bircsak, K.M., Moscovitz, J.E., Wen, X., Archer, F., Yuen, P.Y.S., Mohammed, M., Memon, N., Weinberger, B.I., Saba, L.M., Vetrano, A.M. and Aleksunes, L.M. 2018. Interindividual Regulation of the Breast Cancer Resistance Protein/ABCG2 Transporter in Term Human Placentas. Drug Metab Dispos 46, 619-627.

Biswas, S., Mukherjee, R., Tapryal, N., Singh, A.K. and Mukhopadhyay, C.K. 2013. Insulin regulates hypoxia-inducible factor-1alpha transcription by reactive oxygen species sensitive activation of Sp1 in 3T3-L1 preadipocyte. PloS one 8, e62128.

Bitto, A., Burnett, B.P., Polito, F., Marini, H., Levy, R.M., Armbruster, M.A., Minutoli, L., Di Stefano, V., Irrera, N., Antoci, S., Granese, R., Squadrito, F. and Altavilla, D. 2008. Effects of genistein aglycone in osteoporotic, ovariectomized rats: A comparison with alendronate, raloxifene and oestradiol. Br. J. Pharmacol. 155, 896-905.

Borel, F., Han, R., Visser, A., Petry, H., van Deventer, S.J., Jansen, P.L., Konstantinova, P. and Reseau Centre de Ressources Biologiques Foie, F. 2012. Adenosine triphosphate-binding cassette transporter genes up-regulation in untreated hepatocellular carcinoma is mediated by cellular microRNAs. Hepatology 55, 821-832.

Boswell-Casteel, R.C. and Hays, F.A. 2017. Equilibrative nucleoside transporters-A review. Nucleosides Nucleotides Nucleic Acids 36, 7-30.

Bradfield, C.A., Glover, E. and Poland, A. 1991. Purification and N-terminal amino acid sequence of the Ah receptor from the C57BL/6J mouse. Mol Pharmacol 39, 13-19.

Bravin, F., Duca, R.C., Balaguer, P. and Delaforge, M. 2009. In vitro cytochrome p450 formation of a mono-hydroxylated metabolite of zearalenone exhibiting estrogenic activities: possible occurrence of this metabolite in vivo. International journal of molecular sciences 10, 1824-1837.

Brent, R.L. 2001. The cause and prevention of human birth defects: what have we learned in the past 50 years? Congenital Anomalies 41, 3–21.

Bukovsky, A., Caudle, M.R., Cekanova, M., Fernando, R.I., Wimalasena, J., Foster, J.S., Henley, D.C. and Elder, R.F. 2003a. Placental expression of estrogen receptor beta and its hormone binding variant--comparison with estrogen receptor alpha and a role for estrogen receptors in asymmetric division and differentiation of estrogen-dependent cells. Reprod Biol Endocrinol 1, 36.

Bukovsky, A., Cekanova, M., Caudle, M.R., Wimalasena, J., Foster, J.S., Henley, D.C. and Elder, R.F. 2003b. Expression and localization of estrogen receptor-alpha protein in normal and abnormal term placentae and stimulation of trophoblast differentiation by estradiol. Reprod Biol Endocrinol 1, 13.

C., L., B., E., J., B., J.R., R., M., G., K.R., R. and H., Z. 2016. Exposure of Fischer 344 Rats to Dietary Zeranol During Pregnancy and Lactation Alters Sexual Development in F1 Progeny. Toxicol Sci, Under Review.

Caldwell, R.W., Tuite, J., Stob, M. and Baldwin, R. 1970. Zearalenone production by Fusarium species. Appl Microbiol 20, 31-34.

Camelo Castillo, W., Boggess, K., Sturmer, T., Brookhart, M.A., Benjamin, D.K., Jr. and Jonsson Funk, M. 2014. Trends in glyburide compared with insulin use for gestational diabetes treatment in the United States, 2000-2011. Obstet Gynecol 123, 1177-1184.

Campos, C.R., Schroter, C., Wang, X. and Miller, D.S. 2012. ABC transporter function and regulation at the blood-spinal cord barrier. J Cereb Blood Flow Metab 32, 1559-1566.

Caniggia, I., Winter, J., Lye, S.J. and Post, M. 2000. Oxygen and placental development during the first trimester: implications for the pathophysiology of pre-eclampsia. Placenta 21 Suppl A, S25-30.

Carter, A.M. 2007. Animal models of human placentation--a review. Placenta 28 Suppl A, S41-47.

Cary, P.D., Crane-Robinson, C., Bradbury, E.M. and Dixon, G.H. 1982. Effect of acetylation on the binding of N-terminal peptides of histone H4 to DNA. Eur J Biochem 127, 137-143.

Ceckova, M., Libra, A., Pavek, P., Nachtigal, P., Brabec, M., Fuchs, R. and Staud, F. 2006. Expression and functional activity of breast cancer resistance protein (BCRP, ABCG2) transporter in the human choriocarcinoma cell line BeWo. Clinical and experimental pharmacology & physiology 33, 58-65.

Cerveny, L., Ptackova, Z., Ceckova, M., Karahoda, R., Karbanova, S., Jiraskova, L., Greenwood, S.L., Glazier, J.D. and Staud, F. 2018. Equilibrative Nucleoside Transporter 1 (ENT1, SLC29A1) Facilitates Transfer of the Antiretroviral Drug Abacavir across the Placenta. Drug Metab Dispos 46, 1817-1826.

Chaddha, V., Viero, S., Huppertz, B. and Kingdom, J. 2004. Developmental biology of the placenta and the origins of placental insufficiency. Seminars in fetal & neonatal medicine 9, 357-369.

Chan, G.N., Hoque, M.T. and Bendayan, R. 2013a. Role of nuclear receptors in the regulation of drug transporters in the brain. Trends Pharmacol Sci 34, 361-372.

Chan, Y.Y., Kalpana, S., Chang, W.C., Chang, W.C. and Chen, B.K. 2013b. Expression of aryl hydrocarbon receptor nuclear translocator enhances cisplatin resistance by upregulating MDR1 expression in cancer cells. Mol Pharmacol 84, 591-602.

Chang, C.W., Wakeland, A.K. and Parast, M.M. 2018a. Trophoblast lineage specification, differentiation and their regulation by oxygen tension. J Endocrinol 236, R43-R56.

Chang, K., Kurtz, H.J. and Mirocha, C.J. 1979. Effects of the mycotoxin zearalenone on swine reproduction. Am J Vet Res 40, 1260-1267.

Chang, L., Hu, Z., Zhou, Z. and Zhang, H. 2018b. Linc00518 Contributes to Multidrug Resistance Through Regulating the MiR-199a/MRP1 Axis in Breast Cancer. Cell Physiol Biochem 48, 16-28.

Chang, T.T., Shyu, M.K., Huang, M.C., Hsu, C.C., Yeh, S.Y., Chen, M.R. and Lin, C.J. 2011. Hypoxia-mediated down-regulation of OCTN2 and PPARalpha expression in human placentas and in BeWo cells. Molecular pharmaceutics 8, 117-125.

Chatuphonprasert, W., Jarukamjorn, K. and Ellinger, I. 2018. Physiology and Pathophysiology of Steroid Biosynthesis, Transport and Metabolism in the Human Placenta. Front Pharmacol 9, 1027.

Chen, C.P., Chen, C.Y., Yang, Y.C., Su, T.H. and Chen, H. 2004. Decreased placental GCM1 (glial cells missing) gene expression in pre-eclampsia. Placenta 25, 413-421.

Chen, C.P., Wang, K.G., Chen, C.Y., Yu, C., Chuang, H.C. and Chen, H. 2006. Altered placental syncytin and its receptor ASCT2 expression in placental development and pre-eclampsia. BJOG 113, 152-158.

Chen, L., Wang, Z., Xu, Q., Liu, Y., Chen, L., Guo, S., Wang, H., Zeng, K., Liu, J., Zeng, S. and Yu, L. 2020. The failure of DAC to induce OCT2 expression and its remission by hemoglobin-based nanocarriers under hypoxia in renal cell carcinoma. Theranostics 10, 3562-3578.

Chen, S., Wang, H., Li, Z., You, J., Wu, Q.W., Zhao, C., Tzeng, C.M. and Zhang, Z.M. 2018a. Interaction of WBP2 with ERalpha increases doxorubicin resistance of breast cancer cells by modulating MDR1 transcription. Br J Cancer 119, 182-192.

Chen, Y., Yuan, X., Xiao, Z., Jin, H., Zhang, L. and Liu, Z. 2018b. Discovery of novel multidrug resistance protein 4 (MRP4) inhibitors as active agents reducing resistance to anticancer drug 6-Mercaptopurine (6-MP) by structure and ligand-based virtual screening. PLoS One 13, e0205175.

Chen, Y.J., Huang, W.C., Wei, Y.L., Hsu, S.C., Yuan, P., Lin, H.Y., Wistuba, II, Lee, J.J., Yen, C.J., Su, W.C., Chang, K.Y., Chang, W.C., Chou, T.C., Chou, C.K., Tsai, C.H. and Hung, M.C. 2011a. Elevated BCRP/ABCG2 expression confers acquired resistance to gefitinib in wild-type EGFR-expressing cells. PLoS One 6, e21428.

Chen, Y.M., Ho, S.C., Lam, S.S., Ho, S.S. and Woo, J.L. 2003. Soy isoflavones have a favorable effect on bone loss in Chinese postmenopausal women with lower bone mass: A double-blind, randomized, controlled trial. J. Clin. Endocrinol. Metab. 88, 4740-4747.

Chen, Y.X., Allars, M., Maiti, K., Angeli, G.L., Abou-Seif, C., Smith, R. and Nicholson, R.C. 2011b. Factors affecting cytotrophoblast cell viability and differentiation: Evidence of a link between syncytialisation and apoptosis. Int J Biochem Cell Biol 43, 821-828.

Cheng, G.M. and To, K.K. 2012. Adverse Cell Culture Conditions Mimicking the Tumor Microenvironment Upregulate ABCG2 to Mediate Multidrug Resistance and a More Malignant Phenotype. ISRN Oncol 2012, 746025.

Choi, B.H., Ryoo, I.G., Kang, H.C. and Kwak, M.K. 2014a. The sensitivity of cancer cells to pheophorbide a-based photodynamic therapy is enhanced by Nrf2 silencing. PLoS One 9, e107158.

Choi, B.H., Ryu, D.Y., Ryoo, I.G. and Kwak, M.K. 2017. NFE2L2/NRF2 silencing-inducible miR-206 targets c-MET/EGFR and suppresses BCRP/ABCG2 in cancer cells. Oncotarget 8, 107188-107205.

Choi, Y.H. and Yu, A.M. 2014b. ABC transporters in multidrug resistance and pharmacokinetics, and strategies for drug development. Curr Pharm Des 20, 793-807.

Choudhuri, S. and Klaassen, C.D. 2006. Structure, function, expression, genomic organization, and single nucleotide polymorphisms of human ABCB1 (MDR1), ABCC (MRP), and ABCG2 (BCRP) efflux transporters. Int J Toxicol 25, 231-259.

Chuprin, A., Gal, H., Biron-Shental, T., Biran, A., Amiel, A., Rozenblatt, S. and Krizhanovsky, V. 2013. Cell fusion induced by ERVWE1 or measles virus causes cellular senescence. Genes Dev 27, 2356-2366.

Clarkson, T.B., H., U.W., Allmen, T.I., Aso, T., Barnes, S., Basaria, S.S., Brinton, R.D., M., C.J., Frankenfeld, C.L., Gallagher, J.C., Gold, E.B., Hodis, H.N., Ishimi, Y., Kim, H., Kroenberg, F., Landgren, B.M., Maki, P.M., Messina, M.J., Setchell, K.D., Shu, X.O., Weaver, C.M., Wong, W.W., Goldstein, S.R., Pace, D.T., Shifren, J.L., Clarkson, T.B., Contestabile, E., Gass, M.L., Kagan., R., Maki, P.M., Manson, J.E., Schnatz, P.F., Sievert, L.L., Stuenkel, C.A., Warren, M.P., Schiff, I. and Utian, W.H. 2011. The role of soy isoflavones in menopausal health: Report of the North American Menopause Society/Wulf H. Utian Translational Science Symposium in Chicago, IL (October 2010). Menopause 18, 732-753.

Clayton, A.L., Hebbes, T.R., Thorne, A.W. and Crane-Robinson, C. 1993. Histone acetylation and gene induction in human cells. FEBS Lett 336, 23-26.

Cole, S.P., Bhardwaj, G., Gerlach, J.H., Mackie, J.E., Grant, C.E., Almquist, K.C., Stewart, A.J., Kurz, E.U., Duncan, A.M. and Deeley, R.G. 1992. Overexpression of a transporter gene in a multidrug-resistant human lung cancer cell line. Science 258, 1650-1654.

Coles, L.D., Lee, I.J., Voulalas, P.J. and Eddington, N.D. 2009. Estradiol and progesterone-mediated regulation of P-gp in P-gp overexpressing cells (NCI-ADR-RES) and placental cells (JAR). Mol Pharm 6, 1816-1825.

Collins, T.F., Sprando, R.L., Black, T.N., Olejnik, N., Eppley, R.M., Alam, H.Z., Rorie, J. and Ruggles, D.I. 2006. Effects of zearalenone on in utero development in rats. Food Chem Toxicol 44, 1455-1465.

Colman, P.M. and Lawrence, M.C. 2003. The structural biology of type I viral membrane fusion. Nat Rev Mol Cell Biol 4, 309-319.

Comerford, K.M., Wallace, T.J., Karhausen, J., Louis, N.A., Montalto, M.C. and Colgan, S.P. 2002. Hypoxia-inducible factor-1-dependent regulation of the multidrug resistance (MDR1) gene. Cancer research 62, 3387-3394.

Commision, E. 2006. Commission Regulation (EC) No 1881/2006 of 19 December 2006 setting maximum levels for certain contaminants in foodstuffs. Off. J. Eur. Union L364, 5-24.

Conrad, S., Kauffmann, H.M., Ito, K., Deeley, R.G., Cole, S.P. and Schrenk, D. 2001. Identification of human multidrug resistance protein 1 (MRP1) mutations and characterization of a G671V substitution. J Hum Genet 46, 656-663.

Conrad, S., Kauffmann, H.M., Ito, K., Leslie, E.M., Deeley, R.G., Schrenk, D. and Cole, S.P. 2002. A naturally occurring mutation in MRP1 results in a selective decrease in organic anion transport and in increased doxorubicin resistance. Pharmacogenetics 12, 321-330.

Conseil, G., Deeley, R.G. and Cole, S.P. 2005. Polymorphisms of MRP1 (ABCC1) and related ATP-dependent drug transporters. Pharmacogenet Genomics 15, 523-533.

Constantinou, A.I., White, B.E., Tonetti, D., Yang, Y., Liang, W., Li, W. and van Breemen, R.B. 2005. The soy isoflavone daidzein improves the capacity of tamoxifen to prevent mammary tumours. Eur. J. Cancer. 41, 647-654.

Copsel, S., Garcia, C., Diez, F., Vermeulem, M., Baldi, A., Bianciotti, L.G., Russel, F.G., Shayo, C. and Davio, C. 2011. Multidrug resistance protein 4 (MRP4/ABCC4) regulates cAMP cellular levels and controls human leukemia cell proliferation and differentiation. J Biol Chem 286, 6979-6988.

Cornwell, M.M. 1990. The human multidrug resistance gene: sequences upstream and downstream of the initiation site influence transcription. Cell Growth Differ 1, 607-615.

Correia Carreira, S., Cartwright, L., Mathiesen, L., Knudsen, L.E. and Saunders, M. 2011. Studying placental transfer of highly purified non-dioxin-like PCBs in two models of the placental barrier. Placenta 32, 283-291.

Cortinovis, C., Pizzo, F., Spicer, L.J. and Caloni, F. 2013. Fusarium mycotoxins: effects on reproductive function in domestic animals--a review. Theriogenology 80, 557-564.

Costa, M.A. 2016. The endocrine function of human placenta: an overview. Reproductive biomedicine online 32, 14-43.

Coutifaris, C., Kao, L.C., Sehdev, H.M., Chin, U., Babalola, G.O., Blaschuk, O.W. and Strauss, J.F., 3rd. 1991. E-cadherin expression during the differentiation of human trophoblasts. Development 113, 767-777.

Cronier, L., Guibourdenche, J., Niger, C. and Malassine, A. 1999. Oestradiol stimulates morphological and functional differentiation of human villous cytotrophoblast. Placenta 20, 669-676.

Cui, Y., Konig, J., Buchholz, J.K., Spring, H., Leier, I. and Keppler, D. 1999. Drug resistance and ATP-dependent conjugate transport mediated by the apical multidrug resistance protein, MRP2, permanently expressed in human and canine cells. Mol Pharmacol 55, 929-937.

Cunningham, F.G. 2014. Williams obstetrics, McGraw-Hill Medical, New York.

Cusatis, G., Gregorc, V., Li, J., Spreafico, A., Ingersoll, R.G., Verweij, J., Ludovini, V., Villa, E., Hidalgo, M., Sparreboom, A. and Baker, S.D. 2006. Pharmacogenetics of ABCG2 and adverse reactions to gefitinib. J Natl Cancer Inst 98, 1739-1742.

Dabelea, D., Snell-Bergeon, J.K., Hartsfield, C.L., Bischoff, K.J., Hamman, R.F. and McDuffie, R.S. 2005. Increasing prevalence of gestational diabetes mellitus (GDM) over time and by birth cohort. Diabetes Care 28, 579-584.

Dallmann, A., Liu, X.I., Burckart, G.J. and van den Anker, J. 2019. Drug Transporters Expressed in the Human Placenta and Models for Studying Maternal-Fetal Drug Transfer. J Clin Pharmacol 59 Suppl 1, S70-S81.

Dankers, A.C., Roelofs, M.J., Piersma, A.H., Sweep, F.C., Russel, F.G., van den Berg, M., van Duursen, M.B. and Masereeuw, R. 2013. Endocrine disruptors differentially target ATP-binding cassette transporters in the blood-testis barrier and affect Leydig cell testosterone secretion in vitro. Toxicological sciences : an official journal of the Society of Toxicology 136, 382-391.

Dauchy, S., Miller, F., Couraud, P.O., Weaver, R.J., Weksler, B., Romero, I.A., Scherrmann, J.M., De Waziers, I. and Decleves, X. 2009. Expression and transcriptional regulation of ABC transporters and cytochromes P450 in hCMEC/D3 human cerebral microvascular endothelial cells. Biochemical pharmacology 77, 897-909.

De Baere, S., Osselaere, A., Devreese, M., Vanhaecke, L., De Backer, P. and Croubels, S. 2012. Development of a liquid-chromatography tandem mass spectrometry and ultra-high-performance liquid chromatography high-resolution mass spectrometry method for the quantitative determination of zearalenone and its major metabolites in chicken and pig plasma. Analytica chimica acta 756, 37-48.

Delidaki, M., Gu, M., Hein, A., Vatish, M. and Grammatopoulos, D.K. 2011. Interplay of cAMP and MAPK pathways in hCG secretion and fusogenic gene expression in a trophoblast cell line. Mol Cell Endocrinol 332, 213-220.

Deng, L., Lin-Lee, Y.C., Claret, F.X. and Kuo, M.T. 2001. 2-acetylaminofluorene up-regulates rat mdr1b expression through generating reactive oxygen species that activate NF-kappa B pathway. The Journal of biological chemistry 276, 413-420.

DeSisto, C.L., Kim, S.Y. and Sharma, A.J. 2014. Prevalence estimates of gestational diabetes mellitus in the United States, pregnancy risk assessment monitoring system (PRAMS), 2007-2010. Prev Chronic Dis 11, E104.

Di Pietro, A., Conseil, G., Perez-Victoria, J.M., Dayan, G., Baubichon-Cortay, H., Trompier, D., Steinfels, E., Jault, J.M., de Wet, H., Maitrejean, M., Comte, G., Boumendjel, A., Mariotte, A.M., Dumontet, C., McIntosh, D.B., Goffeau, A., Castanys, S., Gamarro, F. and Barron, D. 2002. Modulation by flavonoids of cell multidrug resistance mediated by P-glycoprotein and related ABC transporters. Cell. Mol. Life Sci. 59, 307-322.

Dietrich, C.G., de Waart, D.R., Ottenhoff, R., Schoots, I.G. and Elferink, R.P. 2001. Increased bioavailability of the food-derived carcinogen 2-amino-1-methyl-6-phenylimidazo[4,5-b]pyridine in MRP2-deficient rats. Mol Pharmacol 59, 974-980.

Ding, R., Jin, S., Pabon, K. and Scotto, K.W. 2016. A role for ABCG2 beyond drug transport: Regulation of autophagy. Autophagy 12, 737-751.

Dokmanovic, M., Clarke, C. and Marks, P.A. 2007. Histone deacetylase inhibitors: overview and perspectives. Mol Cancer Res 5, 981-989.

Doyle, L.A., Yang, W., Abruzzo, L.V., Krogmann, T., Gao, Y., Rishi, A.K. and Ross, D.D. 1998. A multidrug resistance transporter from human MCF-7 breast cancer cells. Proc Natl Acad Sci U S A 95, 15665-15670.

Draheim, V., Reichel, A., Weitschies, W. and Moenning, U. 2010. N-glycosylation of ABC transporters is associated with functional activity in sandwich-cultured rat hepatocytes. Eur J Pharm Sci 41, 201-209.

Dressing, G.E., Hagan, C.R., Knutson, T.P., Daniel, A.R. and Lange, C.A. 2009. Progesterone receptors act as sensors for mitogenic protein kinases in breast cancer models. Endocrine-related cancer 16, 351-361.

Duan, H., Wang, C., Zhou, K., Wang, T., Li, Y., Qiu, D., Li, Q., Zhang, Y. and Hua, Y. 2017a. The effect of histone deacetylase inhibition on the expression of P-glycoprotein in human placental trophoblast cell lines. Placenta 49, 37-47.

Duan, H., Zhou, K., Zhang, Y., Yue, P., Wang, T., Li, Y., Qiu, D., Wu, J., Hua, Y. and Wang, C. 2017b. HDAC2 was involved in placental P-glycoprotein regulation both in vitro and vivo. Placenta 58, 105-114.

Dubey, R., Malhotra, S.S. and Gupta, S.K. 2018. Forskolin-mediated BeWo cell fusion involves down-regulation of miR-92a-1-5p that targets dysferlin and protein kinase cAMP-activated catalytic subunit alpha. Am J Reprod Immunol 79, e12834.

Duley, L. 2009. The global impact of pre-eclampsia and eclampsia. Semin Perinatol 33, 130-137.

Durmus, S., Sparidans, R.W., van Esch, A., Wagenaar, E., Beijnen, J.H. and Schinkel, A.H. 2015. Breast cancer resistance protein (BCRP/ABCG2) and P-glycoprotein (P-GP/ABCB1) restrict oral availability and brain accumulation of the PARP inhibitor rucaparib (AG-014699). Pharm Res 32, 37-46.

Durmus, S., Sparidans, R.W., Wagenaar, E., Beijnen, J.H. and Schinkel, A.H. 2012. Oral availability and brain penetration of the B-RAFV600E inhibitor vemurafenib can be enhanced by the P-GLYCOprotein (ABCB1) and breast cancer resistance protein (ABCG2) inhibitor elacridar. Molecular pharmaceutics 9, 3236-3245.

Ebert, B., Seidel, A. and Lampen, A. 2005. Identification of BCRP as transporter of benzo[a]pyrene conjugates metabolically formed in Caco-2 cells and its induction by Ah-receptor agonists. Carcinogenesis 26, 1754-1763.

Ebert, B., Seidel, A. and Lampen, A. 2007. Phytochemicals induce breast cancer resistance protein in Caco-2 cells and enhance the transport of benzo[a]pyrene-3-sulfate. Toxicol. Sci. 96, 227-236.

Edavana, V.K., Penney, R.B., Yao-Borengasser, A., Williams, S., Rogers, L., Dhakal, I.B. and Kadlubar, S. 2013. Fulvestrant up regulates UGT1A4 and MRPs through ERalpha and c-Myb pathways: a possible primary drug disposition mechanism. Springerplus 2, 620.

Edgar, R., Domrachev, M. and Lash, A.E. 2002. Gene Expression Omnibus: NCBI gene expression and hybridization array data repository. Nucleic acids research 30, 207-210.

Edwards, D.P., Altmann, M., DeMarzo, A., Zhang, Y., Weigel, N.L. and Beck, C.A. 1995. Progesterone receptor and the mechanism of action of progesterone antagonists. The Journal of steroid biochemistry and molecular biology 53, 449-458.

Edwards, S., Cantley, T.C., Rottinghaus, G.E., Osweiler, G.D. and Day, B.N. 1987. The effects of zearalenone on reproduction in swine. I. The relationship between ingested zearalenone dose and anestrus in non-pregnant, sexually mature gilts. Theriogenology 28, 43-49.

Ee, P.L., He, X., Ross, D.D. and Beck, W.T. 2004a. Modulation of breast cancer resistance protein (BCRP/ABCG2) gene expression using RNA interference. Molecular cancer therapeutics 3, 1577-1583.

Ee, P.L., Kamalakaran, S., Tonetti, D., He, X., Ross, D.D. and Beck, W.T. 2004b. Identification of a novel estrogen response element in the breast cancer resistance protein (ABCG2) gene. Cancer research 64, 1247-1251.

Ee, P.L.R., Kamalakaran, S., Tonetti, D., He, X., Ross, D.D. and Beck, W.T. 2004c. Identification of a novel estrogen response element in the breast cancer resistance protein (ABCG2) gene. Cancer Research 64, 1247-1251.

El-Khoury, V., Breuzard, G., Fourre, N. and Dufer, J. 2007. The histone deacetylase inhibitor trichostatin A downregulates human MDR1 (ABCB1) gene expression by a transcription-dependent mechanism in a drug-resistant small cell lung carcinoma cell line model. Br J Cancer 97, 562-573.

El Kasmi, K.C., Anderson, A.L., Devereaux, M.W., Fillon, S.A., Harris, J.K., Lovell, M.A., Finegold, M.J. and Sokol, R.J. 2012. Toll-like receptor 4-dependent Kupffer cell activation and liver injury in a novel mouse model of parenteral nutrition and intestinal injury. Hepatology 55, 1518-1528.

El Kasmi, K.C., Anderson, A.L., Devereaux, M.W., Vue, P.M., Zhang, W., Setchell, K.D., Karpen, S.J. and Sokol, R.J. 2013. Phytosterols promote liver injury and Kupffer cell activation in parenteral nutrition-associated liver disease. Science translational medicine 5, 206ra137.

Eldasher, L.M., Wen, X., Little, M.S., Bircsak, K.M., Yacovino, L.L. and Aleksunes, L.M. 2013. Hepatic and renal Bcrp transporter expression in mice treated with perfluorooctanoic acid. Toxicology 306, 108-113.

Enokizono, J., Kusuhara, H. and Sugiyama, Y. 2007a. Effect of breast cancer resistance protein (Bcrp/Abcg2) on the disposition of phytoestrogens. Mol. Pharmacol. 72, 967-975.

Enokizono, J., Kusuhara, H. and Sugiyama, Y. 2007b. Effect of breast cancer resistance protein (Bcrp/Abcg2) on the disposition of phytoestrogens. Mol Pharmacol 72, 967-975.

Erdei, Z., Sarkadi, B., Brozik, A., Szebenyi, K., Varady, G., Mako, V., Pentek, A., Orban, T.I. and Apati, A. 2013. Dynamic ABCG2 expression in human embryonic stem cells provides the basis for stress response. Eur Biophys J 42, 169-179.

Erkan, E., Devarajan, P. and Schwartz, G.J. 2005. Apoptotic response to albumin overload: proximal vs. distal/collecting tubule cells. American journal of nephrology 25, 121-131.

Errasti-Murugarren, E., Diaz, P., Godoy, V., Riquelme, G. and Pastor-Anglada, M. 2011. Expression and distribution of nucleoside transporter proteins in the human syncytiotrophoblast. Molecular pharmacology 80, 809-817.

Etienne, M. and Jemmali, M. 1982. Effects of zearalenone (F2) on estrous activity and reproduction in gilts. J Anim Sci 55, 1-10.

Evers, R., Cnubben, N.H., Wijnholds, J., van Deemter, L., van Bladeren, P.J. and Borst, P. 1997. Transport of glutathione prostaglandin A conjugates by the multidrug resistance protein 1. FEBS Lett 419, 112-116.

Evseenko, D.A., Murthi, P., Paxton, J.W., Reid, G., Emerald, B.S., Mohankumar, K.M., Lobie, P.E., Brennecke, S.P., Kalionis, B. and Keelan, J.A. 2007a. The ABC transporter BCRP/ABCG2 is a placental survival factor, and its expression is reduced in idiopathic human fetal growth restriction. FASEB journal : official publication of the Federation of American Societies for Experimental Biology 21, 3592-3605.

Evseenko, D.A., Paxton, J.W. and Keelan, J.A. 2006. ABC drug transporter expression and functional activity in trophoblast-like cell lines and differentiating primary trophoblast. American journal of physiology. Regulatory, integrative and comparative physiology 290, R1357-1365.

Evseenko, D.A., Paxton, J.W. and Keelan, J.A. 2007b. Independent regulation of apical and basolateral drug transporter expression and function in placental trophoblasts by cytokines, steroids, and growth factors. Drug Metab Dispos 35, 595-601.

Evseenko, D.A., Paxton, J.W. and Keelan, J.A. 2007c. The xenobiotic transporter ABCG2 plays a novel role in differentiation of trophoblast-like BeWo cells. Placenta 28 Suppl A, S116-120.

Fang, M., Webster, T.F., Ferguson, P.L. and Stapleton, H.M. 2015a. Characterizing the peroxisome proliferator-activated receptor (PPARgamma) ligand binding potential of several major flame retardants, their metabolites, and chemical mixtures in house dust. Environ Health Perspect 123, 166-172.

Fang, M., Webster, T.F. and Stapleton, H.M. 2015b. Activation of Human Peroxisome Proliferator-Activated Nuclear Receptors (PPARgamma1) by Semi-Volatile Compounds (SVOCs) and Chemical Mixtures in Indoor Dust. Environ Sci Technol 49, 10057-10064.

Feige, J.N., Gelman, L., Rossi, D., Zoete, V., Metivier, R., Tudor, C., Anghel, S.I., Grosdidier, A., Lathion, C., Engelborghs, Y., Michielin, O., Wahli, W. and Desvergne, B. 2007. The endocrine disruptor monoethyl-hexyl-phthalate is a selective peroxisome proliferator-activated receptor gamma modulator that promotes adipogenesis. J Biol Chem 282, 19152-19166.

Feinman, M.A., Kliman, H.J., Caltabiano, S. and Strauss, J.F., 3rd. 1986. 8-Bromo-3',5'-adenosine monophosphate stimulates the endocrine activity of human cytotrophoblasts in culture. J Clin Endocrinol Metab 63, 1211-1217.

Feinshtein, V., Erez, O., Ben-Zvi, Z., Eshkoli, T., Sheizaf, B., Sheiner, E. and Holcberg, G. 2013. Cannabidiol enhances xenobiotic permeability through the human placental barrier by direct inhibition of breast cancer resistance protein: An ex vivo study. Am J Obstet Gynecol 209, 573 e571-573 e515.

Feldser, D., Agani, F., Iyer, N.V., Pak, B., Ferreira, G. and Semenza, G.L. 1999. Reciprocal positive regulation of hypoxia-inducible factor 1alpha and insulin-like growth factor 2. Cancer research 59, 3915-3918.

Fernandez, S.B., Hollo, Z., Kern, A., Bakos, E., Fischer, P.A., Borst, P. and Evers, R. 2002. Role of the N-terminal transmembrane region of the multidrug resistance protein MRP2 in routing to the apical membrane in MDCKII cells. J Biol Chem 277, 31048-31055.

Ferrara, A. 2007. Increasing prevalence of gestational diabetes mellitus: A public health perspective. Diabetes Care 30 Suppl 2, S141-146.

Fitzpatrick, D.W., Picken, C.A., Murphy, L.C. and Buhr, M.M. 1989. Measurement of the relative binding affinity of zearalenone, alpha-zearalenol and beta-zearalenol for uterine and oviduct estrogen receptors in swine, rats and chickens: an indicator of estrogenic potencies. Comp Biochem Physiol C 94, 691-694.

Fleck, S.C., Churchwell, M.I., Doerge, D.R. and Teeguarden, J.G. 2016. Urine and serum biomonitoring of exposure to environmental estrogens II: Soy isoflavones and zearalenone in pregnant women. Food and chemical toxicology : an international journal published for the British Industrial Biological Research Association 95, 19-27.

Flens, M.J., Zaman, G.J., van der Valk, P., Izquierdo, M.A., Schroeijers, A.B., Scheffer, G.L., van der Groep, P., de Haas, M., Meijer, C.J. and Scheper, R.J. 1996. Tissue distribution of the multidrug resistance protein. Am J Pathol 148, 1237-1247.

Flowers, B., Cantley, T. and Day, B.N. 1987. A comparison of effects of zearalenone and estradiol benzoate on reproductive function during the estrous cycle in gilts. J Anim Sci 65, 1576-1584.

Fouassier, L., Beaussier, M., Schiffer, E., Rey, C., Barbu, V., Mergey, M., Wendum, D., Callard, P., Scoazec, J.Y., Lasnier, E., Stieger, B., Lienhart, A. and Housset, C. 2007. Hypoxia-induced changes in the expression of rat hepatobiliary transporter genes. American journal of physiology. Gastrointestinal and liver physiology 293, G25-35.

Francois, L.N., Gorczyca, L., Du, J., Bircsak, K.M., Yen, E., Wen, X., Tu, M.J., Yu, A.M., Illsley, N.P., Zamudio, S. and Aleksunes, L.M. 2017. Down-regulation of the placental BCRP/ABCG2 transporter in response to hypoxia signaling. Placenta 51, 57-63.

Frankenfeld, C.L., Patterson, R.E., Horner, N.K., Neuhouser, M.L., Skor, H.E., Kalhorn, T.F., Howald, W.N. and Lampe, J.W. 2003. Validation of a soy food-frequency questionnaire and evaluation of correlates of plasma isoflavone concentrations in postmenopausal women. Am. J. Clin. Nutr. 77, 674-680.

Frommel, T.O., Coon, J.S., Tsuruo, T. and Roninson, I.B. 1993. Variable effects of sodium butyrate on the expression and function of the MDR1 (P-glycoprotein) gene in colon carcinoma cell lines. Int J Cancer 55, 297-302.

Fukuda, R., Hirota, K., Fan, F., Jung, Y.D., Ellis, L.M. and Semenza, G.L. 2002. Insulin-like growth factor 1 induces hypoxia-inducible factor 1-mediated vascular endothelial growth factor expression, which is dependent on MAP kinase and phosphatidylinositol 3-kinase signaling in colon cancer cells. J Biol Chem 277, 38205-38211.

Furukawa, T., Wakabayashi, K., Tamura, A., Nakagawa, H., Morishima, Y., Osawa, Y. and Ishikawa, T. 2009. Major SNP (Q141K) variant of human ABC transporter ABCG2 undergoes lysosomal and proteasomal degradations. Pharm Res 26, 469-479.

Gahir, S.S. and Piquette-Miller, M. 2011. Gestational and pregnane X receptor-mediated regulation of placental ATP-binding cassette drug transporters in mice. Drug metabolism and disposition: the biological fate of chemicals 39, 465-471.

Galanis, E., Jaeckle, K.A., Maurer, M.J., Reid, J.M., Ames, M.M., Hardwick, J.S., Reilly, J.F., Loboda, A., Nebozhyn, M., Fantin, V.R., Richon, V.M., Scheithauer, B., Giannini, C., Flynn, P.J., Moore, D.F., Jr., Zwiebel, J. and Buckner, J.C. 2009. Phase II trial of vorinostat in recurrent glioblastoma multiforme: a north central cancer treatment group study. J Clin Oncol 27, 2052-2058.

Gambino, Y.P., Perez Perez, A., Duenas, J.L., Calvo, J.C., Sanchez-Margalet, V. and Varone, C.L. 2012. Regulation of leptin expression by 17beta-estradiol in human placental cells involves membrane associated estrogen receptor alpha. Biochim Biophys Acta 1823, 900-910.

Gao, H.L., Xia, Y.Z., Zhang, Y.L., Yang, L. and Kong, L.Y. 2019. Vielanin P enhances the cytotoxicity of doxorubicin via the inhibition of PI3K/Nrf2-stimulated MRP1 expression in MCF-7 and K562 DOX-resistant cell lines. Phytomedicine 58, 152885.

Gao, M., Yamazaki, M., Loe, D.W., Westlake, C.J., Grant, C.E., Cole, S.P. and Deeley, R.G. 1998. Multidrug resistance protein. Identification of regions required for active transport of leukotriene C4. J Biol Chem 273, 10733-10740.

Gao, X., Sun, L., Zhang, N., Li, C., Zhang, J., Xiao, Z. and Qi, D. 2017. Gestational Zearalenone Exposure Causes Reproductive and Developmental Toxicity in Pregnant Rats and Female Offspring. Toxins (Basel) 9.

Gapter, L.A., Magnuson, N.S., Ng, K.Y. and Hosick, H.L. 2006. Pim-1 kinase expression during murine mammary development. Biochemical and biophysical research communications 345, 989-997.

Gardner, C.D., Chatterjee, L.M. and Franke, A.A. 2009. Effects of isoflavone supplements vs. soy foods on blood concentrations of genistein and daidzein in adults. J. Nutr. Biochem. 20, 227-234.

Gathiram, P. and Moodley, J. 2016. Pre-eclampsia: its pathogenesis and pathophysiolgy. Cardiovasc J Afr 27, 71-78.

Gedeon, C., Anger, G., Lubetsky, A., Miller, M.P. and Koren, G. 2008a. Investigating the potential role of multi-drug resistance protein (MRP) transporters in fetal to maternal glyburide efflux in the human placenta. J Obstet Gynaecol 28, 485-489.

Gedeon, C., Anger, G., Piquette-Miller, M. and Koren, G. 2008b. Breast cancer resistance protein: mediating the trans-placental transfer of glyburide across the human placenta. Placenta 29, 39-43.

Gedeon, C., Behravan, J., Koren, G. and Piquette-Miller, M. 2006. Transport of glyburide by placental ABC transporters: Implications in fetal drug exposure. Placenta 27, 1096-1102.

Geick, A., Eichelbaum, M. and Burk, O. 2001. Nuclear receptor response elements mediate induction of intestinal MDR1 by rifampin. J Biol Chem 276, 14581-14587.

Genbacev, O., Zhou, Y., Ludlow, J.W. and Fisher, S.J. 1997. Regulation of human placental development by oxygen tension. Science 277, 1669-1672.

Gerbaud, P. and Pidoux, G. 2015a. Review: An overview of molecular events occurring in human trophoblast fusion. Placenta 36 Suppl 1, S35-42.

Gerbaud, P., Tasken, K. and Pidoux, G. 2015b. Spatiotemporal regulation of cAMP signaling controls the human trophoblast fusion. Front Pharmacol 6, 202.

Getsios, S., Chen, G.T. and MacCalman, C.D. 2000. Regulation of beta-catenin mRNA and protein levels in human villous cytotrophoblasts undergoing aggregation and fusion in vitro: correlation with E-cadherin expression. J Reprod Fertil 119, 59-68.

Ghanem, C.I., Rudraiah, S., Bataille, A.M., Vigo, M.B., Goedken, M.J. and Manautou, J.E. 2015. Role of nuclear factor-erythroid 2-related factor 2 (Nrf2) in the transcriptional regulation of brain ABC transporters during acute acetaminophen (APAP) intoxication in mice. Biochemical pharmacology 94, 203-211.

Giacomini, K.M., Balimane, P.V., Cho, S.K., Eadon, M., Edeki, T., Hillgren, K.M., Huang, S.M., Sugiyama, Y., Weitz, D., Wen, Y., Xia, C.Q., Yee, S.W., Zimdahl, H. and Niemi, M. 2013. International Transporter Consortium commentary on clinically important transporter polymorphisms. Clin Pharmacol Ther 94, 23-26.

Glaser, K.B. 2007. HDAC inhibitors: clinical update and mechanism-based potential. Biochem Pharmacol 74, 659-671.

Gluckman, P.D. and Hanson, M.A. 2004. Living with the past: evolution, development, and patterns of disease. Science 305, 1733-1736.

Goldsmith, M.E., Madden, M.J., Morrow, C.S. and Cowan, K.H. 1993. A Y-box consensus sequence is required for basal expression of the human multidrug resistance (mdr1) gene. J Biol Chem 268, 5856-5860.

Goodman, J.E., McConnell, E.E., Sipes, I.G., Witorsch, R.J., Slayton, T.M., Yu, C.J., Lewis, A.S. and Rhomberg, L.R. 2006. An updated weight of the evidence evaluation of reproductive and developmental effects of low doses of bisphenol A. Crit Rev Toxicol 36, 387-457.

Gorczyca, L. and Aleksunes, L.M. 2020. Transcription factor-mediated regulation of the BCRP/ABCG2 efflux transporter: a review across tissues and species. Expert Opin Drug Metab Toxicol 16, 239-253.

Gorlach, A., Diebold, I., Schini-Kerth, V.B., Berchner-Pfannschmidt, U., Roth, U., Brandes, R.P., Kietzmann, T. and Busse, R. 2001. Thrombin activates the hypoxia-inducible factor-1 signaling pathway in vascular smooth muscle cells: Role of the p22(phox)-containing NADPH oxidase. Circ Res 89, 47-54.

Granberg, L., Ostergren, A., Brandt, I. and Brittebo, E.B. 2003. CYP1A1 and CYP1B1 in blood-brain interfaces: CYP1A1-dependent bioactivation of 7,12-dimethylbenz(a)anthracene in endothelial cells. Drug metabolism and disposition: the biological fate of chemicals 31, 259-265.

Gromnicova, R., Romero, I. and Male, D. 2012. Transcriptional control of the multi-drug transporter ABCB1 by transcription factor Sp3 in different human tissues. PLoS One 7, e48189.

Grube, M., Meyer Zu Schwabedissen, H., Draber, K., Prager, D., Moritz, K.U., Linnemann, K., Fusch, C., Jedlitschky, G. and Kroemer, H.K. 2005. Expression, localization, and function of the carnitine transporter octn2 (slc22a5) in human placenta. Drug Metab Dispos 33, 31-37.

Grube, M., Reuther, S., Meyer Zu Schwabedissen, H., Kock, K., Draber, K., Ritter, C.A., Fusch, C., Jedlitschky, G. and Kroemer, H.K. 2007. Organic anion transporting polypeptide 2B1 and breast cancer resistance protein interact in the transepithelial transport of steroid sulfates in human placenta. Drug Metab Dispos 35, 30-35.

Gude, N.M., Roberts, C.T., Kalionis, B. and King, R.G. 2004. Growth and function of the normal human placenta. Thromb Res 114, 397-407.

Guo, J., Yuan, X., Qiu, L., Zhu, W., Wang, C., Hu, G., Chu, Y., Ye, L., Xu, Y. and Ge, R.S. 2012. Inhibition of human and rat 11beta-hydroxysteroid dehydrogenases activities by bisphenol A. Toxicol Lett 215, 126-130.

Gupta, M., Solanki, M.H., Chatterjee, P.K., Xue, X., Roman, A., Desai, N., Rochelson, B. and Metz, C.N. 2014. Maternal magnesium deficiency in mice leads to maternal metabolic dysfunction and altered lipid metabolism with fetal growth restriction. Mol Med 20, 332-340.

Gupta, S.K., Malhotra, S.S., Malik, A., Verma, S. and Chaudhary, P. 2016. Cell Signaling Pathways Involved During Invasion and Syncytialization of Trophoblast Cells. American journal of reproductive immunology 75, 361-371.

Hagiya, Y., Adachi, T., Ogura, S., An, R., Tamura, A., Nakagawa, H., Okura, I., Mochizuki, T. and Ishikawa, T. 2008. Nrf2-dependent induction of human ABC transporter ABCG2 and heme oxygenase-1 in HepG2 cells by photoactivation of porphyrins: biochemical implications for cancer cell response to photodynamic therapy. Journal of experimental therapeutics & oncology 7, 153-167.

Hahnova-Cygalova, L., Ceckova, M. and Staud, F. 2011. Fetoprotective activity of breast cancer resistance protein (BCRP, ABCG2): expression and function throughout pregnancy. Drug Metab Rev 43, 53-68.

Han, Y. and Sugiyama, Y. 2006. Expression and regulation of breast cancer resistance protein and multidrug resistance associated protein 2 in BALB/c mice. Biological & pharmaceutical bulletin 29, 1032-1035.

Harrison, I.F. and Dexter, D.T. 2013. Epigenetic targeting of histone deacetylase: therapeutic potential in Parkinson's disease? Pharmacol Ther 140, 34-52.

Harrison, S.C. 2008. Viral membrane fusion. Nat Struct Mol Biol 15, 690-698.

Hartz, A.M., Madole, E.K., Miller, D.S. and Bauer, B. 2010a. Estrogen receptor beta signaling through phosphatase and tensin homolog/phosphoinositide 3-kinase/Akt/glycogen synthase kinase 3 down-regulates blood-brain barrier breast cancer resistance protein. The Journal of pharmacology and experimental therapeutics 334, 467-476.

Hartz, A.M., Mahringer, A., Miller, D.S. and Bauer, B. 2010b. 17-beta-Estradiol: a powerful modulator of blood-brain barrier BCRP activity. Journal of cerebral blood flow and metabolism : official journal of the International Society of Cerebral Blood Flow and Metabolism 30, 1742-1755.

Hashimoto, K., Uchiumi, T., Konno, T., Ebihara, T., Nakamura, T., Wada, M., Sakisaka, S., Maniwa, F., Amachi, T., Ueda, K. and Kuwano, M. 2002. Trafficking and functional defects by mutations of the ATP-binding domains in MRP2 in patients with Dubin-Johnson syndrome. Hepatology 36, 1236-1245.

Hatherell, K., Couraud, P.O., Romero, I.A., Weksler, B. and Pilkington, G.J. 2011. Development of a three-dimensional, all-human in vitro model of the blood-brain barrier using mono-, co-, and tri-cultivation Transwell models. J Neurosci Methods 199, 223-229.

Hayashi, A., Suzuki, H., Itoh, K., Yamamoto, M. and Sugiyama, Y. 2003. Transcription factor Nrf2 is required for the constitutive and inducible expression of multidrug resistance-associated protein 1 in mouse embryo fibroblasts. Biochemical and biophysical research communications 310, 824-829.

Hayashi, M., Sakata, M., Takeda, T., Yamamoto, T., Okamoto, Y., Sawada, K., Kimura, A., Minekawa, R., Tahara, M., Tasaka, K. and Murata, Y. 2004. Induction of glucose transporter 1 expression through hypoxia-inducible factor 1alpha under hypoxic conditions in trophoblast-derived cells. The Journal of endocrinology 183, 145-154.

He, J., Wei, C., Li, Y., Liu, Y., Wang, Y., Pan, J., Liu, J., Wu, Y. and Cui, S. 2018. Zearalenone and alpha-zearalenol inhibit the synthesis and secretion of pig follicle stimulating hormone via the non-classical estrogen membrane receptor GPR30. Mol Cell Endocrinol 461, 43-54.

Heinonen, S., Ryynanen, M., Kirkinen, P. and Saarikoski, S. 1996. Elevated midtrimester maternal serum hCG in chromosomally normal pregnancies is associated with preeclampsia and velamentous umbilical cord insertion. Am J Perinatol 13, 437-441.

Hellwig-Burgel, T., Rutkowski, K., Metzen, E., Fandrey, J. and Jelkmann, W. 1999. Interleukin-1beta and tumor necrosis factor-alpha stimulate DNA binding of hypoxia-inducible factor-1. Blood 94, 1561-1567.

Hemauer, S.J., Patrikeeva, S.L., Nanovskaya, T.N., Hankins, G.D. and Ahmed, M.S. 2010a. Role of human placental apical membrane transporters in the efflux of glyburide, rosiglitazone, and metformin. Am J Obstet Gynecol 202, 383 e381-387.

Hemauer, S.J., Patrikeeva, S.L., Nanovskaya, T.N., Hankins, G.D.V. and Ahmed, M.S. 2010b. Role of human placental apical membrane transporters in the efflux of glyburide, rosiglitazone, and metformin. American journal of obstetrics and gynecology 202, 383.e381-383.e387.

Hemmings, D.G., Lowen, B., Sherburne, R., Sawicki, G. and Guilbert, L.J. 2001. Villous trophoblasts cultured on semi-permeable membranes form an effective barrier to the passage of high and low molecular weight particles. Placenta 22, 70-79.

Heneweer, M., Houtman, R., Poortman, J., Groot, M., Maliepaard, C. and Peijnenburg, A. 2007. Estrogenic effects in the immature rat uterus after dietary exposure to ethinylestradiol and zearalenone using a systems biology approach. Toxicol Sci 99, 303-314.

Henriksen, U., Gether, U. and Litman, T. 2005. Effect of Walker A mutation (K86M) on oligomerization and surface targeting of the multidrug resistance transporter ABCG2. J Cell Sci 118, 1417-1426.

Hidalgo, I.J., Raub, T.J. and Borchardt, R.T. 1989. Characterization of the human colon carcinoma cell line (Caco-2) as a model system for intestinal epithelial permeability. Gastroenterology 96, 736-749.

Hilakivi-Clarke, L., Cho, E. and Clarke, R. 1998. Maternal genistein exposure mimics the effects of estrogen on mammary gland development in female mouse offspring. Oncology reports 5, 609-616.

Hilf, G. and Merz, W.E. 1985. Influence of cyclic nucleotides on receptor binding, immunological activity, and microheterogeneity of human choriogonadotropin synthesized in placental tissue culture. Mol Cell Endocrinol 39, 151-159.

Hines, M. 2011. Prenatal endocrine influences on sexual orientation and on sexually differentiated childhood behavior. Frontiers in Neuroendocrinology 32, 170-182.

Hirai, T., Fukui, Y. and Motojima, K. 2007. PPARalpha agonists positively and negatively regulate the expression of several nutrient/drug transporters in mouse small intestine. Biol Pharm Bull 30, 2185-2190.

Hirohashi, T., Suzuki, H., Takikawa, H. and Sugiyama, Y. 2000. ATP-dependent transport of bile salts by rat multidrug resistance-associated protein 3 (Mrp3). J Biol Chem 275, 2905-2910.

Hiromori, Y., Nishikawa, J., Yoshida, I., Nagase, H. and Nakanishi, T. 2009. Structure-dependent activation of peroxisome proliferator-activated receptor (PPAR) gamma by organotin compounds. Chem Biol Interact 180, 238-244.

Holobotovskyy, V., Chong, Y.S., Burchell, J., He, B., Phillips, M., Leader, L., Murphy, T.V., Sandow, S.L., McKitrick, D.J., Charles, A.K., Tare, M., Arnolda, L.F. and Ganss, R. 2015. Regulator of G protein signaling 5 is a determinant of gestational hypertension and preeclampsia. Sci Transl Med 7, 290ra288.

Hong, L., Schroth, G.P., Matthews, H.R., Yau, P. and Bradbury, E.M. 1993. Studies of the DNA binding properties of histone H4 amino terminus. Thermal denaturation studies reveal that acetylation markedly reduces the binding constant of the H4 "tail" to DNA. J Biol Chem 268, 305-314.

Hoque, M.T., Robillard, K.R. and Bendayan, R. 2012. Regulation of breast cancer resistant protein by peroxisome proliferator-activated receptor alpha in human brain microvessel endothelial cells. Molecular pharmacology 81, 598-609.

Hoque, M.T., Shah, A., More, V., Miller, D.S. and Bendayan, R. 2015a. In vivo and ex vivo regulation of breast cancer resistant protein (Bcrp) by peroxisome proliferator-activated receptor alpha (Pparalpha) at the blood-brain barrier. J Neurochem 135, 1113-1122.

Hoque, M.T., Shah, A., More, V., Miller, D.S. and Bendayan, R. 2015b. In Vivo and Ex Vivo Regulation of Breast Cancer Resistant Protein (Bcrp) by Peroxisome Proliferator-Activated Receptor Alpha (Pparalpha) at the Blood-Brain Barrier. J Neurochem.

Huang, L., Wang, Y. and Grimm, S. 2006. ATP-dependent transport of rosuvastatin in membrane vesicles expressing breast cancer resistance protein. Drug Metab Dispos 34, 738-742.

Huang, L.E., Arany, Z., Livingston, D.M. and Bunn, H.F. 1996. Activation of hypoxia-inducible transcription factor depends primarily upon redox-sensitive stabilization of its alpha subunit. J Biol Chem 271, 32253-32259.

Huang, W., Wan, C., Luo, Q., Huang, Z. and Luo, Q. 2014. Genistein-inhibited cancer stem cell-like properties and reduced chemoresistance of gastric cancer. Int. J. Mol. Sci. 15, 3432-3443.

Huang, W., Zhang, J., Washington, M., Liu, J., Parant, J.M., Lozano, G. and Moore, D.D. 2005. Xenobiotic stress induces hepatomegaly and liver tumors via the nuclear receptor constitutive androstane receptor. Molecular endocrinology 19, 1646-1653.

Huang, X., Luthi, M., Ontsouka, E.C., Kallol, S., Baumann, M.U., Surbek, D.V. and Albrecht, C. 2016. Establishment of a confluent monolayer model with human primary trophoblast

cells: novel insights into placental glucose transport. Molecular human reproduction 22, 442-456.

Huppertz, B. 2008. The anatomy of the normal placenta. Journal of clinical pathology 61, 1296-1302.

Hussain, M., Banerjee, M., Sarkar, F.H., Djuric, Z., Pollak, M.N., Doerge, D., Fontana, J., Chinni, S., Davis, J., Forman, J., Wood, D.P. and Kucuk, O. 2003. Soy isoflavones in the treatment of prostate cancer. Nutr. Cancer 47, 111-117.

Huuskonen, P., Auriola, S. and Pasanen, M. 2015. Zearalenone metabolism in human placental subcellular organelles, JEG-3 cells, and recombinant CYP19A1. Placenta 36, 1052-1055.

Ibbotson, K., Yell, J. and Ronaldson, P.T. 2017. Nrf2 signaling increases expression of ATP-binding cassette subfamily C mRNA transcripts at the blood-brain barrier following hypoxia-reoxygenation stress. Fluids Barriers CNS 14, 6.

Ietta, F., Wu, Y., Winter, J., Xu, J., Wang, J., Post, M. and Caniggia, I. 2006. Dynamic HIF1A regulation during human placental development. Biology of reproduction 75, 112-121.

Iguchi, T., Tani, N., Sato, T., Fukatsu, N. and Ohta, Y. 1993. Developmental changes in mouse placental cells from several stages of pregnancy in vivo and in vitro. Biol Reprod 48, 188-196.

Ikeda, K., Yamasaki, K., Homemoto, M., Yamaue, S., Ogawa, M., Nakao, E., Fukunaga, Y., Nakanishi, T., Utoguchi, N., Myotoku, M. and Hirotani, Y. 2012. Efflux transporter mRNA expression profiles in differentiating JEG-3 human choriocarcinoma cells as a placental transport model. Pharmazie 67, 86-90.

Imai, Y., Asada, S., Tsukahara, S., Ishikawa, E., Tsuruo, T. and Sugimoto, Y. 2003. Breast cancer resistance protein exports sulfated estrogens but not free estrogens. Molecular pharmacology 64, 610-618.

Imai, Y., Ishikawa, E., Asada, S. and Sugimoto, Y. 2005a. Estrogen-mediated post transcriptional down-regulation of breast cancer resistance protein/ABCG2. Cancer research 65, 596-604.

Imai, Y., Ishikawa, E., Asada, S. and Sugimoto, Y. 2005b. Estrogen-mediated post transcriptional down-regulation of breast cancer resistance protein/ABCG2. Cancer Research 65, 596-604.

Imai, Y., Nakane, M., Kage, K., Tsukahara, S., Ishikawa, E., Tsuruo, T., Miki, Y. and Sugimoto, Y. 2002. C421A polymorphism in the human breast cancer resistance protein gene is associated with low expression of Q141K protein and low-level drug resistance. Mol Cancer Ther 1, 611-616.

Imai, Y., Tsukahara, S., Asada, S. and Sugimoto, Y. 2004. Phytoestrogens/Flavonoids reverse breast cancer resistance protein/ABCG2-mediated multidrug resistance. Cancer Research 64, 4346-4352.

Inadera, H. and Shimomura, A. 2005. Environmental chemical tributyltin augments adipocyte differentiation. Toxicol Lett 159, 226-234.

Inagaki, T., Choi, M., Moschetta, A., Peng, L., Cummins, C.L., McDonald, J.G., Luo, G., Jones, S.A., Goodwin, B., Richardson, J.A., Gerard, R.D., Repa, J.J., Mangelsdorf, D.J. and Kliewer, S.A. 2005. Fibroblast growth factor 15 functions as an enterohepatic signal to regulate bile acid homeostasis. Cell metabolism 2, 217-225.

Ingram, W.J., Crowther, L.M., Little, E.B., Freeman, R., Harliwong, I., Veleva, D., Hassall, T.E., Remke, M., Taylor, M.D. and Hallahan, A.R. 2013. ABC transporter activity linked to radiation resistance and molecular subtype in pediatric medulloblastoma. Exp Hematol Oncol 2, 26.

Inoue, A. and Fujimoto, D. 1969. Enzymatic deacetylation of histone. Biochem Biophys Res Commun 36, 146-150.

Inoue, K. and Creveling, C.R. 1991. Induction of catechol-O-methyltransferase in the luminal epithelium of rat uterus by progesterone. J Histochem Cytochem 39, 823-828.

Inoue, K. and Creveling, C.R. 1995. Induction of catechol-O-methyltransferase in the luminal epithelium of rat uterus by progesterone: inhibition by RU-486. Drug metabolism and disposition: the biological fate of chemicals 23, 430-432.

Iqbal, M., Audette, M.C., Petropoulos, S., Gibb, W. and Matthews, S.G. 2012. Placental drug transporters and their role in fetal protection. Placenta 33, 137-142.

Iqbal, S.Z., Asi, M.R., Jinap, S. and Rashid, U. 2014a. Detection of aflatoxins and zearalenone contamination in wheat derived products. Food Control 35, 223-226.

Iqbal, S.Z., Asi, M.R., Jinap, S. and Rashid, U. 2014b. Detection of aflatoxins and zearalenone contamination in wheat derived products. Food Control 35, 223-226.

Ishikawa, T. and Ali-Osman, F. 1993. Glutathione-associated cis-diamminedichloroplatinum(II) metabolism and ATP-dependent efflux from leukemia cells. Molecular characterization of glutathione-platinum complex and its biological significance. J Biol Chem 268, 20116-20125.

Jacob, A., Potin, S., Saubamea, B., Crete, D., Scherrmann, J.M., Curis, E., Peyssonnaux, C. and Decleves, X. 2015. Hypoxia interferes with aryl hydrocarbon receptor pathway in hCMEC/D3 human cerebral microvascular endothelial cells. Journal of neurochemistry 132, 373-383.

Jacobson, G.F., Ramos, G.A., Ching, J.Y., Kirby, R.S., Ferrara, A. and Field, D.R. 2005. Comparison of glyburide and insulin for the management of gestational diabetes in a large managed care organization. Am J Obstet Gynecol 193, 118-124.

Javam, M., Audette, M.C., Iqbal, M., Bloise, E., Gibb, W. and Matthews, S.G. 2014. Effect of oxygen on multidrug resistance in term human placenta. Placenta 35, 324-330.

Jebbink, J., Veenboer, G., Boussata, S., Keijser, R., Kremer, A.E., Elferink, R.O., van der Post, J., Afink, G. and Ris-Stalpers, C. 2015a. Total bile acids in the maternal and fetal compartment in relation to placental ABCG2 expression in preeclamptic pregnancies complicated by HELLP syndrome. Biochim Biophys Acta 1852, 131-136.

Jebbink, J., Veenboer, G., Boussata, S., Keijser, R., Kremer, A.E., Elferink, R.O., van der Post, J., Afink, G. and Ris-Stalpers, C. 2015b. Total bile acids in the maternal and fetal compartment in relation to placental ABCG2 expression in preeclamptic pregnancies complicated by HELLP syndrome. Biochimica et Biophysica Acta (BBA) - Molecular Basis of Disease 1852, 131-136.

Jedlitschky, G., Burchell, B. and Keppler, D. 2000. The multidrug resistance protein 5 functions as an ATP-dependent export pump for cyclic nucleotides. J Biol Chem 275, 30069-30074.

Jedlitschky, G., Leier, I., Buchholz, U., Hummel-Eisenbeiss, J., Burchell, B. and Keppler, D. 1997. ATP-dependent transport of bilirubin glucuronides by the multidrug resistance protein MRP1 and its hepatocyte canalicular isoform MRP2. Biochem J 327 (Pt 1), 305-310.

Jefferson, W.N., Padilla-Banks, E., Clark, G. and Newbold, R.R. 2002. Assessing estrogenic activity of phytochemicals using transcriptional activation and immature mouse uterotrophic responses. J Chromatogr B Analyt Technol Biomed Life Sci 777, 179-189.

Jeong, H.S., Ryoo, I.G. and Kwak, M.K. 2015. Regulation of the expression of renal drug transporters in KEAP1-knockdown human tubular cells. Toxicology in vitro : an international journal published in association with BIBRA 29, 884-892.

Jeong, W., Bazer, F.W., Song, G. and Kim, J. 2016. Expression of hypoxia-inducible factor-1 by trophectoderm cells in response to hypoxia and epidermal growth factor. Biochem Biophys Res Commun 469, 176-182.

Ji, L., Li, H., Gao, P., Shang, G., Zhang, D.D., Zhang, N. and Jiang, T. 2013. Nrf2 pathway regulates multidrug-resistance-associated protein 1 in small cell lung cancer. PloS one 8, e63404.

Jia, R.Z., Zhang, X., Hu, P., Liu, X.M., Hua, X.D., Wang, X. and Ding, H.J. 2012. Screening for differential methylation status in human placenta in preeclampsia using a CpG island plus promoter microarray. Int J Mol Med 30, 133-141.

Jigorel, E., Le Vee, M., Boursier-Neyret, C., Parmentier, Y. and Fardel, O. 2006. Differential regulation of sinusoidal and canalicular hepatic drug transporter expression by xenobiotics activating drug-sensing receptors in primary human hepatocytes. Drug Metab Dispos 34, 1756-1763.

Jin, S. and Scotto, K.W. 1998. Transcriptional regulation of the MDR1 gene by histone acetyltransferase and deacetylase is mediated by NF-Y. Mol Cell Biol 18, 4377-4384.

Jiraskova, L., Cerveny, L., Karbanova, S., Ptackova, Z. and Staud, F. 2018. Expression of Concentrative Nucleoside Transporters (SLC28A) in the Human Placenta: Effects of Gestation Age and Prototype Differentiation-Affecting Agents. Molecular pharmaceutics 15, 2732-2741.

Johnson, D.R. and Klaassen, C.D. 2002. Regulation of rat multidrug resistance protein 2 by classes of prototypical microsomal enzyme inducers that activate distinct transcription pathways. Toxicol Sci 67, 182-189.

Jones, K., Bray, P.G., Khoo, S.H., Davey, R.A., Meaden, E.R., Ward, S.A. and Back, D.J. 2001. P-Glycoprotein and transporter MRP1 reduce HIV protease inhibitor uptake in CD4 cells: potential for accelerated viral drug resistance? AIDS 15, 1353-1358.

Jonker, J.W., Buitelaar, M., Wagenaar, E., Van Der Valk, M.A., Scheffer, G.L., Scheper, R.J., Plosch, T., Kuipers, F., Elferink, R.P., Rosing, H., Beijnen, J.H. and Schinkel, A.H. 2002. The breast cancer resistance protein protects against a major chlorophyll-derived dietary phototoxin and protoporphyria. Proc Natl Acad Sci U S A 99, 15649-15654.

Jonker, J.W., Smit, J.W., Brinkhuis, R.F., Maliepaard, M., Beijnen, J.H., Schellens, J.H. and Schinkel, A.H. 2000. Role of breast cancer resistance protein in the bioavailability and fetal penetration of topotecan. J Natl Cancer Inst 92, 1651-1656.

Joshi, A.A., Vaidya, S.S., St-Pierre, M.V., Mikheev, A.M., Desino, K.E., Nyandege, A.N., Audus, K.L., Unadkat, J.D. and Gerk, P.M. 2016. Placental ABC Transporters: Biological Impact and Pharmaceutical Significance. Pharm Res 33, 2847-2878.

Jouan, E., Le Vee, M., Denizot, C., Parmentier, Y. and Fardel, O. 2016. Drug Transporter Expression and Activity in Human Hepatoma HuH-7 Cells. Pharmaceutics 9.

Joyeux, C., Rochefort, H. and Chalbos, D. 1989. Progestin increases gene transcription and messenger ribonucleic acid stability of fatty acid synthetase in breast cancer cells. Molecular endocrinology 3, 681-686.

Juhasz, J., Nagy, P., Kulcsar, M., Szigeti, G., Reiczigel, J. and Huszenicza, G. 2001. Effect of low-dose zearalenone exposure on luteal function, follicular activity and uterine oedema in cycling mares. Acta Vet Hung 49, 211-222.

Kafafi, S.A., Afeefy, H.Y., Ali, A.H., Said, H.K. and Kafafi, A.G. 1993. Binding of polychlorinated biphenyls to the aryl hydrocarbon receptor. Environ Health Perspect 101, 422-428.

Kalabis, G.M., Petropoulos, S., Gibb, W. and Matthews, S.G. 2007. Breast cancer resistance protein (Bcrp1/Abcg2) in mouse placenta and yolk sac: ontogeny and its regulation by progesterone. Placenta 28, 1073-1081.

Kallio, P.J., Pongratz, I., Gradin, K., McGuire, J. and Poellinger, L. 1997. Activation of hypoxia-inducible factor 1alpha: posttranscriptional regulation and conformational change by recruitment of the Arnt transcription factor. Proceedings of the National Academy of Sciences of the United States of America 94, 5667-5672.

Kalliokoski, A. and Niemi, M. 2009. Impact of OATP transporters on pharmacokinetics. Br J Pharmacol 158, 693-705.

Kang, H.S., Angers, M., Beak, J.Y., Wu, X., Gimble, J.M., Wada, T., Xie, W., Collins, J.B., Grissom, S.F. and Jetten, A.M. 2007. Gene expression profiling reveals a regulatory role for ROR alpha and ROR gamma in phase I and phase II metabolism. Physiological genomics 31, 281-294.

Kast, H.R., Goodwin, B., Tarr, P.T., Jones, S.A., Anisfeld, A.M., Stoltz, C.M., Tontonoz, P., Kliewer, S., Willson, T.M. and Edwards, P.A. 2002. Regulation of multidrug resistance-associated protein 2 (ABCC2) by the nuclear receptors pregnane X receptor, farnesoid X-activated receptor, and constitutive androstane receptor. J Biol Chem 277, 2908-2915.

Kastner, P., Krust, A., Turcotte, B., Stropp, U., Tora, L., Gronemeyer, H. and Chambon, P. 1990. Two distinct estrogen-regulated promoters generate transcripts encoding the two functionally different human progesterone receptor forms A and B. EMBO J 9, 1603-1614.

Kauffmann, H.M., Pfannschmidt, S., Zoller, H., Benz, A., Vorderstemann, B., Webster, J.I. and Schrenk, D. 2002. Influence of redox-active compounds and PXR-activators on human MRP1 and MRP2 gene expression. Toxicology 171, 137-146.

Kavanaugh, S.M., White, L.A. and Kolesar, J.M. 2010. Vorinostat: A novel therapy for the treatment of cutaneous T-cell lymphoma. Am J Health Syst Pharm 67, 793-797.

Kawabe, T., Chen, Z.S., Wada, M., Uchiumi, T., Ono, M., Akiyama, S. and Kuwano, M. 1999. Enhanced transport of anticancer agents and leukotriene C4 by the human canalicular multispecific organic anion transporter (cMOAT/MRP2). FEBS Lett 456, 327-331.

Kawajiri, K. and Fujii-Kuriyama, Y. 2007. Cytochrome P450 gene regulation and physiological functions mediated by the aryl hydrocarbon receptor. Archives of biochemistry and biophysics 464, 207-212.

Kekuda, R., Leibach, F.H., Furesz, T.C., Smith, C.H. and Ganapathy, V. 2000. Polarized distribution of interleukin-1 receptors and their role in regulation of serotonin transporter in placenta. The Journal of pharmacology and experimental therapeutics 292, 1032-1041.

Kellis, J.T., Jr. and Vickery, L.E. 1987. Purification and characterization of human placental aromatase cytochrome P-450. J Biol Chem 262, 4413-4420.

Kelly, W.K., O'Connor, O.A., Krug, L.M., Chiao, J.H., Heaney, M., Curley, T., MacGregore-Cortelli, B., Tong, W., Secrist, J.P., Schwartz, L., Richardson, S., Chu, E., Olgac, S., Marks, P.A., Scher, H. and Richon, V.M. 2005. Phase I study of an oral histone deacetylase inhibitor, suberoylanilide hydroxamic acid, in patients with advanced cancer. J Clin Oncol 23, 3923-3931.

Kensler, T.W., Wakabayashi, N. and Biswal, S. 2007. Cell survival responses to environmental stresses via the Keap1-Nrf2-ARE pathway. Annual review of pharmacology and toxicology 47, 89-116.

Keskitalo, J.E., Zolk, O., Fromm, M.F., Kurkinen, K.J., Neuvonen, P.J. and Niemi, M. 2009. ABCG2 polymorphism markedly affects the pharmacokinetics of atorvastatin and rosuvastatin. Clin Pharmacol Ther 86, 197-203.

Khan, S., Liu, S., Stoner, M. and Safe, S. 2007. Cobaltous chloride and hypoxia inhibit aryl hydrocarbon receptor-mediated responses in breast cancer cells. Toxicol Appl Pharmacol 223, 28-38.

Khunweeraphong, N., Stockner, T. and Kuchler, K. 2017. The structure of the human ABC transporter ABCG2 reveals a novel mechanism for drug extrusion. Sci Rep 7, 13767.

Kim, S.N., Kim, N.H., Lee, W., Seo, D.W. and Kim, Y.K. 2009. Histone deacetylase inhibitor induction of P-glycoprotein transcription requires both histone deacetylase 1 dissociation and recruitment of CAAT/enhancer binding protein beta and pCAF to the promoter region. Mol Cancer Res 7, 735-744.

Kim, W.Y. and Benet, L.Z. 2004. P-glycoprotein (P-gp/MDR1)-mediated efflux of sex-steroid hormones and modulation of P-gp expression in vitro. Pharm Res 21, 1284-1293.

Klaassen, C.D. and Aleksunes, L.M. 2010. Xenobiotic, bile acid, and cholesterol transporters: function and regulation. Pharmacol Rev 62, 1-96.

Klein, D.M., Wright, S.H. and Cherrington, N.J. 2014. Localization of multidrug resistance-associated proteins along the blood-testis barrier in rat, macaque, and human testis. Drug Metab Dispos 42, 89-93.

Kliewer, S.A., Goodwin, B. and Willson, T.M. 2002. The nuclear pregnane X receptor: a key regulator of xenobiotic metabolism. Endocrine reviews 23, 687-702.

Knauer, M.J., Urquhart, B.L., Meyer zu Schwabedissen, H.E., Schwarz, U.I., Lemke, C.J., Leake, B.F., Kim, R.B. and Tirona, R.G. 2010. Human skeletal muscle drug transporters determine local exposure and toxicity of statins. Circ Res 106, 297-306.

Knerr, I., Beinder, E. and Rascher, W. 2002. Syncytin, a novel human endogenous retroviral gene in human placenta: evidence for its dysregulation in preeclampsia and HELLP syndrome. Am J Obstet Gynecol 186, 210-213.

Knerr, I., Schubert, S.W., Wich, C., Amann, K., Aigner, T., Vogler, T., Jung, R., Dotsch, J., Rascher, W. and Hashemolhosseini, S. 2005. Stimulation of GCMa and syncytin via cAMP mediated PKA signaling in human trophoblastic cells under normoxic and hypoxic conditions. FEBS Lett 579, 3991-3998.

Kobayashi, D., Ieiri, I., Hirota, T., Takane, H., Maegawa, S., Kigawa, J., Suzuki, H., Nanba, E., Oshimura, M., Terakawa, N., Otsubo, K., Mine, K. and Sugiyama, Y. 2005. Functional assessment of ABCG2 (BCRP) gene polymorphisms to protein expression in human placenta. Drug Metab Dispos 33, 94-101.

Koike, K., Conseil, G., Leslie, E.M., Deeley, R.G. and Cole, S.P. 2004. Identification of proline residues in the core cytoplasmic and transmembrane regions of multidrug resistance protein 1 (MRP1/ABCC1) important for transport function, substrate specificity, and nucleotide interactions. J Biol Chem 279, 12325-12336.

Koike, K., Kawabe, T., Tanaka, T., Toh, S., Uchiumi, T., Wada, M., Akiyama, S., Ono, M. and Kuwano, M. 1997. A canalicular multispecific organic anion transporter (cMOAT) antisense cDNA enhances drug sensitivity in human hepatic cancer cells. Cancer Res 57, 5475-5479.

Kondo, C., Suzuki, H., Itoda, M., Ozawa, S., Sawada, J., Kobayashi, D., Ieiri, I., Mine, K., Ohtsubo, K. and Sugiyama, Y. 2004. Functional analysis of SNPs variants of BCRP/ABCG2. Pharm Res 21, 1895-1903.

Kong, B., Luyendyk, J.P., Tawfik, O. and Guo, G.L. 2009. Farnesoid X receptor deficiency induces nonalcoholic steatohepatitis in low-density lipoprotein receptor-knockout mice fed a high-fat diet. The Journal of pharmacology and experimental therapeutics 328, 116-122.

Kong, B., Wang, L., Chiang, J.Y., Zhang, Y., Klaassen, C.D. and Guo, G.L. 2012. Mechanism of tissue-specific farnesoid X receptor in suppressing the expression of genes in bile-acid synthesis in mice. Hepatology 56, 1034-1043.

Konieczna, A., Novakova, V., Medalova, J., Erceg, S. and Klabusay, M. 2015. Thiazolidinediones Regulate the Level of ABC Transporters Expression on Lung Cancer Cells. Klin Onkol 28, 431-438.

Konig, J., Rost, D., Cui, Y. and Keppler, D. 1999. Characterization of the human multidrug resistance protein isoform MRP3 localized to the basolateral hepatocyte membrane. Hepatology 29, 1156-1163.

Kool, M., de Haas, M., Scheffer, G.L., Scheper, R.J., van Eijk, M.J., Juijn, J.A., Baas, F. and Borst, P. 1997. Analysis of expression of cMOAT (MRP2), MRP3, MRP4, and MRP5,

homologues of the multidrug resistance-associated protein gene (MRP1), in human cancer cell lines. Cancer Res 57, 3537-3547.

Kool, M., van der Linden, M., de Haas, M., Scheffer, G.L., de Vree, J.M., Smith, A.J., Jansen, G., Peters, G.J., Ponne, N., Scheper, R.J., Elferink, R.P., Baas, F. and Borst, P. 1999. MRP3, an organic anion transporter able to transport anti-cancer drugs. Proc Natl Acad Sci U S A 96, 6914-6919.

Koraichi, F., Videmann, B., Mazallon, M., Benahmed, M., Prouillac, C. and Lecoeur, S. 2012. Zearalenone exposure modulates the expression of ABC transporters and nuclear receptors in pregnant rats and fetal liver. Toxicol Lett 211, 246-256.

Koritzinsky, M., Magagnin, M.G., van den Beucken, T., Seigneuric, R., Savelkouls, K., Dostie, J., Pyronnet, S., Kaufman, R.J., Weppler, S.A., Voncken, J.W., Lambin, P., Koumenis, C., Sonenberg, N. and Wouters, B.G. 2006. Gene expression during acute and prolonged hypoxia is regulated by distinct mechanisms of translational control. EMBO J 25, 1114-1125.

Kowalska, K., Habrowska-Gorczynska, D.E., Urbanek, K.A., Dominska, K. and Piastowska-Ciesielska, A.W. 2018. Estrogen Receptor alpha Is Crucial in Zearalenone-Induced Invasion and Migration of Prostate Cancer Cells. Toxins (Basel) 10.

Kraemer, J., Klein, J., Lubetsky, A. and Koren, G. 2006. Perfusion studies of glyburide transfer across the human placenta: Implications for fetal safety. Am J Obstet Gynecol 195, 270-274.

Krishnamurthy, P., Ross, D.D., Nakanishi, T., Bailey-Dell, K., Zhou, S., Mercer, K.E., Sarkadi, B., Sorrentino, B.P. and Schuetz, J.D. 2004. The stem cell marker Bcrp/ABCG2 enhances hypoxic cell survival through interactions with heme. J Biol Chem 279, 24218-24225.

Kruh, G.D., Gaughan, K.T., Godwin, A. and Chan, A. 1995. Expression pattern of MRP in human tissues and adult solid tumor cell lines. J Natl Cancer Inst 87, 1256-1258.

Kubota, N., Terauchi, Y., Miki, H., Tamemoto, H., Yamauchi, T., Komeda, K., Satoh, S., Nakano, R., Ishii, C., Sugiyama, T., Eto, K., Tsubamoto, Y., Okuno, A., Murakami, K., Sekihara, H., Hasegawa, G., Naito, M., Toyoshima, Y., Tanaka, S., Shiota, K., Kitamura, T., Fujita, T., Ezaki, O., Aizawa, S., Kadowaki, T. and et al. 1999. PPAR gamma mediates high-fat diet-induced adipocyte hypertrophy and insulin resistance. Mol Cell 4, 597-609.

Kucka, M., Kretschmannova, K., Murano, T., Wu, C.P., Zemkova, H., Ambudkar, S.V. and Stojilkovic, S.S. 2010. Dependence of multidrug resistance protein-mediated cyclic nucleotide efflux on the background sodium conductance. Mol Pharmacol 77, 270-279.

Kudo, Y., Boyd, C.A., Kimura, H., Cook, P.R., Redman, C.W. and Sargent, I.L. 2003. Quantifying the syncytialisation of human placental trophoblast BeWo cells grown in vitro. Biochim Biophys Acta 1640, 25-31.

Kuiper-Goodman, T., Scott, P.M. and Watanabe, H. 1987. Risk assessment of the mycotoxin zearalenone. Regul Toxicol Pharmacol 7, 253-306.

Kuiper, G.G., Lemmen, J.G., Carlsson, B., Corton, J.C., Safe, S.H., van der Saag, P.T., van der Burg, B. and Gustafsson, J.A. 1998. Interaction of estrogenic chemicals and phytoestrogens with estrogen receptor beta. Endocrinology 139, 4252-4263.

Kulczar, C., Lubin, K.E., Lefebvre, S., Miller, D.W. and Knipp, G.T. 2017. Development of a direct contact astrocyte-human cerebral microvessel endothelial cells blood-brain barrier coculture model. J Pharm Pharmacol 69, 1684-1696.

Kullak-Ublick, G.A. and Becker, M.B. 2003. Regulation of drug and bile salt transporters in liver and intestine. Drug Metab Rev 35, 305-317.

Kummu, M., Sieppi, E., Wallin, K., Rautio, A., Vahakangas, K. and Myllynen, P. 2012. Cadmium inhibits ABCG2 transporter function in BeWo choriocarcinoma cells and MCF-7 cells overexpressing ABCG2. Placenta 33, 859-865.

Kumpf, V.J. 2006. Parenteral nutrition-associated liver disease in adult and pediatric patients. Nutrition in clinical practice : official publication of the American Society for Parenteral and Enteral Nutrition 21, 279-290.

Kusuhara, H., Furuie, H., Inano, A., Sunagawa, A., Yamada, S., Wu, C., Fukizawa, S., Morimoto, N., Ieiri, I., Morishita, M., Sumita, K., Mayahara, H., Fujita, T., Maeda, K. and Sugiyama, Y. 2012. Pharmacokinetic interaction study of sulphasalazine in healthy subjects and the impact of curcumin as an in vivo inhibitor of BCRP. British journal of pharmacology 166, 1793-1803.

Lahouar, A., Jedidi, I., Sanchis, V. and Said, S. 2018. Aflatoxin B1, ochratoxin A and zearalenone in sorghum grains marketed in Tunisia. Food additives & contaminants. Part B, Surveillance, 1-8.

Lambot, N., Lebrun, P., Delporte, C., De Vriese, C., Delogne-Desnoeck, J., Vanbellinghen, A.M., Graff, G. and Meuris, S. 2005. Effect of IPs, cAMP, and cGMP on the hPL and hCG secretion from human term placenta. Mol Cell Endocrinol 243, 80-85.

Lan, L., Vinci, J.M., Melendez, J.A., Jeffrey, J.J. and Wilcox, B.D. 1999. Progesterone mediates decreases in uterine smooth muscle cell interleukin-1alpha by a mechanism involving decreased stability of IL-1alpha mRNA. Mol Cell Endocrinol 155, 123-133.

Lang, T., Hitzl, M., Burk, O., Mornhinweg, E., Keil, A., Kerb, R., Klein, K., Zanger, U.M., Eichelbaum, M. and Fromm, M.F. 2004. Genetic polymorphisms in the multidrug resistance-associated protein 3 (ABCC3, MRP3) gene and relationship to its mRNA and protein expression in human liver. Pharmacogenetics 14, 155-164.

Langbein, M., Strick, R., Strissel, P.L., Vogt, N., Parsch, H., Beckmann, M.W. and Schild, R.L. 2008. Impaired cytotrophoblast cell-cell fusion is associated with reduced Syncytin and increased apoptosis in patients with placental dysfunction. Mol Reprod Dev 75, 175-183.

Langer, O., Conway, D.L., Berkus, M.D., Xenakis, E.M.-J. and Gonzales, O. 2000. A comparison of glyburide and insulin in women with gestational diabetes mellitus. New England Journal of Medicine 343, 1134-1138.

Laochariyakul, P., Ponglikitmongkol, M. and Mankhetkorn, S. 2003. Functional study of intracellular P-gp- and MRP1-mediated pumping of free cytosolic pirarubicin into acidic organelles in intrinsic resistant SiHa cells. Can J Physiol Pharmacol 81, 790-799.

Lapaire, O., Grill, S., Lalevee, S., Kolla, V., Hosli, I. and Hahn, S. 2012. Microarray screening for novel preeclampsia biomarker candidates. Fetal Diagn Ther 31, 147-153.

Lee, D.Y., Hayes, J.J., Pruss, D. and Wolffe, A.P. 1993. A positive role for histone acetylation in transcription factor access to nucleosomal DNA. Cell 72, 73-84.

Lee, G., Elwood, F., McNally, J., Weiszmann, J., Lindstrom, M., Amaral, K., Nakamura, M., Miao, S., Cao, P., Learned, R.M., Chen, J.L. and Li, Y. 2002. T0070907, a selective ligand for peroxisome proliferator-activated receptor gamma, functions as an antagonist of biochemical and cellular activities. J Biol Chem 277, 19649-19657.

Lee, X., Keith, J.C., Jr., Stumm, N., Moutsatsos, I., McCoy, J.M., Crum, C.P., Genest, D., Chin, D., Ehrenfels, C., Pijnenborg, R., van Assche, F.A. and Mi, S. 2001. Downregulation of placental syncytin expression and abnormal protein localization in pre-eclampsia. Placenta 22, 808-812.

Lemmen, J., Tozakidis, I.E., Bele, P. and Galla, H.J. 2013a. Constitutive androstane receptor upregulates Abcb1 and Abcg2 at the blood-brain barrier after CITCO activation. Brain Res 1501, 68-80.

Lemmen, J., Tozakidis, I.E. and Galla, H.J. 2013b. Pregnane X receptor upregulates ABC-transporter Abcg2 and Abcb1 at the blood-brain barrier. Brain Res 1491, 1-13.

Leslie, E.M., Haimeur, A. and Waalkes, M.P. 2004. Arsenic transport by the human multidrug resistance protein 1 (MRP1/ABCC1). Evidence that a tri-glutathione conjugate is required. J Biol Chem 279, 32700-32708.

Leslie, E.M., Letourneau, I.J., Deeley, R.G. and Cole, S.P. 2003. Functional and structural consequences of cysteine substitutions in the NH2 proximal region of the human multidrug resistance protein 1 (MRP1/ABCC1). Biochemistry 42, 5214-5224.

Li, H., van Ravenzwaay, B., Rietjens, I.M. and Louisse, J. 2013a. Assessment of an in vitro transport model using BeWo b30 cells to predict placental transfer of compounds. Arch Toxicol 87, 1661-1669.

Li, J., Wang, Y. and Hidalgo, I.J. 2013b. Kinetic analysis of human and canine P-glycoprotein-mediated drug transport in MDR1-MDCK cell model: approaches to reduce false-negative substrate classification. Journal of pharmaceutical sciences 102, 3436-3446.

Li, L. and Schust, D.J. 2015. Isolation, purification and in vitro differentiation of cytotrophoblast cells from human term placenta. Reprod Biol Endocrinol 13, 71.

Li, R., Andersen, C.L., Hu, L., Wang, Z., Li, Y., Nagy, T. and Ye, X. 2019a. Dietary exposure to mycotoxin zearalenone (ZEA) during post-implantation adversely affects placental development in mice. Reproductive toxicology 85, 42-50.

Li, T. and Chiang, J.Y. 2014. Bile Acid Signaling in Metabolic Disease and Drug Therapy. Pharmacological reviews 66, 948-983.

Li, X., Huang, J., Yi, P., Bambara, R.A., Hilf, R. and Muyan, M. 2004. Single-chain estrogen receptors (ERs) reveal that the ERalpha/beta heterodimer emulates functions of the ERalpha dimer in genomic estrogen signaling pathways. Mol Cell Biol 24, 7681-7694.

Li, X., Pan, Y.Z., Seigel, G.M., Hu, Z.H., Huang, M. and Yu, A.M. 2011. Breast cancer resistance protein BCRP/ABCG2 regulatory microRNAs (hsa-miR-328, -519c and -520h) and their differential expression in stem-like ABCG2+ cancer cells. Biochem Pharmacol 81, 783-792.

Li, Y., Guo, Y., Feng, Z., Bergan, R., Li, B., Qin, Y., Zhao, L., Zhang, Z. and Shi, M. 2019b. Involvement of the PI3K/Akt/Nrf2 Signaling Pathway in Resveratrol-Mediated Reversal of Drug Resistance in HL-60/ADR Cells. Nutr Cancer 71, 1007-1018.

Liang, Z., Wu, H., Xia, J., Li, Y., Zhang, Y., Huang, K., Wagar, N., Yoon, Y., Cho, H.T., Scala, S. and Shim, H. 2010. Involvement of miR-326 in chemotherapy resistance of breast cancer through modulating expression of multidrug resistance-associated protein 1. Biochem Pharmacol 79, 817-824.

Lin, L.S., Roberts, V.J. and Yen, S.S. 1995. Expression of human gonadotropin-releasing hormone receptor gene in the placenta and its functional relationship to human chorionic gonadotropin secretion. J Clin Endocrinol Metab 80, 580-585.

Lin, Q., Cong, X. and Yun, Z. 2011. Differential hypoxic regulation of hypoxia-inducible factors 1alpha and 2alpha. Molecular cancer research : MCR 9, 757-765.

Lin, Y., Bircsak, K.M., Gorczyca, L., Wen, X. and Aleksunes, L.M. 2016. Regulation of the placental BCRP transporter by PPAR gamma. Journal of biochemical and molecular toxicology.

Lin, Y., Bircsak, K.M., Gorczyca, L., Wen, X. and Aleksunes, L.M. 2017. Regulation of the placental BCRP transporter by PPAR gamma. J Biochem Mol Toxicol 31.

Liu, F., Soares, M.J. and Audus, K.L. 1997. Permeability properties of monolayers of the human trophoblast cell line BeWo. Am J Physiol 273, C1596-1604.

Liu, F., Yin, R., Chen, X., Chen, W., Qian, Y., Zhao, Y., Jiang, Y., Ma, D., Hu, T., Yu, T., Zhu, Y. and Zhang, Y. 2019. Over-expression of miR-206 decreases the Euthyrox-resistance by targeting MAP4K3 in papillary thyroid carcinoma. Biomed Pharmacother 114, 108605.

Liu, J. and Li, Y. 2015. Trichostatin A and Tamoxifen inhibit breast cancer cell growth by miR-204 and ERalpha reducing AKT/mTOR pathway. Biochem Biophys Res Commun 467, 242-247.

Liu, L., Zhou, L., Hu, S., Zhou, S., Deng, Y., Dong, M., Huang, J., Zeng, Y., Chen, X., Zhao, N., Li, H. and Ding, Z. 2016. Down-regulation of ABCG2 and ABCB4 transporters in the placenta of rats exposed to cadmium. Oncotarget 7, 38154-38163.

Liu, Y., Yin, Y., Sheng, Q., Lu, X., Wang, F., Lin, Z., Tian, H., Xu, A. and Zhang, J. 2014. Association of ABCC2 -24C>T polymorphism with high-dose methotrexate plasma concentrations and toxicities in childhood acute lymphoblastic leukemia. PLoS One 9, e82681.

Liu, Y.H., Di, Y.M., Zhou, Z.W., Mo, S.L. and Zhou, S.F. 2010. Multidrug resistance-associated proteins and implications in drug development. Clin Exp Pharmacol Physiol 37, 115-120.

Livak, K.J. and Schmittgen, T.D. 2001. Analysis of relative gene expression data using real-time quantitative PCR and the 2(-Delta Delta C(T)) Method. Methods 25, 402-408.

Loboda, A., Stachurska, A., Florczyk, U., Rudnicka, D., Jazwa, A., Wegrzyn, J., Kozakowska, M., Stalinska, K., Poellinger, L., Levonen, A.L., Yla-Herttuala, S., Jozkowicz, A. and Dulak, J. 2009. HIF-1 induction attenuates Nrf2-dependent IL-8 expression in human endothelial cells. Antioxidants & redox signaling 11, 1501-1517.

Loe, D.W., Almquist, K.C., Cole, S.P. and Deeley, R.G. 1996. ATP-dependent 17 beta-estradiol 17-(beta-D-glucuronide) transport by multidrug resistance protein (MRP). Inhibition by cholestatic steroids. J Biol Chem 271, 9683-9689.

Loe, D.W., Stewart, R.K., Massey, T.E., Deeley, R.G. and Cole, S.P. 1997. ATP-dependent transport of aflatoxin B1 and its glutathione conjugates by the product of the multidrug resistance protein (MRP) gene. Mol Pharmacol 51, 1034-1041.

Long, G.G., Turek, J., Diekman, M.A. and Scheidt, A.B. 1992. Effect of zearalenone on days 7 to 10 post-mating on blastocyst development and endometrial morphology in sows. Vet Pathol 29, 60-67.

Lopez-Rodas, G., Brosch, G., Georgieva, E.I., Sendra, R., Franco, L. and Loidl, P. 1993. Histone deacetylase. A key enzyme for the binding of regulatory proteins to chromatin. FEBS Lett 317, 175-180.

Loscher, W. and Potschka, H. 2005. Blood-brain barrier active efflux transporters: ATP-binding cassette gene family. NeuroRx 2, 86-98.

Loubiere, L.S., Vasilopoulou, E., Bulmer, J.N., Taylor, P.M., Stieger, B., Verrey, F., McCabe, C.J., Franklyn, J.A., Kilby, M.D. and Chan, S.Y. 2010. Expression of thyroid hormone transporters in the human placenta and changes associated with intrauterine growth restriction. Placenta 31, 295-304.

Lu, X., Wang, R., Zhu, C., Wang, H., Lin, H.Y., Gu, Y., Cross, J.C. and Wang, H. 2017. Fine-Tuned and Cell-Cycle-Restricted Expression of Fusogenic Protein Syncytin-2 Maintains Functional Placental Syncytia. Cell Rep 21, 1150-1159.

Lu, Y., Yan, Y. and Wang, X.F. 2004. Antiepileptic drug-induced multidrug resistance P-glycoprotein overexpression in astrocytes cultured from rat brains. Chin Med J (Engl) 117, 1682-1686.

Lv, Y., Zhao, S., Han, J., Zheng, L., Yang, Z. and Zhao, L. 2015. Hypoxia-inducible factor-1alpha induces multidrug resistance protein in colon cancer. OncoTargets and therapy 8, 1941-1948.

Lye, P., Bloise, E., Dunk, C., Javam, M., Gibb, W., Lye, S.J. and Matthews, S.G. 2013. Effect of oxygen on multidrug resistance in the first trimester human placenta. Placenta 34, 817-823.

Lye, P., Bloise, E., Nadeem, L., Gibb, W., Lye, S.J. and Matthews, S.G. 2018. Glucocorticoids modulate multidrug resistance transporters in the first trimester human placenta. J Cell Mol Med 22, 3652-3660.

MacFarland, A., Abramovich, D.R., Ewen, S.W. and Pearson, C.K. 1994. Stage-specific distribution of P-glycoprotein in first-trimester and full-term human placenta. The Histochemical journal 26, 417-423.

Madden, M.J., Morrow, C.S., Nakagawa, M., Goldsmith, M.E., Fairchild, C.R. and Cowan, K.H. 1993. Identification of 5' and 3' sequences involved in the regulation of transcription of the human mdr1 gene in vivo. J Biol Chem 268, 8290-8297.

Mader, T.L. 1994. Effect of implant sequence and dose on feedlot cattle performance. J Anim Sci 72, 277-282.

Magnarin, M., Rosati, A., De Iudicibus, S., Bartoli, F. and Decorti, G. 2008. Role of ABC Transporters in the BeWo Trophoblast Cell Line. Toxicol Mech Methods 18, 763-769.

Maher, J.M., Aleksunes, L.M., Dieter, M.Z., Tanaka, Y., Peters, J.M., Manautou, J.E. and Klaassen, C.D. 2008. Nrf2- and PPAR alpha-mediated regulation of hepatic Mrp transporters after exposure to perfluorooctanoic acid and perfluorodecanoic acid. Toxicol Sci 106, 319-328.

Maher, J.M., Cheng, X., Slitt, A.L., Dieter, M.Z. and Klaassen, C.D. 2005. Induction of the multidrug resistance-associated protein family of transporters by chemical activators of receptor-mediated pathways in mouse liver. Drug Metab Dispos 33, 956-962.

Maher, J.M., Dieter, M.Z., Aleksunes, L.M., Slitt, A.L., Guo, G., Tanaka, Y., Scheffer, G.L., Chan, J.Y., Manautou, J.E., Chen, Y., Dalton, T.P., Yamamoto, M. and Klaassen, C.D. 2007. Oxidative and electrophilic stress induces multidrug resistance-associated protein transporters via the nuclear factor-E2-related factor-2 transcriptional pathway. Hepatology 46, 1597-1610.

Mahringer, A. and Fricker, G. 2010. BCRP at the blood-brain barrier: genomic regulation by 17beta-estradiol. Molecular pharmaceutics 7, 1835-1847.

Malassine, A., Frendo, J.L. and Evain-Brion, D. 2003. A comparison of placental development and endocrine functions between the human and mouse model. Hum Reprod Update 9, 531-539.

Malhotra, S.S., Suman, P. and Gupta, S.K. 2015. Alpha or beta human chorionic gonadotropin knockdown decrease BeWo cell fusion by down-regulating PKA and CREB activation. Sci Rep 5, 11210.

Maliepaard, M., Scheffer, G.L., Faneyte, I.F., van Gastelen, M.A., Pijnenborg, A.C., Schinkel, A.H., van De Vijver, M.J., Scheper, R.J. and Schellens, J.H. 2001a. Subcellular localization and distribution of the breast cancer resistance protein transporter in normal human tissues. Cancer Res 61, 3458-3464.

Maliepaard, M., Scheffer, G.L., Faneyte, I.F., van Gastelen, M.A., Pijnenborg, A.C.L.M., Schinkel, A.H., van de Vijver, M.J., Scheper, R.J. and Schellens, J.H.M. 2001b. Subcellular localization and distribution of the breast cancer resistance protein transporter in normal human tissues. Cancer Research 61, 3458-3464.

Manceau, S., Giraud, C., Decleves, X., Batteux, F., Chouzenoux, S., Tang, R., Dauchy, S., Scherrmann, J.M., Weill, B., Morini, J.P., Perrot, J.Y. and Treluyer, J.M. 2010. Lack of P-glycoprotein induction by rifampicin and phenobarbital in human lymphocytes. Int J Pharm 395, 98-103.

Mao, Q. 2008. BCRP/ABCG2 in the placenta: expression, function and regulation. Pharmaceutical research 25, 1244-1255.

Mao, Q. and Unadkat, J.D. 2015. Role of the breast cancer resistance protein (BCRP/ABCG2) in drug transport--an update. AAPS J 17, 65-82.

Maran, R.R., Thomas, A., Roth, M., Sheng, Z., Esterly, N., Pinson, D., Gao, X., Zhang, Y., Ganapathy, V., Gonzalez, F.J. and Guo, G.L. 2009. Farnesoid X receptor deficiency in mice leads to increased intestinal epithelial cell proliferation and tumor development. The Journal of pharmacology and experimental therapeutics 328, 469-477.

Marin, J.J., Macias, R.I., Briz, O., Perez, M.J. and Serrano, M.A. 2005. Molecular bases of the excretion of fetal bile acids and pigments through the fetal liver-placenta-maternal liver pathway. Ann Hepatol 4, 70-76.

Marin, S., Ramos, A.J., Cano-Sancho, G. and Sanchis, V. 2013. Mycotoxins: occurrence, toxicology, and exposure assessment. Food Chem Toxicol 60, 218-237.

Marino, M., Galluzzo, P. and Ascenzi, P. 2006. Estrogen signaling multiple pathways to impact gene transcription. Curr Genomics 7, 497-508.

Marshall, S.A., Hannan, N.J., Jelinic, M., Nguyen, T.P.H., Girling, J.E. and Parry, L.J. 2018. Animal models of preeclampsia: translational failings and why. American journal of physiology. Regulatory, integrative and comparative physiology 314, R499-R508.

Martin, P., Riley, R., Back, D.J. and Owen, A. 2008. Comparison of the induction profile for drug disposition proteins by typical nuclear receptor activators in human hepatic and intestinal cells. Br J Pharmacol 153, 805-819.

Martin, P.M., Horwitz, K.B., Ryan, D.S. and McGuire, W.L. 1978. Phytoestrogen interaction with estrogen receptors in human breast cancer cells. Endocrinology 103, 1860-1867.

Mason, C.W., Buhimschi, I.A., Buhimschi, C.S., Dong, Y., Weiner, C.P. and Swaan, P.W. 2011. ATP-binding cassette transporter expression in human placenta as a function of pregnancy condition. Drug Metab Dispos 39, 1000-1007.

Mason, D.L. and Michaelis, S. 2002. Requirement of the N-terminal extension for vacuolar trafficking and transport activity of yeast Ycf1p, an ATP-binding cassette transporter. Mol Biol Cell 13, 4443-4455.

Mathias, A.A., Hitti, J. and Unadkat, J.D. 2005. P-glycoprotein and breast cancer resistance protein expression in human placentae of various gestational ages. American journal of physiology. Regulatory, integrative and comparative physiology 289, R963-969.

Matsuo, H., Takada, T., Ichida, K., Nakamura, T., Nakayama, A., Suzuki, H., Hosoya, T. and Shinomiya, N. 2011. ABCG2/BCRP dysfunction as a major cause of gout. Nucleosides Nucleotides Nucleic Acids 30, 1117-1128.

Matsuura, S., Itakura, A., Ohno, Y., Nakashima, Y., Murata, Y., Takeuchi, M., Kobayashi, M. and Mizutani, S. 2004. Effects of estradiol administration on feto-placental growth in rat. Early Hum Dev 77, 47-56.

Mayhew, T.M. and Barker, B.L. 2001. Villous trophoblast: morphometric perspectives on growth, differentiation, turnover and deposition of fibrin-type fibrinoid during gestation. Placenta 22, 628-638.

Mazur, C.S., Marchitti, S.A., Dimova, M., Kenneke, J.F., Lumen, A. and Fisher, J. 2012. Human and rat ABC transporter efflux of bisphenol a and bisphenol a glucuronide: interspecies comparison and implications for pharmacokinetic assessment. Toxicol Sci 128, 317-325.

McAleer, M.A., Breen, M.A., White, N.L. and Matthews, N. 1999. pABC11 (also known as MOAT-C and MRP5), a member of the ABC family of proteins, has anion transporter activity but does not confer multidrug resistance when overexpressed in human embryonic kidney 293 cells. J Biol Chem 274, 23541-23548.

McCormack, J.T. and Greenwald, G.S. 1974. Evidence for a preimplantation rise in oestradiol-17beta levels on day 4 of pregnancy in the mouse. J Reprod Fertil 41, 297-301.

Mease, K., Sane, R., Podila, L. and Taub, M.E. 2012. Differential selectivity of efflux transporter inhibitors in Caco-2 and MDCK-MDR1 monolayers: A strategy to assess the interaction of a new chemical entity with P-gp, BCRP, and MRP2. J. Pharm. Sci. 101, 1888-1897.

Memon, N., Bircsak, K.M., Archer, F., Gibson, C.J., Ohman-Strickland, P., Weinberger, B.I., Parast, M.M., Vetrano, A.M. and Aleksunes, L.M. 2014. Regional expression of the BCRP/ABCG2 transporter in term human placentas. Reproductive toxicology 43, 72-77.

Mendelson, C.R., Jiang, B., Shelton, J.M., Richardson, J.A. and Hinshelwood, M.M. 2005. Transcriptional regulation of aromatase in placenta and ovary. J Steroid Biochem Mol Biol 95, 25-33.

Merino, G., Alvarez, A.I., Pulido, M.M., Molina, A.J., Schinkel, A.H. and Prieto, J.G. 2006. Breast cancer resistance protein (BCRP/ABCG2) transports fluoroquinolone antibiotics and affects their oral availability, pharmacokinetics, and milk secretion. Drug Metab Dispos 34, 690-695.

Merino, G., Jonker, J.W., Wagenaar, E., van Herwaarden, A.E. and Schinkel, A.H. 2005. The breast cancer resistance protein (BCRP/ABCG2) affects pharmacokinetics, hepatobiliary excretion, and milk secretion of the antibiotic nitrofurantoin. Molecular pharmacology 67, 1758-1764.

Merino, G., Perez, M., Real, R., Egido, E., Prieto, J. and Alvarez, A. 2010. In vivo inhibition of BCRP/ABCG2 mediated transport of nitrofurantoin by the isoflavones genistein and daidzein: A comparative study in Bcrp1 (-/-) mice. Pharm Res 27, 2098-2105.

Meyer zu Schwabedissen, H.E., Grube, M., Dreisbach, A., Jedlitschky, G., Meissner, K., Linnemann, K., Fusch, C., Ritter, C.A., Volker, U. and Kroemer, H.K. 2006. Epidermal growth factor-mediated activation of the map kinase cascade results in altered expression and function of ABCG2 (BCRP). Drug Metab Dispos 34, 524-533.

Meyer Zu Schwabedissen, H.E., Grube, M., Heydrich, B., Linnemann, K., Fusch, C., Kroemer, H.K. and Jedlitschky, G. 2005a. Expression, localization, and function of MRP5 (ABCC5), a transporter for cyclic nucleotides, in human placenta and cultured human trophoblasts: effects of gestational age and cellular differentiation. Am J Pathol 166, 39-48.

Meyer zu Schwabedissen, H.E., Jedlitschky, G., Gratz, M., Haenisch, S., Linnemann, K., Fusch, C., Cascorbi, I. and Kroemer, H.K. 2005b. Variable expression of MRP2 (ABCC2) in human placenta: influence of gestational age and cellular differentiation. Drug Metab Dispos 33, 896-904.

Mi, S., Lee, X., Li, X., Veldman, G.M., Finnerty, H., Racie, L., LaVallie, E., Tang, X.Y., Edouard, P., Howes, S., Keith, J.C., Jr. and McCoy, J.M. 2000. Syncytin is a captive retroviral envelope protein involved in human placental morphogenesis. Nature 403, 785-789.

Midgley, A.R., Pierce, G.B., Jr., Deneau, G.A. and Gosling, J.R. 1963. Morphogenesis of syncytiotrophoblast in vivo: an autoradiographic demonstration. Science 141, 349-350.

Mikheev, A.M., Nabekura, T., Kaddoumi, A., Bammler, T.K., Govindarajan, R., Hebert, M.F. and Unadkat, J.D. 2008. Profiling gene expression in human placentae of different gestational ages: an OPRU Network and UW SCOR Study. Reprod Sci 15, 866-877.

Milane, A., Vautier, S., Chacun, H., Meininger, V., Bensimon, G., Farinotti, R. and Fernandez, C. 2009. Interactions between riluzole and ABCG2/BCRP transporter. Neuroscience letters 452, 12-16.

Minami, S., Ito, K., Honma, M., Ikebuchi, Y., Anzai, N., Kanai, Y., Nishida, T., Tsukita, S., Sekine, S., Horie, T. and Suzuki, H. 2009. Posttranslational regulation of Abcc2 expression by SUMOylation system. Am J Physiol Gastrointest Liver Physiol 296, G406-413.

Minervini, F., Giannoccaro, A., Cavallini, A. and Visconti, A. 2005. Investigations on cellular proliferation induced by zearalenone and its derivatives in relation to the estrogenic parameters. Toxicol Lett 159, 272-283.

Minervini, F., Giannoccaro, A., Fornelli, F., Dell'Aquila, M.E., Minoia, P. and Visconti, A. 2006. Influence of mycotoxin zearalenone and its derivatives (alpha and beta zearalenol) on

apoptosis and proliferation of cultured granulosa cells from equine ovaries. Reprod Biol Endocrinol 4, 62.

Mitra, P. and Audus, K.L. 2010. MRP isoforms and BCRP mediate sulfate conjugate efflux out of BeWo cells. Int J Pharm 384, 15-23.

Moffit, J.S., Aleksunes, L.M., Maher, J.M., Scheffer, G.L., Klaassen, C.D. and Manautou, J.E. 2006. Induction of hepatic transporters multidrug resistance-associated proteins (Mrp) 3 and 4 by clofibrate is regulated by peroxisome proliferator-activated receptor alpha. J Pharmacol Exp Ther 317, 537-545.

Molina-Molina, J.M., Real, M., Jimenez-Diaz, I., Belhassen, H., Hedhili, A., Torne, P., Fernandez, M.F. and Olea, N. 2014. Assessment of estrogenic and anti-androgenic activities of the mycotoxin zearalenone and its metabolites using in vitro receptor-specific bioassays. Food Chem Toxicol 74, 233-239.

Monroe, D.G., Secreto, F.J., Subramaniam, M., Getz, B.J., Khosla, S. and Spelsberg, T.C. 2005. Estrogen receptor alpha and beta heterodimers exert unique effects on estrogen- and tamoxifen-dependent gene expression in human U2OS osteosarcoma cells. Mol Endocrinol 19, 1555-1568.

More, V.R., Campos, C.R., Evans, R.A., Oliver, K.D., Chan, G.N., Miller, D.S. and Cannon, R.E. 2017. PPAR-alpha, a lipid-sensing transcription factor, regulates blood-brain barrier efflux transporter expression. J Cereb Blood Flow Metab 37, 1199-1212.

Morisaki, K., Robey, R.W., Ozvegy-Laczka, C., Honjo, Y., Polgar, O., Steadman, K., Sarkadi, B. and Bates, S.E. 2005. Single nucleotide polymorphisms modify the transporter activity of ABCG2. Cancer Chemother Pharmacol 56, 161-172.

Morito, N., Yoh, K., Itoh, K., Hirayama, A., Koyama, A., Yamamoto, M. and Takahashi, S. 2003. Nrf2 regulates the sensitivity of death receptor signals by affecting intracellular glutathione levels. Oncogene 22, 9275-9281.

Mueller, S.O., Simon, S., Chae, K., Metzler, M. and Korach, K.S. 2004. Phytoestrogens and their human metabolites show distinct agonistic and antagonistic properties on estrogen receptor alpha (ERalpha) and ERbeta in human cells. Toxicol Sci 80, 14-25.

Muerhoff, A.S., Griffin, K.J. and Johnson, E.F. 1992. The peroxisome proliferator-activated receptor mediates the induction of CYP4A6, a cytochrome P450 fatty acid omega-hydroxylase, by clofibric acid. The Journal of biological chemistry 267, 19051-19053.

Mukherjee, D., Royce, S.G., Alexander, J.A., Buckley, B., Isukapalli, S.S., Bandera, E.V., Zarbl, H. and Georgopoulos, P.G. 2014. Physiologically-based toxicokinetic modeling of zearalenone and its metabolites: application to the Jersey girl study. PLoS One 9, e113632.

Myat, T., Hitsumoto, Y., Saheki, S., Kitagawa, H., Yano, J. and Matsuura, S. 1996. Attenuation of human chorionic gonadotropin release by nitric oxide in choriocarcinoma cell lines. J Endocrinol 150, 243-253.

Myint, K., Li, Y., Paxton, J. and McKeage, M. 2015. Multidrug Resistance-Associated Protein 2 (MRP2) Mediated Transport of Oxaliplatin-Derived Platinum in Membrane Vesicles. PLoS One 10, e0130727.

Myllynen, P., Kummu, M. and Sieppi, E. 2010. ABCB1 and ABCG2 expression in the placenta and fetus: an interspecies comparison. Expert Opin Drug Metab Toxicol 6, 1385-1398.

Nagashige, M., Ushigome, F., Koyabu, N., Hirata, K., Kawabuchi, M., Hirakawa, T., Satoh, S., Tsukimori, K., Nakano, H., Uchiumi, T., Kuwano, M., Ohtani, H. and Sawada, Y. 2003. Basal membrane localization of MRP1 in human placental trophoblast. Placenta 24, 951-958.

Nakagawa, H., Wakabayashi-Nakao, K., Tamura, A., Toyoda, Y., Koshiba, S. and Ishikawa, T. 2009. Disruption of N-linked glycosylation enhances ubiquitin-mediated proteasomal

degradation of the human ATP-binding cassette transporter ABCG2. FEBS J 276, 7237-7252.

Nakamura, U. and Kadokawa, H. 2015. The nonsteroidal mycoestrogen zearalenone and its five metabolites suppress LH secretion from the bovine anterior pituitary cells via the estradiol receptor GPR30 in vitro. Theriogenology 84, 1342-1349.

Nakanishi, T. and Ross, D.D. 2012. Breast cancer resistance protein (BCRP/ABCG2): its role in multidrug resistance and regulation of its gene expression. Chin J Cancer 31, 73-99.

Nandivada, P., Potemkin, A.K., Carlson, S.J., Chang, M.I., Cowan, E., O'Loughlin, A.A., Gura, K.M. and Puder, M. 2014. Elevated Alkaline Phosphatase in Infants With Parenteral Nutrition-Associated Liver Disease Reflects Bone Rather Than Liver Disease. JPEN. Journal of parenteral and enteral nutrition.

Naspinski, C., Gu, X., Zhou, G.D., Mertens-Talcott, S.U., Donnelly, K.C. and Tian, Y. 2008. Pregnane X receptor protects HepG2 cells from BaP-induced DNA damage. Toxicol Sci 104, 67-73.

Natarajan, K., Xie, Y., Baer, M.R. and Ross, D.D. 2012. Role of breast cancer resistance protein (BCRP/ABCG2) in cancer drug resistance. Biochemical pharmacology 83, 1084-1103.

Neradugomma, N.K., Liao, M.Z. and Mao, Q. 2016. Buprenorphine, Norbuprenorphine, R-Methadone and S-Methadone Upregulate BCRP/ABCG2 Expression by Activating Aryl Hydrocarbon Receptor in Human Placental Trophoblasts. Molecular pharmacology.

Neradugomma, N.K., Liao, M.Z. and Mao, Q. 2017. Buprenorphine, Norbuprenorphine, R-Methadone, and S-Methadone Upregulate BCRP/ABCG2 Expression by Activating Aryl Hydrocarbon Receptor in Human Placental Trophoblasts. Molecular pharmacology 91, 237-249.

Newhouse, S.M., Davidge, S.T., Winkler-Lowen, B., Demianczuk, N. and Guilbert, L.J. 2007. In vitro differentiation of villous trophoblasts from pregnancies complicated by intrauterine growth restriction with and without pre-eclampsia. Placenta 28, 999-1003.

Ni, X., Li, L. and Pan, G. 2015. HDAC inhibitor-induced drug resistance involving ATP-binding cassette transporters (Review). Oncol Lett 9, 515-521.

Ni, Z., Bikadi, Z., Rosenberg, M.F. and Mao, Q. 2010. Structure and function of the human breast cancer resistance protein (BCRP/ABCG2). Curr Drug Metab 11, 603-617.

Ni, Z. and Mao, Q. 2011. ATP-binding cassette efflux transporters in human placenta. Current pharmaceutical biotechnology 12, 674-685.

Nickel, S. and Mahringer, A. 2014. The xenoestrogens ethinylestradiol and bisphenol A regulate BCRP at the blood-brain barrier of rats. Xenobiotica 44, 1046-1054.

Nigam, S.K., Bush, K.T., Martovetsky, G., Ahn, S.Y., Liu, H.C., Richard, E., Bhatnagar, V. and Wu, W. 2015. The organic anion transporter (OAT) family: a systems biology perspective. Physiol Rev 95, 83-123.

Nikaido, Y., Yoshizawa, K., Danbara, N., Tsujita-Kyutoku, M., Yuri, T., Uehara, N. and Tsubura, A. 2004. Effects of maternal xenoestrogen exposure on development of the reproductive tract and mammary gland in female CD-1 mouse offspring. Reprod Toxicol 18, 803-811.

Ning, Z.F., Huang, Y.J., Lin, T.X., Zhou, Y.X., Jiang, C., Xu, K.W., Huang, H., Yin, X.B. and Huang, J. 2009. Subpopulations of stem-like cells in side population cells from the human bladder transitional cell cancer cell line T24. J Int Med Res 37, 621-630.

Njumbe Ediage, E., Diana Di Mavungu, J., Song, S., Sioen, I. and De Saeger, S. 2013. Multimycotoxin analysis in urines to assess infant exposure: a case study in Cameroon. Environ Int 57-58, 50-59.

Nkabinde, L.A., Shoba-Zikhali, L.N., Semete-Makokotlela, B., Kalombo, L., Swai, H.S., Hayeshi, R., Naicker, B., Hillie, T.K. and Hamman, J.H. 2012. Permeation of PLGA nanoparticles across different in vitro models. Current drug delivery 9, 617-627.

Novakovic, B., Gordon, L., Wong, N.C., Moffett, A., Manuelpillai, U., Craig, J.M., Sharkey, A. and Saffery, R. 2011. Wide-ranging DNA methylation differences of primary trophoblast cell populations and derived cell lines: implications and opportunities for understanding trophoblast function. Molecular human reproduction 17, 344-353.

Ogunyemi, D., Jesse, M. and Davidson, M. 2007. Comparison of glyburide versus insulin in management of gestational diabetes mellitus. Endocr Pract 13, 427-428.

Ogura, K., Sakata, M., Okamoto, Y., Yasui, Y., Tadokoro, C., Yoshimoto, Y., Yamaguchi, M., Kurachi, H., Maeda, T. and Murata, Y. 2000. 8-bromo-cyclicAMP stimulates glucose transporter-1 expression in a human choriocarcinoma cell line. J Endocrinol 164, 171-178.

Ogura, M., Takatori, T., Sugimoto, Y. and Tsuruo, T. 1991. Identification and characterization of three DNA-binding proteins on the promoter of the human MDR1 gene in drug-sensitive and -resistant cells. Jpn J Cancer Res 82, 1151-1159.

Ohashi, R., Tamai, I., Yabuuchi, H., Nezu, J.I., Oku, A., Sai, Y., Shimane, M. and Tsuji, A. 1999. Na(+)-dependent carnitine transport by organic cation transporter (OCTN2): its pharmacological and toxicological relevance. The Journal of pharmacology and experimental therapeutics 291, 778-784.

Ok, H.E., Choi, S.W., Kim, M. and Chun, H.S. 2014. HPLC and UPLC methods for the determination of zearalenone in noodles, cereal snacks and infant formula. Food Chem 163, 252-257.

Olinga, P., Elferink, M.G., Draaisma, A.L., Merema, M.T., Castell, J.V., Perez, G. and Groothuis, G.M. 2008. Coordinated induction of drug transporters and phase I and II metabolism in human liver slices. Eur J Pharm Sci 33, 380-389.

Omata, J., Pierre, J.F., Heneghan, A.F., Tsao, F.H., Sano, Y., Jonker, M.A. and Kudsk, K.A. 2013a. Parenteral nutrition suppresses the bactericidal response of the small intestine. Surgery 153, 17-24.

Omata, W., Ackerman, W.E.t., Vandre, D.D. and Robinson, J.M. 2013b. Trophoblast cell fusion and differentiation are mediated by both the protein kinase C and a pathways. PLoS One 8, e81003.

Orendi, K., Kivity, V., Sammar, M., Grimpel, Y., Gonen, R., Meiri, H., Lubzens, E. and Huppertz, B. 2011. Placental and trophoblastic in vitro models to study preventive and therapeutic agents for preeclampsia. Placenta 32 Suppl, S49-54.

Ortiz, D.F., Li, S., Iyer, R., Zhang, X., Novikoff, P. and Arias, I.M. 1999. MRP3, a new ATP-binding cassette protein localized to the canalicular domain of the hepatocyte. Am J Physiol 276, G1493-1500.

Oscarson, M., Zanger, U.M., Rifki, O.F., Klein, K., Eichelbaum, M. and Meyer, U.A. 2006. Transcriptional profiling of genes induced in the livers of patients treated with carbamazepine. Clin Pharmacol Ther 80, 440-456.

Pan, Y.Z., Morris, M.E. and Yu, A.M. 2009. MicroRNA-328 negatively regulates the expression of breast cancer resistance protein (BCRP/ABCG2) in human cancer cells. Molecular pharmacology 75, 1374-1379.

Park, D., Cheon, M., Kim, C., Kim, K. and Ryu, K. 1996. Progesterone together with estradiol promotes luteinizing hormone beta-subunit mRNA stability in rat pituitary cells cultured in vitro. Eur J Endocrinol 134, 236-242.

Park, Y.J., Lee, E.K., Lee, Y.K., Park do, J., Jang, H.C. and Moore, D.D. 2012. Opposing regulation of cytochrome P450 expression by CAR and PXR in hypothyroid mice. Toxicology and applied pharmacology 263, 131-137.

Pascolo, L., Fernetti, C., Pirulli, D., Crovella, S., Amoroso, A. and Tiribelli, C. 2003. Effects of maturation on RNA transcription and protein expression of four MRP genes in human

placenta and in BeWo cells. Biochemical and biophysical research communications 303, 259-265.

Pasqualini, J.R., Cosquer-Clavreul, C. and Gelly, C. 1983. Rapid modulation by progesterone and tamoxifen of estradiol effects on nuclear histone acetylation in the uterus of the fetal guinea pig. Biochim Biophys Acta 739, 137-140.

Patel, J., Landers, K., Mortimer, R.H. and Richard, K. 2010. Regulation of hypoxia inducible factors (HIF) in hypoxia and normoxia during placental development. Placenta 31, 951-957.

Pathak, P., Li, T. and Chiang, J.Y. 2013. Retinoic acid-related orphan receptor alpha regulates diurnal rhythm and fasting induction of sterol 12alpha-hydroxylase in bile acid synthesis. The Journal of biological chemistry 288, 37154-37165.

Pattabiraman, P.P., Pecen, P.E. and Rao, P.V. 2013. MRP4-mediated regulation of intracellular cAMP and cGMP levels in trabecular meshwork cells and homeostasis of intraocular pressure. Invest Ophthalmol Vis Sci 54, 1636-1649.

Pattillo, R.A. and Gey, G.O. 1968a. The establishment of a cell line of human hormone-synthesizing trophoblastic cells in vitro. Cancer research 28, 1231-1236.

Pattillo, R.A. and Gey, G.O. 1968b. The Establishment of a Cell Line of Human Hormone-synthesizing Trophoblastic Cells in Vitro. Cancer research 28, 1231-1236.

Pattillo, R.A., Gey, G.O., Delfs, E., Huang, W.Y., Hause, L., Garancis, D.J., Knoth, M., Amatruda, J., Bertino, J., Friesen, H.G. and Mattingly, R.F. 1971. The hormone-synthesizing trophoblastic cell in vitro: a model for cancer research and placental hormone synthesis. Ann N Y Acad Sci 172, 288-298.

Pattillo, R.A., Gey, G.O., Delfs, E. and Mattingly, R.F. 1968c. Human hormone production in vitro. Science 159, 1467-1469.

Paulusma, C.C., Bosma, P.J., Zaman, G.J., Bakker, C.T., Otter, M., Scheffer, G.L., Scheper, R.J., Borst, P. and Oude Elferink, R.P. 1996. Congenital jaundice in rats with a mutation in a multidrug resistance-associated protein gene. Science 271, 1126-1128.

Pavek, P., Merino, G., Wagenaar, E., Bolscher, E., Novotna, M., Jonker, J.W. and Schinkel, A.H. 2005. Human breast cancer resistance protein: interactions with steroid drugs, hormones, the dietary carcinogen 2-amino-1-methyl-6-phenylimidazo(4,5-b)pyridine, and transport of cimetidine. J Pharmacol Exp Ther 312, 144-152.

Peekhaus, N.T., Chang, T., Hayes, E.C., Wilkinson, H.A., Mitra, S.W., Schaeffer, J.M. and Rohrer, S.P. 2004. Distinct effects of the antiestrogen Faslodex on the stability of estrogen receptors-alpha and -beta in the breast cancer cell line MCF-7. J Mol Endocrinol 32, 987-995.

Peng, L., Yoo, B., Gunewardena, S.S., Lu, H., Klaassen, C.D. and Zhong, X.-b. 2012. RNA Sequencing Reveals Dynamic Changes of mRNA Abundance of Cytochromes P450 and Their Alternative Transcripts during Mouse Liver Development. Drug Metabolism and Disposition 40, 1198-1209.

Pepling, M.E., Sundman, E.A., Patterson, N.L., Gephardt, G.W., Medico, L., Jr. and Wilson, K.I. 2010. Differences in oocyte development and estradiol sensitivity among mouse strains. Reproduction 139, 349-357.

Perez-Martinez, C., Garcia-Iglesias, M.J., Bravo-Moral, A.M., Ferreras-Estrada, M.C., Martinez-Rodriguez, J.M. and Escudero-Diez, A. 1995. Effect of diethylstilbestrol or zeranol on fetal development, gestation duration, and number of offspring in NMRI mice. Am J Vet Res 56, 1615-1619.

Petrulis, J.R. and Perdew, G.H. 2002. The role of chaperone proteins in the aryl hydrocarbon receptor core complex. Chemico-biological interactions 141, 25-40.

Peyret, B., Collardeau, S., Touzet, S., Loras-Duclaux, I., Yantren, H., Michalski, M.C., Chaix, J., Restier-Miron, L., Bouvier, R., Lachaux, A. and Peretti, N. 2011. Prevalence of liver complications in children receiving long-term parenteral nutrition. European journal of clinical nutrition 65, 743-749.

Pfeiffer, E., Hildebrand, A., Damm, G., Rapp, A., Cramer, B., Humpf, H.U. and Metzler, M. 2009. Aromatic hydroxylation is a major metabolic pathway of the mycotoxin zearalenone in vitro. Molecular nutrition & food research 53, 1123-1133.

Pham, P.A., la Porte, C.J., Lee, L.S., van Heeswijk, R., Sabo, J.P., Elgadi, M.M., Piliero, P.J., Barditch-Crovo, P., Fuchs, E., Flexner, C. and Cameron, D.W. 2009. Differential effects of tipranavir plus ritonavir on atorvastatin or rosuvastatin pharmacokinetics in healthy volunteers. Antimicrob Agents Chemother 53, 4385-4392.

Phillips, J.M., Yamamoto, Y., Negishi, M., Maronpot, R.R. and Goodman, J.I. 2007. Orphan nuclear receptor constitutive active/androstane receptor-mediated alterations in DNA methylation during phenobarbital promotion of liver tumorigenesis. Toxicol Sci 96, 72-82.

Phipps, E.A., Thadhani, R., Benzing, T. and Karumanchi, S.A. 2019. Pre-eclampsia: pathogenesis, novel diagnostics and therapies. Nat Rev Nephrol 15, 275-289.

Pijnenborg, R., Luyten, C., Vercruysse, L. and Van Assche, F.A. 1996. Attachment and differentiation in vitro of trophoblast from normal and preeclamptic human placentas. Am J Obstet Gynecol 175, 30-36.

Pizzo, F., Caloni, F., Schutz, L.F., Totty, M.L. and Spicer, L.J. 2015. Individual and combined effects of deoxynivalenol and alpha-zearalenol on cell proliferation and steroidogenesis of granulosa cells in cattle. Environ Toxicol Pharmacol 40, 722-728.

Poller, B., Gutmann, H., Krahenbuhl, S., Weksler, B., Romero, I., Couraud, P.O., Tuffin, G., Drewe, J. and Huwyler, J. 2008. The human brain endothelial cell line hCMEC/D3 as a human blood-brain barrier model for drug transport studies. J Neurochem 107, 1358-1368.

Pollex, E., Lubetsky, A. and Koren, G. 2008. The role of placental breast cancer resistance protein in the efflux of glyburide across the human placenta. Placenta 29, 743-747.

Pollex, E.K., Anger, G., Hutson, J., Koren, G. and Piquette-Miller, M. 2010. Breast cancer resistance protein (BCRP)-mediated glyburide transport: Effect of the C421A/Q141K BCRP single-nucleotide polymorphism. Drug Metab Dispos 38, 740-744.

Ponniah, M., Billett, E.E. and De Girolamo, L.A. 2015. Bisphenol A increases BeWo trophoblast survival in stress-induced paradigms through regulation of oxidative stress and apoptosis. Chem Res Toxicol 28, 1693-1703.

Poulsen, M.S., Rytting, E., Mose, T. and Knudsen, L.E. 2009. Modeling placental transport: correlation of in vitro BeWo cell permeability and ex vivo human placental perfusion. Toxicology in vitro : an international journal published in association with BIBRA 23, 1380-1386.

Prouillac, C., Videmann, B., Mazallon, M. and Lecoeur, S. 2009. Induction of cells differentiation and ABC transporters expression by a myco-estrogen, zearalenone, in human choriocarcinoma cell line (BeWo). Toxicology 263, 100-107.

Prueksaritanont, T., Chu, X., Gibson, C., Cui, D., Yee, K.L., Ballard, J., Cabalu, T. and Hochman, J. 2013. Drug-drug interaction studies: regulatory guidance and an industry perspective. AAPS J 15, 629-645.

Pulido, M.M., Molina, A.J., Merino, G., Mendoza, G., Prieto, J.G. and Alvarez, A.I. 2006. Interaction of enrofloxacin with breast cancer resistance protein (BCRP/ABCG2): Influence of flavonoids and role in milk secretion in sheep. J. Vet. Pharmacol. Ther. 29, 279-287.

Qian, Y.M., Song, W.C., Cui, H., Cole, S.P. and Deeley, R.G. 2001. Glutathione stimulates sulfated estrogen transport by multidrug resistance protein 1. J Biol Chem 276, 6404-6411.

Qiao, E.Q. and Yang, H.J. 2014. Effect of pregnane X receptor expression on drug resistance in breast cancer. Oncol Lett 7, 1191-1196.

Rajagopal, A. and Simon, S.M. 2003. Subcellular localization and activity of multidrug resistance proteins. Mol Biol Cell 14, 3389-3399.

Rajakumar, C., Guan, H., Langlois, D., Cernea, M. and Yang, K. 2015. Bisphenol A disrupts gene expression in human placental trophoblast cells. Reprod Toxicol 53, 39-44.

Randak, C., Auerswald, E.A., Assfalg-Machleidt, I., Reenstra, W.W. and Machleidt, W. 1999. Inhibition of ATPase, GTPase and adenylate kinase activities of the second nucleotide-binding fold of the cystic fibrosis transmembrane conductance regulator by genistein. Biochem. J. 340 (Pt 1), 227-235.

Rangasamy, T., Cho, C.Y., Thimmulappa, R.K., Zhen, L., Srisuma, S.S., Kensler, T.W., Yamamoto, M., Petrache, I., Tuder, R.M. and Biswal, S. 2004. Genetic ablation of Nrf2 enhances susceptibility to cigarette smoke-induced emphysema in mice. The Journal of clinical investigation 114, 1248-1259.

Ranzenigo, G., Caloni, F., Cremonesi, F., Aad, P.Y. and Spicer, L.J. 2008. Effects of Fusarium mycotoxins on steroid production by porcine granulosa cells. Anim Reprod Sci 107, 115-130.

Reed, M.J., Purohit, A., Woo, L.W., Newman, S.P. and Potter, B.V. 2005. Steroid sulfatase: molecular biology, regulation, and inhibition. Endocr Rev 26, 171-202.

Regazzetti, C., Peraldi, P., Gremeaux, T., Najem-Lendom, R., Ben-Sahra, I., Cormont, M., Bost, F., Le Marchand-Brustel, Y., Tanti, J.F. and Giorgetti-Peraldi, S. 2009. Hypoxia decreases insulin signaling pathways in adipocytes. Diabetes 58, 95-103.

Richard, D.E., Berra, E. and Pouyssegur, J. 2000. Nonhypoxic pathway mediates the induction of hypoxia-inducible factor 1alpha in vascular smooth muscle cells. J Biol Chem 275, 26765-26771.

Rigalli, J.P., Perdomo, V.G., Ciriaci, N., Frances, D.E., Ronco, M.T., Bataille, A.M., Ghanem, C.I., Ruiz, M.L., Manautou, J.E. and Catania, V.A. 2016. The trypanocidal benznidazole promotes adaptive response to oxidative injury: Involvement of the nuclear factor-erythroid 2-related factor-2 (Nrf2) and multidrug resistance associated protein 2 (MRP2). Toxicology and applied pharmacology 304, 90-98.

Rigalli, J.P., Scholz, P.N., Tocchetti, G.N., Ruiz, M.L. and Weiss, J. 2019. The phytoestrogens daidzein and equol inhibit the drug transporter BCRP/ABCG2 in breast cancer cells: potential chemosensitizing effect. Eur J Nutr 58, 139-150.

Rigato, I., Pascolo, L., Fernetti, C., Ostrow, J.D. and Tiribelli, C. 2004. The human multidrug-resistance-associated protein MRP1 mediates ATP-dependent transport of unconjugated bilirubin. Biochem J 383, 335-341.

Ritzel, M.W., Ng, A.M., Yao, S.Y., Graham, K., Loewen, S.K., Smith, K.M., Ritzel, R.G., Mowles, D.A., Carpenter, P., Chen, X.Z., Karpinski, E., Hyde, R.J., Baldwin, S.A., Cass, C.E. and Young, J.D. 2001. Molecular identification and characterization of novel human and mouse concentrative Na+-nucleoside cotransporter proteins (hCNT3 and mCNT3) broadly selective for purine and pyrimidine nucleosides (system cib). J Biol Chem 276, 2914-2927.

Ritzel, M.W., Yao, S.Y., Huang, M.Y., Elliott, J.F., Cass, C.E. and Young, J.D. 1997. Molecular cloning and functional expression of cDNAs encoding a human Na+-nucleoside cotransporter (hCNT1). Am J Physiol 272, C707-714.

Rivera-Nunez, Z., Barrett, E.S., Szamreta, E.A., Shapses, S.A., Qin, B., Lin, Y., Zarbl, H., Buckley, B. and Bandera, E.V. 2019. Urinary mycoestrogens and age and height at menarche in New Jersey girls. Environ Health 18, 24.

Roberts, J.M. and Escudero, C. 2012. The placenta in preeclampsia. Pregnancy Hypertens 2, 72-83.

Rodesch, F., Simon, P., Donner, C. and Jauniaux, E. 1992. Oxygen measurements in endometrial and trophoblastic tissues during early pregnancy. Obstetrics and gynecology 80, 283-285.

Rodway, M., Zhou, F.Z., Benoit, J., Yuen, B.H. and Leung, P.C. 1988. Differential effects of 8-bromo-cyclic AMP on human chorionic gonadotropin (hCG), progesterone and estrogen production by term placental cells. Life Sci 43, 1451-1458.

Rosenberg, M.F., Bikadi, Z., Chan, J., Liu, X., Ni, Z., Cai, X., Ford, R.C. and Mao, Q. 2010. The human breast cancer resistance protein (BCRP/ABCG2) shows conformational changes with mitoxantrone. Structure 18, 482-493.

Rost, D., Konig, J., Weiss, G., Klar, E., Stremmel, W. and Keppler, D. 2001. Expression and localization of the multidrug resistance proteins MRP2 and MRP3 in human gallbladder epithelia. Gastroenterology 121, 1203-1208.

Roth, M., Obaidat, A. and Hagenbuch, B. 2012. OATPs, OATs and OCTs: the organic anion and cation transporters of the SLCO and SLC22A gene superfamilies. British journal of pharmacology 165, 1260-1287.

Roundhill, E.A. and Burchill, S.A. 2012. Detection and characterisation of multi-drug resistance protein 1 (MRP-1) in human mitochondria. Br J Cancer 106, 1224-1233.

Rubinchik-Stern, M. and Eyal, S. 2012. Drug Interactions at the Human Placenta: What is the Evidence? Front Pharmacol 3, 126.

Ruebner, M., Langbein, M., Strissel, P.L., Henke, C., Schmidt, D., Goecke, T.W., Faschingbauer, F., Schild, R.L., Beckmann, M.W. and Strick, R. 2012. Regulation of the human endogenous retroviral Syncytin-1 and cell-cell fusion by the nuclear hormone receptors PPARgamma/RXRalpha in placentogenesis. Journal of cellular biochemistry 113, 2383-2396.

Ruebner, M., Strissel, P.L., Langbein, M., Fahlbusch, F., Wachter, D.L., Faschingbauer, F., Beckmann, M.W. and Strick, R. 2010. Impaired cell fusion and differentiation in placentae from patients with intrauterine growth restriction correlate with reduced levels of HERV envelope genes. J Mol Med (Berl) 88, 1143-1156.

Russel, F.G., Koenderink, J.B. and Masereeuw, R. 2008. Multidrug resistance protein 4 (MRP4/ABCC4): a versatile efflux transporter for drugs and signalling molecules. Trends Pharmacol Sci 29, 200-207.

Ryoo, I.G., Kim, G., Choi, B.H., Lee, S.H. and Kwak, M.K. 2016. Involvement of NRF2 Signaling in Doxorubicin Resistance of Cancer Stem Cell-Enriched Colonospheres. Biomol Ther (Seoul) 24, 482-488.

Sachs, J.A. and Brewerton, D.A. 1978. HLA, ankylosing spondylitis and rheumatoid arthritis. Br Med Bull 34, 275-278.

Sadhasivam, S., Chidambaran, V., Zhang, X., Meller, J., Esslinger, H., Zhang, K., Martin, L.J. and McAuliffe, J. 2015. Opioid-induced respiratory depression: ABCB1 transporter pharmacogenetics. Pharmacogenomics J 15, 119-126.

Saito, J., Hirota, T., Furuta, S., Kobayashi, D., Takane, H. and Ieiri, I. 2013. Association between DNA methylation in the miR-328 5'-flanking region and inter-individual differences in miR-328 and BCRP expression in human placenta. PLoS One 8, e72906.

Saito, S., Iida, A., Sekine, A., Miura, Y., Ogawa, C., Kawauchi, S., Higuchi, S. and Nakamura, Y. 2002. Identification of 779 genetic variations in eight genes encoding members of the ATP-binding cassette, subfamily C (ABCC/MRP/CFTR. J Hum Genet 47, 147-171.

Sakulterdkiat, T., Srisomsap, C., Udomsangpetch, R., Svasti, J. and Lirdprapamongkol, K. 2012. Curcumin resistance induced by hypoxia in HepG2 cells is mediated by multidrug-resistance-associated proteins. Anticancer research 32, 5337-5342.

Salerno, M., Petroutsa, M. and Garnier-Suillerot, A. 2002. The MRP1-mediated effluxes of arsenic and antimony do not require arsenic-glutathione and antimony-glutathione complex formation. J Bioenerg Biomembr 34, 135-145.

Salido, E.C., Yen, P.H., Barajas, L. and Shapiro, L.J. 1990. Steroid sulfatase expression in human placenta: immunocytochemistry and in situ hybridization study. J Clin Endocrinol Metab 70, 1564-1567.

Samangaya, R.A., Mires, G., Shennan, A., Skillern, L., Howe, D., McLeod, A. and Baker, P.N. 2009. A randomised, double-blinded, placebo-controlled study of the phosphodiesterase type 5 inhibitor sildenafil for the treatment of preeclampsia. Hypertens Pregnancy 28, 369-382.

Sampath, J., Adachi, M., Hatse, S., Naesens, L., Balzarini, J., Flatley, R.M., Matherly, L.H. and Schuetz, J.D. 2002. Role of MRP4 and MRP5 in biology and chemotherapy. AAPS PharmSci 4, E14.

Sandusky, G.E., Mintze, K.S., Pratt, S.E. and Dantzig, A.H. 2002. Expression of multidrug resistance-associated protein 2 (MRP2) in normal human tissues and carcinomas using tissue microarrays. Histopathology 41, 65-74.

Sassi, Y., Abi-Gerges, A., Fauconnier, J., Mougenot, N., Reiken, S., Haghighi, K., Kranias, E.G., Marks, A.R., Lacampagne, A., Engelhardt, S., Hatem, S.N., Lompre, A.M. and Hulot, J.S. 2012. Regulation of cAMP homeostasis by the efflux protein MRP4 in cardiac myocytes. FASEB J 26, 1009-1017.

Sassi, Y., Lipskaia, L., Vandecasteele, G., Nikolaev, V.O., Hatem, S.N., Cohen Aubart, F., Russel, F.G., Mougenot, N., Vrignaud, C., Lechat, P., Lompre, A.M. and Hulot, J.S. 2008. Multidrug resistance-associated protein 4 regulates cAMP-dependent signaling pathways and controls human and rat SMC proliferation. J Clin Invest 118, 2747-2757.

Sawai, K., Azuma, C., Koyama, M., Hashimoto, K., Kimura, T., Samejima, Y., Nobunaga, T., Takemura, M. and Saji, F. 1996. The novel role of 3',5'-guanosine monophosphate (cGMP) on the differentiation of trophoblasts: comparison with the effects of 3',5'-adenosine monophosphate (cAMP). Early Pregnancy 2, 244-252.

Sayin, S.I., Wahlstrom, A., Felin, J., Jantti, S., Marschall, H.U., Bamberg, K., Angelin, B., Hyotylainen, T., Oresic, M. and Backhed, F. 2013. Gut microbiota regulates bile acid metabolism by reducing the levels of tauro-beta-muricholic acid, a naturally occurring FXR antagonist. Cell metabolism 17, 225-235.

Sayyed, K., Vee, M.L., Abdel-Razzak, Z., Jouan, E., Stieger, B., Denizot, C., Parmentier, Y. and Fardel, O. 2016. Alteration of human hepatic drug transporter activity and expression by cigarette smoke condensate. Toxicology 363-364, 58-71.

Scharenberg, C.W., Harkey, M.A. and Torok-Storb, B. 2002. The ABCG2 transporter is an efficient Hoechst 33342 efflux pump and is preferentially expressed by immature human hematopoietic progenitors. Blood 99, 507-512.

Schaub, T.P., Kartenbeck, J., Konig, J., Spring, H., Dorsam, J., Staehler, G., Storkel, S., Thon, W.F. and Keppler, D. 1999. Expression of the MRP2 gene-encoded conjugate export pump in human kidney proximal tubules and in renal cell carcinoma. J Am Soc Nephrol 10, 1159-1169.

Scheffer, G.L., Kool, M., de Haas, M., de Vree, J.M., Pijnenborg, A.C., Bosman, D.K., Elferink, R.P., van der Valk, P., Borst, P. and Scheper, R.J. 2002. Tissue distribution and induction of human multidrug resistant protein 3. Lab Invest 82, 193-201.

Schneider, E., Yamazaki, H., Sinha, B.K. and Cowan, K.H. 1995. Buthionine sulphoximine-mediated sensitisation of etoposide-resistant human breast cancer MCF7 cells overexpressing the multidrug resistance-associated protein involves increased drug accumulation. Br J Cancer 71, 738-743.

Schneider, H. 2011. Oxygenation of the placental-fetal unit in humans. Respir Physiol Neurobiol 178, 51-58.

Schollenberger, M., Muller, H.M., Rufle, M., Suchy, S., Planck, S. and Drochner, W. 2005. Survey of Fusarium toxins in foodstuffs of plant origin marketed in Germany. Int J Food Microbiol 97, 317-326.

Schwartz, R.A., Rosenn, B., Aleksa, K. and Koren, G. 2015. Glyburide transport across the human placenta. Obstet Gynecol 125, 583-588.

Schweigmann, H., Sanchez-Guijo, A., Ugele, B., Hartmann, K., Hartmann, M.F., Bergmann, M., Pfarrer, C., Doring, B., Wudy, S.A., Petzinger, E., Geyer, J. and Grosser, G. 2014. Transport of the placental estriol precursor 16alpha-hydroxy-dehydroepiandrosterone sulfate (16alpha-OH-DHEAS) by stably transfected OAT4-, SOAT-, and NTCP-HEK293 cells. J Steroid Biochem Mol Biol 143, 259-265.

Scotto, K.W. 2003. Transcriptional regulation of ABC drug transporters. Oncogene 22, 7496-7511.

Shao, R. 2013. Progesterone receptor isoforms A and B: new insights into the mechanism of progesterone resistance for the treatment of endometrial carcinoma. Ecancermedicalscience 7, 381.

Sharp, A., Cornforth, C., Jackson, R., Harrold, J., Turner, M.A., Kenny, L.C., Baker, P.N., Johnstone, E.D., Khalil, A., von Dadelszen, P., Papageorghiou, A.T., Alfirevic, Z. and group, S. 2018. Maternal sildenafil for severe fetal growth restriction (STRIDER): a multicentre, randomised, placebo-controlled, double-blind trial. Lancet Child Adolesc Health 2, 93-102.

Shi, J.F., Yang, N., Ding, H.J., Zhang, J.X., Hu, M.L., Leng, Y., Han, X. and Sun, Y.J. 2014. ERalpha directly activated the MDR1 transcription to increase paclitaxel-resistance of ERalpha-positive breast cancer cells in vitro and in vivo. Int J Biochem Cell Biol 53, 35-45.

Shier, W.T., Shier, A.C., Xie, W. and Mirocha, C.J. 2001. Structure-activity relationships for human estrogenic activity in zearalenone mycotoxins. Toxicon 39, 1435-1438.

Shin, B.S., Bulitta, J.B., Balthasar, J.P., Kim, M., Choi, Y. and Yoo, S.D. 2011. Prediction of human pharmacokinetics and tissue distribution of apicidin, a potent histone deacetylase inhibitor, by physiologically based pharmacokinetic modeling. Cancer Chemother Pharmacol 68, 465-475.

Shin, B.S., Hong, S.H., Bulitta, J.B., Hwang, S.W., Kim, H.J., Lee, J.B., Yang, S.D., Kim, J.E., Yoon, H.S., Kim, D.J. and Yoo, S.D. 2009. Disposition, oral bioavailability, and tissue distribution of zearalenone in rats at various dose levels. J Toxicol Environ Health A 72, 1406-1411.

Shukalek, C.B., Swanlund, D.P., Rousseau, R.K., Weigl, K.E., Marensi, V., Cole, S.P. and Leslie, E.M. 2016. Arsenic Triglutathione [As(GS)3] Transport by Multidrug Resistance Protein 1 (MRP1/ABCC1) Is Selectively Modified by Phosphorylation of Tyr920/Ser921 and Glycosylation of Asn19/Asn23. Mol Pharmacol 90, 127-139.

Sieppi, E., Vahakangas, K., Rautio, A., Ietta, F., Paulesu, L. and Myllynen, P. 2016. The xenoestrogens, bisphenol A and para-nonylphenol, decrease the expression of the ABCG2 transporter protein in human term placental explant cultures. Mol Cell Endocrinol 429, 41-49.

Sikkel, E., Pasman, S.A., Oepkes, D., Kanhai, H.H. and Vandenbussche, F.P. 2004. On the origin of amniotic fluid bilirubin. Placenta 25, 463-468.

Siman, C.M., Sibley, C.P., Jones, C.J., Turner, M.A. and Greenwood, S.L. 2001. The functional regeneration of syncytiotrophoblast in cultured explants of term placenta. Am J Physiol Regul Integr Comp Physiol 280, R1116-1122.

Simonson, S.G., Raza, A., Martin, P.D., Mitchell, P.D., Jarcho, J.A., Brown, C.D., Windass, A.S. and Schneck, D.W. 2004. Rosuvastatin pharmacokinetics in heart transplant recipients administered an antirejection regimen including cyclosporine. Clinical pharmacology and therapeutics 76, 167-177.

Singh, A., Wu, H., Zhang, P., Happel, C., Ma, J. and Biswal, S. 2010. Expression of ABCG2 (BCRP) is regulated by Nrf2 in cancer cells that confers side population and chemoresistance phenotype. Molecular cancer therapeutics 9, 2365-2376.

Sitras, V., Paulssen, R.H., Gronaas, H., Leirvik, J., Hanssen, T.A., Vartun, A. and Acharya, G. 2009. Differential placental gene expression in severe preeclampsia. Placenta 30, 424-433.

Slobodchikova, I., Sivakumar, R., Rahman, M.S. and Vuckovic, D. 2019. Characterization of Phase I and Glucuronide Phase II Metabolites of 17 Mycotoxins Using Liquid Chromatography-High-Resolution Mass Spectrometry. Toxins (Basel) 11.

Sonagra, A.D., Biradar, S.M., K, D. and Murthy, D.S.J. 2014. Normal pregnancy- a state of insulin resistance. J Clin Diagn Res 8, CC01-03.

Soncin, F., Natale, D. and Parast, M.M. 2015. Signaling pathways in mouse and human trophoblast differentiation: a comparative review. Cell Mol Life Sci 72, 1291-1302.

Song, N.Y., Kim, D.H., Kim, E.H., Na, H.K. and Surh, Y.J. 2009. 15-Deoxy-delta 12, 14-prostaglandin J2 induces upregulation of multidrug resistance-associated protein 1 via Nrf2 activation in human breast cancer cells. Annals of the New York Academy of Sciences 1171, 210-216.

Sparreboom, A., Gelderblom, H., Marsh, S., Ahluwalia, R., Obach, R., Principe, P., Twelves, C., Verweij, J. and McLeod, H.L. 2004. Diflomotecan pharmacokinetics in relation to ABCG2 421C>A genotype. Clin Pharmacol Ther 76, 38-44.

Sparreboom, A., Loos, W.J., Burger, H., Sissung, T.M., Verweij, J., Figg, W.D., Nooter, K. and Gelderblom, H. 2005. Effect of ABCG2 genotype on the oral bioavailability of topotecan. Cancer Biol Ther 4, 650-658.

Spearow, J.L. and Barkley, M. 1999a. Genetic control of hormone-induced ovulation rate in mice. Biol Reprod 61, 851-856.

Spearow, J.L., Doemeny, P., Sera, R., Leffler, R. and Barkley, M. 1999b. Genetic variation in susceptibility to endocrine disruption by estrogen in mice. Science 285, 1259-1261.

Squadrito, F., Marini, H., Bitto, A., Altavilla, D., Polito, F., Adamo, E.B., D'Anna, R., Arcoraci, V., Burnett, B.P., Minutoli, L., Di Benedetto, A., Di Vieste, G., Cucinotta, D., de Gregorio, C., Russo, S., Corrado, F., Saitta, A., Irace, C., Corrao, S. and Licata, G. 2013. Genistein in the metabolic syndrome: Results of a randomized clinical trial. J. Clin. Endocrinol. Metab. 98, 3366-3374.

St-Pierre, M.V., Serrano, M.A., Macias, R.I., Dubs, U., Hoechli, M., Lauper, U., Meier, P.J. and Marin, J.J. 2000. Expression of members of the multidrug resistance protein family in human term placenta. Am J Physiol Regul Integr Comp Physiol 279, R1495-1503.

Stanek, J. 2013. Hypoxic patterns of placental injury: a review. Archives of pathology & laboratory medicine 137, 706-720.

Stejskalova, L., Vecerova, L., Perez, L.M., Vrzal, R., Dvorak, Z., Nachtigal, P. and Pavek, P. 2011. Aryl hydrocarbon receptor and aryl hydrocarbon nuclear translocator expression in human and rat placentas and transcription activity in human trophoblast cultures. Toxicol Sci 123, 26-36.

Stiburkova, B., Pavelcova, K., Zavada, J., Petru, L., Simek, P., Cepek, P., Pavlikova, M., Matsuo, H., Merriman, T.R. and Pavelka, K. 2017. Functional non-synonymous variants of ABCG2 and gout risk. Rheumatology (Oxford) 56, 1982-1992.

Stillerman, K.P., Mattison, D.R., Giudice, L.C. and Woodruff, T.J. 2008. Environmental exposures and adverse pregnancy outcomes: a review of the science. Reprod Sci 15, 631-650.

Stirone, C., Duckles, S.P. and Krause, D.N. 2003. Multiple forms of estrogen receptor-alpha in cerebral blood vessels: regulation by estrogen. Am J Physiol Endocrinol Metab 284, E184-192.

Stokes, W.S. 2004. Selecting appropriate animal models and experimental designs for endocrine disruptor research and testing studies. ILAR J 45, 387-393.

Stolarczyk, E.I., Reiling, C.J., Pickin, K.A., Coppage, R., Knecht, M.R. and Paumi, C.M. 2012. Casein kinase 2alpha regulates multidrug resistance-associated protein 1 function via phosphorylation of Thr249. Mol Pharmacol 82, 488-499.

Strom, S.S., Yamamura, Y., Duphorne, C.M., Spitz, M.R., Babaian, R.J., Pillow, P.C. and Hursting, S.D. 1999. Phytoestrogen intake and prostate cancer: A case-control study using a new database. Nutr. Cancer 33, 20-25.

Sun, M., Kingdom, J., Baczyk, D., Lye, S.J., Matthews, S.G. and Gibb, W. 2006. Expression of the multidrug resistance P-glycoprotein, (ABCB1 glycoprotein) in the human placenta decreases with advancing gestation. Placenta 27, 602-609.

Sundseth, R., MacDonald, G., Ting, J. and King, A.C. 1997. DNA elements recognizing NF-Y and Sp1 regulate the human multidrug-resistance gene promoter. Mol Pharmacol 51, 963-971.

Sung, M.T. and Dixon, G.H. 1970. Modification of histones during spermiogenesis in trout: a molecular mechanism for altering histone binding to DNA. Proc Natl Acad Sci U S A 67, 1616-1623.

Syme, M.R., Paxton, J.W. and Keelan, J.A. 2004. Drug transfer and metabolism by the human placenta. Clin Pharmacokinet 43, 487-514.

Szatmari, I., Vamosi, G., Brazda, P., Balint, B.L., Benko, S., Szeles, L., Jeney, V., Ozvegy-Laczka, C., Szanto, A., Barta, E., Balla, J., Sarkadi, B. and Nagy, L. 2006. Peroxisome proliferator-activated receptor gamma-regulated ABCG2 expression confers cytoprotection to human dendritic cells. J Biol Chem 281, 23812-23823.

Szilagyi, J.T., Gorczyca, L., Brinker, A., Buckley, B., Laskin, J.D. and Aleksunes, L.M. 2019. Placental BCRP/ABCG2 Transporter Prevents Fetal Exposure to the Estrogenic Mycotoxin Zearalenone. Toxicol Sci 168, 394-404.

Szilagyi, J.T., Vetrano, A.M., Laskin, J.D. and Aleksunes, L.M. 2017. Localization of the placental BCRP/ABCG2 transporter to lipid rafts: Role for cholesterol in mediating efflux activity. Placenta 55, 29-36.

Tabe, Y., Konopleva, M., Contractor, R., Munsell, M., Schober, W.D., Jin, L., Tsutsumi-Ishii, Y., Nagaoka, I., Igari, J. and Andreeff, M. 2006. Up-regulation of MDR1 and induction of doxorubicin resistance by histone deacetylase inhibitor depsipeptide (FK228) and ATRA in acute promyelocytic leukemia cells. Blood 107, 1546-1554.

Tachampa, K., Takeda, M., Khamdang, S., Noshiro-Kofuji, R., Tsuda, M., Jariyawat, S., Fukutomi, T., Sophasan, S., Anzai, N. and Endou, H. 2008. Interactions of organic anion transporters and organic cation transporters with mycotoxins. Journal of pharmacological sciences 106, 435-443.

Tache, V., Ciric, A., Moretto-Zita, M., Li, Y., Peng, J., Maltepe, E., Milstone, D.S. and Parast, M.M. 2013. Hypoxia and trophoblast differentiation: a key role for PPARgamma. Stem Cells Dev 22, 2815-2824.

Taher, S.I. and Alalaf, S.K. 2019. Association between serum beta-human chorionic gonadotropin and preeclampsia and its effects on perinatal and maternal outcomes: a case control study. Arch Gynecol Obstet 299, 713-718.

Tait, S., Tassinari, R., Maranghi, F. and Mantovani, A. 2015. Bisphenol A affects placental layers morphology and angiogenesis during early pregnancy phase in mice. J Appl Toxicol 35, 1278-1291.

Takagi, M., Mukai, S., Kuriyagawa, T., Takagaki, K., Uno, S., Kokushi, E., Otoi, T., Budiyanto, A., Shirasuna, K., Miyamoto, A., Kawamura, O., Okamoto, K. and Deguchi, E. 2008. Detection of zearalenone and its metabolites in naturally contaminated follicular fluids by using LC/MS/MS and in vitro effects of zearalenone on oocyte maturation in cattle. Reprod Toxicol 26, 164-169.

Takemura, H., Shim, J.-Y., Sayama, K., Tsubura, A., Ting Zhu, B. and Shimoi, K. 2007a. Characterization of the estrogenic activities of zearalenone and zeranol in vivo and in vitro.

Takemura, H., Shim, J.Y., Sayama, K., Tsubura, A., Zhu, B.T. and Shimoi, K. 2007b. Characterization of the estrogenic activities of zearalenone and zeranol in vivo and in vitro. J Steroid Biochem Mol Biol 103, 170-177.

Takeuchi, Y., Sakakibara, R. and Ishiguro, M. 1990. Synthesis and secretion of human chorionic gonadotropin and its subunits in choriocarcinoma cells: A comparative study with normal placental cells. Mol Cell Endocrinol 69, 145-156.

Tamura, A., Wakabayashi, K., Onishi, Y., Takeda, M., Ikegami, Y., Sawada, S., Tsuji, M., Matsuda, Y. and Ishikawa, T. 2007. Re-evaluation and functional classification of non-synonymous single nucleotide polymorphisms of the human ATP-binding cassette transporter ABCG2. Cancer Sci 98, 231-239.

Tan, K.P., Wang, B., Yang, M., Boutros, P.C., Macaulay, J., Xu, H., Chuang, A.I., Kosuge, K., Yamamoto, M., Takahashi, S., Wu, A.M., Ross, D.D., Harper, P.A. and Ito, S. 2010. Aryl hydrocarbon receptor is a transcriptional activator of the human breast cancer resistance protein (BCRP/ABCG2). Mol Pharmacol 78, 175-185.

Taniguchi, C.M., Finger, E.C., Krieg, A.J., Wu, C., Diep, A.N., LaGory, E.L., Wei, K., McGinnis, L.M., Yuan, J., Kuo, C.J. and Giaccia, A.J. 2013. Cross-talk between hypoxia and insulin signaling through Phd3 regulates hepatic glucose and lipid metabolism and ameliorates diabetes. Nat Med 19, 1325-1330.

Tarrade, A., Schoonjans, K., Guibourdenche, J., Bidart, J.M., Vidaud, M., Auwerx, J., Rochette-Egly, C. and Evain-Brion, D. 2001. PPAR gamma/RXR alpha heterodimers are involved in human CG beta synthesis and human trophoblast differentiation. Endocrinology 142, 4504-4514.

Taylor, R.N., Newman, E.D. and Chen, S.A. 1991. Forskolin and methotrexate induce an intermediate trophoblast phenotype in cultured human choriocarcinoma cells. Am J Obstet Gynecol 164, 204-210.

Teng, S. and Piquette-Miller, M. 2005. The involvement of the pregnane X receptor in hepatic gene regulation during inflammation in mice. The Journal of pharmacology and experimental therapeutics 312, 841-848.

Terranova-Barberio, M., Roca, M.S., Zotti, A.I., Leone, A., Bruzzese, F., Vitagliano, C., Scogliamiglio, G., Russo, D., D'Angelo, G., Franco, R., Budillon, A. and Di Gennaro, E. 2016. Valproic acid potentiates the anticancer activity of capecitabine in vitro and in vivo in breast cancer models via induction of thymidine phosphorylase expression. Oncotarget 7, 7715-7731.

Tiemann, U., Tomek, W., Schneider, F. and Vanselow, J. 2003. Effects of the mycotoxins alpha- and beta-zearalenol on regulation of progesterone synthesis in cultured granulosa cells from porcine ovaries. Reprod Toxicol 17, 673-681.

Tiffon, C., Adams, J., van der Fits, L., Wen, S., Townsend, P., Ganesan, A., Hodges, E., Vermeer, M. and Packham, G. 2011. The histone deacetylase inhibitors vorinostat and romidepsin downmodulate IL-10 expression in cutaneous T-cell lymphoma cells. Br J Pharmacol 162, 1590-1602.

Timsit, Y.E. and Negishi, M. 2007. CAR and PXR: the xenobiotic-sensing receptors. Steroids 72, 231-246.

Tivnan, A., Zakaria, Z., O'Leary, C., Kogel, D., Pokorny, J.L., Sarkaria, J.N. and Prehn, J.H. 2015. Inhibition of multidrug resistance protein 1 (MRP1) improves chemotherapy drug response in primary and recurrent glioblastoma multiforme. Front Neurosci 9, 218.

To, K.K., Polgar, O., Huff, L.M., Morisaki, K. and Bates, S.E. 2008a. Histone modifications at the ABCG2 promoter following treatment with histone deacetylase inhibitor mirror those in multidrug-resistant cells. Mol Cancer Res 6, 151-164.

To, K.K., Robey, R.W., Knutsen, T., Zhan, Z., Ried, T. and Bates, S.E. 2009. Escape from hsa-miR-519c enables drug-resistant cells to maintain high expression of ABCG2. Molecular cancer therapeutics 8, 2959-2968.

To, K.K., Zhan, Z. and Bates, S.E. 2006. Aberrant promoter methylation of the ABCG2 gene in renal carcinoma. Molecular and cellular biology 26, 8572-8585.

To, K.K., Zhan, Z., Litman, T. and Bates, S.E. 2008b. Regulation of ABCG2 expression at the 3' untranslated region of its mRNA through modulation of transcript stability and protein translation by a putative microRNA in the S1 colon cancer cell line. Molecular and cellular biology 28, 5147-5161.

Tompkins, L.M., Li, H., Li, L., Lynch, C., Xie, Y., Nakanishi, T., Ross, D.D. and Wang, H. 2010. A novel xenobiotic responsive element regulated by aryl hydrocarbon receptor is involved in the induction of BCRP/ABCG2 in LS174T cells. Biochemical pharmacology 80, 1754-1761.

Tralamazza, S.M., Bemvenuti, R.H., Zorzete, P., de Souza Garcia, F. and Correa, B. 2016. Fungal diversity and natural occurrence of deoxynivalenol and zearalenone in freshly harvested wheat grains from Brazil. Food Chem 196, 445-450.

Trapani, A., Jr., Goncalves, L.F., Trapani, T.F., Vieira, S., Pires, M. and Pires, M.M. 2016. Perinatal and Hemodynamic Evaluation of Sildenafil Citrate for Preeclampsia Treatment: A Randomized Controlled Trial. Obstet Gynecol 128, 253-259.

Traxler, P., Green, J., Mett, H., Sequin, U. and Furet, P. 1999. Use of a pharmacophore model for the design of EGFR tyrosine kinase inhibitors: Isoflavones and 3-phenyl-4(1H)-quinolones. J Med Chem 42, 1018-1026.

Treins, C., Giorgetti-Peraldi, S., Murdaca, J., Semenza, G.L. and Van Obberghen, E. 2002. Insulin stimulates hypoxia-inducible factor 1 through a phosphatidylinositol 3-kinase/target of rapamycin-dependent signaling pathway. J Biol Chem 277, 27975-27981.

Turner, B.M. 1991. Histone acetylation and control of gene expression. J Cell Sci 99 (Pt 1), 13-20.

Turner, J.G., Gump, J.L., Zhang, C., Cook, J.M., Marchion, D., Hazlehurst, L., Munster, P., Schell, M.J., Dalton, W.S. and Sullivan, D.M. 2006. ABCG2 expression, function, and promoter methylation in human multiple myeloma. Blood 108, 3881-3889.

Uchida, T., Rossignol, F., Matthay, M.A., Mounier, R., Couette, S., Clottes, E. and Clerici, C. 2004. Prolonged hypoxia differentially regulates hypoxia-inducible factor (HIF)-1alpha and HIF-2alpha expression in lung epithelial cells: implication of natural antisense HIF-1alpha. J Biol Chem 279, 14871-14878.

Udasin, R.G., Wen, X., Bircsak, K.M., Aleksunes, L.M., Shakarjian, M.P., Kong, A.N., Heck, D.E., Laskin, D.L. and Laskin, J.D. 2016. Nrf2 Regulates the Sensitivity of Mouse Keratinocytes to Nitrogen Mustard via Multidrug Resistance-Associated Protein 1 (Mrp1). Toxicological sciences : an official journal of the Society of Toxicology 149, 202-212.

Ueda, K., Clark, D.P., Chen, C.J., Roninson, I.B., Gottesman, M.M. and Pastan, I. 1987a. The human multidrug resistance (mdr1) gene. cDNA cloning and transcription initiation. J Biol Chem 262, 505-508.

Ueda, K., Pastan, I. and Gottesman, M.M. 1987b. Isolation and sequence of the promoter region of the human multidrug-resistance (P-glycoprotein) gene. J Biol Chem 262, 17432-17436.

Uehar, M., Arai, Y., Watanabe, S. and Adlercreutz, H. 2000. Comparison of plasma and urinary phytoestrogens in Japanese and Finnish women by time-resolved fluoroimmunoassay. BioFactors 12, 217-225.

Ugele, B., Bahn, A. and Rex-Haffner, M. 2008. Functional differences in steroid sulfate uptake of organic anion transporter 4 (OAT4) and organic anion transporting polypeptide 2B1 (OATP2B1) in human placenta. J Steroid Biochem Mol Biol 111, 1-6.

Ugele, B., St-Pierre, M.V., Pihusch, M., Bahn, A. and Hantschmann, P. 2003. Characterization and identification of steroid sulfate transporters of human placenta. Am J Physiol Endocrinol Metab 284, E390-398.

Urquhart, B.L., Ware, J.A., Tirona, R.G., Ho, R.H., Leake, B.F., Schwarz, U.I., Zaher, H., Palandra, J., Gregor, J.C., Dresser, G.K. and Kim, R.B. 2008. Breast cancer resistance protein (ABCG2) and drug disposition: Intestinal expression, polymorphisms and sulfasalazine as an in vivo probe. Pharmacogenet Genomics 18, 439-448.

USB. 2014. Consumer Attitudes About Nutrition, Health and Soyfoods. United Soybean Board.

USDA. 2008. U.S. Department of Agriculture, Agricultural Research Service Database for the Isoflavone Content of Selected Foods, Release 2.0. Nutrient Data Laboratory Home Page.

Uzan, J., Carbonnel, M., Piconne, O., Asmar, R. and Ayoubi, J.M. 2011. Pre-eclampsia: pathophysiology, diagnosis, and management. Vasc Health Risk Manag 7, 467-474.

Vahakangas, K. and Myllynen, P. 2009. Drug transporters in the human blood-placental barrier. Br J Pharmacol 158, 665-678.

Van Aubel, R.A., Koenderink, J.B., Peters, J.G., Van Os, C.H. and Russel, F.G. 1999. Mechanisms and interaction of vinblastine and reduced glutathione transport in membrane vesicles by the rabbit multidrug resistance protein Mrp2 expressed in insect cells. Mol Pharmacol 56, 714-719.

van de Wetering, K., Burkon, A., Feddema, W., Bot, A., de Jonge, H., Somoza, V. and Borst, P. 2009. Intestinal breast cancer resistance protein (BCRP)/Bcrp1 and multidrug resistance protein 3 (MRP3)/Mrp3 are involved in the pharmacokinetics of resveratrol. Mol Pharmacol 75, 876-885.

Van Den Bemd, G.J., Kuiper, G.G., Pols, H.A. and Van Leeuwen, J.P. 1999. Distinct effects on the conformation of estrogen receptor alpha and beta by both the antiestrogens ICI 164,384 and ICI 182,780 leading to opposite effects on receptor stability. Biochem Biophys Res Commun 261, 1-5.

van Groenigen, M., Valentijn, L.J. and Baas, F. 1993. Identification of a functional initiator sequence in the human MDR1 promoter. Biochim Biophys Acta 1172, 138-146.

van Herwaarden, A.E., Wagenaar, E., Karnekamp, B., Merino, G., Jonker, J.W. and Schinkel, A.H. 2006. Breast cancer resistance protein (Bcrp1/Abcg2) reduces systemic exposure of the dietary carcinogens aflatoxin B1, IQ and Trp-P-1 but also mediates their secretion into breast milk. Carcinogenesis 27, 123-130.

van Hoppe, S., Sparidans, R.W., Wagenaar, E., Beijnen, J.H. and Schinkel, A.H. 2017. Breast cancer resistance protein (BCRP/ABCG2) and P-glycoprotein (P-gp/ABCB1) transport afatinib and restrict its oral availability and brain accumulation. Pharmacol Res 120, 43-50.

Vardhana, P.A. and Illsley, N.P. 2002. Transepithelial glucose transport and metabolism in BeWo choriocarcinoma cells. Placenta 23, 653-660.

Videmann, B., Mazallon, M., Prouillac, C., Delaforge, M. and Lecoeur, S. 2009. ABCC1, ABCC2 and ABCC3 are implicated in the transepithelial transport of the myco-estrogen zearalenone and its major metabolites. Toxicol Lett 190, 215-223.

Vlaardingerbroek, H., Ng, K., Stoll, B., Benight, N., Chacko, S., Kluijtmans, L.A., Kulik, W., Squires, E.J., Olutoye, O., Schady, D., Finegold, M.L., van Goudoever, J.B. and Burrin,

D.G. 2014. New generation lipid emulsions prevent PNALD in chronic parenterally fed preterm pigs. Journal of lipid research 55, 466-477.

Vlaming, M.L., van Esch, A., van de Steeg, E., Pala, Z., Wagenaar, E., van Tellingen, O. and Schinkel, A.H. 2011. Impact of abcc2 [multidrug resistance-associated protein (MRP) 2], abcc3 (MRP3), and abcg2 (breast cancer resistance protein) on the oral pharmacokinetics of methotrexate and its main metabolite 7-hydroxymethotrexate. Drug Metab Dispos 39, 1338-1344.

Vollrath, V., Wielandt, A.M., Iruretagoyena, M. and Chianale, J. 2006. Role of Nrf2 in the regulation of the Mrp2 (ABCC2) gene. The Biochemical journal 395, 599-609.

Vorrink, S.U., Severson, P.L., Kulak, M.V., Futscher, B.W. and Domann, F.E. 2014. Hypoxia perturbs aryl hydrocarbon receptor signaling and CYP1A1 expression induced by PCB 126 in human skin and liver-derived cell lines. Toxicology and applied pharmacology 274, 408-416.

Wada, T., Kang, H.S., Angers, M., Gong, H., Bhatia, S., Khadem, S., Ren, S., Ellis, E., Strom, S.C., Jetten, A.M. and Xie, W. 2008. Identification of oxysterol 7alpha-hydroxylase (Cyp7b1) as a novel retinoid-related orphan receptor alpha (RORalpha) (NR1F1) target gene and a functional cross-talk between RORalpha and liver X receptor (NR1H3). Molecular pharmacology 73, 891-899.

Wadia, P.R., Vandenberg, L.N., Schaeberle, C.M., Rubin, B.S., Sonnenschein, C. and Soto, A.M. 2007. Perinatal bisphenol A exposure increases estrogen sensitivity of the mammary gland in diverse mouse strains. Environ Health Perspect 115, 592-598.

Waitzberg, D.L., Torrinhas, R.S. and Jacintho, T.M. 2006. New parenteral lipid emulsions for clinical use. JPEN. Journal of parenteral and enteral nutrition 30, 351-367.

Wald, N.J. and Morris, J.K. 2001. Multiple marker second trimester serum screening for pre-eclampsia. J Med Screen 8, 65-68.

Wang, B., Cruz Ithier, M., Parobchak, N., Yadava, S.M., Schulkin, J. and Rosen, T. 2018a. Vitamin D stimulates multiple microRNAs to inhibit CRH and other pro-labor genes in human placenta. Endocr Connect 7, 1380-1388.

Wang, F., Li, S.S., Segersvard, R., Strommer, L., Sundqvist, K.G., Holgersson, J. and Permert, J. 2007. Hypoxia inducible factor-1 mediates effects of insulin on pancreatic cancer cells and disturbs host energy homeostasis. The American journal of pathology 170, 469-477.

Wang, F., Xue, X., Wei, J., An, Y., Yao, J., Cai, H., Wu, J., Dai, C., Qian, Z., Xu, Z. and Miao, Y. 2010a. hsa-miR-520h downregulates ABCG2 in pancreatic cancer cells to inhibit migration, invasion, and side populations. Br J Cancer 103, 567-574.

Wang, H., Lee, E.W., Zhou, L., Leung, P.C., Ross, D.D., Unadkat, J.D. and Mao, Q. 2008a. Progesterone receptor (PR) isoforms PRA and PRB differentially regulate expression of the breast cancer resistance protein in human placental choriocarcinoma BeWo cells. Molecular pharmacology 73, 845-854.

Wang, H., Unadkat, J.D. and Mao, Q. 2008b. Hormonal regulation of BCRP expression in human placental BeWo cells. Pharmaceutical research 25, 444-452.

Wang, H., Wu, X., Hudkins, K., Mikheev, A., Zhang, H., Gupta, A., Unadkat, J.D. and Mao, Q. 2006a. Expression of the breast cancer resistance protein (Bcrp1/Abcg2) in tissues from pregnant mice: effects of pregnancy and correlations with nuclear receptors. American journal of physiology. Endocrinology and metabolism 291, E1295-1304.

Wang, H., Zhou, L., Gupta, A., Vethanayagam, R.R., Zhang, Y., Unadkat, J.D. and Mao, Q. 2006b. Regulation of BCRP/ABCG2 expression by progesterone and 17beta-estradiol in human placental BeWo cells. American journal of physiology. Endocrinology and metabolism 290, E798-807.

Wang, H., Zhou, L., Gupta, A., Vethanayagam, R.R., Zhang, Y., Unadkat, J.D. and Mao, Q. 2006c. Regulation of BCRP/ABCG2 expression by progesterone and 17β-estradiol in human placental BeWo cells. Am J Physiol Endocrinol Metab 290, E798-E807.

Wang, L., Ma, L., Lin, Y., Liu, X., Xiao, L., Zhang, Y., Xu, Y., Zhou, H. and Pan, G. 2018b. Leflunomide Increases Hepatic Exposure to Methotrexate and Its Metabolite by Differentially Regulating Multidrug Resistance-Associated Protein Mrp2/3/4 Transporters via Peroxisome Proliferator-Activated Receptor alpha Activation. Mol Pharmacol 93, 563-574.

Wang, L.J., Wang, S.G. and Deng, T.X. 2018c. [Wogonoside reverses cisplatin resistance in SGC7901/cDDP cells through inhibition of PI3K/Akt/Nrf2/ARE signaling pathway]. Sheng Li Xue Bao 70, 397-405.

Wang, X., Campos, C.R., Peart, J.C., Smith, L.K., Boni, J.L., Cannon, R.E. and Miller, D.S. 2014. Nrf2 upregulates ATP binding cassette transporter expression and activity at the blood-brain and blood-spinal cord barriers. The Journal of neuroscience : the official journal of the Society for Neuroscience 34, 8585-8593.

Wang, X., Hawkins, B.T. and Miller, D.S. 2011. Aryl hydrocarbon receptor-mediated up-regulation of ATP-driven xenobiotic efflux transporters at the blood-brain barrier. FASEB J 25, 644-652.

Wang, X., Sykes, D.B. and Miller, D.S. 2010b. Constitutive androstane receptor-mediated up-regulation of ATP-driven xenobiotic efflux transporters at the blood-brain barrier. Molecular pharmacology 78, 376-383.

Wang, X.K., Agarwal, M., Parobchak, N., Rosen, A., Vetrano, A.M., Srinivasan, A., Wang, B. and Rosen, T. 2016. Mono-(2-Ethylhexyl) Phthalate Promotes Pro-Labor Gene Expression in the Human Placenta. PLoS One 11, e0147013.

Wang, Y., Hao, D., Stein, W.D. and Yang, L. 2006d. A kinetic study of Rhodamine123 pumping by P-glycoprotein. Biochim Biophys Acta 1758, 1671-1676.

Wang, Y., Li, L., Wang, C.C. and Leung, L.K. 2013. Effect of zeranol on expression of apoptotic and cell cycle proteins in murine placentae. Toxicology 314, 148-154.

Wang, Z., Wang, B., Tang, K., Lee, E.J., Chong, S.S. and Lee, C.G. 2005. A functional polymorphism within the MRP1 gene locus identified through its genomic signature of positive selection. Hum Mol Genet 14, 2075-2087.

Wareing, M., Myers, J.E., O'Hara, M. and Baker, P.N. 2005. Sildenafil citrate (Viagra) enhances vasodilatation in fetal growth restriction. J Clin Endocrinol Metab 90, 2550-2555.

Warth, B., Preindl, K., Manser, P., Wick, P., Marko, D. and Buerki-Thurnherr, T. 2019. Transfer and Metabolism of the Xenoestrogen Zearalenone in Human Perfused Placenta. Environ Health Perspect 127, 107004.

Washio, I., Nakanishi, T., Ishiguro, N., Yamamura, N. and Tamai, I. 2018. Impact of Breast Cancer Resistance Protein Expression on the In Vitro Efficacy of Anticancer Drugs in Pancreatic Cancer Cell Lines. Drug Metab Dispos 46, 214-222.

Weaver, G.A., Kurtz, H.J., Behrens, J.C., Robison, T.S., Seguin, B.E., Bates, F.Y. and Mirocha, C.J. 1986. Effect of zearalenone on the fertility of virgin dairy heifers. Am J Vet Res 47, 1395-1397.

Wei, B.R., Xu, C. and Rote, N.S. 2012. Increased resistance to apoptosis during differentiation and syncytialization of BeWo choriocarcinoma cells. Adv Biosci Biotechnol 3, 805-813.

Weksler, B., Romero, I.A. and Couraud, P.O. 2013. The hCMEC/D3 cell line as a model of the human blood brain barrier. Fluids Barriers CNS 10, 16.

Weksler, B.B., Subileau, E.A., Perriere, N., Charneau, P., Holloway, K., Leveque, M., Tricoire-Leignel, H., Nicotra, A., Bourdoulous, S., Turowski, P., Male, D.K., Roux, F., Greenwood,

J., Romero, I.A. and Couraud, P.O. 2005. Blood-brain barrier-specific properties of a human adult brain endothelial cell line. FASEB J 19, 1872-1874.

Westlake, C.J., Cole, S.P. and Deeley, R.G. 2005. Role of the NH2-terminal membrane spanning domain of multidrug resistance protein 1/ABCC1 in protein processing and trafficking. Mol Biol Cell 16, 2483-2492.

Westlake, C.J., Qian, Y.M., Gao, M., Vasa, M., Cole, S.P. and Deeley, R.G. 2003. Identification of the structural and functional boundaries of the multidrug resistance protein 1 cytoplasmic loop 3. Biochemistry 42, 14099-14113.

Whitley, G.S. and Cartwright, J.E. 2010. Cellular and molecular regulation of spiral artery remodelling: lessons from the cardiovascular field. Placenta 31, 465-474.

Whyte-Allman, S.K., Hoque, M.T., Jenabian, M.A., Routy, J.P. and Bendayan, R. 2017. Xenobiotic Nuclear Receptors Pregnane X Receptor and Constitutive Androstane Receptor Regulate Antiretroviral Drug Efflux Transporters at the Blood-Testis Barrier. The Journal of pharmacology and experimental therapeutics 363, 324-335.

Wice, B., Menton, D., Geuze, H. and Schwartz, A.L. 1990. Modulators of cyclic AMP metabolism induce syncytiotrophoblast formation in vitro. Exp Cell Res 186, 306-316.

Wielinga, P.R., van der Heijden, I., Reid, G., Beijnen, J.H., Wijnholds, J. and Borst, P. 2003. Characterization of the MRP4- and MRP5-mediated transport of cyclic nucleotides from intact cells. J Biol Chem 278, 17664-17671.

Wijnholds, J., Mol, C., Scheffer, G., Scheper, R. and Borst, P. 1999. Multidrug resistance protein 5, a candidate multispecific organic anion transporter. Proc Am Assoc Cancer Res, p. 315.

Williams, A.F. 1997. Hypoglycaemia of the newborn: A review. Bull World Health Organ 75, 261-290.

Williams, P.J., Mistry, H.D. and Morgan, L. 2012. Folate transporter expression decreases in the human placenta throughout pregnancy and in pre-eclampsia. Pregnancy hypertension 2, 123-131.

Wolf, G. 2005. Role of reactive oxygen species in angiotensin II-mediated renal growth, differentiation, and apoptosis. Antioxidants & redox signaling 7, 1337-1345.

Wolff, M., Kosyna, F.K., Dunst, J., Jelkmann, W. and Depping, R. 2017. Impact of hypoxia inducible factors on estrogen receptor expression in breast cancer cells. Archives of biochemistry and biophysics 613, 23-30.

Wolffe, A.P. 1996. Histone deacetylase: a regulator of transcription. Science 272, 371-372.

Woods, L., Perez-Garcia, V. and Hemberger, M. 2018. Regulation of Placental Development and Its Impact on Fetal Growth-New Insights From Mouse Models. Front Endocrinol (Lausanne) 9, 570.

Woodward, O.M. 2015. ABCG2: the molecular mechanisms of urate secretion and gout. Am J Physiol Renal Physiol 309, F485-488.

Woodward, O.M., Kottgen, A., Coresh, J., Boerwinkle, E., Guggino, W.B. and Kottgen, M. 2009. Identification of a urate transporter, ABCG2, with a common functional polymorphism causing gout. Proc Natl Acad Sci U S A 106, 10338-10342.

Woodward, O.M., Tukaye, D.N., Cui, J., Greenwell, P., Constantoulakis, L.M., Parker, B.S., Rao, A., Kottgen, M., Maloney, P.C. and Guggino, W.B. 2013. Gout-causing Q141K mutation in ABCG2 leads to instability of the nucleotide-binding domain and can be corrected with small molecules. Proc Natl Acad Sci U S A 110, 5223-5228.

Wright, J.A., Haslam, I.S., Coleman, T. and Simmons, N.L. 2011. Breast cancer resistance protein BCRP (ABCG2)-mediated transepithelial nitrofurantoin secretion and its regulation in human intestinal epithelial (Caco-2) layers. Eur J Pharmacol 672, 70-76.

Wu, B., Jiang, W., Yin, T., Gao, S. and Hu, M. 2012a. A new strategy to rapidly evaluate kinetics of glucuronide efflux by breast cancer resistance protein (BCRP/ABCG2). Pharmaceutical research 29, 3199-3208.

Wu, J.C. and Miller, W.L. 1991. Progesterone shortens poly(A) tails of the mRNAs for alpha and beta subunits of ovine luteinizing hormone. Biol Reprod 45, 215-220.

Wu, X., Zhang, X., Sun, L., Zhang, H., Li, L., Wang, X., Li, W., Su, P., Hu, J., Gao, P. and Zhou, G. 2013. Progesterone negatively regulates BCRP in progesterone receptor-positive human breast cancer cells. Cell Physiol Biochem 32, 344-354.

Wu, X., Zhang, X., Zhang, H., Su, P., Li, W., Li, L., Wang, Y., Liu, W., Gao, P. and Zhou, G. 2012b. Progesterone receptor downregulates breast cancer resistance protein expression via binding to the progesterone response element in breast cancer. Cancer Sci 103, 959-967.

Xia, C., Bai, X., Hou, X., Gou, X., Wang, Y., Zeng, H., Huang, M. and Jin, J. 2015. Cryptotanshinone Reverses Cisplatin Resistance of Human Lung Carcinoma A549 Cells through Down-Regulating Nrf2 Pathway. Cell Physiol Biochem 37, 816-824.

Xiao, J., Wang, Q., Bircsak, K.M., Wen, X. and Aleksunes, L.M. 2015a. In Vitro Screening of Environmental Chemicals Identifies Zearalenone as a Novel Substrate of the Placental BCRP/ABCG2 Transporter. Toxicol Res (Camb) 4, 695-706.

Xiao, J., Wang, Q., Bircsak, K.M., Wen, X. and Aleksunes, L.M. 2015b. Screening of Environmental Chemicals Identifies Zearalenone as a Novel Substrate of the Placental BCRP/ Transporter. Toxicology research 4, 695-706.

Xie, M., Rich, T.C., Scheitrum, C., Conti, M. and Richter, W. 2011. Inactivation of multidrug resistance proteins disrupts both cellular extrusion and intracellular degradation of cAMP. Mol Pharmacol 80, 281-293.

Xie, R., Hammarlund-Udenaes, M., de Boer, A.G. and de Lange, E.C. 1999. The role of P-glycoprotein in blood-brain barrier transport of morphine: transcortical microdialysis studies in mdr1a (-/-) and mdr1a (+/+) mice. Br J Pharmacol 128, 563-568.

Xie, Y., Xu, K., Linn, D.E., Yang, X., Guo, Z., Shimelis, H., Nakanishi, T., Ross, D.D., Chen, H., Fazli, L., Gleave, M.E. and Qiu, Y. 2008. The 44-kDa Pim-1 kinase phosphorylates BCRP/ABCG2 and thereby promotes its multimerization and drug-resistant activity in human prostate cancer cells. J Biol Chem 283, 3349-3356.

Xu, K., Liang, X., Shen, K., Cui, D., Zheng, Y., Xu, J., Fan, Z., Qiu, Y., Li, Q., Ni, L. and Liu, J. 2012a. miR-297 modulates multidrug resistance in human colorectal carcinoma by down-regulating MRP-2. Biochem J 446, 291-300.

Xu, X., Chiung, Y.M., Lu, F., Qiu, S., Ji, M. and Huo, X. 2015. Associations of cadmium, bisphenol A and polychlorinated biphenyl co-exposure in utero with placental gene expression and neonatal outcomes. Reprod Toxicol 52, 62-70.

Xu, X., Zhang, Y., Li, W., Miao, H., Zhang, H., Zhou, Y., Li, Z., You, Q., Zhao, L. and Guo, Q. 2014. Wogonin reverses multi-drug resistance of human myelogenous leukemia K562/A02 cells via downregulation of MRP1 expression by inhibiting Nrf2/ARE signaling pathway. Biochemical pharmacology 92, 220-234.

Xu, Y., Jiang, Z., Yin, P., Li, Q. and Liu, J. 2012b. Role for Class I histone deacetylases in multidrug resistance. Exp Cell Res 318, 177-186.

Xu, Y., Xia, F., Ma, L., Shan, J., Shen, J., Yang, Z., Liu, J., Cui, Y., Bian, X., Bie, P. and Qian, C. 2011. MicroRNA-122 sensitizes HCC cancer cells to adriamycin and vincristine through modulating expression of MDR and inducing cell cycle arrest. Cancer Lett 310, 160-169.

Xu, Y.Q., Zhang, D., Jin, T., Cai, D.J., Wu, Q., Lu, Y., Liu, J. and Klaassen, C.D. 2012c. Diurnal variation of hepatic antioxidant gene expression in mice. PloS one 7, e44237.

Yacovino, L.L. and Aleksunes, L.M. 2012. Endocrine and metabolic regulation of renal drug transporters. J Biochem Mol Toxicol 26, 407-421.

Yamamoto, Y., Moore, R., Goldsworthy, T.L., Negishi, M. and Maronpot, R.R. 2004. The orphan nuclear receptor constitutive active/androstane receptor is essential for liver tumor promotion by phenobarbital in mice. Cancer research 64, 7197-7200.

Yang, H. and Wang, H. 2014. Signaling control of the constitutive androstane receptor (CAR). Protein & cell 5, 113-123.

Yang, J., AlTahan, A., Jones, D.T., Buffa, F.M., Bridges, E., Interiano, R.B., Qu, C., Vogt, N., Li, J.L., Baban, D., Ragoussis, J., Nicholson, R., Davidoff, A.M. and Harris, A.L. 2015. Estrogen receptor-alpha directly regulates the hypoxia-inducible factor 1 pathway associated with antiestrogen response in breast cancer. Proceedings of the National Academy of Sciences of the United States of America 112, 15172-15177.

Yang, X., Ma, Z., Zhou, S., Weng, Y., Lei, H., Zeng, S., Li, L. and Jiang, H. 2016. Multiple Drug Transporters Are Involved in Renal Secretion of Entecavir. Antimicrobial agents and chemotherapy 60, 6260-6270.

Yao, J., Wei, X. and Lu, Y. 2016. Chaetominine reduces MRP1-mediated drug resistance via inhibiting PI3K/Akt/Nrf2 signaling pathway in K562/Adr human leukemia cells. Biochem Biophys Res Commun 473, 867-873.

Yasuda, S., Itagaki, S., Hirano, T. and Iseki, K. 2005. Expression level of ABCG2 in the placenta decreases from the mid stage to the end of gestation. Biosci Biotechnol Biochem 69, 1871-1876.

Yasuda, S., Itagaki, S., Hirano, T. and Iseki, K. 2006. Effects of sex hormones on regulation of ABCG2 expression in the placental cell line BeWo. Journal of pharmacy & pharmaceutical sciences : a publication of the Canadian Society for Pharmaceutical Sciences, Societe canadienne des sciences pharmaceutiques 9, 133-139.

Yasuda, S., Kobayashi, M., Itagaki, S., Hirano, T. and Iseki, K. 2009. Response of the ABCG2 promoter in T47D cells and BeWo cells to sex hormone treatment. Molecular biology reports 36, 1889-1896.

Yeboah, D., Sun, M., Kingdom, J., Baczyk, D., Lye, S.J., Matthews, S.G. and Gibb, W. 2006. Expression of breast cancer resistance protein (BCRP/ABCG2) in human placenta throughout gestation and at term before and after labor. Canadian journal of physiology and pharmacology 84, 1251-1258.

You, D., Shin, H.M., Mosaad, F., Richardson, J. and Aleksunes, L. 2019. Brain-region specific regulation of histone acetylation and efflux transporters in mice. J Biochem Mol Toxicol Forthcoming.

Young, L.G. and King, G.J. 1986. Low concentrations of zearalenone in diets of mature gilts. J Anim Sci 63, 1191-1196.

Zamber, C.P., Lamba, J.K., Yasuda, K., Farnum, J., Thummel, K., Schuetz, J.D. and Schuetz, E.G. 2003. Natural allelic variants of breast cancer resistance protein (BCRP) and their relationship to BCRP expression in human intestine. Pharmacogenetics 13, 19-28.

Zamek-Gliszczynski, M.J., Day, J.S., Hillgren, K.M. and Phillips, D.L. 2011. Efflux transport is an important determinant of ethinylestradiol glucuronide and ethinylestradiol sulfate pharmacokinetics. Drug metabolism and disposition: the biological fate of chemicals 39, 1794-1800.

Zampieri, L., Bianchi, P., Ruff, P. and Arbuthnot, P. 2002. Differential modulation by estradiol of P-glycoprotein drug resistance protein expression in cultured MCF7 and T47D breast cancer cells. Anticancer Res 22, 2253-2259.

Zamudio, S., Baumann, M.U. and Illsley, N.P. 2006. Effects of chronic hypoxia in vivo on the expression of human placental glucose transporters. Placenta 27, 49-55.

Zamudio, S., Wu, Y., Ietta, F., Rolfo, A., Cross, A., Wheeler, T., Post, M., Illsley, N.P. and Caniggia, I. 2007. Human placental hypoxia-inducible factor-1alpha expression correlates with clinical outcomes in chronic hypoxia in vivo. The American journal of pathology 170, 2171-2179.

Zelzer, E., Levy, Y., Kahana, C., Shilo, B.Z., Rubinstein, M. and Cohen, B. 1998. Insulin induces transcription of target genes through the hypoxia-inducible factor HIF-1alpha/ARNT. EMBO J 17, 5085-5094.

Zeng, H., Bain, L.J., Belinsky, M.G. and Kruh, G.D. 1999. Expression of multidrug resistance protein-3 (multispecific organic anion transporter-D) in human embryonic kidney 293 cells confers resistance to anticancer agents. Cancer Res 59, 5964-5967.

Zeng, H., Chen, Z.S., Belinsky, M.G., Rea, P.A. and Kruh, G.D. 2001. Transport of methotrexate (MTX) and folates by multidrug resistance protein (MRP) 3 and MRP1: effect of polyglutamylation on MTX transport. Cancer Res 61, 7225-7232.

Zeng, H., Liu, G., Rea, P.A. and Kruh, G.D. 2000. Transport of amphipathic anions by human multidrug resistance protein 3. Cancer Res 60, 4779-4784.

Zhang, H., Jing, X., Wu, X., Hu, J., Zhang, X., Wang, X., Su, P., Li, W. and Zhou, G. 2015a. Suppression of multidrug resistance by rosiglitazone treatment in human ovarian cancer cells through downregulation of FZD1 and MDR1 genes. Anticancer Drugs 26, 706-715.

Zhang, N., Wang, W., Li, W., Liu, C., Chen, Y., Yang, Q., Wang, Y. and Sun, K. 2015b. Inhibition of 11beta-HSD2 expression by triclosan via induction of apoptosis in human placental syncytiotrophoblasts. J Clin Endocrinol Metab 100, E542-549.

Zhang, S., Regnault, T.R., Barker, P.L., Botting, K.J., McMillen, I.C., McMillan, C.M., Roberts, C.T. and Morrison, J.L. 2015c. Placental adaptations in growth restriction. Nutrients 7, 360-389.

Zhang, S., Yang, X. and Morris, M.E. 2004a. Flavonoids are inhibitors of breast cancer resistance protein (ABCG2)-mediated transport. Mol. Pharmacol. 65, 1208-1216.

Zhang, Y. and Klaassen, C.D. 2010. Effects of feeding bile acids and a bile acid sequestrant on hepatic bile acid composition in mice. Journal of lipid research 51, 3230-3242.

Zhang, Y., Schuetz, J.D., Elmquist, W.F. and Miller, D.W. 2004b. Plasma membrane localization of multidrug resistance-associated protein homologs in brain capillary endothelial cells. J Pharmacol Exp Ther 311, 449-455.

Zhang, Y., Wang, H., Unadkat, J.D. and Mao, Q. 2007. Breast cancer resistance protein 1 limits fetal distribution of nitrofurantoin in the pregnant mouse. Drug Metab Dispos 35, 2154-2158.

Zhang, Y., Zhou, G., Wang, H., Zhang, X., Wei, F., Cai, Y. and Yin, D. 2006. Transcriptional upregulation of breast cancer resistance protein by 17beta-estradiol in ERalpha-positive MCF-7 breast cancer cells. Oncology 71, 446-455.

Zhang, Y.K., Guo, G.L. and Klaassen, C.D. 2011. Diurnal variations of mouse plasma and hepatic bile acid concentrations as well as expression of biosynthetic enzymes and transporters. PloS one 6, e16683.

Zhao, Y.Z., Liu, X.L., Shen, G.M., Ma, Y.N., Zhang, F.L., Chen, M.T., Zhao, H.L., Yu, J. and Zhang, J.W. 2014. Hypoxia induces peroxisome proliferator-activated receptor gamma expression via HIF-1-dependent mechanisms in HepG2 cell line. Archives of biochemistry and biophysics 543, 40-47.

Zheng, R., Po, I., Mishin, V., Black, A.T., Heck, D.E., Laskin, D.L., Sinko, P.J., Gerecke, D.R., Gordon, M.K. and Laskin, J.D. 2013. The generation of 4-hydroxynonenal, an electrophilic lipid peroxidation end product, in rabbit cornea organ cultures treated with UVB light and nitrogen mustard. Toxicology and applied pharmacology 272, 345-355.

Zhou, L., Naraharisetti, S.B., Wang, H., Unadkat, J.D., Hebert, M.F. and Mao, Q. 2008a. The breast cancer resistance protein (Bcrp1/Abcg2) limits fetal distribution of glyburide in the pregnant mouse: an Obstetric-Fetal Pharmacology Research Unit Network and University of Washington Specialized Center of Research Study. Molecular pharmacology 73, 949-959.

Zhou, L., Naraharisetti, S.B., Wang, H., Unadkat, J.D., Hebert, M.F. and Mao, Q. 2008b. The breast cancer resistance Protein (Bcrp1/Abcg2) limits fetal distribution of glyburide in the pregnant mouse: An Obstetric-Fetal Pharmacology Research Unit Network and University of Washington Specialized Center of Research Study. Mol Pharmacol 73, 949-959.

Zhu, H., Chen, X.P., Luo, S.F., Guan, J., Zhang, W.G. and Zhang, B.X. 2005. Involvement of hypoxia-inducible factor-1-alpha in multidrug resistance induced by hypoxia in HepG2 cells. Journal of experimental & clinical cancer research : CR 24, 565-574.

Zhu, H., Luo, S.F., Wang, J., Li, X., Wang, H., Pu, W.Y., Zhang, H. and Zhuang, Z.X. 2012a. Effect of environmental factors on chemoresistance of HepG2 cells by regulating hypoxia-inducible factor-1alpha. Chinese medical journal 125, 1095-1103.

Zhu, L., Yuan, H., Guo, C., Lu, Y., Deng, S., Yang, Y., Wei, Q., Wen, L. and He, Z. 2012b. Zearalenone induces apoptosis and necrosis in porcine granulosa cells via a caspase-3- and caspase-9-dependent mitochondrial signaling pathway. J Cell Physiol 227, 1814-1820.

Zhu, Y., Li, F. and Guo, G.L. 2011. Tissue-specific function of farnesoid X receptor in liver and intestine. Pharmacological research : the official journal of the Italian Pharmacological Society 63, 259-265.

Ziegler, T.R. and Leader, L.M. 2006. Parenteral nutrition: transient or permanent therapy in intestinal failure? Gastroenterology 130, S37-42.

Zinedine, A., Soriano, J.M., Moltó, J.C. and Mañes, J. 2007. Review on the toxicity, occurrence, metabolism, detoxification, regulations and intake of zearalenone: An oestrogenic mycotoxin. Food and Chemical Toxicology 45, 1-18.